

---

## **Advanced Characterization Method**

CLUB A

*Monday, July 22 2013, 10:30 am - 12:00 pm*

Chair: **Pam Thomas**  
*University of Warwick*

## Recent progress in dielectric and light scattering spectroscopy of ferroelectric soft modes

Jan Petzelt, Elena Buixaderas, Tetyana Ostapchuk, Dmitry Nuzhnyy, Volodymyr Skoromets, Veronica Goian, Viktor Bovtun, Ivan Gregora, Christelle Kadlec, Filip Kadlec, Stanislav Kamba, Petr Kuzel, Jiri Hlinka

Department of Dielectrics, Institute of Physics, Academy of Sciences of the Czech Republic Na Slovance 2, 18221 Praha 8, Czech Republic

Email: petzelt@fzu.cz

Recent results on ferroelectric soft modes using infrared (IR), time-domain THz and microwave (MW) dielectric spectroscopies as well as Raman and hyper-Raman spectroscopies on single crystals, ceramics and thin films are summarized. In particular, new results obtained on classical perovskite ferroelectrics BaTiO<sub>3</sub> (BTO) single crystals and ceramics, SrTiO<sub>3</sub> (STO) films, PbTiO<sub>3</sub> (PTO) and PbZrO<sub>3</sub> (PZO) single crystals, (Ba,Sr)TiO<sub>3</sub> (BST), (Pb,Zr)TiO<sub>3</sub> (PZT), (Ba,Zr)TiO<sub>3</sub> (BZT) and (K,Na)NbO<sub>3</sub> (KNN) solid solutions, and PbMg<sub>1/3</sub>Nb<sub>2/3</sub>O<sub>3</sub> (PMN) single crystals are emphasized, but also other structure types, as Ruddlesden-Popper phases derived from STO structure and GeTe films are mentioned. The samples for our studies are obtained from several collaborating laboratories.

In the case of BST, the dielectric response is discussed from the point of view of coupled soft and central mode model in the whole composition range and BTO is shown to be the most anharmonic system<sup>1</sup>. The same model approach is successfully applied to tensile strained epitaxial thin STO films on DyScO<sub>3</sub> substrates, which exhibit ferroelectric transition near room temperature; the important impact of Sr stoichiometry on their properties is also studied and discussed. Similar features are revealed in the dynamics of KNN ceramics<sup>2</sup> and in PZT in a broad composition range around the morphotropic phase boundary<sup>3</sup>. In the case of BZT ceramics, the dynamics of both the relaxor and diffuse ferroelectric behavior is studied, consisting of strong softening of an overdamped central-mode component from THz down to GHz range and by almost no phonon softening<sup>4</sup>. In classical relaxor single crystal PMN, the hyper-Raman data reveal a clear splitting of the soft mode in a broad temperature range due to the local symmetry breaking<sup>5</sup>, appearing along with the well-known MW and lower-frequency central-mode type dispersion.

On the other hand, the new hyper-Raman data on paraelectric PTO and IR data on paraelectric PZO single crystals indicate a negligible role of the central mode<sup>6</sup>. In the antiferroelectric PZO, IR and Raman data show several anomalous low-frequency modes for all orthorhombic symmetry types, which are discussed in terms of the recent understanding of the complex phase transition. In conducting thin GeTe films no significant phonon softening is detected; instead a critical THz relaxation is observed in the paraelectric phase with strength comparable to that of the free carrier absorption<sup>7</sup>.

<sup>1</sup> J. Weerasinghe et al., MRS Com., doi 10.1557/mrc.2013.5.

<sup>2</sup> E. Buixaderas et al., J. Appl. Phys. **107**, 014111 (2010).

<sup>3</sup> E. Buixaderas et al., Phys. Rev. B **84**, 184302 (2011).

<sup>4</sup> D. Nuzhnyy et al., Phys. Rev. B **86**, 014106 (2012).

<sup>5</sup> A. Al-Zein et al., Phys. Rev. Lett. **105**, 017601 (2010).

<sup>6</sup> J. Hlinka et al., Phys. Rev. B **87**, 064101 (2013).

<sup>7</sup> F. Kadlec et al., Phys. Rev. B **84**, 205209 (2011).

## A new method of dielectric characterization in the microwave range for tunable high-k ferroelectric thin films

Kevin Nadaud<sup>1</sup>, Raphaël Renoud<sup>1</sup>, Hartmut W. Gundel<sup>1</sup>, Caroline Borderon<sup>1</sup>, Raphaël Gillard<sup>2</sup>

<sup>1</sup>IETR, University of Nantes, Nantes, France

<sup>2</sup>IETR, INSA of Rennes, Rennes, France

E-mail: kevin.nadaud@univ-nantes.fr

Ferroelectric thin films are widely studied for its non constant dielectric permittivity which allows realization of electrically tunable components and devices such as microwave filters, reflectarray antennas, resonators or phase shifters. Depending on the component architecture, the film has to be elaborated either on a conducting electrode or on an insulating substrate. As thin film synthesis, and hence the dielectric properties, strongly depend on the substrate's crystalline structure, it is important to characterize using the same topology as this of the final component.

The method proposed allows measuring the complex permittivity of a ferroelectric thin film in the microwave range using CoPlanar Waveguide (CPW) technology. MIM (Metal Insulator Metal) topology would not be appropriate for the foreseen application (a reconfigurable reflect array cell). Elaboration of the ferroelectric thin film is reported elsewhere<sup>8</sup>. Most characterization methods relying on CPW are based on propagation constant or effective permittivity measurements. In the case of high-k thin films, however, the obtained accuracy is usually poor because the film permittivity does not have a high influence on the effective overall permittivity which also includes the contribution of the thick substrate (of relatively low permittivity).

In the present case, we propose a topology which consists of two CPW transmission lines separated by a gap (Fig. 1). In order to determine the gap-capacitance, a TRL (Thru, Reflect, Line) calibration method is used for the de-embedding of the lines. The permittivity of the thin film can be extracted by full wave simulation or with a mathematical model based on conformal mapping such as in Vendik's *et al.* work<sup>9</sup> that does not use CPW technology. In our case, however, the capacitance also strongly depends on the ferroelectric permittivity because the gap in the center line is very narrow.

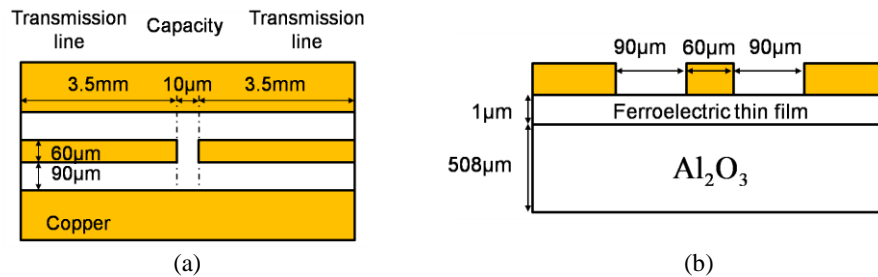


Fig. 1: Illustration of the measuring circuit. Top view (a) of the capacity between two coplanar transmission lines and side view (b) of the ferroelectric thin film deposited on an alumina substrate.

<sup>8</sup> C. Borderon, D. Averty, R. Seveno, H.W. Gundel, "Influence of the morphology of Barium Strontium Titanate thin films on the ferroelectric and dielectric properties", *Integrated Ferroelectrics* **97** (2008) 12-19

<sup>9</sup> O. G. Vendik, S. P. Zubko, and M. A. Nikol'ski "Modeling and calculation of the capacitance of a planar capacitor containing a ferroelectric thin film" *J. Tech. Phy* **44** (1999) 349-355

## Central mode in perovskite ferroelectrics: terahertz spectroscopy and molecular dynamics simulations

P. Kužel<sup>1</sup>, T. Ostapchuk<sup>1</sup>, C. Kadlec<sup>1</sup>, J. Weerasinghe<sup>2</sup>, L. Bellaiche<sup>2</sup> and J. Hlinka<sup>1</sup>

<sup>1</sup>Institute of Physics ASCR, Na Slovance 2, Prague, 182 21, Czech Republic

<sup>2</sup>Department of Physics, University of Arkansas, Fayetteville, Arkansas 72701, USA

Email: kuzelp@fzu.cz

Two limiting cases of structural phase transitions are often distinguished: displacive and order-disorder types. In the displacive case, the equilibrium positions of atoms or ions in the crystal correspond to their average positions. The phase transition is triggered by a change of these positions related to the freezing of a low-frequency phonon mode (called “soft mode”, SM). The order-disorder case involves partially occupied sites given by the potential minima (disorder) and the transition is connected to the symmetry breaking of their spatial distribution (ordering): this is connected to an excitation of the relaxation type (called “central mode”, CM). These excitations are observed by terahertz spectroscopy in ferroelectric perovskite oxides like (Ba,Sr)TiO<sub>3</sub> or K(Ta,Nb)O<sub>3</sub> and they often coexist even in the paraelectric phases and couple to each other<sup>10,11</sup>. The complex dielectric function  $\varepsilon(\omega)$  in the terahertz range then can be usually described by

$$\varepsilon(\omega) = \frac{\Omega_0^2}{\omega_0^2 - \omega^2 - i\omega\Gamma - \delta^2/(1 - i\omega/\gamma)} + \varepsilon_\infty, \quad (1)$$

where  $\Omega_0$ ,  $\omega_0$ ,  $\Gamma$  are the plasma frequency, oscillator frequency and damping constant of the SM, respectively;  $\gamma$  is the bare relaxation frequency of the CM and  $\delta$  is the coupling constant.

The experiments can be confronted with molecular dynamics calculations based on an effective Hamiltonian with parameters derived from first principles. The dynamical degrees of freedom consist of inhomogeneous and homogeneous strain variables and of so called “local soft modes” corresponding to local (within a unit cell) displacements of atoms with the SM eigenvector<sup>1,12</sup>. These degrees of freedom are sufficient to explain that in the studied perovskites the CM suddenly appears in the spectra well above the ferroelectric phase transition. The coexistence of the two spectral features is then an intrinsic property of these materials and a consequence of a complex anharmonic form of the soft mode effective potential.

In this contribution we will compare experimental terahertz dielectric spectra on Ba<sub>x</sub>Sr<sub>1-x</sub>TiO<sub>3</sub> (BST) system with molecular dynamics simulations. The temperature trends of the SM and CM behavior are investigated in the paraelectric phase ( $T > T_C$ ). A transition is observed between high-temperature spectra ( $T > T_{CM}$ ) described by a simple damped harmonic oscillator (SM) and a low-temperature behavior ( $T < T_{CM}$ ) where the spectra fit to the coupled SM-CM model (1). The CM is understood as a thermally activated process of hopping between quasi-stable off-center Ti ionic positions described by Arrhenius-type temperature dependence<sup>3</sup>. This thermal activation process is at the origin of the change of the regime between fast and slow relaxation dynamics which then appears almost as a phase transition in the spectra.

<sup>10</sup>J. Hlinka et al., Phys. Rev. Lett., vol. 101, 167402, 2008.

<sup>11</sup>C. Kadlec et al., Phys. Rev. B, vol. 80, 174116, 2009; V. Skoromets et al., Appl. Phys. Lett., vol. 99, 052908, 2011.

<sup>12</sup>J. Weerasinghe et al., MRS Communications, available online February 2013. doi:10.1557/mrc.2013.5.



## Elastic Anomalies in Ferroelectric Ceramics: $\text{Pb}(\text{Mg}_{1/3}\text{Nb}_{2/3})\text{O}_3$ as Elastic Relaxor, Octahedral Tilts in Tetragonal $\text{Pb}(\text{Zr},\text{Ti})\text{O}_3$ and Magneto-elastic Coupling in $\text{BiFeO}_3$

Hana Ursic<sup>1,2</sup>, Tadej Rojac<sup>1,2</sup>, Li Jin (靳立)<sup>3</sup>, Dragan Damjanovic<sup>4</sup>

<sup>1</sup>Electronic Ceramics Department, Jozef Stefan Institute, Ljubljana, Slovenia

<sup>2</sup>CoE NAMASTE, Ljubljana, Slovenia

<sup>3</sup>Electronic Materials Research Laboratory, Key Laboratory of the Ministry of Education & International Center for Dielectric Research, Xi'an Jiaotong University, Xi'an, China

<sup>4</sup>Ceramics Laboratory, Swiss Federal Institute of Technology in Lausanne - EPFL, Lausanne, Switzerland

Email: dragan.damjanovic@epfl.ch

In the large majority of experimental studies the properties of ferroelectrics are examined through dielectric (polarization-electric field) or piezoelectric (stress/electric field-charge/strain) relations. It is well known and since a long time, however, that elastic (strain-stress) properties of ferroelectrics may be very sensitive at low frequencies to structural phase transitions and domain-walls related processes.<sup>i,ii,iii,iv,v,vi</sup> Elastic studies offer complementary information to more common dielectric- and piezoelectric-oriented investigations and are thus crucial for a better understanding of ferroelectrics.

In this presentation we show results of our recent studies on elastic properties of ferroelectric ceramics. We employed the dynamic mechanical analyzer technique (DMA), in some cases backed by piezoelectric resonance measurements, to study several distinct phenomena in ferroelectrics. We demonstrate that typical relaxor ferroelectric,  $\text{Pb}(\text{Mg}_{1/3}\text{Nb}_{2/3})\text{O}_3$ , exhibits elastic relaxor behavior, which we have measured over two orders of magnitude in frequency. That is,  $\text{Pb}(\text{Mg}_{1/3}\text{Nb}_{2/3})\text{O}_3$  exhibits what is today called the “strain glass-like” behavior.<sup>vii</sup> We show evidence of octahedral tilts in two compositions of tetragonal phase of  $\text{Pb}(\text{Zr}_{1-x}\text{Ti}_x)\text{O}_3$  ( $x=0.55$  and  $58$ ), thus confirming results of earlier infrared spectroscopy study<sup>viii</sup> and ab-initio calculations<sup>ix</sup>. Finally, we give evidence of what appears to be a strong magneto-elastic coupling in  $\text{BiFeO}_3$ .<sup>x</sup>

## Ultrasonic determination of anisotropic elasticity of DyScO3 substrates

Hanus Seiner<sup>1</sup>, Petr Sedlak<sup>1</sup>, Michaela Janovska<sup>1</sup>, Michal Landa<sup>1</sup>,

Pavel Marton<sup>2</sup>, Petr Ondrejko<sup>2</sup> and Jiri Hlinka<sup>2</sup>

<sup>1</sup>Laboratory of Ultrasonic Methods, Institute of Thermomechanics, ASCR,  
Praha, Czech Republic

<sup>2</sup>Department of Dielectrics, Institute of Physics ASCR, Praha, Czech Republic

Email: ML@it.cas.cz

Rare-earth scandate single crystals have become very popular as substrate materials for the epitaxial growth of functional thin films, especially in case of ferroelectric and multiferroic perovskite oxides, such as BiFeO<sub>3</sub>; EuTiO<sub>3</sub>; BaTiO<sub>3</sub>; SrTiO<sub>3</sub> or BiMnO<sub>3</sub>. Hence the elastic constants of the scandates are of high importance for understanding the behavior of the perovskite films and their further development.

The full elastic tensor of orthorhombic dysprosium scandate (DyScO<sub>3</sub>) at room temperature was determined by resonant ultrasound spectroscopy (RUS) complemented by pulse-echo measurement. Measurements (Fig.1) were performed on three 500 um thick substrates with orientations (110), (100) and (001). For this purpose, a modification of the RUS method was developed, enabling simultaneous processing of the resonant spectra of several platelet-shaped samples with different crystallographic orientations.

The obtained results are compared with ab initio calculations and with elastic constants of other rare-earth scandates, and are used for discussion of the in-plane elasticity of the (110)-oriented substrate (Fig2).

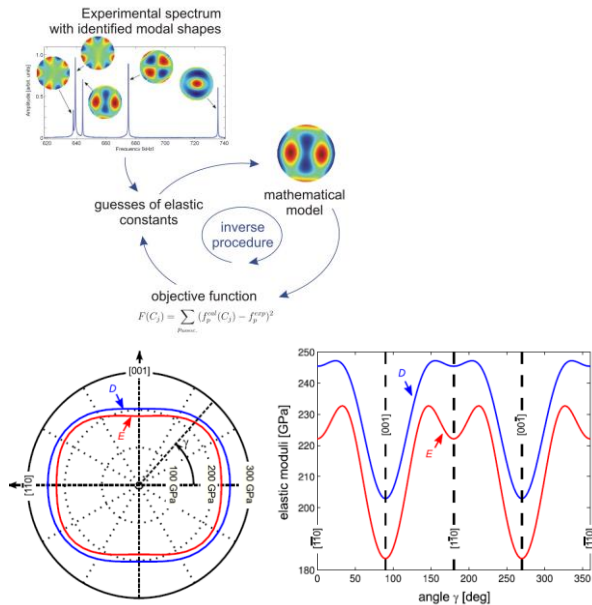


Fig.1. Schema of the modal RUS

Fig.2. Anisotropy of the Young's modulus (E) and the bending rigidity (D) of the (110)-oriented DyScO<sub>3</sub> substrate.

---

## **Piezoelectrics**

CLUB B

*Monday, July 22 2013, 10:30 am - 12:00 pm*

Chair: **Shujun Zhang**  
*Pennsylvania State University*

## Complete Description of Piezoelectric Response in Fundamental Equations

Takaaki Tsurumi, Manabu Hagiwara, Takuya Hoshina and Hiroaki Takeda

Graduate School of Science and Engineering,  
Tokyo Institute of Technology, Meguro, Tokyo, Japan.

Email: ttsurumi@ceram.titech.ac.jp

Promising applications of piezoelectric ceramics have been changing from devices operated under low electric fields in electronic circuits to those driven by high electric fields such as actuators for ink-jet heads, fuel injectors of diesel engines, etc. Under such large-signal operation, response of piezoelectric ceramics deviates from the conventional linear piezoelectric theory, leading to the appearance of nonlinear phenomena which causes the unstable operation and heat generation of the devices. Many researchers have aimed to incorporate the nonlinear and dissipation effects into the piezoelectric theory, but complete theory of the piezoelectric response have not been established yet. In this study, we will propose fundamental equations describing the piezoelectric response under the large-signal operation.

The fundamental equations are based on an assumption to simplify the situation: that is piezoelectric  $e$  coefficient is ‘real and constant’. The piezoelectric  $e$  coefficient is defined by  $D = eS$ , where  $D$  and  $S$  are electric displacement and strain, respectively, and  $D$  can be regarded as polarization  $P$  in piezoelectric ceramics with high permittivity. Thus, the ‘real and constant’  $e$  coefficient means that  $S$  and  $P$  have a linear relationship without a phase lag. This assumption stands to reason, since both  $S$  and  $P$  are originated from crystal lattice deformation (intrinsic effect) and non-180° domain wall motion (extrinsic effect). From a Taylor series expansion of elastic Gibbs energy considering the assumption, we have derived the following nonlinear piezoelectric equations in  $e$ -form:

$$\begin{cases} T = c^{E(1)*} S + c^{E(2)*} S^2 + c^{E(3)*} S^3 - eE - \gamma E^2 \\ D = eS + 2\gamma ES + \varepsilon^{S(1)*} E + \varepsilon^{S(2)*} E^2 + \varepsilon^{S(3)*} E^3 \end{cases}$$

where  $T$  is stress;  $E$  is electric field;  $c^{E(i)*}$  is  $i$ th-order elastic stiffness;  $\varepsilon^{S(i)*}$  is  $i$ th-order permittivity;  $\gamma$  is electrostrictive coefficient. Using the above equations, we analyzed so-called “jump phenomenon” in piezoelectric resonator, which is a discontinuous change of current and/or displacement in piezoelectric resonator at its resonance frequency. As shown in Fig. 1, the resonance curve calculated from the fundamental equations gave a very good agreement with experimental results of PZT-based ceramics driven by high electric field. Moreover, we also found that the proposed fundamental equation could describe waveforms of piezoelectric response distorted by the nonlinear effect.

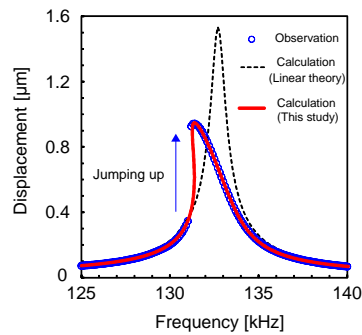


Fig. 1: Resonance curve of PZT-based ceramics (31-mode resonator) driven by high electric field.

## Enhanced Large Signal Performance of PZT Thick Film Actuators for Active Micro-Optics

Dörthe Ernst<sup>1</sup>, Bernhard Bramlage<sup>1</sup>, Sylvia Gebhardt<sup>1</sup>, Oliver Pabst<sup>2</sup>, Andreas Schönecker<sup>1</sup>

<sup>1</sup>Fraunhofer Institute for Ceramic Technologies and Systems (IKTS), Dresden, Germany

<sup>2</sup>Fraunhofer Institute for Applied Optics and Precision Engineering (IOF), Jena, Germany

Email: doerthe.ernst@ikts.fraunhofer.de

In adaptive optics actuators which allow for high precision positioning with short response time are needed. More often complex actuator structures which can be individually driven are beneficial. Piezoceramic thick films offer integrated solutions. By the use of screen printing technology, net-shaped actuator structures can be directly prepared on wafer-level with high accuracy and reproducibility.

At Fraunhofer IKTS piezoceramic thick films based on lead zirconate titanate (PZT) are available. They show excellent small and large signal properties. The paper will report on the performance of bending actuators based on two different PZT compositions. The results lead into the development of complex bending structures (Fig. 1c) which will be used to move micro-lens arrays within a flat-building camera.

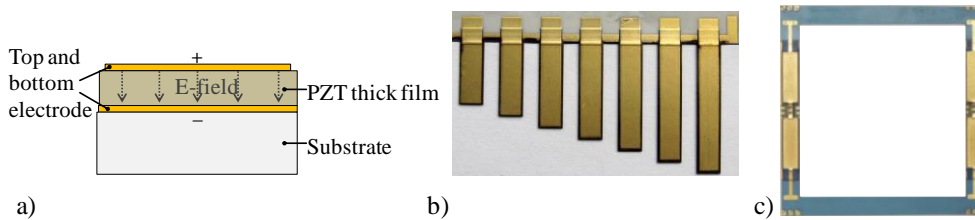


Fig. 2:

a) Schematic cross section of a PZT thick film layer setup, b) screen printed comb structure, c) actuator frame for moveable optical elements

The typical layer setup (Fig. 1a) considered consists of a substrate and two flat electrodes ( $\sim 10 \mu\text{m}$ ) with an intermediate PZT layer ( $\sim 100 \mu\text{m}$ ). In order to increase the performance of such bending actuators we analyzed large signal properties, such as free displacement and blocking force, depending on the substrate material, the cantilever length and the amount of sintering aid. Comb structures with varied cantilever length between 11 and 23 mm as shown in Fig. 1b were built on alumina and Low Temperature Cofired Ceramic (LTCC) substrates. We present the results for two thick film compositions, our standard PZ 5100 and a new composition PZ 5300.

A PZ 5100 cantilever of 4 mm width and 15 mm length with an amount of 10% sintering aid generates blocking forces of 112 mN and 107 mN and free displacements of 42  $\mu\text{m}$  and 106  $\mu\text{m}$  for alumina and LTCC substrates respectively. The new thick film composition PZ 5300, with higher piezoceramic constants reaches an excellent performance with a sintering aid content of 6.5%. Alumina based cantilevers of the same dimensions exhibit free displacements of about 70  $\mu\text{m}$  and blocking forces of about 180 mN. LTCC based cantilevers show values of about 190  $\mu\text{m}$  and 170 mN.

Actuator frames with a size of 45 x 44 mm<sup>2</sup> (Fig. 1c) generate a stroke of about 220  $\mu\text{m}$  at 2 kV/mm. These frames enable an accurate positioning of centrally mounted micro-lens arrays which will be applied to adapt the focal length of flat-building optical elements.

## Microstereolithography of Piezoelectric Components

David I. Woodward<sup>1</sup>, Simon J. Leigh<sup>2</sup>, Connor Watts<sup>1</sup>, Rui Wang<sup>1</sup>, Chris Purssell<sup>2</sup>, Pam A. Thomas<sup>1</sup>,  
Duncan R. Billson<sup>2</sup>

<sup>1</sup>Department of Physics, University of Warwick, Coventry, UK

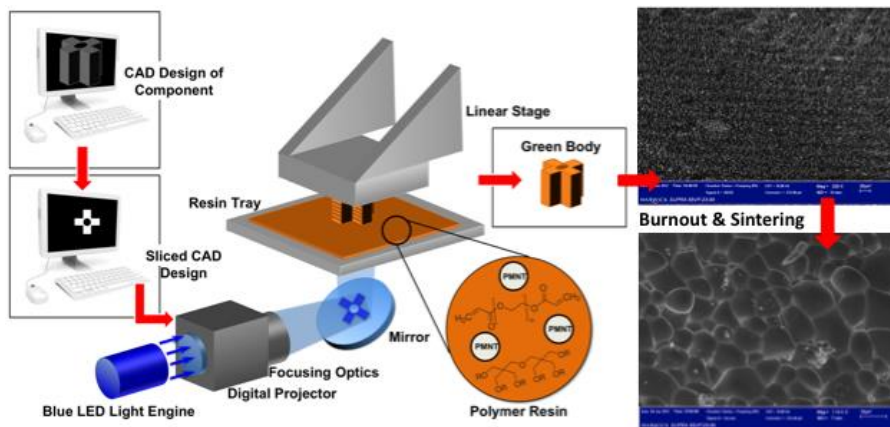
<sup>2</sup>School of Engineering, University of Warwick, Coventry, UK

Email: d.i.woodward@warwick.ac.uk

Microstereolithography (MSL) is an additive manufacturing process whereby a three-dimensional object is created in an additive, layer-by-layer process. The technology can be used to rapidly create complex structures with fine resolution of around 20  $\mu\text{m}$ . The process involves creating a digital design of the final object, slicing this design into a set of cross-sections and then sequentially rendering each cross-section using a thin layer of photosensitive resin. In this way, extremely complex objects such as interlaced lattices can be built with relative ease.

Our work is concerned with the adaptation of this technique to produce functional composites and ceramics. Ferroelectric  $\text{Pb}(\text{Mg}_{1/2}\text{Nb}_{1/2})\text{O}_3\text{-PbTiO}_3$  (PMNT) powder is added to the uncured resin and, once cured, confers the final object with piezoelectric properties. If this composite is heated to the sintering temperature of the PMNT, the organic components are burnt off and the remaining powder densifies, resulting in a miniaturized ceramic version of the original object.

In this talk, recent results will be presented showing the electrical properties of 'piezocomposites' produced by the MSL technique. The effects of sintering will be shown and the effects of modifying the initial chemistry on the density, structure and piezoelectric and ferroelectric characters of these sintered components will be discussed and compared with ceramics of the same composition produced by conventional processes. The application of this technique to the production of devices will be illustrated with some prototype examples.



## Fabrication and Electromagnetic Properties of 3D Photonic Crystals for Microwave Applications

Wei Dai, Hong Wang

Electronic Materials Research Laboratory, Key Laboratory of Ministry of Education, Xi'an Jiaotong University, Xi'an 710049, China

Email: hwang@mail.xjtu.edu.cn

Photonic crystals (PCs) as a new periodical structure material have inspired great interests of scientists and industry for their unique, flexible and desirable photonic band gap properties. On the study of the photonic crystals, it needs to carry out the structure design, in which the main factors influenced the photonic band gap should be investigated. It needs to master the photonic crystals fabrication process and investigate the influences of the various defects introduced into the photonic crystals on the transmission properties of the electromagnetic wave. In this work, the 3D photonic crystals with diamond structure for microwave applications were designed, fabricated and investigated. Through the theory simulation, the main factors influenced the photonic bandgaps have been obtained. The rapid prototyping and gel casting together with the sintering technique were chosen as the main fabrication method. Several kinds of microwave ceramics based PCs had been fabricated and investigated.<sup>13</sup> Then the influence of periodical lattice constant changing PCs on the electromagnetic wave propagating properties was investigated. By introducing the defects into the PCs, the influence of point defects, line defects and planar defects on the electromagnetic wave propagating properties was studied.<sup>14,15,16</sup> The coupling of different defect modes has been also studied and discussed.

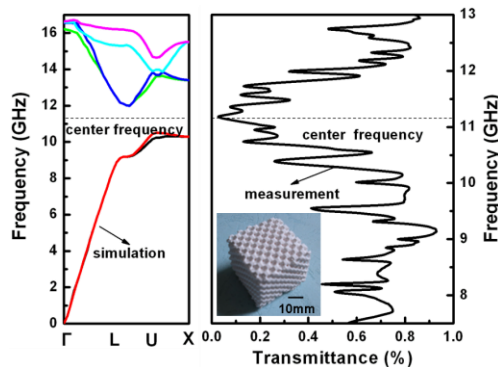


Fig. 3: The simulation and measurement results of the perfect diamond 3D EBGs of Alumina with the lattice constant of 12mm in the dimension of 60 mm× 60 mm× 60 mm. The bandgap is 10.5-12GHz.

<sup>13</sup> Yawen Hu, et.al. "Fabrication of three-dimensional electromagnetic band-gap structure with alumina based on stereolithography and gelcasting", J. Manuf. Sys, vol. 31, p. 22-25, 2012

<sup>14</sup> Wei Dai, et.al. "Effect of point defects on band-gap properties in diamond structure photonic crystals", J. Appl. Phys., vol. 111, p. 023515, 2012.

<sup>15</sup> Wei Dai, et.al. "Bandgap properties of diamond structure photonic crystals with line defects", J. Appl. Phys., vol. 111, p. 083514, 2012.

<sup>16</sup> Wei Dai, et.al. "Planar defects and heterostructure in diamond structure photonic crystals", J. Appl. Phys., vol. 112, p. 113504, 2012.

**Nanoscale Domain Wall Phenomena in Epitaxial Bismuth Ferrite Thin Films**Nagarajan VALANOOR<sup>1#</sup><sup>1</sup>*School of Materials Science and Engineering, University of New South Wales, Australia*<sup>#</sup>*Corresponding author: nagarajan@unsw.edu.au* <sup>+</sup>*Presenter*

In recent years, the control of domains in bismuth ferrite has emerged as a cornerstone of breakthrough science in multiferroic materials. Domain engineering opens up a vast array of physical phenomena, such as band structure manipulation, phase transitions and order parameter couplings that are localised at a nanostructured interface, which can then be harnessed for electronic applications.

This poses a tantalizing new possibility - can the modulation of the physical properties (such as conductance or magnetoresistance) of the domain wall be controlled by the geometry of the wall itself? In this presentation, we report the ability to create domain patterns and modulate conduction in domain walls by patterning the domain walls with specific charge and hence conduction in a multiferroic BiFeO<sub>3</sub> thin-film. Domain phase control is achieved by specific SPM based tip writing. The stability of the phases is rationalized by a phase field model. Secondly by controlling domain wall curvature and the associated divergence in polarization across the wall, a modulation of conduction is achieved along the domain wall. Both ambient and Ultra-high Vacuum (UHV) Scanning probe microscopy (SPM) approaches are employed to show that the conductivity of the fabricated curved domain walls can be modulated by up to 500% in the spatial dimension. Landau-Ginzburg-Devonshire computations reveal that the conduction is a result of carriers or vacancies migrating to neutralize the charge at the formed interface. Polarization dynamics, studied through phase-field models, highlight that anisotropic conduction may arise from even initially uncharged ring-domain structures. These results offer the first proof of concept for modulating charge at interfaces in a multiferroic by SPM and further demonstrate that material and electrical parameters can be extensively controlled at the nanoscale level simply by altering domain geometries. (Vasudevan et al, Nano Letters 2011, 2012)

The presentation is a collaborative effort between the presenting author's group and groups at Oak Ridge National Labs, University of Washington, Ukraine National Academy of Sciences and the National Chiao Tung University. The research at UNSW is supported by the Australian Research Council



## Thermal quench effects on ferroelectric domain walls

P. Paruch<sup>1</sup>, A. B. Kolton<sup>2</sup>, X. Hong<sup>3,4</sup>, C. H. Ahn<sup>3</sup>, T. Giamarchi<sup>1</sup>

<sup>1</sup>MaNEP-DPMC, University of Geneva, Geneva, Switzerland

<sup>2</sup>CONICET, Centro Atómico Bariloche, San Carlos de Bariloche, Argentina

<sup>3</sup>DAP, Yale University, New Haven, CT, USA

<sup>3</sup>present address: DPA, University of Nebraska-Lincoln, Lincoln, NB, USA

Email: patrycja.paruch@unige.ch

Ferroelectric domain walls present a powerful model system for studying the characteristic roughening and complex dynamics of elastic interfaces in disordered media [1,2]. Although the equilibrium properties of such systems are relatively well understood, less is known about their out-of-equilibrium behavior, and a major challenge is understanding the nonsteady slow dynamics associated with aging [3]. Experimentally, an interesting realization of such phenomena is provided by quenches, in which a parameter, such as the temperature of the system, is abruptly varied.

Using piezoresponse force microscopy on epitaxial ferroelectric thin films, we have measured the evolution of domain wall roughening as a result of such heat-quench cycles up to 735 °C, with the effective roughness exponent  $\zeta$  changing from 0.25 to 0.5. We discuss two possible mechanisms for the observed  $\zeta$  increase: a quench from a thermal one-dimensional configuration and from a locally equilibrated pinned configuration with a crossover from a two- to one-dimensional regime. We find that the postquench spatial structure of the metastable states, qualitatively consistent with the existence of a growing dynamical length scale whose ultraslow evolution is primarily controlled by the defect configuration and heating process parameters, makes the second scenario more plausible. This interpretation suggests that pinning is relevant in a wide range of temperatures and, in particular, that purely thermal domain wall configurations might not be observable in this glassy system. We also demonstrate the crucial effects of oxygen vacancies in stabilizing domain structures [4].

[1] T. Tybell et al, PRL 89, 097601 (2002)

[2] P. Paruch et al, PRL 94, 197601 (2005)

[3] L. F. Cugliandolo et al, PRL 96, 217203 (2006)

[4] P. Paruch et al, PRB (2012)

## Disorder and environmental effects on ferroelectric domain wall dynamics

Jill Guyonnet<sup>1</sup>, S. Bustingorry<sup>2</sup>, C. Blaser<sup>1</sup>, E. E. Ferrero<sup>2</sup>, I. Gaponenko<sup>1</sup>, J. Karthik<sup>3</sup>, L. W. Martin<sup>3</sup>, and P. Paruch<sup>1</sup>

<sup>1</sup>DPMC, University of Geneva, Switzerland

<sup>2</sup>CONICET, Centro Atómico Bariloche, San Carlos de Bariloche, Río Negro/Argentina

<sup>3</sup>Department of Materials Science and Engineering and Materials Research Laboratory, University of Illinois, Urbana-Champaign, USA

Email: jill.guyonnet@unige.ch

Domain wall motion in ferroelectric materials is largely determined by the disorder pinning potential, which depends on the nature and density of defects in the sample. Readily controlled with electric fields, and accessible over a large range of length scales and speeds, the domain walls provide an excellent model system for the complex fundamental physics of elastic disordered interfaces. Understanding the microscopic role of defects in domain propagation is also technologically critical in increasingly more miniaturized devices, scaled down to sizes comparable to the extent of individual defects. In this context, scanning probe microscopy (SPM) has emerged as a primary technique for domain engineering, providing a single well-defined nucleation site and nanoscale resolution of the switching dynamics. In such studies, the highly inhomogeneous electric field produced by the SPM tip can however be significantly influenced by the presence of adsorbates on the sample surface, resulting in humidity-dependent domain dynamics [1,2].

Here, we present a systematic study of the interplay between disorder pinning and the screening effects of surface water on the roughness and switching dynamics of SPM-engineered ferroelectric domains in  $\text{Pb}(\text{Zr}_{0.2}\text{Ti}_{0.8})\text{O}_3$  thin films with different defect densities, in ultrahigh vacuum (UHV) and ambient conditions. In samples presenting a low, uniform defect density, the switched domains are circular, with significantly higher growth rates in ambient conditions. In contrast, higher-disorder samples show slow growth rates in both ambient and UHV, with irregular domain shapes in the latter case. These experimental observations are in excellent agreement with Ginzburg-Landau numerical simulations of the localized nucleation and growth of domains under varying disorder and dipolar interaction magnitudes.

These results show that, while domain growth rates and roughness are governed primarily by disorder, electrostatic screening by surface water plays an important role, allowing more rapid domain wall motion in low-disorder samples, and screening the effects of dipolar and disorder forces in high-disorder samples, which otherwise lead to significant domain wall roughness.

[1] D. Dahan, M. Molotskii, G. Rosenman, and Y. Rosenwaks, *Appl. Phys. Lett.* **89**, 152902 (2006).

[2] V. Ya. Shur, A. V. Ievlev, E. V. Nikolaeva, E. I. Shishkin, and M. M. Neradovskiy, *J. Appl. Phys.* **110**, 052017 (2011).

## Direct observation of domain wall pinning and creep in ferroelectric thin film capacitors

Huizhong Zeng, Yao Lei, Wenbo Luo, Wen Huang, Y. Lin

State Key Laboratory of Electronic Thin films and Integrated Devices, University of Electronic Sci. & Tech. of China, Chengdu, P. R. China

Email: zenghz@uestc.edu.cn

The creep-like motion of ferroelectric domain wall (DW) is crucial to understand the role of defect pinning. A nanoscale scanning probe study of DW pinning and creep motion was performed in ferroelectric thin film capacitors. The ferroelectric capacitors are prepared by pulsed laser deposition of  $(\text{Pb}_{0.8}\text{Zr}_{0.2})\text{TiO}_3$  (PZT) and  $\text{SrRuO}_3$  (SRO) electrodes onto  $\text{SrTiO}_3$  single crystal substrates. The ultrathin ( $<10$  nm) SRO top electrode enable piezoresponse force microscope (PFM) to visualize ferroelectric domains in the capacitors, and provide a homogeneous electric field for studying static and dynamic DW properties. From the static domain wall profiles, the averaged roughness exponent is extracted to be  $\sim 0.39$ , indicating a 2D DW in the presence of random bond disorder and long range dipole interaction. By applying the electric pulses ( $E \geq E_c$ ) to the capacitors, creep-like DW motion was directly observed. By measuring the averaged speed of DW, the critical exponent is determined to be  $\mu=1$ , confirming the random bond disorder. However, a DW roughening process was observed when decreasing the pulsed electric field. When further decreasing the pulsed electric field, both creep-like motion and nucleation of bubbles in front of DW were found, indicating the significant role of defect pinning. The transition from creep motion to the bubble formation was discussed. Our results suggest the disordered elastic model oversimplified the DW motion under lower field.

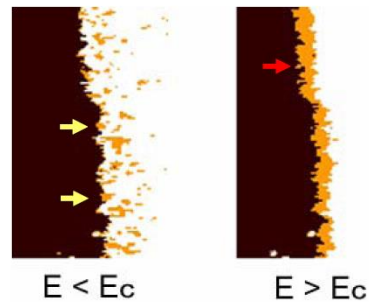


Fig. 4: Motion of domain walls of ferroelectric thin film capacitors under pulsed electric field lower than  $E_c$  (left) and larger than  $E_c$  (right). The DW position before and after electric pulse is colored by dark and orange, respectively. The vertical scan range of PFM is  $6 \mu\text{m}$ .

## PFM at variable temperatures: behavior of domains in BaTiO<sub>3</sub> across its orthorhombic to tetragonal phase transition

T. Limböck, A. Hoffmann, E. Soergel

Institute of Physics, University of Bonn, Wegelerstrasse 8, 53115 Bonn, Germany

Email: soergel@uni-bonn.de

We upgraded a commercial, room-temperature AFM with a home-built temperature-controlled sample holder, allowing for image recording at temperature ranges between  $-80^{\circ}\text{C}$  and  $+120^{\circ}\text{C}$ . We can not only record images at different fixed temperatures but also perform "temperature scans", thereby changing the temperature during the scanning process itself, with the temperature being connected directly to the scanning process. Figure 1 shows a  $20 \times 20 \mu\text{m}^2$  image on BaTiO<sub>3</sub> while in changing the temperature across the orthorhombic to tetragonal phase transition.

Here we report on first results which show that our setup is working reliably across the whole temperature range. We therefore imaged a PPLN sample and showed that the thermal drift is acceptable (few  $\mu\text{m}$ ) and the PFM signals (vertical and lateral) are, as expected, independent on the temperature within the accessible range.

As an interesting candidate for PFM investigations within this temperature range, we chose BaTiO<sub>3</sub>, which is known to exhibit a phase transition at  $\sim 7^{\circ}\text{C}$  from orthorhombic to tetragonal. Both phases are ferroelectric. Whereas the classical, high-temperature orthorhombic phase exhibits 6 directions of the polarization, the tetragonal one has many more. In a first set of experiments, we clarified the situation as to unambiguously assign the direction of polarization in the PFM images recorded for both phases of the crystal. We therefore simultaneously recorded vertical and lateral PFM output channels.

The next goals are (i) the quantitative information of the piezoelectric coefficients of the two phases, (ii) the investigation of the development of the domains across the phase transition, i.e. which are the preferred directions of polarization from a certain starting situation and whether there are domain walls that maintain their position. Finally we (iii) want to find out why, when heating the sample back to room temperature (as we did for the data where only cooling is shown in Fig. 1), the original domain pattern basically is restored.

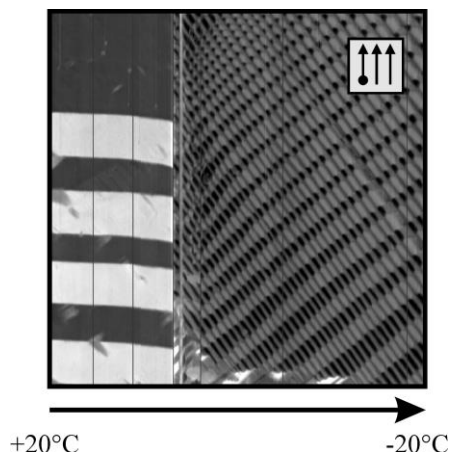


Fig. 5: PFM temperature scan of a BaTiO<sub>3</sub> single crystal across its phase transition clearly showing the alteration of the ferroelectric domain pattern. Image size:  $20\mu\text{m} \times 20\mu\text{m}$ . The arrows in the top right corner indicate the scanning direction.

---

## **Pb-based ceramics: Spectroscopy**

CLUB A

*Monday, July 22 2013, 02:00 pm - 03:30 pm*

Chair: **Jan Petzelt**  
*Institute of Physics ASCR*

## Soft mode in cubic PbTiO<sub>3</sub> by hyper-Raman scattering

Jiri Hlinka<sup>1</sup>, Bernard Hehlen<sup>2</sup>, Antoni Kania<sup>3</sup>, Ivan Gregora<sup>1</sup>

<sup>1</sup>Institute of Physics, Academy of Sciences of the Czech Republic, Prague, Czech Republic

<sup>2</sup>Laboratoire des Colloïdes, Verres et Nanomatériaux (LCVN), UMR CNRS 5587, University of Montpellier II, Montpellier, France

<sup>3</sup>Institute of Physics, University of Silesia, Katowice, Poland

Email: hlinka@fzu.cz

Terahertz-range frequency dispersion of the dielectric permittivity provides the key information needed to understand the potential of practical use of the high permittivity materials.

Therefore, it seems also important to provide clean examples of ferroelectric materials where the THz range permittivity is actually well described by a single polar soft mode excitation.

Hyper-Raman scattering experiments allowed collecting the spectra of the lowest F<sub>1u</sub>-symmetry mode of PbTiO<sub>3</sub> crystal in the paraelectric phase up to  $\approx 930$  K as well as down to about 1 K above the phase transition. It is realized that this mode is fully responsible for the Curie-Weiss behavior of its dielectric permittivity above T<sub>C</sub>. Near the phase transition, this phonon frequency softens down to 17 cm<sup>-1</sup> and its spectrum can be well modelled as a response of a single damped harmonic oscillator. It is concluded that PbTiO<sub>3</sub> constitutes a clean example of a soft mode-driven ferroelectric system. Results of this study are partly available in condmat archive<sup>17</sup>.

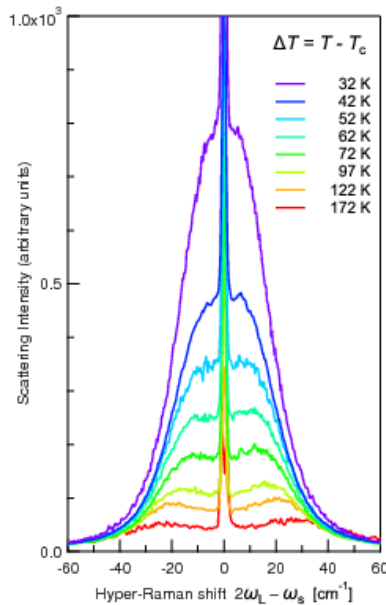


Fig. 6: Unpolarized (V+H) HRS spectra of in paraelectric phase of PbTiO<sub>3</sub> single crystal for several temperatures indicated in the figure with respect to the phase transition (T<sub>C</sub>  $\approx$  760 K).

<sup>17</sup> J. Hlinka, B. Hehlen, A. Kania, and I. Gregora, "Soft mode in cubic PbTiO<sub>3</sub> by hyper-Raman scattering", arXiv:1212.3982v1 [cond-mat.mtrl-sci].

## Infrared and terahertz spectroscopy of antiferroelectric $\text{PbZrO}_3$ single crystals

Tetyana Ostapchuk<sup>1</sup>, Christelle Kadlec<sup>1</sup>, Petr Kužel<sup>1</sup>, Jan Kroupa<sup>1</sup>,

Vladimír Železný<sup>1</sup>, Jan Petzelt<sup>1</sup>, Jiří Hlinka<sup>1</sup>, and Jan Dec<sup>2</sup>

<sup>1</sup>Department of Dielectrics, Institute of Physics, 18221 Prague 8, Czech Republic

<sup>2</sup>Institute of Materials Science, University of Silesia, Bankowa 12, PL-40-007 Katowice, Poland

Email: ostapcuk@fzu.cz

Here, for the first time, we present dielectric dispersion spectra of monodomain  $\text{PbZrO}_3$  single crystals obtained along all three orthorhombic axes from far infrared reflectivity and time-domain terahertz transmission measurements in the 10-500 K temperature range. Within this study we identified the whole set of the modes, predicted by the factor-group analysis for  $Pbam$  structure (11  $B_{1u}(z)$ , 17  $B_{2u}(y)$  and 17  $B_{3u}(x)$ ). As typical for all Pb-based perovskites, the spectra exhibit three main bands with the lowest one corresponding to the Last-type vibrations, the middle (of the largest mode plasma frequency) to the Slater-type, and the highest one - to the Axe-type vibrations<sup>xi</sup>. The Last-type band of  $B_{2u}(y)$ -symmetry demonstrates a significant coupling to the Slater-type band at low temperatures, which gradually vanishes on heating, while in the case of  $B_{1u}(z)$  symmetry this coupling is less pronounced and for the  $B_{3u}(x)$  symmetry practically negligible.

The softening of the lowest Last-type band is observed in all three normal-axes directions, but the largest effect (from  $\sim 75 \text{ cm}^{-1}$  at  $T=10 \text{ K}$  to  $\sim 30 \text{ cm}^{-1}$  at  $T=500 \text{ K}$ ) is found along the [001] direction ( $B_{1u}(z)$  symmetry), which was suggested to be polar (but not ferroelectric) in the earliest structural study<sup>xii</sup>. In this direction we have also discerned a weak central-mode (CM) type dispersion around 0.3 THz, analogous to the previously observed on the multidomain crystal<sup>xiii</sup> and ceramics<sup>xiv</sup>. Its behavior is rather similar to that found in  $\text{BaTiO}_3$  in the [001] direction of the spontaneous polarization<sup>xv</sup>, but its dielectric strength is several times weaker. In the same sub-THz frequency range in  $B_{2u}(y)$ -symmetry spectra we observed a slightly stronger dispersion, which preserves in the terahertz spectra down to the lowest temperatures, and assigned it to a pseudophason response.

## Compositional tunability of phonons in PZT investigated by Raman scattering

Elena Buixaderas, Ivan Gregora, Mael Guennou, Jan Petzelt, Jiří Hlinka

Department of Dielectrics, Institute of Physics, ASCR, Prague, Czech Republic

Email: buixader@fzu.cz

Lattice dynamics of ferroelectric perovskite materials,  $ABO_3$ , is a very fruitful topic of investigation. Due to the combination of cationic shifts and oxygen-octahedra tilts, different structures can be achieved on cooling from the parent cubic high temperature phase. When one of the cationic sites is occupied by two atoms many interesting properties can be achieved. This is the case of one of the most investigated and technologically used materials, the ceramics family  $Pb(Zr_{1-x}Ti_x)O_3$  (PZT 100 $x$ /100(1- $x$ )), which have some of the highest piezoelectric coefficients at room temperature for compositions near  $x = 0.48$ .

We measured the Raman spectra of a broad range of compositions, from the pure rhombohedral ( $x = 0.25$ ) to the pure tetragonal side ( $x = 0.65$ ), crossing the so-called morphotropic phase boundary (MPB), in the 10–800 K temperature range. We also measured single crystals near the MPB down to He temperatures.

Dynamics of the low-frequency vibrations —mainly connected with the Pb atoms— will be discussed and related to the recent far-infrared data obtained for the same samples.<sup>18</sup> Doubling of the unit cell at low temperatures due to the anti-phase tilt of the oxygen octahedra about the polar axis was confirmed for all composition with  $x < 0.60$ .

The middle frequency band (200–400  $cm^{-1}$ ), assigned traditionally to Ti and Zr vibrations, is the key to the transformation from tetragonal to rhombohedral symmetry. The splitting of the  $E(TO_2)$  mode and the gradual weakening of one of its components<sup>19</sup> along with the almost disappearance of the  $A_1(TO_2)$  mode in the rhombohedral samples, are the most striking features of this phase transition across the MPB. The parameters of these modes will be discussed in relation to the symmetry change and to the variation of composition and temperature.

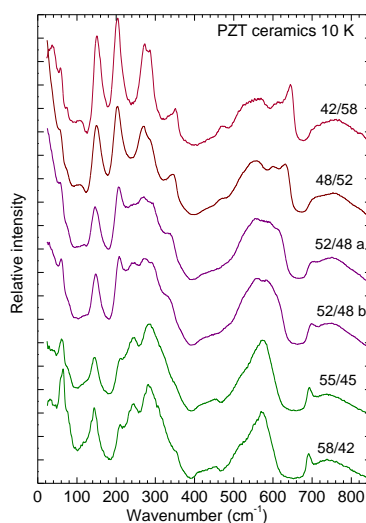


Fig. 7: Raman spectra of several PZT compositions at 10 K.

<sup>18</sup> E. Buixaderas et al., “Polar lattice vibrations and phase transition dynamics in  $Pb(Zr_{1-x}Ti_x)O_3$ ”, Phys. Rev. B, vol. 84, p. 184302, 2011.

<sup>19</sup> E. Buixaderas et al., “Raman spectroscopy of  $Pb(Zr_{1-x}Ti_x)O_3$  graded ceramics around the morphotropic phase boundary”, Phase Transitions, vol. 84, p. 528-541, 2011.



## **PbZrO<sub>3</sub>: nature of the high temperature phase transition**

R. Faye<sup>1</sup>, H. Liu<sup>1</sup>, D. Kajewski<sup>2</sup>, K. Roleder<sup>2</sup>, P. Gemeiner<sup>1</sup>, B. Dkhil<sup>1</sup>, and P.-E. Janolin<sup>1</sup>

<sup>1</sup>SPMS laboratory, UMR CNRS-Ecole Centrale Paris, Chatenay-Malabry, France

<sup>2</sup>Institute of Physics, University of Silesia, Katowice, Poland

Email: romain.faye@ecp.fr

Despite being the archetypal antiferroelectric perovskite the comprehension of lead zirconate (PZO) structure and phase transition(s) is still fragmentary. PZO structure remained elusive between the 50's when its antiferroelectricity was discovered by Shirane<sup>20</sup> and the results of first principles calculations circa 2000<sup>21</sup>. Since then, the description of the AFE phase by a nonpolar Pbam orthogonal space group has been preferred over the polar Pba2 one. Nevertheless a controversy persists over the nature of the high temperature phase transition and the existence of an intermediate stable FE phase<sup>22</sup>. As a consequence, the structure-property relation has so far not been comprehensively established.

We shall aim at providing insights on these points through temperature dependent X-ray diffraction, neutron scattering, Raman spectroscopy, dielectric, pyroelectric, differential scanning calorimetry, and hysteresis loop measurements performed on ceramics and single crystals. The effect of heat, density, time and particle sizes on the FE zone will be considered. In addition, we shall report the results of temperature-dependent X-ray diffraction with *in-situ* AC electric field.

---

<sup>20</sup> G. Shirane, E. Sawaguchi, "Dielectric properties of lead zirconate", Phys. Rev. 84, 476 (1951)

<sup>21</sup> D.J. Singh, "Structure and energetic of antiferroelectric PbZrO<sub>3</sub>", Phys. Rev. B 52, 12559 (1995)

<sup>22</sup> K. Roleder et al. "The first evidence of two phase transitions in PbZrO<sub>3</sub> crystals derived from simultaneous Raman and dielectric measurement", Ferroelectrics 80, 161 (1988)

## Study of ferroelectric-antiferroelectric crossover in PLZT (x/90/10) ceramics

**L. Curecheriu<sup>1</sup>, L. Stoleriu<sup>1</sup>, C. Galassi<sup>2</sup>, F. Fochi<sup>2</sup>, L. Mitoseriu<sup>1</sup>**

<sup>1</sup> Faculty of Physics, Al. I. Cuza Univ., Bv. Carol I no. 11, Iasi 700506, Romania

<sup>2</sup> ISTECCNR, Via Granarolo no. 64, I-48018 Faenza, Italy

Email: lavinia.curecheriu@uaic.ro

(Pb<sub>1-x</sub>La<sub>x</sub>)(Zr<sub>0.90</sub>Ti<sub>0.10</sub>)<sub>1-x/4</sub>O<sub>3</sub> [PLZT x/90/10 with compositions: x=0.0, 2.0, 2.5, 3.0, 3.5, 3.8 and 4.0] solid solutions have been prepared by solid state reaction and sintering at 1250<sup>0</sup>C/2h. The phase purity, crystalline symmetry and microstructures have been investigated. Dense ceramics (relative density above 95-98%) and homogeneous microstructures have been obtained for all the compositions.

The particularities of the switching characteristics at room temperature of these PLZT x/90/10 ceramics were analysed by using the First Order Reversal Curves (FORC) diagrams<sup>1</sup>. The ferro-antiferro crossover with increasing x is probed by the transition from one-component Preisach distribution to a double-maxima symmetric distribution with composition-dependent characteristic bias and coercive fields (Fig. 1 a, c). For composition in range of x=(3.2-3.8%) was obtained a superposition of ferroelectric and antiferroelectric phases characterised by three maxima in the FORC distribution (Fig. 1 b).

Impedance spectroscopy in the temperature range of (20, 250)<sup>0</sup>C demonstrated the shift of the ferro-para phase transition with increasing x towards low temperatures. The superposition of ferro-antiferroelectric states is probed by a small dielectric anomaly in the range 70-90<sup>0</sup>C at high frequencies.

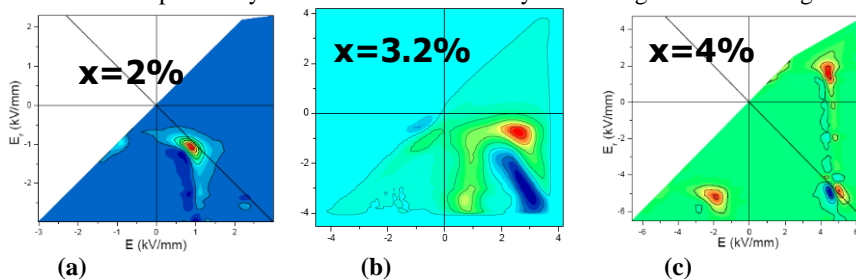


Fig. 1 FORC distribution showing the ferroelectric-antiferroelectric crossover: (a) ferroelectric (x=2), (b) superposition ferroelectric-antiferroelectric (x=3.2) (c) antiferroelectric (x=4).

**Acknowledgements:** The financial support of the PN II-PCE-2011-3-0745 is acknowledged.

## Microwave dielectric properties of relaxor ferroelectric $\text{Pb}(\text{In}_{1/2}\text{Nb}_{1/2})\text{O}_3\text{-Pb}(\text{Mg}_{1/3}\text{Nb}_{2/3})\text{O}_3\text{-PbTiO}_3$ single crystals

Li Jin<sup>1</sup>, Fei Li<sup>1</sup>, Shujun Zhang<sup>2</sup>, Dragan Damjanovic<sup>3</sup>

<sup>1</sup>Electronic Materials Research Laboratory, Key Laboratory of the Ministry of Education & International Center for Dielectric Research, Xi'an Jiaotong University, Xi'an, China

<sup>2</sup>Materials Research Institute, Pennsylvania State University, University Park, Pennsylvania, USA

<sup>3</sup>Ceramics Laboratory, Swiss Federal Institute of Technology in Lausanne - EPFL, Lausanne, Switzerland

Email: ljin@mail.xjtu.edu.cn

Relaxor ferroelectric single crystals with the composition near the morphotropic phase boundary (MPB) region have attracted much attention due to their superior piezoelectric and dielectric properties. Up to date, the routine piezoelectric, dielectric and elastic properties of relaxor ferroelectric single crystals have been studied. Many representative opinions based on intrinsic crystal lattice and extrinsic domain wall motion have been proposed to understand high properties. However, their origin is still under debate.<sup>23,24</sup>

Ferroelectric materials show strong dielectric dispersion in GHz frequency range, which manifests itself as the rapid decrease of the permittivity with increasing the frequency and accompanied with a loss peak.<sup>25,26</sup> This phenomenon is mainly attributed to the domain wall motion and piezoelectric grain resonance.<sup>27</sup> By means of this dielectric dispersion, we could distinguish the intrinsic and extrinsic contribution to the dielectric properties.<sup>28</sup> In this presentation, we show results on microwave dielectric properties of relaxor ferroelectric  $\text{Pb}(\text{In}_{1/2}\text{Nb}_{1/2})\text{O}_3\text{-Pb}(\text{Mg}_{1/3}\text{Nb}_{2/3})\text{O}_3\text{-PbTiO}_3$  (PIN-PMN-PT) single crystals. The dielectric response was studied from 100 kHz to 1.8 GHz at temperatures from -100 to 100 °C. By changing the domain wall density through by gradually depoling samples, we evaluated the domain wall motion contribution to the dielectric properties. A dispersion-free state at GHz range for single domain state was observed, where the value ( $\epsilon' = 160$ ) measured at 1.8 GHz accounts for the intrinsic dielectric response of PIN-PMN-PT single crystals.

<sup>23</sup> D. Damjanovic, IEEE Trans. Ultrason. Ferroelectr. Freq. Control **56**, 1574 (2009).

<sup>24</sup> S. Zhang and F. Li, J. Appl. Phys. **111**, 031301 (2012).

<sup>25</sup> G. Arlt, U. Böttger, and S. Witte, Ann. Phys. **506**, 578 (1994).

<sup>26</sup> M. P. McNeal, S. J. Jang, and R. E. Newnham, J. Appl. Phys. **83**, 3288 (1998).

<sup>27</sup> V. Porokhonsky, L. Jin, and D. Damjanovic, Appl. Phys. Lett. **94**, 212906 (2009).

<sup>28</sup> L. Jin, V. Porokhonsky, and D. Damjanovic, Appl. Phys. Lett. **96**, 242902 (2010).

---

## **Relaxor Materials**

CLUB B

*Monday, July 22 2013, 02:00 pm - 03:30 pm*

Chair: **Takaaki Tsurumi**  
*Tokyo Institute of Technology*

## Similarities between the physic of relaxors and other systems

S. Prosandeev<sup>1,2</sup>, B. Dkhil<sup>3</sup>

<sup>1</sup>Department of Physics, Research Institute of Physics,  
Southern Federal University, Rostov on Don 344090, Russia

<sup>2</sup>Physics Department and Institute for Nanoscience and Engineering,  
University of Arkansas, Fayetteville, AR 72701, USA

<sup>3</sup>Ecole Centrale Paris/CNRS UMR8580, Chatenay-Malabry, France

Email: brahim.dkhil@ecp.fr

In this presentation, the main idea is to demonstrate that relaxors share common features with many other systems; these features being related to various and exotic phenomena like the weak crystallization in lipids, the Bose condensation in Helium II state or the pseudo-gap in superconductors. The tempting proximity of these phenomena will be discussed and used to propose a unified microscopic picture of relaxors. As a matter of fact, two new order parameters will be introduced to characterize the transitions occurring at Burns temperature and that at  $T^*$  which marks the crossover between a spherical glass and a quadrupole glass state.

## Temperature Evolution of Dielectric Relaxation in PMN Single Crystals

Viktor Bovtun, Stanislav Kamba, Jan Petzelt, [Jiri Hlinka](#)

Department of Dielectrics, Institute of Physics ASCR, Prague, Czech Republic

[Email: hlinka@fzu.cz](mailto:hlinka@fzu.cz)

Dielectric relaxation in  $\text{PbMg}_{1/3}\text{Nb}_{2/3}\text{O}_3$  (PMN) was widely studied since 1960. It is observed in broad frequency and temperature ranges, slows down and broadens on cooling, partially freezes out below the freezing temperature  $T_f \approx 200$  K and is characterized by the extremely broad distribution of relaxation times below  $T_f$ . Here we present a detailed analysis of the relaxation based on the complete dielectric spectra from 3 mHz to 3 THz which joined our experimental results<sup>29-6</sup>. Asymmetrical shape of loss spectra  $\epsilon''(\log f)$  indicates the presence of at least two relaxation contributions which are diffuse and overlapped. The Cole-Cole fit allows separation of two contributions (subscripts “1” and “2”) and evaluation of their parameters: dielectric strength, mean relaxation time  $\tau_0$ , relaxation time distribution (RTD) parameter.

Using the uniform RTD function<sup>7</sup>, upper ( $\tau_U$ ) and lower ( $\tau_L$ ) limits of RTD were determined for both Cole-Cole contributions. Temperature dependences of  $\tau_{02}$  and  $\tau_{L2}$  can be fitted to the Arrhenius law, while that of  $\tau_{01}$  and  $\tau_{U1}$  fit well to the Vogel-Fulcher law above 220 K. The longer mean relaxation time  $\tau_{01}$  does not diverge at  $T_f$  and remains finite even below  $T_f$ . We attribute this to the crossover from Vogel-Fulcher to Arrhenius behavior.

As a result of the analysis, we obtained a time-temperature diagram of dielectric relaxation in PMN. According to the diagram, the relaxation dynamics covers a time range limited by the longest relaxation time  $\tau_{U1}$  diverging on cooling according to the Vogel-Fulcher law (or at least approaching the  $T_s$  range at  $T_f$ ) and shortest relaxation time  $\tau_{L2}$  following the Arrhenius law with a small activation energy (i.e. weak temperature dependent in the ps range).

The described evolution of relaxation dynamics corresponds well to the general scheme of dielectric response of relaxor ferroelectrics<sup>1,8</sup> based on the concept of polar nanoclusters (or nanoregions) whose flipping and breathing provide two relaxation contributions. The relation of the relaxation dynamics to the concepts of ferroelectric nanodomains<sup>9</sup> or ion chemistry and environment (based on molecular dynamics simulations<sup>10</sup>) is under discussion.

<sup>29</sup> V. Bovtun, S. Veljko, S. Kamba, J. Petzelt, S. Vakhrušev, et al. - J. Europ. Cer. Soc. 26, 2867-2875, 2006.

<sup>2</sup> V.P. Bovtun, N.N. Krainik, L.A. Markova, Y.M. Poplavko, et al. - Fiz. Tverd. Tela 26, 378 – 381, 1984.

<sup>3</sup> Y.M. Poplavko, V.P. Bovtun, N.N. Krainik, G.A. Smolensky – Fiz. Tverd. Tela 25, 1263-1265, 1985.

<sup>4</sup> E.V. Colla, E.Y. Koroleva, N.M. Okuneva, S.B Vakhrušev - J. Phys.: Cond. Matter 4, 3671–3677, 1992.

<sup>5</sup> V.P. Bovtun, M.A. Leshchenko - Ferroelectrics 190, 185-190, 1997.

<sup>6</sup> V. Bovtun, S. Kamba, A. Pashkin, M. Savinov, P. Samoukhina, et al. – Ferroelectrics 298, 23-30, 2004.

<sup>7</sup> S. Kamba, V. Bovtun, J. Petzelt, I. Rychetsky, et al. - J. Phys.: Cond. Matter 12, 497–519, 2000.

<sup>8</sup> V. Bovtun, J. Petzelt, V. Porokhonsky, S. Kamba, et al. – J. Europ. Ceram. Soc. 21, 1307-1311, 2001.

<sup>9</sup> J. Hlinka – J. Adv. Dielectrics 2, 1241006, 2012.

<sup>10</sup> I. Grinberg, Y.H. Shin, A.M. Rappe – Phys. Rev. Lett. 103, 197601, 2009.

## Acoustic evidence of distinctive temperatures in relaxor-multiferroics

E.Smirnova<sup>1</sup>, A.Sotnikov<sup>1,2</sup>, S.Ktitorov<sup>3</sup>, H.Schmidt<sup>2</sup>, M.Weihnacht<sup>2</sup>

<sup>1</sup>Department of Ferroelectricity, A.F.Ioffe Physical-Technical Institute, St. Petersburg, Russia,

<sup>2</sup>Department of Magnetic and Acoustic Resonances, IFW Dresden, Dresden, Germany,

<sup>3</sup>Department of semiconductors and dielectrics theory, A.F.Ioffe Physical-Technical Institute, St. Petersburg, Russia

E-mail: esmirnoffa@gmail.com

Structurally disordered perovskites - relaxor ferroelectrics with magnetic ordering (relaxor-multiferroics) occupy a special place in the multiferroics family. Coexistence of the relaxor ferroelectric and magnetic subsystems determines their physical properties. The origin of the relaxor state is still controversial in spite of the long time experimental and theoretical studies. The first and very famous approach assumes that unique properties of relaxor ferroelectrics are due to the presence of polar nanoregions (PNR). Some experimental evidences of the creation of PNR in the paraelectric matrix of relaxors around so-called Burns temperature ( $T_B$ ) were obtained from the measurements of the optical refraction index, thermal capacity, and neutron scattering. Scarce results demonstrate acoustic emission signals and small elastic anomalies in the vicinity of  $T_B$ . It is well known that acoustic wave velocity and attenuation are very sensitive to various processes related to phase transitions, relaxations, glass-like behavior, etc. Recently, we have reported that peaks of acoustic attenuation at  $T_B$  and  $T^*$  (temperature of assumed nanoscale phase transition due to random field) are revealed in classic relaxor  $\text{PbMg}_{1/3}\text{Nb}_{2/3}\text{O}_3$  (PMN) and relaxor-multiferroic  $\text{PbFe}_{1/2}\text{Nb}_{1/2}\text{O}_3$  (PFN) [1]. The present study is devoted to dielectric and acoustic properties of relaxors with magnetic ordering  $\text{PbFe}_{1/2}\text{Ta}_{1/2}\text{O}_3$  (PFT) and  $\text{PbFe}_{2/3}\text{W}_{1/3}\text{O}_3$  (PFW) in the temperature range from 100 to 700 K. The samples were prepared by a conventional ceramic technique. Longitudinal ultrasonic wave velocity and attenuation as a function of temperature were determined by ultrasonic pulse-echo method at frequencies of 5 and 10 MHz (PFT) and 10 MHz (PFW). Peaks of attenuation in the vicinity of the dielectric constant maximum temperature  $T_m$ , suggested Burns temperature  $T_B$  and specific temperature  $T^*$  are found for PFT, as well as for PFW.

The results are discussed on the base of PNR model and on the classical idea by Mandelshtam and Leontovich of the slowly relaxing internal parameter. This method being applied to the sound propagation and attenuation problem allows us to describe the acoustic anomaly in the vicinity of Burns temperature. Slowed-down relaxation in the PNRs leads to an incomplete equilibrium of the system, and, therefore, to the energy dissipation. PNRs are considered as randomly distributed short-range relaxing centers interacting with the long-wave acoustic waves. Polarization located in PNR plays a role of such relaxing parameter. PNR are assumed to have a shape of the ellipsoid; the aspect ratio of it determines a relative effectiveness of the polarization interaction with the longitudinal and transverse acoustic waves. Comparison of the results of averaging of the dielectric and acoustic parameters over the PNR's configurations with experimental data gives a possibility to estimate the most probable aspect ratio of the PNR.

<sup>1</sup> E.Smirnova, S.Ktitorov, A.Sotnikov, H.Schmidt, M.Weihnacht, "High Temperature Acoustic Effects in Relaxors  $\text{PbMg}_{1/3}\text{Nb}_{2/3}\text{O}_3$  and  $\text{PbFe}_{1/2}\text{Nb}_{1/2}\text{O}_3$ ", Proceedings ISAF/ECAPD/PFM 2012, #6297789, 2012

## Relaxation of Polarized State Created by Local Electric Field in SBN Single Crystals

Shikhova Vera<sup>1</sup>, Shur Vladimir<sup>1</sup>, Shvartsman Vladimir<sup>2</sup>, Lupascu Doru<sup>2</sup>, Ievlev Anton<sup>1</sup>,  
Neradovskiy Maxim<sup>1</sup>, Pelegov Dmitry<sup>1</sup>, Lebedev Vasily<sup>3</sup>, Ivleva Lyudmila<sup>4</sup>, Dec Jan<sup>5</sup>

<sup>1</sup>Ferroelectric laboratory, Ural Federal University, Ekaterinburg, Russia

<sup>2</sup>Institute for Materials Science, University of Duisburg-Essen, Essen, Germany

<sup>3</sup>Faculty of Materials Science, Moscow State University, Moscow, Russia

<sup>4</sup>General Physics Institute of the Russian Academy of Sciences, Moscow, Russia

<sup>5</sup>Institute of Materials Science, University of Silesia, Katowice, Poland

Email: vera.shikhova@labfer.usu.ru

The temperature and temporal relaxation of the polarized state created by application of the local electric field using conductive tip of the scanning probe microscope was investigated in pure and doped by Ce single crystals of relaxor ferroelectric  $\text{Sr}_x\text{Ba}_{1-x}\text{Nb}_2\text{O}_6$  (SBN) with  $x = 0.61$  and  $0.75$ .

The 0.5-mm-thick plates of SBN single crystals were cut normally to the polar axis and carefully polished. The samples before measurements were treated by two alternative procedures: (1) thermal depolarization (creation of the multi-domain state) by heating up to  $200^\circ\text{C}$  and zero-field cooling, (2) creation of the single domain state by application of 30–50 bipolar triangular or rectangular field pulses with amplitude and duration sufficient for complete polarization reversal at room temperature using liquid electrodes.

The polarized areas were created under the action of local electric field of both directions with amplitude ranged from 40 to 100 V and duration from 1 ms to 1 s at room temperature and at elevated temperature up to  $100^\circ\text{C}$  (above freezing temperature for all compositions). The difference between piezoelectric responses in the polarized areas produced by application of the field of opposite sign (“contrast”) has been obtained. The temporal relaxation of the contrast value has been measured at various temperatures.

It was shown that increasing of the field amplitude and pulse duration leads to higher stability of the polarized state (increasing of the relaxation time constant). The polarized state created in the crystals in the single domain state was remarkably more stable than in the crystals in the multi-domain state.

Moreover it has been shown that the diameter of the area created at elevated temperatures decreasing with increasing the temperature. The average value of the induced contrast decreased gradually during heating and with the increase of the creation temperature for all investigated crystals.

The obtained effects have been attributed to field induced partial polarization of the multidomain state and important role of the backswitching under the action of depolarization field leading to relaxation of the piezoresponse value. The acceleration of backswitching at the temperatures above freezing point has been attributed to additional input of the phase boundaries.

The equipment of the UCSU “Modern Nanotechnology”, Institute of Natural Sciences, UrFU has been used. The research was made possible in part by RFBR (Grants 13-02-01391-a, 11-02-91066-CNRS-a, 12-02-31377); by Ministry of Education and Science (Contracts 14.513.12.0006, 16.740.11.0585), by OPTEC LLC and UrFU development program.



## Structural Origins of Strain and Fatigue in 94%(Bi<sub>1/2</sub>Na<sub>1/2</sub>)TiO<sub>3</sub>-6%BaTiO<sub>3</sub>

Hugh Simons<sup>1</sup>, John E. Daniels<sup>2</sup>, Julia Glaum<sup>2</sup>, Jacob L. Jones<sup>3</sup>, Andrew J. Studer<sup>4</sup>, Mark Hoffman<sup>2</sup>

<sup>1</sup>Department of Physics, Technical University of Denmark, Lyngby 2800, Denmark

<sup>2</sup>School of Materials Science & Engineering, University of New South Wales, Sydney, NSW 2052, Australia

<sup>3</sup>Department of Materials Science & Engineering, University of Florida, Gainesville, FL 32611, USA

<sup>4</sup>Bragg Institute, Australian Nuclear Science & Technology Organisation, Kirrawee, NSW 2234, Australia

Email: husimo@fysik.dtu.dk

94%(Bi<sub>1/2</sub>Na<sub>1/2</sub>)TiO<sub>3</sub>-6%BaTiO<sub>3</sub> (BNT-6BT) remains one of the most intensively studied lead-free ferroelectric composition for high-strain applications<sup>30</sup>. At elevated temperatures ( $T > 75^\circ\text{C}$ ), large recoverable strains ( $S_{\text{max}} \sim 0.4\%$ ) can be attained with low hysteretic loss, accompanied by a reversible electric-field-induced relaxor-to-ferroelectric transition. However, its ultimate applicability is hindered by uncertainties regarding the role of this structural transformation on the strain mechanism and fatigue life. Here, we describe the temperature-dependence of this transition from  $25^\circ\text{C}$  to  $100^\circ\text{C}$ , and its influence on the macroscopic strain and fatigue.

Orientation-dependent structural measurements were carried out using neutron diffraction under *in situ* electric fields and elevated temperatures, requiring the development of specialized sample environments and analysis processes. By calculating domain switching fractions as a function of temperature and electric field amplitude, the large recoverable strain observed at elevated temperature was shown to be associated with the reversible nature of the field induced phase transformation<sup>31</sup>. In addition, structural transformation occurring during bipolar electrical fatigue was investigated using a similar technique, highlighting a fatigue mechanism by which domains are progressively pinned and fragmented<sup>32</sup>. When heated close to the ferroelectric-relaxor transition temperature, the fatigue degradation reduced significantly, an improvement attributed to the unstable domain structure near the relaxor transition.

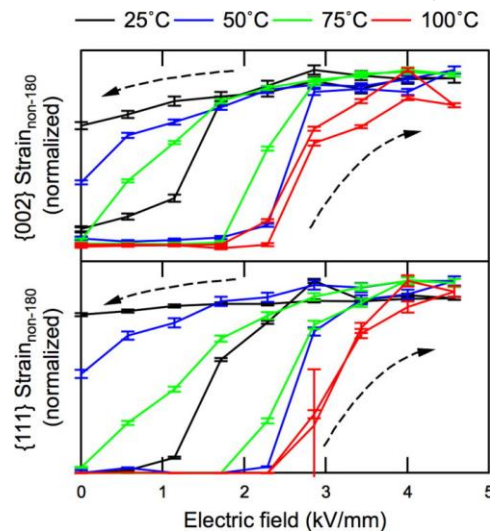


Fig. 8: Normalized strain from the contribution of non- $180^\circ$  domain wall motion in the tetragonal and rhombohedral phases. The strain is calculated from the relative positions and intensities of the  $\{002\}_{\text{pc}}$  and  $\{111\}_{\text{pc}}$  reflections respectively.

<sup>30</sup> W. Jo, R. Dittmer, M. Acosta, J. Zang, C. Groh, E. Sapper, K. Wang, and J. Rödel, "Giant electric-field-induced strains in lead-free ceramics for actuator applications – status and perspective", *J. Electroceram.* **29**, 71 (2012)

<sup>31</sup> H. Simons, J.E. Daniels, J. Glaum, A.J. Studer, J.L. Jones and M. Hoffman, "Origin of large recoverable strain in 94%(Bi<sub>1/2</sub>Na<sub>1/2</sub>)TiO<sub>3</sub>-6%BaTiO<sub>3</sub> near the ferroelectric-relaxor transition", *Appl. Phys. Lett.* **102**, 062902 (2013)

<sup>32</sup> H. Simons, J. Glaum, J.E. Daniels, A.J. Studer, A. Liess, J. Rodel, and M. Hoffman, "Domain fragmentation during cyclic fatigue in 94%(Bi<sub>1/2</sub>Na<sub>1/2</sub>)TiO<sub>3</sub>-6%BaTiO<sub>3</sub>" *J. Appl. Phys.* **112**, 044101 (2012)

Julia Glaum<sup>1</sup>, Hugh Simons<sup>1,3,4</sup>, Mark Hoffman<sup>1</sup>  
Matias Acosta<sup>2</sup>

*1 School of Materials Science and Engineering, University of New South Wales, NSW 2052, Australia*

*2 Institute of Materials Science, Ceramics Group, Technische Universität Darmstadt, Germany*

*3 School of Physics, Technical University of Denmark, Lyngby, Denmark*

*4 European Synchrotron Radiation Facility, Grenoble 38000, France*

*j.glaum@unsw.edu.au*

#### Temperature-dependency of the relaxor-ferroelectric transition in BNT-BZT ceramics

Piezoelectric ceramics are used in a wide range of actuating applications, utilizing their characteristic to transform electrical power into mechanical strain. In pure ferroelectric compositions the strain mechanism is based on the reorientation of ferroelectric domains and the intrinsic elongation of the unit cells along the direction of the applied field. However, in relaxor-type ceramics a third mechanism can contribute to the strain. It is based on an electric-field-induced transformation between the macroscopically non-polar relaxor state and the polar ferroelectric state and the associated high degree of domain alignment. In these materials the maximum unipolar strain is achieved at temperatures close to the transition temperature  $T_{F-R}$  where the ferroelectric state becomes unstable in the absence of an external electric field.

One of the most promising lead-free piezoelectric systems is  $(\text{Bi}_{1/2}\text{Na}_{1/2})\text{TiO}_3$ -6BaTiO<sub>3</sub> (BNT-6BT) with electromechanical properties similar to the widely used Pb(Zr,Ti)O<sub>3</sub> system. It exhibits relaxor characteristics and a ferroelectric state can be induced by electric field application. The transition temperature for BNT-6BT ceramics appears to be around 80°C. Doping with small amounts of Zr was found to increase the maximum strain, which makes this modification of BNT-BT interesting for high-strain applications.

This study investigates the influence of Zr-doping on the electric field induced relaxor-ferroelectric transition of the system BNT-6BT. Zr addition leads to a de-stabilization of the induced ferroelectric order, resulting in a lower transition temperature  $T_{F-R}$  and a corresponding increase in unipolar strain. However, the electric field  $E^*$  needed to induce this transition appears to be only slightly temperature dependent. Temperature dependent polarization and permittivity measurements will be utilized to explore the temperature-electric field diagram.

---

**PFM2**

CLUB C

*Monday, July 22 2013, 02:00 pm - 03:30 pm*

Chair: **To Be Announced**

## Electrical Modulation of the Local Conduction at BiFeO<sub>3</sub>-CoFe<sub>2</sub>O<sub>4</sub> Tubular Oxide Interface

Ying-Hao Chu

Department of Materials Science and Engineering, National Chiao Tung University, Hsinchu, Taiwan 30010, R.O.C.

Email: [yhc@nctu.edu.tw](mailto:yhc@nctu.edu.tw)

Complex oxide interfaces emerge as one of the most exciting subjects among condensed matters due to their unique physical properties and new possibilities for next-generation electronic devices. Three types of complex oxide interfaces have been established. Among them, the most explored interface is the artificially constructed heterointerfaces. Various interactions at the interface have resulted in a number of exciting discoveries, such as highly mobile quasi-two dimensional electron gas (2DEG) forms between two band insulators (LaAlO<sub>3</sub> and SrTiO<sub>3</sub>). Moreover, in ferroic oxides, domain walls dictate natural homo-interfaces as a consequence of the minimization of electrostatic and elastic energies. Several key studies have pointed out interesting observations, such as local conduction, on domain walls in multiferroics. Recently, new tubular oxide interface has been developed in the self-assembled heterostructures and the local conduction at the tubular interfaces of BiFeO<sub>3</sub> (BFO)-CoFe<sub>2</sub>O<sub>4</sub> (CFO) heterostructure was found. Such results create a huge playground to explore and design intriguing properties of complex oxide interfaces. However, in the push for practical applications, it is desirable to have the control of the interface functionalities through external stimulus. An electrical modulation of the local conduction at the homo- (BFO domain walls) and hetero-interfaces (LaAlO<sub>3</sub>/SrTiO<sub>3</sub>) was demonstrated recently. In this study, we went back to the BFO-CFO tubular interfaces and showed the interface conduction can be modulated non-volatile and reversibly via an external electric field by using conducting AFM (Figure 1). A memristive-like electronic conduction was observed, that is strongly correlated to the motion of oxygen vacancies (donor impurities) at the interface and in turn modifies the junction characteristics between the measurement tip and interface. Our results complete the control of the conduction at complex oxide interfaces and suggest the possibility for new devices based on complex oxide interfaces.

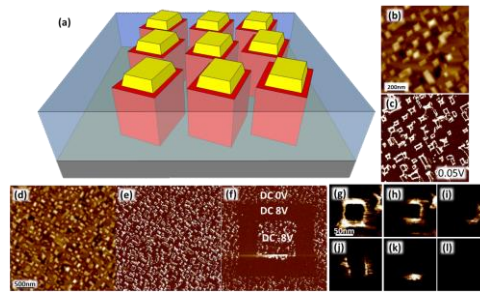


Figure 1. (a) The diagram of BFO-CFO nanostructures. CFO nanopillars (yellow) are embedded in the BFO matrix (blue), and hence the tubular interfaces (Red) form between these two materials. (b) The topography and (c) the current image of BCFO are gained simultaneously under the CAFM mode where the current is read by applied +0.05V sample bias. (d)~(f) the conduction currents at tubular interfaces can be turn on and off by applying larger DC bias (8 V) of different polarity. (g)~(l) currents at four sides of the tubular interface can be switched individually.

## Anomalous Photovoltaic effect in BiFeO<sub>3</sub>

Akash Bhatnagar, Marin Alexe  
Max Planck Institute of Microstructure Physics  
Weinberg 1, 06120 Halle (Saale), Germany  
e-mail: [malexe@mpi-halle.mpg.de](mailto:malexe@mpi-halle.mpg.de)

In the recent past, the entire field of photo-ferroelectrics has been revitalized by the reports of photovoltaic (PV) effect in BFO. Unlike traditional semiconductors the open circuit voltages in BFO are not limited by band gap. Initial investigations assumed that the PV effect in BFO is primarily due to the presence of a potential step at the domain wall which enables a more efficient separation of charge carriers [<sup>xvi</sup>]. However, in a recent work [<sup>xvii</sup>] it was observed that the generation and recombination of photo-generated non-equilibrium carriers in a BFO single crystal are primarily affected by the presence of shallow energy levels and the domain walls might not playing a major in the corresponding PV effect, as initially proposed. Thus, till now there is not yet a clear model of the PV effect in BFO. In this work, in order to get a further insight into the actual mechanism for the generation of PV effect in epitaxial BFO thin films, time and temperature resolved measurements have been performed. Time resolved measurements, namely photo induced transient spectroscopy (PITS) bring valuable data regarding generation and recombination of the photo-excited carriers. Providing that the ferroelectric domain configuration in BFO does not change at low temperature, variable temperature measurements of PV effect can provide information on details regarding the electronic structure of BFO, respectively shallow or deep levels in the band gap, that may affect the conduction mechanism as reported in [2].

## Optimization of carbon nanotube tips for improved scanning probe microscopy studies of ferroic thin films

Yuliya Lisunova<sup>1\*</sup>, J. Heidler<sup>2</sup>, I. Levkivskiy<sup>3</sup>, I. Gaponenko<sup>1</sup>, A. Weber<sup>2</sup>, L.J. Heyderman<sup>2</sup>, C. Cailler<sup>1</sup>, M. Klau<sup>4</sup> and P. Paruch<sup>1</sup>

<sup>1</sup>DPMC-MaNEP, University of Geneva, 24 Quai Ernest-Ansermet, 1211 Geneva 4, Switzerland

<sup>2</sup>Paul Scherrer Institut, 5232 Villigen PSI, Switzerland

<sup>3</sup>DPT, University of Geneva, 24 Quai Ernest-Ansermet, 1211 Geneva 4, Switzerland

<sup>4</sup>University of Mainz, Institute of Physics, Staudinger Weg 7, 55128 Mainz, Germany

Email: yuliya.lisunova@unige.ch

Scanning probe microscopy is an essential research tool for both fundamental and technology-driven studies, mapping diverse functional properties in a wide range of materials with a nanoscale resolution, defined by the specific tip geometry and properties. Its imaging capacity can be significantly enhanced by carbon-nanotube-based (CNT) tips [1], whose small size and outstanding mechanical and electrical properties improve resolution in topographical, electrostatic and surface potential microscopy modes. Further modification of the CNT tips [2-3] extends their application to magnetic force microscopy, when ferromagnetically coated, and to contact-based techniques, when rigidified with an insulating silicon dioxide layer. In the rapidly developing field of domain wall nanoelectronics [4], such ultra-high resolution tips could provide unprecedented access to the novel and highly localized functional properties of domain walls in ferroelectric and magnetic materials.

Here, we report on extended studies of such CNT tips, benchmarking their properties against commercially available tips on ferroic thin films. Introducing molecular beam epitaxy deposition of cobalt on single-walled CNT, we demonstrate sub-10 nm resolution in hard magnetic samples, and non-perturbative magnetic force microscopy imaging of complex domain and domain wall (DW) structures in micropatterned permalloy, both at ambient conditions [5]. We also develop theoretical models allowing us to extract the key imaging parameters and their dependence on the tip properties, and tailor the tip design to optimize resolution under given measurement conditions [5]. Integrating rigidified tips in ferroelectric thin film studies, we demonstrate more precise spatial resolution of the conducting region, allowing us to determine the minimal separation of DW in potential nanoelectronic devices, and the writing and reading of ferroelectric domain structures. These results are expected to have an impact on future probe-based technology, data storage and material characterization.

### References

- [1] J.H. Hafner et al. *J. Am. Chem. Soc.* 121, 9750 (1999)
- [2] H. Kuramochi et al. *Nanotechnology*. 16, 24 (2005)
- [3] N. Tayebi et al. *Appl. Phys. Lett.* 93, 103112 (2008)
- [4] G. Catalan et al. *Rev. Mod. Phys.* 84, 119 (2012)
- [5] Y. Lisunova et al. *Nanotechnology* 24 105705 (2013)

## Characterizing piezoelectric MEMs displacement

J. Evans, S. Chapman

Radiant Technologies, Inc., Albuquerque, NM USA

Email: sframboss@ferrodevices.com

Piezoforce Response Microscopy is a popular tool for studying ferroelectric and piezoelectric materials at the nanometer level.<sup>33,34</sup> Progress in piezoelectric MEMs (pMEMs) fabrication is highlighting the need to characterize *absolute* displacement at the nanometer and Ångstrom scales, something AFM might do but PFM cannot. The lack of calibration standards for atomic force microscopes at those scales plus high ambient noise levels exceeding the maximum displacement under study make accurate displacement characterization difficult. Nevertheless, once acceptable accuracy has been achieved it becomes possible to measure converse  $d_{33}$  for thin piezoelectric films and to determine the motions of MEMs structures that are far too complex to accurately simulate using finite element analysis tools. Absolute displacement measurement at the pMEMs level must target electroded devices. A major issue is that the demand for electrical current by electroded ferroelectric capacitors easily destroys the lightly metalized conductive cantilever tips used for PFM studies. This issue requires the development of more robust cantilevers to actuate pMEMs capacitors. Reliable conductive cantilevers make possible long term studies of actuator reliability, uniformity, and yield, all of which are prerequisites for manufacturing. As fully integrated pMEMs devices become available, the top electrode metal will be passivated by glass or other layers. Conductive cantilevers will no longer be needed since electrical connections will occur through the sample chuck to the pMEMs package pins. These extra layers above the actuator capacitor are necessary for long term product reliability but they will greatly complicate modeling device performance in product form. The results of on-going research by the authors on pMEMs characterization progress and challenges will be presented.

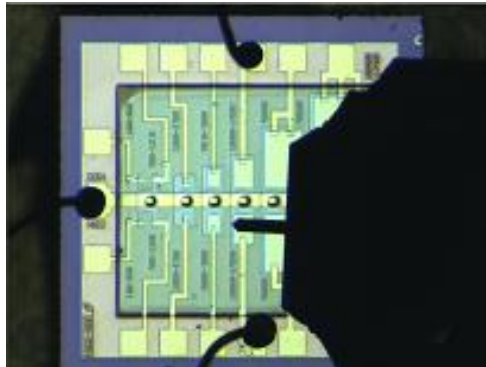


Fig. 9: 1-micron-thick niobium-doped PZT capacitor and its displacement butterfly loop.

<sup>33</sup> S. V. Kalinin and A. Gruverman, "Scanning Probe Microscopy of Functional Materials, Nanoscale Imaging and Spectroscopy", Springer, 2011

<sup>34</sup> M. Alexe and A. Gruverman, "Nanoscale Characterization of Ferroelectric Materials: Scanning Probe Microscopy Approach", Springer, 2004

---

## **Lead-free ceramics: Structure**

CLUB A

*Monday, July 22 2013, 04:30 pm - 06:00 pm*

Chair: **Jacob Jones**  
*University of Florida*



## Tilted or Distorted Octahedra in Perovskite Structures - what is the limit of what we can learn from powder diffraction?

Pam Thomas<sup>1</sup>, Mike Glazer<sup>1&2</sup>, Dean Keeble<sup>1</sup>, David Woodward<sup>1</sup>

<sup>1</sup> Department of Physics, University of Warwick, Coventry CV4 7AL, UK

<sup>2</sup> Clarendon Laboratory, Parks Road, Oxford OX1 3PU, UK

Email: p.a.thomas@warwick.ac.uk

Powder diffraction, whether by x-rays or neutrons, is well known as a technique for “finger-printing” crystal structures of all sorts, with automated search-match procedures and databases such as the ICDD making this practice relatively routine in many cases. However, when dealing with highly pseudo-symmetric structures that are derived either actually or theoretically from a cubic aristotype, powder diffraction patterns must be scrutinized with considerable rigour and one must rationally discriminate between very similar refinement fits to derive the correct structural model. In so doing, factors such as the resolution of the experiment and the broadening contributed by the sample must also be correctly accounted for.

In perovskite structures it has well been known since the seminal work of Glazer in the 1970's, that the structure can distort *via* tilting (rotating) of the oxygen octahedra about the unit cell axes of the parent phase. These tilts can be classified according to the Glazer notation and their effects on the powder pattern calculated. In particular, different systems of oxygen octahedral tilts lead to doublings of the unit cell, which are detected *via* super-structure peaks (often called “tilt peaks” in common parlance). It is usual for materials scientists (physicists, chemists *etc*) to look for particular super-structure peaks e.g.  $\frac{3}{2} \frac{3}{2} \frac{1}{2}$  or  $\frac{3}{2} \frac{1}{2} 0$  in a powder pattern to conclude that they have antiphase or in-phase octahedral tilts, respectively.

In recent work on refinements of the crystal structure of the archetypal lead-free piezoelectric sodium bismuth titanate,  $\text{Na}_{0.5}\text{Bi}_{0.5}\text{TiO}_3$  (NBT), in its tetragonal phase (at  $T > 673\text{K}$ ), we have discovered a previously unconsidered characteristic of powder patterns for perovskites. In this talk, we will show how there is a degeneracy in the powder patterns for (a) a tilted octahedral model of the structure or (b) a distorted but untilted octahedral model of the structure. The effect of this is that the computed powder patterns of these two quite different structures are virtually indistinguishable from each other, a very unusual situation in powder diffraction! The implications of this for the wider interpretation of powder diffraction data for a range of perovskite structures, including some fluorides—with highly distorted (fluorine) octahedra, are discussed.

## Lead-free Piezoelectric Ceramics ( $\text{Na}_{0.5}\text{K}_{0.5}\text{NbO}_3$ ) doped with $\text{LiTaO}_3$ and $\text{BiScO}_3$

Fangyuan ZHU<sup>1</sup>, Jing-Feng Li<sup>1</sup>, Michael B. Ward<sup>2</sup>, Tim P. Comyn<sup>2</sup>, Andrew J. Bell<sup>2</sup> and Steven J. Milne<sup>2</sup>

<sup>1</sup>School of Materials Science and Engineering, Tsinghua University, Beijing, China

<sup>2</sup>Institute for Materials Research, SPEME, University of Leeds, Leeds, UK

Email: [jessie-zhufangyuan@hotmail.com](mailto:jessie-zhufangyuan@hotmail.com)

A series of compositions along the compositional join in the ternary NKN-LT-BS system, extending from  $0.98\text{Na}_{0.5}\text{K}_{0.5}\text{NbO}_3$ - $0.02\text{BiScO}_3$  toward  $\text{LiTaO}_3$  have been prepared and characterized. A composition  $[\text{NKN}_{0.98}(\text{LiTaO}_3)_{0.02}]_{0.98}[\text{BiScO}_3]_{0.02}$  showed enhanced piezoelectric properties, relative to similar compositions, with  $d_{33}$  values of 215 pC/N. This can be attributed to a phase content of mixed orthorhombic (or monoclinic) and tetragonal phases at ambient temperatures. Variable temperature X-ray diffraction (XRD), and dielectric measurements as a function of temperature, indicated phase transitions (on heating) from an orthorhombic (or monoclinic) crystal system to tetragonal and then cubic crystal systems at  $\sim 25^\circ\text{C}$  and  $\sim 370^\circ\text{C}$  respectively.

Different types of dielectric behavior were observed on increasing the LT content. A NKN-5%LT-2%BS composition exhibited twin dielectric peaks at high temperatures ( $\sim 370^\circ\text{C}$  and  $\sim 470^\circ\text{C}$ ), along with broad X-ray diffraction peaks and a fine grain size,  $< 0.5 \mu\text{m}$ . The twin dielectric peaks suggest that chemical inhomogeneities may have been present; this was examined using transmission electron microscopy (TEM) with energy dispersive X-ray analysis (EDX). Elemental segregation was observed within individual grains, such that a core-shell grain structure was evident. Subsequently, a series of other compositions were prepared in the wider  $\text{Na}_{0.5}\text{K}_{0.5}\text{NbO}_3$ - $\text{LiTaO}_3$ - $\text{BiScO}_3$  ternary system.

Considering the combined data from XRD, dielectric measurements, SEM, TEM and piezoelectric properties for a wide range of compositions within the NKN-rich region of the NKN-LT-BS system, materials may be grouped into three categories, exhibiting the following defining characteristics.

**Type I:** single, sharp dielectric Curie peak ( $\sim 370^\circ\text{C}$ ); single phase by XRD; large grain size (5-10  $\mu\text{m}$ ); chemically uniform by TEM-EDX.

**Type II:** broad, single dielectric peak ( $\sim 350^\circ\text{C}$ ); single phase by XRD; large grain size; no obvious chemical segregation.

**Type III:** twin, broad dielectric peak(s) ( $\sim 370^\circ\text{C}$  and  $\sim 470^\circ\text{C}$ ); broad XRD peaks; small grain size ( $\sim 0.5 \mu\text{m}$ ); chemical segregation (core-shell structure) identified by TEM-EDX.

## Breaking of the centric symmetry in ferroelectric and paraelectric phases of unpoled ceramics.

Alberto Biancoli<sup>1</sup> and Dragan Damjanovic<sup>1</sup>

<sup>1</sup>Ceramics Laboratory, Swiss Federal Institute of Technology in Lausanne –EPFL, Switzerland.

Email: [alberto.biancoli@epfl.ch](mailto:alberto.biancoli@epfl.ch)

In the recent years, flexoelectricity attracted a growing interest as an electro-mechanical coupling mechanism alternative to piezoelectricity and electrostriction. Flexoelectric polarization is proportional to elastic strain gradient, which scales inversely with the size of sample, and thus was in general expected to play a major role only on nano-scale. In the past decade however, the experimental finding of large apparent flexoelectric coefficients in bulk ferroelectrics (three to four order of magnitude larger than theoretically predicted) raised the hope to exploit flexoelectricity for practical applications in bulk materials as well.

On the other hand, the recent observation of piezoelectric and pyroelectric-like responses in unpoled ferroelectric and paraelectric phases of ceramics suggests a breaking of the macroscopic centric symmetry caused by a mechanism other than the already known symmetry breaking induced under electric field. An insight into the origin of this breaking of the symmetry would have important implications on the understanding of the flexoelectric effect in bulk materials and may provide an explanation for the unexpectedly high apparent flexoelectric polarization reported for some bulk materials.

We report here on investigations of the described spontaneous symmetry breaking in unpoled ceramics. Materials examined include  $\text{BaTiO}_3$ ,  $\text{SrTiO}_3$ ,  $\text{Ba}_{1-x}\text{Sr}_x\text{TiO}_3$ ,  $(\text{Ba,Ca})(\text{Zr,Ti})\text{O}_3$  and  $\text{PbZr}_{1-x}\text{Ti}_x\text{O}_3$  solid solutions. Barium titanate,  $\text{Ba}_{1-x}\text{Sr}_x\text{TiO}_3$ ,  $(\text{Ba,Ca})(\text{Zr,Ti})\text{O}_3$  were examined both below and above their Curie temperature. A number of systematic studies were performed in a search for a possible driving force for the symmetry breaking.

The influence of dielectric permittivity, temperature, surface electrodes and grain size on apparent electro-mechanical and pyroelectric response of unpoled ferroelectric and paraelectric samples were studied. Grain size of a  $\text{BaTiO}_3$  sample could be changed by thermal annealing. A fine-grained  $\text{BaTiO}_3$  sample with a large permittivity exhibits a lower pyroelectric response than the same sample with a larger grain size and a lower permittivity. Response in  $\text{BaTiO}_3$  and  $\text{SrTiO}_3$  ceramics was compared to that in respective single crystals. Both ceramics and single crystals of  $\text{BaTiO}_3$  exhibit nonzero piezoelectric and pyroelectric signals above the Curie temperature. Within resolution of our measurements, neither single crystal nor ceramics of  $\text{SrTiO}_3$  show any symmetry breaking at room temperature. Pressing and sintering conditions for ceramics were analyzed and it was found that the cooling rate after sintering does not significantly affect the response.

## Laser Beam Scanning Microscopy Observation of Domain Switching in $\text{NaNbO}_3$ Epitaxial Film

Ichiro Fujii, Akihiro Kohori, Seiji Yamazoe, and Takahiro Wada

Department of Materials Chemistry, Ryukoku University, Otsu, Shiga, Japan

Email: ifujii@rins.ryukoku.ac.jp

Domain switching, or polarization reversal, substantially affects the dielectric and piezoelectric properties of ferroelectric materials. Thus, it is important to understand how the domain structure changes with the electric field amplitude. Laser beam scanning microscopy (LSM) with a polarizer is a methodology that allows us to see domain patterns and their polarization directions.<sup>35, 2</sup> We applied this technique to a 001-oriented  $\text{NaNbO}_3$  (NN) film, and observed a drastic change in the domain structure after a large electric field of 230 kV/cm was applied. In this study, evolution of the domain patterns of ferroelectric 001-oriented NN film was observed using LSM *during* application of ac electric fields with smaller amplitudes, and the domain structures were analyzed.

Before deposition of the NN film, we deposited  $\text{SrRuO}_3$  (SRO) film as a bottom electrode on (001)  $\text{SrTiO}_3$ (STO) substrate by pulsed laser deposition (PLD). Then, a 001-oriented NN film was prepared on a (001) SRO/(001)STO substrate by PLD. Pt top electrodes were formed on the NN film by sputtering. An electric field large enough to induce the ferroelectric response was applied by measuring polarization – electric field ( $P$ - $E$ ) loops with a ferroelectric tester. The domain structures were observed by LSM during the application of a triangular electric field. Here, a polarizer was placed between the film and the objective lens, and rotated to see the polarization directions of the domains.

A ferroelectric  $P$ - $E$  loop was observed for the NN film when an ac electric field amplitude of 100 kV/cm was applied. Figure 1 (a) shows a representative LSM image of the NN film. Rotation of the polarizer found that the domain structure consisted of the vertical and horizontal domains and the slanted domains, illustrated in Fig. 1 (b). When the electric field decreased from maximum electric field ( $+E_{\text{max}}$ ) to minimum electric field ( $-E_{\text{max}}$ ), two different domain-switching routes were observed. One is that the slanted domains changed to vertical and horizontal domains, which then reverted to slanted domains. These changes indicated that the polarization direction, for example, changed from out-of- $[101]$  to in-plane  $[110]$  and to out-of-plane  $[10-1]$ . The other route will be also discussed.

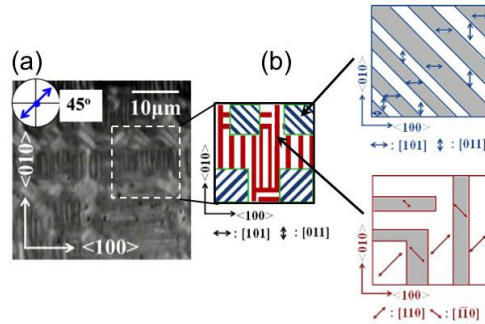


Fig. 1: (a) LSM image of NN film using 45° polarized laser beam, and (b) schematics of polarization directions of domains. plane  $[10-1]$ .

<sup>35</sup> S. Yamazoe, H. Sakurai, T. Saito, and T. Wada, Appl. Phys. Lett., **96**, 092901 (2010).

<sup>2</sup> S. Yamazoe *et al.*, J. Appl. Phys. 112, 052007 (2012).

---

## **Materials for High Power and High Temperature Applications**

CLUB B

*Monday, July 22 2013, 04:30 pm - 06:00 pm*

Chair: **Ian Reaney**  
*University of Sheffield*

## BaTiO<sub>3</sub> – Bi(Zn<sub>1/2</sub>Ti<sub>1/2</sub>)O<sub>3</sub> – NaNbO<sub>3</sub> Dielectric Ceramics for Advanced Capacitor Applications

Natthaphon Raengthon<sup>1</sup>, Harlan J. Brown-Shaklee<sup>2</sup>, Geoff L. Brennecke<sup>2</sup> and David P. Cann<sup>1</sup>

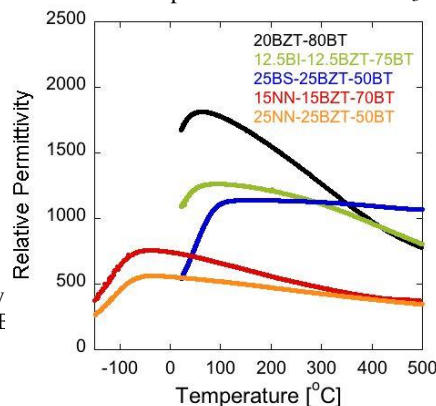
<sup>1</sup>Materials Science, School of Mechanical, Industrial, and Manufacturing Engineering,  
Oregon State University, Corvallis, OR, USA

<sup>2</sup>Electronic, Optical, and Nanostructured Materials Department, Sandia National Laboratories,  
Albuquerque, NM, USA

Email: raengthn@onid.orst.edu

Dielectric ceramics for high temperature electronics are desired for advanced technologies since existing technologies of ceramic capacitors (X7R or NP0) are not compatible with extreme environments, especially at temperatures higher than 200 °C. In recent years, several research groups have developed new BaTiO<sub>3</sub> – based materials that exhibit promising dielectric properties for high temperature applications. Previous studies on BaTiO<sub>3</sub> – Bi(Zn<sub>1/2</sub>Ti<sub>1/2</sub>)O<sub>3</sub> – BiScO<sub>3</sub> ceramics demonstrated that a temperature-stable permittivity can be obtained over a broad temperature range<sup>36</sup>. However, a large change in permittivity between room temperature and 100 °C persisted which might limit the usage of the material over that temperature range. Therefore, BaTiO<sub>3</sub> – Bi(Zn<sub>1/2</sub>Ti<sub>1/2</sub>)O<sub>3</sub> – NaNbO<sub>3</sub> ceramic solid solutions were investigated. The effects of BaTiO<sub>3</sub> and NaNbO<sub>3</sub> additions on the dielectric properties of ternary compounds are of interest. A broadening of the temperature-dependent permittivity maximum and a decrease in overall permittivity were observed when the content of BaTiO<sub>3</sub> decreased while the Bi(Zn<sub>1/2</sub>Ti<sub>1/2</sub>)O<sub>3</sub>:NaNbO<sub>3</sub> ratios were kept constant. A shift in the temperature of the maximum permittivity (T<sub>max</sub>) down to -103 °C was achieved when substituting Bi(Zn<sub>1/2</sub>Ti<sub>1/2</sub>)O<sub>3</sub> with NaNbO<sub>3</sub> for the compositions with constant BaTiO<sub>3</sub> concentration. A broad permittivity peak was observed in several compositions that was comparable to other BaTiO<sub>3</sub> – Bi(Zn<sub>1/2</sub>Ti<sub>1/2</sub>)O<sub>3</sub> based ceramics as shown in Figure 1. The dielectric characteristics of the 50BT-25BZT-25NN composition also satisfies the X9R standard ( $\Delta C/C_{25} = \pm 15\%$  over a range of -55 to 200 °C). A linear dielectric response is also presented under high electric fields at various temperatures. In conclusion, the investigation of BT-BZT-NN compounds resulted in promising dielectric properties with broad temperature ranges with a high permittivity, which is of interest for advanced capacitor applications.

Figure 1. Temperature dependence of relative permittivity compounds (BZT: Bi(Zn<sub>1/2</sub>Ti<sub>1/2</sub>)O<sub>3</sub>, BT: BaTiO<sub>3</sub>, BI: F



<sup>36</sup>N. Raengthon, T. Sebastian, D. Cumming, I. M. Reaney, and D. P. Cann, "BaTiO<sub>3</sub> – Bi(Zn<sub>1/2</sub>Ti<sub>1/2</sub>)O<sub>3</sub> – BiScO<sub>3</sub> Ceramics for High-Temperature Capacitor Applications", *J. Am. Ceram. Soc.*, 95[11] 3554-3561 (2012).

Sandia National Laboratories is a multi-program laboratory managed and operated by Sandia Corporation, a wholly owned subsidiary of Lockheed Martin Corporation, for the U.S. Department of Energy's National Nuclear Security Administration under contract DE-AC04-94AL85000. This work was supported by the Department of Energy's Office of Electricity Delivery and Energy Reliability, Energy Storage Systems program managed by Dr. Imre Gyuk.

## Large Field Property Assessment of Mn:PIN-PMN-PT Crystals for High Power Transducers

Jun Luo<sup>1</sup>, Sam Taylor<sup>1</sup>, Shujun Zhang<sup>2</sup> and W. Hackenberger<sup>1</sup>

<sup>1</sup>TRS Technologies, Inc, State College, PA 16801

<sup>2</sup>Material Research Institute, Pennsylvania State University, PA16801

Email: jun@trstechnologies.com

The third generation of advanced relaxor-PT piezoelectric single crystals, Mn:PIN-PMN-PT (manganese doped  $\text{Pb}(\text{In}_{1/2}\text{Nb}_{1/2})\text{O}_3\text{-Pb}(\text{Mg}_{1/3}\text{Nb}_{2/3})\text{O}_3\text{-PbTiO}_3$ ), has attracted broad attention for the high power transducers due to their greatly reduced mechanical loss but well-maintained, extremely high electromechanical coupling coefficient. Small signal characterization of Mn:PIN-PMN-PT crystals have been extensively studied. However, systematic large signal tests of Mn:PIN-PMN-PT crystals were urgently needed for further assessing the properties for high power transducer operation.

A systematic large signal, quasistatic measurement has been conducted for Mn:PIN-PMN-PT crystals under variable prestress, temperature and electric field. Preliminarily optimized operation domains for high power transducer design have been revealed for [001]-poled crystals for achieving maximum acoustic power density with low hysteretic losses caused by nonlinearity and phase transitions. It was proved that the uniaxial prestress can stabilize the rhombohedral phase and suppress the electric field induced phase transition. Furthermore, driven by a combination of a bipolar AC field and a positive DC bias field, the crystals exhibit a broader range of linear strain and polarization response under uniaxial prestress, which means, at room temperature, a positive DC bias field (applied in the same direction with the poling field) expands the linear range of strain response under a bipolar AC field (1Hz). As shown in Fig. 1, for a +4kV/cm DC bias, the crystal was driven by a  $\pm 6$ kV/cm bipolar AC field with no domain switch. A larger AC field driving range may benefit the high power transducer applications.

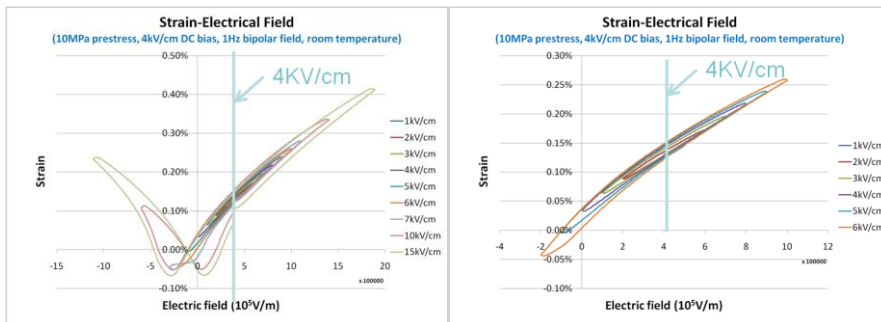


Fig. 1: S-E loops of a Mn: PIN-PMN-PT crystal sample measured under 10MPa prestress and 4kV/cm external DC bias: (a) for 1-15kV/cm bipolar fields and (b) for 1-6kV/cm bipolar fields

## Effects of excess Bi on high-temperature dielectric and piezoelectric properties of lead-free $0.75\text{BiFeO}_3\text{-}0.25\text{BaTiO}_3$ ceramics

Jianguo Chen, Jinrong Cheng<sup>1</sup>

<sup>1</sup> School of Materials Science and Engineering, Shanghai University, Shanghai, People's Republic of China

Email: [chenjianguo@shu.edu.cn](mailto:chenjianguo@shu.edu.cn)

$0.75\text{BiFeO}_3\text{-}0.25\text{BaTiO}_3$  (BF-BT) ceramics with different excess Bi contents were prepared by solid state reaction method. The effects of excess Bi content on the structure, dielectric and piezoelectric properties of BF-BT ceramics were studied. XRD results indicated that the modified BF-BT ceramics exhibited single perovskite structure with rhombohedral symmetry. The introduction of excess Bi in the solid solutions showed positive effects on both dielectric and piezoelectric properties. The Curie temperature  $T_c$ , dielectric constant  $\epsilon$  and loss  $\tan\delta$  (1 kHz), piezoelectric constant  $d_{33}$ , and planner electromechanical coupling factor  $k_p$  of BF-BT ceramics with 1 % excess Bi were 514 °C, 230, 440, 4.6 %, 115 pC/N and 0.28, respectively. The piezoelectric constant  $d_{33}$ , and planner electromechanical coupling factor  $k_p$  of BF-BT ceramics with 1 % excess Bi were stable up to 450 °C, about 300 °C higher than that of PZT-based ceramics. The combination of improved piezoelectric constant  $d_{33}$  and temperature stability indicated that BF-BT ceramics with excess Bi were promising candidates for high-temperature and lead-free piezoelectric applications.



## Novel high temperature BiFeO<sub>3</sub>-(K<sub>0.5</sub>Bi<sub>0.5</sub>)TiO<sub>3</sub>-PbTiO<sub>3</sub> piezoceramics

Jim Bennett<sup>1</sup>, Andrew.J.Bell<sup>1</sup>, Tim.J.Stevenson<sup>1</sup> and Tim.P.Comyn<sup>1</sup>

<sup>1</sup>Institute for Materials Research, University of Leeds, Leeds, UK

Email: pm07jb@leeds.ac.uk

There is currently a need for high strain piezoelectric actuators that are capable of operating under extreme temperatures and pressures in applications such as aerospace, deep sea oil drilling and in chemical processing. PZT is currently the dominant piezoelectric ceramic material in actuators, sensors and transducers, however, PZT has a restricted operating temperature.

Ceramics belonging to the  $(1-x-y)\text{BiFeO}_3-x(\text{K}_{0.5}\text{Bi}_{0.5})\text{TiO}_3-y\text{PbTiO}_3$  system have been fabricated. X-ray diffraction was utilized along with PUND, strain-field, polarization-field and high temperature electrical measurements in order to characterize the new materials. The Curie temperatures,  $T_C$ , of the compositions presented far exceed those of PZT, coupled with piezoelectric coefficients in the region of 152-225 pC/N. A link was found to exist between the  $c/a$  ratio of the tetragonal phase across the MPB and  $T_C$ .

This work also examines the extrinsic piezoelectric effect as a function of temperature using the piezoelectric Rayleigh relations. The effects of composition upon intrinsic contributions,  $d_{33}$  and  $E_C$  are also detailed. The  $d_{33}$ , intrinsic and extrinsic contributions of these materials were found to increase up to 150 °C while adhering to the Rayleigh model. The composition with the highest room temperature  $d_{33}$  was found to have a Rayleigh coefficient of  $58.83 \times 10^{-18} \text{ (m}^2/\text{V}^2\text{)}$ , an order of magnitude increase compared to La-doped BiFeO<sub>3</sub>-PbTiO<sub>3</sub>.

Ternary and pseudoquaternary systems have recently been subject to large amounts of research as many of the possible binary systems have been explored. This has led to a raft of materials with reported high piezoelectric coefficients; these are often electrostrictive or have limited operating temperatures. This system shows that with only small amounts of a third end member such as potassium bismuth titanate in BFPT, the electrical properties of a binary system can be drastically altered.

**Clive Randall**<sup>1</sup>, Dennis P. Shay<sup>1</sup>, Russell Maier<sup>1</sup>, Doo Hyun Choi<sup>2</sup>, Michael Lanagan<sup>3</sup>

<sup>1</sup>*Materials Science and Engineering, The Pennsylvania State University, University Park, PA, USA*, <sup>2</sup>*Materials Science and Engineering, The Pennsylvania State University, University Park, PA, USA*, <sup>3</sup>*Engineering Science and Mechanics, The Pennsylvania State University, University Park, PA, USA*

### Designing Dielectric Materials for High Power and Energy Density-a New Era for Capacitor Based Applications

This paper will develop a rationale for new dielectric materials that are required for new high temperature and high energy density capacitors. We will consider the voltage saturation issues in nonlinear dielectrics, degradation, and breakdown processes. We will also consider the impact of coupled dipole mechanisms on energy density and power density behavior of selected dielectric materials. These new insights into high energy density capacitors could be applied to electrochemical and hybrid capacitor designs.

---

## **PFM3**

CLUB C

*Monday, July 22 2013, 04:30 pm - 06:00 pm*

Chair: **Patrycja Paruch**  
*University of Geneva*

**Interplay of polarization dynamic and surface electrochemistry in ferroelectrics: from ionic transport to chaotic dynamics and fractal growth**

S.V. Kalinin,<sup>1</sup> A. Morozovska,<sup>2</sup> and V. Shur<sup>3</sup>

sergei2@ornl.gov

<sup>1</sup> The Center for Nanophase Materials Sciences, Oak Ridge National Laboratory,  
Oak Ridge, TN 37922

<sup>2</sup> Ferroelectric Laboratory, Institute of Natural Sciences, Ural Federal University,  
620000 Ekaterinburg, Russia

<sup>3</sup> Institute of Physics, National Academy of Sciences of Ukraine, 46, pr. Nauki, 03028 Kiev, Ukraine

Polarization switching in ferroelectric materials is inseparable from the screening processes, which in many cases are realized by mobile surface ions. In this presentation, I will discuss experimental evidence for the existence and slow dynamics of these ions based on variable temperature Kelvin Probe Microscopy data, and present experimental strategies for exploring the injection and ionic transport phenomena based on the time-resolved KPFM. The nontrivial effects of the ionic dynamics on domain structure and dynamics in ferroelectric thin films and crystals, including metastable nanoscale phase separated domain states, slow switching dynamics, and formation of fractal domains and chaotic dynamics during switching are discussed.

This work is supported by the Center for Nanophase Materials Sciences which is sponsored by the Scientific User Facilities Division, Office of Basic Energy Sciences, U.S. Department of Energy

## Nanoscale electrochemical diode in proton-exchanged LiNbO<sub>3</sub>

Michele Manzo,<sup>1</sup> Nina Balke,<sup>2</sup> Amit Kumar,<sup>2</sup> Stephen Jesse,<sup>2</sup> Sergei V. Kalinin,<sup>2</sup>  
Brian J. Rodriguez,<sup>3</sup> and Katia Gallo<sup>1</sup>

<sup>1</sup> Dept. of Applied Physics, KTH - Royal Institute of Technology, Stockholm, Sweden

<sup>2</sup> The Center for Nanophase Materials Sciences, Oak Ridge National Laboratory, Oak Ridge, Tennessee, USA

<sup>3</sup> School of Physics, University College Dublin, Belfield, Dublin 4, Ireland

Email: manzo@kth.se

Gaining deeper understanding of nanoscale ionic transport in solid-state materials is a key aspect towards more efficient energy harvesting, storage, and conversion devices, as well as progress in other applications, such as memristors and holographic memories. LiNbO<sub>3</sub> (LN) is an artificial ferroelectric (widely used in the context of nonlinearity and electro-optics)<sup>xviii</sup> where such insights are furthermore relevant for an even broader range of applications, encompassing also photonics. Through macroscopic studies on LN crystals of different stoichiometry, a clear correlation of its electrical conductivity to the hydroxyl content has been established.<sup>xix</sup> However, such analyses are performed at high temperatures (400–1000 K) where conductivity is associated with thermal-activated ionic mobility. On the other hand, estimations at room temperature report extremely low values (10<sup>-18</sup> mS/cm) and hence are usually assessed by indirect methods.

Here we present room-temperature conductivity measurements on congruent LN substrates in which protons have been controllably introduced via selective periodic proton-exchange (PE). The electrical excitation was applied via a nanoscale contact, by means of conductive atomic force microscopy (c-AFM), on wedge-polished samples as in Fig. 1a. This offered the direct assessment on the mechanisms for ionic transport in

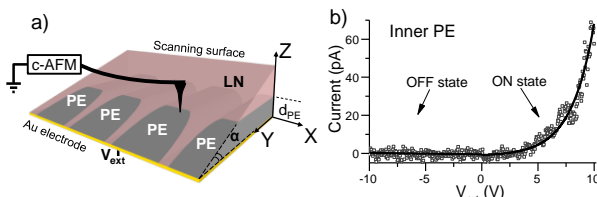


Fig. 10 a) 3D sketch of the periodic PE:LN wedged sample with which PE and LN regions were probed by c-AFM. b) Current flowing through the sample plotted as a function of the DC-bias voltage ( $V_{ext}$ ) applied to the crystal (bottom electrode in 1a). Measurements performed at the center of the PE region.

LN, highlighting conductivity enhancements up to four orders of magnitude localized at the core of the PE regions. Furthermore, a strongly unipolar response of the measured currents as a function of the applied voltage was observed (Fig. 1b). The effect was modeled by the Butler-Volmer equations<sup>xx</sup> and ascribed to the interplay of both electrically-activated ionic transport of interstitial protons in the core-PE region and surface nanoscale electrochemical reactions occurring at the c-AFM tip. This response was also systematically compared to the one arising in LN and regions with much lower proton content.

The study presented in this work opens a new approach to investigate and engineer at the nanoscale the interplay among ionic motion, electrochemical, and photochemical phenomena on ferroelectric surfaces.

## Formation of Ordered and Disordered Nanodomain Chains as a Result of Switching by Conductive Tip of Scanning Probe Microscope

Ievlev Anton<sup>1</sup>, Shur Vladimir<sup>1</sup>, Neradovskiy Maxim<sup>1</sup>,  
Morozovska Anna<sup>2</sup>, Eliseev Eugene<sup>2</sup>, and Kalinin Sergei<sup>3</sup>

<sup>1</sup>Ferroelectric Laboratory, Ural Federal University, Ekaterinburg, Russia

<sup>2</sup>Lashkaryov Institute of Semiconductor Physics, National Academy of Sciences of Ukraine,  
Kiev, Ukraine

<sup>3</sup>The Center for Nanophase Materials Sciences and Technology Division,  
Oak Ridge National Laboratory, Oak Ridge, TN, USA

Email: anton.ievlev@labfer.usu.ru

Formation of the domain chains under the action of electric field produced by conductive tip of scanning probe microscope (SPM) has been studied in 20  $\mu\text{m}$ -thick z-cut plate of congruent lithium niobate. Switching was carried out by bipolar triangular pulses with amplitude  $U_{sw}$  ranged from 20 V to 100 V and duration 250 ms. The chain period  $d$  ranged from 100 nm to 1  $\mu\text{m}$ . The uniform, ordered and disordered nanodomain chains was created in different switching conditions.

Uniform chains of non-interacted domains appeared for switching with periods above 300 nm (for  $U_{sw} = 50\text{V}$ ) (Fig. 1a). Decreasing of the period led to change of the nanodomain chains types due to domain-domain interaction. Weak interaction at shorter periods ( $300\text{ nm} > d > 250\text{ nm}$ ) led to formation of the uniform chains with larger first domain. Further decrease of the period to 150 nm led to formation of ordered and disordered chains (Fig. 1c,d). At the periods below 150 nm the domain merging started (Fig. 1b). Moreover the strong influence of the temperature and humidity in the SPM chamber on the chain parameters has been revealed.

Experimental results were attributed to influence of the residual depolarization field of older domain, which suppresses the domain growth at short distances and stimulate nucleation at proper distance. The proposed model has been confirmed by calculation of the spatial distribution of electric field in the vicinity of the isolated needle-like domain both by computer simulation and analytically.

Equipment of the Center of Nanophase Material Science of Oak Ridge National Laboratory was used (project CNMS2012-113). The research was made possible in part by RFBR (Grants 13-02-01391-a, 11-02-91066-CNRS-a), by Ministry of Education and Science (Contract 14.513.12.0006).

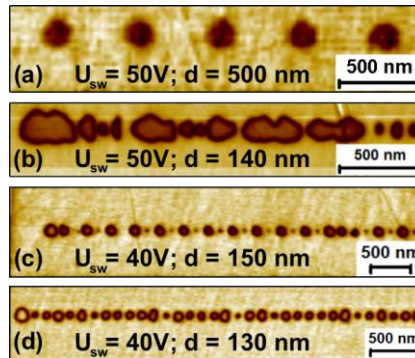


Fig. 11: Different types of nanodomain chains formed after local switching with different parameters. (a) Uniform chain; (b) merging of domains in the chain; (c), (d) intermittent switching in the chain.

## Towards a Better Understanding of Lateral Piezoresponse Force Microscopy

Shiming Lei<sup>1,2</sup>, Ryan C. Haislmaier<sup>1</sup>, Tom T. A. Lummen<sup>1</sup>, Wenwu Cao<sup>2,3</sup>, Venkatraman Gopalan<sup>1</sup>

<sup>1</sup>Materials Research Institute and Department of Materials Science and Engineering, Pennsylvania State University, University Park, Pennsylvania, USA

<sup>2</sup>Condensed Matter Science and Technology Institute and Department of Physics, Harbin Institute of Technology, Harbin, People's Republic of China

<sup>3</sup>Materials Research Institute and Department of Mathematics, Pennsylvania State University, University Park, Pennsylvania 16802, USA

Email: [sul46@psu.edu](mailto:sul46@psu.edu)

Piezoresponse Force Microscopy (PFM) has been widely used for probing and imaging domain structures of ferroelectric materials. In order to obtain a comprehensive information of probed polar materials, both vertical and lateral signals are necessary to be used. In this sense, it is of vital importance to bridge the PFM signal correctly to the corresponding properties of the probed materials.

Our previous theoretical calculations systematically analyzed the mechanisms of lateral and vertical PFM response for Lithium Niobate single crystal ( $\text{LiNbO}_3$ )<sup>37</sup>. But for the realistic experimental signals, they are always contaminated by the frequency-dependent background noise, which is inherent to the experimental setup<sup>2</sup>. Jungk et al. proposed an effective treatment to recover vertical contrast. However, to our best knowledge, no effective background noise treatment has been proposed for the lateral signal so far, which undoubtedly holds back the quantitative understanding of lateral PFM signals. Here we reported an effort towards eliminating the background noise in the lateral PFM signal. The results after this treatment showed an excellent agreement with theoretical calculations. In addition, the 90° lateral PFM signal scanning across the anti-parallel  $\text{LiNbO}_3$  domain wall, which was dismissed as an artefact before, is confirmed with repeatable results in the present effort.

---

<sup>37</sup>Lei et al, "Origin of piezoelectric response under a biased scanning probe microscopy tip across a 180° ferroelectric domain wall", PHYSICAL REVIEW B 86, 134115 (2012)

<sup>2</sup>Jungk et al, "Quantitative analysis of ferroelectric domain imaging with piezoresponse force microscopy", Appl. Phys. Lett. 89 163507 (2006).

## Application of Atomic Force Acoustic Microscopy and Ultrasonic Piezoelectric Force Microscopy to Characterization of Bismuth-Based Piezoelectric Ceramics

Ute Rabe, Leonardo Batista, Sigrun Hirsekorn

Fraunhofer Institute for Non Destructive Testing (IZFP), Saarbruecken, Germany

Email: [Ute.Rabe@izfp.fraunhofer.de](mailto:Ute.Rabe@izfp.fraunhofer.de)

The combination of ultrasonics with scanning force microscopy allows one to exploit the bending modes of Atomic Force Microscope (AFM) cantilevers for material characterization with a local resolution in the nm range. In Atomic Force Acoustic Microscopy (AFAM) the resonances of the cantilevers vibrating in contact with the sample surface are evaluated to image local elasticity qualitatively and/or quantitatively. The contact resonances are furthermore used for contrast enhancement in Ultrasonic Piezoelectric Force Microscopy (UPFM). In the framework of a European/Mexican project, Bismuth-based epitaxial thin films have been investigated and evaluated by different operation modes of an AFM (Fig. 1)<sup>38</sup>. Especially, dynamic modes in the ultrasonic frequency range such as AFAM and UPFM have been used. Ferroelectric materials have found many useful applications for example as sensors, actuators, transducers, and memories. However, most of these materials are based on toxic elements, e.g., Lead (Pb). With the new European regulations restricting the use of such toxic elements, the need arises for new materials which provide the same or better functional properties. These properties such as piezoelectric constants, polarizability and high electromechanical coupling factors are mostly determined by the microstructure and the arrangement of the ferroelectric domains.

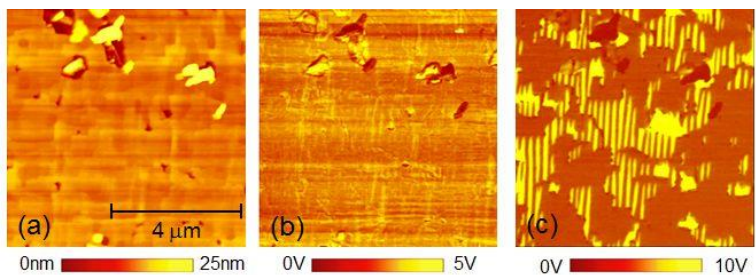


Fig. 12: (a) AFM topography image, (b) AFAM amplitude image and (c) UPFM image of the same surface area of a  $\text{BiFeO}_3$  thin film on  $\text{SrTiO}_3$  (100)<sup>1</sup>

The macroscopic properties of Bismuth-based, polarized bulk samples  $\text{Na}_0.5\text{Bi}_0.5\text{TiO}_3$  (NBT) and  $0.94\text{Na}_0.5\text{Bi}_0.5\text{TiO}_3-0.06\text{BaTiO}_3$  (NBT-BT) were also examined. The piezoelectric activity was characterized by impedance and 3D laser vibrometer measurements. Furthermore, the Young's modulus and the shear modulus were calculated from the longitudinal and transverse wave sound velocities and the density. Using these data and the geometrical parameters of the samples, the first thickness and radial resonance frequencies were calculated and compared to experimental spectra.

<sup>38</sup> R. P. Fernandes, L. Batista, A. C. G. Castro, L. Salamanca-Riba, M. P. Cruz, F. J. Espinoza-Beltrán, S. Hirsekorn, U. Rabe, J. Muñoz-Saldaña, G. A. Schneider, Mater. Res. Soc. Symp. Proc. Vol. 1477, DOI: 10.1557/opl.2012.1701 (2012).



---

## **ISAF Group 1 Posters**

Forum Hall

*Monday, July 22 2013, 01:00 pm - 04:30 pm*

## Ultrahigh superelastic and actuation strains in BaTiO<sub>3</sub> crystals by reversible electromechanical domain switching

Yingwei. Li<sup>1</sup>, Faxin. Li<sup>1,4</sup>, Xiaobing. Ren<sup>3</sup>, Haosu. Luo<sup>5</sup>, Daining. Fang<sup>2</sup>

<sup>1</sup>State Key Lab for Turbulence and Complex Systems, College of Engineering, Peking University, Beijing, 100871, China

<sup>2</sup>Department of Aeronautics & Astronautics, College of Engineering, Peking University, Beijing, 100871, China

<sup>3</sup>Materials Physics Group, National Institute for Materials Science, Tsukuba, 305-0047, Ibaraki, Japan

<sup>4</sup>HEDPS, Center for Applied Physics and Technologies, Peking University, Beijing, China

<sup>5</sup>Shanghai Institute of Ceramics, Chinese Academy of Sciences, Shanghai, 200050, China

Email: yingweili@pku.edu.cn

Superelasticity (SE), characterized by large recoverable hysteretic stress-strain curve, has been observed in shape memory alloys and other smart materials including the relaxor ferroelectrics via reversible phase transformation, while it has rarely been realized in normal ferroelectrics. Theoretically, SE could appear in polyaxial ferroelectrics via reversible ferroelastic domain switching but should be under a bias electric field because different domains are by default energetically identical. Chaplya and Carman realized SE under electromechanical loading by non-180° ferroelastic domain switching in Lead Titanate Zirconate ceramics; however, influenced by the interaction between grains, SE was realized only under large external preload bias electric fields and compressive stresses. In this work, by using BaTiO<sub>3</sub> crystal, we realized ultrahigh superelastic strain of up to 0.85% in a pre-poled BaTiO<sub>3</sub> crystal under uni-axial electromechanical loading. The superelasticity was realized under bias electric fields of only 200V/mm during compression with the maximum stress at 15MPa. More importantly, it was tunable by the applied electric field, making it very promising for advanced damping applications. In addition, when keeping the compression and making unipolar electric fields cycling, an actuation strain of 0.93%, which is larger than the previous reported value of ~0.8% by Bucsu et al, was obtained at 800V/mm. These characteristics stem from the reversible 90° domain switching under the competition of electrical and mechanical loading. A unified incremental switching criterion was proposed to depict the domain switching process.

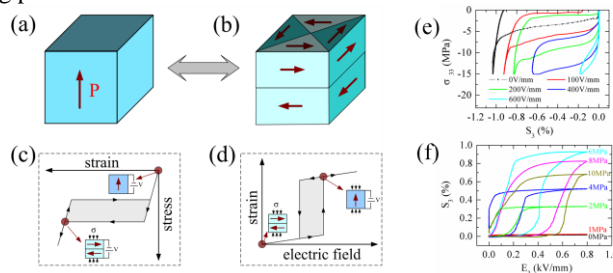


Fig 1. Principle of realization of superelasticity and actuation in a poled BTO crystal via reversible 90° domain switching under electromechanical loading (a-d), and the measured experimental results (e-f).

## 2D Ferroelectrics – Material for Future Memory Devices?

Vilgelmina Stepkova<sup>1</sup>, Pavel Marton<sup>1</sup>, Jiri Hlinka<sup>1</sup>

<sup>1</sup>Department of Dielectrics, Institute of Physics, Academy of Sciences of the Czech Republic,  
Prague, Czech Republic

Email: stepkova@fzu.cz

Ferroelectric materials are characterized by existence of spontaneous polarization, which can be reoriented by application of electric field. The dependence of polarization on electric field magnitude is described by hysteresis loop in analogy to ferromagnets. Typically, ferroelectric structure splits into domains – the regions which differ by the direction of spontaneous polarization. These properties give an opportunity to store information.

It is already well known that ferroelectric memory devices have a variety of advantages, such as non-volatility, low energy consumption, fast information writing, large number of rewriting cycles, etc. However, the already existing ferroelectric random access memory (FeRAM) is not very popular nowadays due to its low density of information arrangement, high cost and limited capacity.

Present work is devoted to the investigation of recently predicted new type of ferroelectric domain walls, so-called “Bloch walls”<sup>39,40,41,42</sup> in analogy to ferromagnets. These walls are characterized by nonzero out of plane component ( $P_t$ ) (see Fig.1), which has an orientation perpendicular to spontaneous polarization. The idea for new type of memory devices lies in switching of this polarization out of plane component within the wall, not whole domain state, which requires much lower energy losses and in principle allow higher density of information arrangement.

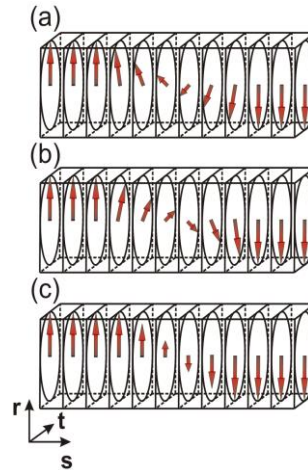


Fig. 13: Variation of polarization  $\mathbf{P}$  within Bloch- and Ising-type domain walls. The Bloch-type structure (a,b) conserves the magnitude of the local vectorial order parameter.

<sup>39</sup> P. Marton, I. Rychetsky, and Jiri Hlinka, “Domain walls of ferroelectric within the Ginzburg-Landau-Devonshire phenomenological model”, Phys. Rev. B, vol. 81, p.144125, 2010.

<sup>40</sup> J. Hlinka, V. Stepkova, P. Marton, I. Rychetsky, V. Janovec, and P. Ondrejko “Phase-field modelling of 180° “Bloch walls” in rhombohedral BaTiO<sub>3</sub>”, Phase Transitions, vol. 84, p. 738-746, 2011.

<sup>41</sup> V. Stepkova, P. Marton, and J. Hlinka “Stress-induced phase transition in ferroelectric domain walls of BaTiO<sub>3</sub>”, J. Phys: Condens. Matter, vol. 24, p. 212201, 2012.

<sup>42</sup> M. Teherinejad, D. Vanderbilt, P. Marton, V. Stepkova and J. Hlinka, “Bloch-type domain walls in rhombohedral BaTiO<sub>3</sub>”, Phys. Rev. B, vol. 86, p. 155138, 2012.

## Electrostrictive effect of PMN-PT crystals

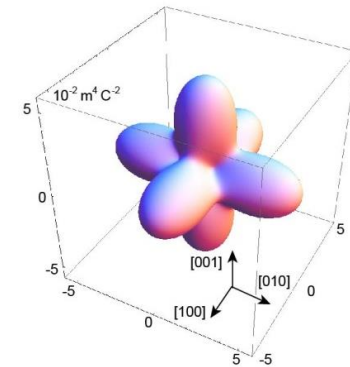
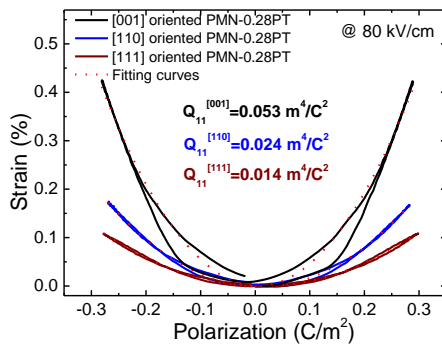
Fei Li<sup>1</sup>, Li Jin<sup>1</sup>, Zhuo Xu<sup>1</sup>, and Shujun Zhang<sup>1,2</sup>

<sup>1</sup>Electronic Materials Research Laboratory, Key Laboratory of the Ministry of Education and International Center for Dielectric Research, Xi'an Jiaotong University, Xi'an 710049, China

<sup>2</sup>Materials Research Institute, Pennsylvania State University, University Park, Pennsylvania 16802, USA

Email: ful5@mail.xjtu.edu.cn

For exploring high performance piezoelectric materials, researchers generally resort to the ferroelectric phase transition regions in perovskite solid solutions, where the polarization can be easily changed by external field, leading to high dielectric and piezoelectric responses. This approach, however, improves the piezoelectricity at the cost of thermal stability. In addition, over the development of last sixty years, there is limited space to enhance the piezoelectric activity through this method. The electrostrictive effect, which is a critical factor for controlling the piezoelectric response in ferroelectrics, on the other hand, has received limited attention. With the aim of searching alternative approaches to enhance the piezoelectric response, the electrostrictive effect was studied in  $\text{Pb}(\text{Mg}_{1/3}\text{Nb}_{2/3})\text{O}_3\text{-PbTiO}_3$  relaxor ferroelectric crystal, a representative high performance piezoelectric material, with respect to orientation, temperature and composition. The electrostrictive coefficients  $Q_{11}^C$ ,  $Q_{12}^C$  and  $Q_{44}^C$  of PMN- $x$ PT ( $x=0.25\text{-}0.37$ ) crystals are found to be about 0.055, -0.024 and 0.020  $\text{m}^4 \text{C}^{-2}$  respectively. The maximum and minimum  $Q_{33}^*$  is found to be along  $\langle 001 \rangle$  and  $\langle 111 \rangle$  directions, being about 0.055 and 0.014  $\text{m}^4 \text{C}^{-2}$ , respectively. The relation between piezoelectric and electrostrictive effects is discussed for domain engineered PMN- $x$ PT crystals. Based on this research, it is expected that the piezoelectric activity of relaxor- $\text{PbTiO}_3$  crystals can be greatly enhanced by improving their electrostrictive coefficients to the typical level of classical perovskite crystals.



## Formation of Nanodomain Structure in Front of Moving Domain Wall in Proton Exchanged Lithium Niobate

Mikhail Dolbilov<sup>1</sup>, Vladimir Shur<sup>1</sup>, Ekaterina Shishkina<sup>1</sup>, Ekaterina Angudovich<sup>1</sup>, Andrey Ushakov<sup>1</sup>, Pascal Baldi<sup>2</sup>, Marc P. De Micheli<sup>2</sup>, Emmanuel Quillier<sup>2</sup>

<sup>1</sup>Ferroelectric laboratory, Ural Federal University, Ekaterinburg, Russia

<sup>2</sup>Laboratory of condensed matter physics, University of Nice Sophia-Antipolis, Nice, France

E-mail: mikhail.dolbilov@labfer.usu.ru

Formation and evolution of the bands with nanodomain structure in front of the moving domain wall were studied in a field range in the congruent lithium niobate  $\text{LiNbO}_3$  single crystals modified by proton exchange (CLN-PE). PE method is a well-developed technique which can produce the surface layers with step profile of spontaneous polarization and refractive index<sup>43</sup>.

Continuous motion of the domain wall led to the smooth switching current was optically observed in CLN-PE in contrast to CLN. This process was caused by formation of with nanodomain structures in front of the wall which was revealed by Raman confocal microscopy (RCM). The averaged width of the nanodomain bands grew with increasing of the external field.

For switching in constant field the domain structure evolution strongly depends on the applied field value. Three different types of evolution were obtained: 1) continuous growth of the hexagon domains at low field (21.0 kV/mm) (Fig. 1a); 2) formation and growth of the wide domain wall in medium field (21.5 kV/mm) (Fig. 1b); 3) growth of micro- and nanodomain ensembles in high field (22.0 kV/mm) (Fig. 1c). The discrete switching being the origin of all obtained effects is caused by retardation of the depolarization field screening in the crystal with the surface dielectric layer<sup>44</sup>. The fitting of the measured field dependence of the nanodomain front propagation allowed to extract the value of the threshold and activation fields.

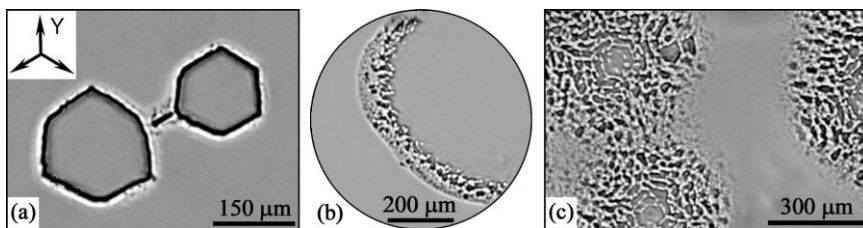


Fig. 14: Domain structure evolution during switching in constant field:  
(a) 21.0 kV/m, (b) 21.5 kV/m, (c) 22.0 kV/m

The equipment of the UCSU “Modern Nanotechnology”, Institute of Natural Sciences, UrFU has been used. The research was made possible in part by RFBR (Grants 13-02-01391-a, 11-02-91066-CNRS-a, 12-02-31731-mol-a), by Ministry of Education and Science (Contract 14.513.12.0006), by UrFU development program.

<sup>43</sup> M.P. De Micheli, *Ferroelectrics*, vol. 340, p. 49, 2006.

<sup>44</sup> V.Ya. Shur, *Journal of Materials Science*, vol. 41, p.199, 2006.

## Forming a regular domain structures at 127° Y'-cut of a LiTaO<sub>3</sub> crystal by using direct e-beam writing

Evgeny Emelin<sup>1</sup>, Dmitrii Roshchupkin<sup>1</sup>, Sergey Lavrov<sup>2</sup>, Nikita Ilyin<sup>2</sup>, Andrey Kudryavtsev<sup>2</sup>

<sup>1</sup>Institute of Microelectronics Technology and High-Purity Materials Russian Academy of Sciences/Chernogolovka/Russian Federation

<sup>2</sup>Moscow Institute of Radioengineering, Electronics and Automation/Moscow/Russian Federation

Email: EEmelin@iptm.ru

Regular domain structures (RDS) were formed at the 127° Y'-cut of a LiTaO<sub>3</sub> crystal by direct e-beam writing. The period of RDS was 2 and 10 μm. After e-beam writing process the optical contrast was observed at the irradiated surface without chemical etching and was stable for at least several months. To visualize the formed domain structures two methods were used:

1) selective chemical etching in a HF+2HNO<sub>3</sub> solution for 60 s at 110 °C. In this case domains of differing signs were revealed due to different etching rates on surface areas of opposite polarity<sup>45</sup>. Fig.1 shows both irradiated and opposite crystal surfaces after the etching process. As can be seen from Fig.1, the reliefs formed on the irradiated and the back sides of the crystal after etching are shifted with respect to each other. The domains distribution inside the 127° Y'-cut of a LiTaO<sub>3</sub> occurs at the angle 37° to the irradiated surface;

2) generation of the second harmonics of optic radiation on the RDS (Fig.2). This method enables nondestructive study of the domain structure. The sensitivity of the method is sufficient to resolve the domain structure lines. The domain lines consist of single domain of triangle shapes merged together (base-to-apex).

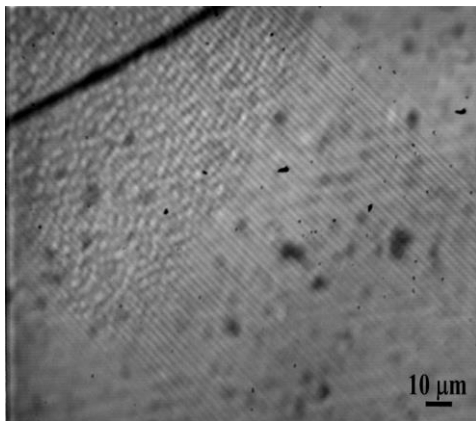


Fig.1. A regular domain structure inside the 127° Y'-cut of LiTaO<sub>3</sub> crystal with the period 2 μm.

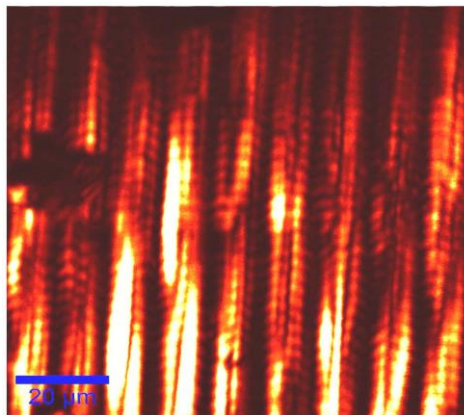


Fig.2. Second harmonic generation of optic radiation at the irradiated surface of 127° Y'-cut of LiTaO<sub>3</sub> crystal. The period of RDS was 10 μm.

<sup>45</sup> O. Norio, I. Takashi, "Etching study of microdomains in LiNbO<sub>3</sub> single crystals", J. Appl. Phys., vol. 46, p. 1063, 1975.

## Phase Transitions and Electrocaloric Effect in Ca modified $\text{Na}_{1/2}\text{Bi}_{1/2}\text{TiO}_3\text{-SrTiO}_3\text{-PbTiO}_3$ Solid Solutions

Marija Dunce<sup>1</sup>, Eriks Birks<sup>1</sup>, Jani Peräntie<sup>2</sup>, Juha Hagberg<sup>2</sup>, Maija Antonova<sup>1</sup>, Andris Sternberg<sup>1</sup>

<sup>1</sup>Department of Ferroelectrics, Institute of Solid State Physics, University of Latvia, Riga, Latvia

<sup>2</sup>Microelectronics and Material Physics Laboratories, University of Oulu, Oulu, Finland

Email: marija.dunce@cfi.lu.lv

$\text{Na}_{1/2}\text{Bi}_{1/2}\text{TiO}_3$  (NBT) and its solid solutions attract interest mostly as an alternative for nowadays widely used ferroelectrics with high lead content, use of which is gradually limited due to environmental considerations. According to our previous studies, composition  $0.4\text{NBT}-0.4\text{SrTiO}_3-0.2\text{PbTiO}_3$  is located in the region of the (T,x) phase diagram of  $0.4\text{NBT}-(0.6-x)\text{SrTiO}_3-x\text{PbTiO}_3$  solid solution where stability of relaxor state, evaluated as width of temperature region between the maximum of dielectric permittivity  $T_m$  and the temperature of spontaneous phase transition between relaxor and ferroelectric states  $T_t$ , diminishes.

In the present work dielectric properties, electric field-induced phase transitions and electrocaloric effect (ECE) are studied in  $0.4\text{NBT}-0.4\text{SrTiO}_3-0.2\text{PbTiO}_3$ , if Sr in this composition is gradually replaced by Ca. At low concentrations of Ca, stability of the phase transition temperature (Fig. 1) and polarization as a function

of Ca content, on the one hand, and steep decreasing of dielectric properties, on the other hand, is explained assuming that at these concentrations Ca resides inside polar nanoregions, stabilizing them and preventing their reorientation in weak external electric field, leaving the surrounding media free from Ca.

Electric field-induced 1<sup>st</sup> order phase transition between relaxor and ferroelectric states is studied both by means critical fields, obtained from double polarization hysteresis loops, and ECE. Behaviour of ECE at low Ca concentrations resembles pure  $0.4\text{NBT}-0.4\text{SrTiO}_3-0.2\text{PbTiO}_3$ , reaching value of 1.1 °C at the electric field-

induced phase transition. Like for  $T_t$  as a function of Ca content, remarkable decreasing of the maximal value of ECE starts at 15at% of Ca, while polarization at high electric field remains weakly dependent on concentration up to 30at% of Ca.

Apparently decreasing of ECE indicates that concentration of polar nanoregions, which do not contribute to ECE at the electric field-induced phase transition, increases at higher content of Ca.

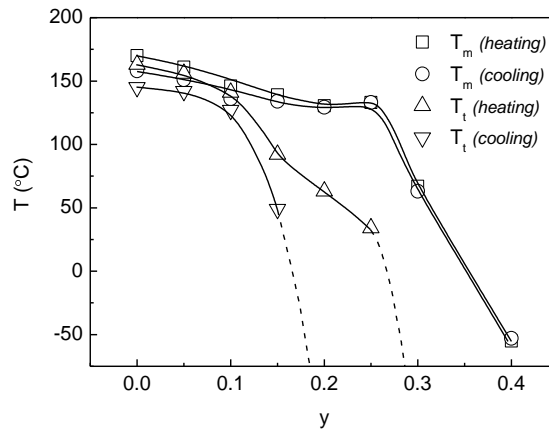


Fig. 15: Temperatures of maximum of dielectric permittivity  $T_m$  and spontaneous phase transition between relaxor and ferroelectric states  $T_t$  as functions of Ca concentration  $y$  in  $0.4\text{NBT}-(0.4-y)\text{SrTiO}_3-0.2\text{PbTiO}_3-y\text{CaTiO}_3$ , measured both on heating and cooling at 1 kHz.

## X-Ray, Dielectric, Piezoelectric and Mossbauer Studies of $\text{PbFe}_{0.5}\text{Ta}_{0.5}\text{O}_3$ Multiferroic

A.V. Blazhevich<sup>1</sup>, I.P. Raevski<sup>1</sup>, M. S. Molochev<sup>2</sup>, S.V. Mişjul<sup>3</sup>, S.P. Kubrin<sup>1</sup>,  
E.I. Sitalo<sup>1</sup>, S. I.Raevskaya<sup>1</sup>, V.V. Titov<sup>1</sup>, D.A. Sarychev<sup>1</sup>, M.A. Malitskaya<sup>1</sup>

<sup>1</sup>Faculty of Physics and Research Institute of Physics,  
Southern Federal University, Rostov-on-Don / Russia

<sup>2</sup>Kirensky Institute of Physics, Siberian Branch of the  
Russian Academy of Sciences, Krasnoyarsk/ Russia

<sup>3</sup>Institute of Engineering Physics and Radio Electronics,  
Siberian Federal University, Krasnoyarsk/ Russia

Email: [ablagh@gmail.com](mailto:ablagh@gmail.com)

X-ray, dielectric, piezoelectric, and Mossbauer studies of  $\text{PbFe}_{0.5}\text{Ta}_{0.5}\text{O}_3$  (PFT) powder and highly-resistive Li-doped PFT ceramics have been carried out. X-ray powder diffraction studies

confirmed symmetry changes on cooling from cubic to tetragonal at 270 K and then to monoclinic at 220 K, reported earlier for PFT crystals<sup>46</sup>. Temperature dependence of the monoclinic angle exhibits an anomaly in the vicinity of mean temperature of the antiferromagnetic phase transition  $T_N \approx 180$  K determined from the temperature dependence of the doublet relative intensity  $\eta$  in the  $^{57}\text{Fe}$  Mossbauer spectra<sup>2</sup>. Permittivity maximum is well below the cubic-tetragonal transition and shows a strong frequency dependence (Fig.1) well described by a Vogel-Fulcher law. This relaxor-like behavior seems to be due to coexistence of tetragonal and cubic phases in a wide temperature range. This assumption correlates with a plateau of piezoelectric modulus, within the range of tetragonal phase (Fig.1).  $T_N$  values of PFT powders and ceramics studied varied from 120 to 190 K depending on the sintering conditions. This dependence may be attributed to the changes in the degree of Fe clustering<sup>3</sup> or Fe and Ta ordering.

This study was partially supported by RFBR grant 12-08-00887.

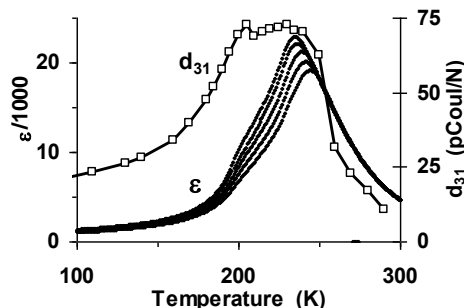


Fig. 16: Temperature dependences of dielectric permittivity  $\epsilon$  measured at frequencies  $10^2$ ,  $10^3$ ,  $10^4$ ,  $10^5$  and  $10^6$  Hz and piezoelectric modulus  $d_{31}$  for poled Li-doped PFT ceramics.

<sup>46</sup> N Lampis, P. Sciau, A.G. Lehmann, "Rietveld refinements of the paraelectric and ferroelectric structures of  $\text{PbFe}_{0.5}\text{Ta}_{0.5}\text{O}_3$ ", J. Phys.:Condens. Matter., vol. 12, p. 2367–2378, 2000.

<sup>2</sup> I. P. Raevski, S. P. Kubrin, S. I. Raevskaya, V.V. Stashenko, D. A. Sarychev, M. A. Malitskaya, M. A. Seredkina, V. G. Smotrakov, I. N. Zakharchenko, V. V. Eremkin, "Dielectric and Mossbauer studies of perovskite multiferroics", Ferroelectrics, vol. 373, p.121-126, 2008.

<sup>3</sup> I. P. Raevski, S. P. Kubrin, S. I. Raevskaya, D. A. Sarychev, S. A. Prosandeev, M. A. Malitskaya, "Magnetic Properties of  $\text{PbFe}_{1/2}\text{Nb}_{1/2}\text{O}_3$ : Mossbauer Spectroscopy and First Principles Calculations", Phys. Rev. B., vol. 85, p.224412-1 - 224412-5, 2012.



## Linear and nonlinear optical properties of congruent LiNbO<sub>3</sub>

Arthur Riefer, Simone Sanna, Arno Schindelmayer, Wolf Gero Schmidt

Theoretische Physik, Universität Paderborn, Warburger Str. 100,  
33100 Paderborn, Germany

Email: riefer@mail.uni-paderborn.de

Lithium niobate (LN) is one of the most important ferroelectric materials and the most important optical material. Recently, the linear<sup>49,50,51</sup> and nonlinear<sup>5,52</sup> optical properties of highly ordered stoichiometric LN (SLN) have been investigated theoretically. However, the technologically relevant material is the congruently melting LN (CLN), containing up to 6% empty Li sites. In this work, we have investigated the linear and the nonlinear optical properties of congruent LN from first-principles. Thereby CLN is simulated both within the established Li and the Nb site vacancy models<sup>53</sup> [in Fig. 1 denoted by CLN(Li) and CLN(Nb)]. Our approach allows us to calculate the dielectric function as well as the second harmonic generation spectra within the independent particle approximation. The influence of the intrinsic defects on the optical and electronic properties of LN is discussed. The results are compared with experimental measurements<sup>1,2,54</sup>.

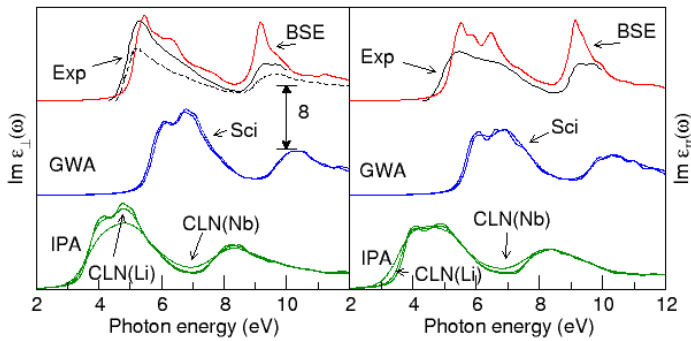


Fig. 17: Imaginary part of the ordinary and extraordinary dielectric function of SLN calculated within the independent-particle approximation (IPA), including quasiparticle self-energy effects calculated either within the GW approximation (GWA) or obtained from a scissors operator (Sci) and including electron-hole attraction and local-field effects from the solution of the Bethe-Salpeter equation (BSE). Also shown are IPA calculations for CLN and experimental data (solid line<sup>47</sup>, dashed line<sup>48</sup>).

<sup>47</sup> E. Wiesendanger and G. Güntherodt, Sol. State Commun. 14, 303 (1974).

<sup>48</sup> A. M. Mamedov, M. A. Osman, and L. C. Hajieva, Appl. Phys. A 34, 189 (1984).

<sup>49</sup> W. G. Schmidt *et al.*, Phys. Rev. B 77, 035106 (2008).

<sup>50</sup> C. Thierfelder *et al.*, phys. stat. sol. (c) 7, 362 (2010).

<sup>51</sup> A. Riefer *et al.*, IEEE Trans. on Ultrasonics, Ferroelectrics and Frequency Control 59, 1929 (2012).

<sup>52</sup> S. Cabuk, Central European Journal of Physics 10, 239 (2012).

<sup>53</sup> T. Volk *et al.*, Lithium Niobate, Berlin Springer, 2008.

<sup>54</sup> D.A. Roberts, IEEE J. of Quantum Electronics 28, 2057 (1992).

## Dynamic Denisyuk holograms in photorefractive crystals: fundamental physical properties and applications for interferometry

Pavel V. Zuev<sup>1</sup>, Stanislav M. Shandarov<sup>1</sup>, Sergey S. Shmakov<sup>1</sup>, Nikolay I. Burimov<sup>1</sup>, Vitaly I. Bykov<sup>1</sup>, Alexander E. Urban, Yury F. Kargin<sup>2</sup>, Vasilij V. Shepelevich<sup>3</sup>

<sup>1</sup>Department of Electronic Devices, Tomsk State University of Control System and Radioelectronics, Tomsk 634050, Russia

<sup>2</sup>Baikov Institute of Metallurgy and Materials Science Sciences of the RAS, Moscow 119991, Russia

<sup>3</sup>Department of Theoretical Physics, I.P. Shamyakin Mozyr State Pedagogical University, Mozyr 247760, Belarus

Email: [zuev.p.v@gmail.com](mailto:zuev.p.v@gmail.com)

We report on adaptive interferometry based on dynamic reflection holograms in photorefractive crystals. The basic physical principles of the interaction of two counterpropagating light waves on dynamic reflection gratings formed in the Denisyuk scheme in photorefractive crystals due to the diffusion mechanism of the charge transfer are considered. We analyze the nonlinear response relating to both phase (photorefractive) and amplitude (absorption) components of the reflection grating. Along with conventional linear electro-optic effect the additional elasto-optic contributions to the phase grating induced by secondary phenomena are taken into account. We consider two converse effects, piezoelectric and flexoelectric ones, as the causes of existence of the elastic-strain gratings in the electro-optic (photorefractive) crystals.

The peculiarity of reflection volume holograms, which formed by interaction of waves from visible region, is the small spatial period assuming values about  $100 \text{ nm}^{55}$ . In this case the reflection holograms are accompanied by electric-field gradient may be as high as several  $\text{TV/m}^2$ . It is shown that owing to converse flexoelectric effect, these giant gradient values are capable of generation in photorefractive crystal the appreciable elastic strains. We have considered the contradirectional interaction between a strong stationary reference wave and a weak phase-modulated signal wave on a reflection grating in the X-cut piezoelectric (electro-optic) crystals belonging to the point symmetry groups  $23$ ,  $\bar{4}3m$ ,  $\bar{4}2m$ ,  $422$ ,  $622$ , and  $222$ . It was shown that qualitative distinctions in photorefractive response induced by linear electro-optic effect and by converse flexoelectric effect together with the elasto-optic one are exhibited at phase demodulation in an adaptive interferometric setup utilizing interaction of two counterpropagating light beams on the reflection holograms. Based on the experiments with such interaction in the (100)-cut  $\text{Bi}_{12}\text{TiO}_{20}:\text{Fe,Cu}$  crystals we established that their flexoelectric coefficient  $f_{11}$  can be estimated as the value in the range from 1.9 to  $5.3 \text{ nC/m}^2$ .

This work was supported in part by the Russian Foundation for Basic Research (grant No 12-02-90038\_Bel\_a), and by the Belarusian Republican Foundation for Fundamental Research (grant No F12R-222).

<sup>55</sup> S.M. Shandarov, S.S. Shmakov, N.I. Burimov, O.S. Syuvaeva, Yu.F. Kargin, and V.M. Petrov, "Detection of the contribution of the inverse flexoelectric effect to the photorefractive response in a bismuth titanium oxide single crystal," JETP Letters, vol. 95, p. 699–702, 2012.

## Modeling of switching and piezoelectric phenomena in PVDF

Vladimir Bystrov<sup>1,2</sup>, Ekaterina Paramonova<sup>2</sup>, Varsenik Gevorkyan<sup>3</sup>, Leon Avakyan<sup>3</sup>, Igor Bdikin<sup>4</sup>, Robert Pullar<sup>1</sup> and Andrei Kholkin<sup>1</sup>

<sup>1</sup>Department Materials Eng. and Ceramics & CICECO, University of Aveiro, Aveiro, Portugal

<sup>2</sup>Institute of Mathematical Problems of Biology, Rus. Academy of Sciences, Pushchino, Russia

<sup>3</sup>Physics Faculty, Southern Federal University, Rostov-on-Don, Russia

<sup>4</sup>Centre for Mechanical Technology and Automation, University of Aveiro, Aveiro, Portugal

Email: [vsbys@mail.ru](mailto:vsbys@mail.ru) , [bystrov@ua.pt](mailto:bystrov@ua.pt)

At the present work we consider the molecular model of ferroelectric polymer polyvinylidene fluoride (PVDF) film, consisting from one, two chains  $[-\text{CH}_2-\text{CF}_2-]_n$  and for PVDF unit cell. The main software was HyperChem 8.0 for all models as for quantum calculations as well for molecular mechanics. First principle calculations were employed, using various quantum-chemical methods (QM), including semi-empirical (PM3) and various density functional theory (DFT) approaches, and in addition combined with molecular mechanics (MM) methods in complex joint approaches (QM/MM). The first model, is limited by  $n=6$  elementary units  $\text{CH}_2\text{CF}_2$ . The first principle approach PM3 and molecular dynamic run were applied for investigation of the switching and its kinetics for these models. It is revealed, that kinetics of polarization switching shows a homogeneous critical behavior with critical point at Landau-Ginzburg-Devonshire (LGD) coercive field  $E = E_C$ . Two types of 2 PVDF chains behavior were established: simultaneous and consequence rotation in low and high electric field for two chains model. Our modeling and first principle calculation for one chain model was obtained hysteresis loop for PVDF with LGD intrinsic coercive field  $E_C \sim 1$  GV/m and for two chains it is confirmed with  $E_C \sim 2 \dots 2.5$  GV/m. These obtained results are compared with experimental data at the nano-scale level by the atomic force microscopy. These data are related also with arisen of the PVDF piezoelectric effects, especially of the negative piezoelectric coefficients. Performed detailed molecular modeling was applied to study the nature of this negative piezoelectric effect in PVDF, and these results confirmed by actual nanoscale measurements. Both PVDF molecular chains and a unit cell of crystalline  $\beta$ -phase PVDF were modelled. This computational molecular exploration clearly shows that the nature of the so-called negative piezo-electric effect in the ferroelectric PVDF polymer has a self-consistent quantum nature, and is related to the redistribution of the electron molecular orbitals (wave functions), leading to the shifting of atomic nuclei and reorganization of all total atomic charges to the new, energetically optimal positions, under an applied electrical field. As a results, complex cooperative dipole reorganization occurs on the bonded molecular chain under the action of this applied electrical field. Complicated non-uniform and nonlinear anisotropy deformations in the PVDF molecular chain result, involving both individual interactions of  $\text{C}_2\text{H}_2\text{F}_2$  dipoles, as well as the whole PVDF unit cell, leading to negative deformation in relation to the applied field. Molecular modeling and first principles calculations show that the piezoelectric coefficient  $d_{33}$  has negative values in the range  $d_{33} \sim -16.5 \dots -33.5$  pC/N (pm/V), corresponding to known data, and allowing us to explain the reasons for the negative sign of the piezo-response. For value of  $\varepsilon \sim 5$ , we obtained a value of another oriented coefficient  $d_{31} \sim +15.5$  pC/N (with a positive sign). This computational study is corroborated by measured nanoscale data obtained by atomic force and piezo-response force microscopy (AFM / PFM). This study could be useful as a basis for further insights into organic and molecular ferroelectrics.

## Dielectric properties of ferroelectric thin films with full and partial depletion and the possible inversion of the thickness effect in the presence of impurities

I. B. Misirlioglu, M. Yildiz

Faculty of Engineering and Natural Sciences, Sabancı University, Istanbul, Turkey

Email: burc@sabanciuniv.edu

Interfaces in ferroelectric structures are important not only because these are the boundaries at which the regular structure of the crystal terminates but also because of the termination of the polar arrangement and nature of the contact with the electrodes if the system is electroded. Therefore, the treatment of ferroelectrics as polar semiconductors becomes inevitable when examining polarization stability and dielectric properties especially in reduced dimensions. In this work, we study the effect of electrical boundary conditions on ferroelectrics in thin film form and possible scenarios in case the ferroelectric has moderate to high densities of vacancies or impurities. Our recent findings reveal the extent of coupling between the dielectric response and depletion charges and how depletion charges alter the Curie point in fully and partially depleted films, a phenomena often neglected in discussing size effects in films. The possibility that high densities of depletion charges might invert the thickness effect concerning the stability of polarization in ferroelectric films is demonstrated where thicker films have a higher dielectric response with respect to thinner ones for the same impurity density (Fig. 1). We also investigate the effect of line defects on depletion charge and impurity distribution as a function of film thickness to shed light on the possible impact of line defects on leakage currents in ferroelectric thin films.

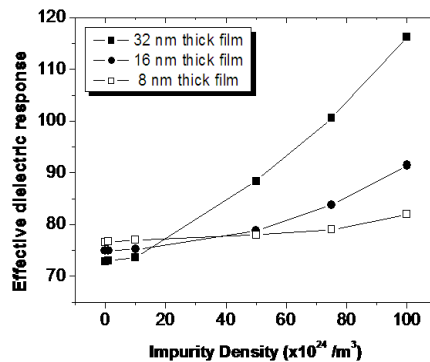


Fig. 1: Computed thickness dependence of the small signal dielectric response at zero bias for BaTiO<sub>3</sub> sandwiched between Pt electrodes on SrTiO<sub>3</sub> as a function of impurity density<sup>56</sup>. The lines are guides for the eyes.

<sup>56</sup> I. B. Misirlioglu, M. Yildiz, "Dielectric response of fully and partially depleted ferroelectric thin films and inversion of the thickness effect", J. Phys. D: Appl. Phys., vol. 46, p.125301-11, 2013.

# Influence of the piezoelectric effect on ferroelectric properties and phase transition

Andreas Leschhorn<sup>1</sup>, Herbert Kliem<sup>1</sup>

<sup>1</sup>Institute of Electrical Engineering Physics, Saarland University, Saarbruecken, Germany

Email: a.leschhorn@lusi.uni-sb.de

The Weiss model for magnetization can also be applied to the polarization of ferroelectrics<sup>57</sup>. In this model, the local field is the superposition of the applied field  $E_a$  and of a field proportional to the polarization  $P$ :

$$E_{loc} = E_a + \alpha P. \quad (1)$$

The coupling parameter  $\alpha$  describes the coupling between the dipoles by the electrostatic fields. The dipoles with moment  $p$  are assumed to fluctuate thermally activated in double well potentials yielding (temperature  $T$ , dipole density  $n$ )

$$P = np \cdot \tanh\left(\frac{pE_{loc}}{k_B T}\right). \quad (2)$$

With (1) and (2) we have a feedback loop for the polarization. In this form the model predicts several properties of ferroelectric materials like the polarization hysteresis and the phase transition from ferroelectric to paraelectric at the Curie temperature. However, the model only yields a ferro- to paraelectric transition of the second type.

The type 2 transition can be converted into a type 1 transition by introducing the piezoelectric effect<sup>58</sup>. Simultaneously the single hysteresis of polarization splits into a double hysteresis loop close to the Curie point.

With the piezoelectric effect the distances inside the sample depend on the polarization. In this way some parameters in (1) and (2) are functions of  $P$ , namely the dipole moment  $p$ , the density  $n$  and the coupling parameter  $\alpha$ . If the length of the sample is changed due to the polarization the distances between the dipoles are altered and e.g. the coupling constant  $\alpha$  is also varied like (piezo coefficient  $\zeta$ )

$$\alpha(P) = \alpha_0(1 + \zeta P). \quad (3)$$

Combining (1), (2) and (3) yields the ferro- to paraelectric transition of the first order. In an analogous way also the variation of  $p$  and/or  $n$  with the polarization  $P$  can cause this change from type 2 to type 1 transition.

*Acknowledgement:* This work is supported by the Deutsche Forschungsgemeinschaft.

<sup>57</sup> J. C. Burfoot, G. W. Taylor, "Polar Dielectrics", MacMillan Press, London, 1979.

<sup>58</sup> H. Kliem, "Strain induced change from second order to first order ferroelectric phase transition", Ferroelectrics, vol. 425, p. 54-62, 2011.

## Modeling and Numerical Study of Electroacoustic Behavior of Lithium Niobate Under an Initial Electrical Stress

Domenjoud Mathieu<sup>1</sup>, Lematre Michaël<sup>2</sup>, Fortineau Jérôme<sup>2</sup>, Feuillard Guy<sup>2</sup> and Tran-Huu-Hue Louis-Pascal<sup>2</sup>

<sup>1</sup>GREMAN, UMR CNRS 7347, University of Tours, Tours, France

<sup>2</sup>GREMAN, UMR CNRS 7347, ENIVL, Blois, France

Email: mathieu.domenjoud@univ-tours.fr

Piezoelectric materials are frequently used for various applications, such as sensors, actuators or transducers, many of which imply operation under harsh environmental conditions like high temperature, high pressure, external electrical DC bias field or mechanical stress. For instance, Tonpilz piezoelectric transducers are built in such a way that a stress-bolt assembly maintains the piezoelectric stacks under compression, leading to an increased efficiency and lifetime. Conversely, in high power ultrasonic transducers used for therapy, the electroacoustic response can be improved by applying a static electrical field. However, the presence of high external (mechanical or electrical) stress induces non-linear effects that significantly modify the piezoelectric characteristics through a shift of material properties from their stress-free values. The improvement of electromechanical performance due to external prestress is not very well known and designers of systems, who have to deal with difficulties to evaluate piezoelectric material properties in real operating conditions, often rely on empirical considerations.

Recently, we developed a second order formalism of piezoelectric structures under an external (mechanical or electrical) stress in the natural (nondeformed) and current (predeformed) coordinate systems<sup>59</sup>. Here, our formalism is used to evaluate the effect of an applied electrical stress on the electroacoustic behavior of piezoelectric materials. Knowing the coercitive field of lithium niobate material, we numerically quantify nonlinearities induced by an electrical prestress on the deformations, wave velocities and coupling coefficients for a lithium niobate plate. Evolutions of these parameters are studied in the two coordinate systems as a function of the azimuthal and elevation angles as well as electrical prestress values.

We show that the contribution of nonlinearity to deformation reaches 22.5% in a specific cut plane. Moreover, the maximum shift in wave velocities induced by prestress is found to be 33 and 9 m/s for quasi-longitudinal and quasi-transversal modes respectively. Numerical studies of electromechanical coupling coefficients show that the electrical prestress is able to produce an increase of about +1.1%. Finally, we show that electrical prestress in specific cut planes significantly increases longitudinal wave velocities and electromechanical coupling coefficients. This study shows that, by designing an electrical prestressed transducer using a piezoelectric material in well determined cuts, it is possible to increase the performance and that this can be predicted.

---

<sup>59</sup> M. Lematre, M. Domenjoud and L. P. Tran-Huu-Hue, "Exact second order formalism for the study of electro-acoustic properties in piezoelectric structure under an initial mechanical stress", *Ultrasonics*, vol. 51, p 898-910, 2011.

## **The abnormal polarization switching of relaxor terpolymer films at low temperature**

B. B. Tian, X. L. Zhao, B. L. Liu, J. L. Wang, J. L. Sun, X. J. Meng and J. H. Chu

<sup>1</sup>State Key Laboratory of Infrared Physics, Shanghai Institute of Technical Physics, Chinese Academy of Sciences, Yu Tian Road 500, Shanghai 200083, China

### **Abstract**

The ferroelectricity of the Poly(vinylidene fluoride-trifluoroethylene-chlorofluoroethylene) terpolymer films fabricated by the Langmuir–Blodgett (LB) technology were investigated from 180 to 300 K. The temperature dependence of the remanent polarization and the dielectric response shows a broad peak at ~ 270 K, suggesting a ferroelectric phase transition. Contrary to the perovskite relaxor, a deviation from the Merz's law is observed in the relation between the coercive field and frequency for the relaxor terpolymer. The particular ferroelectricity of the relaxor terpolymer is considered to be associated with the distinct structure and the dynamics of its typical molecular conformations.

## Effect of grain size on the microwave dielectric properties of $\beta$ -BZN ceramics

Gao-qun Zhang<sup>1</sup>, Hong Wang<sup>1</sup>, Di Zhou<sup>1</sup>, Jing Guo<sup>1</sup>

<sup>1</sup>Electronic Materials Research Laboratory, Key Laboratory of Ministry of Education,  
Xi'an Jiaotong University, Xi'an 710049, China

Email: gaoqunzhang2012@gmail.com

In this study,  $\beta$ -BZN ceramics were prepared by the traditional solid state method. The samples sintered at 930 °C for 2 h possessed a relative permittivity of 74 and a Q×f value of 3740 GHz. The grain size of  $\beta$ -BZN ceramics was regulated by changing sintering temperature and heat preservation time. When the sintering temperature was increased from 780 °C to 990 °C, the grain grew from 0.7  $\mu$ m to 1.9  $\mu$ m as approximate exponential function. Grain growth mechanism of  $\beta$ -BZN ceramic with sintering temperature was discussed. The function

$$\ln(1000 \times l_p^3 / t) = 3e^{(T/1000)^3}$$

about the relationship between the grain size of  $\beta$ -BZN and sintering temperature was obtained by simulation, whose results were in accord with experimental values. For the samples at different heat preservation time, there was deviation between experimental values and results from theory model formula

$$\bar{G}^2 - \bar{G}_0^2 = Ct.$$

For well dense  $\beta$ -BZN, the grain size has little effect on the relative permittivity. And the Q×f value increased with increasing grain size from 0.7  $\mu$ m to 1.2  $\mu$ m, but for  $\beta$ -BZN ceramics of the average grain size above 1.2  $\mu$ m, the Q×f value decreased. When the grains grew from 0.7  $\mu$ m to 1.2  $\mu$ m, there was a uniform microstructure, and a reduction in the number of grain boundaries per unit volume would result in material with a lower loss. When the average size of the grains was more than 1.2  $\mu$ m, some large grains appeared, which introduced more defect and deteriorated the quality factor.



# Density Functional Theory Calculations of Doped Perovskite Barium Titanate ( $\text{BaTi}_{0.6}\text{Nb}_{0.2}\text{Fe}_{0.1}\text{O}_3$ ): Structural Deformations and Ferroelectric Properties

Piyarat Nimmanpipug<sup>1,2</sup>, Wiranwit Wankawee<sup>1</sup>, Laongnuan Srisombat<sup>1,2</sup>, Yongyut Laosiritaworn<sup>1,2</sup>

<sup>1</sup>Computational Simulation and Modelling Laboratory (CSML), Department of Chemistry, Faculty of Science, Chiang Mai University, Chiang Mai 50200, Thailand

<sup>2</sup>Thailand Center of Excellence in Physics (ThEP), Commission on Higher Education, Bangkok 10400, Thailand

Email: piyarat.n@cmu.ac.th, piyaratn@gmail.com

The structural deformations and ferroelectric properties of doped barium titanate were theoretically analyzed using density functional theory (DFT). Niobium ( $\text{Nb}^{5+}$ ) and ferrous ( $\text{Fe}^{2+}$ ) ion were substituted in all possible titanium sites to evaluate all possible structures. The distortion of octahedral hole was found depending on size of dopant and neighboring atoms. The direction of atomic displacement in octahedral holes were investigated and related to the direction of polarization. The splitting of phonon modes was observed in doped barium titanate indicating ferroelectric instability of the structure. The electronic band structure and density of states (DOS) indicate decrease of energy band gap in doped structures. The hybridization of the Ti-3d, Nb-4d and Fe-3d with the O-2p orbitals was remarked corresponding with the shift in the frequency of phonon modes.

## Free energy of BaTiO<sub>3</sub> single crystal

Raphaël Renoud<sup>1</sup>, Mostafa Ragheb<sup>1</sup>, Gilles Damamme<sup>2</sup>, Caroline Borderon<sup>1</sup>, Hartmut Gundel<sup>1</sup>

<sup>1</sup>IETR, University of Nantes, Nantes, France

<sup>2</sup>CEA/DAM, centre de Gramat, Gramat, France

E-mail: raphael.renoud@univ-nantes.fr

The thermodynamic description of a ferroelectric material is generally done using the approach of Landau. This latter is based on the development of the free energy around the para/ferro-electric transition temperature. Following the formulation of Devonshire (1949) [1], many authors have tried to improve the description level. In this context, the free energy due to the elastic behavior of the material has been included in models. In the case of BaTiO<sub>3</sub>, for example, we can hold work of Li *et al.* [2], Bell [3] or Wang *et al.* [4]. Despite this progress, the development of the free energy in successive power of the polarization still depends on parameters that must be set in an *ad hoc* manner. We propose here a formulation of the free energy for displacive ferroelectrics which takes direct account of the polarization but also of the coupling with temperature and of the electrostrictive coupling. We apply this formalism to the case of BaTiO<sub>3</sub> single crystal. A comparison with experiment and with previous works [2-4] is performed. The proposed approach allows for example to properly account for the evolution of the spontaneous polarization [5-6] and lattice parameters [7] as a function of temperature in all polar phases.

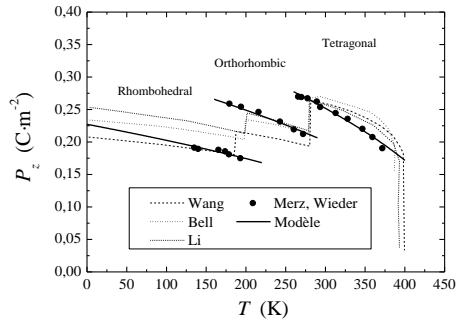


**Fig. 1:** Spontaneous polarization  $P_z$  as a function of the temperature  $T$ . Comparison of the model with the approach of Li *et al.* [2], Bell [3] and Wang *et al.* [3]. Comparison with experimental data of Merz [5] and Wieder [6]

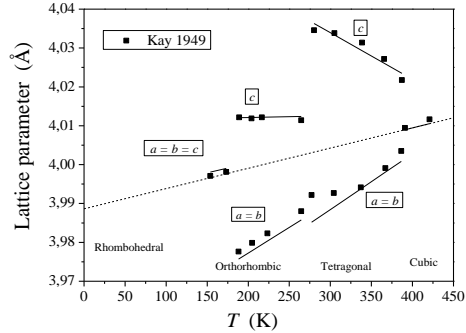


**Fig. 2:** Lattice parameter as a function of the temperature. Comparison of the model with experimental data of Kay and Vousden [7]

[1] A.F. Devonshire, *Phil. Mag.* **40** (1949) 1040

[2] Y.L. Li, L.E. Cross, L.Q. Chen, *J. Appl. Phys.* **98** (2005) 064101

[3] A.J. Bell, *J. Appl. Phys.* **89** (2001) 3907

[4] Y.L. Wang, A.K. Tagantsev, D. Damjanovic, N. Setter, V.K. Yarmarkin, A.I. Sokolov, I.A. Lukyanchuk, *J. Appl. Phys.* **101** (2007) 104115

[5] W.J. Merz, *Phys. Rev.* **91** (1953) 513

[6] H.H. Wieder, *Phys. Rev.* **99** (1955) 1161

[7] H.F. Kay, P. Vousden, *Phil. Mag.* **40** (1949) 1019

## Ferroelectric domain engineering in tricolour superlattices

C. Hubault<sup>1,5</sup>, I. C. Infante<sup>2</sup>, A. Boulle<sup>3</sup>, N. Boudet<sup>4</sup>, C. Davoisne<sup>5</sup>, L. Dupont<sup>5</sup>, V. Demange<sup>6</sup>, A. Perrin<sup>6</sup>, B. Gautier<sup>7</sup>, M.G. Karkut<sup>1</sup> and N. Lemée<sup>1\*</sup>

<sup>1</sup>LPMC, Université de Picardie Jules Verne, Amiens, France

<sup>2</sup>SPMS, CNRS UMR 8580, Ecole Centrale Paris, France

<sup>3</sup>SPCTS, CNRS UMR 7315, Limoges, France

<sup>4</sup>D2AM-CRG, ESRF and Institut Néel, CNRS, Grenoble, France

<sup>5</sup>LRCS, CNRS UMR 7314, Amiens, France

<sup>6</sup>USCR, CNRS UMR 6226, Rennes, France

<sup>7</sup>INL, CNRS UMR 5270, INSA, Villeurbanne, France

Email: [nathalie.lemee@u-picardie.fr](mailto:nathalie.lemee@u-picardie.fr)

Functional properties of perovskite ferroelectric thin films are highly influenced by their domain structure which is determined both by epitaxial strain and depolarizing fields. Ferroelectric superlattices can provide a way to disentangle the competition between the elastic and electrostatic energy. Recently we have applied tensile in-plane strain to  $\text{PbTiO}_3$  (PT) by combining PT,  $\text{PbZr}_{0.2}\text{Ti}_{0.8}\text{O}_3$  (PZT 20-80) and  $\text{SrTiO}_3$  (STO) in tricolour superlattices<sup>60</sup>. In bicolour PT/PZT 20-80 SLs, an *a/c* polydomain structure was evidenced<sup>61</sup>. In tricolor PT/STO/PZT superlattices, the introduction of ultrathin layers of STO (2-3 unit cells) between each ferroelectric layer seems to play a significant role in the decoupling of ferroelectric interactions. Indeed, the insertion of STO layers induces a strong decrease in the tetragonality of the overall superlattice, and inhibits this 90° polydomain formation. X-ray diffraction measurements evidence the presence of satellites around the *out-of-plane* SL Bragg peaks. This modulation is characteristic of 180° ferroelectric domains of alternate “up” and “down” polarization, presumably produced to minimize the electric field arising from the STO induced depolarizing field. Their polar origin is clearly confirmed by their disappearance close to the superlattice ferroelectric transition temperature. In order to investigate the *in-plane* polar structure, reciprocal space maps were realized using grazing incidence diffraction at beamline BM2-D2AM at ESRF. The period  $\Lambda$  of the observed satellites is consistent with the polar modulation measured around the specular reflections. These measurements show that in the tricolour PT/STO/PZT 20-80 superlattices the polarization has both in-plane and out-of-plane components, which is an argument in favour of a polarization rotation away from the normal. Using piezo-force microscopy, it is possible to write and image polarization domains, confirming that the piezoelectric response of the sample is still retained with the 180° nanodomain formation. This work demonstrates that such tricolour ferroelectric superlattices provide a powerful tool to study the role of electrostatic and strain effects in the control of polarization orientation.

<sup>60</sup> C. Hubault *et al.*, J. Appl. Phys., vol. 112, 114102, 2012

<sup>61</sup> C. Hubault *et al.*, Appl. Phys. Lett., vol. 99, 052905, 2011

## Modeling of Glycine polymorphic and switching properties

Vladimir Bystrov<sup>1</sup>, Ensieh Hosseini<sup>1</sup>, Igor Bdikin<sup>2</sup>, Svitlana Kopyl<sup>2</sup> and Andrei Kholkin<sup>1</sup>

<sup>1</sup>Department Materials Eng. and Ceramics & CICECO, University of Aveiro, Aveiro, Portugal

<sup>2</sup>Centre for Mechanical Technology and Automation, University of Aveiro, Aveiro, Portugal

Email: [bystrov@ua.pt](mailto:bystrov@ua.pt)

Polymorphism of glycine nano-crystal structure is known – it could exist in  $\alpha$ ,  $\beta$ ,  $\gamma$  and in several cases as  $\delta$  modification. The most interest for nano-electronic present non-centro-symmetric structures:  $\beta$ -glycine (space group  $P2_1$ ) and  $\gamma$ -glycine (space group  $P3_2$ ). These structures reveal piezoelectric and polar properties. But the value of polarization is not clear as well its switching behaviour. In this work computational modelling of both glycine polymorphic crystal structures were performed using combined method with LDA first principle calculations of atomic optimized crystal structures on Linux cluster and with molecular semi-empirical calculations by HyperChem 8.0 software. Figure show both molecular nano-crystal structures in two projections with hydrogen bonds net and total dipole. The main difference for these structures consist that for  $\gamma$ -glycine we have very strong oriented along OZ axis hydrogen-bonded net with total dipole moment preferably oriented in this direction. Computed value of polarization by PM3 method is  $P \sim P_z = 0.17 \text{ C/m}^2$ . But for the  $\beta$ -glycine we have layered structure with hydrogen bonds in XOZ plane, while total dipole moment has several components and polarization is oriented under angle to main axis. Computed values of polarization components are smaller and have average  $P \sim 0.025 \text{ C/m}^2$ . The orientation of polarization vector could provide several components ( $P_z$ ,  $P_y$ ,  $P_x$ ) and piezo-response, while  $\gamma$ -glycine could have only Z-component. Estimation of coercive electric field for  $\gamma$ -glycine have high value  $E_c \sim 3 \text{ GV/m} = 30 \text{ MV/cm}$ , oriented along OZ axis, and it made non-possible polarization and piezo-response switching in this case. For  $\beta$ -glycine we obtain 10 times less value of coercive electric field  $E_c \sim 0.4 \text{ GV/m} = 4 \text{ MV/cm}$  for different polarization components, which make possible for switching phenomena. For these estimations we use value of dielectric permittivity for glycine  $\epsilon \sim 6$ . These computed data and obtained switching properties for both models of  $\beta$  and  $\gamma$  glycine polymorphic structures are confirmed by AFM/PFM measurements. As result, we can conclude that namely  $\beta$ -glycine could demonstrate ferroelectric properties.

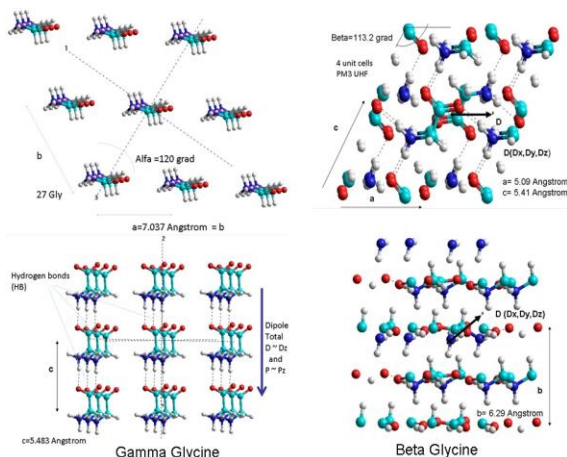


Figure: Computed molecular models of two polymorphic glycine structures:  $\gamma$ -glycine and  $\beta$ -glycine.

## Domain Kinetics in Lithium Niobate Single Crystals Inhomogeneously Modified by Annealing in Vacuum

Alikin Denis, Pryakhina Victoria, Shur Vladimir, Negashev Stanislav, Palitsin Ilya

Ferroelectric laboratory, Institute of the Natural Science, Ekaterinburg, Russia

Email: denis.alikin@labfer.usu.ru

It is known that annealing of the lithium niobate (LN) crystals in vacuum leads to sufficient increase of the bulk conductivity caused by out-diffusion of oxygen ions<sup>62</sup>. We present experimental study of the polarization reversal in the single crystalline plates of congruent LN annealed in vacuum in different temperature-time regimes: 300°C, 1h, 300°C, 10 h and 850°C, 15 min.

The polarization reversal was carried out by application of electric field using liquid electrolyte (aqua solution of LiCl). Instantaneous domain patterns were *in situ* visualized by polarized optical microscope (Carl Zeiss LMA 10, Germany). The static domain patterns revealed by chemical etching were observed by optical microscopy. Nondestructive high resolution domain visualization was achieved by piezoresponse force microscopy and Raman confocal microscopy (NT-MDT NanoLaboratories NTEGRA Aura and NTEGRA Spectra, Russia).

Annealing at 300°C during 1 h didn't change the domain kinetics remarkably. The annealing at the same temperature during 10 h leads to domain kinetics with formation of the residual domains and traces of the domain walls typical for modification of the thin surface layer<sup>63</sup>.

Annealing at high temperature (850°C) drastically modified the domain kinetics and leads to smooth isotropic motion of the domain walls in the bulk (Fig. 1). The stable domain structure with charged domain walls appeared over the whole switched area. The obtained switching in the bulk and isotropic domain growth was attributed to inhomogeneous field distribution caused by inhomogeneous bulk conductivity.

The equipment of the UCSU "Modern Nanotechnology", Institute of Natural Sciences, UrFU has been used. The research was made possible in part by RFBR (Grants 13-02-01391-a, 12-02-31377, 11-02-91066-CNRS-a), by Ministry of Education and Science (Contract 14.513.12.0006).

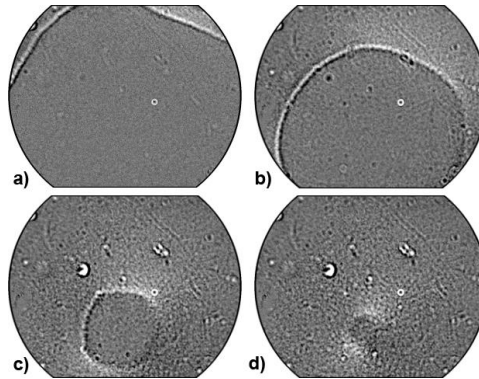


Fig.1. Domain kinetics in vacuum annealed lithium niobate (850 °C, 15 min). Time form the beginning of the pulse: (a) 48.8 s, (b) 51.6 s, (c) 53.2 s, (d) 53.6 s.

<sup>62</sup> P.F. Bordui, D.H. Jundt, E.M. Standifer, R.G. Norwood, R.L. Sawin, J.D. Galipeau, "Chemically reduced lithium niobate single crystals: Processing, properties and improved surface acoustic wave device fabrication and performance", Appl. Phys, vol. 85, p. 3766 – 3769, 1999

<sup>63</sup> D.O. Alikin, V.Ya. Shur, V.I. Pryakhina, N.V. Gavrilov, M. Carrascosa, J. Olivares, The Domain Kinetics in Congruent Lithium Niobate Modified by Low and High Energy Ion Irradiation, Ferroelectrics, vol. 441, p. 17-24, 2012

## Polarization Reversal Process in Lithium Niobate Single Crystals with Photoresist Dielectric Layer

Shur Vladimir<sup>1,2</sup>, Akhmatkhanov Andrey<sup>1,2</sup>, Baturin Ivan<sup>1,2</sup>, Zorikhin Dmitriy<sup>1,2</sup>, Chuvakova Mariya<sup>1</sup>, Lukmanova Almira<sup>1</sup>, Zelenovskiy Pavel<sup>1</sup>, Neradovskiy Maxim<sup>1</sup>.

<sup>1</sup>Ferroelectrics laboratory, Ural Federal University, Ekaterinburg, Russia

<sup>2</sup>Labfer Ltd., Ekaterinburg, Russia

Email: ahmathanov@labfer.usu.ru

The creation of the tailored periodic domain structure in lithium niobate (LiNbO<sub>3</sub>, LN) single crystals is widely used technique for efficient conversion of the laser light frequency based on quasi-phase-matching effect. The regular domain structure in LN is usually created by application of inhomogeneous external electric field through the photoresist mask using liquid electrodes. Thus the study of domain kinetics in LN covered by photoresist film is of the great practical importance for developing the methods of domain engineering.

The domain structure evolution during polarization reversal has been investigated in congruent LN (CLN) single crystals covered by photoresist dielectric film. The films with thickness ranged from 0.5 to 5.5 μm of positive (AZ-series) and negative (nLOF) photoresist were spin coated on Z+ polar CLN surface. The polarization reversal process has been studied by *in situ* optical visualization of the domain kinetics and analysis of the switching current data

It was revealed that the domain structure evolution changes drastically for film thickness about 2 μm. The conventional growth of hexagonal domains by jump-like motion of the plane domain walls oriented along Y crystallographic directions accompanied by isolated pulses of switching current was observed for film thickness below 2 μm. In contrast the continuous domain wall motion and the smooth current shape have been revealed for film thickness above 2 μm caused by formation of the isolated nanodomains in front of the moving domain wall.

The experimental switching current data was successfully fitted by Kolmogorov-Avrami formula modified for switching in linearly increasing electric field in finite media<sup>xxi</sup>. Two stages of the switching process representing "continuous nucleation" and "growth only" processes revealed by fitting of the switching current data were confirmed by *in situ* observation of the domain kinetics.

The complex study of the obtained static domain structures by optical, scanning probe and Raman confocal microscopy allowed to reconstruct the unusual domain evolution scenario during polarization reversal in CLN covered by thick photoresist film. The obtained results are important for creation of the periodically poled CLN crystals.

The equipment of the UCSU "Modern Nanotechnology", Institute of Natural Sciences, UrFU has been used. The research was made possible in part by RFBR (Grants 13-02-01391-a, 11-02-91066-CNRS-a), by Ministry of Education and Science (Contract 14.513.12.0006), by OPTEC LLC and in terms of Ural Federal University development program with the financial support of young scientists.

## Structural, elastic, and vibrational properties of Topological Insulators on $A_2^5B_3^6$ compound based

H. Koc<sup>64</sup>, Amirullah M. Mamedov<sup>2</sup>, Ekmel Ozbay<sup>2</sup>

<sup>1</sup> Department of Physics, Siirt University, 56100 Siirt, Turkey

<sup>2</sup> Nanotechnology Research Center (NANOTAM), Bilkent University, 06800 Bilkent, Ankara, Turkey

Email: mamedov@bilkent.edu.tr

We have performed a first principles study of structural and elastic properties of rhombohedral  $Sb_2Te_3$  and  $Bi_2Te_3$  compounds using the density functional theory within the local density approximation. The lattice parameters, bulk modulus, and its pressure derivatives of considered compounds have been calculated. The second-order elastic constants have been calculated, and the other related quantities such as the Young's modulus, shear modulus, Poisson's ratio, anisotropy factor, sound velocities, Debye temperature, and hardness have also been estimated in the present work. The phonon dispersion curves are derived using the direct method. The present results demonstrate that this compound is dynamically stable.

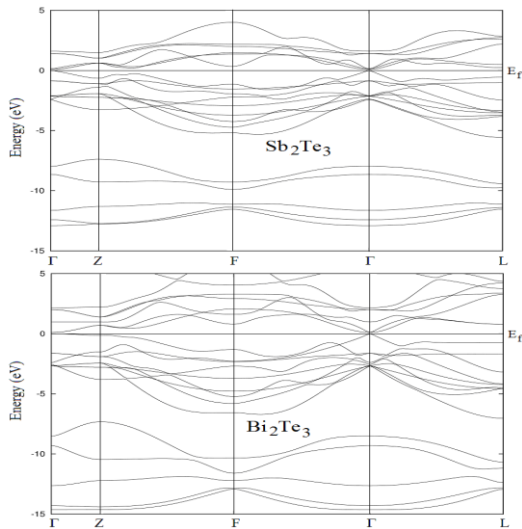


Fig. 1: Energy band structure for  $Sb_2Te_3$  and  $Bi_2Te_3$ . The calculated electronic band structure shows that  $Sb_2Te_3$  and  $Bi_2Te_3$  compounds have a direct band gap with the value 0.093 eV and 0.099 eV, respectively.

<sup>64</sup> H. Koc, E. Deligöz, Amirullah M. Mamedov, "The elastic, electronic, and optical properties of PtSi and PtGe compounds" Philophysical Magazine, Vol. 91, p. 3093-3107, 2011.

## Linear and Non-Linear Optical Properties of $\text{AgBO}_3$ (B=Nb, Ta): First Principle Study

Sevket Simsek, Amirullah M. Mamedov, Ekmel Ozbay

Nanotechnology Research Center (NANOTAM), Bilkent University 06800, Bilkent, Ankara, Turkey

Email: mamedov@bilkent.edu.tr

The linear and nonlinear optical properties of ferroelectrics  $\text{AgBO}_3$  (B=Ta, Nb) are studied by density functional theory (DFT) in the local density approximation (LDA) expressions based on first principle calculations without the scissor approximation. Specially, we present calculations of the frequency- dependent complex dielectric function  $\varepsilon(\omega)$ , and the second harmonic generation response coefficient  $\chi^{(2)}(-2\omega, \omega, \omega)$  over a large frequency range in rhombohedral phase for the first time. The electronic linear electrooptic susceptibility  $\chi^{(2)}(-\omega, \omega, 0)$  is also evaluated below the band gap. These results are based on a series of the LDA calculation using DFT. Our goals are to give the details of the calculations for linear and nonlinear optical properties, including the linear electro-optic (EO) tensor for some  $\text{ABO}_3$  structures with oxygen octahedral structures using first-principles methods<sup>65, 66</sup>.

---

<sup>65</sup> S. Cabuk and S. Simsek, "First-principles calculation of the linear and nonlinear optical properties of  $\text{LiTaO}_3$ ", Phys. Scr., Vol. 81, p. 055703-055710, 2010.

<sup>66</sup> H. Akkus, Amirullah M. Mamedov, "Linear and Nonlinear Optical Properties of  $\text{SbSI}$ : First-Principle Calculation", Ferroelectrics, Vol. 352, p.148–152, 2007.



## One and Two-Dimensional Ferroelectric LiNbO<sub>3</sub> Photonic Crystal

Sevket Simsek, Amirullah M.Mamedov, Ekmel Ozbay

Nanotechnology Research Center (NANOTAM), Bilkent University 06800, Bilkent, Ankara, Turkey

Email: mamedov@bilkent.edu.tr

In this report, we present an investigation of the optical properties and band structure calculations for the photonic crystal structures (PCs) based on one-dimensional (1D) and two-dimensional (2D) ferroelectric LiNbO<sub>3</sub> crystal<sup>67</sup>. Here we use 1D and 2D periodic crystal structure of dielectric rods and layers in air background. We have theoretically calculated photonic band structure and optical properties of 1D and 2D LiNbO<sub>3</sub> PCs. Beside, we have calculated affect PBG properties of different parameters such as filling fraction and the shape. In order to get photonic gap map, we have calculated the gaps as a function of radius of the rods. We have also investigated the nature of guided modes in line defect waveguide. In our simulation, we employed the finite-difference time domain (FDTD) technique which implies the solution of Maxwell equations with centered finite-difference expressions for the space and time derivatives. FDTD schemes are especially promising for the investigation of PBG structures, as they provide an opportunity of analyzing the spatial distribution of the electromagnetic field in PBG structure.

---

<sup>67</sup> S. Simsek, Amirullah M. Mamedov, E. Ozbay “Two-Dimensional Ferroelectric Photonic Crystals: Optics and Band Structure”, *Ferroelectrics* (in pres: accepted for publ).

## Lattice Dynamics of Alkali Halides in the Anharmonic Regime

M. Kempa<sup>1</sup>, J. Hlinka<sup>1</sup>, P. Ondrejko<sup>1</sup>, P. Marton<sup>1</sup>

<sup>1</sup> Department of Dielectrics, Institute of Physics AS CR, Prague, Czech Republic

Email: kempa@fzu.cz

Simple alkali halides, such as NaI or KBr, have been model examples of ionic crystals for decades, being studied both experimentally and theoretically. Recently, renewed interest in dynamics of alkali halides appeared: Among others, incorporation of three-body interactions into the polarizable shell model has been shown to improve considerably the agreement between lattice dynamic calculations and experimental results on phonon dispersion<sup>6,8</sup>. Furthermore, an intrinsic localized mode (breather) was discovered in the phonon gap of NaI doped by Tl [2] at high temperatures. Breathers can be regarded as dynamic nanoclusters, they have been discussed in the context of relaxors<sup>3,4</sup>, and it would be very interesting to observe them in simple systems. Such an anharmonic lattice mode could be the same as the locally excited vibrational mode that causes photoluminescence quenching in alkali halides doped by  $ns^2$  ions<sup>5,6</sup>, and had been theoretically predicted<sup>7</sup>, but never experimentally observed before in such a simple structure.

In this contribution, we present our inelastic neutron scattering data on both pure and doped KBr and NaI, at room and high temperatures, as well as our first-principles calculations based on density functional theory within the local-density approximation. The position and size of the energy gap in the phonon density of states in a wide range of temperatures from 10 to 700 K are discussed in connection with a pronounced temperature effect which effectively leads to closure of the phonon gap at high temperatures<sup>8</sup>. The results are also discussed in the context of studies of possible intrinsic localized modes in the phonon gap of alkali halides. We have also attempted to induce the anharmonic lattice modes at low temperatures by UV excitation of the impurity electronic states of Tl<sup>+</sup> substitution centers<sup>9</sup>.

<sup>6,8</sup> U.C. Srivastava, R.S. Pandey, K.S. Upadaya, Int. J. Phys. Sci. 5, 972 (2010).

<sup>2</sup> M.E. Manley, A.J. Sievers, J.W. Lynn, S.A. Kiselev, N.I. Agladze, Y. Chen, A. Llobet, A. Alatas, Phys. Rev. B 79, 134304 (2009).

<sup>3</sup> A. Bussmann-Holder, A. R. Bishop, J. Phys.: Condens. Matter 16, L313 (2004).

<sup>4</sup> A. Bussmann-Holder, A. R. Bishop, T. Egami, Europhys. Lett., 71, 249 (2005).

<sup>5</sup> J. Hlinka, E. Mihokova, M. Nikl, Physica Status Solidi (b) 166, 503 (1991).

<sup>6</sup> E. Mihokova, L.S. Schulman, J. Phys. A: Math. Theor. 43, 183001 (2010).

<sup>7</sup> S.A. Kiselev, A.J. Sievers, Phys. Rev. B 55, 5755 (1997).

<sup>8</sup> M. Kempa, P. Ondrejko, P. Bourges, J. Ollivier, S. Rols, J. Kulda, S. Margueron, J. Hlinka, J. Phys.: Condens. Matter 25, 055403 (2013).

<sup>9</sup> M. Kempa, P. Ondrejko, J. Ollivier, S. Rols, J. Kulda, S. Margueron, M. Fernandez, J. Hlinka, Ferroelectrics 440, 42 (2012).

## Electrical properties of ferroelectric composites described in terms of local field inhomogeneity

L. Padurariu<sup>1</sup> and L. Mitoseriu<sup>1</sup>

<sup>1</sup>*Faculty of Physics, Alexandru Ioan Cuza University, 11 Bv. Carol I, 700506 Iasi, Romania*

In last years, the material scientists attention was focused in investigation of new dielectric materials with tailored properties: permittivity, tunability, P(E), etc. for specific applications. Unfortunately, the required electrical properties are not usually accomplished in single phase systems, and the solution was the development of multiphase composite materials. By comparison with a single phase material, a composite is characterized by the presence of interfaces separating regions with different permittivities, which induce the formation of local inhomogeneous fields which should be taken into account when a theoretical model is proposed.

The aim of this work is the theoretical investigation of the role of the local electric field inhomogeneity on different electric properties of composites: effective permittivity, nonlinear tunability and P(E) response. The local field calculations were performed by Finite Element Method (FEM), by solving the Laplace's equation:  $\nabla \cdot (\varepsilon \nabla V) = 0$ , where  $\varepsilon$  is the local permittivity,  $V$  is the local potential and the local field is the potential derivative  $\vec{E} = -\nabla V$ .

Different structures with various microstructure particularities were generated and investigated by FEM analysis in order to estimate different properties. A remarkable agreement between the experimental tunability features and the model calculations was obtained in nanostructured BaTiO<sub>3</sub> ceramics (composite with di-similar grain bulk and grain boundary regions) with grain size between 5000 to 90 nm and for porous PZT materials (composite with ceramic bulk and air pores) with different porosity levels [1,2]. Others satisfactory results were derived for a combined FEM-Preisach model applied to estimate the field-dependence of the polarization (MHL and FORC) in ferroelectric composites (particular case: porous PZTN ceramics).

### Acknowledgments:

The financial support of the CNCS-UEFISCDI Projects No. PN-II-ID-PCE-2011-3-0745 and PCCE II-2011-0006 are highly acknowledged.

### References:

- [1] L. Padurariu et al. Phys.Rev.B **85**, 224111 (2012)
- [2] L. Padurariu et al. Appl.Phys.Lett. **100**, 252905 (2012)

**CALCULATION OF THE DAMPING CONSTANT AND THE ORDER PARAMETER  
FOR THE LATTICE MODES IN FERROELECTRIC PbTiO<sub>3</sub>**

A. Kiraci and H. Yurtseven\*  
Department of Physics,  
Middle East Technical University,  
06531, Ankara-Turkey

\*Corresponding author: hamit@metu.edu.tr

**ABSTRACT**

The temperature dependences of the damping constant and the order parameter are calculated for the lattice modes A<sub>1</sub>(1TO) and E (1TO) in PbTiO<sub>3</sub> using the experimental data by the soft mode- hard mode coupling model and the energy fluctuation model. Calculation of the damping constant of both lattice modes is performed in the temperature range of 400-490 °C close to the ferroelectric-paraelectric transition (T<sub>C</sub>=493 °C) in PbTiO<sub>3</sub>. By relating the frequency to the order parameter (spontaneous polarization), the temperature dependences of the frequencies for the A<sub>1</sub>(1TO) and E (1TO) modes in the ferroelectric phase of PbTiO<sub>3</sub> are calculated from the mean field theory.

Our calculated values for the damping constant and the order parameter describe the observed behaviour of PbTiO<sub>3</sub> close to the ferroelectric-paraelectric transition adequately. Our predicted values for the damping constant of the A<sub>1</sub>(1TO) lattice mode can be compared with the experimental bandwidths of this mode when this data is available in the literature.

## Magnetically induced change of polarization due internal magnetoelectric coupling in PFW-PT ceramics

Bárbara Fraygola<sup>1,2</sup>, José A. Eiras<sup>1</sup>

<sup>1</sup>Universidade Federal de São Carlos, Departamento de Física, Grupo de Cerâmicas Ferroelétricas, São Carlos –SP - Brazil

<sup>2</sup> École Polytechnique Fédérale de Lausanne, Material Institute, Ceramic Laboratory LC, Lausanne, Switzerland.

Email: barbara.fraygola@epfl.ch

The magnetoelectric (ME) coupling in a material can be either extrinsic (obtained by applying fields) or intrinsic (characteristic of the material). Multiferroic materials do not necessarily exhibit extrinsic effect. Their characteristic feature is the presence of, together (or not) with ME effects induced by an external fields, intrinsic ME effects due to the interaction of strong internal electric and magnetic fields. These spontaneous effects are manifested at electric and magnetic phase transitions, mediated by an elastic contribution. A concomitance of magnetism and ferroelectricity then has to rely on more subtle microscopic coupling mechanisms, driven by spin-orbit coupling in the form of Dzyaloshinskii-Moriya interactions or exchange-striction, generally obtained in materials with complicated structure and low order temperature. For example,  $\text{TbMnO}_3$  and other spin-induced ferroelectrics exhibit relatively large ME coupling. Another option looking for materials with a large ME coupling goes to mixed solid solutions. In this work, a polarization study was done in  $\text{Pb}(\text{Fe}_{2/3}\text{W}_{1/3})_{1-x}\text{Ti}_x\text{O}_3$  ( $x=0.15, 0.17, 0.20$ ) ceramics looking for the temperature dependence around the para-antiferromagnetic transition temperature, in which the multiferroic state is established, with a G-type antiferromagnetic structure. The results were complemented with elastics, magnetic and dielectric properties.

Fig. 1 shows the obtained temperature dependence of the electric polarization for PFW-17PT as an example. The sample was cooled down to 10 K under an electric field of 0.5 kV/mm and then the current flow from the sample was recorded upon heating without the electric field. A series of large decreases of polarization occurs as the temperature is increased: at 235K, at the ferroelectric phase transition ( $\Delta P_{\text{FE}}=26\mu\text{C}/\text{cm}^2$ ) and around 143 K ( $\Delta P_{\text{AFM}}=24\mu\text{C}/\text{cm}^2$ ), which is the magnetic transition temperature, showing that an additional magnetic contribution to the ferroelectric polarization occurred and not only the intrinsic ferroelectric one. These results can be explained by the governing equations for magnetoelastically coupled materials and an interpretation of the increase in the electric polarization in the antiferromagnetic phase transition is proposed on the foundation of general phenomenological basis. The changes in AFM phase transition observed in PFW-PT are considered to be the result of a renormalization of the FE constants by the magnetoelectric interaction, and are compared with colossal values.

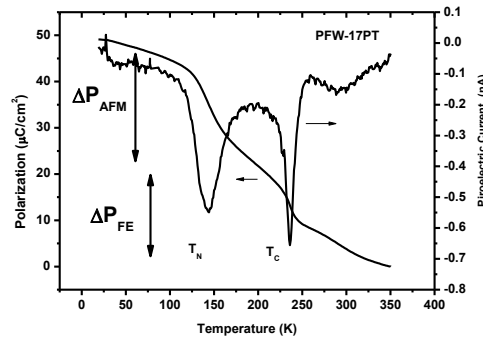


Fig. 18: Pyroelectric current and spontaneous polarization as a function of the temperature for PFW-17PT ceramic.

# Magnetolectric Coupling of Multiferroic Composites under Combined Thermal-Mechanical-Magnetic loadings

Fang Fei<sup>1</sup>, Xu Yantao, Zhou Yangyang, Jing Wenqi, Yang Wei

School of Aerospace, Tsinghua University, Beijing 100084

Email: fangf@mail.tsinghua.edu.cn

Extensive scientific and technological interests have been drawn by multiferroic materials since their versatile combinations of ferroelectricity, ferromagnetism and ferroelasticity. In multiferroic composites, the ME coupling is a strain mediated product effect achieved via the interfaces between the magnetic and electrical subsystems through elastic deformation. Due to the strong ME coupling, multiferroic composites are suitable for applications such as magnetic field sensors, transformers and microwave resonators. Such applications frequently involve environments where the temperature alters and/or suffer from the variation of the mechanical loads.

In this presentation, we will focus on three aspects of our recent developments on ME coupling for multiferroic composites. Firstly, a multi-peak phenomenon of ME coupling are reported which is very promising for applications in double-band ME resonators and filters, etc (Fig. 1). An theoretical analysis was carried out, which agrees well with the experimental observations and enables us to conclude the resonance modes. Secondly, investigations on the temperature or mechanical effects on ME coupling are carried out. The study aims at exemplifying the temperature or mechanical sensitivity of ME coupling for the composites, as well as exploring the particular material parameter(s) which plays a dominant role. Thirdly, an intriguing phenomenon of four-state ME coupling is reported for embedded composites (Fig. 2). A geometric factor  $k$  is proposed which captures the size effect on the ME behavior for the embedded composites. Finite element analysis is performed, which fits well with the experimental data and enables us to deduce the underlying mechanism of the four-state ME coupling.

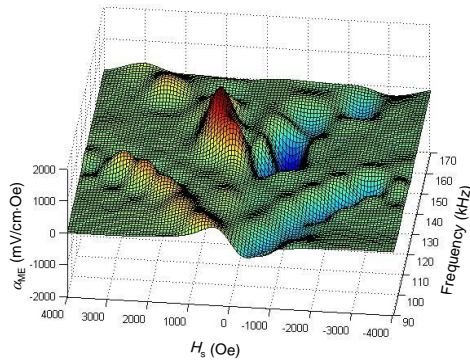


Fig. 1 A 3-D surface chart of ME coupling versus frequency and  $H_s$ .

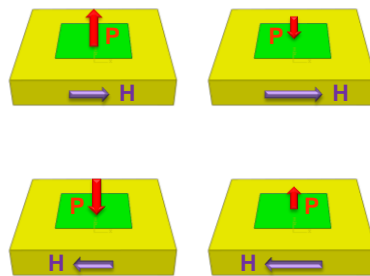


Fig. 2 Schematics of the four-state magnetolectric coupling.

# Phase transitions of high insulating rhombohedral $\text{Bi}_{1-x}\text{La}_x\text{Fe}_{1-y}\text{Ti}_y\text{O}_3$ multiferroic ceramics

Jian Yu and Linlin Zhang

Functional Materials Research Laboratory, Tongji University, Shanghai 200092, China

Email: [jyu@tongji.edu.cn](mailto:jyu@tongji.edu.cn)

$\text{BiFeO}_3$  is the only known high temperature single-phased multiferroic material, which exhibits coexistence of ferroelectric and antiferromagnetic ordering below Néel temperature of  $370^\circ\text{C}$ . Owing to thermodynamic instability of  $\text{BiFeO}_3$  compound, it is very difficult to prepare phase pure samples, often accompanying with impurities of  $\text{Bi}_{25}\text{FeO}_{39}$  and  $\text{Bi}_2\text{Fe}_4\text{O}_9$ . Meanwhile, synthesization of high insulating  $\text{BiFeO}_3$  ceramics is a major challenge for material scientists.

In this report,  $\text{Bi}_{1-x}\text{La}_x\text{Fe}_{1-y}\text{Ti}_y\text{O}_3$  multiferroic ceramics with  $0.02 \leq x \leq 0.12$  and  $0.01 \leq y \leq 0.08$  were prepared with refined electroceramic processing of traditional solid state reaction method. It was found experimentally that La/Ti-codoping stabilizes rhombohedral  $\text{BiFeO}_3$  through forming ternary solid solution. Then the electrical properties of robust insulating with resistivity of  $\sim 10^{11} \Omega\cdot\text{m}$  under 90 kV/cm electric field and low dielectric loss below 0.03 over the frequency range of 20 - 1M Hz were obtained for all composition studied here. Their robust insulating property was also able to be demonstrated by poling experiments, for example, the  $\text{Bi}_{0.98}\text{La}_{0.02}\text{Fe}_{0.99}\text{Ti}_{0.01}\text{O}_3$  ceramics bore more than 5kV DC electric field at  $120^\circ\text{C}$  and then exhibited piezoelectric constant of  $d_{33} = 0.6 \text{ pC/N}$ . The mechanisms for high insulating and low dielectric loss were also experimentally investigated and discussed relating to defect and thermodynamic stability of  $\text{BiFeO}_3$ .

For these rhombohedral  $\text{Bi}_{1-x}\text{La}_x\text{Fe}_{1-y}\text{Ti}_y\text{O}_3$  multiferroic ceramics, differential thermal analysis, temperature-dependent X-ray diffraction and magnetization measurements probe four structural phase transitions, e.g.  $T_H = 305^\circ\text{C}$ ,  $T_N = 365^\circ\text{C}$ ,  $T_C = 810^\circ\text{C}$  and  $T_S = 830^\circ\text{C}$  observed in the  $\text{Bi}_{0.98}\text{La}_{0.02}\text{Fe}_{0.99}\text{Ti}_{0.01}\text{O}_3$ , which are reasonably attributed to antiferromagnetic-helimagnetic, helimagnetic-paramagnetic, ferroelectric-paraelectric and rhombohedral-cubic lattice structural phase transition, respectively. With increasing  $x$  and  $y$  in our experiments,  $T_H$  and  $T_N$  changes little but  $T_C$  and  $T_S$  decrease gradually. The change of magnetic phase transition from second-order to first-order and emergence of helimagnetic ordering phase was attributed to  $\text{Ti}^{3+}$   $d^1$  disordered distribution in the  $-\text{Fe}^{3+}d^5\text{-O-Fe}^{3+}d^5\text{-O-Fe}^{3+}d^5\text{-O-}$  chains.

The rhombohedral  $\text{Bi}_{1-x}\text{La}_x\text{Fe}_{1-y}\text{Ti}_y\text{O}_3$  multiferroic ceramics with robust insulating and low dielectric loss may be able to find possible applications as microwave dielectrics, different from those normal diamagnetic dielectrics.

## Mixtures of the ferroelectric liquid crystal and magnetic nanoparticles: New Soft Magnetolectrics

Brigita Rožič<sup>1,2</sup>, Marko Jagodič<sup>3,4</sup>, Sašo Gyergyek<sup>1</sup>, George Cordoyiannis<sup>1,2,5</sup>, Mihael Drogenik<sup>1</sup>, Zvonko Jagličić<sup>3,6</sup>, Samo Kralj<sup>7</sup>, Vassilios Tzitzios<sup>8</sup> and Zdravko Kutnjak<sup>1,2,9</sup>

<sup>1</sup>Jozef Stefan Institute, Jamova cesta 39, 1000 Ljubljana, Slovenia

<sup>2</sup>Centre of Excellence Namaste, Jamova cesta 39, 1000 Ljubljana, Slovenia

<sup>3</sup>Institute of Mathematics, Physics and Mechanics, Jadranska 19, 1000 Ljubljana, Slovenia

<sup>4</sup>EN-FIST Centre of Excellence Namaste, Dunajska 156, 1000 Ljubljana, Slovenia

<sup>5</sup>Department of Physics, University of Athens, 15784 Athens, Greece

<sup>6</sup>Faculty of Civil and Geodetic Engineering, Jamova cesta 2, 1000 Ljubljana

<sup>7</sup>Faculty of Natural Science and Mathematics, Koroška cesta 160, 2000 Maribor, Slovenia

<sup>8</sup>National Centre for Scientific Research Demokritos, Aghia Paraskevi 15310, Greece

<sup>9</sup>Jozef Stefan International Postgraduate School, 1000 Ljubljana, Slovenia

Email: brigita.rozic@ijs.si

Magnetolectrics have recently attracted significant attention due to their properties and potential for various applications<sup>69</sup>. So far the main focus remains on solid magnetolectrics, but in our case we focused on the magnetolectric effect in a soft material based on mixtures of a ferroelectric liquid crystal (FLC) and magnetic nanoparticles (MNPs).

In this work we report the theoretical estimation and experimental observation of the magnetolectric effect in similar systems of two different FLCs, i.e., SCE9 and Felix 015/100, and two different ferromagnetic NPs, i.e., maghemite and magnetite magnetic NPs<sup>70,71,72</sup>. NPs were weakly anisotropic with an average size of 20 nm and coated with an oleic acid to avoid instability of the suspension in the toluene. The high resolution calorimetry, dielectric spectroscopy and magnetic susceptibility measurements were performed in the vicinity of the ferroelectric phase transition. Similar disordering effects on the ferroelectric phase transition were found as in the case of the aerosils<sup>73</sup> and the impact of the MNPs on the dielectric response was observed. Measurements of the impact of the electric field on the magnetic susceptibility via SQUID-based magnetometer confirmed the indirect coupling between the NP's magnetic moments and LC's electric polarization.

Obtained experimental results are in good agreement with the theoretical predictions and they provide a strong support for the generally expected behavior in such mixtures. This enhances the chance to engineer the soft composite magnetolectrics.

<sup>69</sup> W. Erenstein et al., "Multiferroic and magnetolectric materials", *Nature*, vol. 442, 05023, 2006.

<sup>70</sup> B. Rožič et al., "Orientational order-magnetization coupling in mixtures of magnetic nanoparticles and the ferroelectric liquid crystal", *Ferroelectrics*, vol. 410, p. 37-41, 2011.

<sup>71</sup> B. Rožič et al., "Multiferroic behavior in mixtures of the ferroelectric liquid crystal and magnetic nanoparticles", *Mol. Cryst. Liq. Cryst.*, vol. 545, p. 99-104, 2011.

<sup>72</sup> B. Rožič et al., "Mixtures of magnetic nanoparticles and ferroelectric liquid crystal: New soft magnetolectrics", *Ferroelectrics*, vol. 431, p. 150-153, 2012.

<sup>73</sup> G. Cordoyiannis et al., "Pretransitional effects near the smectic A-smectic C\* phase transition of hydrophilic and hydrophobic aerosil networks dispersed in ferroelectric liquid crystals", *Phys. Rev. E*, vol. 75, 021702, 2007.



## Epitaxial (Sr<sub>1-x</sub>Ba<sub>x</sub>)MnO<sub>3</sub> thin films: towards strain-induced ferroelectricity

L. Maurel<sup>1,2</sup>, J. A. Pardo<sup>1,3,\*</sup>, M. Algueró<sup>4</sup>, C. Becher<sup>5</sup>, E. Langenberg<sup>1</sup>, J. Blasco<sup>2,6</sup>, C. Magén<sup>1,2</sup>, P. Ramos<sup>7</sup>, R. Jiménez<sup>4</sup>, J. Ricote<sup>4</sup>, P. Štrichovanec<sup>1</sup>, I. Lucas<sup>2,6</sup>, L. Morellón<sup>1,2</sup>, M. Fiebig<sup>5</sup>, M. R. Ibarra<sup>1,2</sup>, P. A. Algarabel<sup>2,6</sup>

<sup>1</sup>INA, University of Zaragoza, Spain. <sup>2</sup>Condensed Matter Physics Dept., University of Zaragoza, Spain. <sup>3</sup>Materials Science Dept., University of Zaragoza, Spain. <sup>4</sup>ICMM-CSIC, Cantoblanco, Spain. <sup>5</sup>Materials Dept., ETH, Switzerland. <sup>6</sup>ICMA-CSIC, Zaragoza, Spain. <sup>7</sup>Dpto. Electrónica, UAH, Alcalá de Henares, Spain

(\*) [email: jpardo@unizar.es](mailto:jpardo@unizar.es)

Recent theoretical predictions and experimental results suggest that paraelectric SrMnO<sub>3</sub> with the ABO<sub>3</sub> perovskite structure could become ferroelectric upon artificial expansion of the unit cell, either by epitaxial strain<sup>1</sup> or partial substitution of Ba for Sr (ref.<sup>2</sup>). This would give rise to a new class of multiferroic perovskites where ferroelectricity would be driven by off-centring of the magnetic cation Mn<sup>4+</sup>.

Here we have investigated the effect of both Ba doping and epitaxial strain on the structure and electric properties of SrMnO<sub>3</sub> thin films. Pulsed laser deposition with in situ RHEED monitoring was used to grow strained (Sr<sub>1-x</sub>Ba<sub>x</sub>)MnO<sub>3</sub>, 0 ≤ x ≤ 0.5 (SBMO) thin films on (001)-oriented perovskite substrates, with strain ranging from -1% (compressive) to +3% (tensile). X-ray diffraction shows that, under appropriate deposition conditions, the perovskite pseudocubic phase is stabilized over the hexagonal phase, despite the latter being favored with increasing Ba content. Optimized films show fully coherent cube-on-cube epitaxial growth and are chemically homogeneous and defect-free, as determined by scanning transmission electron microscopy and electron energy loss spectroscopy.

Nonlinear optics measurements reveal that some of our SBMO films emit optical second harmonic generation signal, pointing to spatial inversion symmetry being broken (necessary condition for ferroelectricity). Electric measurements and piezoresponse force microscopy were used to investigate the ferroelectric properties of epitaxially strained SBMO films.

---

<sup>1</sup> J. H. Lee and K. M. Rabe, *Phys. Rev. Lett.* **104**, 207204 (2010)

<sup>2</sup> H. Sakai et al., *Phys. Rev. Lett.* **107**, 137601 (2011)

## The Magnetoelectric Coupling in a Self-Assembled Epitaxial Nano-composite Driven by Chemical Interaction

Wen-I Liang<sup>1</sup>, Yuanming Liu<sup>2</sup>, Wei-Cheng Wang<sup>3</sup>, Heng-Jui Liu<sup>1</sup>, Sheng-Chieh Laio<sup>4</sup>, Hong-Ji Lin<sup>3</sup>,  
Chih-Huang Lai<sup>4</sup>, Elke Arenholz<sup>5</sup>, Jaingyu Li<sup>2</sup>, Ying-Hao Chu<sup>1</sup>

<sup>1</sup>Department of Materials Science and Engineering, National Chiao Tung University, HsinChu, 30010, Taiwan

<sup>2</sup>Department of Mechanical Engineering, University of Washington, Seattle, WA 98195, USA

<sup>3</sup>National Synchrotron Radiation Research Center, Hsinchu 30076, Taiwan

<sup>4</sup>Department of Materials Science and Engineering, National Tsing Hua University, Hsinchu 30013, Taiwan

<sup>5</sup>Advanced Light Source, Berkeley, CA 94720, USA

Email: [yhc@nctu.edu.tw](mailto:yhc@nctu.edu.tw)

Complex oxide heterostructures have triggered a plethora of studies with novel phenomena in condensed matter physics because it provides the possibility to integrate dissimilar oxide with diverse functionalities. Among them, self-assembled vertical nano-composite, as one approach to build heterostructure, has enlarged the playground of complex oxide heterostructure due to structural, physical and chemical interactions between dissimilar oxides. From the previous studies, the structural and physical interactions are demonstrated comprehensively; however, the information of chemical interaction, or atomic diffusion, which is more or less inevitable in two-phase system, is still missing so far. In this study, it is designed the chemical-interaction-induced magnetoelectric coupling effect exhibits in two antiferromagnetic materials: BiFeO<sub>3</sub> and LiMn<sub>2</sub>O<sub>4</sub> vertical nano-composite.

The self-assembled (BiFeO<sub>3</sub>)<sub>x</sub>:(LiMn<sub>2</sub>O<sub>4</sub>)<sub>1-x</sub> vertical heterostructure with different composition ratio were grown by pulse laser deposition. Via the scrutiny of scanning electron microscope, X-ray diffraction, nano Auger and high resolution transmission electron microscope, a fundamental view between the inter-diffusion and the composition ratio is visualized. Based on this chemical interaction, we have found the both ferroelectricity and ferromagnetism coexist in the (BiFeO<sub>3</sub>)<sub>0.75</sub>:(LiMn<sub>2</sub>O<sub>4</sub>)<sub>0.25</sub> nano-heterostructure. Furthermore, in order to understand this behavior, a concrete connection between chemical diffusion and the induced magnetic moment is proposed when we conduct soft x-ray circular dichroism to investigate the local environment of transition metals. The last part of this study shows the strong magnetoelectric coupling effect between these two chemical phases. Thus, in this study, we have manipulated successively the chemical interaction between dissimilar oxides heterostructure to demonstrate the new-emerged physical properties and its coupling effect, which would be a key study to extend the practical value in vertical nanoheterostructure.

## Effect of composition on functional properties of ferroelectric-ferrite composite systems

Cristina Elena Ciomaga<sup>1</sup>, Mihai Valentin Pop<sup>1</sup>, Leontin Padurariu<sup>1</sup>, Mirela Airimioaei<sup>2</sup>, Carmen Galassi<sup>3</sup> and Liliana Mitoseriu<sup>1</sup>

<sup>1</sup>Faculty of Physics, "Al. I. Cuza" University of Iasi 700506, Romania

<sup>2</sup>Faculty of Chemistry, "Al. I. Cuza" University of Iasi 700506, Romania

<sup>3</sup>CNR -ISTEC, Via Granarolo no. 64, I-48018 Faenza, Italy

E-mail: cristina.ciomaga@uaic.ro

The ferroelectric, dielectric and magnetic properties related to the microstructures in the  $x\text{NiFe}_2\text{O}_4-(1-x)\text{Pb}_{0.988}(\text{Zr}_{0.52}\text{Ti}_{0.48})_{0.976}\text{Nb}_{0.024}\text{O}_3$  ( $x\text{NF}-(1-x)\text{PZTNb}$ ) magneto-electric composites with  $x= 2, 5, 10, 20, 30, 40, 50, 60, 70$  and 100 wt% are investigated. The di-phase ceramics prepared *in situ* by sol-gel method present homogeneous microstructures, higher density and a better mixing of the two phases.

The temperature dependence of dielectric properties showed a sharp ferroelectric to paraelectric phase transition peak at around 360°C for low NF concentrations and a diffuse phase transition at around 330°C for high amounts of ferrite in the composites. Thus, the addition of NF phase induces a microscopic heterogeneity in composites and a distribution of different localized Curie points. From frequency dependence of the complex dielectric permittivity it was observed a dispersive behavior, due to Maxwell-Wagner effect. The higher degree addition of magnetic phase contributes to the interfacial polarization, causing a significant increase of the real part of permittivity for frequencies below 1 kHz. The ferroelectric properties reveal that with increasing the NF concentration in the composites it was obtained flattened P-E loops with smaller values of the remnant polarization. In contrast, the magnetic properties improve with addition of ferrite phase. However the coercitive field ( $H_c$ ) for all the composite samples is larger than that of pure  $\text{NiFe}_2\text{O}_4$  phase.

For describing the dependence of the polarization on the applied electric field, a combined model based on Classical Preisach Model (CPM) and Finite Element Method (FEM) was developed and compared with the experimental data.

**Acknowledgements:** These works were financial supported by CNCSIS-UEFISCSU, projects number PN II-RU TE code 187/2010 and PN-II-ID-PCE-2011-3-0745.

## Influence of substrate–film interface engineering on the multiferroic BiFeO<sub>3</sub>

Alim Solmaz<sup>1</sup>, Mark Huijben<sup>1</sup>, Beatriz Noheda<sup>2</sup>, Guus Rijnders<sup>1</sup>

<sup>1</sup>Mesa+ Institute for Nanotechnology, University of Twente, Enschede, The Netherlands

<sup>2</sup>Zernike Institute for Advanced Materials, University of Groningen, Groningen, The Netherlands

Email: [a.solmaz@utwente.nl](mailto:a.solmaz@utwente.nl)

Multiferroics, such as BiFeO<sub>3</sub>, which simultaneously exhibit multiple order parameters such as antiferromagnetism and ferroelectricity, enable the development of novel magnetoelectric devices by utilizing the intrinsic magnetoelectric coupling in which one can control the electric polarization by applied magnetic fields or the magnetism by applied electric fields. This could lead to new applications in magnetic data storage, spintronics, and high-frequency magnetic devices, which do not require large currents and magnetic fields for operation.

In bulk, BiFeO<sub>3</sub> is a rhombohedrally distorted perovskite crystal where the ferroelectricity arises due to the displacement of Bi ions with respect to FeO<sub>6</sub> octahedra. This results in an electrical polarization that lies along the  $\langle 111 \rangle_{pc}$  directions and, thereby, to formation of three types of domain walls i.e. 71°, 109° and 180°, each of which show distinctive properties such as conductivity and magnetism. In addition to that, the antiferromagnetic properties of BiFeO<sub>3</sub> are exploited in order to create an exchange bias with a ferromagnetic layer such that two coupling effects can be used to manipulate the ferromagnetic state by electric field<sup>74</sup>. Additionally, it has been shown that a ferromagnetic state can be induced at the interface between BiFeO<sub>3</sub> and La<sub>0.7</sub>Sr<sub>0.3</sub>MnO<sub>3</sub> thin films<sup>75</sup>. Thus it is important to have atomic level control of the growth of BiFeO<sub>3</sub> thin films in order to obtain specific properties at domain walls and interfaces.

In our work, we focus on the heteroepitaxial growth of BiFeO<sub>3</sub> single crystal thin films on SrTiO<sub>3</sub> substrates by pulsed laser deposition. We demonstrate that the initial BiFeO<sub>3</sub> growth is very sensitive to the terminating layer of the substrate. Singly TiO<sub>2</sub>-terminated substrates can be switched to SrO termination by interval deposition with the assistance of Reflective High Energy Electron Diffraction (RHEED) technique. BiFeO<sub>3</sub> thin films grown on SrO and TiO<sub>2</sub> singly-terminated substrates show different morphologies as well as different ferroelectric domains. This indicates that the sticking of bismuth oxide species on TiO<sub>2</sub>-terminated surfaces is different than that of iron oxide on SrO terminated surfaces. This determines the interface quality between the BiFeO<sub>3</sub> thin film and the substrate. Keeping in mind that the interfaces become more influential as the film gets thinner, we emphasize the importance of interface engineering for highly controlled multiferroic devices. We claim that, in BiFeO<sub>3</sub> thin film growth, the atomic terminating layer of the substrate should be taken into account as well, next to other factors that are known to influence the ferroelectric domain formation, such as screening charges, lattice mismatch or substrate miscut.

<sup>74</sup> Chu Y. et al., Electric-field control of local ferromagnetism using a magnetoelectric multiferroic, *Nat. Mater.*, 7, 478- (2008).

<sup>75</sup> Yu P. et al, Interface Ferromagnetism and Orbital Reconstruction in BiFeO<sub>3</sub>-LaSrMnO Heterostructures, *PRL* 105, 27201 (2010).

## Optimal Layout Design of Magnetolectric Laminates : Effects of Mechanical Boundary Conditions

Kyung Ho Sun<sup>1</sup>, Jae Eun Kim<sup>2</sup>, Yoon Young Kim<sup>3</sup>

<sup>1</sup>Department of System Dynamics, Korea Institute of Machinery & Materials,

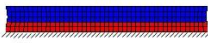
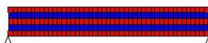
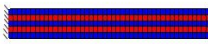
<sup>2</sup>Faculty of Mechanical and Automotive Engineering, Catholic University of Daegu,

<sup>3</sup>School of Mechanical and Aerospace Engineering, Seoul National University

Email: sunkh@kimm.re.kr

Recently, multiferroic or magneto-electro-elastic composites, made of piezoelectric and magnetostrictive materials, have received a significant research interest for potential applications in novel multifunctional devices. These multiferroic composites exhibit an additional functionality: the extrinsic magnetolectric (ME) effect via elastic mediation. In such composite materials, the performance is critically dependent on the composition of constituent materials and their structural configuration. The authors first proposed the design method of multiferroic composites by topology optimization and provided the understanding of the maximized ME effects<sup>76</sup>. In this investigation, a practical layout design approach to find optimal ME laminates (2-2 type) using the genetic algorithm will be presented. The multiferroic BaTiO<sub>3</sub>-CoFe<sub>2</sub>O<sub>4</sub> composite is analyzed by a

two-dimensional finite element formulation and the magnetolectric coupling factor by some stored energy expressions is considered as an objective function to evaluate the magnetolectric effect. Since ME effect is the stress-mediated phenomenon, the performance of ME laminates is highly dependent on mechanical boundary conditions. Figure 1 shows the optimized piezoelectric/magnetostrictive phase sequence by the proposed design method. A comparison of results indicates that the ME composites should have different layouts with each boundary condition. From this study, a design guideline on how to enhance the ME effects in terms of the applied mechanical boundary conditions can be gained.

Mechanical B.C.	Optimized layouts (deformed shape)	Layout sequence (from bottom)
Bottom-fixed		p p m m m
Simply supported		p m p m p
Left-fixed		m p m p m

(p: piezoelectric, m: magnetostrictive)

Fig. 19: The optimized ME laminates with 5 layouts under three mechanical boundary conditions. Note that optimal layout sequence is different according to the given mechanical boundary conditions.

<sup>76</sup> K. H. Sun and Y. Y. Kim, "Design of magnetolectric multiferroic heterostructures by topology optimization", J. Phys. D: Appl. Phys., vol. 44, 185003, 2011.

## Angular Dispersion of Oblique Phonon Modes in BiFeO<sub>3</sub> from micro-Raman scattering

J. Hlinka<sup>1</sup>, J. Pokorný<sup>1,2</sup>, F. Borodavka<sup>1</sup>, E. Simon<sup>1</sup>, I. Gregora<sup>1</sup>, S. Karimi<sup>2</sup>, I. M. Reaney<sup>2</sup>

<sup>1</sup>Institute of Physics, Academy of Sciences of the Czech Republic, Prague, Czech Republic

<sup>2</sup>Dept. of Materials Science and Engineering, The University of Sheffield, Sheffield, UK

Email: pokorny@fzu.cz

Bismuth ferrite (BiFeO<sub>3</sub>) is a prototypical multiferroic system, ferroelectric up to  $T_C \sim 1100$  K and antiferromagnetic up to  $T_N \sim 640$  K. It exhibits rhombohedrally distorted perovskite structure with R3c symmetry at room temperature. Characterisation of polar phonon modes is essential for understanding its dielectric and electromechanical behaviour.

Assigning Raman spectra of BiFeO<sub>3</sub> is a complex task due to mixing of vibrational modes caused by general orientation of naturally grown crystal facets. The measured *oblique* phonon modes do not coincide with any pure TO or LO mode and their frequencies continuously vary with the orientation of the phonon propagation vector (*angular dispersion*). For an optically uniaxial single crystal, modes can be assigned by analysing a set of spectra taken for different angles between the phonon propagation vector and the optical axis. To avoid demanding experiment on de-twinned single crystal, we collected a large enough set of micro-Raman spectra obtained within different randomly oriented grains of bulk ceramics. The data were curve fitted to a sum of damped harmonic oscillators and sorted by frequency evolution of one of the clearly distinct modes. The angle between the phonon propagation vector and the vector of the spontaneous polarisation (optical axis) was obtained numerically<sup>xxii</sup> using initial TO and LO frequencies from DFT calculated data. The obtained *angular dispersion* of the phonon mode parameters then enabled full mode assignment.

This work was supported by EPSRC Grant No. EP/H048049/1, by Project GACR P204/10/0616 and by AV0Z10100520.

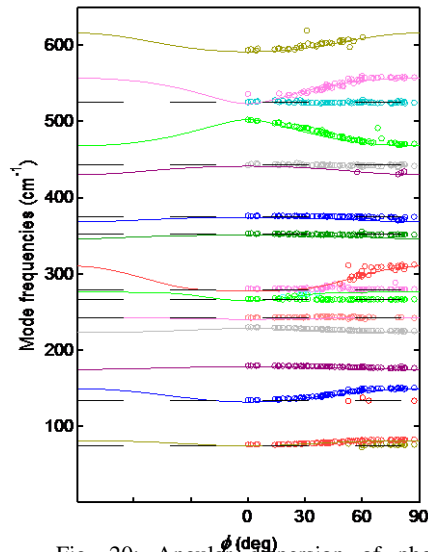


Fig. 20: Angular dispersion of phonon modes in BiFeO<sub>3</sub>. Solid lines represent the computed angular dispersion curves, open circles are the experimental fitted mode frequencies as a function of grain orientation.

## Structural Phase Transitions in $\text{Bi}_{1-x}\text{Ca}_x\text{FeO}_3$ Multiferroics

V. A. Khomchenko<sup>1</sup>, I. O. Troyanchuk<sup>2</sup>, D. M. Többens<sup>3</sup>, V. Sikolenko<sup>4</sup>, J. A. Paixão<sup>1</sup>

<sup>1</sup>CEMDRX/Department of Physics, University of Coimbra, Coimbra, Portugal

<sup>2</sup>SSPA “Scientific-Practical Materials Research Centre of NAS of Belarus”, Minsk, Belarus

<sup>3</sup>Helmholtz-Zentrum-Berlin for Materials and Energy, Berlin, Germany

<sup>4</sup>Laboratory for Neutron Scattering, Paul Scherrer Institute, Villigen, Switzerland

Email: uladzimir@fis.uc.pt

$\text{BiFeO}_3$  perovskite remains one of the most popular objects of condensed matter research. Indeed, the coexistence of spin and electric dipole ordering observed in this material in a broad temperature range and giving rise to the promising cross-coupling effects is interesting from the viewpoint of both fundamental and applied physics.  $\text{BiFeO}_3$  crystallizes in a rhombohedral  $R3c$  structure permitting the polar ionic displacements along the  $\langle 111 \rangle_c$  direction of the parent cubic perovskite cell. To be suitable for applications, the polarization should be coupled to the net magnetization, which is, however, locked in the cycloidal modulation superimposed on the  $G$ -type antiferromagnetic (with a weak ferromagnetic component) structure. One of the ways allowing the modulation to be suppressed is a chemical substitution.

In present work, the neutron powder diffraction and magnetization measurements of the  $\text{Bi}_{1-x}\text{Ca}_x\text{FeO}_3$  ( $0.05 \leq x \leq 0.14$ ) compounds belonging to the intermediate concentration range separating the polar antiferromagnetic ( $x \sim 0$ ) and nonpolar antiferromagnetic ( $x \sim 0.2$ ) phases have been carried out. It has been shown that Ca substitution induces appearance of weak ferromagnetism in the initial ferroelectric  $R3c$  phase, but modifies the picture of polar displacements, so the *average*  $\text{PbZrO}_3$ -like antiferroelectric structure (S.G. *Pbam*) is stabilized at  $x=0.11$ . Further increase of the Ca content leads to the transformation of the antipolar ionic shifts to give rise to the  $Pbam \rightarrow Imma$  transition near  $x=0.14$ . A structural study performed for the  $x=0.05$  compound at high temperature reveals the heating-induced  $R3c \rightarrow Pnma$  phase transition. Analysis of the compositional dependence of the spontaneous magnetization and polarization in the  $R3c$  phase shows that  $\text{Ca}^{2+}$  substitution ensures a balanced influence on the magnetic and ferroelectric subsystems of  $\text{BiFeO}_3$  allowing its multiferroic behavior to be improved.

This work is supported by funds from FEDER (Programa Operacional Factores de Competitividade COMPETE) and from FCT-Fundação para a Ciência e a Tecnologia under the project PEst-C/FIS/UI0036/2011.

## DIELECTRIC AND IMPEDANCE SPECTROSCOPY OF Fe DOPED 0.94(Na<sub>0.5</sub>Bi<sub>0.5</sub>TiO<sub>3</sub>)-0.06BaTiO<sub>3</sub> CERAMICS

Kęstutis Bučinskas<sup>1</sup>, Maksim Ivanov<sup>1</sup>, Robertas Grigalaitis<sup>1</sup>, Jūras Banys<sup>1</sup>, Eva Sapper<sup>2</sup>, Jürgen Rödel<sup>2</sup>

<sup>1</sup>Faculty of Physics, Vilnius University, Lithuania

<sup>2</sup>Institute of Materials Science, Technische Universität Darmstadt, Germany

Email: maksim.ivanov@ff.vu.lt

Ever since the discovery of piezoelectric effect, piezoelectric materials have been rapidly developed and widely used. The most widely used piezoelectric materials are Pb(Zr,Ti)O<sub>3</sub>(PZT)-based ceramics because of their superior piezoelectric properties. However due to legislative enforcements, representatively the European RoHS/WEEE regulations<sup>77</sup>, lead-free piezoelectric materials have been extensively studied last decade. Among the studied materials, (1-x)(Na<sub>0.5</sub>Bi<sub>0.5</sub>TiO<sub>3</sub>)-xBaTiO<sub>3</sub> ceramic family has been of particular interest because of the similar piezoelectric properties to PZT ceramics<sup>78</sup>.

In the present work the dielectric and impedance properties of Fe doped 0.94(Na<sub>0.5</sub>Bi<sub>0.5</sub>TiO<sub>3</sub>)-0.06BaTiO<sub>3</sub> ceramics in 20Hz-1GHz frequency range and 300-500K temperature range are investigated. The measurements of dielectric permittivity were performed during freezing cycle with 1K/min temperature variation rate. Conductivity was calculated using dielectric permittivity data. Fig. 1 shows frequency dependency of the real part of complex conductivity. Experimental data was fitted with generalized universal Jonscher's law<sup>79</sup>. The best fits were obtained for 403K-500K temperature range. One conductivity process was distinguished with Arrhenius behavior of  $\sigma_{DC}$  and possible cause of conductivity process is discussed.

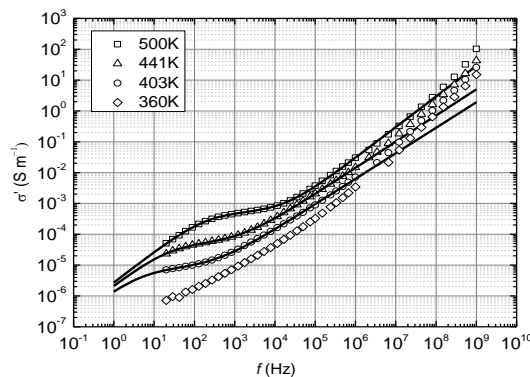


Fig. 21: Frequency dependency of real part of complex conductivity of Fe doped 0.94(Na<sub>0.5</sub>Bi<sub>0.5</sub>TiO<sub>3</sub>)-0.06BaTiO<sub>3</sub> ceramics

<sup>77</sup> EU-Directive 2002/95/EC: Restriction of the use of certain hazardous substances in electrical and electronic equipment (RoHS). Official Journal of the European Union 46 (L37) pp. 19-23,2003.

<sup>78</sup> Thomas R. Shrout, Shujun J. Zhang, "Lead-free piezoelectric ceramics: Alternatives to PZT?" J. Electroceram. 19, pp 111-124, 2007.

<sup>79</sup> I. I. Popov, R. R. Nigmatullin, A. A. Khamzin, and I. V. Lounev, "Conductivity in disordered structures: Verification of the generalized Jonscher's law on experimental data", J. Appl. Phys. 112, 094107, 2012.



## Proton Diffusion as an Origin of Dielectric Properties of Water and Ice

Alexander Volkov<sup>1</sup>, Vasily Artemov<sup>1</sup>, Artem Pronin<sup>1,2</sup>

<sup>1</sup> A. M. Prokhorov Institute of General Physics, RAS, 119991 Moscow, Russia

<sup>2</sup> Dresden High Magnetic Field Laboratory, HZ Dresden-Rossendorf, 01314 Dresden, Germany

Email: [aavol@bk.ru](mailto:aavol@bk.ru)

Despite of ubiquity of water and ice and a very long history of investigations of their physical properties, the microscopic origins of the electrodynamic properties of these substances are still in focus of sharp scientific debates [1]. It is generally accepted that both, water and ice, are dielectrics with unexpectedly high proton dc conductivity and high static permittivity, the origin of which is not fully understood. The orientational motion of the dipole moments of H<sub>2</sub>O molecules is traditionally related to the static permittivity, while the dc conductivity is explained by the ability of a H<sub>2</sub>O molecule to self-dissociate. To a large extent, these two directions of research (orientation → permittivity, ionization → conductivity) are being developed independently and hardly overlap. The first of them deals not only with water, but also with other substances, particularly with hydrogen-bonded ferroelectrics, such as KDP [2]. The second direction is closely related to the chemical acid-base index, the pH [3].

Recently, from our analysis of broad-band panoramas of dielectric response (Fig. 1), we have found an approach, which offers a uniform explanation for both, the permittivity and the conductivity spectra [4]. The new approach reveals the Debye relaxation and the dc conductivity to be two manifestations of a single microscopic mechanism – the diffusion of protons, generated via self-ionization of H<sub>2</sub>O

molecules. In Ref. [4], we developed a phenomenological model of Brownian-like diffusion and showed that the static permittivity of water results from flickering of separated charges with a fast recombination rate, while the dc conductivity is due to diffusion with a much slower recombination rate. These long-living charges are eventually responsible for pH = 7.

In this presentation, we apply our model to the case of solid ice and compare the obtained parameters for ice and water. We show that the dielectric spectra of ice can be scaled up to the liquid-water spectra (Fig. 1), using a single parameter, the activation energy for diffusion. The ice lattice is appeared to be inherently filled with a giant amount of ionic defects.

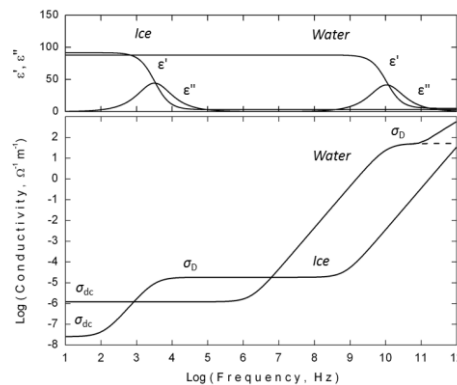


Fig. 22: Dielectric response of water and ice at 0 °C in terms of the dielectric function (top) and the dynamical conductivity (bottom).

<sup>1</sup> A. von Hippel, “The Dielectric Relaxation Spectra of Water, Ice, and Aqueous Solutions,

and their Interpretation”, IEEE Transactions on Electrical Insulation, vol. 23, p. 801-816, 1988.

<sup>2</sup> R. Blinc, B. Žekš, “Soft modes in ferroelectrics and antiferroelectrics”, p. 317, North-Holland, Amsterdam, 1974

<sup>3</sup> D. Marx, “Proton Transfer 200 Years after von Grothuss: Insights from Ab Initio Simulations”, ChemPhysChem, Vol. 7, p. 1855-1870, 2006.

<sup>4</sup> A. A. Volkov, V. G. Artemov, A. V. Pronin, “Proton Electrostatics in Liquid Water”, arXiv:1302.5048, 2013.

## Study of the ferroelectric phase transition in GeTe using time-domain THz spectroscopy

C. Kadlec, F. Kadlec, P. Kužel and J. Petzelt

Institute of Physics, Academy of Sciences, Prague, Czech Republic

Email: kadlecch@fzu.cz

Germanium telluride (GeTe) is a narrow-gap semiconductor with conducting properties important for potential applications. It belongs to so-called phase change materials: its crystalline form exhibits an electrical conductivity orders of magnitude higher than the amorphous one. The unit cell of crystalline GeTe includes two atoms only, thus it is the simplest known ferroelectric (FE). Upon heating, it becomes paraelectric (PE) at  $T_c \approx 350^\circ\text{C}$ . However, a controversy persists about the character of its FE phase transition (PT). While Raman spectra showed phonon softening in the FE phase and suggested a displacive character of the PT, there is no such evidence above  $T_c$ . Recent XANES data<sup>80</sup> showed no anomaly of the Ge-Te bond length at  $T_c$ , which indicates an order-disorder behavior. The question about the PT character is of fundamental interest.

The free charge carriers prevent the use of traditional spectroscopic techniques on bulk crystals. We present results of high-temperature measurements of GeTe thin films by means of time-domain terahertz spectroscopy. We were able to detect the IR active excitations; both FE and PE phases were studied. The PT manifests itself in a change of slope in the THz conductivity  $\sigma_{\text{THz}}(T)$ . Above  $T_c$ , we detected an excitation located in the sub-THz range. This mode is absent in the FE phase and unambiguously present in the PE phase (see Fig. 1).

The complex permittivity spectra  $\varepsilon(\omega)$  were determined numerically from the complex transmittance. We set up a model of  $\varepsilon(\omega)$  with the high-frequency limit  $\varepsilon_\infty$ , one harmonic oscillator, one Drude term due to carriers and, in the PE phase, one relaxator:

$$\varepsilon_{\text{PE}}(\omega) = \varepsilon_\infty + \frac{\Delta\varepsilon\omega_0^2}{\omega_0^2 - \omega^2 - i\omega\Gamma} + \frac{\omega_p^2}{\omega^2 - i\omega\gamma} + \frac{\Delta\varepsilon_r\omega_r}{\omega_r - i\omega}$$

where  $\omega_0$ ,  $\omega_p$  and  $\omega_r$  are the oscillator, free carrier plasma and relaxation frequencies, respectively,  $\Gamma$  and  $\gamma$  denote the oscillator and plasma damping and  $\Delta\varepsilon$ ,  $\Delta\varepsilon_r$  are the contributions to  $\varepsilon(\omega)$  due to the oscillator and relaxator, respectively. The relaxator parameters in the PE phase are compatible with the Curie-Weiss law:  $\Delta\varepsilon_r = C/(T - T_c)$  with  $C \approx 10^5$  K.

To summarize, we performed the first time-domain THz spectroscopy study of the FE PT in GeTe thin films. In the PE phase, we observed a relaxation typical for an order-disorder behavior. Moreover, only a limited softening of the lowest-lying phonon occurs. Therefore, our experimental data indicate the mixed (displacive and order-disorder) nature of the PT<sup>81</sup>.

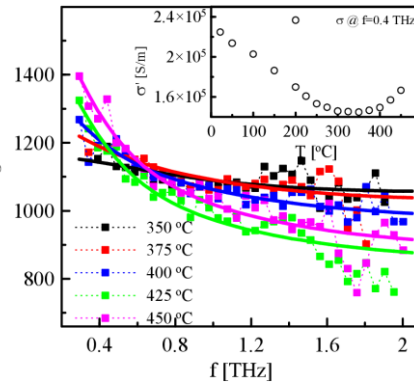


Fig. 1: THz spectra of real permittivity of GeTe in the PE phase; symbols: experimental data, lines: fits. Inset: conductivity at 0.4 THz with a minimum

<sup>80</sup>P. Fons et al., 'Phase transition in crystalline GeTe: Pitfalls of averaging effects', Phys. Rev. B 82, 155209, 2010

<sup>81</sup>F. Kadlec et al., 'Study of the FE PT in GeTe using THz spectroscopy', Phys. Rev. B 84, 205209, 2011

## Thermal evolution of crystal structure of $\text{Bi}_{1-x}\text{Pr}_x\text{FeO}_3$ ceramics across rhombohedral-orthorhombic phase boundary

D.V. Karpinsky, A.L. Kholkin

CICECO/Department of Materials and Ceramics Engineering, University of Aveiro, 3810-193 Aveiro, Portugal

Email: karpinski@ua.pt

Enhanced ferroic properties expected in  $\text{BiFeO}_3$ -based multiferroics near the morphotropic phase boundaries still attract continuous interest, while an origin of such improvement is still ambiguous [1, 2]. Assuming a close correlation between the enhanced ferroic properties and specific structural phases we focused our study on thermally driven phase transition of  $\text{Bi}_{1-x}\text{Pr}_x\text{FeO}_3$  compounds with chemical composition within the phase boundary region.

Room temperature XRD patterns of  $\text{Bi}_{1-x}\text{Pr}_x\text{FeO}_3$  ceramics prove the following sequence of the phase transitions with increasing  $x$ : rhombohedral polar (R) – orthorhombic antipolar (O2) – orthorhombic nonpolar (O1) [3]. The crystal structure of the selected compound  $\text{Bi}_{0.875}\text{Pr}_{0.125}\text{FeO}_3$  is characterized by a coexistence of the rhombohedral (R) and the orthorhombic (O2) phases. An analysis of the variable temperature diffraction data testifies a decrease of the antipolar orthorhombic phase fraction with temperature growth. The antipolar phase remains at temperatures above  $350^\circ\text{C}$ , whereas at  $400^\circ\text{C}$  a strong evidence of new nonpolar orthorhombic phase has been revealed, thereby at the temperatures about  $400^\circ\text{C}$  all three phases coexist.

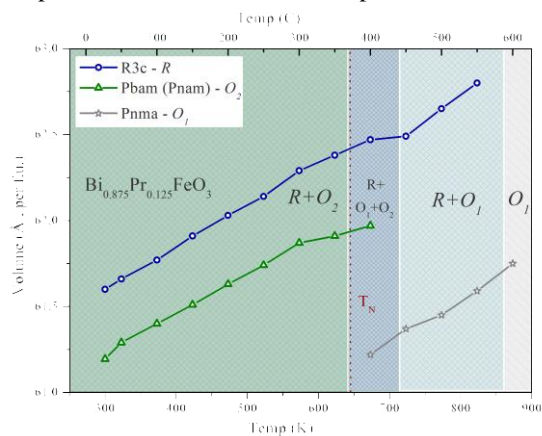


Fig.1: Structural phase diagram of  $\text{Bi}_{0.875}\text{Pr}_{0.125}\text{FeO}_3$  compound showing phase coexistence regions along with the evolution of the unit cell volume.

The structural phase transition occurring in the vicinity of the triple point is of particular interest as its mechanism can decipher a driving force of the polar - nonpolar phase transformations. Taking into account available structural data for RE-doped  $\text{BiFeO}_3$  solid solutions [4] and the evolution of crystal structure estimated for  $\text{Bi}_{0.875}\text{Pr}_{0.125}\text{FeO}_3$  compound we consider the dominant role of the chemical bond peculiarities associated with orbital hybridization along with the size effect in the structural phase transitions in  $\text{BiFeO}_3$  based materials.

1. Y. H. Chu, Q. Zhan, C.-H. Yang et al., Appl. Phys. Lett. **92** (2008) 102909.
2. G. L. Yuan, S. W. Or, J. M. Liu, Z. G. Liu, Appl. Phys. Lett. **89** (2006) 052905.
3. D.V. Karpinsky, I.O. Troyanchuk, O.S. Mantyskaya et al., Solid State Commun. **151** (2011) 1686.
4. I.O. Troyanchuk, D.V. Karpinsky, M.V. Bushinsky et al., J. Am. Ceram. Soc. **94** (2011) 4502.

## High temperature single-phased magnetic ferroelectrics: $\text{BiFeO}_3\text{-Bi}(\text{Zn}_{1/2}\text{Ti}_{1/2})\text{O}_3\text{-PbTiO}_3$ ceramics

Linlin Zhang, Xianbo Hou, Jian Yu\*

Functional Materials Research Laboratory, Tongji University, Shanghai, China

Email: [0zhanglinlin0621@tongji.edu.cn](mailto:0zhanglinlin0621@tongji.edu.cn) \*[jyu@tongji.edu.cn](mailto:jyu@tongji.edu.cn)

Multiferroic materials have been attracting an increasingly fundamental and practical interest. Owing to the lacking of high-temperature single-phased ferromagnetic-ferroelectric multiferroics with strong linear magnetoelectric coupling effect, these materials have not been widely applied yet. Meanwhile, synthesization of pure single-phased and high insulating material is a major challenge for material scientists. Here, perovskite-structured  $\text{BiFeO}_3\text{-Bi}(\text{Zn}_{1/2}\text{Ti}_{1/2})\text{O}_3\text{-PbTiO}_3$  solid solutions, fabricated with conventional electroceramic processing and sintered at temperature around  $890^\circ\text{C}$ , were systematically investigated. The authors reported on the dielectric, ferroelectric and magnetic properties of the ternary solid solutions. It was found that high insulating and low dielectric loss ceramics are obtained for the  $(1-2x)\text{BiFeO}_3\text{-xBi}(\text{Zn}_{1/2}\text{Ti}_{1/2})\text{O}_3\text{-xPbTiO}_3$  ceramics ( $0.05 \leq x \leq 0.25$ ). Pure rhombohedral phase of  $0.7\text{BiFeO}_3\text{-0.14Bi}(\text{Zn}_{1/2}\text{Ti}_{1/2})\text{O}_3\text{-0.16PbTiO}_3$  was obtained, with the dielectric loss below  $0.04@1\text{kHz}$ , which bore  $4\text{kV DC}$  electric field at  $100^\circ\text{C}$  and exhibited piezoelectric constant of  $d_{33} = 0.5 \text{ pC/N}$ . Two ferroic phase transition temperatures of  $T_N \sim 330^\circ\text{C}$  and  $T_C \sim 810^\circ\text{C}$  were detected from DSC and DTA measurements, respectively. The magnetic and electrical properties were also studied under different heat treatments. Our researching is to design high temperature high performed perovskite-structured magnetic-ferroelectric multiferroic compounds.

## Does the lithium niobate Z cut surface reconstruct?

Rebecca Hölscher, Simone Sanna, Wolf Gero Schmidt

Computational Materials Science Group, University of Paderborn, Germany

Email: reh@mail.upb.de

LiNbO<sub>3</sub> (LN) is a frequently used material for optical and acoustic applications due to its strong piezoelectric, pyroelectric, and photorefractive properties. As for other ferroelectric materials, the surface reactivity can be manipulated by polarization reversal. This opens the possibility for the realization of devices like molecular detectors<sup>82</sup>.

Unfortunately, there are only few data about the microscopic structure of the surface available. While most existing studies<sup>83</sup>, do not find surface periodicities other than the 1x1 bulk-truncated structure, there are very recent indications that at elevated temperatures large surface reconstructions might occur for both the positive and the negative Z cut<sup>84</sup>.

Here surface phase diagrams calculated from first principles are presented. Thereby a large number of structures of different morphology and stoichiometry are investigated by means of density functional theory within the generalized gradient approximation (DFT-GGA). In contrast to earlier work<sup>85</sup>, the possibility of large surface reconstructions is taken into account. Interestingly, we find that for certain preparation conditions indeed large surface reconstructions may be stable. Their formation is rationalized in terms of surface electrostatic interactions.

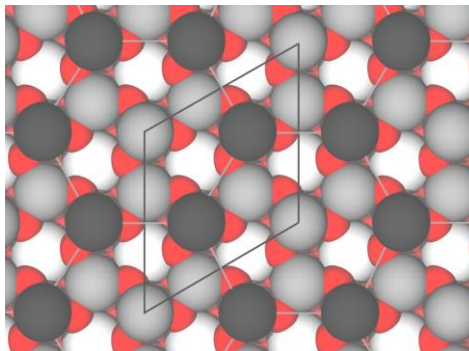


Fig. 23: Top view of one of the possible reconstructions on the LiNbO<sub>3</sub> (0001) surface, lithium atoms are shown in grey (light and dark), niobium atoms in white and oxygen atoms in red, the surface unit cell is outlined in dark grey.

<sup>82</sup> D. Li, M. H. Zhao, J. Garra, et al., “Direct *in situ* determination of the polarization dependence of physisorption on ferroelectric surfaces”, *Nature Materials*, vol. 7, p. 473-477, 2008.

<sup>83</sup> S. Rode, R. Hölscher, S. Sanna, et al., “Atomic-resolution imaging of the polar (0001) surface of LiNbO<sub>3</sub> in aqueous solution by frequency modulation atomic force microscopy”, *Physical Review B*, vol. 86, p. 075468, 2012.

<sup>84</sup> A. Kühnle, S. Klassen, S. Rode, Private communication

<sup>85</sup> S. Sanna, W. G. Schmidt, “Lithium niobate X-cut, Y-cut, and Z-cut surfaces from *ab initio* theory”, *Physical Review B*, vol. 81, p. 214116, 2010.

# Behavior of Polar Nanoregions in Lead Free Relaxor Ferroelectrics

Chandra Shekhar Pandey<sup>1</sup>, Juergen Schreuer<sup>1</sup>, Manfred Buriánek<sup>2</sup>, Manfred Muehlberg<sup>2</sup>

<sup>1</sup>Institute of Geology, Mineralogy, & Geophysics, Crystallography, Ruhr University Bochum, Bochum, Germany

<sup>2</sup>Institute of Crystallography, University of Cologne, Cologne, Germany

Email: chandrashekhar.pandey@rub.de

An understanding on how the polar nanoregions (PNRs) affect on the properties of materials is a subject of great curiosity, challenge and one of the key parameters of interest to the materials scientist as well as condensed matter physicist. PNRs observed in relaxor ferroelectrics (hereafter relaxors) are an example of this type of challenge.

Behavior of polar nanoregion and hence relaxor behavior of lead free relaxor ferroelectrics will be explained incorporating elastic properties, and Czochralski grown  $\text{Ca}_{0.28}\text{Ba}_{0.72}\text{Nb}_2\text{O}_6$  (CBN-28) as an example. CBN-28 belongs to the partially filled tetragonal tungsten bronze (TTB) family. The unit cell of the TTB-structure contains two voids of type A1 and A2, and four small voids of type C. Consequently, the general formula for niobates with TTB-structure is  $(A1)_2(A2)_4C_4\text{Nb}_{10}\text{O}_{30}$ . Recently, we have reported the relaxor behavior of CBN-28 with the evidence of the existence of the Burns temperature  $T_B$ , and the intermediate characteristic temperature  $T^*$ .<sup>86</sup> In the present work, we show that the dynamics of polar nanoregions (and hence the relaxor behavior) strongly varies with the variation of composition<sup>87</sup> (see Fig. 1), and doping<sup>88</sup>. Evidence is found for a more pronounced relaxor behavior with increasing A1 site content. Curie temperature ( $T_C$ ) and the Burns temperature are also very sensitive to the composition, whereas the  $T^*$  appears unaffected with composition variation and doping. Presented results open the perspective to understand the relaxor behavior of many lead free relaxors with composition variation, and doping above  $T_C$ .

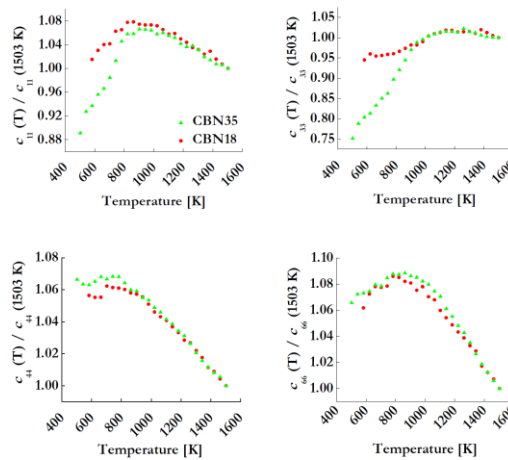


Fig. 24: Temperature evolution of the  $c_{ij}$  (in relative scale) for CBN- $x$  in its paraelectric phase.

<sup>86</sup> Pandey *et. al.*, Anomalous elastic behavior of relaxor ferroelectric  $\text{Ca}_{0.28}\text{Ba}_{0.72}\text{Nb}_2\text{O}_6$  single crystals, Phys. Rev. B **84**, 174102, 2011.

<sup>87</sup> Pandey *et. al.*, Relaxor behavior of  $\text{Ca}_x\text{Ba}_{1-x}\text{Nb}_2\text{O}_6$  tuned by Ca/Ba ratio and investigated by resonant ultrasound spectroscopy, Phys. Rev. B (Accepted for publication, in press), 2013.

<sup>88</sup> Pandey *et. al.*, Anomalous elastic behavior of relaxor ferroelectric  $\text{Ca}_{0.28}\text{Ba}_{0.72}\text{Nb}_2\text{O}_6:\text{Ce}$  studied by resonant ultrasound spectroscopy, Appl. Phys. Lett. **99**, 252901, 2011.

## Ferroelectric and dielectric properties of solid solutions in the system $x\text{Bi}_{0.5}\text{K}_{0.5}\text{TiO}_3 - (100-x)\text{Bi}_{0.5}\text{Na}_{0.5}\text{ZrO}_3$

Espen Tjønneland Wefring, Maxim I. Morozov, Mari-Ann Einarsrud, Tor Grande

Department of Materials Science and Engineering,  
Norwegian University of Science and Technology, Trondheim, Norway

Email: tor.grande@ntnu.no

Development of lead-free piezoelectric ceramics has attained significant attention in recent years as there are environmental concerns related to the lead containing  $\text{Pb}(\text{Zr}_{1-x}\text{Ti}_x)\text{O}_3$  commonly used today.<sup>89</sup> One prominent class of lead-free alternatives is mixed bismuth-alkali titanates such as  $\text{Bi}_{0.5}\text{K}_{0.5}\text{TiO}_3$  and  $\text{Bi}_{0.5}\text{Na}_{0.5}\text{TiO}_3$ , both in their pure state and as a solid solution. Substitution of Zr for Ti in these materials has not been studied widely earlier. Here we report on synthesis and characterization of the  $x\text{Bi}_{0.5}\text{K}_{0.5}\text{TiO}_3 - (100-x)\text{Bi}_{0.5}\text{Na}_{0.5}\text{ZrO}_3$  (BKT-BNZ) materials system.

Conventional solid state synthesis was used to fabricate dense and phase pure ceramics. Structural characterization was done using x-ray diffraction both at room temperature (RT, Fig. 1) and elevated temperatures (RT - 600°C). A transition from tetragonal BKT to pseudo cubic xBKT was identified for  $x \leq 90$ . Dielectric properties were studied with respect to both temperature (RT - 600°C) and frequency ( $10^a$  Hz,  $a = \{6, \dots, 0\}$ ) and the electric field induced strain response of the materials was investigated at RT. All materials studied show relaxor-like behaviour with a frequency dispersion of the dielectric constant, and the maximum dielectric constant was observed for 85BKT (Fig. 2). The maximum strain response of the composition joint was seen for 90BKT. Both compositions of maximum performance are close to where the phase transition from tetragonal to pseudo cubic crystal structure was observed.

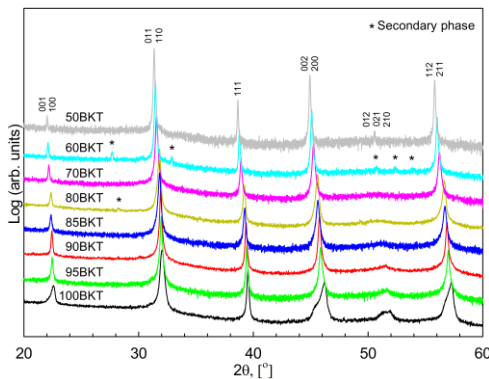


Fig. 25: X-ray diffractograms of compositions 100BKT-50BKT

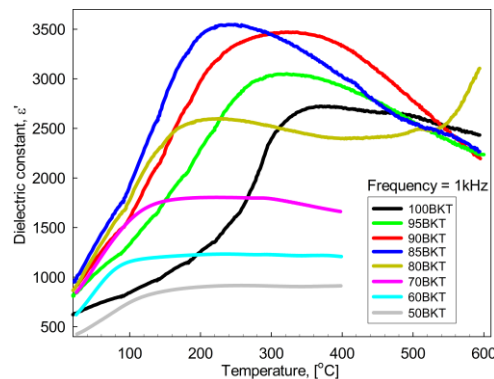


Fig. 2: Temperature dependence of the dielectric constant for 100BKT - 50BKT at 1 kHz

<sup>89</sup> J. Rödel, W. Jo, et al. "Perspective on the Development of Lead-free Piezoceramics.", J. Am. Ceram. Soc., vol. 92(6), p. 1153-1177, 2009.



## Influence of Plasma-Source Ion Irradiation on Formation of Domain Structure in MgO:LiNbO<sub>3</sub> Single Crystals

Shur Vladimir, Pryakhina Victoria, Alikin Denis, Negashev Stanislav, Besedina Nadezhda

Ferroelectric Laboratory, Institute of Natural Sciences, Ural Federal University,  
Ekaterinburg, Russia

Email: victoria.pryahina@labfer.usu.ru

We have studied the formation of the domain structure with charged domain walls (CDW) under application of the inhomogeneous electric field in MgO doped LiNbO<sub>3</sub> single crystals after plasma-source ion irradiation.

The investigated samples represented 1-mm-thick plates of single-crystalline LiNbO<sub>3</sub> doped by 5% MgO (MgO:LN) cut normal to the polar axis. The irradiation of Z+ polar surface was done by Ar<sup>+</sup> ions with energy ranged from 2 to 5 keV (flux 0.5 μA/cm<sup>2</sup>, fluence (1-6)·10<sup>17</sup> cm<sup>-2</sup>, time 5 min, vacuum 10<sup>-4</sup> Torr). The maximal temperature caused by radiation heating ranged from 400 to 600°C. The sample was fixed on the metal substrate by silver paste to prevent modification of the opposite polar surface.

It was shown that plasma-source ion irradiation of MgO:LN drastically increases the bulk conductivity due to out-diffusion of oxygen in vacuum<sup>90</sup>. The spatially inhomogeneous sample conductivity leads to dependence of the switching field in the bulk on the depth. The field distribution in the bulk and its time dependence has been extracted from the recorded interferometry pattern on the YZ side of the sample. The variation of the irradiation energy and duration allows to change the field value and distribution.

Kinetics of the domain structure during polarization reversal under application of triangular and rectangular field pulses has been studied by recording of instantaneous domain images. The switching field was applied using liquid electrolyte (saturated LiCl water solution). The formation and growth of domains with CDW<sup>91</sup> have been observed. Interaction between approaching domain walls leads to formation of the dense net of residual domains.

The position and the shape of the stable CDW have been studied by confocal Raman spectroscopy and domain visualization on YZ cross-sections. The correlation between domain structure and field distribution has been revealed.

The equipment of the UCSU “Modern Nanotechnology”, Institute of Natural Sciences, UrFU has been used. The research was made possible in part by RFBR (Grants 13-02-01391-a, 12-02-31377, 11-02-91066-CNRS-a), by Ministry of Education and Science (Contracts 14.513.12.0006, 16.740.11.0585).

<sup>90</sup> V.I. Pryakhina, V.Ya. Shur, D.O. Alikin, S.A. Negashev, “Polarization reversal in MgO:LiNbO<sub>3</sub> single crystals modified by plasma-source ion irradiation”, *Ferroelectrics*, vol. 439, p. 20-32, 2012.

<sup>91</sup> V.Ya. Shur, E.L. Rumyantsev, E.V. Nikolaeva, E.I. Shishkin, “Formation and evolution of charged domain walls in congruent lithium niobate”, *Appl. Phys. Lett.*, vol. 77, p. 3636-3638, 2000.



# Interface Control of Surface Photochemical Reactivity in Ultrathin Epitaxial Ferroelectric Films

Jason Chen<sup>1,5\*</sup>, Haidong Lu<sup>2</sup>, Heng-Jui Liu<sup>3</sup>, Ying-Hao Chu<sup>3</sup>, Steve Dunn<sup>4</sup>, Kostya (Ken) Ostrikov<sup>5,6</sup>, Alexei Gruverman<sup>2</sup>, and Nagarajan Valanoor<sup>1</sup>

<sup>1</sup>School of Materials Science and Engineering, University of New South Wales, Sydney, New South Wales 2052, Australia

<sup>2</sup>Department of Physics and Astronomy University of Nebraska Lincoln, Lincoln, NE 68588, United States

<sup>3</sup>Department of Materials Science and Engineering, National Chiao Tung University, Hsinchu, Taiwan

<sup>4</sup>School of Engineering and Materials, Queen Mary University of London, Mile End Road, E1 4NS, London

<sup>5</sup>CSIRO Materials Science and Engineering, P. O. Box 218, Lindfield, New South Wales 2070, Australia

<sup>6</sup>School of Physics, The University of Sydney, Sydney, New South Wales 2006, Australia

**Email:** jason.chen1@student.unsw.edu.au

Asymmetrical electrical boundary conditions in (001)-oriented  $\text{Pb}(\text{Zr}_{0.2}\text{Ti}_{0.8})\text{O}_3$  (PZT) epitaxial ultrathin ferroelectric films are exploited to control surface photochemical reactivity determined by the sign of the surface polarization charge. The preferential orientation of polarization in the as-grown PZT layer can be manipulated by choosing an appropriate type of the bottom electrode material. Photochemical activity of the PZT surfaces with different surface polarization charges has been tested by studying deposition of silver nanoparticles from  $\text{AgNO}_3$  solution under UV irradiation. We found that PZT surfaces with preferential  $\text{C}^+$  orientation possess a more active surface for metal reduction than their  $\text{C}^-$  counterparts, evidenced by large differences in the concentration of deposited silver nanoparticles. This effect is attributed to band bending at the bottom interface which varies depending on the difference in work functions of PZT and electrode materials. A full description of the band profile will be presented to explain the observed effects.

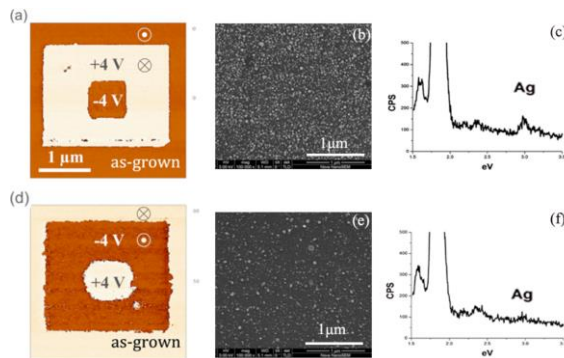


**Figure 1.** PFM (a, d), SEM (b, e) and EDX (c, f) data acquired in PZT/SRO/STO (a-c) and PZT/LSCO/STO (d-f). The PFM images demonstrate that the bottom electrode controls the as-grown polarization orientation. The SEM images obtained after UV irradiation show the appearance of particulates with the particle density being visibly higher on PZT/SRO/STO. EDX scans confirm the presence of Ag on both samples after UV irradiation with the intensity of the Ag signal being more prominent in PZT/SRO/STO.

*This work is supported by Australian Research Council (ARC), Australian Nanotechnology Network (ANN), EPSRC, National Science Foundation - Materials Research Science and Engineering Center (NSF grant DMR-080521). J.C. thanks CSIRO for OCE Ph.D. top-up scholarship support.*

\* jason.chen1@student.unsw.edu.au

## Multiscale modeling of multiferroic nanocomposites

Prokhorenko Sergei, Igor Kornev

Laboratoire Structure, Propriétés et Modélisation des Solides, Ecole Centrale Paris

Email: [sergei.prokhorenko@ecp.fr](mailto:sergei.prokhorenko@ecp.fr)

Multiferroic and magnetoelectric crystals form a very specific class of materials with possibly wide range of applications in novel electronic devices, such as next-generation biomagnetic sensors, actuators, energy storage and tunable microwave devices. Owing to coexistence of several order parameters of different nature and various coupling mechanisms between them, modeling of multiferroic compounds becomes one of the main challenges in the field of material-design.

Leaving aside the problem of pure single-phase multiferroics, our study focuses on nanocomposites comprising multiferroic and ferroelectric compounds with perovskite structure. Taking as a base an existing *ab initio* effective Hamiltonian model<sup>92</sup>, we develop a new methodological extension targeting better consideration of local and global symmetry of the supercell structure. As a consequence, short-range intersite dynamical matrix obtains a bigger set of independent coefficients<sup>93</sup> and thus encodes the local morphology of the material, while dipole-dipole interaction symmetry captures the global structure, e.g. connectivity of the composite.

The developed computational scheme is then applied to  $\text{BiFeO}_3$  based nanocomposites. It is shown that by varying geometrical characteristics of the structure such as connectivity of inclusion components, surface area of the hetero-interface or fractality of the host matrix, one can drastically change energy balance between short-range and long-range interactions allowing for transition temperature tuning, control of the symmetry of the ordered phases, and change of coupling between different order parameters. For instance,  $\text{BiFeO}_3$ - $\text{BaTiO}_3$  nanocomposites with different connectivities and nanoscale morphology show rich crossover behavior patterns (Fig.1).

The obtained results show that the developed methodology captures main features of nanocomposites systems, opening a new path to optimization and design of multiferroic materials. This work is supported by ERA.Net RUS, STProject-133, Nano-C grant.

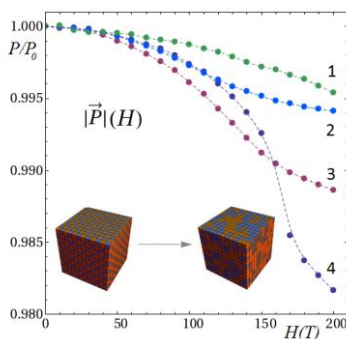


Fig.1  $(\text{BiFeO}_3)_{0.5}(\text{BaTiO}_3)_{0.5}$ ; Magnetolectric effect dependency on geometry during “Checkerboard”- “Disordered mixture” crossover. This figure shows dependence of normalized polarization on applied external magnetic field for structures with different texture. While in checkerboard structure (curve 1) the coupling between polarization and magnetic field is purely defined by interaction of electric dipoles at the interface, the disordered mixture (curve 4) exhibits behavior close to  $\text{BiFeO}_3$  nanoclusters embedded in polarizable matrix.

<sup>92</sup> Zhong, D. Vanderbilt, K. Rabe *Phys. Rev. Lett.* **73**, 1861 (1994); *Phys. Rev. B* **52**, 6301 (1995)

<sup>93</sup> A. A. Maradudin, S. H. Vosko *Rev. Mod. Phys.* **40**, 1 (1968)

---

## **PFM Poster**

Forum Hall

*Monday, July 22 2013, 01:00 pm - 04:30 pm*

## Piezo- and ferroelectricity of cellular polypropylene electrets films characterized by piezoresponse force microscopy

Faxin Li<sup>1</sup>, Chenhong Miao<sup>1</sup>, Yao Sun<sup>1</sup>, Yongping Wan<sup>2</sup>

<sup>1</sup>State Key Lab for Turbulence and Complex Systems, College of Engineering, Peking University, Beijing, 100871, China

<sup>2</sup>School of Aeronautics and Astronautics, Tongji University, Shanghai, 200050, China

Email: lifaxin@pku.edu.cn

Cellular electrets polymer is a new ferroelectret material exhibiting large piezoelectricity and has attracted considerable attentions in research and industries. Property characterization is very important for this material and current investigations are mostly on macroscopic properties. In this work, we conduct nanoscale piezoelectric and ferroelectric characterizations of cellular polypropylene (PP) films using piezoresponse force microscopy (PFM). First, both the single-frequency (or conventional) PFM and the dual frequency resonance-tracking PFM testing were conducted to map the converse piezoelectric constant  $d_{33}$  of the cellular PP film, which is only 13-18pC/N for the former and 7-11C/N for the latter, strongly dependent of the vibration amplitude (or pressing force). Then, using the switching spectroscopy PFM (SS-PFM), we studied ferroelectricity of the cellular PP films. Results show that it exhibits the typical ferroelectric-like phase hysteresis loops and butterfly-shaped amplitude loops, which is similar to that of a poly(vinylidene fluoride) (PVDF) ferroelectric polymer film (See Fig.1). However, both the phase and amplitude loops of the PP film are intensively asymmetric, which is thought caused by the nonzero remnant polarization after poling. Finally, the  $D-E$  hysteresis loops of both the cellular PP film and PVDF film were measured by a ferroelectric analyzer, using the same wave form as that in the SS-PFM, and show significant differences. In conclusion, we suggest that the ferroelectric-like behavior of cellular electrets polymers can well be distinguished from that of typical ferroelectrics, both macroscopically and microscopically.

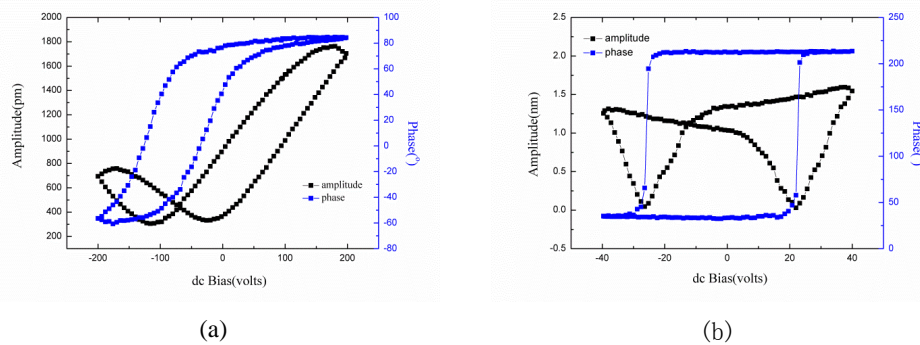


Fig.1 Phase hysteresis loops and amplitude butterfly loops of (a) cellular PP films and (b) PVDF films characterized by switching spectroscopy PFM

## Nanoscale switching behavior of BiFeO<sub>3</sub> film investigated by PFM and CAFM

W. Luo<sup>1,2</sup>, H. Zeng<sup>1</sup>, Y. Shuai<sup>1,2</sup>, C. Wu<sup>1</sup>, W. Zhang<sup>1</sup>, S. Zhou<sup>2</sup>, S. Gemming<sup>2</sup>, N. Du<sup>3</sup>, H. Schmidt<sup>3</sup>

<sup>1</sup>State Key Lab. of Electronic Thin Films and Integrated Devices, UESTC, Chengdu, China

<sup>2</sup>Institute of Ion Beam Physics and Materials Research, HZDR, Dresden, Germany.

<sup>3</sup>Department of Materials for Nanoelectronics, Technical University Chemnitz, Germany

**Email:** luowb@uestc.edu.cn

In this contribution, BiFeO<sub>3</sub> (BFO) polycrystalline thin films have been grown on Pt/Ti/SiO<sub>2</sub>/Si and BFO epitaxial film were deposited on SrRuO<sub>3</sub> coated SrTiO<sub>3</sub> substrates by pulsed laser deposition. Nonvolatile<sup>94</sup>, bipolar, and multilevel<sup>2</sup> resistive switching has been observed in polycrystalline thin films as shown in fig.1 (a). In contrast, the I-V loops of Au/BFO/SRO structure, shown as fig.2 (a), exhibited different RS behavior like a switchable diode. Piezoelectric force microscopy (PFM) and current atomic force microscopy (CAFM) using Pt coated tips were combined to study the obscure connection between RS and ferroelectric polarization in both polycrystalline and epitaxial BFO film. A ferroelectric-related resistive switching behavior has been observed in both the BFO/Pt and BFO/SRO structures. As it can be seen from figure 1, the conductive paths nucleated at almost the same position as the nucleation site of ferroelectric domain. As shown in fig.2 (c), the BFO epitaxial film show well defined surface step structure, which can eliminate the interfere factors on PFM and CAFM measurements from surface roughness. The BFO films were electrically switched with a set of positive and negative voltages. For these regions, local current were measured by the CAFM with a voltage of -2V. The CAFM images revealed that the conducting state of the green area shown in fig.2 (d) was modulated by about two orders of magnitude after the polarization direction was switched upwards shown as yellow area in fig.2 (c). These results demonstrated that the RS of BFO is close related to ferroelectric polarization and the barrier height of the top and bottom contact.

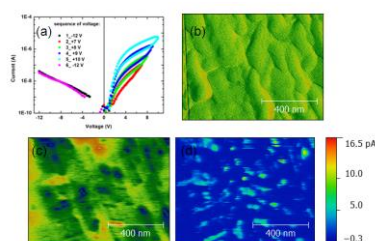


Fig. 26: multilevel resistive switching I-V plots (a), surface morphology (b), ferroelectric domain structure (c), and local current image drawn in a log scale (d) of BFO polycrystalline films deposited on Pt/Ti/SiO<sub>2</sub>/Si substrate, respectively.

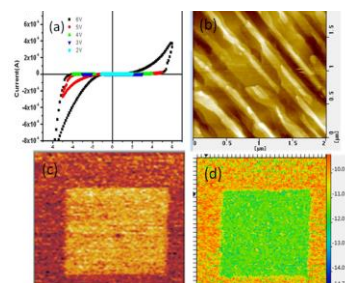


Fig. 2: Switchable diode I-V curves (a) surface morphology (b), ferroelectric domain structure (c), and local current image drawn in a log scale (d) of BFO films deposited on SrRuO<sub>3</sub> coated SrTiO<sub>3</sub> substrate, respectively.

<sup>1</sup> Y. Shuai, S. Zhou, C. Wu, W. Zhang, D. Bürger, S. Slesazek, T. Mikolajick, M. Helm, and H. Schmidt, Control of rectifying and resistive switching behavior in BiFeO<sub>3</sub> thin films, Appl. Phys. Express 4, p. 095802, 2011.

<sup>2</sup> Y. Shuai, X. Ou, W. Luo, N. Du, C. Wu, W. Zhang, D. Burger, C. Mayr, R. Schuffny, S. Zhou, M. Helm, and H. Schmidt, Nonvolatile multilevel resistive switching in Ar<sup>+</sup> irradiated BiFeO<sub>3</sub> thin films, IEEE Elec. Dev. Lett., vol. 34, p. 54-56, 2013.

## Force microscopy study of Magnetoelectric coupling in perovskite FM/FE thin films heterostructures

P. Mirzadeh Vaghefi<sup>1</sup>, C. A. P. Alves<sup>1</sup>, F. Figueiras<sup>1</sup>, A.C. Lourenço<sup>1</sup>, V. S. Amaral<sup>1</sup>

<sup>1</sup> Department of Physics & CICECO, University of Aveiro, 3810-193 Aveiro,

Email: pegah.mirzadeh@ua.pt

The coupling of magnetic, strain and dielectric degrees of freedom and the potential multifunctionalities revived the interest on multiferroics oxides<sup>95,96,97</sup>. Understanding dynamic coupling between order parameters on the local scale is a major problem in Condensed Matter Physics and will also be the key to future device applications of Strongly Correlated Electron (SCE) oxide materials. These applications of ferroelectric materials for electronic devices require the quantitative study of local switching behaviour.

In this work  $\text{La}_{1-x}\text{Ba}_x\text{MnO}_3$  (33nm)/ $\text{BaTiO}_3$  (34nm)/ $\text{La}_{1-x}\text{Ba}_x\text{MnO}_3$  (33nm) trilayer films were grown coherently on Si (100) and  $\text{Al}_2\text{O}_3$  (001) oriented substrates by UHV RF-magnetron sputtering. X-ray diffraction was used to analyse film growth orientation and texture. Considering that the polarization can exist at a nanoscale volume, we used the piezo-force and magnetic force scanning probe microscopies (PFM/MFM) for studying local electrical and electromechanical properties of the manganite overlayer and to study the modification of trilayers with application of local-bias. Local poling is also used to modify nearby magnetic areas via mechanical stress and field effects at voltages,  $-/+30$ ,  $-/+20$  and  $-/+10$  V, as shown in figure 1. Local piezoelectric hysteresis measurements detect electric field-induced deformation at a nanoscale. We observe a clear modification of the piezo-response of trilayer surface encompassing local piezoelectric hysteresis measurements which detect electric field-induced deformation on the nanoscale and contrast change in magnetic areas via mechanical stress and field effects, which make them interesting issues to continue work on them. Also, no deformation of topography was observed at  $-/+10$  V.

The work was partially supported by FCT projects PTDC/FIS/105416/2008, PTDC/CTM/099415/2008 – FCOMP-01-0124-FEDER-009368 and PEst-C/CTM/LA0011/2011

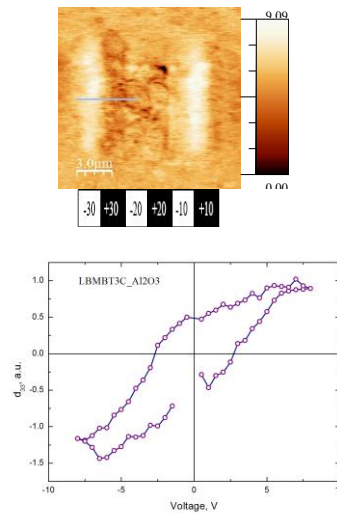


Figure 1: (a) PFM image of the area after poling of -30, 30, -20, 20, -10 and 10V from left to right, on trilayer film deposited on oriented  $\text{Al}_2\text{O}_3$  substrate, (b) hysteresis loop of trilayer on  $\text{Al}_2\text{O}_3$  substrate.

<sup>95</sup> W. Eerenstein, N. D. Mathur and J. F. Scott, , Nature, 442, 7104, 759-765, 2006.

<sup>96</sup> S. W. Cheong and M. Mostovoy, , Nature Materials, 6, 1, 13-20, 2007.

<sup>97</sup> R. Ramesh and N. A. Spaldin, , Nature Materials, 6, 1, 21-29, 2007.

## SPM study of localized magnetoelectric effect in BaTiO<sub>3</sub>/Hexaferrite composite ceramics

Harsh Trivedi<sup>1</sup>, Vladimir V. Shvartsman<sup>1</sup>, Doru C. Lupascu<sup>1</sup>, Robert C. Pullar<sup>2,3</sup>, Andrei Kholkin<sup>2,3</sup>

<sup>1</sup>Institute for Materials Science, University of Duisburg-Essen, Essen, Germany

<sup>2</sup>CICECO, University of Aveiro, Aveiro, Portugal

<sup>3</sup>Department of Materials and Ceramic Engineering, University of Aveiro, Aveiro, Portugal

Email: harsh.trivedi@uni-due.de

Composite multiferroics are the materials with Piezoelectric and magnetostrictive constituent phases, with an indirect stress mediated coupling at the interface resulting in a bulk magnetoelectric effect. As compared to the single phase multiferroics the coupling in composites is usually large and exists at room temperature, however due to general conducting nature of the magnetic phase in composites, bulk measurements of ferroelectric properties is difficult. In this study, composite ceramics with a homogeneous distribution of piezoelectric (BaTiO<sub>3</sub>) and magnetostrictive hexaferrite (BaFe<sub>12</sub>O<sub>19</sub>/SrFe<sub>12</sub>O<sub>19</sub>) phases were investigated locally using Scanning Probe Microscopy (SPM) techniques like MFM (Magnetic Force Microscopy) and PFM (Piezoresponse Force Microscopy). The domain patterns of each constituent phase (Viz. Magnetic and Ferroelectric) were observed under applied conjugate (Electric/Magnetic) fields and correlated with the virgin state of the domains. Apparent direct and indirect coupling effects were observed in the form of restructuring of magnetic domain and changes in the switching properties of ferroelectric domains. In the end an analysis for magnetic domain wall motion is presented considering the Bloch-wall case.

## Modulating domain wall conduction in epitaxial $\text{Pb}(\text{Zr}_{0.2}\text{Ti}_{0.8})\text{O}_3$ thin films by varying oxygen vacancy densities

Gaponenko Iaroslav<sup>1</sup>, Karthik Jambunathan<sup>2</sup>, Martin Lane W.<sup>2</sup>, Paruch Patrycja<sup>1</sup>

<sup>1</sup>MaNEP-DPMC, University of Geneva, Geneva, Switzerland, CH-1205

<sup>2</sup>DMRL, University of Illinois, Urbana, IL, USA 61801

Email: [iaroslav.gaponenko@unige.ch](mailto:iaroslav.gaponenko@unige.ch)

Electrical conduction at domain walls in otherwise insulating ferroelectric or multiferroic materials has been variously explained as intrinsic – with local structural changes decreasing the band gap [1], extrinsic – where defects preferentially accumulating at domain walls allow a conduction pathway across the sample [2], or as a dynamical phenomenon related to (ir)reversible microscopic displacements of the domain walls in an applied electric field [3]. In particular in  $\text{BiFeO}_3$ , recent studies have highlighted the importance of oxygen vacancies for the observed conduction, both at domain walls [4] and at more complex closure/vortex structures [5].

Here, we report on the significant role of oxygen vacancies in the domain wall conduction we have previously demonstrated at  $180^\circ$  domain walls in epitaxial  $\text{Pb}(\text{Zr}_{0.2}\text{Ti}_{0.8})\text{O}_3$  thin films [6]. For these studies, we compare the conduction behavior of two different types of epitaxial PZT thin films grown on  $\text{SrRuO}_3$  electrodes: the first grown by off-axis RF magnetron sputtering on  $\text{SrTiO}_3$  (STO), the second grown by pulsed laser deposition (PLD) on  $\text{DyScO}_3$  (DSO). Both types of samples present a smooth surface with a slightly granular morphology and a RMS roughness of 0.3 nm, but the Czochralski-grown DSO substrates show higher crystalline quality and less dislocations than Verneuil-grown STO, and present much lower densities of oxygen vacancies.

Using piezoresponse force microscopy (PFM) and conductive atomic force microscopy(c-AFM) we show that contrary to the case of sputtered films, which show domain wall conduction as-grown, no domain-wall-specific current is observed in the PLD grown films at low-medium voltages. At high voltages, displacement currents related to the nucleation and growth of new domains are observed throughout the whole sample, not specifically at the domain wall, together with static hot-spots of localized current possibly related to pin-hole defects. However, after high-vacuum annealing of the PLD-grown films at  $300^\circ\text{C}$  for 30 minutes, domain wall conduction is recovered, and shows qualitatively similar behavior to that observed in the sputtered films.

These results suggest that a threshold density of oxygen vacancies – naturally occurring in the case of sputtered films, or engineered artificially for the PLD films – is needed for conduction at the domain walls.

[1] J. Seidel *et al*, Nature Mater. **8**, 229-234 (2009)

[2] J. Seidel *et al*, Phys. Rev. Lett. **105**, 197603 (2010)

[3] P. Maksymovych *et al*, Nano Lett. **11**, 1906 (2011)

[4] S. Farokhipoor *et al*, J. Appl. Phys. **112**, 052003 (2012)

[5] N. Balke *et al*, Nature Physics **8**, 81-88 (2012)

[6] J. Guyonnet *et al*, Adv. Mater. **23**, 5377 (2011)



## Piezoresponse force microscopy study of doped (K,Na)NbO<sub>3</sub>-based ceramics for piezoactuator applications

Danka Gobeljic<sup>1</sup>, Vladimir Shvartsman<sup>1</sup>, Ke Want<sup>2</sup>, Wook Jo<sup>3</sup>, Jing-Feng Li<sup>2</sup>, Jürgen Rödel<sup>3</sup>, Doru C. Lupascu<sup>1</sup>

<sup>1</sup>Institute for Materials Science, Universität Duisburg-Essen, Essen, Germany

<sup>2</sup>State Key Laboratory of New Ceramics and Fine Processing, Tsinghua University, Beijing, P.R. China

<sup>3</sup>Institute of Materials Science, Technische Universität Darmstadt, Darmstadt, Germany

Email: danka.gobeljic@uni-due.de

A current development of potential lead-free alternatives to Pb(Zr,Ti)O<sub>3</sub> (PZT) suggests (K,Na)NbO<sub>3</sub> (KNN)-based materials as one of the most promising, lead-free piezoceramics. Owing to its excellent electromechanical properties, particular dopants-modified KNN is suitable for high-precision, temperature-stable actuator applications. Material, besides high piezoelectric constant  $d_{33}$ , exhibits high field-induced strain of significant stability in a range from room temperature up to 175 °C<sup>98</sup>.

Here, we demonstrate results of a Piezoresponse Force Microscopy (PFM) study on 0.95(Na<sub>0.49</sub>K<sub>0.49</sub>Li<sub>0.02</sub>)(Nb<sub>0.8</sub>Ta<sub>0.2</sub>)O<sub>3</sub>-0.05CaZrO<sub>3</sub> ceramics. Investigation of the temperature dependent domain evolution, indicating a sequence of phase transformation responsible for enhanced piezoelectric properties, is revealed. Correspondingly, locally obtained longitudinal piezoelectric coefficient shows comparable temperature behavior as macroscopic small piezoelectric coefficient,  $d_{33}$ .

Demonstrated study provides nanoscopic insight on mechanisms of enhanced electromechanical properties in the studied KNN-based ceramics, establishing correlation with macroscopically determined material properties.

---

<sup>98</sup> K. Wang, F. Yao, W. Jo, D. Gobeljic, V. V. Shvartsman, D. C. Lupascu, J.F. Li and J. Rödel, "Temperature-Insensitive (K,Na)NbO<sub>3</sub>-based Lead-free Piezo Actuator Ceramics", Accepted by Adv. Funct. Mat. 2013.

## PFM images of non-ferroelectric thin films

Borowiak Alexis<sup>1</sup>, Vilquin Bertrand<sup>2</sup>, Baboux Nicolas<sup>1</sup>, Brice Gautier<sup>1</sup>

<sup>1</sup>Institut des Nanotechnologies de Lyon, INSA de Lyon, 20, avenue Albert Einstein, 69621 Villeurbanne, France

<sup>2</sup>Institut des Nanotechnologies de Lyon, Ecole Centrale de Lyon, 36 avenue Guy de Collongue, 69134 Ecully cedex, France

Email: [alexis.borowiak@insa-lyon.fr](mailto:alexis.borowiak@insa-lyon.fr)

Piezoresponse Force Microscopy (PFM) is a powerful tool for the characterization of ferroelectric materials thanks to its ability to map and control in a non destructive way domain structures in ferroelectric films<sup>99</sup>.

Most of the time, the ferroelectric behaviour of a film is tested by writing domains of opposite polarisation with the Atomic Force Microscope (AFM) tip and/or by performing hysteresis loops with the AFM tip as a top electrode. A given sample is declared ferroelectric when domains of opposite direction have been detected, corresponding to zones of distinct contrast on the PFM image, or when an open hysteresis loop is obtained. More prudently in certain cases, the ferroelectricity is at last attested only when the contrast is stable within several hours<sup>100</sup>.

But as the thickness of the films studied by PFM decrease, data become difficult to interpret. In particular, charges trapped after current injection due to leakage currents may contribute in a non-negligible way to the final contrast of PFM images. As a result a convincing PFM contrast has been recently observed in non-ferroelectric oxides such as SrTiO<sub>3</sub><sup>101</sup>, (La<sub>x</sub>Sr<sub>1-x</sub>)MnO<sub>3</sub><sup>102</sup> and CaCu<sub>3</sub>Ti<sub>4</sub>O<sub>12</sub><sup>103</sup>. This is not disturbing when the sample under consideration is known to be paraelectric but it may become a real problem when very thin layers of a well-known ferroelectric material are under study.

In this communication, we will show that the standard procedure used in order to show the ferroelectricity of a film can be applied to a non-ferroelectric sample with apparently the same results. To do so, we use a LaAlO<sub>3</sub> amorphous dielectric film and apply similar voltages as for artificially written ferroelectric domains. The resulting pattern is imaged by PFM and exhibit zones of distinct PFM contrasts, stable with time, similar to the one obtained with ferroelectric samples.

We will explain these results, try and choose the experimental parameters which minimize these effects, and compare with results obtained on BaTiO<sub>3</sub> thin films prepared by Molecular Beam Epitaxy which are supposed to be ferroelectric. The aim of this study is to establish a reliable procedure which would remove any ambiguity in the characterization of the ferroelectric nature of such samples.

<sup>99</sup> A. Gruverman, O. Auciello, H. Tokumoto, "Scanning force microscopy for the study of domain structure in ferroelectric thin films", J. Vac. Sci. Technol. B., vol. 14 (2), p. 602-605, 1996.

<sup>100</sup> V. Garcia, S. Fusil, K. Bouzouane, S. Enouz-Vedrenne, N. D. Mathur, A. Barthélémy, M. Bibes, "Giant tunnel electroresistance for non-destructive readout of ferroelectric states", Nature, vol. 460, p. 81-84, 2009.

<sup>101</sup> A. Kholkin, I. Bdikin, T. Ostapchuk, J. Petzelt, "Room temperature surface piezoelectricity in SrTiO<sub>3</sub> ceramics via piezoresponse force microscopy", Appl. Phys. Lett., vol. 93, 222905, 2008.

<sup>102</sup> R. F. Mamin, I. K. Bdikin, A. L. Kholkin, "Locally induced charged states in La<sub>0.89</sub>Sr<sub>0.11</sub>MnO<sub>3</sub> single crystals", Appl. Phys. Lett., vol. 94, 222901, 2009.

<sup>103</sup> R. Tararam, I.K. Bdikin, N. Panwar, J. A. Varela, P. R. Bueno, A. L. Kholkin, "Nanoscale electromechanical properties of CaCu<sub>3</sub>Ti<sub>4</sub>O<sub>12</sub> ceramics", J. Appl. Phys., vol. 110, 052101, 2011.

## Morphological and Ferroelectric Studies of LiNbO<sub>3</sub> Films Prepared by a Sputtering Deposition

D.A. Kiselev, R.N. Zhukov, A.S. Bykov, M.D. Malinkovich, Yu.N. Parkhomenko

Department of the Material Science of Semiconductors and Dielectrics  
National University of Science and Technology "MISiS"  
Leninskiy pr. 4, 119049 Moscow, Russian Federation  
Email: dm.kiselev@misis.ru

Lithium niobate (LiNbO<sub>3</sub>) has been one of the promising ferroelectric materials for potential applications in the area of modulators, switches, actuators, surface acoustic wave devices, sensors, and wave guides because of its high piezoelectric, photorefractive, and nonlinear optical properties. However, thin films are advantageous over their bulk counterparts for various device applications. From a technological point of view, the prospect of LiNbO<sub>3</sub> thin films on Si substrates is particularly attractive in view to combine the ferro- and piezoelectric processing capabilities of with lithium niobate the obvious advantages of Si. Indeed, Si technology continues to dominate the microelectronics market, providing a rigid substrate ideal for lithographic techniques. This will make possible the development of integrated devices in which sources, detectors and electronics, as well as ferroelectric and waveguiding components may be produced on the same wafer.

The studied LiNbO<sub>3</sub> films were deposited by radio-frequencies magnetron sputtering of the single-crystalline target in Ar/O=1 atmosphere (0.6 Pa) on n-type Si (100) and Si (111) substrates ( $\rho = 2 \Omega \cdot \text{cm}$ ) with SiO<sub>2</sub> buffer layer (thickness ~ 5 nm). The subsequent thermal annealing of the obtained structures has been done in air at 700 °C. Atomic force microscopy measurements indicate that the surface roughness of the LiNbO<sub>3</sub> thin films was 4-10 nm, which meets the demands for practical waveguiding devices. The ferroelectric properties have been studied by visualization of the as-growth domain structure (vertical and lateral component polarization), recording induced ferroelectric states and the hysteresis loops by piezoresponse force microscopy (PFM) using Scanning probe laboratory NTEGRA-Prima (NT MDT, Russia). Also, Kelvin probe force microscopy (KPFM) was used extensively for determining electric properties in these heterostructures.

The research was financially supported by the Ministry of Education and Science of the Russian Federation out using the equipment of Common-Use Scientific Center "Material Science and Metallurgy" at NUST "MISiS" and by the Program for Creation and Development of the National University of Science and Technology "MISiS".

## Local stress enhancement of ferroelectricity in GFO thin films

<sup>1</sup>Maksym Iazykov, <sup>2</sup>Alexandre Thomasson, <sup>1</sup>Brice Gautier, <sup>2</sup>Natalie Viart

<sup>1</sup> Institut des Nanotechnologies de Lyon, Villeurbanne/France

<sup>2</sup> Institut de Physique et Chimie des Matériaux de Strasbourg, Strasbourg/France

Email: maksym.iazykov@insa-lyon.fr

Today multiferroics become more and more attractive materials because of their fundamental ability to combine ferroelectric and magnetic properties<sup>1</sup>. In recent years, multiferroics have been intensively investigated. However, most of the reported materials demonstrate coupling of the magnetic and ferroelectric order parameters at the temperatures much lower or higher than room temperature<sup>2,3</sup>.

The promising candidate for potential application is Ga<sub>2-x</sub>Fe<sub>x</sub>O<sub>3</sub> (GFO) oxides which show ferromagnetic, ferroelectric and ferroelastic properties at near-ambient temperatures<sup>4,5</sup>. This phenomenon gives them great potential in technological application<sup>6,7</sup>. However, physical properties of GFO oxides have been proved for single-crystal samples whereas the device integration requires using of thin films of these materials which were rarely reported until now<sup>8-10</sup>.

In this work we performed local probe electrical characterization of GFO thin films. Conductive AFM measurements showed strong leakage currents when sufficiently high voltages were applied to the sample. This fact makes impossible domain switching by Piezoresponse Force Microscopy (PFM). The direct mechanical domain writing has not provided switching of polarization. Despite this, we showed that possible ferroelectricity of GFO can be studied using the Atomic Force Microscope (AFM) as instrument for local stress enhancement of ferroelectricity. Such method allowed us relatively easy writing of the ferroelectric domains avoiding the problem of the leakage currents. We hope that this approach will lead to better understanding of current and capacitance measurements at the microscopic level that is critical for possible improvement of the magnetoelectric properties of GFO.

<sup>1</sup>N.A. Hill, J. Phys. Chem. B 104, 6694, 2000

<sup>2</sup>A.M. dos Santos, S.Parashar, A.R.Raju et al, Solid State Comm. 122(1-2) 49-52, 2002

<sup>3</sup>N.Hur, S.Park, P.A.Sharma, J.S.Ahn, S.Guha and S.W.Cheong, Nature. 429 392-5, 2004

<sup>4</sup>J.P.Remeika, J. Appl. Phys. 31 263S, 1960

<sup>5</sup>G.T.Rado, Phys. Rev. Lett. 13 335, 1964

<sup>6</sup>J.H. Jung, M. Matsubara, T. Arima, J.P. He, Y. Kaneko, Y. Tokura, Phys.Rev. Lett. 93, 037 403, 2004

<sup>7</sup>A.M. Kalashnikova, R.V. Pisarev, L.N. Bezmaternykh, V.L. Temerov, A. Kirilyuk, T. Rasing, JETP Lett. 81, 452, 2005

<sup>8</sup>D. C. Kundaliya, S. B. Ogale, S. Dhar, et al., J. Magn. Magn. Mater. 299 307-311, 2006

<sup>9</sup>Z. H. Sun, Y. L. Zhou, S. Y. Dai, et al., Appl. Phys. A: Mater. Sci. Process. 91 97-100, 2008

<sup>10</sup>M. Trassin, N. Viart, G. Versini, et al., Journal of Materials Chemistry 19 8876-8880, 2009

## Buffer layer effect on microstructures and properties of Pb(Zr,Ti)O<sub>3</sub>-CoFe<sub>2</sub>O<sub>4</sub> layered thin films

Hongcai He, Feifei Luo, Neng Qian, Ning Wang

State Key Laboratory of Electronic Thin Films and Integrated Devices and School of Microelectronics and Solid-State Electronics, University of Electronic Science and Technology of China, Chengdu 610054, P. R. China

### Abstract:

The conductive oxide LaNiO<sub>3</sub> thin film was selected as a buffer layer and a bottom electrode for the Pb(Zr,Ti)O<sub>3</sub>-CoFe<sub>2</sub>O<sub>4</sub> composite films derived from the sol-gel method in our previous work. This LaNiO<sub>3</sub> buffer obviously enhanced the magnetoelectric response of the Pb(Zr,Ti)O<sub>3</sub>-CoFe<sub>2</sub>O<sub>4</sub> bi-layered thin films. Deeper work will be introduced in this work. The LaNiO<sub>3</sub> thin films with different thickness, surface morphology, preferred orientation and conductivity are deposited on Si substrate as buffer layers to deposit Pb(Zr,Ti)O<sub>3</sub>-CoFe<sub>2</sub>O<sub>4</sub> composite films. XRD, SEM / EDS and AFM were used to characterize films microstructure. Magnetic force microscopy (MFM) and piezo-force response microscopy (PFM) were used to characterize the composite film at the local scale. Ferroelectric hysteresis loops and ferromagnetic hysteresis loops were macroscopically measured. The direct ME measurement was done in terms of the variation in the induced voltage by the applied magnetic field using a self-made equipment. The results are compared and discussed in relation to the microstructure and properties of LaNiO<sub>3</sub> buffer layers.

Acknowledgement: This work has been supported by Natural Science Foundation of China (51002020, 51272035).

## PFM study of size effects on lead-free ceramics and films of $(\text{Bi}_{0.5}\text{Na}_{0.5})_{1-x}\text{Ba}_x\text{TiO}_3$ with compositions around the morphotropic phase boundary

Norberto Salazar<sup>1</sup>, Dulce Pérez-Mezcua<sup>2</sup>, M. Lourdes Calzada<sup>2</sup>, Adriana Gil<sup>1</sup>, Jesús Ricote<sup>2</sup>

<sup>1</sup>Nanotec Electrónica S.L., Tres Cantos, Madrid, Spain

<sup>2</sup>Instituto de Ciencia de Materiales de Madrid, CSIC, Madrid, Spain

Email: norberto.salazar@nanotec.es

The increasing interest in the development of lead-free piezoelectric materials has drawn the attention to solid solutions such as  $1-x(\text{Bi}_{0.5}\text{Na}_{0.5})\text{TiO}_3-x\text{BaTiO}_3$  (BNBT). Enhanced dielectric, ferroelectric and piezoelectric properties have been observed for bulk ceramics with compositions close to the morphotropic phase boundary (MPB) between rhombohedral and tetragonal phases<sup>104</sup>. The preparation of these materials in thin film form is indispensable for their integration into microelectronic devices. However a drastic decrease in the remnant polarization of BNBT thin films respect to their bulk counterparts is reported<sup>105</sup>. This has been attributed to size effects, as the reduction of dimensions in thin films leads to smaller grains, which determines the nature of the ferroelectric domain configuration<sup>106</sup>.

In order to understand the mechanisms that lead to the size effects responsible for the reduction of the remnant properties, ceramics and films of BNBT with different grain sizes are analyzed by Piezoresponse Force Microscopy. Materials are prepared from sol-gel derived solutions<sup>107</sup>. The comparison between the results obtained in micro- and nanometric grain size materials allows us to discuss the effects of the grain size on the ferroelectric domain configuration, and to relate it to the properties. Besides, the measurement of local piezoelectric loops and the study of the mobility of the domain walls under an electric field will shed light onto the role of the grain boundaries. All measurements were carried out with a Nanotec<sup>®</sup> scanning force microscope.

<sup>104</sup> T. Takenaka, K.I. Maruyama, K. Sakata, “ $(\text{Bi}_{1/2}\text{Na}_{1/2})\text{TiO}_3\text{-BaTiO}_3$  System for Lead-Free Piezoelectric Ceramics”, Jap. J. Appl. Phys., vol 30, p. 2236-2239, 1991.

<sup>105</sup> I. Bretos, D. Alonso-San José, R. Jiménez, J. Ricote, M.L. Calzada, “Evidence of morphotropic phase boundary displacement in lead-free  $(\text{Bi}_{0.5}\text{Na}_{0.5})_{1-x}\text{Ba}_x\text{TiO}_3$  polycrystalline thin films”, Mater. Lett., vol 65, p. 2714-2716, 2011.

<sup>106</sup> M. Algueró, J. Ricote, R. Jiménez, P. Ramos, J. Carreaud, J.M. Kiat, B. Dkhil, J. Holc, M. Kosec, “Size effect in morphotropic phase boundary  $\text{PbMg}_{1/3}\text{Nb}_{2/3}\text{O}_3\text{-PbTiO}_3$ ”, Appl. Phys. Lett., vol. 91, p. 112905, 2007.

<sup>107</sup> D. Alonso-San José, R. Jiménez, I. Bretos, M.L. Calzada, “Lead-free ferroelectric  $(\text{Na}_{1/2}\text{Bi}_{1/2})\text{TiO}_3\text{-BaTiO}_3$  thin films in the morphotropic phase boundary composition: solution processing and properties”, J. Amer. Ceram. Soc., vol. 92, p. 2218-2225, 2009.

## Quantification of Electromechanical Coupling Measured with Piezoresponse Force Microscopy

Serban Lepadatu<sup>1</sup>, Markys Cain<sup>1</sup>

<sup>1</sup>National Physical Laboratory, Hampton Road, Middlesex, TW11 0LW

Email: serban.lepadatu@npl.co.uk

In this work we propose a measurement procedure for calibrating against various artifacts affecting PFM measurements using a standard procedure and sample. Further inter-laboratory comparisons should reveal any systematic differences in PFM measurements, working towards a commonly accepted PFM standard.

Piezoresponse force microscopy (PFM) is an invaluable tool for measuring the piezoresponse of functional materials at the nanoscale, allowing for high resolution measurements of the electromechanical coupling of thin films. In this work we address the challenges facing quantification of PFM by developing standards both through in-house work and inter-laboratory comparisons.

PZT 20-80 epitaxial thin films have been grown to 100 nm thickness on  $10 \times 10 \text{ mm}^2$  1 at% Nb-doped  $\text{SrTiO}_3$  substrates and poled along the c-axis which lies perpendicular to the substrate plane. Optical lithography was used to define a series of top electrodes with varying dimensions, capacitance values, proximity and thickness. By varying the top electrode structure various effects are quantified and calibrated, including substrate bending, electrode clamping, electric field non-uniformity, tip-surface contact resistance and PFM tip displacement. Laser Doppler vibrometry (LDV) measurements of circular capacitor structures have shown uniform displacement amplitude, linearly dependent on driving voltage amplitude. For  $10 \mu\text{m}$  diameter top electrode typically  $d_{33} = 41 \pm 1 \text{ pm/V}$ . Good agreement of LDV and PFM measurements was obtained where the tip displacement is measured for driving voltage applied directly to the electrodes, resulting in  $d_{33} = 39 \pm 3 \text{ pm/V}$ , as shown in Figure 1.

Calibrating for the tip-surface contact resistance and modelling of the tip-surface interaction allows for measurements of  $d_{33}$  values when driving the voltage through the PFM tip both on the capacitor structures and on the PZT thin film in scanning mode.

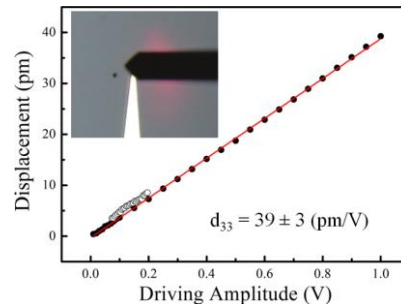


Fig. 27: PFM measurements of capacitor structure with PFM tip placement shown in the inset. Variation of vertical displacement amplitude with driving amplitude at 30 kHz is shown with solid circles for voltage applied directly to the capacitor structure (●) and open circles for voltage applied through the PFM tip (○). Linear fitting of data points gives the  $d_{33}$  value as  $39 \pm 3 \text{ pm/V}$ .

## **Nanoscale piezoresponse and thermal behavior of ferroelectric domain in multiferroic BiFeO<sub>3</sub> thin film**

Huarong Zeng, Senxing Hui, Kunyu Zhao, Guorong Li, Qingrui Yin

Key Laboratory of Inorganic Functional Materials and Devices, Shanghai Institute of Ceramics, Chinese Academy of Sciences, Shanghai 200050, China

Email: [huarongzeng@mail.sic.ac.cn](mailto:huarongzeng@mail.sic.ac.cn)

Multiferroic materials exhibit simultaneous ferroelectric and magnetic orders, which enable the coupling interaction between ferroelectric and magnetic orders. This coupling interaction produces various possibilities in the realization of mutual control and detection of electrical polarization and magnetism. Recent advances of multiferroelectrics have offered an imperative need to develop high resolution tool for in-situ investigating ferroelectric/ferromagnetic domain configurations and local physical properties. Here we introduce piezoresponse force microscopy (PFM) and  $3\omega$ -scanning thermal microscopy ( $3\omega$ -SThM) to characterize local piezoresponse and thermal behavior of nanoscale domains in multiferroic BiFeO<sub>3</sub> (BFO) thin film. The  $3\omega$ -SThM, developed based on the customer-developed PFM, provides a powerful tool for imaging locally thermal distributions and characterizing local thermal conductivity. Ultrahigh resolution PFM imaging reveals that ferroelectric domain wall width is around 2.18 nm for multiferroic BiFeO<sub>3</sub> thin film, which is well consistent with the upper limit values of 2 nm via first principle study [1]. Good polarization retention behavior was also demonstrated in the BFO thin film by the PFM tip fields. Local thermal conductivity of ferroelectric domains of BFO thin film was firstly performed by  $3\omega$ -SThM, and was found to be 1.525 W/m·K. The local thermal conductivity dependence of the domain switching behavior was also investigated and discussed in the present study.



## The kinetics of the domain structure of TGS crystals investigated near phase transition temperature by means of AFM

O.M.Golitsyna, V.O.Chulakova, S.N.Drozhdin

Voronezh State University / Voronezh / Russia

Email: golitsynaom@yandex.ru

Formation of the domain structure of triglycine sulfate crystals (TGS) after their rapid cooling from the paraelectric to the ferroelectric phase is essentially non-equilibrium process, which has been studied in detail<sup>1,2</sup> in the temperature range of stability of the spontaneous polarization  $P_S$ , i.e. far from the phase transition temperature  $T_C$ . It is of interest to study this process in the vicinity of the phase transition, where the fluctuations of  $P_S$  can significantly affect the kinetics of forming and evolution of the domain structure. The analysis of the literature shows that to date, such experimental studies have not been carried out at temperatures close to  $T_C$ . In this paper the evolution of the domain structure of both nominally pure TGS and TGS doped with L, $\alpha$ -alanine was investigated at temperatures near  $T_C$ .

The visualization of the domain structure of the polar cuts of these crystals was carried out by means of atomic force microscopy (AFM) in contact mode of piezoelectric response (microscope Solver P47 Pro, cantilevers NSG 11/TiN). The samples were transferred into the paraelectric phase and after 30 minutes of exposure at  $\approx 333$  K cooled at a rate of 10 K / min to the desired temperature. The accuracy of temperature stabilizing was equal to  $\pm 0,05$  K. At a given temperature  $T \leq T_C - 1.0$  K the evolution of freshly formed domain structure was observed.

The kinetics of the formation of the domain structure was studied by means of calculations of the space-time correlation function  $C(r, t) = \langle S(r, t)S(0, t) \rangle$ , where  $S(r, t) = +1$  or  $-1$ , depending on the sign of the domain at the point with coordinate  $r$ . The following parameters of the domain structure also were calculated:

1) average characteristic correlation length  $L$ , defined as the distance at which the correlation function takes the value of  $C(r = L(t), t) = 1/2$  with respect to its original value at  $r = 0$ , 2) the total perimeter of the domain walls, 3) areas of the domains of opposite sign, and the coefficient of static unipolarity.

It was found that near  $T_C$  the forming of a stable domain configuration occurs with a significantly different kinetic parameters comparing with those calculated in<sup>1,2</sup>. It was found that the formation of the domain structure in nominally pure and doped TGS is described by different kinetic parameters. The general tendency of investigated processes of domain structure evolution is their slowing down with the distance from the Curie temperature.

<sup>1</sup> H.Orihara, N.Tomita, Y. Ishibashi. Ferroelectrics, vol.95, p.45-48, 1989.

<sup>2</sup> V. Likodimos, M. Labardi, M. Allegrini. Physical Review B66, p.024104-1-02410407, 2002.

## Piezo Force Microscopy as a Fundamental Tool for Characterization of Nanoporous PbTiO<sub>3</sub> Thin Films

Alichandra Castro,<sup>1</sup> Paula Ferreira,<sup>1</sup> Brian Rodriguez<sup>2</sup>, Paula M. Vilarinho<sup>1</sup>

<sup>1</sup>Department of Materials and Ceramic Engineering, University of Aveiro, Aveiro, Portugal

<sup>2</sup>Conway Institute of Biomolecular and Biomedical Research, University College Dublin, Dublin, Ireland

Email: alichandra@ua.pt

Nowadays, due to the increasing demand on portable electronic devices with ultrahigh density data storage and lower power consumption, the miniaturization of the ferroelectric has become an important issue. This progressive development requires the morphology control of materials and the understanding the effects of size reduction on properties at the nanoscale, namely the ferroelectric properties. Within this context, we have been exploiting nano and mesoporosity in ferroelectric materials, because ordered meso and nano porous thin film arrays may be used as ferroelectric platforms for the conception of new multifunctional materials, such as multiferroics. Multiferroics materials are currently of great interest for applications in microelectronics. However, preparing nanoporous oxide thin films is not a trivial task and the influence of porosity on the piezo and ferroelectric properties of these ferroelectric matrices is practically unknown. Due to exceptional spatial resolution, Scanning Probe Microscopy (SPM) techniques and in particular Piezoresponse Force Microscopy has become an important high resolution characterization tool for visualization of domain structures in ferroelectric thin films at the nanoscale.

Thus, in this work, Vertical Piezoresponse Force Microscopy (VPFM), Lateral Piezoresponse Force Microscopy (LPFM), and Switching Spectroscopy Piezoresponse Force Microscopy (SSPFM) are used to characterize the piezoelectric and ferroelectric properties of mesostructured PbTiO<sub>3</sub> thin films prepared by sol-gel and evaporation-induced self-assembly methodologies.<sup>108</sup> The porous PbTiO<sub>3</sub> thin films were thermally treated at different temperatures in order to assess the effect of the microstructure crystallization evolution on the ferroelectric properties and the results obtained for nanoporous thin films are compared with PbTiO<sub>3</sub> dense thin films prepared under the same conditions. Scanning electron microscopy (SEM) and PFM results clearly demonstrate the existence of two distinct areas, which exhibit different crystallinity and consequently different local piezoelectric properties. The area with strong out-of-plane piezoresponse increases with the thermal treatment temperature, as well as the tetragonal phase. In addition, at a more local scale it is also observed that the regions near the pores exhibit a higher piezoresponse that is possibly associated with a higher degree of crystallinity in these regions. The ferroelectric behaviour in these samples was also demonstrated by the typical square-shaped piezoelectric hysteresis loops. Some of these hysteresis loops exhibit imprint and the relation between this vertical and lateral shift is related to the processing conditions and porosity. We evaluated also the piezoelectric and switching properties in different grains using PFM and SS-PFM. The size influence of each grains on electric properties was discussed as a function of coercive bias, imprint voltage and saturation response. Microstructural details were analyzed by Scanning Electron Microscopy (SEM), Transmission Electron Microscopy and Ultra-Raman. X-ray diffraction (XRD) analyses were used to characterize the phase content, lattice parameters and mesoporosity.

### Acknowledgements

The authors thank FCT and FEDER (QREN – COMPETE) for funding the project PTDC/CTM/098130/2008 and to the FCT for the Doctoral fellowship SFRH/BD/67121/2009. We thank also to the COST Action MP0904 SIMUFER for funding the STSM in Dublin.

<sup>108</sup> P. Ferreira, R. Z. Hou, A. Wu, M.-G. Willinger, P. M. Vilarinho, J. Mosa, C. Laberty-Robert, C. Boissière, D. Grosso, C. Sanchez, "Nanoporous Piezo- and Ferroelectric Thin Films", *Langmuir*, vol. 28, p. 2944-2949, 2012.

## Local Polarization Reversal in the Vicinity of 180° Domain Wall in Lithium Niobate

Ievlev Anton<sup>1</sup>, Shur Vladimir<sup>1</sup>, Neradovskiy Maxim<sup>1</sup>, Turigin Anton<sup>1</sup>,  
Morozovska Anna<sup>2</sup>, Eliseev Eugene<sup>2</sup>, and Kalinin Sergei<sup>3</sup>

<sup>1</sup>Ferroelectric Laboratory, Ural Federal University, Ekaterinburg, Russia

<sup>2</sup>Lashkaryov Institute of Semiconductor Physics, National Academy of Sciences of Ukraine,  
Kiev, Ukraine

<sup>3</sup>The Center for Nanophase Materials Sciences and Technology Division,  
Oak Ridge National Laboratory, Oak Ridge, TN, USA

Email: maxim.neradovskiy@labfer.usu.ru

Local polarization reversal under the action of local electric field produced by conductive tip of scanning probe microscope has been studied in the vicinity of the existing flat domain wall in 30- $\mu\text{m}$ -thick single crystalline plate of periodically poled congruent lithium niobate (CLN). The polarization reversal has been carried out on different distances from existing domain wall.

Two modes of tip motion between switching points were used. **Non-contact mode** represents tip motion at distance about 2  $\mu\text{m}$  over the sample surface. Polarization reversal at distances above 250 nm from the wall led to formation of isolated domains (Fig 1a) with linear dependence of radius on pulse amplitude. Switching at distance < 250 nm from the wall led to round shaped shifts of the wall (Fig. 1b,c). **Contact mode** uses the motion of the grounded tip in contact with the surface. Formation of prolate triangular shifts (length 350 nm) (Fig 1d) and nanodomain chains with period 100 nm (Fig 1e,f) was observed for the tip motion across the wall.

The observed domain kinetics has been explained by polarization reversal under the action of residual depolarization field and stimulation of polarization reversal along the path of grounded SPM tip due to effective external screening. Analytical and numerical simulations of the spatial distribution of residual depolarization field in the vicinity of the isolated needle-like domain justified the proposed model.

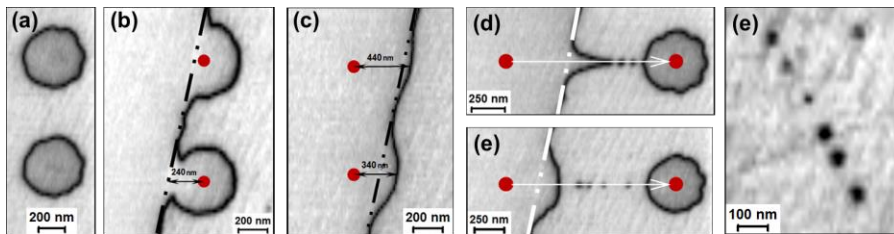


Figure 1. Domain structures formed as a result of local switching near the flat 180° domain wall. (a) isolated domains; (b), (c) round-shaped shifts of the wall; (d) prolate triangular shift; (e), (f) nanodomain chains.

The equipment of the UCSU “Modern Nanotechnology”, Institute of Natural Sciences, UrFU has been used. The research was made possible in part by RFBR (Grants 12-02-31377-mol-a, 13-02-01391-a, 11-02-91066-CNRS-a), by Ministry of Education and Science (Contracts 14.513.12.0006 and 16.740.11.0585).

## Size effect of the space charge modulation in semiconductor caused by ferroelectric domain structure

Anna N. Morozovska,<sup>1</sup> Eugene A. Eliseev,<sup>2</sup> Olexander V. Varenyk<sup>3</sup>, and Sergei V. Kalinin<sup>4</sup>,

<sup>1</sup> Institute of Physics, National Academy of Sciences of Ukraine,  
41, pr. Nauki, 03028 Kiev, Ukraine

<sup>2</sup> Institute for Problems of Materials Science, National Academy of Sciences of Ukraine,  
3, Krjijanovskogo, 03142 Kiev, Ukraine

<sup>3</sup> Taras Shevchenko Kiev National University, Radiophysical Faculty  
4g, pr. Akademika Hlushkova, 03022 Kiev, Ukraine

<sup>4</sup> The Center for Nanophase Materials Sciences, Oak Ridge National Laboratory,  
Oak Ridge, TN 37831

Email: [morozo@i.com.ua](mailto:morozo@i.com.ua)

We consider a typical heterostructure “domain patterned ferroelectric film – ultra-thin physical gap (dielectric layer) – semiconductor (electrolyte)”, where the semiconductor can be an incipient ferroelectric, high-k narrow-gap semiconductors, covered with water adsorbents. Unexpectedly we have found that the space charge modulation profile and amplitude in the semiconductor, that screens the spontaneous polarization of a 180-degree domain structure of ferroelectric, nonlinearly depends on the domain structure period  $a$ , dielectric layer thickness  $h$  and semiconductor screening radius  $R_d$  in a rather non-trivial way. Multiple size effects appearance and manifestation are defined by the relationship between  $a$ ,  $h$  and  $R_d$ . Under the absence of the dielectric layer the space charge amplitude very slowly saturates to a spontaneous polarization value with the domain size increase. When the dielectric layer is present, the amplitude saturates to the smaller values, at that the saturation value essentially decreases with the layer thickness increase, but the saturation rate is almost independent on the thickness in the actual range of parameters. The space charge amplitude strongly vanishes with the dielectric thickness increase only for small domain period, but remains almost constant for wide domains. We show that the concept of effective gap  $h^*$  can be introduced in a simple way only for a single-domain limit. Depth distribution of electric potential is nonlinear inside ferroelectric, while it is linear inside the dielectric and exponentially vanishes inside the semiconductor as anticipated. Obtained exact analytical results open the way for understanding of complex current-AFM measurements of contaminated ferroelectric surfaces in ambient atmosphere with moderate humidity.

## Study of ferroelectric nanodomains in epitaxial PbTiO<sub>3</sub> films by PFM and Raman spectroscopy

Fedir Borodavka<sup>1</sup>, Ivan Gregora<sup>1</sup>, Ausrine Bartasyte<sup>2</sup>, Samuel Margueron<sup>3</sup> and Jiří Hlinka<sup>1</sup>

<sup>1</sup>Institute of Physics, Prague, Czech Republic

<sup>2</sup>Institute Jean Lamour, Nancy, France

<sup>3</sup>Université de Lorraine and Supélec, Metz, France

Email: borodav@fzu.cz

Investigation of the domain structure in ferroelectric thin films is helpful for elucidating the interfacial processes in these materials and for finding possible ways of their applications.

Domain structure of 320 nm thin films of ferroelectric lead titanate (PTO) grown using the metalorganic chemical vapour deposition method (MOCVD) on TbScO<sub>3</sub>(TSO) and SmScO<sub>3</sub>(SSO) perovskite substrates have been studied with the help of piezoresponse force microscopy (PFM) and Raman spectroscopy techniques.

PFM (Fig.1) and Raman show that PTO films grown on SSO have preferentially a-domain orientation (in-plane orientation of spontaneous polarization  $P_S$ ), while films grown on TSO substrate have dominantly c-domain orientation (out-of-plane orientation of  $P_S$ ). The striking difference between the two domain structures can be assigned to the opposite sign of the epitaxial misfit strain at the deposition temperature 650°C ( $a'_{TSO} < a'_{PTO} < a'_{SSO}$ ).

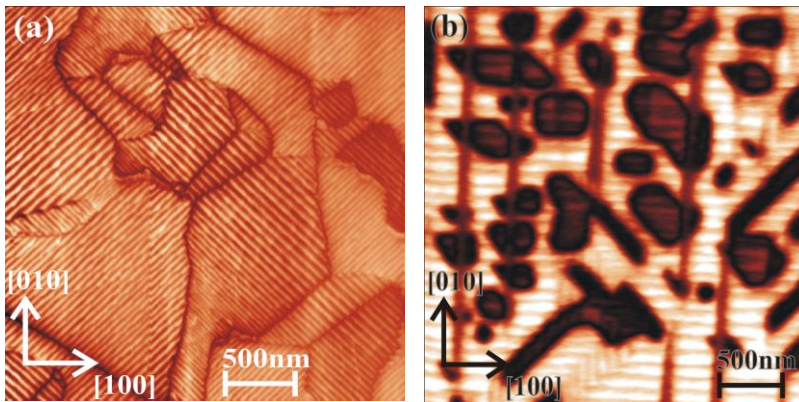


Fig. 28: PFM images of 320 nm thin PbTiO<sub>3</sub> film on SmScO<sub>3</sub> (a) and TbScO<sub>3</sub> (b) substrates. Edges of the scanned area are roughly parallel to pseudocubic axes of the substrate.

## Li diffusion and electrochemical activity in commercial LiMn<sub>2</sub>O<sub>4</sub> battery cathode by Electrochemical Strain Microscopy

Sergey Luchkin<sup>1</sup>, Andrei Kholkin<sup>1</sup>, Nina Balke<sup>2</sup>

<sup>1</sup>Dept. of Materials and Ceramics Engng. & CICECO, University of Aveiro, 3810-193 Aveiro, Portugal

<sup>2</sup>The Center for Nanophase Materials Science, Oak Ridge National Laboratory, Oak Ridge, Tennessee 37831, USA

Email: luchkin@ua.pt

Fast growth of popularity of green technologies leads to a wider use of Li batteries in applications that require high power density. High charging and discharging rates result in intensive degradation of battery materials. Deep understanding of the degradation mechanisms associated with Li transport is essential to engineer new battery materials with long life and excellent reliability. These studies should be done on a nanoscale to identify the defect sites responsible for degradation. For this, we used Electrochemical Strain Microscopy (ESM) [1], a technique similar to Piezoresponse Force Microscopy (PFM) where ionic diffusion is responsible for measurable surface displacements. Li diffusivity and electrochemical activity was studied in commercial LiMn<sub>2</sub>O<sub>4</sub> cathodes. Typical cathode consists of LiMn<sub>2</sub>O<sub>4</sub> oxide particles and conductive carbon black particles distributed in PVDF binder. In the cathodes we observed clear ESM response on the active oxide particles that is a representation of the local molar volume change caused by Li diffusion. Conductive nanoparticle distribution in the binder PVDF was detected by PFM. We used both the ESM time voltage spectroscopies to measure electrochemical activity of Li ions on the active particles. The obtained results are discussed based on the current understanding of Li diffusion mechanism in Li cathode materials. This research was supported by the European project «Nanomotion» (FP7-People-2011-ITN-290158). The authors gratefully acknowledge A. Hugues-Yanis and D. Rosato (Robert Bosch GmbH) for providing samples and valuable discussions.

1. A. N. Morozovska, E. A. Eliseev, N. Balke, and S. V. Kalinin, «Local probing of ionic diffusion by electrochemical strain microscopy: Spatial resolution and signal formation mechanisms», J. Appl. Phys. 108, 053712, 2010.

# Nanoscale Crystallization of Piezoelectric Polymer and Its Electromechanical Properties Studied by Atomic Force Microscopy

Gun Ahn<sup>1,2</sup>, [Seungbum Hong](#)<sup>1,2</sup>, [Kwangsoo No](#)<sup>1</sup>

<sup>1</sup>Department of Materials and Science Engineering, KAIST, South Korea

<sup>2</sup>Nanoscience and Technology Division, Argonne National Laboratory, USA

Email: [hong@anl.gov](mailto:hong@anl.gov), [ksno@kaist.ac.kr](mailto:ksno@kaist.ac.kr)

Piezoelectric polymers have attracted great attentions due to its potential applications to bio-compatible actuators, wireless sensors, and energy harvesting devices. However, the crystallization process and subsequent electrical poling, which are essential in realizing such devices, have been the most difficult challenges. Here, we suggest a novel method to control the crystallization process by using atomic force microscopy (AFM) equipped with a nanoscale tip of various coatings, which we can use to confine the mechanical load, electrical field and temperature gradient. Furthermore, we will present the AFM tip-induced nanoscale crystallization under different ambient condition by changing the purging gas into a sealed sample holder to study the impact of surrounding gas or water molecules on the electromechanical properties of the piezoelectric polymers.

## Measurement Anomaly of Step Width using Atomic Force Microscopy

Gun Ahn<sup>1,2</sup>, Dean J. Miller<sup>3</sup>, Kwangsoo No<sup>2</sup>, Seungbum Hong<sup>1,2</sup>

<sup>1</sup>Nanoscience and Technology Division, Argonne National Laboratory, USA

<sup>2</sup>Department of Materials and Science Engineering, KAIST, South Korea

<sup>3</sup>Electron Microscopy Center, Argonne National Laboratory, USA

Email: [hong@anl.gov](mailto:hong@anl.gov), [ksno@kaist.ac.kr](mailto:ksno@kaist.ac.kr)

We imaged the topography of silicon grating having a pitch of 10  $\mu\text{m}$  with different pixel pitch to find the optimum resolution using atomic force microscopy (AFM). We found that the step width decreased from 1300 to 108 nm and the step height increased from 172 to 184 nm when a pixel pitch in fast scan axis decreased from 625 nm to 3.9 nm. We also measured the step width and height of etched silicon grating by a focused ion beam (FIB) using Scanning Electron Microscopy (SEM) and compared the measured step height and width with AFM data. The obtained values from SEM image were 187.3 nm  $\pm$  6.2 nm and 116 nm  $\pm$  10.4 nm, which were in agreement with AFM data with 39 nm and 23 nm of pixel pitches, respectively. Lastly, our findings that RMS roughness varied less than 1 nm and converged at the value of 77.6 nm with any pixel pitch suggest we can use the RMS roughness obtained with any resolution. Based on the assumption that our results scale linearly with the size of the features of interest, we believe that one can use the optimal pixel resolution for fast and reliable topography acquisition and surface roughness analysis.



## Calibration and Correction of Signals in Piezoresponse Force-Microscopy (PFM)

Leonard F Henrichs, Andrew J Bell

Institute for Materials Research, University of Leeds, Leeds, United Kingdom

Email: pmlfh@leeds.ac.uk

Piezoresponse force-microscopy (PFM) has become a very powerful technique to study ferroelectric domains and probe local properties in polar materials. However, reliable data acquisition was often reported to be difficult. This also poses a problem for quantitative data acquisition and in fact, most of PFM data published to date are qualitative. The frequency-dependent background-signal that was found by Soergel et al., was identified as one of the problems for reliable data acquisition. Here, we confirm the existence and consequences of the background-signal. Furthermore, we show that other instabilities in PFM also have a similar effect like the background-signal. A new calibration method is presented to quantify the X-Amplitude PFM signal and subtract the background-signal in a single step by using periodically poled lithium niobate as a reference sample.

Furthermore, a simple scheme to generate background-signal free R-Amplitude and phase images out of X-Amplitude images using a freeware software is presented.

The method of calibration and correction is applied to PFM images of several ferroelectric samples.

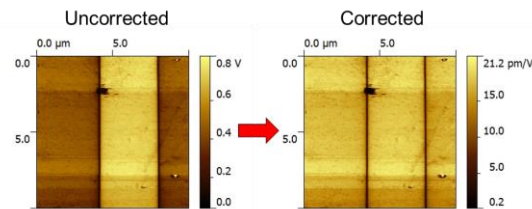


Fig. 29: Uncorrected (left) and corrected (right) PFM-Amplitude of contaminated periodically poled lithium niobate.

**Roger Prokschi**

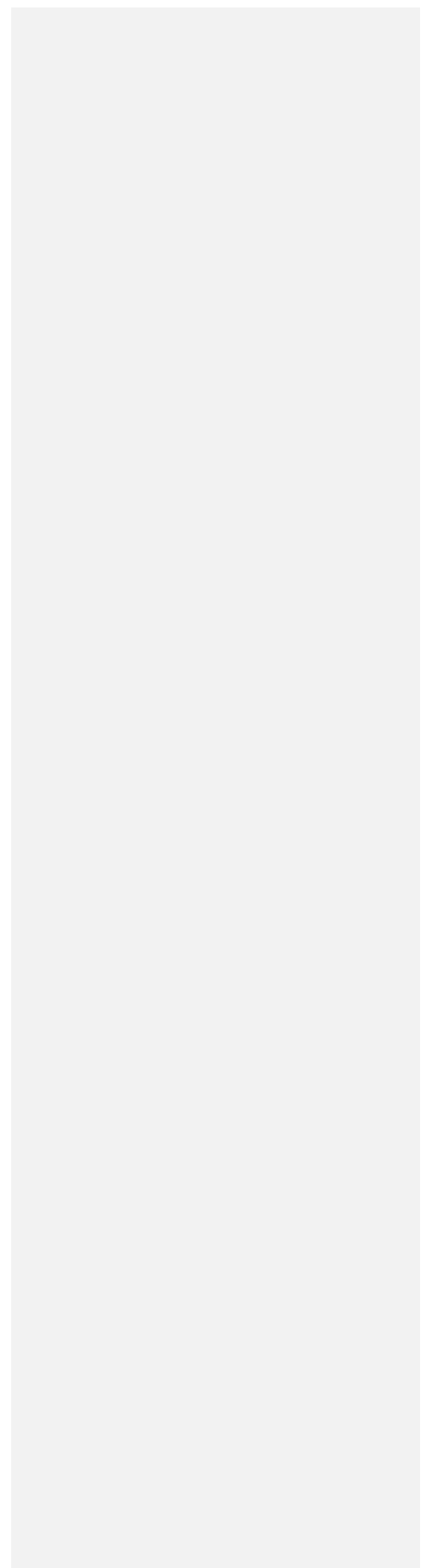
*Asylum Research, USA*

Piezoresponse Force Microscopy (PFM) and Electrochemical Strain Microscopy (ESM) have led to significant progress in our understanding of the nano-electromechanical origins of functionality in a large variety of materials. For example, hysteresis has been considered the “smoking gun” that demonstrates ferroelectricity in PFM measurements. The cantilever is an extended mechanical object with normal modes that depend on the boundary conditions both of the cantilever structure itself and on the boundary conditions imposed by the tip-sample interactions. By using the encoded and motorized optical beam controls on a commercial microscope we have been able to directly measure the extended shape of the cantilever as it interacts with various samples and in a variety of measurement modes. Integration of the laser scanning mechanism directly in the AFM has enabled these shape measurements during normal AFM operation in a variety of imaging modes ranging from force curves and contact modes to AC modes. This presentation will focus on contact and force curves measurement modes. In many cases of interest, the response of a cantilever does not behave as a simple, single-mode system. To elucidate the effects of local and long-ranged drive mechanisms on the multi-modal cantilever probe, the response of the cantilever as a function of both frequency and optical beam spot position has been measured in-situ while the cantilever is directly probing a functional material, either with PFM or ESM. Two interesting results are (i) the crossover between the dc and first contact mode is measurable at surprisingly low frequencies, and (ii) contrary to initial expectations, operating on resonance actually provides more stable and reliable quantification of the cantilever drive. This is explained in terms of the high Q-factor of the resonance. The crossover frequency is affected by the boundary conditions, specifically the tip-sample stiffness. Because of this, electrochemical interactions at the tip can lead to a measured change in the amplitude and phase of the cantilever, even when the response of the sample remains unchanged. In particular, this in turn can cause measured 180 degree phase shifts in the measured response. This phase shift – stemming from a change in the tip-sample stiffness – is indistinguishable from a phase shift originating from a change in the polarization of the sample. We will show simulations and experimental data that illustrate this crosstalk. In addition, we will discuss methods to remove separate these two effects.

**ISAF Student poster competition**

Forum Hall

*Monday, July 22 2013, 01:00 pm - 02:00 pm*



## Electric Field-Induced Deformation Behavior In Mixed $\text{Bi}_{0.5}(\text{Na}_{0.8}\text{K}_{0.2})_{0.5}\text{TiO}_3$ and $\text{Bi}_{0.5}(\text{Na}_{0.385}\text{K}_{0.09}\text{Li}_{0.025})(\text{Ti}_{0.975}\text{Ta}_{0.025})\text{O}_3$

Dae-Jun Heo, Chang-Ho Yoon, Changhyo Hong, Hyoung-Su Han, Hyun-Young Lee, and Jae-Shin Lee

School of Materials Science and Engineering, University of Ulsan, Ulsan, Republic of Korea

Email: hdj0804@hanmail.net

Recently,  $0.82(\text{Bi}_{1/2}\text{Na}_{1/2})\text{TiO}_3$ - $0.18(\text{Bi}_{1/2}\text{K}_{1/2})\text{TiO}_3$  solid solution (BNKT) ceramics attract great attention because of their large electric field-induced strains (EFIS) at relaxor (R) – ferroelectric (FE) phase boundaries. However, a critical problem that hinders their practical application to actuators is probably originated from the fact that a high electric-field required to induce the phase transition accompanying a large strain. In this study, a method to reduce the field for the R-FE transition is proposed. This study investigated the electrical and EFIS properties of BNKT ceramics-embedded  $\text{Bi}_{0.5}(\text{Na}_{0.385}\text{K}_{0.09}\text{Li}_{0.025})(\text{Ti}_{0.975}\text{Ta}_{0.025})\text{O}_3$  (BNKL-TT) ceramics, in which the fraction of BNKT was varied from 0 to 30 wt%. The normalized strain  $S_{max}/E_{max}$  of a single phase BNKT-TT ceramics was  $608 \text{ pm/V}$  at  $4 \text{ kV/mm}$ , however, it was enhanced up to  $761 \text{ pm/V}$  by embedding 30 wt% BNKT particles.

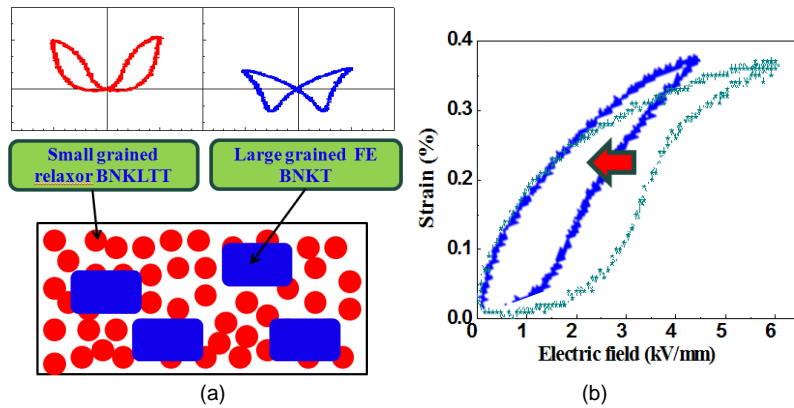


Fig. 1. Schematic of a relaxor ceramic matrix ferroelectric-relaxor composite (a) and its electric field-induced strain behavior (b) in comparison with that of a homogeneous BNKT relaxor

## Temperature Dependence of Domain Contributions to Piezoelectric Activity in the Soft- & Hard-doped Lead Zirconate Titanate and La-doped Bismuth Ferrite Lead Titanate Systems

Sayyed Adam Qaisar<sup>1</sup>, Andrew J Bell<sup>2</sup>, Timothy P Comyn<sup>3</sup>

<sup>1</sup>Institute for Materials Research, University of Leeds, Leeds, United Kingdom

Email: s.a.qaisar06@leeds.ac.uk

Previous investigations have established the significance of the Rayleigh law to explaining intrinsic and extrinsic contributions to activity in piezoelectric ceramics[1–4]. Typically investigations of domain wall contributions to the piezoelectric effect require the use of synchrotron time. Presented is a technique using a combination of weak-signal & direct-effect measurements in addition to electrical characterization to elude to the reversible and irreversible domain contributions to the piezoelectric effect in lead zirconate titanate (PZT) and bismuth ferrite lead titanate (BFPT) systems.

A new experimental apparatus has been constructed, allowing for investigation of cycling electric field & stress effects at selected temperatures on the degradation of  $d_{33}$  in piezoelectric materials. Furthermore, the device has been used to investigate the intrinsic and extrinsic contributions to the direct piezoelectric effect in PZT & La-doped BFPT. Supported by using weak-signal measurements, the domain wall behaviour and piezoelectric activity at elevated temperatures has been investigated for these material systems in addition to activity degradation.

Data from the new apparatus is presented and further discussed in relation to previously observed behaviour in PZT[5][6][7], highlighting the enhanced mechanical properties of BFPT over PZT and comparing the temperature dependence of domain contributions in both material systems

- [1] D. Damjanovic and M. Demartin, *Journal of Physics: Condensed Matter*, vol. 9, no. 23, pp. 4943–4953, Jun. 1997.
- [2] R. E. Eitel, T. R. ShROUT, and C. A. Randall, *Journal of Applied Physics*, vol. 124110, 2006.
- [3] A. Pramanick, D. Damjanovic, J. E. Daniels, J. C. Nino, and J. L. Jones, *Journal of the American Ceramic Society*, vol. 94, no. 2, pp. 293–309, Feb. 2011.
- [4] M. Davis, D. Damjanovic, and N. Setter, *Journal of Applied Physics*, vol. 084103, 2006.
- [5] J. Nuffer, *Acta Materialia*, vol. 48, no. 14, pp. 3783–3794, Sep. 2000.
- [6] H. Wang, A. a. Wereszczak, and H.-T. Lin, *Journal of Applied Physics*, vol. 105, no. 1, p. 014112, 2009.
- [7] M. Liu and K. J. Hsia, *Applied Physics Letters*, vol. 83, no. 19, p. 3978, 2003.

## General Behavior of Soft Mode and Central Mode in Strained SrTiO<sub>3</sub>/DyScO<sub>3</sub> multilayers

Volodymyr Skoromet<sup>1</sup>, Christelle Kadlec<sup>1</sup>, Jürgen Schubert<sup>2</sup>, Gregor Panaitov<sup>2</sup>, and Petr Kužel<sup>1</sup>

<sup>1</sup>Department of dielectrics, Institute of Physics, Academy of Sciences of the Czech Republic, Prague, Czech Republic

<sup>2</sup>Institute of Bio and Nanosystems, Research Centre Jülich, JARA-Fundamentals of Future Information Technology, Jülich, Germany

Email: skoromet@fzu.cz

Strontium titanate (SrTiO<sub>3</sub>, STO) single crystal is an incipient ferroelectric; its THz and sub-THz dielectric behavior is nearly entirely governed by the ferroelectric soft mode (SM). It has been shown<sup>109</sup> that the ferroelectric phase transition can be induced near the room temperature in strained epitaxial STO films if the substrate is suitably chosen, e.g. DyScO<sub>3</sub> (DSO).

It is known that the strain induced by the substrate gradually relaxes with increasing thickness of the film. To overcome this problem we prepared several heterostructures consisting of  $n \times$ STO/DSO bilayers on (110) DSO substrates by pulsed laser deposition. The thickness of each individual layer is of 50 nm, since the strain relaxation mainly occurs for thicker STO films<sup>110</sup>. The DSO layers are intended to maintain the strain over an increased total STO thickness ( $n = 2-8$ ). Interdigitated metallic electrode structure deposited on each sample allowed application of a bias electric field.

The time-domain THz spectroscopy was used to measure the temperature and electric-field dependence of the complex dielectric spectra of the samples. Two main features are observed: a ferroelectric SM and a central mode (CM), which are described by a general model consisting of a harmonic oscillator coupled with a Debye relaxation. The SM frequency  $\omega_0(T, E)$  is the key parameter which describes the temperature ( $T$ ) and electric-field ( $E$ ) evolution of the permittivity; some examples of the behavior of  $\omega_0$  are shown in Fig. 1. A comprehensive comparison of the dielectric behavior of all the structures and the underlying lattice dynamics will be discussed in the conference contribution.

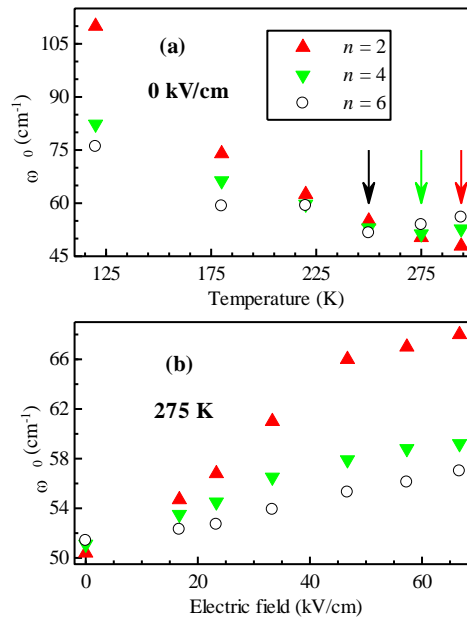


Fig. 30: (a) Temperature (at 0 kV/cm) and (b) field dependence (at 275 K) of the SM frequency for selected samples. Arrows denote the phase transition.

<sup>109</sup> J. H. Haeni et al., "Room-temperature ferroelectricity in strained SrTiO<sub>3</sub>", Nature, vol. 430, p. 758-761, 2003

<sup>110</sup> Z. Y. Zhai et al., "Dislocation density and strain distribution in SrTiO<sub>3</sub> film grown on (110) DyScO<sub>3</sub> substrate", J. Phys. D: Appl. Phys., vol. 42, 105307, 2009

## **Fabrication and characterization of BaTiO<sub>3</sub> ultrathin ferro-electric layers to investigate the origin and characteristics of domain wall conductivity.**

Alan Douglas<sup>1</sup>, Li-Wu Chang<sup>1</sup>, Marty Gregg<sup>1</sup>

<sup>1</sup>Centre for Nanostructured Media, Queens University Belfast, Belfast, Northern Ireland

Email: adouglas08@qub.ac.uk

An investigation into the fabrication and characterization of ferroelectric heterostructures was carried out. The materials of choice were a combination of ultrathin Barium Titanate (BTO) and Strontium Ruthenate (SRO), a ferroelectric and bottom electrode layer respectively; these layers were deposited on a substrate of Strontium Titanate (STO) by Pulsed Laser Deposition (PLD).

The films were then characterized by in-house measurements through Atomic Force Microscopy (AFM), Piezoresponse Force Microscopy (PFM), Transmission Electron Microscopy (TEM), and X-Ray Diffraction (XRD). Such techniques allowed the fabrication method to continually be adapted until the production high quality ultra-thin ferroelectric BTO films was achieved.

Domains and domain walls within the ultrathin ferroelectric layer were then investigated using both PFM and Scanning Tunneling Microscopy (STM), with the intention of being able to measure domain wall conductivity and investigate the factors which control conductivity. The use of STM has not been widely utilized for domain wall studies<sup>11</sup> but should allow both high-resolution conductivity mapping and direct probing of the densities of states within the domain walls.

Striving for a better understanding and control over ferroelectric domain walls will no doubt prove of use, as it will enable us to better integrate such components into a newly emerging generation of nanoscale electronic devices.

---

1. Chiu, Y.P. *et al.* "Atomic-Scale Evolution of Local Electronic Structure Across Multiferroic Domain Walls." *Advanced Materials* **23**, 1530–1534 (2011).

## Compositional dependence of PMN-PT thin films prepared by combinatorial sputtering

Fumiya Kurokawa<sup>1</sup>, Kohei Tomioka<sup>2</sup>, Hirotaka Hida<sup>1</sup>, Isaku Kanno<sup>1</sup>

<sup>1</sup> Mechanical Engineering, Kobe University, Kobe City, Hyogo, Japan

<sup>2</sup> Micro Engineering, Kyoto University, Kyoto City, Kyoto, Japan

Email: funyayorozu1112@gmail.com

In this study, we deposited  $\text{Pb}(\text{Mg}_{1/3}\text{Nb}_{2/3})\text{O}_3\text{-PbTiO}_3$  (PMN-PT) thin films on Pt/Ti/Si substrates by combinatorial sputtering to optimize the composition ratio of PMN-PT thin films. We confirmed that relative dielectric constants increase with decreasing PT ratio in PMN-PT films. On the other hand, the PMN-PT thin films showed the maximum piezoelectric coefficients  $|e_{31,f}| = 7 \sim 8 \text{ C/m}^2$  around PMN-0.45PT.

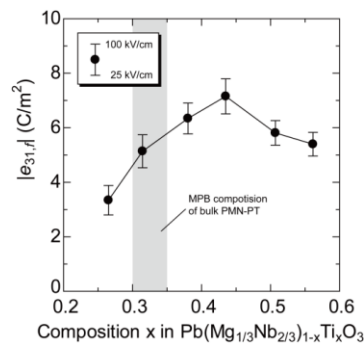
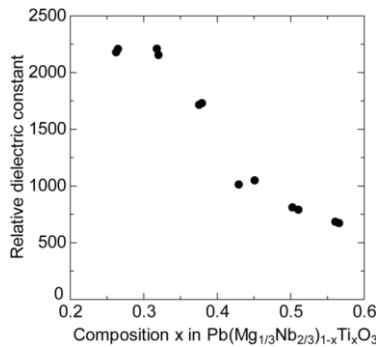


Fig.1 Relative dielectric constants of PMN-PT thin films dependence on compositional ratio

Fig.2 Piezoelectric coefficient  $|e_{31,f}|$  of PMN-PT thin films dependence on compositional ratio

Optimization of PMN/PT compositional ratio is one of important parameters for PMN-PT thin films to maximize piezoelectric properties. In this study, we deposited PMN-PT thin films by combinatorial sputtering and evaluated compositional dependence of dielectric and piezoelectric properties precisely<sup>112</sup>. Compositional gradient PMN-PT thin films were deposited by multi target co-sputtering, and pyrochlore-free PMN-PT thin films with random orientation were prepared on Pt/Ti/Si substrates. PT compositional ratio is ranging from 0.25 to 0.57, which covered MPB composition of bulk PMN-PT ceramics<sup>113</sup>. Measurement results of relative dielectric constants and transverse piezoelectric coefficients  $|e_{31,f}|$  dependence on PMN/PT compositional ratio are shown in Fig.1 and Fig.2. Relative dielectric constants increase with decreasing PT ratio, and peaked at around PMN-0.30PT which is consistent with the MPB composition of bulk PMN-PT ceramics. On the other hand, piezoelectric coefficient shows maximum value  $|e_{31,f}| = 7 \sim 8 \text{ C/m}^2$  at PMN-0.45PT, which is shifted from MPB composition of PMN-PT bulk ceramics. This shift phenomenon might be attributed to residual stress of resulting PMN-PT thin films.

<sup>112</sup> K. Tomioka, et al, "Composition dependence of piezoelectric properties of  $\text{Pb}(\text{Zr,Ti})\text{O}_3$  films prepared by combinatorial sputtering", Jpn. J. Appl. Phys., vol. 51, 09LA12, 2012.

<sup>113</sup> B. Noheda, et al, "Phase diagram of the ferroelectric relaxor  $(1-x)\text{Pb}(\text{Mg}_{1/3}\text{Nb}_{2/3})\text{O}_3\text{-xPbTiO}_3$ ", Phys. Rev. B., vol. 66, 054104, 2002.



## Processing ceramic (Bi,Sm)FeO<sub>3</sub>: comparing two methods of synthesis by microstructure, phase evolution, polarization and strain behavior

Julian Walker<sup>1,3</sup>, Peter Bryant<sup>2</sup>, Valsala Kurusingal<sup>2</sup>, Charles C. Sorrell<sup>1</sup>,

Tadej Rojac<sup>3</sup> and Nagarajan Valanoor<sup>1</sup>

<sup>1</sup>Materials Science and Engineering, University of New South Wales, Sydney, NSW, Australia

<sup>2</sup>Thales Australia, Rydalmere, Sydney, NSW, Australia

<sup>3</sup>Jozef Stefan Institute, Ljubljana, Slovenia

Email: [julian.walker@unsw.edu.au](mailto:julian.walker@unsw.edu.au)

Samarium substitution in bismuth ferrite (Bi,Sm)FeO<sub>3</sub> has been studied as a means of inducing a morphotropic phase boundary between polar rhombohedral R3c and non-polar orthorhombic Pnma structures. In such compositions there have been observations of enhanced remnant polarization, reduced coercive field and increased piezoelectric response with respect to pure BiFeO<sub>3</sub>. However these properties are published for thin film materials, while for bulk ceramics the switching behavior, which is most often studied by means of polarization- and strain-electric-field hysteresis loops, and the weak-field piezoelectric response, are mostly unknown.

In this work we present details of two processing methods utilizing surfactant addition during milling to reduce agglomerate formation and improve homogeneity of oxide mixtures. While both methods use a reaction sintering technique one method involves the use of mechanochemical activation to enhance homogeneity and reactivity of mixtures. We show that activation effectively reduces the temperatures required to complete the diffusion of Sm<sup>+3</sup> into the R3c crystal structure.

These processing methods can produce samples with high dielectric breakdown (> 180kV/cm) at fields more than double the coercive field (≈80kV/cm). At these high fields we measured large strains of up to 0.3 % within the range of 0.1-100 Hz frequencies (Fig. 1.), while polarization loops up to 500 Hz display moderate leakage and good saturation (insert of Fig. 1.). Previously piezoelectric data for these (Bi,Sm)FeO<sub>3</sub> systems have been obtained only from thin films and we now provide for the first time, a comprehensive study of piezoelectric behaviour also in bulk ceramic materials.

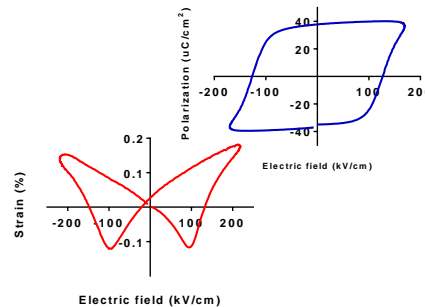


Fig. 31: Strain-electric-field hysteresis loop of reaction sintered (Bi<sub>0.88</sub>Sm<sub>0.12</sub>)FeO<sub>3</sub> measured at 220 kV/cm and 0.1Hz. Insert: Polarization-electric-field loop at 160 kV/cm and 100Hz for the same composition.

## Textured $\text{K}_{0.5}\text{Na}_{0.5}\text{NbO}_3$ thin films by aqueous chemical solution deposition on $\text{SrTiO}_3$ substrates

Ky-Nam Pham<sup>1</sup>, Maxim Morozov<sup>1</sup>, Thomas Tybell<sup>2</sup>, Tor Grande<sup>1</sup>, Mari-Ann Einarsrud<sup>1</sup>

<sup>1</sup> Department of Material Science and Engineering, Norwegian University of Science and Technology, Trondheim, Norway

<sup>2</sup> Department of Electronics and Telecommunications, Norwegian University of Science and Technology, Trondheim, Norway

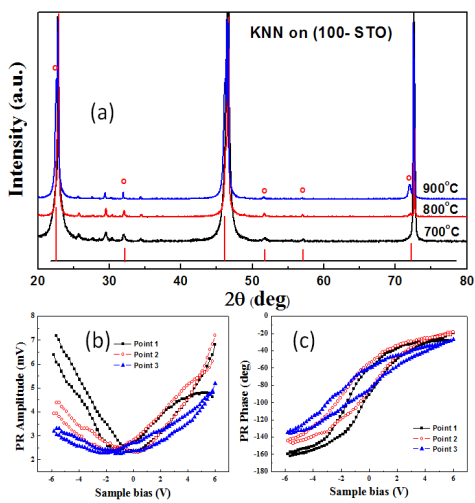
Email: pham.ky-nam@ntnu.no

The search for lead-free alternatives to PZT materials is currently going on worldwide.  $\text{Na}_{0.5}\text{K}_{0.5}\text{NbO}_3$  (KNN) thin films were fabricated on (100) and (110) oriented  $\text{SrTiO}_3$  substrates by chemical solution deposition. Stable environmentally friendly aqueous KNN precursor solutions were prepared from Na-acetate, K-acetate and Nb-ammonium oxalate and deposited onto  $\text{SrTiO}_3/\text{Nb}:\text{SrTiO}_3$  substrates by spin coating at 2500-3000 rpm for 20-40 s. The films were dried at 200 °C for 2 min using a hotplate and then pyrolysed at 400 °C for 5 min. The film thickness could be controlled by repeating the spin coating procedure. The final films were sintered at 600-900 °C for 5 min in oxygen by rapid thermal processing (RTP) with heating rate of 40 °C/s. To aid texturing of the KNN-based films, Dissolution/reprecipitation of KNN in a molten mixture of NaCl/KCl was tested to enhance texturing by incorporating salts in the solution or deposition of salt layers between the KNN layers, which could be washed away after the thermal treatment.

Homogeneous films with an average grain size down to 60 nm were prepared after heat treatment at 900 °C. The high degree of texture was confirmed by XRD, Fig. a). The intensity of the KNN (100) reflection for films on (100) oriented substrates increased with increasing sintering temperature up to 900 °C, while for KNN films deposited on (110)-oriented substrate the (110) reflect that texture could be controlled by the crystal orientation of the substrate.

The ferroelastic and piezoelectric properties of the film was confirmed by PFM, see Fig. b) and c). Local piezoelectric properties of selected films will be discussed in relation to the processing conditions, effect of the molten salts, microstructure and orientation of the substrate. The high degree of texture and the fine-grained microstructure of the KNN nano-crystalline thin films demonstrate that this environmentally friendly synthesis method is applicable for fabrication of textured lead-free ferroelectric thin films.

Fig. 32: (a) XRD patterns for the KNN thin film deposited on (100) SrTiO<sub>3</sub> substrate, sintered at various temperature as well as local piezoresponse (b) amplitude, (c) phase of the KNN thin films was sintered at 800 °C.



## Growth and Piezo-/Ferroelectric Properties of $\text{Pb}(\text{Mg}_{1/3}\text{Nb}_{2/3})\text{O}_3$ - $\text{PbTiO}_3$ - $\text{Bi}(\text{Zn}_{1/2}\text{Ti}_{1/2})\text{O}_3$ Ternary Single Crystals

Reagan Belan, Hamel Tailor, Zuo-Guang Ye

Department of Chemistry and 4D LABS, Simon Fraser University,  
Burnaby, BC, V5A 1S6, Canada

Email: rab11@sfu.ca

Single crystals of relaxor-based perovskite solid solutions, namely  $\text{Pb}(\text{Mg}_{1/3}\text{Nb}_{2/3})\text{O}_3$ - $\text{PbTiO}_3$  [PMN-PT] and  $\text{Pb}(\text{Zn}_{1/3}\text{Nb}_{2/3})\text{O}_3$ - $\text{PbTiO}_3$  [PZN-PT], show extraordinary piezoelectric performance, enabling them to be the leading choice of materials for the next generation of electromechanical transducers in a broad range of applications<sup>1</sup>. However, these materials suffer from some drawbacks, in particular, a low Curie temperature ( $T_C$ ) and a low coercive field ( $E_c$ ). In order to overcome these shortages,  $\text{Bi}(\text{Zn}_{1/2}\text{Ti}_{1/2})\text{O}_3$  [BZT] was added to ‘harden’ the PMN-PT system and the ternary solid solution system of  $\text{Pb}(\text{Mg}_{1/3}\text{Nb}_{2/3})\text{O}_3$ - $\text{PbTiO}_3$ - $\text{Bi}(\text{Zn}_{1/2}\text{Ti}_{1/2})\text{O}_3$  [PMN-PT-BZT] was prepared in our laboratory in the form of ceramics and single crystals<sup>2,3</sup>. In this work, we report the growth of the single crystals of this ternary solid solution by the high temperature solution (flux) method using a  $\text{PbO}$  and  $\text{H}_2\text{BO}_3$  mixture as flux. By varying both the temperature profile of the growth and the nominal composition of charge, large and good-quality multinucleated crystals of PMN-PT-BZT were obtained. The domain structure and phase transitions of the PMN-PT-BZT crystals are characterized by polarized light microscopy (PLM) and piezoresponse force microscopy (PFM), providing insights into the crystal growth behavior of the ternary system. The dielectric and ferroelectric properties of the crystals are also investigated, confirming that the ternary single crystals exhibit enhanced piezoelectric performance compared to their ceramic counterparts.

*This work is supported by the Office of Naval Research (Grants No. N00014-11-1-0552 and N00014-12-1-1045) and the Natural Science and Engineering Research Council of Canada.*

<sup>1</sup>Z.-G. Ye, *Mater. Res. Soc. Bull.*, Vol. **34**, No. 4, pp. 277-283 (2009).

<sup>2</sup>H. N. Tailor, A. A. Bokov, Z.-G. Ye, *Ferroelectrics*, **405**, 67-75 (2010).

<sup>3</sup>R. Belan, H. N. Tailor, X. Long, A. A. Bokov and Z.-G. Ye, *J. Cryst. Growth*, **318**, 839-845 (2011)

## Enhanced Flexoelectric Effect in a Non-ferroelectric composite

Yong Li<sup>1</sup>, Hong Wang<sup>1</sup>, Feng Xiang<sup>1</sup>, Longlong Shu<sup>1</sup>, Xiaoyong Wei<sup>1</sup>

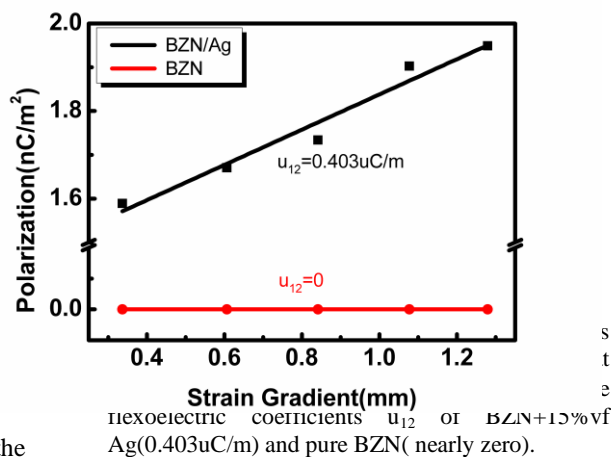
<sup>1</sup>Electronic Materials Research Laboratory, Key Laboratory of Ministry of Education, Xi'an Jiaotong University, Xi'an 710049, China

Email: liyong0509@stu.xjtu.edu.cn

Direct flexoelectric effect was investigated in a non-ferroelectric composite  $(\text{Bi}_{1.5}\text{Zn}_{0.5})(\text{Zn}_{0.5}\text{Nb}_{1.5})\text{O}_7/\text{Ag}$  (BZN/Ag) where the structure symmetry  $\infty\infty m$  permits no macro-piezoelectricity. The flexoelectric coefficient of the BZN/Ag composite was measured using beam bending method at room temperature and the value is up to  $0.4\mu\text{C}/\text{m}$ . This value is 3-4 orders magnitude higher than those of common dielectrics.

In the past few years, most of the researches on flexoelectricity were focused on ferroelectrics. We first experimentally studied the flexoelectric effect in non-ferroelectrics. In our research, the composite of BZN+15%vf Ag was prepared by solid state sintering method. The dielectric constant of the composite is above 720, and the loss below 6% at the frequency of 1kHz. The doping of silver to BZN enlarged the permittivity and  $\gamma$  value of the composite, making the flexoelectric effect enhanced.

Our study indicates that non-ferroelectrics can also have enhanced flexoelectric effect and that composite materials with high flexoelectric effect can be designed.



S  
t  
e

## High frequency magneto-impedance effects in multiferroic CoTiO<sub>2</sub>-Bi<sub>4</sub>Ti<sub>3</sub>O<sub>12</sub> multilayer films

Hanae Kijima<sup>1,3</sup>, Zhang Yiwen<sup>1</sup>, Nobukiyo Kobayashi<sup>2</sup>, Shigehiro Ohnuma<sup>1,2</sup>, Nava Setter<sup>3</sup>, Paul Muralt<sup>3</sup> and Hiroshi Masumoto<sup>1</sup>

<sup>1</sup> Center for Interdisciplinary Research, Tohoku University, Sendai, Japan

<sup>2</sup> Research Institute for Electromagnetic Materials RIEM, Sendai, Japan

<sup>3</sup> Laboratoire de Céramique, Ecole Polytechnique Fédérale de Lausanne EPFL, Lausanne, Switzerland

Email: kijima@cir.tohoku.ac.jp

Multiferroic thin film structures are of great interest for applications in the lower GHz frequency range. In our study, we combine soft magnetic thin films exhibiting a strong magneto impedance (MI) effect with ferroelectric thin films. The impedance change upon application of an external magnetic field ( $H_{ex}$ ) is supposed to occur also in magnetic-ferroelectric multilayers. It is expected that the MI effect can be suitably enhanced at magnetic resonances occurring at a few GHz.

In expectation of high permeability ( $\mu$ ) and dielectric permittivity ( $\epsilon$ ) at GHz frequencies, CoTiO<sub>2</sub> and Bi<sub>4</sub>Ti<sub>3</sub>O<sub>12</sub> are selected for the soft magnetic and dielectric layers, respectively. In this study, we present a strong resonance effect in  $\mu$  measurements, and a significant magneto-impedance effect in CoTiO<sub>2</sub>- Bi<sub>4</sub>Ti<sub>3</sub>O<sub>12</sub> multilayer films in the frequency range of 0.1-10 GHz at room temperature.

50 nm thick ferromagnetic CoTiO<sub>2</sub> layers were intercalated with Bi<sub>4</sub>Ti<sub>3</sub>O<sub>12</sub> dielectric thin films. Both were grown by rf magnetron sputtering. The frequency dependence of  $\mu$  was investigated by using the shielded parallel line method in the frequency range of 0.1-10 GHz. The  $H_{ex}$  was applied parallel to rf-magnetic field in the film plane. For the high frequency impedance analysis, micro MIM capacitors were fabricated by lithography and wet etching processes. The complex admittance ( $Y = G+iB$ ) of the film under various  $H_{ex}$  were measured by using calibrated 50 Ohm probes for the desired frequency range. The measurements are carried out at room temperature.

Figure 1 presents the frequency dependence of real and imaginary part of  $\mu$ , and  $G$  and  $B$  of CoTiO<sub>2</sub>- Bi<sub>4</sub>Ti<sub>3</sub>O<sub>12</sub> multilayer films at various  $H_{ex}$ -fields. The  $\mu''$  shows a clear peak at the ferromagnetic resonance ( $f_r$ ) at 3.76 GHz. The intensity of the peak decreases from 94.8 to nearly zero when applying a  $H_{ex}$  of 334 Oe. Interestingly,  $G$  and  $B$  values around  $f_r$  also change with varying  $H_{ex}$ . The maximum increase of  $B$  (by 12.3 %) was observed at 3.76 GHz in a magnetic field of  $H_{ex} = 96$  Oe.

### Acknowledgement

We wish to thank Dr. S. Takada for his cooperation of high frequency  $\mu$  measurement. The authors would like to thank for much help and technical assistance of Mr. [R. M. Aghdam](#) (EPFL),

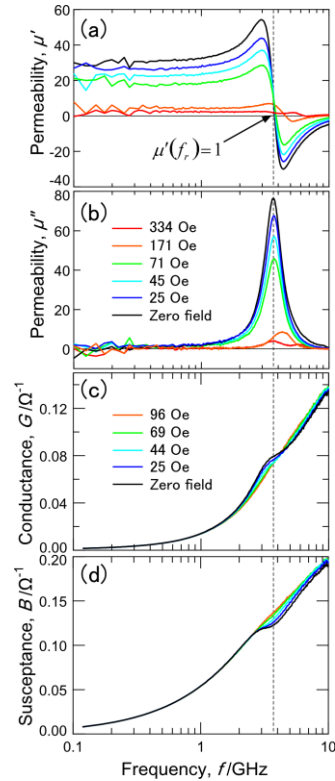


Fig. 33: The frequency dependence of  $\mu'$ (a),  $\mu''$  (b),  $G$  (c) and  $B$ (d) measured at various values of  $H_{ex}$ .

Mr. M. Murakami (RIEM) and Mr. M. Iwasa (RIEM).

## Large and stable actuation strain by reversible 90° domain switching in 0.62%PMN-0.38%PT crystal under electromechanical loading

Yingwei Li, Faxin Li

State Key Lab for Turbulence and Complex Systems, College of Engineering, Peking University, Beijing, 100871, China

Email: yingweili@pku.edu.cn

Ferroelectric actuators are characterized by their peculiar electromechanical energy conversion efficiency, ultra-fast response, and compact size, etc. However, their wide application is limited by the small piezoelectric strains of ferroelectric materials. Therefore, intensive efforts have been made in this aspect. The biggest breakthrough was achieved by Park and Shrout in 1990s. They obtained large actuation strains of  $\sim 1.7\%$  in relaxor ferroelectric crystals via phase transformation. However, the actuation ability of relaxor ferroelectric crystals decreases to  $0.2\sim 0.4\%$  within the up-operation field limit in the vicinity of  $1.5\sim 2.0\text{ kV/mm}$ . Large reversible actuation strains of  $\sim 0.8\%$  were also realized by using the huge strain accompanied with  $90^\circ$  domain switching via point-defect mediation or via electromechanical loading. For the former, further investigations concerned its stability is still needed before utilizing due to the intrinsic dissipation property of the point defects. As for the latter, their practical applications were inconvenienced by the compressive stress sensitivity of the actuation strains, the brittleness of BaTiO<sub>3</sub> crystals, and the requirement of large bipolar field power amplifier. Here we report that a pre-poled 0.62%PMN-0.38PT crystal can generate large strains of 0.65% at uni-polar electric fields of 1.8kV/mm with uniaxial pre-compression. Such large strains stem from the reversible  $90^\circ$  domain switching under the competition between compressive stresses and electric fields. Additionally, the actuation strain is stable. It only decreases about 7.7% after one thousand cycle's electric fields loading. On the other hand, the actuation strains can be larger than 0.42% in a wide range of compressive stresses (12MPa $\sim$ 40MPa). These characteristics make it suitable for practical applications.

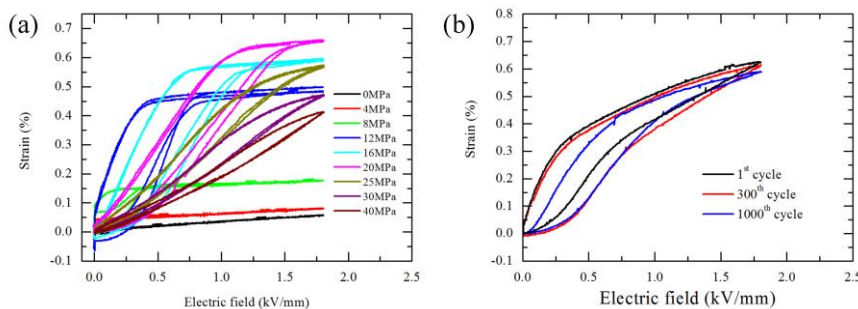


Fig 1. (a) Electric field vs. strain (E-S) curves for PMN-PT crystal during unipolar electric fields loading at different levels of compressive stress, (b) Evolution of the electric field vs. strain curve under cycle's electric fields loading (The compressive stress is at 20MPa).



## A MEMS AlN transducer array for use as a cochlear implant

Katherine Knisely and Karl Grosh

Mechanical Engineering, University of Michigan, Ann Arbor, MI

Email: kknisely@umich.edu

Aluminum nitride (AlN) has emerged as an excellent material for a variety of MEMS applications because of its high electrical resistance, low dielectric loss, and high sound velocity. Recently, MEMS sensors using AlN in a bimorph cantilever configuration have been demonstrated with low noise floors and good sensitivity<sup>114</sup>. Because of its very low dielectric loss factor and relatively simple deposition process as a thin film, AlN is an excellent material for microphones. The cantilever configuration has many benefits, including a more linear response, control of the frequency response using simple changes to the beam geometry, and simple adaptation from microphone to hydrophone.

We present an array of AlN bimorph cantilevers, fabricated using MEMS batch processing techniques, with applications both as a hydrophone array and as a completely implantable cochlear implant (CI). A silicon backbone supports five 400 $\mu\text{m}$  wide, 5 $\mu\text{m}$  thick bimorph (Platinum/aluminum nitride (AlN) stack) cantilevers, each of which is designed to have a resonance, in water, that corresponds to its tonotopic location in the guinea pig cochlea (20-40kHz). A 1mm wide, 10 $\mu\text{m}$  thick parylene and gold ribbon cable extends 3cm from the probe to an electrode bay, where electrical connections to each cantilever are accessed. The frequency response of a cantilever in a viscous fluid is predicted using a modified Euler-Bernoulli equation that includes fluid loading and viscous damping<sup>115</sup>, and is measured in air using a laser vibrometer and in water using a calibrated underwater transducer pair.

Unlike traditional CIs, this probe is designed to transduce mechanical vibrations of the cochlear fluid into electrical signals that stimulate the auditory nerves without the use of an external sound processing unit. Vibrations in the cochlear fluid deflect the cantilevers, resulting in a potential forming on the outer electrode layers of the cantilever. The outer electrodes are in electrical contact with the ionic fluid of the cochlea, producing a current in the cochlear fluid that is passed to the auditory nerves. In this design the energy is locally sensed and converted into stimulation within the cochlea, therefore our design does not require the traditional signal processing unit, microphone, and transceiver that current CIs employ. Benefits of this design include lower power, smaller size, and lower latency when compared with current commercial CIs.

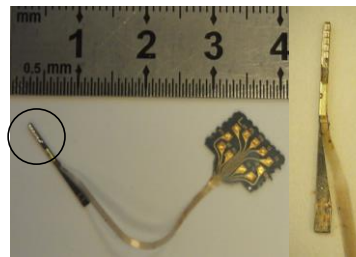


Fig. 34: The fabricated device. The cantilever array (left, circled, with a closeup on the right ) is connected to an electrode bay for external electrical monitoring by a flexible parylene-gold ribbon cable.

<sup>114</sup> R. Littrell and K. Grosh, *Journal of Microelectromechanical Systems* 21(2), 406 (2012).

<sup>115</sup> JE Sader. *Journal of Applied Physics*, 84:64–76, 1998.



## Piezoelectric Films for High Density Switching Arrays for Logic

R. Keech<sup>1</sup>, S. Shetty<sup>1</sup>, S. Trolier-McKinstry<sup>1</sup>, D. Newns<sup>2</sup>, and G. Martyna<sup>2</sup>

<sup>1</sup>Department of Materials Science and Engineering, Pennsylvania State University  
Millennium Sciences Complex, State College, PA, 16802

<sup>2</sup>IBM TJ Watson Research Center  
Yorktown Heights, PA 10598

A fast, low power, transistor-type switching device has been proposed in which piezoelectric and piezoresistive materials are employed in a stacked sandwich structure of nanometer dimension. Of particular interest to this program is the functionality of the high aspect ratio piezoelectric  $70\text{Pb}(\text{Mg}_{1/3}\text{Nb}_{2/3})\text{O}_3\text{-}30\text{PbTiO}_3$  (PMN-PT) component. Dense PMN-PT films of approximately 350 nm in thickness were made by a 2MOE solvent sol-gel route. These films were phase pure and strongly 100 oriented by XRD with dielectric constants exceeding 1300 and loss tangents of approximately 0.01. The films showed slim hysteresis loops with remanent polarizations of about  $10 \mu\text{C}/\text{cm}^2$  and breakdown field of over 1500 kV/cm. The films exhibited large signal strain of over 1% with clamped, large signal  $d_{33,f}$  of approximately 90 nm/V. Reactive ion etching (RIE) has been employed to pattern features in the PMN-PT film down to one micron in spatial scale with vertical sidewalls. Upon lateral scaling, a small increase in small signal electrical properties has been observed. The paper will describe the evolution in properties that develop as the films are further laterally subdivided into small driving pixels.

*Corresponding author:*

Ryan R. Keech  
Department of Material Science and Engineering  
Pennsylvania State University  
N-225 Millennium Science Complex  
State College, PA, 16801  
Phone: (207) 651-8804  
E-mail: ryk5144@psu.edu

## **Pb(In<sub>1/2</sub>Nb<sub>1/2</sub>)-Pb(Mg<sub>1/3</sub>Nb<sub>2/3</sub>)-PbTiO<sub>3</sub> single crystal monomorph with perpendicular electrode connections for sensing and energy harvesting**

Ming Ma, Zhenrong Li, Zhuo Xu, Xi Yao

Electronic Materials Research Laboratory, Key Laboratory of Education Ministry; International Center for Dielectric Research, Xi'an Jiaotong University, Xi'an 710049, China

Email: zhrli@mail.xjtu.edu.cn

Piezoelectric monomorph, which has only one element, is one kind of potential structure for piezoelectric applications in some extreme conditions. However the traditional parallel electrode connection is not effective for sensing and energy harvesting because of the restriction of the strain neutral layer. In this paper, the perpendicular electrode connections were used to make the monomorph avoid the restriction of the strain neutral layer. And Pb(In<sub>1/2</sub>Nb<sub>1/2</sub>)-Pb(Mg<sub>1/3</sub>Nb<sub>2/3</sub>)-PbTiO<sub>3</sub> single crystal monomorph with perpendicular electrodes was studied. By comparing seven forms of perpendicular electrode connections with the traditional parallel electrode connection, the whole superposed perpendicular electrode connection is considered as the optimal output way for the monomorph. The 27.2V peak to peak voltage in open circuit and the 71.5μW maximum power with the matching resistance at the resonance frequency can be produced by the whole superposed perpendicular electrode connection, which are much more than 3.2V and 1.5μW that produced by the parallel electrode connection.

## **Al<sub>1-x</sub>Sc<sub>x</sub>N thin films as promising non-ferroelectric materials for energy harvesting**

Ramin Matloub<sup>1</sup>, Gilles Moulard<sup>2</sup>, Thomas Metzger<sup>2</sup> and Paul Muralt<sup>1</sup>

<sup>1</sup>**Ceramics Laboratory, Ecole Polytechnique Fédérale de Lausanne, Lausanne, Switzerland**

<sup>2</sup>**TDK-EPC Corporation, Munich**

Email: [ramin.matloub@epfl.ch](mailto:ramin.matloub@epfl.ch)

Aluminum nitride (AlN) thin films have become a standard material for RF filters in mobile phones exploiting thickness mode resonances based on the longitudinal piezoelectric effect. Recently it was shown that by partial substitution of Al by Sc, a factor 4 increase of this longitudinal effect was observed in Sc<sub>0.43</sub>Al<sub>0.57</sub>N (Akiyama et. al). The question is how much the transverse piezoelectric effect is increasing in Sc<sub>x</sub>Al<sub>1-x</sub>N alloys. This is of interest for many MEMS applications including vibration energy harvesting. In this case the coefficient of interest is  $e_{31,f}$  describes the stress that can be created in the film plane (coordinates 1, 2) of a parallel plate capacitor structure under the condition that the film is free to move in the third direction (vertical to the film plane). In this work, the transverse piezoelectric coefficient,  $e_{31,f}$ , of Al<sub>1-x</sub>Sc<sub>x</sub>N thin films was investigated as a function of composition. It increased by nearly 50 % from x=0 to x=0.17. As the increase of the dielectric constant is only moderate we observed a more than 60 % increase of the electrical energy content to be harvested. The energy harvesting FOM of 18.0 (GJ/m<sup>3</sup>) for Al<sub>0.83</sub>Sc<sub>0.17</sub>N is comparable to good PZT thin films with an  $e_{31,f}$  of 16 C/m<sup>2</sup> and a dielectric constant of 1600. We shall show that the harvesting efficiency is potentially increased by more than 60 % as compared to pure AlN. Going to even higher Sc concentrations, a doubling of the harvested power is conceivable.

---

## **Ferroelectrics Awrads, ISAF Plenary Talk**

CH

*Tuesday, July 23 2013, 08:30 am - 10:00 am*

## Piezoelectric Actuator Renaissance

Kenji Uchino

ONR Global-Asia, Office of Naval Research, Roppongi, Minato-Ku, Tokyo 106-0032, Japan; & Int'l Ctr. for Actuators & Transducers, The Penn State Univ., University Park, PA 16802, USA

Email: [kenji.uchino.ngo@mail.mil](mailto:kenji.uchino.ngo@mail.mil) & [kenjiuchino@psu.edu](mailto:kenjiuchino@psu.edu)

Actuator applications of piezoelectrics started in late 1970s, and enormous investment was installed on practical developments during '80s, aiming at consumer applications such as precision positioners with high strain materials, multilayer device designing and mass-fabrication processes for portable electronic devices, ultrasonic motors for micro-robotics and smart structures. After the slump due to the worldwide economic recession in late '90s, we are now facing a sort of "Renaissance" of piezoelectric actuators according to the social environmental changes. This paper reviews the recent advances in materials, designing concepts, and new applications of piezoelectric actuators, and describes the future perspectives of this area.

The 21st century faces to a "*sustainable society*". Global regulations are strongly called on ecological and human health care issues, and the government-initiated technology (i.e., "*politico-engineering*") has become essential. Because of significantly high energy efficiency of piezoelectrics in comparison with other actuators such as chemical engines and electromagnetic components, piezoelectric actuators have been re-focused most recently in the sustainable society (i.e., "Renaissance" in piezoelectric actuators).

I will discuss five key trends in this paper for providing the future perspectives; "*Performance to Reliability*", "*Hard to Soft*", "*Macro to Nano*", "*Homo to Hetero*" and "*Single to Multi-functional*". First in the materials trend, the worldwide toxicity regulation is accelerating the development of Pb-free piezoelectrics for replacing the conventional PZTs. Second, high power piezoelectrics with low loss have become a central research topic from the energy-efficiency improvement viewpoint; that is to say, "real (strain magnitude) to imaginary performance (heat generation reduction)". Third, we are facing the revival polymer era after '80s because of their elastically soft superiority. Larger, thinner, lighter and mechanically flexible human interfaces are the current necessity in the portable electronic devices, leading to the development in elastically soft displays, electronic circuits, and speakers/microphones. Polymeric and polymer-ceramic composite piezoelectrics are reviving and commercialized. PZN-PT or PMN-PT single crystals became focused due to the rubber-like-soft piezo-ceramic strain after 25 years of the discovery. In the MEMS/NEMS area, piezo MEMS is one of the miniaturization targets for integrating the piezo-actuators in a micro-scale devices, aiming at bio/medical applications for maintaining the human health. "Homo to hetero" structure change is also a recent research trend: Stress-gradient in terms of space in a dielectric material exhibits piezoelectric-equivalent sensing capability (i.e., "flexoelectricity"), while electric-field gradient in terms of space in a semiconductive piezoelectric can exhibit bimorph-equivalent flextensional deformation ("monomorph"). New functions can be realized by coupling two effects. Magnetolectric devices (i.e., voltage is generated by applying magnetic field) were developed by laminating magnetostrictive Terfenol-D and piezoelectric PZT materials, and photostriction was demonstrated by coupling photovoltaic and piezoelectric effects in PLZT. In the application area, the global regime for "ecological sustainability" particularly accelerated new developments in ultrasonic disposal technology of hazardous materials, diesel injection valves for air pollution, and piezoelectric renewable energy harvesting systems.

---

## **Marija Kosec Memorial Electroceramic Processing**

CLUB A

*Tuesday, July 23 2013, 10:30 am - 12:00 pm*

Chair: **Nava Setter**  
*Swiss Federal Institute of Technology – EPFL, nava.*



# Mechanochemistry as an Efficient Way to Chemically Homogeneous Ferroelectric Ceramics: Case Studies of (K,Na)NbO<sub>3</sub>- and BiFeO<sub>3</sub>-Based Materials

Tadej Rojac<sup>1,2</sup>, Andreja Bencan<sup>1</sup>, Dragan Damjanovic<sup>3</sup>, Barbara Malic<sup>1</sup>

<sup>1</sup>Electronic Ceramics Department, Jozef Stefan Institute, Ljubljana, Slovenia

<sup>2</sup>CoE NAMASTE, Ljubljana, Slovenia

<sup>3</sup>Ceramics Laboratory, Swiss Federal Institute of Technology – EPFL, Lausanne, Switzerland

Email: tadej.rojac@ijs.si

*Dedicated to the memory of the late Prof. Marija Kosec*

In many cases, the conventional solid-state processing fails to provide ceramics of complex oxides with sufficiently high compositional homogeneity. Mechanochemical processing, an alternative approach often referred to as the “high-energy milling”, is a simple milling method that is capable to provide powders with superior homogeneity and sinterability. The aim of this contribution is to review the role and benefits of mechanochemistry in the processing of ferroelectric oxides through two known examples: (K,Na,Li)(Nb,Ta)O<sub>3</sub> and BiFeO<sub>3</sub>. After revising the main processing issues associated with these two oxides, we will show how key problems, such as achieving high homogeneity and reducing the number of processing steps, are overcome by introducing the mechanochemical approach. In addition, we will gain insight into the reaction mechanisms, revealing the origins of the high reactivity of the mechanochemically processed powders.

One of the main issues in the processing of the Li- and Ta-modified (K,Na)NbO<sub>3</sub> (KNLNT) ceramics is achieving high compositional homogeneity, particularly at the B-site of the perovskite ABO<sub>3</sub> lattice. The reason lies in the low diffusivity of Nb<sup>5+</sup> and Ta<sup>5+</sup>, which prevents complete homogenization of the two cations in the solid solution during calcination and subsequent sintering. In contrast to the thermally activated solid-state reaction, which is governed by diffusion processes, the mechanochemical treatment of the initial powder mixture of alkaline carbonates and transition-metal oxides is characterized by the formation of an amorphous carbonate complex. This phase, which was identified by means of infrared spectroscopy analysis, consists of CO<sub>3</sub><sup>2-</sup> groups coordinated to the Nb<sup>5+</sup> and Ta<sup>5+</sup> cations. The complex thus provides direct chemical binding between the alkaline ions and transition-metal ions via the carbonate group. Through systematic studies, we will show that this phase is largely responsible for the high level of chemical homogeneity of the activated powder and, consequently, of the resulting KNLNT ceramics.

Despite being compositionally simpler than KNLNT, the synthesis of phase-pure BiFeO<sub>3</sub> is extremely difficult. The persistence of the secondary phases, i.e., Bi<sub>25</sub>FeO<sub>39</sub> and Bi<sub>2</sub>Fe<sub>4</sub>O<sub>9</sub>, in the final ceramics is frequently reported in the literature and it is most probably associated with the particular thermodynamics and reaction kinetics of this system. We recently developed a two-step synthesis route for BiFeO<sub>3</sub>, involving mechanochemical activation of the Bi<sub>2</sub>O<sub>3</sub>–Fe<sub>2</sub>O<sub>3</sub> powder mixture, followed by reactive sintering. The resulting BiFeO<sub>3</sub> ceramics were able to withstand high electric fields, i.e., as high as 180 kV/cm, allowing us to pole the ceramics and study systematically the piezoelectric properties. Some of these results will be presented and discussed as well.

## Influence of Ca/Zr Substitution on Grain Size Effect of BaTiO<sub>3</sub>-Based Ceramics

Takuya Hoshina, Tsutomu Furuta, Takahiro Yamazaki, Hiroaki Takeda, Takaaki Tsurumi

Nano-Phonics Lab., Graduate School of Science and Engineering,  
Tokyo Institute of Technology, Meguro, Tokyo, Japan

Email: thoshina@ceram.titech.ac.jp

BaTiO<sub>3</sub> is typical ferroelectrics with high permittivity and have been used as materials for dielectric devices such as multilayered ceramic capacitors (MLCCs). In ferroelectrics, it is known that dielectric permittivity depends on the grain size.<sup>116</sup> This phenomenon is called the grain size effect, which is a significant problem to development next-generation dielectric devices. BaTiO<sub>3</sub>-based ceramics such as (Ba,Ca)TiO<sub>3</sub> and Ba(Zr,Ti)O<sub>3</sub> ceramics have been expected as materials for MLCCs. However, the grain size effects of (Ba,Ca)TiO<sub>3</sub> and Ba(Zr,Ti)O<sub>3</sub> ceramics, including these mechanisms, remain unclear. In this study, we investigated the influence of Ca/Zr substitution on the grain size effect of BaTiO<sub>3</sub>-based ceramics.

Highly dense BaTiO<sub>3</sub>-based ceramics with micrometer- and nanometer-sized grains were fabricated by a two-step sintering method and aerosol deposition (AD) method, respectively. The two-step sintering is a promising technique for obtaining highly dense ceramics without significant grain growth. The AD method is a unique technique that enables nanograined ceramic fabrication at room temperature. Figure 1 shows the grain size dependence of dielectric permittivity of BaTiO<sub>3</sub>-based ceramics.<sup>1,117</sup> The permittivity of BaTiO<sub>3</sub> ceramics increased with decreasing grain size when the grain size was more than 1 μm, whereas it decreased when the grain size was below 1 μm. The permittivity of Ba<sub>0.92</sub>Ca<sub>0.08</sub>TiO<sub>3</sub> ceramics is much smaller than that of Ba<sub>0.92</sub>Ca<sub>0.08</sub>TiO<sub>3</sub> ceramics at micrometer-sized grains. In contrast, the permittivity of Ba<sub>0.92</sub>Ca<sub>0.08</sub>TiO<sub>3</sub> ceramics is almost the same as that of BaTiO<sub>3</sub> ceramics at nanometer-sized grains. The permittivity of the BaZr<sub>x</sub>Ti<sub>1-x</sub>O<sub>3</sub> ceramics markedly decreased with decreasing grain size below 3 μm. The permittivity of the BaZr<sub>x</sub>Ti<sub>1-x</sub>O<sub>3</sub> nanograined ceramics decreased with increasing Zr content and was much smaller than the permittivity of the BaTiO<sub>3</sub> nanograined ceramics. These results indicated that the BaZr<sub>x</sub>Ti<sub>1-x</sub>O<sub>3</sub> ceramics were more susceptible to the grain size effect than the pure BaTiO<sub>3</sub> ceramics.

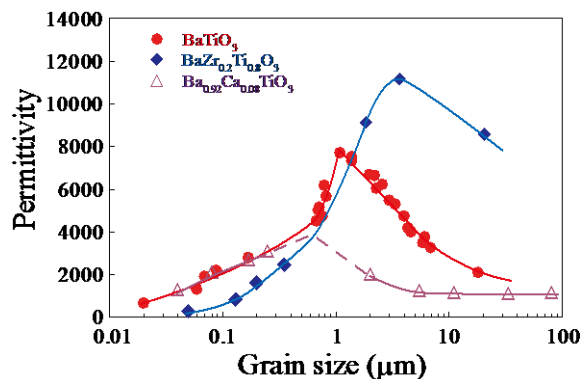


Fig. 35: Grain size dependence of permittivity of BaTiO<sub>3</sub>-based ceramics.

<sup>116</sup> T. Hoshina, "Size effect of barium titanate: fine particles and ceramics", J. Ceram. Soc. Jpn., vol. 121, p. 156-161, 2013.

<sup>117</sup> T. Hoshina, T. Furuta, T. Yamazaki, H. Takeda, and T. Tsurumi, "Grain Size Effect on Dielectric Properties of Ba(Zr,Ti)O<sub>3</sub> Ceramics", Jpn. J. Appl. Phys., vol. 51, 09LC04, 2012.



## Processing of $\text{Bi}(\text{Zn}_{1/2}\text{Ti}_{1/2})\text{O}_3\text{-BaTiO}_3$ dielectrics for reliable high field operation

Geoff L. Brennecke<sup>1</sup>, Harlan J. Brown-Shaklee<sup>1</sup>, Natthaphon Raengthon<sup>2</sup>, Mia A. Blea<sup>1</sup>, David I. Shahin<sup>3</sup>, David P. Cann<sup>2</sup>, Wayne Huebner<sup>3</sup>

<sup>1</sup>Electronic, Optical, and Nanostructured Materials, Sandia National Laboratories, Albuquerque, NM, USA

<sup>2</sup>Mechanical, Industrial, and Manufacturing Engineering, Oregon State University, Corvallis, OR, USA

<sup>3</sup>Materials Science and Engineering, Missouri University of Science and Technology, Rolla, MO, USA

Email: [glbrenn@sandia.gov](mailto:glbrenn@sandia.gov)

Weakly-coupled relaxor systems based on modifications of  $\text{BaTiO}_3$  with Bi-based perovskites are of interest for a variety of capacitor applications because of their ability to maintain relatively large permittivity, low loss tangents, and high resistivity values under large electric fields and/or at elevated temperatures<sup>118</sup>. Our work focuses on relatively large (>100nF) capacitors for high voltage (>1kV) operation (Figure 1) to address the need for reliable high-operating-temperature capacitors for emerging power electronics systems based on wide bandgap semiconductors. We report here on effects of compositional variation and processing parameters on microstructure as well as various electrical parameters of materials in the  $\text{Bi}(\text{Zn}_{1/2}\text{Ti}_{1/2})\text{O}_3\text{-BaTiO}_3$  system.

Bi-based additives assist in densification at reasonable temperatures but also greatly complicate cofiring of these systems with desired electrodes. In addition to the volatility of Bi during sintering,  $\text{Bi}_2\text{O}_3$  is unstable in contact with metallic Ni, offers a vanishingly-small thermodynamic stability window with regard to metallic Cu, and tends to alloy with Pt and Pd at temperatures commonly used for densification of free-standing ceramic pellets. Nevertheless, we show here that BZT-BT MLCCs can be successfully cofired with both Pt and Ag-Pd electrodes and can provide reliable performance under high field and high operating temperatures. We also discuss the effects of various processing parameters including contaminants, sintering conditions, electrode interactions, and liquid phase

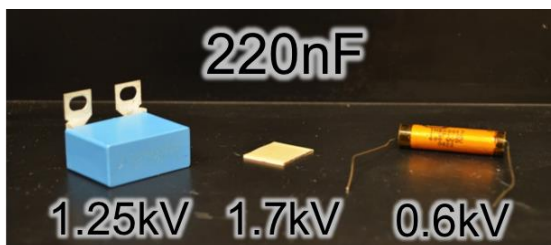


Fig. 36:  $\text{Bi}(\text{Zn}_{1/2}\text{Ti}_{1/2})\text{O}_3\text{-BaTiO}_3$ -based MLCC (center) shown with two similar polymer film capacitors (left and right) of the same capacitance value (220nF) at rated operating voltage for ambient conditions (shown below each part). The MLCC also operates at temperatures

<sup>118</sup> N. Raengthon, T. Sebastian, D. Cumming, I.M. Reaney, D.P. Cann, "BaTiO<sub>3</sub>-Bi(Zn<sub>1/2</sub>Ti<sub>1/2</sub>)O<sub>3</sub>-BiScO<sub>3</sub> Ceramics for High-Temperature Capacitor Applications", J. Am. Ceram. Soc., vol. 95, p. 3554-3561, 2012.

Sandia National Laboratories is a multi-program laboratory managed and operated by Sandia Corporation, a wholly owned subsidiary of Lockheed Martin Corporation, for the U.S. Department of Energy's National Nuclear Security Administration under contract DE-AC04-94AL85000. This work was supported by the Department of Energy's Office of Electricity Delivery and Energy Reliability, Energy Storage Systems program managed by Dr. Imre Gyuk.

additives, on permittivity, resistivity and degradation mechanisms.

**Electromechanical Properties of Hard  
Lead-free Bi<sub>0.5</sub>Na<sub>0.5</sub>TiO<sub>3</sub>-based Ceramics**

E. Taghaddos, M. Hejazi, and A. Safari  
Glenn Howatt Electroceramics Laboratory  
Department of Materials Science and Engineering, Rutgers University  
607 Taylor Rd, Piscataway, NJ 08854

It has been previously shown that in a ternary system of  $x[\text{Bi}_{0.5}\text{Na}_{0.5}\text{TiO}_3]-y[\text{Bi}_{0.5}\text{K}_{0.5}\text{TiO}_3]-(1-x-y)[\text{Bi}_{0.5}\text{Li}_{0.5}\text{TiO}_3]$ , the highest mechanical quality factor ( $Q_m$ ) is obtained at a composition with  $x$  and  $y$  values of 0.88 and 0.08, respectively. In this work, processing and electro-mechanical properties of Mn-doped  $0.88[\text{Bi}_{0.5}\text{Na}_{0.5}\text{TiO}_3]-0.08[\text{Bi}_{0.5}\text{K}_{0.5}\text{TiO}_3]-0.04[\text{Bi}_{0.5}\text{Li}_{0.5}\text{TiO}_3]$  ceramics prepared by mixed oxide route have been comprehensively studied. Different amount of Mn (0.01, 0.014, 0.015, 0.01625, 0.0175, 0.02, and 0.022) was added to the ceramics either in form of a dopant (B-site substitution) or as an additive after calcination. Pressed samples were sintered at different temperatures (1075-1150 °C) and time. It was found that Mn-addition did not exhibit any hardening effect and in fact led to an increase in the dielectric loss. On the other hand,  $Q_m$  was remarkably increased by Mn-doping in the B-site. Mn-doping was also resulted in decreasing in planar coupling coefficient, dielectric constant, and dielectric loss which are common effects in hard ferroelectrics doped with an acceptor. The  $Q_m$ ,  $d_{33}$ ,  $k_p$ ,  $\epsilon_r$  and  $\tan\delta$  values for 0.015 Mn doped sample were 950, 85 pC/N, 0.218, 310, and 0.009, respectively. Sintering temperature in Mn doped BNKLT ceramics were slightly lower than undoped samples..

## Poling below Coercive Field for Large Piezoelectricity

Xiaoli Tan, Hanzheng Guo, Cheng Ma, Xiaoming Liu

Department of Materials Science and Engineering, Iowa State University, Ames, Iowa/USA

Email: xtan@iastate.edu

Piezoelectric materials are key to many important technologies, including energy harvesting, noise cancellation, and minimally invasive surgery. The dominant piezoelectric materials in industry are polycrystalline ferroelectrics, which must be poled by electric fields to exhibit piezoelectricity. During electrical poling, the originally randomly oriented polarizations are aligned by the poling field, forming the macroscopic non-centrosymmetry that is required for piezoelectricity. Therefore, it is commonly believed that poling fields have to be much greater than the coercive field  $E_C$ , which characterizes the difficulty of polarization reversal in ferroelectrics. Such an empirical rule is based on and supported by numerous experimental observations on all the widely studied piezoelectrics so far. Poling fields below or around  $E_C$  only yield very small piezoelectric coefficient  $d_{33}$  values that are close to zero.

In the present work, we report that well-developed piezoelectric properties are measured in certain lead-free  $(1-x)(\text{Bi}_{1/2}\text{Na}_{1/2})\text{TiO}_3-x\text{BaTiO}_3$  compositions even when they are poled at fields significantly below their measured coercive fields. Prior to poling, these compositions are in the morphotropic phase boundary region and display a relaxor behavior with the ferroelectric  $P4bm$  structure. Electric field *in-situ* transmission electron microscopy experiments reveal that this unusual behavior is originated from the poling of the non-ergodic relaxor ferroelectric phase where  $P4bm$  nanodomains irreversibly coalesce and form extremely thin lamellar domains. Similar behavior is also confirmed in a lead-containing relaxor ferroelectric  $(\text{Pb}_{0.92}\text{La}_{0.08})(\text{Zr}_{0.65}\text{Ti}_{0.35})\text{O}_3$ .

---

## **Domain engineering**

CLUB B

*Tuesday, July 23 2013, 10:30 am - 12:00 pm*

Chair: **To Be Announced**



**Investigation of intrinsic domains in PbTiO<sub>3</sub> ultrathin films: from nanodots to nanostripes**  
**Céline Lichtensteiger, Pavlo Zubko and Jean-Marc Triscone**

*DPMC – University of Geneva, 24 Quai Ernest Ansermet, CH – 1211 Genève 4*

Email: celine.lichtensteiger@unige.ch

In ferroelectric ultrathin films, the depolarization field arising from bound charges on the surface of the film and at the interface with the substrate can be partially screened by free charges from metallic electrodes, ions from the atmosphere, or mobile charges from within the semiconducting ferroelectric itself. Even in structurally perfect metallic electrodes, the screening charges will spread over a small but finite length, giving rise to a nonzero effective screening length that will dramatically alter the properties of an ultrathin film. In the absence of sufficient free charges, a ferroelectric has several other ways of minimizing its energy while preserving its polar state, e.g., by forming domains of opposite polarization, or rotating the polarization into the plane of the thin ferroelectric slab<sup>119</sup>.

Using piezo-force microscopy (PFM), we investigate the intrinsic nanodomain structure of PbTiO<sub>3</sub> ultrathin films at room temperature.

By changing the degree of screening, the domain structure can be modified or even suppressed in favour of a uniform monodomain state.

Focusing on the effect of film thickness, we observe the evolution of the size and shape of the domains from large nanodots to small stripes as the PbTiO<sub>3</sub> films thickness decreases.

---

<sup>119</sup> Ferroelectricity in ultrathin-film capacitors, C. Lichtensteiger et al, Ch. 12 in Oxide Ultrathin Films, Science and Technology, Wiley (2011) ([arXiv:1208.5309v1](https://arxiv.org/abs/1208.5309v1) [[cond-mat.mtrl-sci](#)])

## Ferroelectric Domain Wall Injection via Electric Field Engineering

J. R. Whyte<sup>1</sup>, R. G. P. McQuaid<sup>1</sup>, P. Sharma<sup>2</sup>, C. Canalias<sup>3</sup>, J. F. Scott<sup>4</sup>, A. Gruverman<sup>2</sup> and J. M. Gregg<sup>1</sup>

<sup>1</sup>School of Mathematics and Physics, Queen's University Belfast, Belfast, United Kingdom

<sup>2</sup>Department of Physics and Astronomy, University of Nebraska, Lincoln, Nebraska, USA

<sup>3</sup>Department of Applied Physics, Royal Institute of Technology, Stockholm, Sweden

<sup>4</sup>Department of Physics, Cavendish Laboratory, Cambridge, England, UK

Email: [jwhyte05@qub.ac.uk](mailto:jwhyte05@qub.ac.uk)

The discovery of enhanced conductivity in ferroelectric domain walls has prompted a number of ideas for new electronic devices, such as transistors and memristors, which operate through the existence or otherwise of domain wall-based conducting channels between electrodes. For such devices to work, complete control over where domain walls nucleate and how they subsequently move is crucial<sup>120</sup>.

Here, we demonstrate how engineering of the local electric field, using focused ion beam-milled defects, can be used to allow site-specific domain wall injection in thin single crystal lamellae of the uniaxial ferroelectric  $\text{KTiOPO}_4$  (KTP). We also show how designed variations in local field can dictate subsequent domain wall mobility. Defect-related field engineering is thus demonstrated as a new paradigm for domain wall control as part of a journey towards realizing domain wall nanoelectronic devices.

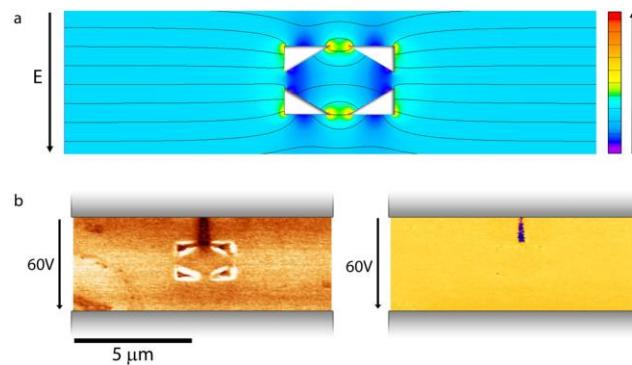


Fig. 37: (a) Electric field model of KTP lamella under the application of 100 V with field hotspots positioned at inside vertices of triangular holes. (b) Amplitude (left) and phase (right) images show the appearance of a new domain nucleating from one of the hot-spots post application of 60 V, implying that the production of field hotspots can control the exact location of reverse domain nucleation.

<sup>120</sup> H. Béa, P. Paruch, "Multiferroics: A way forward along domain walls", *Nature Mater.*, vol 8, p. 168–169, 2009.

## Breathing mode of domain wall motion and spatial energy landscapes in ferroelectric BiFeO<sub>3</sub> films

Jong-Gul Yoon<sup>1</sup>, Tae Heon Kim<sup>2</sup>, S. H. Baek<sup>3</sup>, S. M. Yang<sup>2</sup>, J.-S. Chung<sup>4</sup>, C. B. Eom<sup>3</sup>, and T. W. Noh<sup>2</sup>

<sup>1</sup>Department of Physics, University of Suwon, Gyunggi-do 445-743, Korea

<sup>2</sup>IBS-CFI-CES, Seoul National University, Seoul 151-747, Korea

<sup>3</sup>Department of Materials Science and Engineering, University of Wisconsin, Madison, WI 53706, USA

<sup>4</sup>Department of Physics, Soongsil University, Seoul 156-743, Republic of Korea

Email: jgyoon@suwon.ac.kr

We investigated a breathing mode of ferroelectric domain wall motion in an epitaxial BiFeO<sub>3</sub> film grown on a vicinal SrTiO<sub>3</sub> (001) substrate by monitoring ferroelectric domain evolution under successive pulse fields with piezoresponse force microscopy. An anisotropic domain growth, which should be caused by a structurally-driven symmetry breaking,<sup>121</sup> resulted in the breathing mode of sideways domain wall motion with the alternative application of negative and positive electric pulse fields. The domain-shape-preserving breathing mode of domain wall motion indicated that the domain shape should be governed by the spatial energy landscapes, which would be determined by the corresponding domain wall energies as well as the distribution of defects acting as pinning sites. With the theoretical results of domain wall energies in BiFeO<sub>3</sub>, we showed that 109 and 180° domain walls critically affect the polarity dependence of various dynamics properties, such as domain shape, nucleation sites, and domain wall velocity. The domain-shape-preserving breathing mode can be exploited for ferroelectric domain wall motion devices.

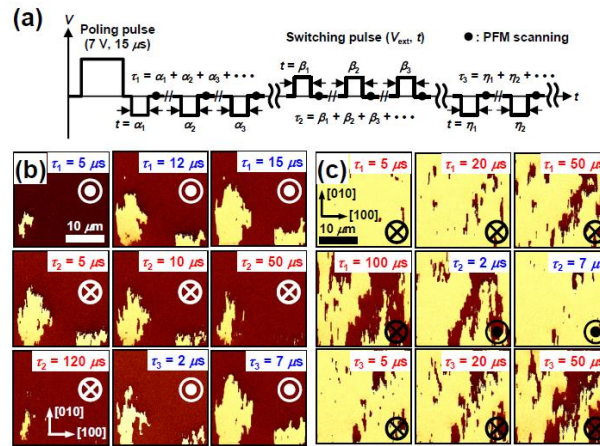


Fig. 38: (a) Pulse sequences for observing breathing mode of domain wall motion. [(b) and (c)] Successive out-of-plane PFM phase images of the domain evolution induced by the pulse fields. ⊙ and ⊗ represent the direction of the applied upward and downward electric field, respectively. The bright and dark regions represent ferroelectric domains with upward and downward polarization, respectively.

<sup>121</sup> T. H. Kim et al., “Electric-field-controlled directional motion of ferroelectric domain walls in multiferroic BiFeO<sub>3</sub> films”, Appl. Phys. Lett. Vol. 95, p. 262902, 2009.



## Multiscaling analysis and thermal quench effects of domain walls in epitaxial BiFeO<sub>3</sub> thin films

Benedikt Ziegler<sup>1</sup>, Ingrid Infante<sup>2</sup>, Stephane Fusil<sup>2</sup>, Manuel Bibes<sup>2</sup> and Patrycja Paruch<sup>1</sup>

<sup>1</sup>MaNEP-DPMC, University of Geneva, Geneva, Switzerland

<sup>2</sup>Unité Mixte de Physique CNRS/Thales, Palaiseau Cedex, France

Email: benedikt.ziegler@unige.ch

The coexistence of ferroelectric and antiferromagnetic ordering at room temperature have led to intense research on multiferroic BiFeO<sub>3</sub>. In addition, the recent discoveries of interesting new phenomena like conducting ferroelectric domain walls<sup>122</sup> make it a promising candidate for nanoelectronic applications<sup>123</sup>.

Here, we present our study of the microscopic behavior of such domain walls within the broader framework of elastic disordered systems, using vertical and lateral piezoresponse force microscopy to study the roughness of artificially written and intrinsic domain walls in ambient conditions and under thermal cycling. A multiscaling analysis of the domain walls can be used to discriminate between different kinds of disorder. While this analysis was previously applied to artificially written ferroelectric domain walls<sup>124</sup>, we use it here to study intrinsic stripe-like 71° multiferroic domain walls, which are potentially better equilibrated and have a richer internal structure due to strain and potentially also electromagnetic coupling. From these studies we extract a characteristic length scale, below which the domain walls show a mono-affine scaling, usually an indication of weak collective pinning in random disorder. However, unlike for the individual artificially written walls, in this case long-range interactions between the domain walls appear to dominate the effective elastic behavior. The domain walls show higher roughening than purely artificially written ferroelectric domain walls. Independently, we also present the evolution of domain wall roughness with thermal cycling<sup>125</sup> in artificially written walls in BiFeO<sub>3</sub>.

---

<sup>122</sup> Seidel, J., et al., Nature Mater. 8, 229, 2009

<sup>123</sup> Catalan, G., et al., Rev. Mod. Phys. 84, 119-156, 2012

<sup>124</sup> Guyonnet, J., et al., Phys. Rev. Lett. 109, 147601, 2012

<sup>125</sup> Paruch, P., et al., Phys. Rev. B 85, 214115, 2012

## Nanodomain Structuring of Uniaxial Ferroelectrics. Achievements in Nanodomain Engineering

Shur Vladimir<sup>1,2</sup>

<sup>1</sup>Ferroelectric Laboratory, Ural Federal University, Ekaterinburg, Russia

<sup>2</sup>Labfer Ltd., Ekaterinburg, Russia

Email: [vladimir.shur@usu.ru](mailto:vladimir.shur@usu.ru)

Nanodomain engineering is the important modern target of the ferroelectric science and technology. The production of ferroelectric crystals with periodical tailored stable domain structure used for spatial modulation of their electro-optic, nonlinear optical and piezoelectric properties allow to manufacture various devices with upgraded performance. The fabrication of sub-micron-pitch quasi-regular domain gratings and engineered structures with nanoscale precision for photonic applications needs the deeper research of domain formation with submicron spatial resolution.

The set of modern high-resolution methods including piezoresponse force microscopy, scanning electron microscopy and confocal Raman microscopy applied for domain study in nanoscale has allowed to reveal the important role of nanodomain kinetics and to investigate the evolution of self-assembled nanodomain structures. The recent important achievements in studying of the nanodomain structure evolution obtained in highly non-equilibrium switching conditions realized by various methods and characterized by ineffective screening of depolarization fields has been reviewed. Several new effects leading to formation of the quasi-regular dendrite nanodomain structures has been demonstrated.

The crystals of lithium niobate and lithium tantalate family were studied both as the model ferroelectrics and as the most important for application nonlinear optical materials. Their simple domain structure and ability to change the bulk screening rate in wide range by heating allows to realize the nanodomain structuring.

The nanodomain kinetics has been studied in the samples with the surface layer modified by proton exchange and during switching by pyroelectric field during cooling after multiply pulse laser heating. The types of nanoscale domain structures and original scenarios of their evolutions have been singled out. The unique information about evolution of the nanodomain structures has been revealed by analysis of the domain images at different depth in the bulk obtained by scanning laser confocal Raman microscopy. The stable self-assembled stripe domain structures with periods about 20 nm has been produced.

The obtained knowledge opens the new approach to the nanodomain engineering. The high-efficient crystals for laser light frequency conversion in spectral range from 0.4 to 4  $\mu\text{m}$  have been manufactured.

The equipment of the UCSU "Modern Nanotechnology", Institute of Natural Sciences, UrFU has been used. The research was made possible in part by RFBR (Grants 13-02-01391- a , 12-02-31377, 11-02-91066-CNRS- a ), by Ministry of Education and Science (Contract 14.513.12.0006).

---

## High Temperature Piezoelectrics

CLUB C

*Tuesday, July 23 2013, 10:30 am - 12:00 pm*

Chair: **David Cann**  
*Oregon State University*

## High Temperature Piezoelectric Crystals: Recent Developments and Application Specifications

Shujun Zhang<sup>1,2</sup>, Fapeng Yu<sup>3</sup>, Thomas R. Shrout<sup>2</sup>

<sup>1</sup>Electronic Materials Research Laboratory, Xi'an Jiaotong University, Xi'an, China

<sup>2</sup>Materials Research Institute, Pennsylvania State University, University Park, PA, US

<sup>3</sup>Institute of Crystal Materials, Shandong University, Ji'nan, China

Email: shujunzhang@gmail.com

Piezoelectric materials that can function at high temperatures without failure are desired for structural health monitoring and/or nondestructive evaluation of the next generation turbines, more efficient jet engines, electrical and nuclear power plants. The operational temperature range of the smart transducers is limited by the sensing capability of the piezoelectric material at elevated temperatures, increased conductivity and mechanical attenuation, variation of the piezoelectric properties with temperature. This paper discusses properties relevant to sensing applications, including ferroelectric materials and non-ferroelectric piezoelectric crystals.

Recent developments in advanced piezoelectrics are highlighted in the figure, showing piezoelectric activity versus maximum usage temperature range for various piezoelectric materials. The relaxor-PT ferroelectric crystals with perovskite structure were found to possess the highest piezoelectric properties, with  $d_{33}$  values being on the order of  $>2000$  pC/N, however, their usage temperature range is limited by the low ferroelectric phase transition  $T_{RTS}$ <sup>126</sup>. Perovskite polycrystalline ceramics, including PMNT, PZT and BSPT, have sensitivities in the range of 200 pC/N to 900 pC/N, with a usage temperature range of 100-400°C, restricted by thermally activated aging behavior at temperatures far below their  $T_C$ . Ferroelectric materials with the tungsten bronze and Aurivillius structures possess medium piezoelectric properties, ranging from 10 pC/N to 100 pC/N, with usage temperatures up to 550°C, limited by  $T_C$  or low electrical resistivity at elevated temperatures. It should be noted that though LN crystals possess a  $T_C$  of 1150°C, their low resistivities and oxygen loss at elevated temperature restrict applications to  $< 600$ °C.

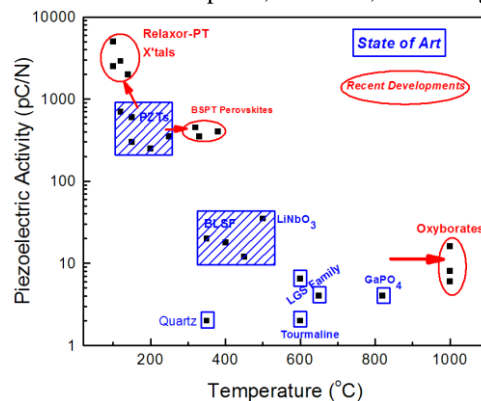


Figure. Piezoelectric activity as function of usage temperature range for different piezoelectrics.

<sup>126</sup> S. Zhang and F. Li, "High performance ferroelectric relaxor-PT single crystals: status and perspective," J. Appl. Phys., Vol.111, 031301, 2012.



Generally, nonferroelectric piezoelectric single crystals possess low sensitivity, falling in the range of 1-20pC/N, however, their ultralow mechanical and dielectric losses, and high electrical resistivities, make them ideal candidates for ultra-high temperature sensing applications<sup>127</sup>.

---

<sup>127</sup> S. Zhang and F. Yu, "Piezoelectric materials for high temperature sensors," J. Am. Ceram. Soc., Vol.94, pp.3153-3170, 2011.

## High Temperature Behaviors of Piezoelectric Sorosilicate Single Crystals

H. Takeda<sup>1</sup>, M. Hagiwara<sup>1</sup>, H. Noguchi<sup>1</sup>, T. Hoshina<sup>1</sup>, N. Kodama<sup>2</sup> and T. Tsurumi<sup>1</sup>

<sup>1</sup>Tokyo Institute of Technology, 2-12-1 Ookayama, Meguro, Tokyo 152-8550, Japan.

<sup>2</sup>Akita University, 1-1 Tegata-gakuencho, Akita 010-8502, Japan

E-mail: htakeda@ceram.titech.ac.jp

High temperature piezoelectric materials are highly demanded for gas sensors, combustion pressure sensors (CPS) and gas injectors directly placed in the cylinder part of engines. For the CPS use, the material need possess a low temperature dependence of the piezoelectric properties and a high electric resistivity at high temperature. Currently, there are four candidates of piezoelectric materials such as gallium phosphate ( $\text{GaPO}_4$ ), langasite ( $\text{La}_3\text{Ga}_5\text{SiO}_{14}$ ) family, rare-earth calcium oxoborate ( $\text{YCa}_4\text{O}(\text{BO}_3)_3$ ), and aluminum nitride ( $\text{AlN}$ ). Among of them, the most promising candidates are langasite type single crystals because the crystals with large size can be synthesized by melt growth technique. However, these crystals need still improvement of electric resistivity. In this study, we have demonstrated the possibility of sorosilicate-type single crystal for high temperature use. Material constants of the crystal were determined at the driving temperature (@400°C). Resistivity measurement was also conducted up to 700°C. The sorosilicate crystal showed ten times higher resistivity than those of langasite family as shown in Fig. 1. We have constructed measurement system of direct piezoelectric effect at high temperature and characterized the crystals under pseudo combustion environment in the engine cylinder. Output charge against applied stress was properly detected at 400°C. The sorosilicate-type crystal showed better performance than other piezoelectric materials.

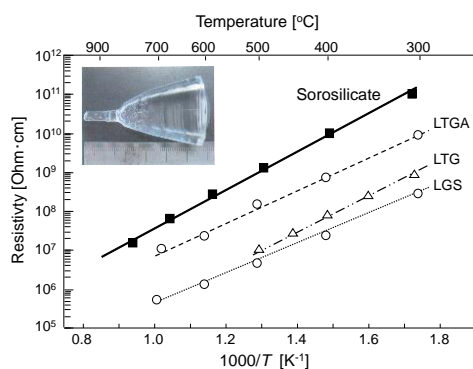


Fig. 1. Temperature dependence of resistivity of sorosilicate-type crystal and langasite family crystals (LTGA: Al-doped  $\text{La}_3\text{Ta}_{0.5}\text{Ga}_{5.5}\text{O}_{14}$ , LTG:  $\text{La}_3\text{Ta}_{0.5}\text{Ga}_{5.5}\text{O}_{14}$ , LGS:  $\text{La}_3\text{Ga}_5\text{SiO}_{14}$ ). The inset is a photograph of the sorosilicate-type crystal grown by Czochralski technique.

## Bi(B'B'')O<sub>3</sub> – PT based High Temperature Piezoelectrics

Ben Kowalski<sup>1</sup>, Alp Sehirlioglu<sup>1</sup>

<sup>1</sup>Materials Science and Engineering, Case Western Reserve University, Cleveland, OH/USA

Email: bak121@case.edu

High temperature piezoelectrics are sought after for ultrasonic drilling on the surface of Venus, dampening of turbine blades in hot regions, and energy harvesting in a thermoacoustic engine, etc. Previous studies by Grinberg and Eitel have predicted Curie temperatures ( $T_c$ ) greater than that of Pb(Zr,Ti)O<sub>3</sub> (PZT) through solid solutions of Bi(B'B'')O<sub>3</sub> with PbTiO<sub>3</sub>(PT).<sup>128,129</sup> In this work, doping for the B-site cations is explored through combination of the ternary (1-x-y)BiScO<sub>3</sub>–(x)Bi(Zn<sub>0.5</sub>,Zr<sub>0.5</sub>)O<sub>3</sub>–(y)PbTiO<sub>3</sub> (BS-BZZ-PT) with In, Mn, Sb, Sn, Ga, and Sm. These systems are being investigated via weak and high field studies to establish dielectric and electromechanical properties as a function of temperature, frequency, and electric field.

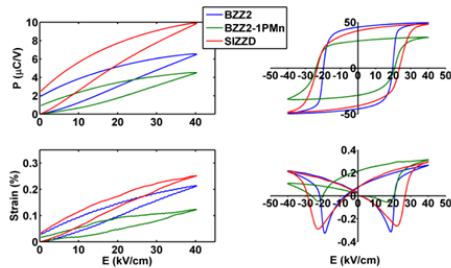


Fig. 1: Unipolar and bipolar polarization and strain for 3 compositions.

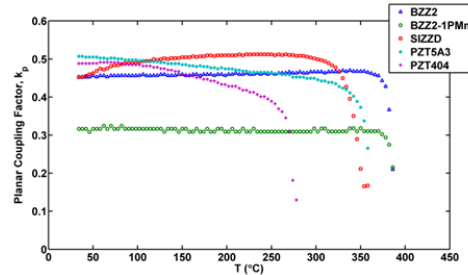


Fig. 2: Planar coupling factor vs. temperature for 5 compositions.

Room temperature examples of hysteresis/strain loops are shown in Fig. 1 for unmodified **BZZ2** (37.5BS-2.5BZZ-60PT) and two modified compositions, **BZZ2-1PMn** (1Mn for 1Ti) and **SIZZD** (30BS-5BZZ-5BI-60PT). Planar coupling factor vs. temperature is compared in Fig. 2 for the three previous compositions as well as two commercial PZT's. The Bi-based compositions have superior temperature stability for  $k_p$  as well as other properties. Aliovalent doping of Mn for Ti (**1PMn**) increases the mechanical quality factor ( $Q_m$ ), decreases the  $\tan\delta$  with no loss in  $T_c$ , but a drop in  $k_p$  does occur. Trading out 5BS for 5BI (**SIZZD**) increases  $k_p$ , increases the  $d_{33}$  from 430 to 630 pm/V, but reduces the  $T_c$  by  $\sim 20^\circ\text{C}$ . Doping schemes will be shown to design piezoelectrics for different applications by modifying  $k_p$ ,  $\epsilon_r$ ,  $Q_m$ ,  $\tan\delta$ , and  $d_{33}$ .

<sup>128</sup> J. Appl. Phys. 98, (2005)

<sup>129</sup> Jpn. J. Appl. Phys. Vol. 40 (2001)

## **Pb(Yb<sub>1/2</sub>Nb<sub>1/2</sub>)O<sub>3</sub>-PbTiO<sub>3</sub>, structure-property relation in a high temperature piezoelectric material**

Charlotte Cochard<sup>1,2</sup>, Christine Bogicevic<sup>1</sup>, Xavier Brill<sup>1</sup>, Nicolas Guiblin<sup>1</sup>, Florence Porcher<sup>3</sup>, Orland Guedes<sup>2</sup>, Pierre-Eymeric Janolin<sup>1</sup>

<sup>1</sup> Laboratoire SPMS, UMR CNRS-École Centrale Paris, Châtenay-Malabry, France

<sup>2</sup> Schlumberger, Clamart, France

<sup>3</sup> Laboratoire LLB, CEA, Saclay, France

Email: [Charlotte.Cochard@ecp.fr](mailto:Charlotte.Cochard@ecp.fr)

Piezoelectricity has attracted a considerable amount of work due to the variety of possible applications such as accelerometers, gyroscopes or transducers. Solid solutions of relaxors and classical ferroelectrics are known to exhibit enhanced piezoelectric properties close to the morphotropic phase boundary (MPB) compared to the pure materials counterpart. Therefore, materials such as Pb(Mg<sub>1/3</sub>Nb<sub>2/3</sub>)O<sub>3</sub>-PbTiO<sub>3</sub> or Pb(Zn<sub>1/3</sub>Nb<sub>2/3</sub>)O<sub>3</sub>-PbTiO<sub>3</sub> have been extensively studied over the last 50 years. On the contrary, Pb(Yb<sub>1/2</sub>Nb<sub>1/2</sub>)O<sub>3</sub>-PbTiO<sub>3</sub> (PYN-PT) which is long known to have good piezoelectric properties ( $d_{33}=510\text{pC/N}$ ) and a relatively high Curie temperature ( $\sim 370^\circ\text{C}$  at the MPB) has not been examined so extensively probably because of the scarcity of single crystals

In this work, we will present experimental data obtained on PYN-PT of different compositions close to the MPB. These data were obtained by X-ray diffraction, neutron scattering as well as dielectric and piezoelectric measurement as a function of temperature, enabling a clearer picture of the structure-property relation around the MPB to emerge in this material of crucial importance for high-temperature applications.

## Piezoceramic Materials for High-Temperature & High-Pressure Applications in Oilfield Exploration & Production

Kenneth Liang<sup>1</sup>, Wanda Wolny<sup>2</sup>, Dragan Damjanovic<sup>3</sup>, Torsten Bove<sup>2</sup>

<sup>1</sup>Schlumberger-Doll Research, Cambridge, MA, USA

<sup>2</sup>Meggitt A/S, Kvistgaard, Denmark

<sup>3</sup>Institute of Materials, EFPL, Lausanne, Switzerland

Email: [kliang@slb.com](mailto:kliang@slb.com)

Ultrasonic measurements play important roles in many oilfield services applications. With oil wells reaching ever increasing depths, the operating environment is characterized by high temperature and high pressure (175°C, 20,000psi and beyond). Ultrasonic transducers typically operate into a liquid-filled borehole. Lead metaniobate, mainly due to its low acoustic impedance and despite its low  $k_t$ , is used where both efficiency and bandwidth are required. There is ongoing effort though to seek equivalent and better substitute materials. This work is a continuation of a previous study carried out on Pz31 and Pz36, two PZT-based materials developed by Meggitt A/S with engineered porosity<sup>130</sup>. While these materials are well-behaved with temperature, both tend to depole when subjected to 15,000psi, with Pz31 being more susceptible to depoling than Pz36. The polarization can be restored by repoling afterwards, indicating that depoling is due *only* to rearrangement of polarization within samples and *not* mechanical failure. The depoling mechanism is not understood and the difference in vulnerability to static pressure appears to be inconsistent with the relative degree of hardness of, and the rhombohedral and tetragonal structures of Pz31 and Pz36 respectively. To develop insight, we carried out identical temperature and pressure tests on the fully densified versions of Pz31 and Pz36, Pz24 and Pz26 respectively. The experimental setup is described and the results and analyses are given.

A bismuth titanate based material, Pz46, has also been studied for its suitability under extreme conditions. It exhibits  $k_t \sim 0.2$ , slightly higher acoustic impedance than lead metaniobate, Curie temperature in excess of 600°C, and is highly resistant to shock. The material has been temperature cycled up to 200°C with no degradation and results of pressure cycling to assess its field worthiness will be reported and discussed.

---

<sup>130</sup> Bove, Liang, Wolny, "Experimental Study of Temperature & Pressure Effects on High-Porosity PZT Materials," IEEE Ultrasonics Symposium Proceedings, Dresden, 2012

---

## **Lead-free ceramics: E-field Effects**

CLUB A

*Tuesday, July 23 2013, 02:00 pm - 03:30 pm*

Chair: **Xiaoli Tan**  
*Iowa State University*

## ***In situ* diffraction reveals the dependence of BaTiO<sub>3</sub> grain size on domain wall motion and relation to macroscopic properties**

Jacob L. Jones<sup>1</sup>, Dipankar Ghosh,<sup>1</sup> Akito Sakata,<sup>1</sup> Jared Carter,<sup>1</sup> Hyuksu Han,<sup>1</sup> Juan C. Nino,<sup>1</sup> and Pam A. Thomas<sup>2</sup>

<sup>1</sup> Department of Materials Science and Engineering, University of Florida, Gainesville, FL 32611, USA

<sup>2</sup> Department of Physics, University of Warwick, Coventry, CV4 7AL, UK

Email: jjones@mse.ufl.edu

It is now widely accepted that polycrystalline barium titanate (BaTiO<sub>3</sub>) exhibits maximum room temperature relative permittivity ( $\epsilon_r$ ) at a grain size of approximately 1-2  $\mu\text{m}$  and  $\epsilon_r$  decreases below and above this grain size. Some limited studies have also shown analogous behavior of the piezoelectric coefficients,  $d_{33}$  or  $d_{31}$ , with grain size. Two widely accepted theories attribute this behavior to either internal residual stress or non-180° domain wall motion, though a direct measurement of the exact origin of such grain size effects has, to date, elucidated researchers.

Using an *in situ* high-energy X-ray diffraction (XRD) technique in transmission mode during application of high external electric fields, we show conclusive and direct evidence that 90° domain wall motion in BaTiO<sub>3</sub> is present under high electric fields across the grain size range 0.2  $\mu\text{m}$  to 3.5  $\mu\text{m}$  and, most notably, is maximum at a grain size of approximately 2  $\mu\text{m}$ . Measurements of  $\epsilon_r$  and  $d_{33}$  in these same samples show that the properties also peak at 2  $\mu\text{m}$  (Figure 1).

X-ray measurement of the unit cell volume and spontaneous lattice strain also indicates that the degree of residual internal stress due to changing domain wall density is measurable though small. The current investigation thus conclusively attributes 90° domain wall motion to the grain size dependence of BaTiO<sub>3</sub> ceramics in the 0.2-3.5  $\mu\text{m}$  range.

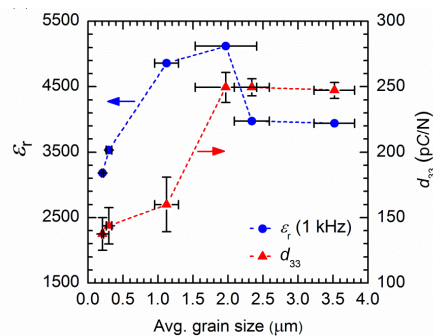


Fig. 39: Relative permittivity and longitudinal piezoelectric coefficient measurements of the samples synthesized for the present work.

## High-speed data capture of the electric field induced phase transition in potassium sodium bismuth titanate

Tim P. Comyn<sup>1</sup>, Andrew J. Bell<sup>1</sup>, Annette Kleppe<sup>2</sup>

<sup>1</sup>Institute for Materials Research, University of Leeds, Leeds, UK

<sup>2</sup>Diamond Light Source, Harwell Science Campus, Didcot, Oxfordshire, UK

Email: [t.p.comyn@leeds.ac.uk](mailto:t.p.comyn@leeds.ac.uk)

The lead free system KNBT ( $x\text{K}_{1/2}\text{Bi}_{1/2}\text{TiO}_3-(1-x)\text{Na}_{1/2}\text{Bi}_{1/2}\text{TiO}_3$ ) exhibits an electric field induced phase transition from rhombohedral to mixed phase rhombohedral and tetragonal, for  $x=0.2$ , as confirmed using in-situ synchrotron experiments. Here, we track the phase transition at high speed, using a state of the art Pilatus x-ray detector. Strobing has been used by other groups to track ferroelectric materials driven around major and minor hysteresis loops, using synchrotron and neutron radiation, but such techniques are not appropriate here. The phase transition which occurs in KNBT during poling is irreversible, except by heating to above 400 °C.

Data collected at 100 Hz shows that an electric field induced strain precedes the phase transition. The detector was synchronized with the electric drive field. The complexities of the experiment, and further improvements are discussed.



Effect of Applied Field Direction in  $\{001\}_{pc}$  Oriented  
 $\text{Bi}_{0.5}\text{Na}_{0.5}\text{TiO}_3\text{-}7\text{BaTiO}_3\text{-}2\text{K}_{0.5}\text{Na}_{0.5}\text{NbO}_3$  Bulk Ceramics

<sup>a</sup>Chris M. Fancher, <sup>a</sup>John E. Blendell, and <sup>a,b</sup>Keith J. Bowman

α) Σχημολ οφ Ματεριαλσ Ενγινεερινγ, Πυρδυε Υνιπερσιτυ, Ωεστ  
Λαφαψεττε 47907, ΥΣΑ

β) Mechanical, Materials & Aerospace Engineering, Illinois Institute of  
Technology, Chicago, Illinois 60616, USA

The high strain response of the  $\text{Bi}_{0.5}\text{Na}_{0.5}\text{TiO}_3\text{-}y\text{BaTiO}_3\text{-}x\text{K}_{0.5}\text{Na}_{0.5}\text{NbO}_3$  system has been attributed to a reversible electric-field-induced phase transformation from a pseudocubic to a distorted polar structure. A recent *in situ* experiment has reported BNT-6BT-2KNN to transform from an undistorted tetragonal into a phase mixture of distorted rhombohedral and tetragonal phases. In this work, the effect that crystallographic texture and texture symmetry have on the field-induced phase transformation of BNT-7BT-2KNN bulk ceramics was investigated. Bulk BNT-7BT-2KNN ceramics with a 8.6 multiples of a random distribution (MRD)  $\{001\}_{pc}$  fiber texture were prepared using the tape-casting method with a 5wt% template fraction. Texturing improved the high field strain response of BNT-7BT-2KNN by 47%. To understand the origin of this improvement, the effect texture symmetry has on the strain response was investigated by applying an electric field parallel or perpendicular to the  $\{001\}_{pc}$  fiber texture axis. Applying the electric field perpendicular to the fiber axis resulted in a high field strain response that was 16% lower compared to the strain response for a field applied along the fiber axis. Field direction did not affect the volume expansion during electric cycling; suggesting the field-induced phase transformation is independent of the applied field direction. *In situ* diffraction showed that field direction does not effect the induced phase formation; however, field direction did affect the ferroelastic texture and electric field required to induce the polar phase.

## Electric Field-Induced Polarization and Strain in $94(\text{Bi}_{1/2}\text{Na}_{1/2})\text{TiO}_3$ - 0.06BaTiO<sub>3</sub> Under Uniaxial Stress

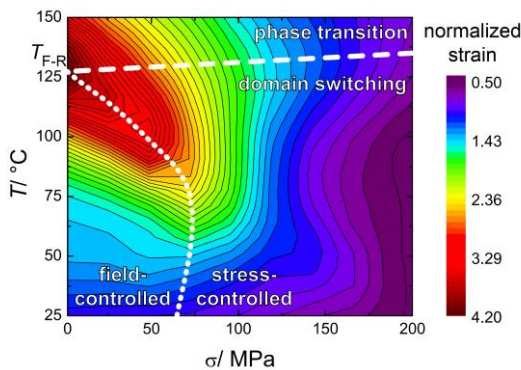
Robert Dittmer<sup>1</sup>, Kyle G. Webber<sup>1</sup>, Emil Aulbach<sup>1</sup>, Wook Jo<sup>1</sup>, Xiaoli Tan<sup>2</sup>, and Jürgen Rödel<sup>1</sup>

<sup>1</sup>Institute of Materials Science, Technische Universität Darmstadt, Darmstadt, Germany

<sup>2</sup>Department of Materials Science and Engineering, Iowa State University, Ames, IA, USA

Email: dittmer@ceramics.tu-darmstadt.de

Solid solutions based on  $\text{Bi}_{1/2}\text{Na}_{1/2}\text{TiO}_3$  (BNT) are capable of producing large strains that rival PZT at high electric fields. In application an actuator has to produce large displacements against an external mechanical load. Blocking stress measurements demonstrated that  $0.94\text{Bi}_{1/2}\text{Na}_{1/2}\text{TiO}_3$ - $0.06\text{BaTiO}_3$  (BNT-6BT) can provide a large maximum stress  $\sigma_B$  of 102 MPa at 125 °C. The addition of 2 mol%  $\text{K}_{0.5}\text{Na}_{0.5}\text{NbO}_3$  affords a large  $\sigma_B$  of 124 MPa even at room temperature. However, the effect of stress on the unipolar large-signal behavior remains unknown. In this study we present for the first time the complex field-, stress- and temperature-dependent large-signal properties of a lead-free piezoceramic. Polarization and strain hystereses have been obtained for the model material BNT-6BT during unipolar electric field loading from room temperature to 150 °C under uniaxial compressive stress up to 446 MPa. For low temperatures the maximum strain peaks at a certain stress due to enhanced non-180° domain switching. At 125 °C a large strain with a large-signal piezoelectric coefficient  $d_{33}^*$  of  $884 \text{ pm}\cdot\text{V}^{-1}$  is observed, which decreases upon the application of stress. This behavior is rationalized with a change in the primary strain mechanism from domain switching at low temperatures to a reversible electric field-induced transition from an ergodic relaxor state to a long-range order at high temperatures (see Figure). In addition, the energy terms for the output mechanical work and the charged electrical energy density are analyzed and used to define a large-signal efficiency.



Strain normalized to room temperature strain at zero-field as a function of stress for BNT-6BT.

## Exploration of Microscopic Mechanisms of the Polarization Switching in Lead-free BZT-xBCT Ferroelectrics

Sergey Zhukov, Yuri Genenko, Matias Acosta, Heide Humburg, Wook Jo and Heinz von Seggern

<sup>1</sup>Institut für Materialwissenschaft, TU Darmstadt, Darmstadt, Germany

Email: zhukov@e-mat.tu-darmstadt.de

Nowadays lead-free ferroelectric materials are receiving considerable attention as replacement for the market dominating, toxic lead-containing PZT ceramics. Recently discovered  $\text{Ba}(\text{Zr}_{0.2}\text{Ti}_{0.8})\text{O}_3-x(\text{Ba}_{0.7}\text{Ca}_{0.3})\text{TiO}_3$  compositions show piezoelectric properties comparable to that of PZT.<sup>131</sup> Similar to PZT, BZT-xBCT possesses a morphotropic phase boundary (MPB) where piezoelectric properties peak. At room temperature this boundary is at  $x = 50\%$  between the rhombohedral BZT and the tetragonal BCT.

In the current research the polarization switching process in different BZT-xBCT compositions ( $0.3 < x < 0.6$ ) has been studied over a broad time domain covering range from  $1\mu\text{s}$  to 100s. For all compositions investigated the temporal evolution of the switched polarization exhibits a rather complex shape which cannot be rationalized by the classical switching concept of nucleation and grow of reversed domains known also as the Kolmogorov-Avrami-Ishibashi (KAI) model. Unlike the KAI approach, the recently developed Inhomogeneous Field Mechanism (IFM) model<sup>132,133</sup> provides an adequate fit to the experimental results. Moreover, the experimentally obtained dependencies of the switching time on the electric field strongly suggest the existence of two distinct switching mechanisms in different field regions. The microscopic origin of both mechanisms as well as the evolution of their parameters with composition, microstructure and temperature will be discussed.

<sup>131</sup> W.F. Liu, X.B. Ren, "Large Piezoelectric Effect in Pb-Free Ceramics", *Phys. Rev. Lett.*, 103, 257602, 2009.

<sup>132</sup> S. Zhukov, Y. A. Genenko, O. Hirsch, J. Glaum, T. Granzow, H. von Seggern, "Dynamics of polarization reversal in virgin and fatigued ferroelectric ceramics by inhomogeneous field mechanism", *Phys. Rev. B*, 82, 014109, 2010.

<sup>133</sup> Y. A. Genenko, S. Zhukov, S.V. Yampolskii, J. Schüttrumpf, R. Dittmer, W. Jo, H. Kungl, M.J. Hoffmann, H. von Seggern, "Universal Polarization Switching Behavior of Disordered Ferroelectrics", *Adv. Funct. Mater.*, 22, 2058-2066, 2012.

## Electric Field Effects on Domain Processes and Properties in $\text{Ba}(\text{Zr}_{0.2}\text{Ti}_{0.8})\text{O}_3\text{-x}(\text{Ba}_{0.7}\text{Ca}_{0.3})\text{TiO}_3$ Piezoceramics

Matthias C. Ehmke<sup>1</sup>, John E. Blendell<sup>1</sup>, Keith J. Bowman<sup>1,2</sup>

<sup>1</sup>Materials Engineering, Purdue University, West Lafayette, IN 47907, USA

<sup>2</sup>Mechanical, Materials & Aerospace Engineering, Illinois Institute of Technology, Chicago, IL 60616, USA

Email: ehmke@purdue.edu

The lead-free  $\text{Ba}(\text{Zr}_{0.2}\text{Ti}_{0.8})\text{O}_3\text{-x}(\text{Ba}_{0.7}\text{Ca}_{0.3})\text{TiO}_3$  (BZT-BCT) system has been demonstrated to show attractive piezoelectric performance at the strongly temperature dependent morphotropic phase boundary (MPB) and is discussed in the literature as a possible alternative to lead based piezoceramics. Structural reports suggest the coexistence of rhombohedral and tetragonal phases at the MPB that result in the impressive properties.<sup>134</sup>

In the present study compositions across the MPB are investigated ranging from single rhombohedral to single tetragonal symmetries, including one MPB composition. The individual 180° and non-180° domain processes are studied as a function of the electric poling history by means of large signal polarization and strain, small signal permittivity and piezoelectric coefficients, as well as *in situ* synchrotron x-ray diffraction. Non-180° (ferroelastic) domain processes can be clearly identified by electric field dependent small signal permittivity measurements as well as by electric field dependent XRD.

Rietveld analysis of diffraction data using "Materials Analysis Using Diffraction" (MAUD)<sup>135</sup> reveals a very large electrically induced ferroelastic domain texture. For an applied electric field the domain alignment exceeds 85% in tetragonal BZT-BCT materials. At zero field a large relaxation of the domain texture is observed, which suggests that each field cycle leads to a strong ferroelastic domain reorientation. Moreover, the refined lattice parameters enable quantification of intrinsic and extrinsic contributions to the piezoelectric coefficient as a function of orientation. The large macroscopic piezoelectric response observed from electric measurements is discussed and related to the complex strain anisotropy in the microstructure and the extraordinary domain alignment developed under field as observed from *in situ* XRD. The results presented give insight into the design objectives of new lead-free piezoelectric materials.

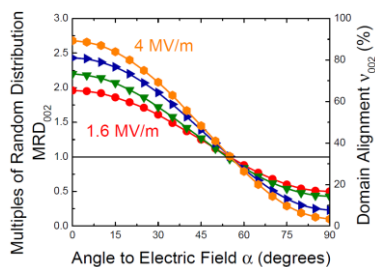


Fig. 40: Development of a large ferroelastic domain texture for an applied electric field, with domain alignment of over 85%.

<sup>134</sup> W. Liu and X. Ren, Phys. Rev. Lett. **103**, 257602 (2009).

<sup>135</sup> L. Lutterotti, M. Bortolotti, G. Ischia, I. Lonardelli, and H. R. Wenk, Zeitschrift für Kristallographie Supplements **2007**, 125 (2007).

---

## **Multiferroics**

CLUB B

*Tuesday, July 23 2013, 02:00 pm - 03:30 pm*

Chair: **Ruediger-A. Eichel**  
*Forschungszentrum Juelich*

## Direct Observation of Electric and Magnetic Field induced Ferroelectric Switching in a Room Temperature Multiferroic

D. M. Evans<sup>1\*</sup>, M. Arredondo<sup>1</sup>, A. Schilling<sup>1</sup>, Ashok Kumar<sup>2,3</sup>, D. Sanchez<sup>2</sup>, N. Ortega<sup>2</sup>, R. S. Katiyar<sup>2</sup>, J. F. Scott<sup>4</sup> and J. M. Gregg<sup>1</sup>

<sup>1</sup> School of Mathematics and Physics, Queen's University Belfast, Belfast, N. Ireland, BT7 1NN, UK.

<sup>2</sup> Department of Physics and Institute of Multifunctional Materials, University of Puerto Rico, San Juan, P.R., USA.

<sup>3</sup> Materials Physics and Engineering Division, National Physical Laboratory, New Delhi-110012, India

<sup>4</sup> Department of Physics, Cavendish Laboratory, J. J. Thomson Ave., Cambridge, CB3 0HE, UK.

Email: [devans92@qub.ac.uk](mailto:devans92@qub.ac.uk)

For any material to realize a multiferroic device there must be coupling between the ferromagnetism and ferroelectricity. This has been shown at low temperature by switching magnetically and electrically as far back as the 60s [1]. However, it was not until 2006 that any form of coupling was demonstrated at room temperature [2]. Zhao *et al.* switched antiferromagnetic domains in BiFeO<sub>3</sub> using an electric field. Despite this progress in switching antiferromagnetic domains no one has directly observed switching, at room temperature, of ferromagnetic domains by using an electric field, or ferroelectric domains by using a magnetic field.

In this talk, we will show electrical switching in a co-planar geometry, imaged with a PFM, we then show how a comparable remanent ferroelectric domains pattern can be achieved with a magnetic field; the authors believe this is the first demonstration of equivalence between electric and magnetic field at room temperature. TEM is used to investigate the domain hierarchy and to look at preliminary evidence that coupling occurs on the lowest level of hierarchy, on a scale of order tens of nanometers. Finally we gain an order of magnitude estimate for the effective magnetoelectric coupling coefficient[4] and compare it to other values in the literature. All our samples are single crystal slabs of ca. (PbZr<sub>0.53</sub>Ti<sub>0.47</sub>O<sub>3</sub>)<sub>0.6</sub>-(PbFe<sub>0.5</sub>Ta<sub>0.5</sub>O<sub>3</sub>)<sub>0.4</sub> cut from single grains of bulk multiferroic ceramics [3] by using a Focused Ion Beam Microscope.

[1] E. Ascher *et al.*, *J. Appl. Phys.* **37**, 1404-1405, 1966

[2] T. Zhao *et al.*, *Nat. Mater.* **5**, 823 – 829, 2006

[3] D. Sanchez *et al.*, *AIP Adv.* **1**, 042169, 2011

[4] D. M. Evans *et al.*, *Nat. Comms.* **4**, 1534 (2013)

## Influence of Composition on the Multiferroic Properties of 5-layer $\text{Bi}_6\text{Ti}_x\text{Fe}_y\text{Mn}_z\text{O}_{18}$ Aurivillius Phase Thin Films

Lynette Keeney<sup>1</sup>, Ahmad Faraz<sup>1</sup>, Nitin Deepak<sup>1</sup>, Tuhin Maity<sup>1</sup>, Michael Schmidt<sup>1</sup>, Andreas Amann<sup>1,2</sup>, Nikolay Petkov<sup>1</sup>, Saibal Roy<sup>1</sup>, Martyn E. Pemble<sup>1,3</sup>, Roger W. Whatmore<sup>1,3</sup>.

<sup>1</sup>Tyndall National Institute, University College Cork, Cork, Ireland

<sup>2</sup>School of Mathematical Sciences, University College Cork, Cork, Ireland

<sup>3</sup>Department of Chemistry, University College Cork, Cork, Ireland

Email: lynette.keeney@tyndall.ie

Single-phase, room temperature magnetoelectric multiferroic materials are of considerable interest for potential applications in sensors and spin-based memory/logic devices<sup>136</sup> as a result of their ability to induce a change in magnetization by an applied electric field or electric polarization by a magnetic field. However, such materials are exceptionally scarce. Recently<sup>137</sup>, Aurivillius phase thin films prepared by a chemical solution deposition method, having an average film composition of  $\text{Bi}_6\text{Ti}_{2.8}\text{Fe}_{1.52}\text{Mn}_{0.68}\text{O}_{18}$  (B6TFMO), demonstrated both ferroelectric and ferromagnetic hysteresis at room temperature. Microstructural analysis concluded that the multiferroic behaviour does not originate from impurity phases to a confidence level of 99.5%. Piezoresponse force microscopy (PFM) investigations as a function of applied magnetic field demonstrated magnetic field induced switching of ferroelectric polarisation in individual grains at room temperature (Fig. 1). This present work will report the effect of Ti/Fe/Mn compositional ratios on the multiferroic properties of B6TFMO thin films prepared on sapphire substrates by chemical solution deposition. Structural, ferroelectric (PFM), magnetic (superconducting quantum interference device magnetometry) and magnetoelectric (PFM under magnetic field) properties are assessed and an optimised B6TFMO composition selected for the growth of thin films with controlled orientation and texture by atomic vapour deposition (AVD).<sup>138</sup>

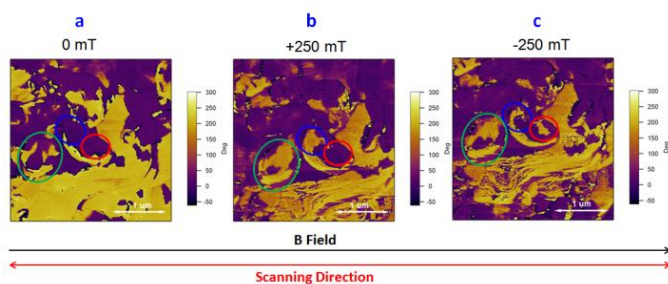


Fig. 1: Representative PFM phase images of B6TFMO thin films on *c*-plane sapphire under (a) 0 mT, (b) 250 mT and (c)

<sup>136</sup> Emerging Research Device Materials, ITRS, 2007 Edition

<sup>137</sup> L. Keeney, T. Maity, M. Schmidt, A. Amann, N. Deepak, N. Petkov, S. Roy, M. E. Pemble and R. W. Whatmore, "Magnetic-Field-Induced Ferroelectric Switching in Multiferroic Aurivillius Phase Thin Films at Room Temperature", *submitted*.

<sup>138</sup> The support of SFI under the FORME SRC Award number 07/SRC/I1172 and FP7-PEOPLE-2011 under the NANOMOTION Grant Agreement Number 290158 is gratefully acknowledged.

## Application of PMN-PT ferroelectric relaxor for multiferroic random access memory cell

Nicolas Tiercelin<sup>1</sup>, Yannick Dusch<sup>1</sup>, Alexey Klimov<sup>2</sup>, Stefano Giordano<sup>1</sup>, Arnaud Stolz<sup>1</sup>, Vladimir Preobrazhensky<sup>3</sup> and Philippe Pernod<sup>1</sup>

International Associated Laboratory LICS/LEMAC :

<sup>1</sup>IEMN UMR CNRS 8520, PRES Lille Nord de France, ECLille, Villeneuve d'Ascq, France

<sup>2</sup>V. A. Kotel'nikov Institute of Radioengineering and Electronics, 125009 Moscow, Russia

<sup>3</sup>Wave Research Center, GPI RAS, Moscow, Russia

Email: Nicolas.tiercelin@iemn.univ-lille1.fr - Preobr@newmail.ru

The renaissance of multiferroics<sup>139</sup> has triggered a quest for magnetoelectric memories, offering non-volatility, endurance, high switching speeds and ultra-low power operation. In 2010, Tiercelin *et al.*<sup>140</sup> proposed a concept for magnetoelectric random access memory (MELRAM) based on stress-mediated composite multiferroic. Theoretical studies of the expected performances have been presented<sup>141</sup> and a macroscopic proof of the concept was provided<sup>142</sup>. In this system electric field allows switching between two orthogonal magnetic states "0" or "1" in plane of magnetostrictive subsystem. In order to be successfully integrated in practical devices, one must find an efficient way to generate inplane anisotropic stress in a simple planar structure with vertical dielectric polarisation. We show here that the ferroelectric relaxors of the PMN-PT type, cut in the  $\langle 011 \rangle$  plane are suitable candidates for MELRAM cell design. For demonstration we sputtered the magnetostrictive nanostructure  $10 \times [(TbCo_2)_{5nm}/(FeCo)_{5nm}]$  on commercial  $\langle 011 \rangle$  PMN-PT single crystal substrate (fig.1). A magnetic easy axis (EA) was induced in plane by application of static magnetic field during sputtering. External magnetic field  $H_s$  perpendicular to the EA created two energetically equivalent magnetic states. Application of a positive voltage pulse to the planar electrodes induced orientation of magnetisation in the position "1", whereas a negative pulse switched magnetisation to the position "0". The switching process was detected by magneto-optic Kerr effect (MOKE). The results of MOKE signal measurements are shown on fig.1. The

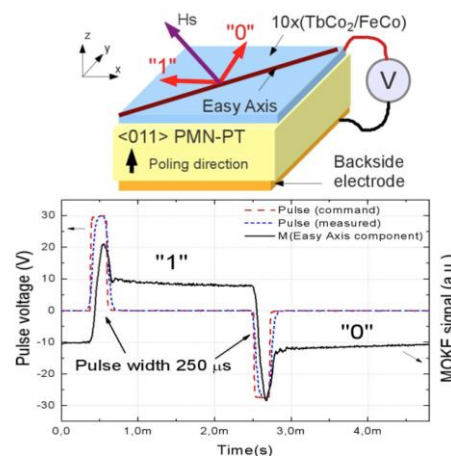


Fig. 41: Prototype of MELRAM cell and experimental evidence of by electric field magnetisation switching in magnetostrictive nanostructure deposited on single crystal PMN-PT

<sup>139</sup> N. Spaldin, and M. Fiebig, Science, 309 (5733), 391-392, 2005.

<sup>140</sup> N. Tiercelin, Y. Dusch, V. Preobrazhensky, and P. Pernod, J. Appl. Phys. 109, 07D726, 2011.

<sup>141</sup> S. Giordano, Y. Dusch, N. Tiercelin, P. Pernod and V. Preobrazhensky, Phys.Rev.B 85, 155321, 2012.

<sup>142</sup> N. Tiercelin, Y. Dusch, A. Klimov, S. Giordano, V. Preobrazhensky, P. Pernod, Appl.Phys.Lett. 99, 192507, 2011



characteristics of cell and prospective of MELRAM technology are discussed.

## Spin dynamics controlled by strain in BiFeO<sub>3</sub> films

Daniel Sando<sup>1</sup>, Arsène Agbelele<sup>3</sup>, Dovran Rahmedov<sup>4</sup>, Ingrid C. Infante<sup>2</sup>, Alexander Pyatakov<sup>6</sup>, Laurent Bellaïche<sup>4</sup>, Stéphane Fusil<sup>1</sup>, Cecile Carretero<sup>1</sup>, Eric Jacquet<sup>1</sup>, Cyrile Deranlot<sup>1</sup>, Sergey Lisenkov<sup>7</sup>, Dawei Wang<sup>8</sup>, Jean-Marie Le Breton<sup>3</sup>, Maximilien Cazayous<sup>5</sup>, Alain Sacuto<sup>5</sup>, Jean Juraszek<sup>3</sup>, Anatoly Zvezdin<sup>6</sup>, Agnès Barthélémy<sup>1</sup>, Brahim Dkhil<sup>2</sup>, Manuel Bibes<sup>1</sup>

<sup>1</sup>Unité Mixte de Physique CNRS/Thalès UMR137, Palaiseau, France

<sup>2</sup>Ecole Centrale Paris/CNRS UMR8580, Chatenay-Malabry, France

<sup>3</sup>Université de Rouen/CNRS UMR6634, Rouen, France

<sup>4</sup>Physics Department, University of Arkansas, Fayetteville, Arkansas, United States

<sup>5</sup>Université Paris 7/CNRS UMR7162, Paris, France

<sup>6</sup>Russian Academy of Sciences, Moscow, Russian Federation

<sup>7</sup>University of South Florida, Tampa, FL, United States

<sup>8</sup>Xi'an Jiaotong University, Xi'an, China

Email: [ingrid.canero-infante@ecp.fr](mailto:ingrid.canero-infante@ecp.fr)

Multiferroics are considered as ideal materials to combine magnetic control of polarization and conversely, electric control of magnetization, as they show (within the same phase) ferroelectric and magnetic orders. Among these materials, BiFeO<sub>3</sub> has been by far the most investigated, mainly because it is one of the few room temperature multiferroics. Bulk BiFeO<sub>3</sub> is characterized by a large ferroelectric polarization coexisting with a G-type antiferromagnetic order and a spin cycloid. When grown in thin film form, the epitaxial strain has been shown to induce important distortions on unit cell causing a drift of the ferroelectric transition<sup>143</sup> and eventually the stabilization of new phases<sup>144</sup>.

In the present work<sup>145</sup>, we explore the less studied effects of epitaxial strain on spin dynamics of BiFeO<sub>3</sub> films. By combining Mössbauer and Raman spectroscopies with Landau-Ginzburg and effective Hamiltonian calculations, we have evidenced that a spin cycloid modulation exists in BiFeO<sub>3</sub> thin films at small and moderate strains and disappears at high tensile and compressive strains. We have also observed that the average spin orientation evolves from in-plane to out of plane directions when the strain changes from compressive to tensile, which leads to a strong modification of spin dynamics in these films. The interface effects and coupling to other ferromagnetic layers through exchange bias effects will also be presented and discussed in the spirit of proposing and proving direct applications in tuning the conduction in giant magnetoresistive spin valves.

---

<sup>143</sup> I. C. Infante et al. Phys. Rev. Lett. **105**, 057601 (2010)

<sup>144</sup> R. J. Zeches et al. Science **326**, 977 (2009) ; B. Dupé et al., Phys. Rev. B **81**, 144128 (2010)

<sup>145</sup> D. Sando et al., Nature Materials, in press

## On the chemical stability and charged point defects in BiFeO<sub>3</sub>-materials

Tor Grande<sup>1</sup>

<sup>1</sup>Department of Materials Science and Engineering,  
Norwegian University of Science and Technology, NO-7491 Trondheim, Norway

Email: grande@ntnu.no

The rhombohedral perovskite BiFeO<sub>3</sub> has become the centre of research on multiferroics due to its robust room-temperature multiferroism with a Néel temperature of 370 °C and a Curie temperature of 820–830 °C.<sup>146</sup> Beside the multiferroic properties BiFeO<sub>3</sub> is also interesting because of its high intrinsic polarization of  $\sim 100 \mu\text{C}/\text{cm}^2$ , which is along the pseudocubic (111) direction. A tremendous amount of work has been reported on BiFeO<sub>3</sub> thin films, single crystals and bulk ceramics,<sup>1</sup> but particularly the investigations on bulk BiFeO<sub>3</sub> ceramics have been hampered by the severe difficulties to prepare single phase materials and the problems with dielectric loss caused by the high electronic conductivity of BiFeO<sub>3</sub>.

We will first focus on the thermodynamic stability of BiFeO<sub>3</sub>, particularly with respect to the competing reaction to form the phases Bi<sub>25</sub>FeO<sub>39</sub> and Bi<sub>2</sub>Fe<sub>4</sub>O<sub>9</sub> on the expense of BiFeO<sub>3</sub>.<sup>147</sup> The thermodynamic stability of BiFeO<sub>3</sub> and related Bi-based perovskites is discussed in relation to Goldschmidt tolerance factor and the influence of pressure/strain and chemical substitution.

The thermodynamic stability and properties of BiFeO<sub>3</sub> is also influenced by the volatility of Bi<sub>2</sub>O<sub>3</sub> at elevated temperatures. The corresponding loss of PbO in PZT materials is known to have a pronounced effect on the functional properties of traditional lead-based ferroelectric materials, and here will discuss possible influence of charged point defects in the BiFeO<sub>3</sub>-materials due to loss of Bi<sub>2</sub>O<sub>3</sub>. Volatilization of Bi<sub>2</sub>O<sub>3</sub> will create charged point defects in the perovskite lattice, more precisely Bi and O vacancies. These point defects may have detrimental effects on the properties of bulk BiFeO<sub>3</sub> ceramics mainly due to two different reasons.

First, the oxygen vacancies formed due to Bi<sub>2</sub>O<sub>3</sub> loss may influence on the oxidations state Fe and thereby on the electrical conductivity of BiFeO<sub>3</sub>. Iron is Fe<sup>3+</sup> in stoichiometric BiFeO<sub>3</sub>, but may oxidize to Fe<sup>4+</sup> due to available oxygen vacancies leading to increasing p-type conductivity.<sup>148</sup> We will discuss the influence of the atmosphere during thermal annealing by examples from (1-x) Bi<sub>0.5</sub>K<sub>0.5</sub>TiO<sub>3</sub> – x BiFeO<sub>3</sub> (BKT-BFO) solid solutions.<sup>149</sup>

Finally, point defects may also strongly influence on the domain wall mobility in BiFeO<sub>3</sub>, as recently discussed by Rojac *et al.*<sup>150</sup> Strategies to reduce the influence of point defects and thereby

<sup>146</sup> G. Catalan, J.F. Scott “Physics and applications of bismuth ferrite”, *Adv. Mater.*, vol. 21, p. 2463-2485, 2009.

<sup>147</sup> S.M. Selbach *et al.* “On the thermodynamic stability of BiFeO<sub>3</sub>”, *Chem. Mater.*, vol. 21, p. 169-173, 2009.

<sup>148</sup> S.M. Selbach, T. Tybell, M.-A. Einarsrud, T. Grande “Phase transitions, electrical conductivity and chemical stability of BiFeO<sub>3</sub> at high temperature”, *J. Solid State Chem.*, vol. 183, p. 1205-1208, 2010.

<sup>149</sup> M. I. Morozov, M.-A. Einarsrud, T. Grande., “Polarization and strain response in Bi<sub>0.5</sub>K<sub>0.5</sub>TiO<sub>3</sub> – BiFeO<sub>3</sub> ceramics”, *Appl. Phys. Lett.*, vol. 101, 252904, 2012.

<sup>150</sup> T. Rojac, M. Kosec, B. Budic, N. Setter, D. Damjanovic “Strong ferroelectric domain-wall pinning in BiFeO<sub>3</sub> ceramics”, *J. Appl. Phys.* vol. 108, 074107, 2010.

softening of  $\text{BiFeO}_3$  is discussed with particular emphasis on the atmosphere during annealing and chemical substitution of Fe with Ti, which reduces the oxygen vacancy concentration.

---

**PFM4**

CLUB C

*Tuesday, July 23 2013, 02:00 pm - 03:30 pm*

Chair: **To Be Aannounced**

## **Polarization-Related Electronic Properties of Complex Oxides**

**Alexei Gruverman**

*Department of Physics and Astronomy, University of Nebraska, Lincoln, NE 68588, USA*

Recently it was demonstrated that the conductivity of the  $\text{LaAlO}_3/\text{SrTiO}_3$  (LAO-STO) interface can be reversibly tuned through a switchable electromechanical response arising from the LAO overlayer in the LAO-STO heterostructures. Bulk  $\text{LaAlO}_3$  (LAO) is a typical perovskite, which shows paraelectric behavior at room temperature. In this study, we have investigated switchable dielectric properties of the LAO ultrathin (several unit cells) films grown on top of lattice-matched conducting oxide  $\text{Sr}_{0.2}\text{Ca}_{0.8}\text{RuO}_3$  (SCRO) on the (001)  $(\text{LaAlO}_3)_{0.3}-(\text{Sr}_2\text{AlTaO}_6)_{0.7}$  (LSAT) substrate. Piezoresponse force microscopy (PFM) studies performed on the LAO/SCRO/LSAT heterostructures show a genuine switchable hysteretic electromechanical behavior resembling that one observed in ferroelectric films associated with induced polarization in the LAO layer. An insight into the underlying mechanism of such behavior has been gained by using temperature-dependent PFM spectroscopic, dielectric and structural measurements. The effect of inhomogeneous strain gradient induced by the PFM probe on polarization in LAO has been also studied. The proposed mechanism of switchable electromechanical response should be active in many other oxide heterosystems, but its detailed manifestation likely depends on a number of subtleties, such as oxygen octahedra rotations and distortions, strain, and lattice coupling at the nanoscale. Control of this phenomenon will enable new structures and devices that exploit nanoscale electromechanical coupling.

## Minimum domain size and stability in carbon nanotube-ferroelectric devices

Cédric Blaser and Patrycja Paruch

MaNEP-DPMC, University of Geneva, Switzerland

Email: cedric.blaser@unige.ch

When combining carbon nanotubes (CNTs) with ferroelectric materials, the small size and exceptional electronic properties of the former makes them extremely interesting as local field sources for nanoscale ferroelectric polarization switching. Meanwhile, the ferroelectric polarization can be used to modulate the electronic behavior of an adjacent CNT, leading to potentially multifunctional devices.

We deposited single-walled CNTs from aqueous suspension onto patterned epitaxial ferroelectric  $\text{Pb}(\text{Zr}_{0.2}\text{Ti}_{0.8})\text{O}_3$  (PZT) thin films. Using this device, PFM is used to probe domain switching in three different electrode configurations, using an AFM tip, edges of macroscopic planar electrodes and CNTs on the ferroelectric surface as electric field sources, allowing us to separately consider the effects of the separation between two straight domain walls, and the radius of curvature on domain stability<sup>151</sup>.

Domain growth dynamics in the three configurations are discussed using finite element analysis of the vertical electric field vs. distance dependence, and in comparison with previously reported ferroelectric nanodomains and thermodynamic models of switching.

In 270 nm thick films, we demonstrate domain sizes down to 9 nm half-width using a CNT electrode (see Fig. 1) and 14.5 nm radius with the AFM tip as electrode, two times smaller than the minimum domain size predicted from thermodynamic models. The observed domains remained stable over 20 months. These results suggest that the internal defect structure plays a significant role in the dynamic and stability of ferroelectric nanodomains.

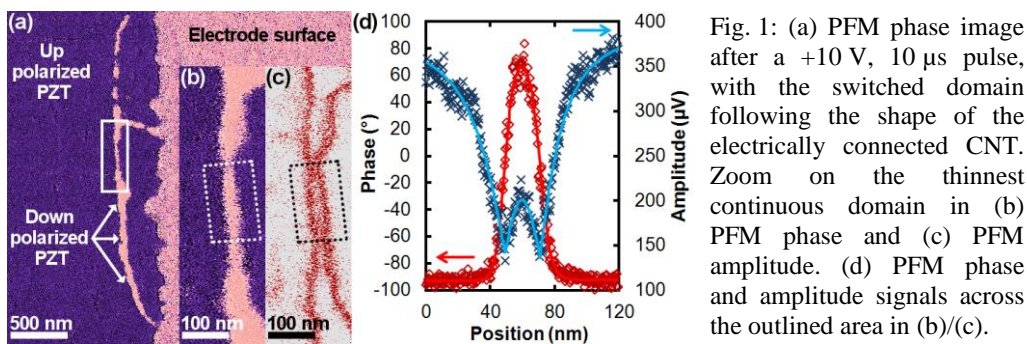


Fig. 1: (a) PFM phase image after a +10 V, 10 µs pulse, with the switched domain following the shape of the electrically connected CNT. Zoom on the thinnest continuous domain in (b) PFM phase and (c) PFM amplitude. (d) PFM phase and amplitude signals across the outlined area in (b)/(c).

<sup>151</sup> C. Blaser and P. Paruch, "Minimum domain size and stability in carbon nanotube-ferroelectric device", Appl. Phys. Lett., vol. 101, p. 142906, 2012.





## Piezo and ferroelectric phases of glycine

Ensieh Hosseini<sup>1</sup>, Igor Bdikin<sup>2</sup>, Budhendra Singh<sup>2</sup>, Vladimir Bystrov<sup>1</sup>, Andrei Kholkin<sup>1</sup>

<sup>1</sup> CICECO & Department of Materials and Ceramics Engineering, University of Aveiro, Aveiro, Portugal

<sup>2</sup> TEMA & Department of Mechanical Engineering, University of Aveiro, Aveiro, Portugal

Email: Seyedhosseini@ua.pt

Creating artificial biomimetic materials with multiple functions similar to those of living bodies, is an important frontier for advanced society in near future. Recently, electromechanical coupling in many bio-organic materials has been revisited and several materials demonstrated properties similar to their inorganic counterparts. Glycine (the simplest amino acid) is one of basic and important elements in biology as it serves as building block for proteins. Several polymorphic forms with completely different physical properties are possible in glycine. In this work, glycine microcrystals were grown on a conductive substrate under different conditions. The influence of various parameters (e.g. concentration of solution, solvent, volume of microdroplets, temperature, humidity, and type of substrates) on the formation of polymorph phases was evaluated using powder X-ray diffraction. The results indicated that the saturated solution and lower temperature lead to formation of  $\gamma$  phase whereas the  $\beta$  phase can be grown from low concentrated solution.

The piezoelectric response and ferroelectric domains of the different polymorphic forms of glycine crystals have been investigated locally by using Piezoresponse Force Microscopy (PFM). The domain switching properties are studied for crystals by applying a dc voltage to a localized area. The results showed that the switching domains growth in different shape depends on the polarization direction of the sample.

In addition, a molecular dynamics simulation was used for modeling the crystal structure of glycine and the spontaneous polarization was determined and compared with experimental results. Also, the mechanisms of polarization switching on the nanoscale level were investigated via this model.

The major part of this work was supported by the Marie-Curie ITN project “Nanomotion”

## Piezoelectricity in Biopolymers and DNA Nucleobase Crystals

Brian J. Rodriguez<sup>1</sup>

<sup>1</sup>School of Physics, University College Dublin, Ireland

Email: brian.rodriguez@ucd.ie

Piezoelectricity is a property of many organic and biological materials, including collagen, nucleobase crystals, and peptide nanostructures. Recent progress in understanding the origin and role of piezoelectricity and possible ferroelectricity in these materials will be discussed. Piezoelectric properties of collagen, etc. can be measured using piezoresponse force microscopy (PFM), which is a voltage-modulated contact mode atomic force microscopy technique that allows bias-induced surface deformations via the converse piezoelectric effect to be detected. Thus, PFM makes it possible to investigate electromechanical coupling in biosystems and organic materials at the nanoscale.

Recently, PFM was used to study polar ordering in tendon, eye tissues, and collagen hydrogels.<sup>152,153</sup> Collagen shear piezoelectricity is a functional property that may be associated with bone remodeling, however, the biofunctional implications of piezoelectricity in collagen and other biomaterials has yet to be clearly demonstrated. A preliminary step towards this goal is to determine if collagen is piezoelectric in physiological conditions, which involves understanding the role of pH and moisture content. Here, we investigate the structure and piezoelectric properties of aligned collagen membranes before and after a neutralization process, which alters the pH from acidic to neutral conditions. Electromechanical properties of the collagen membranes have been further investigated under controlled humidity conditions to probe whether collagen is piezoelectric in moisture rich environments. In addition, the orientation dependence of collagen fibril piezoresponse is explored using cross sections of embedded tendons.

An early biopolymer identified as being piezoelectric was deoxyribonucleic acid (DNA).<sup>154</sup> DNA comprises the nucleobases adenine, cytosine, guanine, and thymine, which are held by backbones of deoxyribose and phosphate. Thymine and other nucleobase crystals grown from solutions during evaporation have been found to exhibit piezoelectricity, and in some cases contain domains which can be switched via external field. The results are complemented using second harmonic generation measurements.

The discovery of piezoelectricity in peptide nanotubes has helped to propel the field of PFM of biomaterials. Peptides are short chains of amino acids and are the building blocks of all structural tissues and are inherently “biocompatible.” Not only are peptide nanotubes piezoelectric but so are dried peptide hydrogels. The differences in piezoresponse from the two materials will be analyzed.

---

<sup>152</sup> D. Denning et al. “Visualizing Molecular Polar Order in Tissues via Electromechanical Coupling”, *J. Struct. Bio.*, vol. 180, p. 409–419, 2012.

<sup>153</sup> D. Denning et al. “Electromechanical properties of dried tendon and iso-electrically focused collagen hydrogels”, *Acta Biomater.*, vol. 8, p. 3073–3079, 2012.

<sup>154</sup> E. Fukada “History and recent progress in piezoelectric polymers”, *IEEE Trans. Ultra. Ferro. Freq. Control*, vol. 47, 1277-1290 2000.

Furthermore, the outlook for future measurements and applications of piezoelectric collagen, nucleobase crystals, and peptide nanostructures will be discussed.

---

## **Lead-free ceramics: Spectroscopy**

CLUB A

*Tuesday, July 23 2013, 04:30 pm - 06:00 pm*

Chair: **Jirka Hlinka**  
*Institute of Physics, Czech Academy of Sciences*

## Two excitations below phonon frequencies in broad-band dielectric response of Ba(Zr,Ti)O<sub>3</sub> ceramics

Dmitry Nuzhnyy<sup>1</sup>, Jan Petzelt<sup>1</sup>, Maxim Savinov<sup>1</sup>, Viktor Bovtun<sup>1</sup>, Martin Kempa<sup>1</sup>,  
Giovanna Canu<sup>2</sup>, Maria Teresa Buscaglia<sup>2</sup>, Vincenzo Buscaglia<sup>2</sup>

<sup>1</sup>Department of Dielectrics, Institute of Physics, Academy of Sciences of the Czech Republic,  
Prague, Czech Republic

<sup>2</sup>Electroceramic Department, Institute for Energetics and Interphases, National Research Council  
Genoa, Italy

Email: nuzhnyj@fzu.cz

Lead-free perovskite systems attract attention due to their potential use in a wide range of applications (piezoelectric transducers, phase shifters, tunable filters etc.). They are considered as good candidates for the replacement of lead-based materials. Dielectric properties of the Ba(Zr,Ti)O<sub>3</sub> solid solution are changing dramatically with the ratio of Zr/Ti-ions. This allows for tuning the dielectric properties from slightly incipient ferroelectric behaviour (BaZrO<sub>3</sub>) through relaxor to diffuse and normal ferroelectric behavior (BaTiO<sub>3</sub>).

We have already investigated a set of Ba(Zr,Ti)O<sub>3</sub> ceramics<sup>155</sup> and observed an excitation which softened from THz either to GHz (BaZr<sub>0.2</sub>Ti<sub>0.8</sub>O<sub>3</sub>) or to MHz (BaZr<sub>0.4</sub>Ti<sub>0.6</sub>O<sub>3</sub>) range where it merged into a constant-loss background. This feature in dielectric response we considered as one overdamped excitation associated with local hopping of Ti-ions among their off-centered sites. To prove this picture, we needed similar data for smaller Ti concentration, since the hopping dynamics of Ti ions is not expected to be much dependent on the size of the Ti clusters. In order to obtain these data we prepared another set of Ba(Zr,Ti)O<sub>3</sub> ceramics with higher concentration of Zr (x=0.6, 0.7, 0.8) using solid-state reaction technique. These compounds were studied in 5 - 500 K temperature range using Fourier-transform infrared reflectivity, time-domain THz transmission spectroscopy, high-frequency - microwave coaxial technique, and standard low-frequency capacitance spectroscopy. This enabled us to obtain the dielectric response in the whole range from 1Hz to 100 THz and fit it with phenomenological models.

Even though there is a gap in our experimental data ( $\sim 10^9$ - $10^{11}$  Hz), careful fitting of the data at various temperatures led us to the conclusion that two relaxations are needed to fit the dielectric response in the whole frequency range. The high frequency relaxation ( $\sim 10^{10}$ - $10^{11}$  Hz) is almost temperature independent for all investigated compounds, while another broad relaxation is thermally activated, showing considerable softening on cooling from GHz range, similar for all compositions in agreement with the Ti-hopping picture.

---

<sup>155</sup> D. Nuzhnyy, J. Petzelt, M. Savinov, T. Ostapchuk, V. Bovtun, M. Kempa, J. Hlinka, V. Buscaglia, M. T. Buscaglia, and P. Nanni, "Broadband dielectric response of Ba(Zr,Ti)O<sub>3</sub> ceramics: From incipient via relaxor and diffuse up to classical ferroelectric behavior", Phys. Rev. B, vol. 86, p. 014106(1)- 014106(9), 2012.

## Impedance spectroscopy studies on Mn doped $K_{0.5}Na_{0.5}NbO_3$ lead-free ferroelectric ceramics

Paula Maria Vilarinho, Muhammad Asif Rafiq, Maria Elisabete Costa,

Department of Materials and Ceramics Engineering, Centre for Research in Ceramics and Composite Materials, CICECO, University of Aveiro, 3810-193 Aveiro, Portugal

Email: paula.vilarinho@ua.pt

This talk is about a systematic study carried out by impedance spectroscopy to identify defects and describe their role in the conduction behaviour of undoped and Mn doped KNN ceramics. Oxygen vacancies located at the grain boundaries were identified as responsible for the decrease of the conductivity at room temperature and a less leaky behaviour of Mn doped KNN and also for the conduction increase at elevated temperatures for these ceramics. The importance of this work resides on the fact that  $K_{0.5}Na_{0.5}NbO_3$  (KNN) is one of the leading lead free piezoelectric materials being considered as an alternative to  $Pb(Zr_{1-x}Ti_x)O_3$  (PZT), which is currently the most widely used material for electromechanical applications<sup>156</sup>.

Smart materials like piezoelectrics and ferroelectrics are crucial in applications such as sensors and actuators, radio-frequency switching, drug delivery, chemicals detection, and power generation and storage. Although pure KNN has inferior electromechanical properties compared to PZT, efforts are on going to tailor and improve its ferroelectric and piezoelectric coefficients by doping and texturing<sup>1</sup>. Earlier reports have shown that the remnant polarization ( $P_r$ ) values of KNN ceramics may exceed the saturation polarization value<sup>157</sup>, thus indicating the presence of leakage current and space charge contributions either in undoped or doped KNN (doped with Li and Ta, Li and Sb) ceramics. Mn dopant has been used to reduce the leakage current in KNN single crystals but its effects on the electrical properties of KNN ceramics have not yet been properly addressed and thus remain unclear.

In this work Impedance spectroscopy (IS) is used to get a deeper insight into the electrical behaviour of undoped and Mn doped KNN ceramics by assessing and distinguishing contributions to the ceramic impedance arising from different regions, bulk and grain-boundary. Ac conductivity dependence on the temperature showed that resistivity of Mn doped ceramics increased at room temperature while the reverse was observed for temperature higher than 200 °C. Activation energy values showed that hopping mechanism at room temperature and mobile oxygen vacancies are the main charge carrier at high temperature ( $T > 200$  °C). Impedance spectroscopy revealed the main location of the defects and the dependence of their contribution on the temperature. For low temperatures, Mn decreases the conductivity of KNN and for high temperatures due to the increased mobility of oxygen vacancies mainly located at the grain boundaries, the conductivity of Mn doped KNN increases. This work is expected to contribute to the pool of knowledge on KNN materials making them useable for industrial applications.

<sup>156</sup> Y. Saito, H. Tani, et al., Lead-free piezoceramics. *Nature*, 432(7013), p. 84-87, 2004

<sup>157</sup> H.E. Mgbemere, M. Hinterstein, et al., Structural phase transitions and electrical properties of  $(K_xNa_{1-x})NbO_3$  based ceramics modified with Mn. *Journal of the European Ceramic Society*, 32(16), p. 4341-4352, 2012



## defect-structure – property relationships: fundamental differences between $\text{Pb}[\text{Zr},\text{Ti}]\text{O}_3$ and ‘lead-free’ alternative compounds

Rüdiger-A. Eichel

Forschungszentrum Jülich, Institut für Energie und Klimaforschung (IEK-9), Germany

Email: r.eichel@fz-juelich.de

In order to meet the sometimes stringent requirements for specific piezoelectric applications, the materials properties of ferroelectric oxides may be tailored by means of *aliovalent* doping with transition-metal or rare-earth ions. The main effect of aliovalent doping is to control the defect structure in terms of the generation or annihilation of lattice vacancies<sup>158</sup>, which renders compounds with so-termed ‘hard’ or ‘soft’ ferroelectric properties. With that respect, the hardening mechanism is attributed to the formation of dipolar complexes between the acceptor ion and charge compensating oxygen vacancies. As a result, the orientation of spontaneous polarization in the neighbouring unit cells as well as the domain structure and domain-wall mobility are impacted.

By using multi-frequency electron paramagnetic resonance (EPR) spectroscopy<sup>159</sup>, local information at the (paramagnetic) dopant sites can be gathered, including information about the dopant site with respect to domain walls or grain boundaries<sup>160</sup>. Recent results allow to monitor the formation of defect complexes between acceptor-type dopants and charge-compensating oxygen vacancies. Furthermore, a complete defect chemical description upon aliovalent doping emerges from the EPR results.

Most interestingly, the results obtained for the pseudo-binary solid-solution system  $\text{Pb}[\text{Zr}_{1-x}\text{Ti}_x]\text{O}_3$  (PZT) cannot simply be transferred to ‘lead-free’ alternative compounds, such as  $[\text{K}_{0.5}\text{Na}_{0.5}]\text{NbO}_3$  (KNN)<sup>161</sup> or  $[\text{Bi}_{0.5}\text{Na}_{0.5}]\text{TiO}_3$  (BNT)<sup>162</sup> for instance. Differences in defect structure also impact the dynamic properties as function of switching upon external poling<sup>163</sup>.

---

<sup>158</sup> E. Erdem, P. Jakes, S.K.S. Parashar, K. Kiraz, M. Somer, A. Rüdiger, R.-A Eichel, *J. Phys.: Condens. Matter* **22** (2010) 345901.

<sup>159</sup> R.-A. Eichel, *Phys. Chem. Chem. Phys.*, **13** (2011) 368–384.

<sup>160</sup> P. Jakes, E. Erdem, R.-A. Eichel, L. Jin, D. Damjanovic, *Appl. Phys. Lett.* **98** (2011) 072907.

<sup>161</sup> E. Erüinal, P. Jakes, S. Körbel, J. Acker, H. Kungl, C. Elsässer, M.J. Hoffmann, R.-A. Eichel, *Phys. Rev. B* **84** (2011) 184113.

<sup>162</sup> E. Aksel, P. Jakes, E. Erdem, D.M. Smyth, A. Ozarowski, J. van Tol, J.L. Jones, R.-A. Eichel, *J. Am. Ceram. Soc.*, **94** (2011) 1363–1367.

<sup>163</sup> L.X. Zhang, E. Erdem, X. Ren, R.-A. Eichel, *Appl. Phys. Lett.* **93** (2008) 202901



## Ferroelectric Phase Transition in nanostructured BaTiO<sub>3</sub> studied by Raman scattering and second harmonic generation.

A. M. Pugachev<sup>1</sup>, V. I. Kovalevskii<sup>1</sup>, V. K. Malinovsky<sup>1</sup>, N. V. Surovtsev<sup>1</sup>, Yu. M. Borzdov<sup>2</sup>

<sup>1</sup>Institute of Automation and Electrometry, Russian Academy of Sciences, Novosibirsk, Russia

<sup>2</sup>V. S. Sobolev Institute of Geology and Mineralogy, Russian Academy of Sciences, Novosibirsk, Russia

E-mail [apg@iae.nsk.su](mailto:apg@iae.nsk.su)

It is widely known that the ferroelectric phase transition from tetragonal to cubic phase in BaTiO<sub>3</sub> ceramics and powders is strongly suppressed compared with the crystals. In our study the features of this transition were investigated by low - frequency Raman scattering and second harmonic generation (SHG) techniques. The samples were prepared from the BaTiO<sub>3</sub> powder pressed by using a uniaxial pressure of 600 MPa, 3\*10<sup>3</sup> MPa and 4\*10<sup>3</sup> MPa. Raman scattering spectra were measured in a spectral range 1.5 – 650 cm<sup>-1</sup> by a triple-grating spectrometer TRIVISTA 777 for temperature range from 300 K to 800 K, covering both ferroelectric and paraelectric phases. Over the entire temperature range a well pronounced central peak (CP) was detected. It was previously shown<sup>1,2</sup> that in BaTiO<sub>3</sub> crystals the central peak in a spectral density presentation  $I_n(\nu, T) = I(\nu, T) / (n(\nu) + 1) \nu$  (here  $n(\nu)$  is the Bose factor) is well fitted by Lorentz contour (single relaxation time approximation) and its width demonstrated a critical slowing down in the vicinity of the Curie temperature. In the case of single relaxation time the low frequency part of CP in a susceptibility presentation is described by power law:  $I_r(\nu, T) = I_n(\nu, T) \nu \propto \nu^\alpha$  where  $\alpha = 1$ . In contrast to crystals the CP in a spectral density presentation in a pressed powder can not be fitted by Lorentz function and  $I_r(\nu, T) \propto \nu^\alpha$  where  $\alpha \approx 0.07$  in ferroelectric phase and increased up to 0.8 with increasing the temperature up to 800 K in paraelectric phase. Such behavior of the parameter  $\alpha$  indicates that the relaxation process in the pressed powder can not be described by a single relaxation time. The temperature dependence of  $\alpha$  is typical for ferroelectrics with a diffuse phase transition (relaxors) as shown by the example of crystals SBN 61<sup>3</sup> and PMN<sup>4</sup>. A study of second harmonic generation (SHG) in BaTiO<sub>3</sub> pressed powder has been carried out by the procedure described in<sup>5</sup>. It was found that the broadening of the phase transition is significantly increased with the application of mechanical stress and increases monotonically with increasing stress up to Burns temperature (~ 600 K). The experimental data confirm that BaTiO<sub>3</sub> ceramics and powders in paraelectric phase exhibit much greater SHG intensity than in the crystals because of the existence of the polar nanoregions in the paraelectric phase. The obtained results of Raman and SHG experiments are interpreted as a relaxor - like behavior of BaTiO<sub>3</sub> pressed powder.

1. J.H. Ko, T. H.Kim, K. Roleder, D. Rytz, S. Kojima, "Precursor dynamics in the ferroelectric phase transition of barium titanate single crystals studied by Brillouin light scattering" Phys. Rev. B **84**, 094123, 2011
2. V. K. Malinovsky, A. M. Pugachev, V.A. Popova, N. V. Surovtsev, S. Kojima "Low frequency Raman scattering in BaTiO<sub>3</sub> crystal", Ferroelectrics, in press
3. Koreeda, H. Taniguchi, S. Saikan, and M. Itoh "Fractal Dynamics in a Single Crystal of a Relaxor Ferroelectric", PRL, **109**, 197601, 2012
4. V. K. Malinovsky, A. M. Pugachev, N. V. Surovtsev "Study of the Central Peak in Raman Spectra of SBN Crystals" Bulletin of the Russian Academy of Sciences: Physics, **74**, No. 9, pp. 1231–1234, 2010.

5. Pugachev A.M., Kovalevskii V.I., Surovtsev N.V., Kojima S., Prosandeev S.A., Raevski I.P., Raevskaya S.I. "Broken local symmetry in paraelectric BaTiO<sub>3</sub> proved by second harmonic generation", P.R.L., v.108., 247601, 2012 .

## Non-linear Coupling between the Primary and Secondary Order Parameters of Strontium Titanate Ceramics

Ali Al-Zein<sup>1</sup>, Bernard Hehlen<sup>2</sup>, Christine Bogicevic<sup>3</sup>, Pascale Gemeiner<sup>3</sup>, Jean-Michel Kiat<sup>3,4</sup>

<sup>1</sup>European Synchrotron Radiation Facility, 6 Rue Jules Horowitz, Grenoble, France

<sup>2</sup>Laboratoire Charles Coulomb (LCC), CNRS-UMR 5221, Université Montpellier II, France

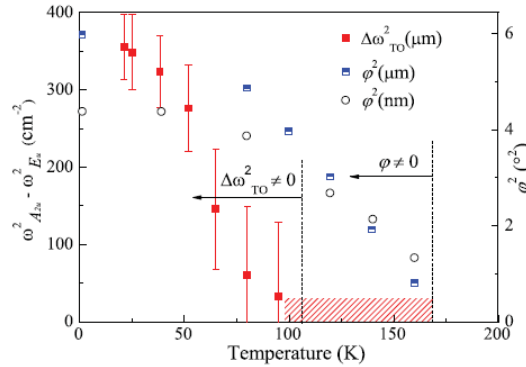
<sup>3</sup>Laboratoire Structures, Propriétés et Modélisation des Solides, Ecole Centrale Paris, CNRS-UMR8580, Châtenay Malabry, France

<sup>4</sup>Laboratoire Léon Brillouin, CE Saclay CNRS-UMR12, Gif-Sur-Yvette, France

Email: alzein@esrf.fr

SrTiO<sub>3</sub> (STO) is a textbook example of quantum paraelectric materials with very high value of the dielectric constant at low temperature. It exhibits an anti-ferrodistortive cubic (*Pm-3m*) to tetragonal (*I4mcm*) phase transition at  $T_a = 105$  K [1]. In bulk material, its primary (rotation angle  $\varphi$  of the TiO<sub>6</sub> octahedra) and secondary (spontaneous strain  $c/a-1$ ) order parameters are linearly coupled with  $\varphi^2 \propto c/a-1$ . In STO ceramics, a core-shell structure was assumed to interpret the behavior of the low-temperature permittivity, with probably a static polarization in the shell and large stress fields affecting the core grain [2].

Neutron diffraction, Raman and hyper-Raman (HRS) scattering have been used to study the structural and vibrational properties of micrograin and nanograin STO ceramics. HRS spectroscopy of micrograin STO ceramics revealed a splitting of the soft  $F_{1u}$  mode into a  $A_{2u}$  and  $E_u$  vibrations [3]. This was not observed by previous Raman scattering or infrared absorption studies. Interestingly, this splitting occurs at about 90 K that is, at a much lower temperature than 160 K [4] at which the tilting of the TiO<sub>6</sub> octahedra starts growing. This observation suggests a nonlinear coupling between the two order parameters (Figure) [3]. Such behavior possibly arises from the strain field the shell imposes on the core grain and one therefore expects that it is strongly dependent on the synthesis route and grain size.



[1] K.A. Muller, W. Berlinger, and F. Waldner, Phys. Rev. Lett. **21**, 814 (1968).

[2] J. Petzelt, T. Ostapchuk, I. Gregora, P. Kuzel, J. Liu, and Z. Shen, J. Phys.: Condens. Matter. **19**, 196222 (2007).

[3] B. Hehlen, A. Al-Zein, C. Bogicevic, P. Gemeiner, and J.-M. Kiat, Phys. Rev. B **87**, 014303 (2013).

[4] J. M. Kiat, C. Bogicevic, P. Geimener, A. Al-Zein, F. Karolak, N. Guiblin, F. Porcher, B. Hehlen, Ll. Yedra, S. Estradé, F. Peiro and R. Haumont, *Phys. Rev. B.* **87**, 024106 (2013).

---

## **Multiferroics**

CLUB B

*Tuesday, July 23 2013, 04:30 pm - 06:00 pm*

Chair: **Tor Grande**  
*Norwegian University of Science and Technology*

## Raman spectroscopy for characterization of crystalline phases and phase transformations in BiVO<sub>4</sub> and BiFeO<sub>3</sub> films

D. A. Tenne<sup>1</sup>, A. K. Farrar<sup>1</sup>, J. B. Romero<sup>1</sup>, D. A. Hillsberry<sup>1</sup>, S. Stoughton,<sup>2</sup> M. Showak,<sup>2</sup> C. Heikes<sup>2</sup>, J. H. Lee<sup>2</sup>, A. Melville<sup>2</sup>, C. Adamo<sup>2</sup>, Q. Mao,<sup>3</sup> L. F. Kourkoutis,<sup>3</sup> D. A. Muller,<sup>3</sup> C. Beekman<sup>4</sup>, W. Siemons,<sup>4</sup> T.Z. Ward<sup>4</sup>, M. Chi,<sup>4</sup> J. Howe,<sup>4</sup> M.D. Biegalski<sup>5</sup>, N. Balke<sup>5</sup>, P. Maksymovych<sup>5</sup>, H. M. Christen<sup>4</sup>, and D. G. Schlom<sup>2</sup>

<sup>1</sup>Department of Physics, Boise State University, Boise, ID 83725, USA

<sup>2</sup>Department of Materials Science and Engineering, Cornell University, Ithaca, NY 14853, USA

<sup>3</sup>School of Applied and Engineering Physics, Cornell University, Ithaca, NY 14853, USA

<sup>4</sup>Materials Science and Technology Division, Oak Ridge National Laboratory, Oak Ridge, TN, 37831, USA

<sup>5</sup>Center for Nanophase Materials Sciences, Oak Ridge National Laboratory, Oak Ridge, TN, 37831, USA

Email: [dmitritenne@boisestate.edu](mailto:dmitritenne@boisestate.edu)

Raman spectroscopy is a technique capable of distinguishing crystalline polymorphs and detecting phase transitions between different crystal structures in bulk and thin film solids. In this work it was applied to study strained thin films of photocatalytic BiVO<sub>4</sub> and multiferroic BiFeO<sub>3</sub>. Bulk BiVO<sub>4</sub> is known to exist in several crystalline forms (polymorphs), and the monoclinic polymorph of BiVO<sub>4</sub> is believed to have the best photocatalytic properties for water splitting using solar energy. The BiVO<sub>4</sub> films studied were grown by molecular beam epitaxy on yttria-stabilized cubic zirconia substrate. Raman spectra were measured at 10 and 300 K with several excitation laser lines in the range from 325 to 514.5 nm, and 441.6 nm line was found to produce the strongest Raman signal from BiVO<sub>4</sub>, because of its proximity to the resonance with the bandgap of BiVO<sub>4</sub>. The analysis of the Raman spectra indicated that the film was of monoclinic structure, as expected for the growth conditions used and consistent with x-ray diffraction and scanning transmission electron microscopy data.

Coherently strained BiFeO<sub>3</sub> films were grown by molecular beam epitaxy and pulsed laser deposition on various substrates including YAlO<sub>3</sub>, LaAlO<sub>3</sub>, NdGaO<sub>3</sub>, SrTiO<sub>3</sub>, and ReScO<sub>3</sub> (Re = Pr, Sm, Gd, Tb, Dy). These substrates induce lattice-mismatch biaxial strain in BiFeO<sub>3</sub> films spanning a range from -6.7% to +1.4%. The films have been studied by variable-temperature Raman spectroscopy with ultraviolet excitation (325 nm) in order to reduce the substrate contribution to spectra. At low temperatures, a large number of BiFeO<sub>3</sub> phonon peaks observed in spectra indicates the structure to be monoclinically distorted (*Cc*). Temperature evolution of Raman spectra from BiFeO<sub>3</sub> films under large compressive strain (above 4%) indicates the phase transitions to another monoclinic phase, then to tetragonal phase (at ~ 730 K for the films on LaAlO<sub>3</sub>). Raman spectra (measured up to 950 K), demonstrate that the high temperature phases are still polar; a linear extrapolation of Raman intensities yields an estimated Curie temperature at 867 ± 100 °C for BiFeO<sub>3</sub> under 4.4% compressive strain. Tensile-strained films (on PrScO<sub>3</sub> substrates, strain +1.4%) undergo a transition from monoclinic rhombohedral-like to orthorhombic-like phase at about 550–600 K. The temperature dependence of Raman intensities of certain characteristic peaks indicates the possibility of coexisting phases in the temperature range 400–550 K.

Supported in part by the National Science Foundation through the Grant DMR-1006136.

## Electromagnons and sequence of structural and magnetic phase transitions in multiferroic $\text{CaMn}_7\text{O}_{12}$

S. Kamba<sup>1</sup>, V. Goian<sup>1</sup>, F. Kadlec<sup>1</sup>, J. Hejtmánek<sup>1</sup>, M. Savinov<sup>1</sup>, P. Vaněk<sup>1</sup>, and M. Orlita<sup>2</sup>

<sup>1</sup>Institute of Physics, Academy of Sciences of the Czech Republic, Prague, Czech Republic

<sup>2</sup>Grenoble High Magnetic Field Lab, Grenoble, France

Email: kamba@fzu.cz

$\text{CaMn}_7\text{O}_{12}$  is an unusual material which exhibits a rich sequence of structural, ferroelectric and magnetic phase transitions. At high temperatures,  $(\text{CaMn}_3)\text{Mn}_4\text{O}_{12}$  crystallizes in the cubic perovskite structure (space group  $\bar{I}m\bar{3}$ ) and upon cooling below  $T_{c1} \sim 450$  K charge ordering occurs which induces a structural transition to a trigonal phase with the space group  $R\bar{3}$  ( $Z=3$ ). Below  $T_{c2} = 250$  K, orbital ordering occurs and the trigonal structure becomes incommensurately modulated with a propagation vector  $\mathbf{q}_c = (0, 0, 2.077)$ .<sup>164</sup> Upon further cooling below  $T_{N1} = 90$  K, an incommensurately modulated magnetic structure emerges with a magnetic modulation vector  $\mathbf{q}_m = \frac{1}{2}\mathbf{q}_c$ .<sup>164</sup> Very recently, it was reported<sup>165</sup> that the magnetic structure is also ferroelectric with a spontaneous polarization attaining up to  $\mathbf{P}_s = 2870 \mu\text{Cm}^{-2}$  oriented parallel to the  $c$  axis. This is the highest spin-induced polarization among all multiferroics. At  $T_{N2} = 50$  K, another magnetic transition occurs, giving rise to a second propagation vector along the  $c$  axis. Both propagation vectors  $\mathbf{q}_{m1}$  and  $\mathbf{q}_{m2}$  change with temperature, but their average value corresponds exactly to  $\frac{1}{2}\mathbf{q}_c$ .

We have investigated far-IR reflectivity and time-domain THz transmission spectra of  $\text{CaMn}_7\text{O}_{12}$  between 10 and 550 K and found significant changes in the spectra at structural and magnetic phase transitions. The IR reflectivity changes abruptly at  $T_{c1} = 450$  K, giving evidence of the first-order character of the phase transition. Moreover, the conductivity seen in the high-temperature IR spectra disappears below  $T_{c1}$ , proving the metal-insulator character of this phase transition due to charge ordering. New polar phonons appear in the spectra in the incommensurate phase below 250 K due to a change of IR selection rules. Close to  $T_{N1}$ , a new mode develops near  $50 \text{ cm}^{-1}$ ; another one near  $30 \text{ cm}^{-1}$  appears below  $T_{N2}$ . Since the modes appear near the magnetic phase transitions, they can be spin waves (magnons). Nevertheless, IR reflectivity spectra reveal a transfer of the oscillator strengths from the phonons to the excitations seen below  $50 \text{ cm}^{-1}$ . Thus, the modes at 30 and  $50 \text{ cm}^{-1}$  contribute to the dielectric permittivity and not to the magnetic susceptibility. This is a typical signature of electromagnons, i.e. electric active magnons, which are activated in THz dielectric spectra due to dynamical magnetoelectric coupling. The origin of magnetoelectric coupling in  $\text{CaMn}_7\text{O}_{12}$  will be analyzed and discussed.

Low-temperature far-IR transmission spectra measured under magnetic field up to 12 T revealed significant shifts of electromagnon frequencies with magnetic field. These shifts are responsible for a large dependence of low-frequency dielectric permittivity on applied static magnetic field (magneto-dielectric effect), which we as well investigated.

<sup>164</sup> N.J. Perks, R.D. Johnson, C. Martin, L.C. Chapon, and P.G. Radaeli, "Magneto-orbital helices as a route to coupling magnetism and ferroelectricity in multiferroic  $\text{CaMn}_7\text{O}_{12}$ ", *Nature Commun.* vol. 3, p. 1277, 2012.

<sup>165</sup> R.D. Johnson, L.C. Chapon, D.D. Khalyavin, P. Manuel, P.G. Radaeli, and C. Martin, "Giant improper ferroelectricity in the ferroaxial magnetic  $\text{CaMn}_7\text{O}_{12}$ ", *Phys. Rev. Lett.* vol. 108, p. 067201 (2012).



## Electromagnon in the pyroelectric ferrimagnet $\epsilon$ -Fe<sub>2</sub>O<sub>3</sub>

Filip Kadlec<sup>1</sup>, Christelle Kadlec<sup>1</sup>, Veronica Goian<sup>1</sup>, Martí Gich<sup>2</sup>, Martin Kempa<sup>1</sup>, Stéphane Rols<sup>3</sup>, Maxim Savinov<sup>1</sup>, Jan Prokleška<sup>4</sup>, Milan Orlita<sup>5</sup> and Stanislav Kamba<sup>1</sup>

<sup>1</sup>Institute of Physics, Academy of Sciences of the Czech Republic, Na Slovance 2, 182 21 Prague 8, Czech Republic

<sup>2</sup>Institut de Ciència de Materials de Barcelona, Campus UAB, 08193, Bellaterra, Spain

<sup>3</sup>Institut Laue-Langevin, BP 156, 38042 Grenoble Cedex 9, France

<sup>4</sup>Faculty of Mathematics and Physics, Charles Univ., Ke Karlovu 5, 121 16 Prague 2, Czech Rep.

<sup>5</sup>Grenoble High Magnetic Field Lab, CNRS - 25, avenue des Martyrs, Grenoble Cedex 9, France

Email: kadlec@fzu.cz

Spin waves excited in crystals by the electric component of electromagnetic radiation are called electromagnons (EMs), in contrast to magnons, which are linked to the magnetic component. The EMs can be detected in the far-infrared (IR) permittivity spectra; typically, a transfer of dielectric strength from phonons to EMs upon temperature or magnetic field change is observed<sup>166</sup>. EMs are known from multiferroics whose ferroelectric polarization is induced by a spin order.

We report a discovery of an EM in the far-IR spectra of  $\epsilon$ -Fe<sub>2</sub>O<sub>3</sub> nanograin ceramics, appearing below 100 K.  $\epsilon$ -Fe<sub>2</sub>O<sub>3</sub> is a less known phase of iron oxide with the space group *Pna2<sub>1</sub>*, stable only in the form of nanoparticles with a size of about 30 nm (see Fig. 1). It is a charge transfer insulator, exhibiting, at room temperature, a collinear spin structure and a record value<sup>167</sup> of the coercive field,  $H_c \approx 20$  kOe. Below 110 K, its ferrimagnetic structure becomes incommensurately modulated. We have performed temperature-dependent IR reflectivity measurements, which revealed a transfer of phonon strength to the EM peak emerging near 10 meV (see Fig. 1). Terahertz time-domain spectroscopy shows a temperature- and magnetic-field-dependent ferromagnetic resonance near 0.5 meV and reveals that the EM peak is sensitive to the external magnetic field. Inelastic neutron scattering data (see Fig. 1) show that the peak scattering frequency corresponds to a magnon from the Brillouin zone boundary<sup>168</sup>.

Our dielectric impedance measurements show that the spontaneous polarization of  $\epsilon$ -Fe<sub>2</sub>O<sub>3</sub>, which has a non-centrosymmetric lattice, cannot be switched by electric field. Thus, the compound is pyroelectric and it does not belong to classical multiferroics; the data show that the existence of EMs is not limited to spin-induced ferroelectrics. We suggest that at low temperatures, the Dzyaloshinskii-Moriya interaction is activated, tilts the spins and activates the EM via magnetostriction.

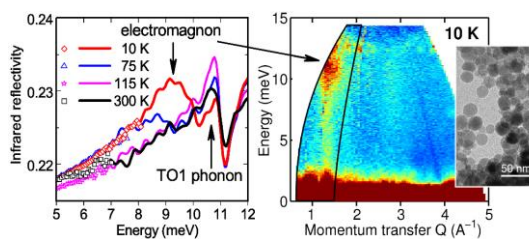


Fig. 42: Left: temperature-dependent far-IR reflectivity (lines) and data from THz transmission spectroscopy (symbols). Right: Inelastic neutron scattering map of the powdered sample (pictured in the inset). The framed area marks the mixed magnon-EM branch.

<sup>166</sup>R. Valdés Aguilar & al., "Colossal magnon-phonon coupling in Eu<sub>0.75</sub>Y<sub>0.25</sub>MnO<sub>3</sub>", Phys.Rev.B, vol.76, 60404(R), 2007

<sup>167</sup>J. Tuček & al., "ε-Fe<sub>2</sub>O<sub>3</sub>: An advanced nanomaterial ...", Chem. Mater. vol. 22, p. 6483-6505, 2010

<sup>168</sup>C. Kadlec & al., "Electromagnon in ferrimagnetic ε-Fe<sub>2</sub>O<sub>3</sub> nanograin ceramics", submitted to Phys. Rev. Lett.



### Magnetic field enhanced structural instability in almost multiferroic $\text{EuTiO}_3$

Z. Guguchia<sup>1</sup>, H. Keller, J. Köhler<sup>2</sup>, and A. Bussmann-Holder<sup>2</sup>

<sup>1</sup>Physik-Institut der Universität Zürich, Winterthurerstr. 190, CH-8057 Zürich, Switzerland

<sup>2</sup>Max-Planck-Institut für Festkörperforschung, Heisenbergstr. 1, D-70569 Stuttgart, Germany

$\text{EuTiO}_3$  undergoes a structural phase transition from cubic to tetragonal at  $T_S=282\text{K}$  [1] which is not accompanied by any long range magnetic order. However, it is related to the oxygen octahedra rotation driven by a zone boundary acoustic mode softening [2]. Here we show that this displacive second order structural phase transition can be shifted to higher temperatures by the application of an external magnetic field ( $\Delta T_S \sim 4\text{K}$  for  $\mu_0 H=9\text{T}$ ) [3]. This observed field dependence is in agreement with theoretical predictions based on a coupled spin-anharmonic-phonon interaction model. The observed magnetic field dependence of  $T_S$  (Figure 1) demonstrates that a strong spin-phonon coupling is present in this compound already at high temperatures which suggests that spin fluctuations are present at these temperatures most likely driven by the oxygen ion octahedral rotation.

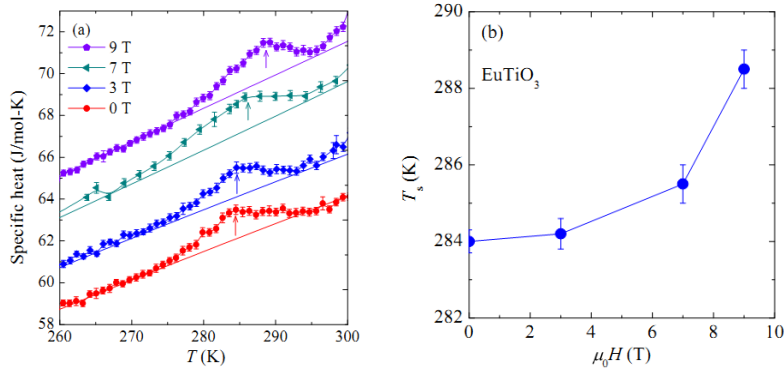


**Fig. 1** a) The specific heat of ETO as a function of temperature within a limited temperature regime around the structural phase transition temperature  $T_S$  for fields of 0, 3, 7, 9T. For clarity the data are shifted by 2 J/mol-K relative to each other with increasing magnetic field. b)  $T_S$  as a function of H as derived from Fig. 1a.

1. [A. Bussmann-Holder, J. Köhler, R. K. Kremer, and J. M. Law](#), Phys. Rev. B **83**, 212102 (2011).
2. J. L. Bettis, M.-H. Whangbo, J. Köhler, A. Bussmann-Holder, and A. R. Bishop, Phys. Rev. B **84**, 184114 (2011).
3. [Guguchia, H Keller, J Köhler and A Bussmann-Holder](#) *J. Phys.: Condens. Matter* **24**, 492201 (2012).

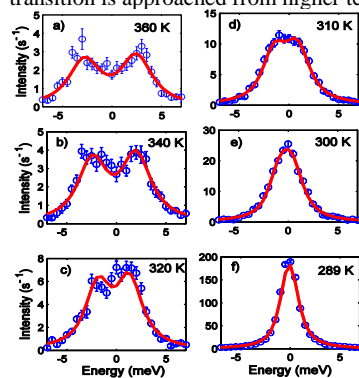
05:45 pm Vibrations in Europium Titanate

David. S. Ellis<sup>1</sup>, Hiroshi Uchiyama<sup>1,2</sup>, Satoshi Tsutsui<sup>1,2</sup>, Kuniyoshi Sugimoto<sup>2</sup>, Kenichi Kato<sup>3</sup>, Alfred Q.R. Baron<sup>1,2</sup><sup>1</sup>Materials Dynamics Laboratory, RIKEN SPring-8 Center, <sup>2</sup>Research and Utilization Division, SPring-8/JASRI<sup>3</sup>Structural Materials Science Laboratory, RIKEN SPring-8 Center, Sayo, Hyogo, Japan

60 years ago, divalent europium was formed in an oxide lattice for the first time [1]. The result was  $\text{EuTiO}_3$ , a compound isostructural to  $\text{SrTiO}_3$ , with apparently no structural phase transitions down to  $\sim 108$  K. Besides the discovery of a magnetic ordering below 5 K in the following decade [2], the material had all but disappeared from the publications. With the onset of the new millennium, experiments demonstrating coupling between the dielectric and magnetic states in  $\text{EuTiO}_3$  [3-4] led to a flurry of theoretical and experimental works showing its remarkable properties and potential for practical multiferroics and other diverse uses, ranging from magnetic field dependent polarization rotators to studying the fundamental properties of electrons [5-11] (not an exhaustive list!). And as it turned out, there *is* a phase transition, in fact near room temperature [12]. In this talk we review recent developments in  $\text{EuTiO}_3$ , including our study of its lattice vibrations with inelastic x-ray scattering [13], which give a dynamical view of the structural phase transition and ferroelectric properties.

[1] Brous et al, *Acta Crystallographica* **6** 67 (1953)[2] McGuire et al., *Journal of Applied Physics* **37** 981 (1966)[3] Katsufuji and Tokura, *Physical Review B (Rapid Com.)* **60** 15021 (1999)[4] Katsufuji and Takagi, *Physical Review B* **64** 054415 (2001)[5] Fennie and Rabe, *Physical Review Letters* **97** 267602 (2006), [6] Kamba et al, *European Physics Letters***80** 27002 (2007), [7] Lee et al, *Nature*, **466** 954 (2010), [8] Ryan et al, *Nature Communications*, **4** 1334(2013), [9] Kim et al., *Physical Review Letters* **110** 027201 (2013), [10] Mechelen et al., *Physical**Review Letters* **106** 217601 (2011), [11] Rushchanskii et al., *Nature Materials* **9** 649 (2012)[12] Bussmann-Holder et al., *Physical Review B* **83** 212102 (2011)[13] Ellis et al., *Physical Review B (Rapid Com.)* **86** 220301 (2012)

Figure to right : Condensation of soft phonon mode of  $\text{EuTiO}_3$  into a Bragg reflection as the structural phase transition is approached from higher temperature (from [13]).



---

## **PZT film processing**

CLUB C

*Tuesday, July 23 2013, 04:30 pm - 06:00 pm*

Chair: **Nazanin Bassiri-Gharb**  
*Georgia Institute of Technology*

## Solution Chemistry, Substrate, and Processing Effects on Chemical Homogeneity of PZT Thin Films

Jon F. Ihlefeld,<sup>1</sup> Paul G. Kotula,<sup>1</sup> Geoff L. Brenneka,<sup>1</sup> Christopher T. Shelton,<sup>1</sup> Bonnie B. McKenzie,<sup>1</sup> Bryan Gauntt,<sup>1</sup> Dara V. Gough,<sup>1</sup> Ping Lu,<sup>1</sup> and Erik D. Spoeke<sup>1</sup>

<sup>1</sup>Sandia National Laboratories, Albuquerque, New Mexico/USA

Email: jihlefe@sandia.gov

In this presentation we explore the contributing factors toward preparing high-quality chemically-homogeneous lead zirconate titanate (PZT) thin films via chemical solution routes. Principle to this study is the selection of an adhesion layer that forms a low energy interface with platinum on SiO<sub>2</sub>/Si substrates, resulting in improved dielectric and ferroelectric responses of PbZr<sub>0.52</sub>Ti<sub>0.48</sub>O<sub>3</sub>. PZT films deposited on substrates with ZnO adhesion layers have 35% and 21% percent enhancements over traditional titanium adhesion layers in remanent polarization and permittivity, respectively, with values of 32 μC/cm and 1950 measured. Enhanced responses have been ascribed to films deposited on ZnO-buffered substrates possessing no composition gradients as determined from chemical mapping utilizing quantitative Energy Dispersive Spectroscopy within in a Scanning Transmission Electron Microscope. Films prepared on traditional substrates possess significant gradients in the Ti/Zr concentrations. To understand this observation we have explored the effects of solution chemistry (traditional sol-gel versus chelate), pyrolysis temperature, substrate adhesion layer, and crystallization anneal heating rate on chemical gradient formation and subsequent properties in PZT films. In the course of this study, we have found that films prepared on Pt/ZnO/SiO<sub>2</sub>/Si substrates possess homogeneous distributions of zirconium and titanium through the film thickness regardless of solution chemistry and pyrolysis condition. PZT films prepared on conventional Pt/Ti/SiO<sub>2</sub>/Si substrates possess enriched concentrations of titanium near the PZT/Pt interface in all cases. We will show that this chemical gradient is driven by diffusion of titanium from the adhesion layer through the platinum bottom electrode. Finally, we will show our most recent studies investigating the effect of crystallization heating rate within a rapid thermal annealer on the gradient formation for films prepared on Pt/ZnO/SiO<sub>2</sub>/Si substrates. Sandia National Laboratories is a multi-program laboratory managed and operated by Sandia Corporation, a wholly owned subsidiary of Lockheed Martin Corporation, for the U.S. Department of Energy's National Nuclear Security Administration under contract DE-AC04-94AL85000.

## PZT-based high coupling with low permittivity thin films

Kiyotaka Wasa<sup>1</sup>, Tomoaki Matsushima<sup>1</sup>, Hideaki Adachi<sup>2</sup>, Toshifumi Matsunaga<sup>2</sup>,  
Takahiko Yanagitani<sup>3</sup>, Takashi Yamamoto<sup>4</sup>, and Susan Trolier-McKinstry<sup>5</sup>

<sup>1</sup> Micro-Engineering, Kyoto University, Kyoto, Japan

<sup>2</sup> Panasonic Co., Osaka, Japan

<sup>3</sup> Nagoya Institute of Technology, Nagoya, Japan

<sup>4</sup> The National Defense Academy, Yokosuka, Japan

<sup>5</sup> Materials Research Institute and Materials Science and Engineering. Department, Penn State University, PA., USA

Email: [kiyotaka.wasa@gmail.com](mailto:kiyotaka.wasa@gmail.com)

Piezoelectric thin films of high coupling and/or high piezoelectricity with low permittivity are essential for better piezoelectric thin film MEMS<sup>1</sup>. However, high coupling/high piezoelectric PZT based thin films show high permittivity similar to bulk PZT ceramics. Most of the PZT based thin films are polycrystalline with domain structure. We have epitaxially grown single c-domain/single crystal modified PZT based thin films, xPb(Mn,Nb)O<sub>3</sub>-(1-x)PZT(PMnN-PZT),<sup>2</sup> for fabricating high coupling/high piezoelectric thin films with low permittivity. Table 1 shows their dielectric and piezoelectric properties in comparison with recent reported piezoelectric thin films<sup>3-9</sup>. It is seen the single crystal PMnN-PZT thin films at optimum chemical composition exhibit reasonable high coupling with extra low permittivity which could not be observed in bulk PZT materials. The PMnN-PZT thin films exhibit extraordinary large  $e_{31,f}^2/\epsilon$  with high  $Q_m$ . These unique properties are mainly resulted from the domain free single crystal structure. Present PMnN-PZT thin films are applicable for better energy harvesting devices<sup>7</sup> and/or GHz wide band filters<sup>9</sup>. The mechanism of the unique dielectric and piezoelectric properties of the single crystal PMnN-PZT thin films will be discussed.

Table 1. Dielectric and piezoelectric properties of conventional ZnO and PZT-based thin films

Materials	ZnO	AlN	PZT	PMN-PT	PMN-PT	PMnN-PZT	PMnN-PZT
Structure	poly	epi	epi	epi	epi	epi	poly
$\epsilon/\epsilon_0$	10.9	9.5	200	800	500	100	850
$e_{31,f}$ (Cm <sup>-2</sup> )	-1.0	-1.37	-6.2	-27	-10.6	-12	-16.9
$e_{31,f}^2/\epsilon$ (GPa)	10.3	22.3	20.5	50	25.4	163	38
$Q_m$	100<	<100		20	180		
Ref.	[4]	[4]	[8]	[5]	[3]	Present [7,9]	[6]

[1] S. Trolier-McKinstry & P. Muralt, J. Electroceram., vol. 12, pp7-17,2004..

[2] K. Wasa et al., IEEE Trans. UFFC, vol.59,pp.6-13, 2012.

[3] K. Wasa et al., Appl. Phys. Lett., vol.88, pp.122903, 2006.

[4] S. Trolier-McKinstry et al., IEEE Trans. UFFC., vol.58pp.1782-1792,2011.

[5] S.H. Baek et al., Science, vol.334, pp.958-961, 2011. [6] T. Zhang et al., Appl. Phys. Lett., vol.94122909, 2009.

[7] K. Wasa et al., J. Microelectromechanical Systems, vol.21,pp.451-457 2012. [8] Conventional PZT thin films.

[9] N. Yamauchi et al., Appl. Phys. Lett., vol.94, pp.172903, 2009.

## PLD Growth and PFM Study of Self-poled, Mono-crystalline PZT Thin Films: Control of Polarization Direction by Dopants and Bottom Electrode

Mahamudu Mtebwa<sup>1</sup>, Ludwig Feigl<sup>1</sup>, Nava Setter<sup>1</sup>

<sup>1</sup>Ceramic Laboratory, Swiss Federal Institute of Technology of Lausanne, CH-1015 Lausanne, Switzerland

Email: mahamudu.mtebwa@epfl.ch

Experimental works have established that self-polarization in thin films is associated with the existence of built-in field resulting from charge carriers such as oxygen or lead vacancies and high trap density at the bottom interface, that is, difference in electrical boundary conditions between top and bottom film interface<sup>169</sup>. Theoretical works have shown that the built-in field is also associated with mismatch between the film and the substrate<sup>170</sup>. Self-polarization has been studied in polycrystalline thick films using macroscopic techniques including P-V hysteresis loops and Laser Intensity Modulation Method (LIMM). In thin films self-polarization was observed by PFM<sup>171</sup> but not systematically investigated.

In this work we report the growth of high quality, fully epitaxial, mono-crystalline Pb(Zr<sub>0.5</sub>Ti<sub>0.5</sub>)O<sub>3</sub> thin films with step flow growth mode by PLD. For the first time the study of self-polarization in doped mono-crystalline PZT thin films using PFM is presented. In addition to electrical boundary conditions, the direction of polarization is controlled by acceptor and donor dopants. Furthermore the dependence of self-polarization on film thickness is presented.

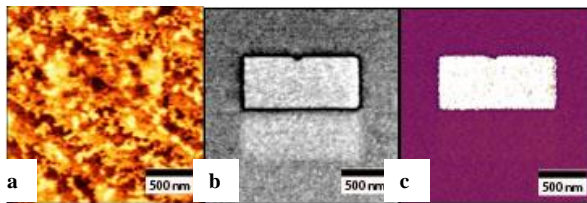


Figure 43: A 30nm thick 1% Fe doped Pb(Zr<sub>0.5</sub>Ti<sub>0.5</sub>)O<sub>3</sub> thin film. (a) AFM image, (b) PFM amplitude, (c) PFM phase. Fe doped PZT thin films grow self-poled with polarization pointing downwards. The rectangular region shows polarization switching when negatively biased dc voltage is applied on the AFM tip.

<sup>169</sup> V. P. Afanasjev, A. A. Petrov, I. P. Pronin, et al., "Polarization and self-polarization in thin PbZr<sub>1-x</sub>Ti<sub>x</sub>O<sub>3</sub>", J. Appl. Phys. Condens. Matter, vol. 13, p. 8755-8763, 2001.

<sup>170</sup> M. D. Glinchuk, A. N. Morozovska, "Ferroelectric Thin Film self-Polarization Induced by Mismatch Effect", Ferroelectrics, vol. 317, p.125-133, 2005.

<sup>171</sup> C. S. Ganpule, V. Nagarajan, H. Li, et al., Pole of 90° Domains in Lead Zirconate Titanate thin Films, vol. 77, p.292-297, 2000.



## Chemical Solution Deposited PZT Thin Films on Silicon Substrates with Thin Intermediate Buffer Layer

J. P. George<sup>1,2,4</sup>, J. Beeckman<sup>1,4</sup>, W. Woestenborghs<sup>1,4</sup>, P.F. Smet<sup>3,4</sup>, W. Bogaerts<sup>2,4</sup> and K. Neyts<sup>1,4</sup>

<sup>1</sup>Department of ELIS, Ghent University, Sint-Pietersnieuwstraat 41, 9000 Gent, Belgium

<sup>2</sup>Department of INTEC, Ghent University, Sint-Pietersnieuwstraat 41, 9000 Gent, Belgium

<sup>3</sup>Department of Solid State Sciences, Ghent University, Krijgslaan 281, 9000 Gent, Belgium

<sup>4</sup>Center for Nano- and Biophotonics (NB-Photonics), Ghent University, 9000 Gent, Belgium

Email: John.PuthenParampilGeorge@elis.ugent.be

The epitaxial deposition of ferroelectric thin films on silicon is a key technology to develop future electronic and photonic devices on CMOS fabrication platform. The inter-diffusion of the constituent elements and the reactions at the Si/thin film interface impose a challenge on the epitaxial growth and limit the application of these films on silicon substrates. Different techniques have already been proposed and demonstrated to aid the thin film growth with either a seed or an intermediate barrier layer.

In this work, we show the epitaxial growth of Lead zirconate titanate (PZT) thin films on bare silicon substrate with conventional 2-methoxy ethanol based chemical solution deposition<sup>1</sup>. We have used a lanthanum oxide nitrate intermediate buffer layer to promote the thin film growth on the silicon substrate. The influence of intermediate barrier layers as small as 2.5 – 10 nm on the crystallization, micro-structural, dielectric, and ferroelectric properties of the PZT thin films have been investigated in detail. Our experiments show that a buffer layer as thin as 4.4 nm can efficiently promote the thin film growth with a preferential orientation. The annealing temperature and buffer layer heat treatment are optimized, to obtain an oriented stoichiometric PZT thin film, with desired properties. The X-ray diffractogram show a preferential PZT growth along the  $\langle 100 \rangle$  crystallographic orientation, having single perovskite phase with either tetragonal or rhombohedral geometry. The SEM top and cross section image of the PZT films grown on silicon substrate show a nano-columnar crystal growth with polygonal crystal grains (see Fig. 1). The SEM and AFM measurements indicate the presence of smooth, crack free, uniform layers, with densely packed PZT crystal grains of size 40 - 100 nm, with an average surface roughness less than 5 nm. The electrical properties of the film are investigated with electric field dependant polarization (P-E) hysteresis and capacitance-voltage (C-V) measurements. The PZT film annealed at 525 °C, with a buffer layer of 6 nm shows a dielectric constant of 460, remnant polarization ( $2P_r$ ) of 18  $\mu\text{C}/\text{cm}^2$ , and coercive field ( $E_c$ ) of 80 kV/cm.

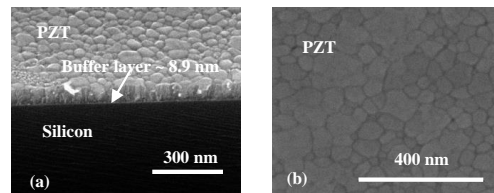


Fig. 44: Cross section (a) and top (b) image of the PZT thin film deposited on silicon substrate with a buffer layer of 8.9 nm and annealed at 600 °C.

<sup>1</sup> Chen YN, Wang ZJ "Rapid Microwave Annealing of Amorphous Lead Zirconate Titanate Thin Films Deposited by Sol-Gel Method on LaNiO<sub>3</sub>/SiO<sub>2</sub>/Si Substrates". *J. Am. Ceram. Soc.* 96:90-5, 2013.

## Nb doped PZT thin films grown by CSD

N. Chidambaram<sup>1</sup>, A. Mazzalai<sup>1</sup>, C. Sandu<sup>1</sup>, D. Balma<sup>1</sup>, D. Faralli<sup>2</sup>, L. Colombo<sup>2</sup>, M. Fusi<sup>2</sup>, and P. Muralt<sup>1</sup>

<sup>1</sup>Laboratoire de Céramique, École Polytechnique Fédérale de Lausanne EPFL, Lausanne, Switzerland.

<sup>2</sup>ST-Microelectronics, Via C. Olivetti, Agrate Brianza, Italy.

Email: nachiappan.chidambaram@epfl.ch

Niobium doping is known to have a beneficial effect on many properties of PZT ceramics. Substituting Ti or Zr on a B-site by Nb ions, form positive point defects that repel oxygen vacancies. As a consequence PZT domains move more easily. Nb doped ceramics excel in high piezoelectric coefficients  $d_{ij}$  and  $e_{ij}$ , and high permittivities. Nb doping is not so well studied with sol-gel processed PZT thin films. To date, the main interest in Nb doped films was to reduce leakage. Nb doping tends to increase the break-down field, which is of course very interesting for MEMS applications. In this work, we investigated concentration limits, gradient issues, dielectric and piezoelectric properties of such films.

The concentration limit for pyrochlore free, phase pure perovskite was identified. The {100}-texture of the PZT films could be maintained also for the Nb containing films. It is supposed that this texture results in the best possible piezoelectric performance. The Nb doped films showed a slight tetragonal splitting, indicating that Nb deviates the system rather to tetragonal symmetry than to rhombohedral symmetry. As it is known that sol-gel processing tends to form Zr/Ti gradients, it was of interest to know whether Nb forms gradients as well by being accumulated ahead of the perovskite growth front in the amorphous matrix. Such a behavior was indeed observed. Ferroelectric and piezoelectric behaviors of different Nb doped films were characterized. The  $e_{31,f}$  measured with a measurement of the direct effect was smaller than the one of the reverse effect. It seems that it is difficult to pole Nb doped films sufficiently well. The results of the first series allowed us to fine-tune the CSD precursor solutions for further improvements. The PZT film resulting from this optimized process, was deeply characterized and compared with standard PZT sol-gel films, showing an increased piezoelectric performance and reliability.

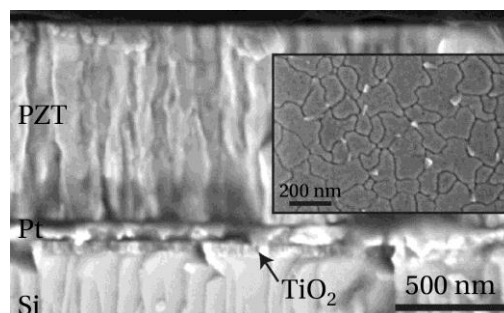


Fig. 45: Shows the cross section SEM micrograph of Nb doped film grown by CSD. Fully dense microstructure was observed. Inset shows the SEM top view, here as well one could observe phase pure Nb doped PZT without pyrochlore. Bright spots in the top view SEM are platinum residues from lift off process.

---

## **ISAF Group 2 Posters**

Forum Hall

*Tuesday, July 23 2013, 01:00 pm - 04:30 pm*

## Two-Stage Sintering of Multiferroic PZT-Based Ceramics

Supon Ananta<sup>1</sup>, Orawan Khamman<sup>1</sup>, Penphitcha Amonpattaratkit<sup>1</sup>

<sup>1</sup>Department of Physics and Materials Science, Faculty of Science, Chiang Mai University, Chiang Mai, Thailand

Email: suponananta@yahoo.com

Highly dense and pure phase of nanograin ceramics are of current scientific and technological interest, especially for utilization in electromagnetic components in which miniaturization and integration are essential. In this respect, the processing challenge is to produce dense and pure phase ceramics at low temperature, preferably without any additives and pressure, and with the least amount of coarsening of the initial microstructure. Recently, the potential of a two-stage sintering technique for the production of dense and pure phase ceramics with fine grain size has been demonstrated by our group, especially in the area of electroceramics such as BaTiO<sub>3</sub><sup>172</sup>, PbTiO<sub>3</sub>, Pb(Fe<sub>1/2</sub>Nb<sub>1/2</sub>)O<sub>3</sub>, Pb(Mg<sub>1/3</sub>Nb<sub>2/3</sub>)O<sub>3</sub><sup>173</sup> and Zn<sub>3</sub>Nb<sub>2</sub>O<sub>8</sub><sup>174</sup> ceramics. In this work, a two-stage sintering, which exploits the difference in the kinetics between grain boundary diffusion and grain boundary migration, was further employed to produce pure phase of perovskite multiferroic PZT-based ceramics to high density with fine grain size, by suppressing grain growth in the final stage of densification. It was found that this technique also offers an additional advantage as it requires a substantially lower sintering temperature than conventional sintering.

---

<sup>172</sup>W. Chaisan *et al.*, "Two-stage sintering of barium titanate and resulting characteristics", *Ferroelectrics.*, vol. 346, pp. 84-92, 2007.

<sup>173</sup>R. Wongmaneerung *et al.*, "Effect of two-stage sintering on phase formation, microstructure and dielectric properties of perovskite PMN ceramics derived from a corundum Mg<sub>4</sub>Nb<sub>2</sub>O<sub>9</sub> precursor", *Mater. Chem. Phys.*, vol. 114, pp. 569-575, 2009.

<sup>174</sup>P. Amonpattaratkit *et al.*, "Microstructure and dielectric properties of Zn<sub>3</sub>Nb<sub>2</sub>O<sub>8</sub> ceramics prepared by a two-stage sintering method", *Ceram. Inter.*, 2013, in press.

# Synthesis, Formation and Characterization of Perovskite Ferroelectric PZT-PZN Powders Derived from a Novel $Zn_2Nb_{34}O_{87}$ Precursor

Penphitcha Amonpattaratkit, Supon Ananta

Department of Physics and Materials Science, Faculty of Science,  
Chiang Mai University, Chiang Mai 50200 Thailand

Email: p.amonpattaratkit@gmail.com

Recently, there have been a great deal of interest in complex perovskite lead zirconate titanate-lead zinc niobate or PZT-PZN systems because of their high dielectric, piezoelectric and ferroelectric properties suitable for applications in multilayer capacitors, sensors and energy harvesting devices.<sup>1,2</sup> Moreover, it is well documented that the inhomogeneous mixing in the conventional solid state reaction process and firing temperature leads to formation of secondary phase (i.e. pyrochlore) and subsequent deterioration of electrical properties in PZT-PZN ceramics.<sup>2,3</sup> In this study, a combination of piezoelectric PZT perovskite phase stabilizers and novel  $Zn_2Nb_{34}O_{87}$  B-site precursor is employed for the fabrication of  $Pb(Zr_{0.44}Ti_{0.56})O_3$ - $Pb(Zn_{0.33}Nb_{0.67})O_3$  powders. Effects of calcination temperature on phase formation, crystal structure, morphology and microchemical composition of calcined PZT-PZN powders synthesized by a solid-state reaction were carefully examined via a combination of X-ray diffraction (XRD), scanning electron microscopy (SEM), transmission electron microscopy (TEM), particle size analyzer and energy-dispersive X-ray (EDX) techniques. This study has demonstrated a successful fabrication of pure-perovskite phase PZT-PZN powders via a combination of piezoelectric PZT perovskite phase stabilizers and novel  $Zn_2Nb_{34}O_{87}$  B-site precursor. Moreover, with increasing calcination temperature, the perovskite phase content, cell parameters, degree of tetragonality, particle size and degree of agglomeration tend to increase.

---

<sup>1</sup> E. Fernandez, W.D. Mechtaly, M.Q. Lopez, B. Gnade, E.L. Salguero, P. Shah and H.N. Alshareel, "Synthesis and Characterization of  $Pb(Zr_{0.53}Ti_{0.47})O_3$ - $Pb(Nb_{1/3}Zn_{2/3})O_3$  Thin Film Cantilevers for Energy Harvesting Applications", *Smart. Mater. Res.*, vol. 2012 (doi:10.1155/2012/872439).

<sup>2</sup> A. Ngamjarrojana, O. Khamman, S. Ananta and R. Yimnirun, "Synthesis, Formation and Characterization of Lead Zinc Niobate-Lead Zirconate Titanate Powders Via a Rapid Vibro-Milling Method", *J. Electroceram.*, vol. 21 p. 786-790, 2008.

<sup>3</sup> N. Vittayakorn, G. Rujijanagul, X. Tan, H. He, M.A. Marquardt and D.P. Cann, "Dielectric Properties and Morphotropic Phase Boundaries in the  $xPb(Nb_{1/3}Zn_{2/3})O_3$ -(1-x) $Pb(Zr_{0.5}Ti_{0.5})O_3$  Pseudo-Binary System", *J. Electroceram.*, vol. 16 p. 141-149, 2006.

## Influences of PZT Addition on the Phase Formation and Multiferroic Properties of PFN-Based Ceramics

Penphitcha Amonpattaratkit, Supon Ananta  
Department of Physics and Materials Science, Faculty of Science,  
Chiang Mai University, Chiang Mai 50200 Thailand

Email: p.amonpattaratkit@gmail.com

Recently, many electromagnetic ceramics which are promising multiferroic candidate for various electronic applications including transducers, capacitors and magnetoresistive random access memory have been developed from binary systems containing a combination of relaxor and normal ferroelectric materials.<sup>1</sup> In connection with this,  $\text{Pb}(\text{Fe}_{0.5}\text{Nb}_{0.5})\text{O}_3$  or PFN ceramics and their solid solutions are one of the most promising multiferroic materials with a perovskite structure.<sup>2</sup> However, the formation of unwanted phases especially the pyrochlores are one of the major problems in the preparation of these PFN-based compounds.<sup>3</sup> To solve this matter, in this study, a combination of perovskite stabilizer  $\text{Pb}(\text{Zr}_{0.44}\text{Ti}_{0.56})\text{O}_3$  or PZT and a wolframite-type  $\text{FeNbO}_4$  *B*-site precursor was employed for the fabrication of PFN-PZT ceramics. The phase formation, microstructure and multiferroic properties of ceramics in the  $(1-x)\text{PFN}-x\text{PZT}$  ( $x = 0.1-0.5$ ) system were investigated by using a combination of X-ray diffraction (XRD), scanning electron microscopy (SEM), energy-dispersive X-ray (EDX) analyzer and the multiferroic measurement techniques. Phase-pure perovskite of the PFN-PZT ceramics was obtained. These ceramics exhibit first-order ferroelectric phase transition of typical normal ferroelectrics, where the dielectric response peaks are narrow, sharp and without frequency dispersion, and the dielectric constant above Curie temperature ( $T_C$ ) can be fitted well by Curie law. With the increase of PZT content, tetragonality value of the PFN-PZT ceramics was found to increase slightly accompanied by the variation of cell volume, whilst the P-E ferroelectric hysteresis loops become narrower accompanied by the decrease of remanent polarization ( $P_r$ ) and coercive field ( $E_C$ ).

---

<sup>1</sup> R. Wongmaneerung, P. Jantaratana, R. Yimnirun, S. Ananta, "Phase Formation and Magnetic Properties of Bismuth Ferrite-Lead Titanate Multiferroic Composites", J. Supercond. Nov. Magn., 2013 in press.

<sup>2</sup> B. Fang, Y. Shan, K. Tezuka, H. Imoto, "High Curie Temperature  $\text{Pb}(\text{Fe}_{1/2}\text{Nb}_{1/2})\text{O}_3$ -Based Ferroelectrics:  $0.40\text{Pb}(\text{Fe}_{1/2}\text{Nb}_{1/2})\text{O}_3-0.34\text{PbZrO}_3-0.26\text{PbTiO}_3$ ", Phys. Stat. Sol., vol. 202 p. 481-489, 2005.

<sup>3</sup> A. Prasatkhetragarn, "Synthesis and Dielectric Properties of  $0.9\text{Pb}(\text{Zr}_{1/2}\text{Ti}_{1/2})\text{O}_3-0.1\text{Pb}(\text{Fe}_{1/3}\text{Nb}_{2/3})\text{O}_3$  Ceramics", Ferroelectrics., vol. 416 p. 35-39, 2011.

## (001)-Oriented Sol-Gel Epitaxial BiFeO<sub>3</sub> Thin Films using Stoichiometric Precursor

Qi Zhang<sup>1</sup>, Owen Standard<sup>1</sup>, Hsin-hui Huang<sup>1</sup>, Nagarajan Valanoor<sup>1</sup>

<sup>1</sup> School of Materials Science and Engineering, The University of New South Wales, Sydney, New South Wales 2052, Australia  
 Email: peggy.zhang@unsw.edu.au

Preparation of epitaxial BiFeO<sub>3</sub> (BFO) thin film by chemical routes is a challenging process as it is difficult to control the Bi:Fe stoichiometry precisely. Often the imprecision of the starting chemical composition and the volatilisation of Bi during high-temperature annealing leads to secondary phases or highly conductive films with very poor leakage resistance. To counter this problem, excessive Bi is often added to the starting reagents but this can lead to the formation of bismuth rich phases as well. Therefore a question to ask is: Can we make epitaxial BFO films by precise control of precursor chemistry?

This question is answered in this presentation. We demonstrate phase pure epitaxial BFO thin films (ranging from 45 to 100 nm in thickness) prepared on (100) SrTiO<sub>3</sub> substrates by a non-aqueous sol-gel deposition process. The first part of the presentation details the sol-gel chemistry of the process used and explains how stoichiometric precursors can be used to obtain high quality films. Starting solutions consisting of Bi- and Fe-nitrates dissolved in 2-methoxyethanol (2-MOE) solvent were deposited onto substrates by spin-coating. Fourier transform infrared (FTIR) analysis of the as-deposited coatings indicated polymerisation type reactions, notably esterification and aldehyde formation, during drying/gelation. Depending on the drying temperature (50–90°C), resultant films were either pure polymerised gels or powdery with areas of well-developed crystals. Given that 2-MOE is both a solvent for the system and a precursor for polymerisation, gelation versus crystal formation in the films is explained in terms of a competition between the rate of 2-MOE evaporation and the rate of 2-MOE gelation.

Phase composition and crystallographic orientation were characterised (for uniform gelated films) as a function of precursor stoichiometry (stoichiometric/Bi-excess), temperature (450–850°C), and annealing atmosphere (air/oxygen) to determine an optimum synthesis route for the formation of phase-pure epitaxial BFO films (Fig.1). Square polarization hysteresis loops of optimised films were obtained at room temperature with a maximum  $2P_r$  of 55  $\mu\text{C}/\text{cm}^2$  for the best performing samples with an obvious domain switching behaviour. The as grown samples show a polydomains state unlike counterpart films made by pulsed laser deposition. The electromechanical behavior of the BFO thin films (in terms of thickness, orientations, domain structure and dopant compositions) will be presented in detail as a function of selected processing parameters.

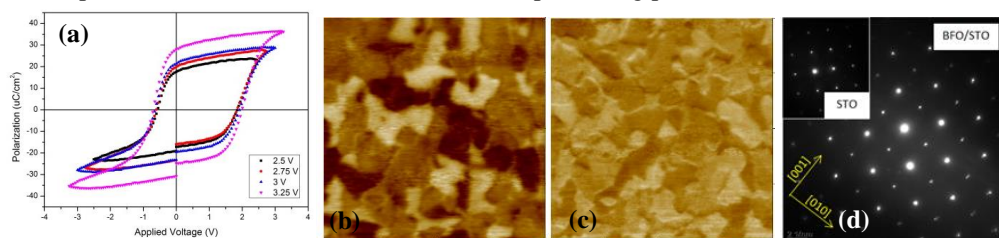


**Fig.46: (a) Ferroelectric hysteresis of BFO/LSMO/STO(100) thin film measured at a frequency of 10 kHz at room temperature; (b) Out-of-plane PFM and (c) In-plane PFM images of BFO/LSMO/STO(100) thin film (1  $\mu\text{m} \times 1 \mu\text{m}$ ); (d) TEM diffraction pattern of BFO/STO(100) thin film**

**Comment [NV1]:** Caption does not make sense. Make caption point 10 and bold. Does the sample not have a bottom electrode?



## Production and characterization of organic polar nanofibers produced by electrospinning

Ricardo Lima, Tiago Monteiro, Pedro Sá, Etelvina de Matos Gomes, Bernardo Almeida and Dmitry Isakov.

University of Minho, Center of Physics, Campus de Gualtar, 4710-059 Braga, Portugal

Email: [dmitry@fisica.uminho.pt](mailto:dmitry@fisica.uminho.pt)

Electrospinning is a versatile cost-effective bottom-up nanomanufacturing process, allowing for the fabrication of continuous nanofibers with diameters ranging from a few nanometers up to micrometers. In the last decade the interest in the electrospinning process and in the application of electrospun nanofibers is exponentially growing, due to their potential applicability as active material in electronic and sensor devices. The unique characteristics of electrospun nanofibers are their high surface-to-volume ratio, intrinsic 3D topography, biochemical flexibility and the possibility of obtaining extremely long fibers—all features which are strategically important for a remarkable variety of technological applications. Additionally, functional embedded dopants (included inorganic nanoparticles, carbon nanotubes, light-emitting molecules, cell-directing proteins, conjugated polymers etc.) may greatly expand the use of electrospun nanofibers. The recent success in the electrospinning of peptides and polymer-free materials is very encouraging for the consideration of electrospinning as a bottom-up process for fabrication of various 1D organic stand-alone nanofibers with strong  $\pi$ – $\pi$  or h-bonding interactions served as molecular entanglements for the stabilization of the continuous fiber-like structure.

Among the polar materials acting as functional elements in nanoelectronic devices, organic polar materials are of special interest due to their attractive multifunctional capacity, making them very attractive for a broad spectrum of potential applications in various fields such as thermoelectricity, electromechanics, electro-optics etc. The attractiveness of nanosized polar materials results also from the strong influence of the dimensionality on device performance and from the possibility of tuning their polar properties by changing the molecular structure.

Here, we present an extended number of polar organic materials that can be successfully electrospun. The materials under investigation include potassium sodium tartrate, triglycine sulphate, glycine, DL-alanine, urea, L-cistine and sucrose. All materials are embedded into electrospun nanofibers (with diameters in range of 200-600 nm) and possess strong dipolar orientation along the fiber direction which were confirmed by X-ray diffraction measurements. Aligned arrays of such obtained nanofibers present a mesocrystalline structure with highly anisotropic responses. The study of polar properties such as ferroelectricity, pyroelectricity, piezoelectricity and optical second harmonic generation are presented and discussed. All nanofibers reveal an enhancement of polar responses as compared with their bulk counterparts. We propose that the intrinsic orientation of polar molecules along electrospun nanofibers enhance the observed cooperative phenomena.

### Dielectric Properties of $\text{Ba}_{1-x}\text{La}_x\text{TiO}_3$ Ceramics Prepared by Two-Step Sintering Method

Ferroelectric perovskite ( $\text{ABO}_3$ ) materials play an important role in modern electronics and electronic engineering (capacitors, microwave technologies, etc.). Barium titanate ( $A = \text{Ba}$ ,  $B = \text{Ti}$ ) has a special place in this group of compounds since solid solutions with high electrophysical and ferroelectric properties based on it are obtained. Therefore, along with the constant improvement in the technology of ceramic materials, an important area of modification of electrophysical characteristics of the considered systems is doping by different iso- and heterovalent additives in A- and B-sites, both separately and together. Rare earth elements are found to be more efficient in comparison with other dopant additives. It was determined that the introduction of heterovalent cations into the  $\text{BaTiO}_3$  lattice in A- and B- sites causes a significant change in its electrophysical characteristics. The purpose of this work was to investigate the structure and dielectric properties of  $\text{Ba}_{1-x}\text{La}_x\text{TiO}_3$  ceramics prepared by two-step sintering method.

By means of two-step sintering method  $\text{Ba}_{1-x}\text{La}_x\text{TiO}_3$  ( $x = 0-0.05$ ) ceramics with sub-micron grain size was obtained. The grain size was 200–400 nm at  $x = 0.025$  and 300–700 nm at  $x = 0.05$ . Phase transition temperature was lowered with the growth of lanthanum concentration at the rate of  $\sim 25^\circ\text{C}/\text{mol}\%$ . Despite the small grain size the value of dielectric permittivity of the prepared samples were increased ( $\epsilon_{\text{max}} \approx (1.7-2.4) \times 10^4$  for  $x = 0.025$  and  $\approx (3.3-4.7) \times 10^4$  for  $x = 0.05$ ) as compared with large grain materials sintered by standard technique (with grain size  $> 1 \mu\text{m}$ ). Dielectric losses were at an acceptable level ( $\tan\delta \sim 0.05-0.15$ ).

## Effect of Oxygen Addition in the sputtering Gas on the Structures and Dielectric Properties of $\text{Bi}_2\text{Zn}_{2/3}\text{Nb}_{4/3}\text{O}_7$ Thin Films

M. Saeed Khan<sup>1,2</sup>, Wei Ren<sup>1,2</sup>, Peng Shi<sup>1,2</sup> and Xiaoqing Wu<sup>1,2</sup>

<sup>1</sup>Electronic Materials Research Laboratory, Xi'an Jiaotong University, Xi'an, Shaanxi, China

<sup>2</sup> International Center for Dielectric Research, Xi'an Jiaotong University, Xi'an, Shaanxi, China

Email: [wren@mail.xjtu.edu.cn](mailto:wren@mail.xjtu.edu.cn), [sonykhan\\_007@yahoo.com](mailto:sonykhan_007@yahoo.com)

$\text{Bi}_2\text{Zn}_{2/3}\text{Nb}_{4/3}\text{O}_7$  (BZN) thin films were deposited by RF magnetron sputtering technique onto Pt/TiO<sub>2</sub>/SiO<sub>2</sub>/Si substrates at room temperature, without any intentional heating of substrate, as a function of Ar/O<sub>2</sub> atmosphere. As-deposited thin films were post-annealed at a temperature  $\leq 200$  °C, which is compatible with the printed circuit board (PCB) substrates. The effect of Ar/O<sub>2</sub> gas ratio on structures, surface morphologies, dielectric and electrical properties of thin films were studied to produce dielectric thin films with suitable characteristics for application as an embedded capacitor. Surface roughness increased with increasing the concentration of oxygen in Ar/O<sub>2</sub> gas ratio but the deposition rate reduced. Moderate oxygen enrichment is helpful for the stoichiometry in the BZN films, which reduced the leakage current losses and the concentration of charge carriers produced from oxygen vacancies. The dielectric properties were improved with varying the Ar/O<sub>2</sub> gas ratio from 100/0 to 85/15 but no further significant improvement occurred with further variation of the Ar/O<sub>2</sub> gas ratio. The dielectric constant increased with increasing annealing temperature up to 150 °C due to the much stronger establishment of bismuth oxide into the thin film and then decreases with further increase of temperature due to the Bi migration at high temperature. 200 nm-thick BZN thin film deposited under Ar/O<sub>2</sub> gas ratio of 85/15 and later post annealed at 150 °C had a dielectric constant of 60.1 with a very low loss of 0.006, measured at 10 kHz. The leakage current density was  $6.7 \times 10^{-7}$  A/cm<sup>2</sup> at an applied bias field 400 kV/cm.

## Electrical Activity of Ferroelectric Biomaterials

Přemysl Vaněk<sup>1</sup>, Zdeňka Kolská<sup>2</sup>, Jan Petzelt<sup>1</sup>

<sup>1</sup>Institute of Physics ASCR, Prague, Czech Republic

<sup>2</sup>J.E. Purkyně University, Ústí nad Labem, Czech Republic

Email: vanek@fzu.cz

It is well known that bone is electrically active under mechanical loading, due to the piezoelectricity of collagen and the movement of ionic fluids within the bone structure. Electrical potentials in mechanically loaded bone have been linked to the mechanical adaptation of bone in response to loading, leading to the suggestion that the addition of an electrically active component to an implant material may improve healing and adaptation of the surrounding tissue. Recently, interest has grown in exploiting this phenomenon to develop electrically active ceramics for implantation in hard tissue, which may induce improved biological responses.

Ferroelectric (i.e. also piezoelectric) ceramics, which produce electrical potentials under stress, have been among others studied in order to determine the possible benefits of using electrically active bioceramics as implant materials. Most of the piezoelectric ceramics proposed for implant use contain barium titanate ( $\text{BaTiO}_3$ ). In vivo and in vitro investigations have indicated that ceramics of this kind are biocompatible and induce improved bone formation around implants. Nevertheless, the results are somewhat ambiguous. In majority of them, a negative charge on the surface is preferred for cell growth but in some cases a positive charge is preferred.

However, previous studies have not taken into account the fact that the charge at the surface of ferroelectrics is always quickly compensated (screened) by the opposite charge from the surroundings. Kalinin<sup>1</sup> showed that the charge at the surface of polarized  $\text{BaTiO}_3$  (or the ferroelectric domain) is fully screened by adsorbed charges at room temperature in air, so that the charge on the surface is opposite to that of the polarization. If a ferroelectric is immersed in a liquid (e.g. tissue fluid) it is obvious that an electric double layer and a diffusion layer are formed at its surface. The charge distribution in these layers can be characterized in a simplified way by zeta potential (potential at the „slipping“ plane). The zeta potential and its dependence on pH were frequently measured on colloidal ferroelectric  $\text{BaTiO}_3$  particles because the zeta potential is crucial for the stability of colloidal suspensions. However, the dependence of zeta potential on the polarity of the surface of poled ferroelectrics has not been measured until now. Therefore it is not clear if the spontaneous polarization in ferroelectrics can really have any influence on their bioactive behavior. We shall measure the zeta potential in dependence of the surface polarity and pH on poled single crystalline plates of ferroelectric  $\text{LiNbO}_3$  and  $\text{BaTiO}_3$ .  $\text{LiNbO}_3$  will be used because of its good stability of polarization,  $\text{BaTiO}_3$  because of its known biocompatibility. The zeta potential will be determined by measurement of streaming potential with an electrolyte flowing in the gap between two parallel ferroelectric plates.

---

<sup>1</sup>S.V. Kalinin and D.A. Bonnell, “Local potential and polarization screening on ferroelectric surfaces”, Phys. Rev. B, vol. 63, p. 125411-1-13, 2001.



## Effect of Nb substitution on (Pb,Ba)ZrO<sub>3</sub> ceramics

Barbara Fraygola<sup>1,2</sup>, Ulises Salazar<sup>3</sup>, Alberto Biancoli<sup>1</sup>, Dragan Damjanovic<sup>1</sup> and Nava Setter<sup>1</sup>

<sup>1</sup> École Polytechnique Fédérale de Lausanne, Material Institute, Ceramic Laboratory LC, Lausanne, Switzerland.

<sup>2</sup> Universidade Federal de São Carlos, Departamento de Física, Grupo de Cerâmicas Ferroelétricas, São Carlos –SP - Brazil

<sup>3</sup> Univeridad Autónoma de Puebla, Instituto de Física de la Benemérita, México.

Email: barbara.fraygola@epfl.ch

Lead zirconate, PbZrO<sub>3</sub>, is the first antiferroelectric identified and one end member of the highly useful solid-solution series PbZrO<sub>3</sub>–PbTiO<sub>3</sub>. At room temperature PZ is antiferroelectric but at elevated temperatures, it is ferroelectric over a very narrow temperature range (230–233 °C). The ferroelectric phase can become dominant by partial replacement of Zr<sup>4+</sup> ions for Ti<sup>4+</sup> ions (PZT ceramics) and also by partially replacing Pb<sup>2+</sup> by Ba<sup>2+</sup> ions (PBZ). The temperature range of this intermediate phase increases with increased Ba concentration.

The electromechanical properties of ferroelectric materials can be modified by doping in order to meet the requirements for various applications. This is well known in PZT ceramics, in which even a very small amount of the dopant element affects macroscopic properties and makes the ferroelectric hard or soft. We investigate whether hard and soft behavior occurs also due to doping of PBZ, which, to the best of our knowledge, has not been studied before.

Pb<sub>0.77</sub>Ba<sub>0.23</sub>ZrO<sub>3</sub> ceramics with 1-mol%-PbO-excess have been prepared with various Nb-dopant concentrations between 0.05 and 2 mol% by the mixed-oxide route. The densification behavior and the microstructural development, as well as ferroelectric, dielectric, and piezoelectric properties were measured and analyzed. The phase analysis of the sintered solid solutions revealed single-phase perovskite for all concentrations. The results showed a different relative density and grain size dependence for samples containing >0.5 mol% additives compared to samples with <0.5 mol% Nb. Nb doping influenced significantly the electrical characteristics. Softening and a very marked increase in the dielectric and piezoelectric characteristics were obtained for low concentrations of Nb<sup>5+</sup>. The influence of the dopants and associated defects on the physical, microstructural and electrical characteristics was investigated and well correlated.

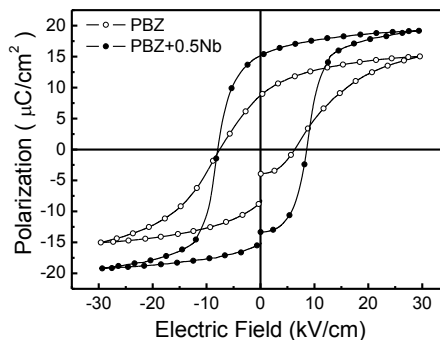


Fig. 47: Ferroelectric Hysteresis loops for pure and 0.5% Nb doped (Pb,Ba)ZrO<sub>3</sub> ceramics.

## Comparative study of synthesis and properties of multiferroic BiFeO<sub>3</sub> nano-objects

X. F. Bai<sup>1</sup>, I. C. Infante<sup>1</sup>, C. Bogicevic<sup>1</sup>, S. Gonzalez<sup>2</sup>, C. Mathieu<sup>2</sup>, N. Barrett<sup>2</sup>, and B. Dkhil<sup>1</sup>

<sup>1</sup>SPMS laboratory, UMR 8580 Ecole Centrale Paris-CNRS, Châtenay-Malabry, France

<sup>2</sup>DSM/IRAMIS/SPCSI, CEA-Saclay, Gif-sur-Yvette, France

Email: xiaofei.bai@ecp.fr

Bismuth ferrite (BiFeO<sub>3</sub>) has received a lot of attention as it is one of the rare multiferroic material showing simultaneously ferroelectric and antiferromagnetic orders at room temperature. Remarkably, because of its small band gap (~2.2eV) and good chemical stability, it was recently demonstrated to have significant photocatalytic and photovoltaic properties which make it a very interesting material for developing potential photoferroelectric applications in the UV and visible light range.

This work is devoted to study this multiferroic material at the nanoscale. We will show results on the synthesis and characterization of nano-objects of BiFeO<sub>3</sub>. The fabrication of pure and Ca-doped BiFeO<sub>3</sub> nano-objects have been performed using different methods (soft chemical route, sol-gel synthesis, co-precipitation and hydrothermal process, solid-state reaction) in order to investigate the influence of the shape and preparation conditions on the nano-object properties. These different routes have been adapted to tune and obtain particles of different morphology and size. Through studying the functional properties, the optimized fabrication conditions will be proposed. The ferroelectric domains and surface chemistry of different BiFeO<sub>3</sub>-nano-objects have been investigated using local electron microscopy (SEM, TEM and LEEM) to understand their influence on functional properties. Their ferroelectric and magnetic properties and first measurements on the photocatalytic and photovoltaic properties will be presented. We will discuss on the effect of the chemistry, structure and ferroelectric domain arrangement of these nano-objects on their macroscopic photoferroelectric properties. Perspectives on future applications of BiFeO<sub>3</sub>-based materials will be presented.

### Preparation and electrical properties of multilayered $\text{BaTi}_{1-x}\text{Zr}_x\text{O}_3$ composite ceramics

The study of  $\text{ABO}_3$ -type solid solutions based on perovskite-structured  $\text{BaTiO}_3$  has so far been of great interest as it offers the possibility to optimize several electrical properties for the manufacture of a number of devices. Nevertheless, pure  $\text{BaTiO}_3$  shows large changes in permittivity around the phase transitions temperatures. This characteristic is a problem for many applications and many kinds of dopants have been added to depress and/or broaden the maximum permittivity. Nowadays, graded ferroelectric ceramics are established as an attractive class of materials in which is possible to create a gradient of properties that cannot be attained in any homogeneous materials<sup>175</sup>. Thus, in the present work, the preparation and characterization of  $\text{BaTiO}_3/\text{BaTi}_{0.95}\text{Zr}_{0.05}\text{O}_3/\text{BaTi}_{0.85}\text{Zr}_{0.15}\text{O}_3$  composite dielectric ceramics is reported. The graded ceramic materials were prepared by powder-stacking method and uniaxially pressing process, followed by sintering at  $1320^\circ\text{C}/2\text{h}$ . A variety of concentrations and number of layers were studied. The final density of each sintered specimen was determined by the Archimedes method, showing values above 95% of the  $\text{BaTiO}_3$ 's theoretical density in all cases. The interfaces between the layers were studied by micro-Raman spectroscopy and scanning electron microscopy. The signals obtained from the interfaces show a  $\sim 20\mu\text{m}$  diffusion layer between the phases. Grain size of the ceramics was evaluated by the intercept method on the SEM images. Electrical measurements were carried out with a Solartron SI1260 impedance/gain-phase analyzer over a wide temperature range (25 to  $400^\circ\text{C}$ ). The temperature dependence of permittivity curve (1 kHz) shows a flat temperature dependence within the range. According to the series mixing rules these curves were simulated with the permittivity and the volume fraction of each phase. A good correlation with the experimental data was observed and the composites permittivity decrease smoothly to minimum value of each phase. The dielectric spectra of the composites are characterized by dielectric peaks that correspond to the sum of each ferroelectric-to-paraelectric phase transitions in the isolated compositions. In addition, the nature of these transitions is seen to change from normal (sharp-like dielectric peak) to diffuse (broad-like dielectric peak). On the other hand, the temperature dependence of permittivity recorded at various frequencies for the composite show also a change from normal (frequency independent) to relaxor (frequency dependent) phase transition develops.

<sup>175</sup> S. Markovic, M. Mitric, N. Cvjeticanin, D. Uskokovic, Preparation and properties of  $\text{BaTi}_{1-x}\text{Sn}_x\text{O}_3$  multilayered Ceramics, *J. Eur.Ceram. Soc.*, vol. 27, p. 505-509, 2007.



## Fabrication of lead-free ferroelectric (Na,K)NbO<sub>3</sub> thin films by Pulsed Laser Deposition

Tomohiro Nako<sup>1</sup>, Natsuki Koyama<sup>1</sup>, Ichiro Fujii<sup>1</sup>, Takahiro Wada<sup>1</sup>

<sup>1</sup> Department of Materials Chemistry, Ryukoku University, Japan

Email: t12m082@mail.ryukoku.ac.jp

Pb-based ferroelectric materials have drawbacks from an environmental standpoint. Therefore, lead-free ferroelectric materials have been attracting attention as environmentally benign compounds. We fabricated NaNbO<sub>3</sub>(NN) thin films on (001), (110) and (111) SrTiO<sub>3</sub> (STO) substrates using pulsed laser deposition (PLD).<sup>1</sup> It is well known that (Na,K)NbO<sub>3</sub>(NKN) solid solution has better ferroelectric properties than NN. In this study, we fabricated (Na<sub>1-x</sub>K<sub>x</sub>)NbO<sub>3</sub> thin films with  $x=0.1$ (NKN10), 0.2(NKN20) and 0.3(NKN30) on STO substrate by PLD.

NKN thin films were fabricated using this ceramics target by PLD. We deposited NKN films in the following conditions: O<sub>2</sub> partial pressure of about 225 mTorr and substrate temperature of 850°C. Fabricated NKN thin films had about 1-2- $\mu$ m thickness. The crystalline structures of the films were measured by  $\theta/2\theta$  X-ray diffraction (XRD) analysis. The  $P$ - $E$  hysteresis loops were observed using a ferroelectric tester.

The NKN films were epitaxially grown on (001), (110) and (111) substrates. Figure 1 shows XRD patterns of NKN30 films deposited on (001), (110) and (111) STO substrates. The NKN film on (001) STO had a smooth surface, the film on (110) STO had a striped pattern, and that on (111) STO had trigonal pyramid-like structures. The  $P$ - $E$  hysteresis of (Na,K)NbO<sub>3</sub> thin films increased with increased K content.  $P$ - $E$  hysteresis of NKN30 films fabricated on (001), (110) and (111) STO substrates is shown in Fig. 2. All of the NKN30 films show single hysteresis (ferroelectricity). The  $P$ - $E$  hysteresis of NKN30 film on (111) STO substrate shows a very large hysteresis loop and

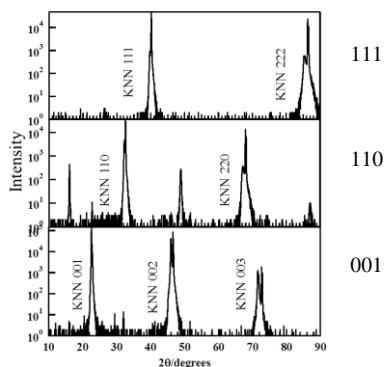


Fig.1. XRD patterns of (Na<sub>0.7</sub>K<sub>0.3</sub>)NbO<sub>3</sub> films deposited on (001), (110) and (111)SrTiO<sub>3</sub> substrates.  
remnant polarization  $P_r$  of 69  $\mu$ C/cm<sup>2</sup>.

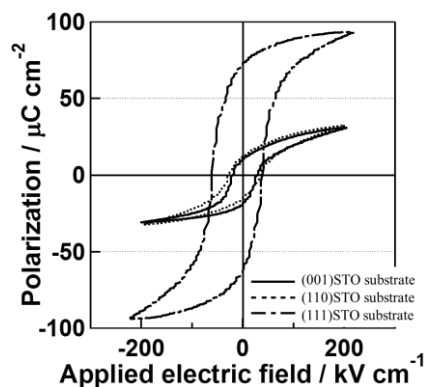


Fig.2.  $P$ - $E$  hysteresis of (Na<sub>0.7</sub>K<sub>0.3</sub>)NbO<sub>3</sub> films deposited on (001), (110) and (111)SrTiO<sub>3</sub> substrates.

<sup>1</sup> S. Yamazoe, H. Sakurai, M. Fukada, H. Adachi, and T. Wada, *Appl. Phys. Lett.* , **95**, 062906 (2009).

## Effects of $\text{InNbO}_4$ fabrication on perovskite PIN-PMN-PT

Linghang Wang<sup>1</sup>, Zhuo Xu<sup>1</sup>

<sup>1</sup>*Electronic Materials Research Laboratory, Key Laboratory of Ministry of Education & International Center for Dielectric Research, Xi'an Jiaotong University, Xi'an 710049, P. R. China*

Email: uswlh@yahoo.com.cn

Due to the superior piezoelectric properties compared to ceramics and thin films, such as its ultrahigh piezoelectric coefficients ( $d_{33} > 1500 \text{ pC/N}$ ) and electromechanical coupling factors ( $k_{33} > 90$ ), the ferroelectric single crystals are regarded as the promising new materials used for electroacoustic, hydroacoustic or ultrasonic transduction devices. The relaxor-based ferroelectric ternary  $\text{Pb}(\text{In}_{1/2}\text{Nb}_{1/2})\text{O}_3\text{-Pb}(\text{Mg}_{1/3}\text{Nb}_{2/3})\text{O}_3\text{-PbTiO}_3$  (PIN-PMN-PT) crystals have the better properties at higher temperature, whose Curie temperature is about  $200^\circ\text{C}$  with the piezoelectric constant  $d_{33}$  about  $2000 \text{ pC/N}$ , as compared with the binary  $\text{Pb}(\text{Mg}_{1/3}\text{Nb}_{2/3})\text{O}_3\text{-PbTiO}_3$  (PMN-PT) single crystals and  $\text{Pb}(\text{In}_{1/2}\text{Nb}_{1/2})\text{O}_3\text{-PbTiO}_3$  (PIN-PT) single crystals for the applications in the high temperature transduction devices. For PIN-PMN-PT crystal growth, however, the perovskite PIN-PMN-PT raw materials are very critical. In this paper, we presented effects of  $\text{InNbO}_4$  (IN) fabrication on the perovskite PIN-PMN-PT. Excess of  $\text{In}_2\text{O}_3$  and annealing on the phases of synthesized IN were investigated. The pre-sintered IN and unsintered IN powders on the phases of PIN-PMN-PT were discussed. The experimental results indicated that excess of  $\text{In}_2\text{O}_3$  did not have influences on the phase of IN due to higher chemical activity of  $\text{In}_2\text{O}_3$ , IN powder with 3%  $\text{In}_2\text{O}_3$  excess was in grey because of the reaction,  $\text{In}_2\text{O}_3 \rightarrow \text{In}_2\text{O}$ , annealing at  $850^\circ\text{C}$  could make grey IN powder into white. It is apparent that unsintered IN could obtain the pyrochlore-free PIN-PMN-PT rather than pre-sintered IN powders. An improved way for preparing PIN-PMN-PT raw materials is developed.

## Synthesis of Needle-like $\text{NaNbO}_3$ Particles by Hydrothermal Process

Ebru Mensur Alkoy<sup>1</sup>, Sedat Alkoy<sup>2,3</sup>, Yağız Özeren<sup>2</sup>,

<sup>1</sup>Faculty of Engineering and Natural Sciences, Maltepe University, Maltepe, Istanbul, Turkey

<sup>2</sup>Dept. Materials Sci. & Eng., Gebze Institute of Technology, Gebze, Kocaeli, Turkey

<sup>3</sup>ENS Piezodevices Ltd., Gebze, Kocaeli, Turkey

Email: ebrualkoy@maltepe.edu.tr

In recent years, great efforts have been spent on to develop lead-free piezoelectric ceramics, which exhibits high piezoelectric and ferroelectric properties, due to the restrictions on the use of lead and other hazardous substances. One way to obtain enhanced piezoelectric properties in lead-free piezoceramics is to fabricate them with grain orientation and crystallographic texture. Potassium sodium niobate – KNN,  $[(\text{K},\text{Na})\text{NbO}_3]$ , is one of the leading lead-free composition that have been investigated in texture studies in detail.<sup>176</sup> However, all of these templated grain growth (TGG) studies use plate-like sodium niobate – NN,  $[\text{NaNbO}_3]$ , templates and align these templates using tape casting process.

The final objective of our study is to obtain grain oriented and textured KNN fibers that will be used in the fabrication of KNN based 1-3 piezocomposites. NN templates with needle-like morphology are required to induce a fiber texture in KNN. NN templates are known to grow with a plate-like morphology, when synthesized through the molten salt synthesis and topotactical transformation method. Thus, in this study, sodium niobate (NN) particles were synthesized by hydrothermal process. Since the aim of this study is to obtain anisometric morphology, various hydrothermal treatment temperatures and durations, as well as OH and Nb molarity have been investigated.

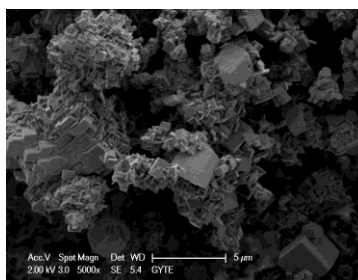
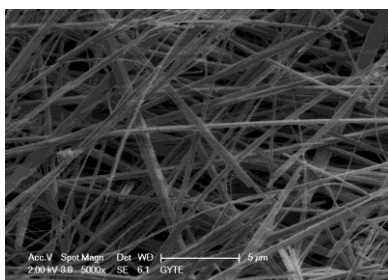


Fig. 1: SOMS with needle-like morphology (T=150°C) Fig. 2: NN with cubic morphology (T=160°C)

The  $\text{Na}_8\text{Nb}_6\text{O}_{19} \cdot 13\text{H}_2\text{O}$  phase with needle-like morphology was obtained at 120°C, the Sandia Octahedral Molecular Sieve (SOMS) morphology started to form at 130°C and was fully obtained at 150°C (Fig. 1), whereas the perovskite  $\text{NaNbO}_3$  particles with cubic morphology was obtained at

<sup>176</sup> Saito, Y., H. Takao, T. Tani, T. Nonoyama, K. Takatori, T. Homma, T. Nagaya, M. Nakamura, —Lead-free piezoceramics, Nature, vol. 432, pp. 84-87, 2004.

160°C (Fig. 2). Needle-like morphology was retained after annealing at 400-800°C. The results of the hydrothermal treatment process will be presented in details.

## Grain oriented $(\text{K}_{0.5}\text{Na}_{0.5})\text{NbO}_3$ -based piezoelectric ceramics prepared by reactive template grain growth method

**A. Hussain<sup>1</sup>, T. K. Song<sup>1</sup>, M. H Kim<sup>1</sup> and W. J. Kim<sup>2</sup>**

<sup>1</sup>*School of Nano & Advanced Materials Engineering, Chanwon National University, Gyeongnam 641-773, Republic of Korea*

<sup>2</sup>*Department of Physics, Changwon National University, Gyeongnam 641-773, Republic of Korea*

Lead-base piezoelectric materials such as  $\text{Pb}(\text{Zr},\text{Ti})\text{O}_3$  (PZT) are widely utilized in electrical devices because of their excellent properties. However, legislations such as RoHS/WEEE (restriction of hazardous substances/waste electrical and electronic equipment) demand for the development of lead-free piezoelectric materials. Lead-free  $(\text{K}, \text{Na})\text{NbO}_3$  (KNN) perovskite system is currently under study as strong potential candidate for environmentally benign piezoelectric devices. However, pure KNN ceramics are difficult to sinter by conventional methods, and show inferior properties. To improve the performance of KNN ceramic system, different techniques for their fabrication such as spark plasma sintering, screen printing, templated grain growth, and reactive templated growth have been employed. Among these techniques, the reactive templated grain growth (RTGG) has proved to be more effective in improving the piezoelectric performance.

In this work, lead-free non-stoichiometric  $(\text{K}_{0.470}\text{Na}_{0.545})(\text{Nb}_{0.55}\text{Ta}_{0.45})\text{O}_3$  (KNNT) textured ceramics were prepared by RTGG method using  $\text{NaNbO}_3$  (NN) templates. The Plate-like  $\text{NaNbO}_3$  (NN) templates were synthesized from bismuth layer-structured  $\text{Bi}_{2.5}\text{Na}_{3.5}\text{Nb}_5\text{O}_{18}$  (BNN) particles by a topochemical microcrystal conversion (TMC) method. Using 5 wt% of NN templates, textured KNNT ceramics were fabricated, and their crystal structure, microstructure, dielectric and piezoelectric properties were compared with non-textured KNNT ceramics prepared by a conventional solid state reaction method. The textured KNNT ceramics exhibited high grain orientation and high dielectric constant. In addition, piezoelectric properties of textured KNNT ceramics were improved, giving a high piezoelectric coefficient  $d_{33} = 390$  pC/N and piezoelectric coupling coefficient  $k_p = 0.60$ .

Corresponding author: Ali Hussain

E.mail: [alihussain\\_phy@yahoo.com](mailto:alihussain_phy@yahoo.com)

## **0.6(Bi<sub>0.85</sub>La<sub>0.15</sub>)FeO<sub>3</sub>-0.4PbTiO<sub>3</sub> Multiferroic Ceramics by Tape Casting**

JIN Guo-xi, BU Shun-dong, Wang Da-Lei, Dai Rui, CHENG Jin-rong

School of Materials Science and Engineering/Shanghai University, Shanghai/China

Email: jrcheng@shu.edu.cn

For meeting the needs of function-structure integration design in ceramics, new shaping technology should be applied into modern ceramic materials. In this letter, BFPT-based multiferroic specimens formed by tape casting method were studied. Firstly, 0.6(Bi<sub>0.85</sub>La<sub>0.15</sub>)FeO<sub>3</sub>-0.4PbTiO<sub>3</sub> powders were obtained by solid state reaction calcined at 750°C. Then the powders were mixed with ethanol, polyvinylbutyral(PVB), dibutyl phthalate(DBP)-polyethylene glycol(PEG) and Triethylamine(TEA) to form tape casting slurry with viscosity range from 650 to 2700 mPa.s. Filming and rheological properties of slurry was studied by adjusting the components content. High quality casting films were obtained when the ratio of DBP-PEG/PVB was 1.5 with 1% TEA in slurry. Casting films were dried, cut and laminated into disks. The effects of forming process on densification and dielectric properties were studied via controlling forming pressure. Ceramics formed by 200MPa with T<sub>c</sub>=410 °C, tanδ=2.2%, ε<sub>r</sub>=480 at 1kHz while Pr=5.5μC/cm<sup>2</sup> at 20kV/cm were obtained.

## **Controllable Synthesis of Different Bismuth Ferrites by an EDTA-assisted Hydrothermal Method and Photocatalytic Characterization**

Tong Tong, Dengren Jin and Jinrong Cheng\*

School of materials science and engineering, Shanghai University, Shanghai 200072, P.R.China

\*corresponding author: [jrcheng@shu.edu.cn](mailto:jrcheng@shu.edu.cn)

Bismuth ferrites crystallites were synthesized by an EDTA-assisted hydrothermal method using  $\text{Fe}(\text{NO}_3)_3 \cdot 9\text{H}_2\text{O}$  and  $\text{Bi}(\text{NO}_3)_3 \cdot 5\text{H}_2\text{O}$  as starting materials with NaOH as the mineralizer. Different phases of bismuth ferrites including sillenite  $\text{Bi}_{25}\text{FeO}_{40}$ , perovskite  $\text{BiFeO}_3$  and orthorhombic  $\text{Bi}_2\text{Fe}_4\text{O}_9$  were obtained respectively in the process of hydrothermal reactions by adjusting the process parameters, such as NaOH concentration, reaction temperature and duration time et al. The analysis revealed that EDTA played an important role in the phase evolution of bismuth ferrites and intensely influenced the morphology of bismuth ferrites powders. The mechanism of forming different bismuth ferrites in the hydrothermal process was also investigated and discussed. Moreover, photocatalytic properties of the bismuth ferrites crystallites were explored as well. The as-prepared powders performed a good degradation effect at visible light region, suggesting their promising applications as photocatalysts.

*Keywords: Bismuth ferrites; Hydrothermal synthesis; EDTA; Photocatalysis*



NANOPARTICLES TRANSPORT IN CERAMIC MATRIXES:  
A NOVEL APPROACH FOR CERAMIC MATRIX COMPOSITE FABRICATION

Andrey N. Rybyanets, Anastasia A. Naumenko

*Institute of Physics, Southern Federal University  
Rostov on Don, Russia  
[arybyantes@gmail.com](mailto:arybyantes@gmail.com)*

Nanoparticles are perfect building blocks offering a wide variety of compositions, structures and properties, ideally suited to designing functional nanomaterials and nanodevices. Nanoparticles can be embedded in various matrixes; however, a major technological problem is spontaneous aggregation of nanoparticles which, as a result, lose their unique properties. Recently polymer nano- and microgranules filled with nanoparticles (magnetic, metal, oxides etc.) start widely used as a delivery means of nanosubstances in medical, biotechnology and chemical applications. Very recently, there was a tendency to fix (immobilize) particles on the surface of spherical polymeric microgranules. Such composite micro-nano systems offer a number of significant advantages. When fixed to a surface or embedded in microgranules, nanoparticles lose their tendency to readily aggregate but retain their reactivity and, for the most part, their physical properties. Besides, microgranules are easier to manipulate than nanoparticles. Microgranules, coated or filled with nanoparticles can be used to produce "homogeneous" disperse systems, such as sols and aerosols, and fabricate films, coatings or bulk materials.

A novel approaches for fabrication of nano- and microporous piezoceramics as well as *ceramic matrix* piezocomposites (CMC's) are proposed in this work. The technique is based on nanoparticles transport in ceramic matrixes using polymer nanogranules, coated or filled by a various chemicals, as a porosifiers at standard ceramics fabrication process. Resulting CMC's are composed by super lattices of closed pores filled or coated by nanoparticles of metals, oxides, ferromagnetics etc., embedded in piezoceramic matrix. Pilot samples of nano and microporous ceramics and CMC's were fabricated using different piezoceramics compositions as a ceramic matrix. Two types of polymer microgranules were used for a nanoparticles transport: polystyrene microgranules filled by magnetite nanoparticles and polytetrafluoroethylene microgranules coated by metal nanoparticles. Parent microgranules and nanoparticles as well as resulting CMS's were examined using transmission and scanning electron microscopy (TEM and SEM). New family of nano- and microporous piezoceramics and CMC's are characterized by a unique spectrum of the electrophysical properties unachievable for standard PZT ceramic compositions and fabrication methods, including combination of piezoelectric, magnetic and electrets properties, giant dielectric

relaxation, giant piezoelectric and electrocaloric effects, as well as a possibility of controllable changes of the main properties within a wide range.

## Synthesis and Electromechanical Investigations of Tb Substituted $\text{Bi}_4\text{Ti}_3\text{O}_{12}(\text{BiFeO}_3)_m$ Aurvillius Phase Thin Films

Ahmad Faraz<sup>1</sup>, Nitin Deepak<sup>1</sup>, Tuhin Maity<sup>1</sup>, Saibal Roy<sup>1</sup>, Martyn E. Pemble<sup>1,2</sup>, Lynette Keeney<sup>1</sup>

<sup>1</sup>Tyndall National Institute, University College Cork, Cork, Ireland

<sup>2</sup>Department of Chemistry, University College Cork, Cork, Ireland

**Email:** ahmad.faraz@tyndall.ie

Lead-based piezoelectric materials are the most extensively used materials for piezoelectric and ferroelectric applications due to their strong piezoelectric responses<sup>1</sup>. However, due to toxicological and environmental concerns, there is a strong impetus to identify and replace Pb-base materials with new materials having comparable piezoelectric properties for use as piezoelectric actuators, sensors and transducers, especially for use at elevated temperatures in applications such as engines<sup>2</sup>. Bismuth layer-structured ferroelectric materials in the Aurvillius phase are considered as potential candidates to replace Pb-base materials with high Curie temperatures ( $T_c$  generally over 500°C) and fatigue-free switching for memories. These materials are naturally 2-*D* nanostructured, consisting of  $(\text{Bi}_2\text{O}_2)^{2+}$  layers alternating with  $n\text{ABO}_3$  perovskite units, described by the general formula  $\text{Bi}_2\text{O}_2(\text{A}_{n-1}\text{B}_n\text{O}_{3n+1})$ . On increasing the number of perovskite layers ( $n$ ), the microstructural, ferroelectric, magnetic and other physical properties can be altered significantly. They also offer the desirable quality of accommodating various cations in their crystal structure.

In this work we report the synthesis and electromechanical investigations of novel 5-layered Tb substituted  $\text{Bi}_4\text{Ti}_3\text{O}_{12}(\text{BiFeO}_3)_2$  thin films (TbB5FTO) on  $\text{La}_{0.7}\text{Sr}_{0.3}\text{MnO}_3$  electrodes/c-plane sapphire substrates by chemical solution deposition (CSD). Structural and morphological analyses confirm that films are single phase with no additional detectable impurity phases.

Piezoresponseforce microscopy (PFM) was used as a characterization tool to confirm in-plane and out-of-plane piezoelectric behaviour. Local hysteresis loops were generated by switching-spectroscopy SS-PFM and information on local ferroelectric behavior in these materials as a function of temperature is presented. Magnetic measurements were performed using SQUID (superconducting quantum interference device) magnetometry and the potential of TbB5FTO thin films as candidate multiferroics is discussed.

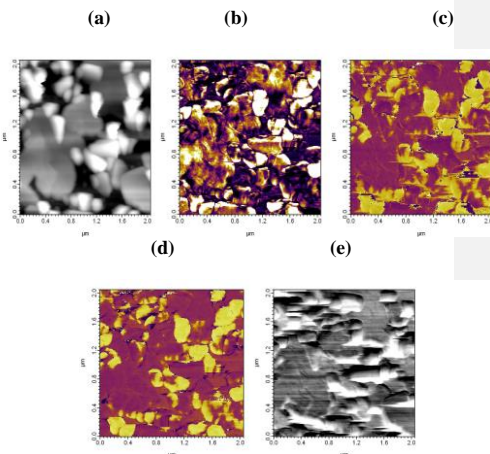


Fig. 1: Vertical DART PFM micrographs TbB<sub>5</sub>TFO films on C- plane (0001) Sapphire substrate (a) Height response (b) Amp response (c) Phase-1 response (d) Phase-2 response (e)

<sup>177</sup> Y. Saito, H. Takao<sup>1</sup>, T. Tani, T. Nonoyama, K. Takatori<sup>1</sup>, T. Homma<sup>1</sup>, T. Nagaya, M. Nakamura, Lead-free piezoceramics, nature vol 432 Nov 2004

<sup>2</sup>M. Demartin Maeder, D. Damjanovic, N. Setter, Lead Free Piezoelectric Materials J. Electrocer. 13, 385–392, 2004

## Hexagonal Ferrite and Ferroelectric Perovskite Magnetoelectric Composites

Robert C. Pullar<sup>\*</sup>, Marco Medeiros, Dmitry V. Karpinsky and Andrei L. Kholkin

*Department of Materials and Ceramic Engineering and CICECO, University of Aveiro,  
Campus Universitário de Santiago, Aveiro, 3810-193, Portugal*

<sup>\*</sup>Presenting author, email: [rpullar@ua.pt](mailto:rpullar@ua.pt)

There has been a great deal of interest in the possibility of coupling between magnetic and electrical properties in multiferroic and magnetoelectric (ME) ceramics. Because of the inherent problems in establishing good magnetic and dielectric/ferroelectric properties in a single multiferroic material, we are investigating the manufacture of magnetoelectric composite materials consisting of separate magnetic and dielectric/ferroelectric ceramic components, and potential coupling between such components at up to microwave (GHz) frequencies. In this paper we will report our investigations of composites consisting of the ferrites BaM (BaFe<sub>12</sub>O<sub>19</sub>), SrM (SrFe<sub>12</sub>O<sub>19</sub>), Co<sub>2</sub>Z (Ba<sub>3</sub>Co<sub>2</sub>Fe<sub>24</sub>O<sub>41</sub>) or SrZ (Sr<sub>3</sub>Co<sub>2</sub>Fe<sub>24</sub>O<sub>41</sub>) combined with the ferroelectrics BT (BaTiO<sub>3</sub>) or KN (KNbO<sub>3</sub>). The ferrites were produced by various methods – sol-gel, citrate combustion and solid state ceramics – and the results compared. This is first time such composites have been made with the Z ferrites or potassium niobate perovskites. The synthesis and properties of the composites were investigated by XRD, SEM, VSM, PFM/MFM and dielectric measurements.

## Study of polar and electrical properties of Hydroxyapatite: Modeling and data analysis

Anna Bystrova<sup>1</sup>, Yuri Dekhtyar<sup>1</sup>, Svitlana Kopyl<sup>2</sup>, Igor Bdikin<sup>2</sup>, Vladimir Bystrov<sup>3</sup>, Alla Saprionova<sup>4</sup> and Andrei Kholkin<sup>3</sup>

<sup>1</sup>Institute of Biomedical Eng. and Nanotechnology, Riga Technical University, Riga, Latvia

<sup>2</sup>Centre for Mechanical Technology and Automation, University of Aveiro, Aveiro, Portugal

<sup>3</sup>Department Materials Eng. and Ceramics & CICECO, University of Aveiro, Aveiro, Portugal

<sup>4</sup>Bergen Center for Computational Science, Unifob AS, N-5008 Bergen, Norway

Email: [bystrov@ua.pt](mailto:bystrov@ua.pt)

1. Non-homogeneity of hydroxyapatite (HAP) surface structure was shown by atomic force microscopy (AFM) with formation of nano-crystals area of ~ 500...1000 nm.
2. These formations could be connected with HAP polymorphism – two phases (hexagonal and monoclinic) are co-existed, as was shown by our computational modeling (HyperChem 8.0) and first principles LDA calculations. The unit cell parameters are different for these phases, as results the area's height on surface of various phases are altered. This alteration could generate variation of surface potential, which could be registered by Kelvin probe scanning, and must be create the local change of work function. It is first reason of local electrical and polar HAP surface peculiarities influenced on osteoblastes attachment and proliferation.
3. Defects formations (such as oxygen vacancy or hydrogen interstices) change unit cell total energy and surface potential. Modeling and first principle calculations show that energy changes/per HAP crystal cell unit are approximately ~ 0.1...0.2 eV for these defects. These changes coincide with experimentally measured work functions alteration on HAP surface. It must be second reason for influence of nano-interaction with living cells on the HAP surface.
4. Such defects could be arisen by hydrogenation processes under hydrogen introducing during high pressure treatment, conjugated with following microwave irradiation. Such insertion could switch OH dipole orientation and as results change the H-OH ordering along OH-column in HAP structures and creates non-centrosymmetric polar and piezoelectric local areas on HAP structure and its surface. This technology was apply now for HAP surface modification and insertion of the negative electrical charges on the HAP surface layer, that change locally of HAP surface potential (and consequence its polar properties), which is very influenced on the cell's adhesion and proliferation of these living cell, e.g. osteoblasts. Common cumulative effect from reasons 1 and 2 could be estimated by introducing of nano-interaction's correlation length, which value ~ 200...500 nm correspond to sizes of specific osteoblast's filaments (such as cell's leg/stem) and HAP surface non-homogeneities area.
5. The experimental data of synchrotron illuminations and registered absorption peaks are investigated and compared with computational estimation of surface potential and work functions changes under formations of various types of such defects for each HAP crystal phases.

## **Effect of B<sub>2</sub>O<sub>3</sub> Addition on Dielectric and Ferroelectric Properties of BiFeO<sub>3</sub> Ceramic**

Thanatep Phatunghane, Gobwute Rujijanagul

Department of Physics and Materials Science, Faculty of Sciences, Chiangmai University,  
Chiangmai, Thailand

Email: rujijanagul@yahoo.com

In the present work, the effect of B<sub>2</sub>O<sub>3</sub> addition on sintering behavior, dielectric and ferroelectric properties of BiFeO<sub>3</sub> (BFO) ceramics was investigated. These ceramics were prepared successfully by a solid state reaction technique for the first time. Phase formations of the obtained ceramics were investigated by x-ray diffraction technique (XRD). The morphology of the B<sub>2</sub>O<sub>3</sub> added BFO ceramics was characterized by electron microscopy (SEM). The dielectric and ferroelectric properties of the ceramics were also investigated. Pure phase perovskite was observed. Our work indicates that the ceramics exhibit good dielectric and ferroelectric behavior.

### **Acknowledgements**

This work was supported by The Royal Golden Jubilee Ph.D. Program, The Thailand Research Fund (TRF), Faculty of Science and Graduate School Chiang Mai University and National Research University (NRU), Office of the Higher Education Commission (OCHE) Thailand.

## Shift of morphotropic phase boundary in PNZT epitaxial films processed by sol-gel approach

Qi Yu<sup>1</sup>, Jing-Feng Li<sup>1</sup>, Yuanming Liu<sup>2</sup>, Jiangyu. Li<sup>2</sup>

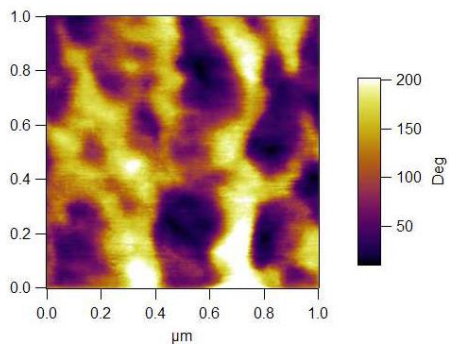
<sup>1</sup>State Key Laboratory of New Ceramics and Fine Processing, School of Materials Science and Engineering, Tsinghua University, 100084 Beijing, People's Republic of China.

<sup>2</sup>Department of Mechanical Engineering, University of Washington, Seattle, Washington 98195-2600, United States

Email: [jingfeng@mail.tsinghua.edu.cn](mailto:jingfeng@mail.tsinghua.edu.cn)

Motivated by the miniaturized trend on the next-generation electronic devices, Pb(Zr,Ti)O<sub>3</sub>-based thin films had been treated as a predominant selection among aspects so far due to the overwhelming piezoelectric and ferroelectric properties especially for the composition situating at morphotropic phase boundary (MPB). It has been widely accepted that epitaxial films could enable higher performance as well as numerous fancy phenomena potentially associated with a closer structure to real single crystals as well as subtle effects originated from constraint of single-crystalline substrate. In this study, 2% Nb-doped Pb(Zr, Ti)O<sub>3</sub> thin films [abbreviated as "PNZT"] along a wide composition range were deposited onto SrTiO<sub>3</sub> single-crystalline substrates with various cutting directions including [100], [110] and [111] through a facile sol-gel route. Based on X-ray diffraction, Raman spectroscopy, ferroelectric test together with piezoresponse measurement at nanoscale, deviations of MPB from the critical ratio of Zr/Ti=52/48 in bulks were confirmed in PNZT epitaxial thin films with [001], [110] and [111] preferred orientations. It was found that the MPB moved to Ti-rich region in both [110] and [111]-oriented system, while to the opposite Zr-rich region in [001]-oriented ones. Optimum electrical properties could be obtained at the location of the shifted MPB composition. Mapping of domains structure and switching was also carried out on scanning probe microscopy platform, which should be helpful to reveal internal mechanisms of domain configurations and kinetics in PZT-based epitaxial films with various crystallographic orientations.

Fig. 1: Nanoscale mapping of piezoresponse phase configuration of PNZT epitaxial films (Zr/Ti=30/70, 001-oriented).





## Microstructure and Optical Properties of $\text{Er}_2\text{O}_3$ - Doped Potassium Sodium Niobate-Tellurite Glass-ceramics

P. Yongsiri<sup>1</sup>, and K. Pengpat<sup>1,2</sup>

<sup>1</sup> Department of Physics and Materials Science, Faculty of Science,  
Chiang Mai University, Chiang Mai, 50200, Thailand

<sup>2</sup> Materials Science Research Center, Faculty of Science, Chiang Mai, 50200, Thailand

Email: kamonpan.p@cmu.ac.th

Ferroelectric glass-ceramics have been extensively studied as they possess the properties of non-porous glasses as well as ferroelectric crystals, giving rise to materials that have the good mechanical properties of glass and the electro-optical properties of ferroelectric crystals. In this work, ferroelectric potassium sodium niobate [ $(\text{K}_{0.5}\text{Na}_{0.5})\text{NbO}_3$  or KNN] crystals are of interest because of their distinct electrical properties<sup>1</sup> and non-linear optical properties<sup>2</sup>. Many researchers have attempted to produce glass-ceramics with the ferroelectric<sup>178</sup> KNN phase<sup>3-4</sup>. The difficult part of preparing this glass type is to crystallize the KNN single phase. The idea of combining potassium sodium niobate crystals in some selected glasses has therefore been developed and called the incorporation method<sup>5</sup>. In the present study, KNN crystals were firstly introduced to tellurite base glasses. Transparent glasses of erbium oxide ( $\text{Er}_2\text{O}_3$ )-doped KNN-tellurite glasses were then successfully prepared by using the incorporation method. Experiments started with the preparation of KNN powder by simple mixed oxide method using calcination temperature of  $900^\circ\text{C}$  for 5 h. Then, the calcined KNN powder was mixed with  $\text{TeO}_2$  and 0.5-1 mol%  $\text{Er}_2\text{O}_3$  dopant. Each batch was subsequently melted at  $800^\circ\text{C}$  for 15 min in a platinum crucible using an electric furnace. The quenched glasses were then subjected to heat treatment at various temperatures for 4 h in order to form glass-ceramics with the desired crystal phases. X-ray diffraction (XRD) results showed that KNN solid solution distributed over the glass-ceramic samples. Scanning electron microscopy (SEM) revealed that nano-crystals of KNN and some secondary crystals precipitated in the glass-ceramics. Crystal sizes increased with increasing heat treatment temperatures. The optical and physical properties of the prepared glass-ceramics were measured. The values of refractive index ( $n$ ) ranged between 1.99 and 2.15, while that of density ( $\rho$ ) ranged between  $4.70\text{--}5.18\text{ g/cm}^3$ . Energy band gap from the transmission cut-off wavelength ( $\text{Eg}$ ) was measured as  $3.14\text{--}3.20\text{ eV}$ .

<sup>178</sup> M. Ichiki, L. Zhang, M. Tanaka and R. Maeda, "Electrical properties of piezoelectric sodium-potassium niobate", *J. Eur. Ceram. Soc.*, Vol. 24, Issue 6, p. 1693–1697, 2004.

<sup>2</sup> A. Aronne, E. Fanelli, P. Pernice, S. Peli, C. Giannetti and G. Ferrini, "Crystallization and second harmonic generation in potassium–sodium niobosilicate glasses", *J. Solid State Chem.*, Vol. 182, p. 2796–2800, 2009.

<sup>3</sup> A. Aronne, E. Fanelli, P. Pernice, S. Peli, C. Giannetti and G. Ferrini, "Crystallization and second harmonic generation in potassium–sodium niobosilicate glasses", *J. Solid State Chem.*, Vol. 182, p. 2796–2800, 2009.

<sup>4</sup> D. E. Vernacotola, S. Chatlani, J. E. Shelby, "Ferroelectric sodium-potassium-niobium silicate glass ceramics", proceedings of the 2000 12th IEEE international symposium on application of ferroelectrics, Vol. 2, p. 829, 2000.

<sup>5</sup> P. Yongsiri, S. Eitssayeam, G. Rujjanagul, S. Sirisoonthorn, T. Tunkasiri and K. Pengpat, "Fabrication of transparent lead-free KNN glass-ceramics by incorporation method", *Nanoscale. Res. Lett.*, Vol. 7, p. 136, 2012.



## Sputtered Pb(Zr,Ti)O<sub>3</sub> piezoelectric films for MEMS application

Hiroki Kobayashi<sup>1</sup>, Mitsunori Henmi<sup>1</sup>, Mitsutaka Hirose<sup>1</sup>, Isao Kimura<sup>1</sup>, Takehito Jinbo<sup>1</sup>,  
Koukou Suu<sup>1</sup>

<sup>1</sup> Institute of Semiconductor and Electronics Technologies, ULVAC Inc.,  
1220-1 Suyama Susono, Shizuoka, Japan

Email: hiroki2\_kobayashi@ulvac.com

One of the difficulties in PZT film deposition by sputtering method is to keep the stability in the lead content which is volatile element and deposition rate with the passage of sputtering time. Another would be how to obtain higher piezoelectric coefficient  $e_{31}$  of PZT film for high-performance devices such as sensor and actuator. In this work, some key technologies for perovskite oxide thin-film production including production tool technologies, their performances of sputtering, and improvement of properties of PZT film will be introduced.

A multi-chamber type mass production sputtering systems for electronic devices SME-200E (ULVAC Inc.) equipped with an exclusive sputtering module was used. When insulating PZT film adhered to the shields of the ground potential, charge-up occurred, the impedance of the system changed, plasma was pushed to the center of the chamber, exposure to plasma was enhanced, and as a consequence, Pb content within film reduced. In order to stabilize the status of plasma, we installed a stable anode, that is, an anode that avoided charge-up due to the adhesion of insulating PZT film and maintained the role as an anode [1]. As a result that a stable anode was installed, the change in the Pb composition was  $1.0 \pm 0.6\%$  by the evaluation until end of target life (total wafer; 400 pieces @2  $\mu\text{m}$  thickness PZT). And the change in the deposition rate was  $3.8 \mu\text{m/h} \pm 1.4\%$  and uniformity of within wafer was less than  $\pm 5\%$  by the evaluation until end of target life. As a result that a stable anode was installed, stability of Pb content and deposition rate within film in continuous sputtering has been confirmed.

PZT films have been deposited on 8inch diameter Pt(111)/TiO<sub>x</sub>/SiO<sub>2</sub>/Si substrates. The PZT films were deposited under Ar/O<sub>2</sub> mixed gas atmosphere of 0.5 Pa. Substrate temperature was heated up to around 580°C. PZT films were deposited with relatively high growth rate about 3.8  $\mu\text{m/h}$  and these thicknesses was 2.0  $\mu\text{m}$ . PZT film oriented PZT(001)/(100) preferably, and the pyrochlore phase cannot be detected. We also note that *post in-situ treatment* [2] has been recently established, aiming to improve crystalline property and piezoelectric coefficient in our PZT films. After in-situ treatment, piezoelectric coefficient  $e_{31}$  increased up to  $-19.2 \text{ C/m}^2$ , which is remarkably improved compared to  $e_{31}$  of  $-14.7 \text{ C/m}^2$  as deposited. We have established both mass production capability and advanced process capability for MEMS devices.

[1] United States Patent, US 6,521,105 B2 (2003)

[2] Kobayashi et.al in preparation

## Structural, ferroelectric and piezoelectric properties of composition spread $\text{Bi}_{1-x}\text{Ga}_x\text{FeO}_3$ thin films

N. Jaber<sup>1</sup>, J. Wolfman<sup>1</sup>, C. Daumont<sup>1</sup>, B. Négulescu<sup>1</sup>, A. Ruyter<sup>1</sup>, G. Feuillard<sup>1</sup>, J. Fortineau<sup>1</sup>,  
T. Sauvage<sup>2</sup>, B. Courtois<sup>2</sup>, C. Autret-Lambert<sup>1</sup>, F. Gervais<sup>1</sup>

<sup>1</sup> GREMAN laboratory, UMR7347 CNRS, Université François Rabelais, Tours, France

<sup>2</sup> CEMHTI laboratory, UPR3079 CNRS, Orléans, France

Email: [wolfman@univ-tour.fr](mailto:wolfman@univ-tour.fr)

The coexistence in some oxide materials of distinct ferroic orders (ferroelectricity, ferromagnetism, ferroelasticity) open the way to new multifunctional applications. Among those materials, PZT  $[(\text{PbZrO}_3)_{1-x}(\text{PbTiO}_3)_x]$  and PMNPT  $[(\text{PbMg}_{1/3}\text{Nb}_{2/3}\text{O}_3)_{1-x}(\text{PbTiO}_3)_x]$  solid solutions exhibit the highest ferroelectric-ferroelastic coupling and are widely used as piezoelectric sensors or more recently for energy harvesting applications. However lead-based compounds are about to be banished by European RoHS regulation and a lead-free replacement is required. An important piezoelectric effect has recently been shown in  $\text{Bi}_{1-x}\text{Re}_x\text{FeO}_3$  (Re : rare earth) thin films solid solutions<sup>1</sup>, related with the occurrence of a morphotropic phase boundary (MPB), as it is the case for PZT and PMNPT. In this work, we report the exploration of  $\text{Bi}_{1-x}\text{Ga}_x\text{FeO}_3$  (BGFO) phase diagrams. Composition spread epitaxial BGFO thin films were grown by pulsed laser deposition onto  $\text{La}_{0.8}\text{Sr}_{0.2}\text{MnO}_3$  electrodes. Composition gradients were characterized by EDX and RBS while phase analysis was realized by X-Ray micro-diffraction (XRMD). Impedance spectroscopy, ferroelectric cycles and XRMD versus temperature were used to identify phase transitions and MPBs locations in the composition spread films. Cartographies of the effective  $d_{33}$  measured at various length scales with PFM (a few nm), laser interferometry (a few  $\mu\text{m}$ ) and XRMD (a few 100  $\mu\text{m}$ ) across composition spread will be presented and compared.

# Magnetoelectric Coupling of $\text{Pb}(\text{Zr}_{0.52}\text{Ti}_{0.48})\text{O}_3/\text{Pt}/\text{CuFe}_2\text{O}_4$ Multilayer Thin Films

Sung-Ok Hwang<sup>1</sup>, Chang Young Koo<sup>1</sup>, You Jeong Eum<sup>1</sup>, Jungho Ryu<sup>2</sup>, Hee Young Lee<sup>1,\*</sup>

<sup>1</sup>School of Materials Science and Engineering, Yeungnam University,  
Gyeongsan, 712-749, Korea

<sup>2</sup>Functional Ceramics Research Group, Korea Institute of Materials Science (KIMS),  
Gyeongnam, 641-831, Korea

\*Email: [hyulee@yu.ac.kr](mailto:hyulee@yu.ac.kr)

The multiferroic materials and/or multilayer structure of ferroelectric/ferromagnetic materials can be used for sensors, memory storage devices, energy harvesting devices and so on due to their magnetoelectric(M-E) coupling properties. But single-phase multiferroic materials such as BFO( $\text{BiFeO}_3$ ) still have shown lower M-E coupling properties than multilayer structured ones. Therefore, the hybrid structured ferroelectric/magnetic materials have received a great deal of attention because their high M-E performances, but it's also still restricted to bulk materials. In this regards, we have prepared multilayer thin film structure with PZT and Cu-ferrite.

Polycrystalline  $\text{Pb}(\text{Zr}_{0.52}\text{Ti}_{0.48})\text{O}_3$ (PZT)/Pt/ $\text{CuFe}_2\text{O}_4$  multilayer thin films on quartz(or  $\text{SiO}_2/\text{Si}$ ) substrate. The film structure is tri-layered type,  $\text{CuFe}_2\text{O}_4$  film was deposited by using pulsed laser deposition (PLD) method. In order to investigate annealing effect on film microstructure, ferroelectric and ferromagnetic properties of multilayer thin films,  $\text{CuFe}_2\text{O}_4$  layer was heat-treated at various temperatures. For measuring their electrical and magnetoelectric properties, Pt electrode layer was deposited on the  $\text{CuFe}_2\text{O}_4$  layers by sputtering. PZT layers were fabricated by sol-gel method on Pt interlayer. And Pt top electrodes were also deposited using by sputtering with shadow mask. Structural and microstructural properties of PZT/Pt/ $\text{CuFe}_2\text{O}_4$  multilayer thin films were observed by XRD and SEM. Ferroelectric and ferromagnetic behaviors of multilayer films were examined by measuring polarization and magnetization – electric and magnetic field hysteresis. Magnetoelectric coefficients were calculated by measured magnetoelectric voltages using magnetoelectric measurement system.

We'll discuss the annealing effect on ferroelectric and ferromagnetic properties of multilayer films, and also discuss the M-E coupling properties as a function of annealing temperatures in detail.

## Microstructure and kHz- and GHz- Range Dielectric properties of Polycrystalline $\text{Ba}_{0.5}\text{Sr}_{0.5}\text{TiO}_3$ Thin Films

Tanja Pečnik<sup>1,2</sup>, Sebastjan Glinšek<sup>3,4</sup>, Brigita Kmet<sup>1,4</sup>, Barbara Malič<sup>1,2,4</sup>

<sup>1</sup>Electronic Ceramics Department, Jožef Stefan Institute, Jamova cesta 39, 1000 Ljubljana, Slovenia

<sup>2</sup>Jožef Stefan International Postgraduate School, Jamova cesta 39, 1000 Ljubljana, Slovenia

<sup>3</sup>School of Engineering, Brown University, 184 Hope Street, Providence, Rhode Island 02912, USA

<sup>4</sup>Centre of Excellence SPACE-SI, Aškerčeva cesta 12, 1000 Ljubljana, Slovenia

Email: tanja.pecnik@ijs.si

The  $\text{Ba}_x\text{Sr}_{1-x}\text{TiO}_3$  ( $x=0-1$ ) solid solution is suitable for tunable microwave applications, such as phase shifters, tunable resonators, etc. Its main advantage is composition-tunable functional response, i.e., high dielectric permittivity, relatively low dielectric losses and high tunability at microwave frequencies<sup>179</sup>. In the case of solution-derived thin films, knowledge and control of the microstructure-dielectric properties relations is of crucial importance for the integration into devices. In this contribution we present the processing of  $\text{Ba}_{0.5}\text{Sr}_{0.5}\text{TiO}_3$  (BST) thin films on polycrystalline alumina substrates and the study of the relationships between the microstructure and the RF- and MW-range dielectric properties in these films.

The 0.25 M solutions were prepared via alkoxides-based route from alkaline earth acetates and Ti-butoxide, which were dissolved in the 2-methoxyethanol-acetic acid mixture. The precursor solutions were spin-coated on the alumina substrates and the as-deposited films were dried at 200 °C, pyrolyzed at 350 °C and annealed in a rapid thermal annealing furnace at 900 °C. The deposition-annealing steps were repeated several times to achieve the final thickness of the films. According to the XRD analysis, the films crystallize in the randomly oriented perovskite phase. The SEM analysis revealed uniform in-plane microstructures, with grains of a few 10 nm and about 100 nm in 170 nm- and 500 nm- thick films, respectively.

For the RF-range dielectric characterization the planar capacitor structures were deposited using the lift-off photolithography, while the split-post dielectric resonators were used for MW measurements. The about 170 nm thick films reached the values of the dielectric permittivity, dielectric losses and tunability ( $\epsilon_{0V}/\epsilon_{40V}$ ) of 994, 0.01 and 1.63, measured at 100 kHz. The dielectric properties of the films with different thicknesses, from about 100 nm to 600 nm, and microstructures, will be presented in the contribution.

<sup>179</sup> M. J. Lancaster, "Thin-film ferroelectric microwave devices", *Supercond. Sci. Technol.*, vol. 11, p. 1323-1334, 1998.



## Effects of Thermal Treatment on the Properties of Zirconium Doped Barium Titanate Ceramics

Parkpoom Jarupoom<sup>1</sup>, Anocha Munpakdee<sup>2</sup>, Sukum Eitssayeam<sup>3</sup>, Kamonpan Pengpat<sup>3</sup>,  
Pongthep Arkornsakul<sup>3</sup>, Gobwute Rujjanagul<sup>3</sup>

<sup>1</sup>Department of Industrial Engineering, Faculty of Engineering, Rajamangala University of  
Technology Lanna (RMUTL), Chiang Mai, 50300, Thailand

<sup>2</sup>General Science Department, Faculty of Science, Srinakharinwirot University,  
Bangkok, 10110, Thailand

<sup>3</sup>Department of Physics and Materials Science, Faculty of Science, Chiang Mai University, Chiang  
Mai, 50200, Thailand

Email: [rujjanagul@yahoo.com](mailto:rujjanagul@yahoo.com)

In this work, zirconium doped barium titanate ceramics were prepared via a solid state technique. After sintering at 1,450 °C for 2h, the ceramics were annealed at 1,200 °C for 4-16 h. Effects of the thermal treatment on the electrical properties of the ceramics was investigated. An improvement in strain level, ferroelectric properties and piezoelectric coefficient were observed for the 8 h sample. High strain level and calculated  $d_{33}$  ( $d_{33}^*$ ) of 0.26% and 326 pm/V were also obtained for this sample. The electrical properties were found to correlate with the densification and second phase formation.

Acknowledgement: The authors would like to thank the Graduate School of Srinakharinwirot University.



## Electrical Properties of (1-x)BCZT-xBZT Lead-Free Ceramics

Piewpan Parjansri<sup>1</sup>, Sukum Eitssayeam<sup>1,2</sup>

<sup>1</sup>Department of Physics and Materials Science, Faculty of Science, Chiang Mai University, Chiang Mai 50200, Thailand

<sup>2</sup>Materials Science Research Center, Faculty of Science, Chiang Mai 50200, Thailand

Email: [sukum99@yahoo.com](mailto:sukum99@yahoo.com)

The aim of this study was to investigate the electrical properties of (1-x)[Ba<sub>0.85</sub>Ca<sub>0.15</sub>Zr<sub>0.1</sub>Ti<sub>0.9</sub>]O<sub>3</sub>-x[(BiZn<sub>0.5</sub>Ti<sub>0.5</sub>)O<sub>3</sub>] ceramics system for x = 0.00-0.10. The (1-x)BCZT-xBZT ceramics were fabricated via solid state reaction technique. The samples were calcined and sintered at 925 °C for 6 h and 1370 °C for 3 h, respectively. Phase formation and microstructure of (1-x)BCZT-xBZT ceramics were studied using an X-ray diffractometer (XRD) and scanning electron microscope (SEM). The physical properties and electrical properties, such as dielectric properties and ferroelectric properties were examined. It was found that all the samples show pure perovskite phase. Grain size and density value were in the range of 2.18-13.30 μm and 5.61-5.77 g/cm<sup>3</sup>, respectively. The BZT content lead to the change and improved of the dielectric properties of ceramic samples. The dielectric loss values were lower than 0.01 (at 1 kHz) for all samples. The samples show higher degree of the relaxor like behavior with higher BZT content. In addition, the ferroelectric properties were found to depend on the BZT content.

## Relationship of Microstructure and Electrical Properties in Sol-Gel PZT Films

Konstantin Vorotilov<sup>1</sup>, Alexander Sigov<sup>1</sup>, Dmitry Seregin<sup>1</sup>, Yury Podgorny<sup>1</sup>, Olga Zhigalina<sup>2</sup>,  
Dmitry Khmelenin<sup>2</sup>

<sup>1</sup>Moscow State Technical University of Radioengineering, Electronics and Automation (MIREA),  
Moscow, Russia

<sup>2</sup>Shubnikov Institute of Crystallography, Russian Academy of Sciences, Moscow, Russia

Email: vorotilov@mirea.ru

Thin PZT films are a prominent material for ferroelectric random access memory (FRAM), MEMS and other integrated ferroelectric devices<sup>180</sup>.

Despite the fact that formation of perovskite phase in PZT films prepared by sol-gel techniques has been the subject of investigation since 1990s, mechanisms of fine crystalline structure formation, nucleation and growth processes are as yet not fully understood. A comparison between results reported by different authors is complicated due to various precursor chemistry and preparation conditions. A comprehensive discussion of different approaches to sol-gel synthesis of PZT films and nucleation processes was made recently in refs.<sup>181,182</sup>.

In this work we try to establish main regular trends in formation of fine crystalline structure (with the use of TEM techniques) of sol-gel PZT thin films annealed at different temperatures and its effect on electrical properties of the films.

For this purpose in addition to the range of annealing temperatures  $T_a = 600 - 750^\circ\text{C}$  commonly used for preparation of sol-gel PZT films, we have studied both the film annealed at low temperature  $T_a = 550^\circ\text{C}$ , where perovskite phase has not completely arisen, and one annealed at high temperature  $T_a = 900^\circ\text{C}$ , that leads to degradation of multilevel heterostructure as a result of diffusion processes.

The structure of the films was studied by transmission electron microscopy (TEM), electron and X-ray diffraction; electrical properties were characterized by Sawyer-Tower, capacitance-voltage and current-voltage techniques.

Experimental data on film microstructure (grain size, texture, pyrochlore inclusions, interfaces), changes in structure and composition of the underlying layers are discussed in association with electrical properties of the films.

---

<sup>180</sup>N. Setter, D. Damjanovic, L. Eng, et al. "Ferroelectric thin films: Review of materials, properties, and applications", J. Appl. Phys., vol. 100, p. 051606, 2006.

<sup>181</sup>T. Schneller, and R. Waser, "Chemical modifications of  $\text{Pb}(\text{Zr}_{0.3}\text{Ti}_{0.7})\text{O}_3$  precursor solutions and their influence on the morphological and electrical properties of the resulting thin films", J. Sol-Gel Sci. Techn., vol. 42, p. 337-352, 2007.

<sup>182</sup>A. C. Dippel, T. Schneller, R. Waser, D. Park, and J. Mayer, "Formation sequence of lead platinum interfacial phases in chemical solution deposition derived  $\text{Pb}(\text{Zr}_{1-x}\text{Ti}_x)\text{O}_3$  thin films", Chem. Mater., vol. 22, p. 6209 – 6211, 2010.



## Fabrication and Characterization of PZT-PAni/PVDF Based Nanocomposite

Oliveira Cibele<sup>1</sup>, Fuzari Jr, Gilberto de C.<sup>3</sup>, Sakamoto, Walter<sup>2</sup>, Longo Elson<sup>1</sup>, Zaghete, Maria A.<sup>1</sup>.

<sup>1</sup> Depto de Bioquímica e Tecnologia Química, Instituto de Química/ Univ. Estadual Paulista – UNESP, Araraquara, S P/ Brasil

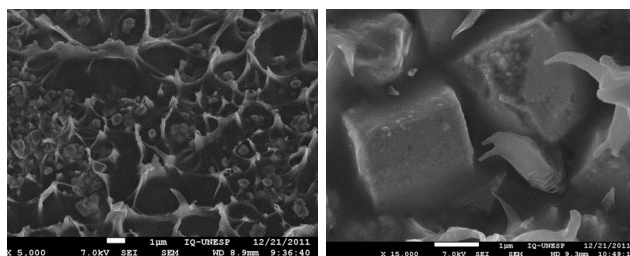
<sup>2</sup> Depto de Física e Química, Faculdade de Engenharia/ Univ. Estadual Paulista - UNESP, Ilha Solteira, S P/Brasil

<sup>3</sup> Instituto de Ciências Exatas e da Terra (ICET)/ Univ. Federal de Mato Grosso-UFMT/ Barra do Garças, MT – Brasil

Email: zaghete@iq.unesp.br

This work presents the preparation and characterization of PZT ceramic obtained by different methods. The influence of the synthesis method on the grain size and the morphology are also object of study. The fabrication and characterization of composite films with 0-3 connectivity, immersing nanoparticles of PZT into the non-polar poly(vinylidene fluoride) – PVDF as the polymer matrix were presented. For comparison there are results obtained with composite samples made of ceramic particles unrecovered and recovered with a conducting polymer. In this sample the PZT grain was partially covered by PAni, which allowed better distribution of grains in the polymer matrix avoiding a continuous electrical flux path which does not allow the polarization process of the composite sample. The use of this composite as sensor and power converter is an indicative that it is a good alternative for technological applications. The concept of energy harvesting must be related to capture the ambient energy and convert it into usable electrical energy without environment attack i.e., a clean electric energy. Although there are a number of sources of harvestable ambient energy, such as solar energy and energy from wind, piezoelectric materials are very interesting due to their ability to convert applied strain energy into usable electric energy<sup>1</sup>. For material to be used as a sensor, the relationship between output voltage and input power should be linear, i.e., the responsivity should remain constant. And regarding the magnitude of responsivity, it may indicate the quality of the sensor, i.e. the larger the magnitude, more input signal is being converted into output signal. Samples of PZT/PVDF 30/70 vol.% without and with PAni (PZT-PAni/PVDF), previously polarized with a electric field of 5 MV/m for 15 min were characterized. A analysis of the results allows observing that the composite with polyaniline (PAni) was superior in all respects in comparison to the other composite. It can easily be observed when comparing the two composites 30/70 vol.% that PZT-PAni/PVDF presents better results<sup>2</sup>.

Fig.1. FE-SEM images of composite PZT – Pani / PVDF with PZT nanostructures synthesized by (a) Pechini method (b) hydrothermal microwave method



## Ultrathin BaTiO<sub>3</sub>/Fe bilayer obtained by Atomic Layer Deposition for magnetoelectric devices

E. Martinez-Guerra<sup>1</sup>, Paul P. Horley<sup>1</sup>

<sup>1</sup> Centro de Investigación en Materiales Avanzados (CIMAV S.C.), Chihuahua/Monterrey, 31109 Chihuahua, México.

Email: eduardo.martinez@cimav.edu.mx

Ferroelectric ultrathin BaTiO<sub>3</sub> (BTO) films in contact with Fe underlayer have been grown by Atomic Layer Deposition (ALD) on silicon substrates. In this work Ba-Ti-O films were deposited at 380 °C using Ba cyclopentadienyl precursors and titanium alkoxides. Binary reactions of Ba(<sup>t</sup>Bu<sub>3</sub>C<sub>5</sub>H<sub>2</sub>)<sub>2</sub> and H<sub>2</sub>O are first studied separately in BaO deposition and are found to result in a hydration/dehydration cycle, which is strongly influenced by temperature. Self-limiting growth of amorphous barium titanate films becomes possible when Ti(OMe)<sub>4</sub>-H<sub>2</sub>O growth cycles are mixed as well as possible with Ba(<sup>t</sup>Bu<sub>3</sub>C<sub>5</sub>H<sub>2</sub>)<sub>2</sub>-H<sub>2</sub>O cycles. The formation of Ba(OH)<sub>2</sub> is an issue for deposition of Ba-containing materials with H<sub>2</sub>O as the oxygen source, and can be severe at low temperatures. The high growth rates up to 1.0 Å/cycle in this preliminary study were most likely due to a surface hydroxide contribution to the film growth and thermal decomposition of Ti(O<sup>i</sup>Pr)<sub>4</sub>. A strong influence of water purging time was found in growth at 235 °C. The addition of titanium methoxide-water cycles is effective in stopping a BaO/(Ba(OH)<sub>2</sub>(H<sub>2</sub>O)<sub>n</sub> hydration/dehydration cycle and thus makes self-limiting growth of Ba-Ti-O films possible. Even though fairly uniform films could be grown with fixed precursor pulse lengths and sufficiently long H<sub>2</sub>O purge times, the required H<sub>2</sub>O purge time was seen to increase with longer Ba(<sup>t</sup>Bu<sub>3</sub>C<sub>5</sub>H<sub>2</sub>)<sub>2</sub> pulses, resulting in nearly doubled growth rates in the 1–5 second pulse and purge timescale often used in practical ALD. Low temperature ALD of barium-containing oxides with H<sub>2</sub>O can thus be both difficult and time consuming. The situation was improved considerably in higher temperature processing with Ti(OMe)<sub>4</sub> as the titanium source, and self-limiting conditions were found. In general it can be assumed that Ba-Ti-O growth with H<sub>2</sub>O as the oxygen source becomes easier with lower Ba content in the film and with as high as possible process temperature, as long as precursor self-decomposition is avoided. The as-deposited amorphous films are crystallized by post-deposition annealing at 700 °C. Once the BTO films were crystallized Fe films were prepared by DC-Ion Sputtering on Si/BTO substrates. Fe films were patterned to form bands by using a shadow mask. The magnetoelectric effect (ME) was measured with a variation of magnetic field up to 366.07 kA/m and superimposed by a modulation magnetic field of 0.80 kA/m. These magnetic fields were supplied by an electromagnet with a modulated Helmholtz coil and the voltage was detected by a lock-in amplifier. The ME coefficient was calculated as a variation of the electric field in response to the applied magnetic field. The effect of the modulation frequency was studied by making ME measurements at 7 different frequencies from 400 to 1000 Hz. We also study theoretically the multiferroic dynamics in a composite one-dimensional system consisting of BaTiO<sub>3</sub> multiferroically coupled to an iron chain<sup>1</sup>. These theoretical results are useful to describe multiferroic interaction at the interface.

<sup>1</sup> Paul P. Horley, "Influence of magnetoelectric coupling on electric field induced magnetization reversal in a composite unstrained multiferroic chain", PHYSICAL REVIEW B 85, 054401 (2012).

## Preparation and Energy Storage Properties of Barium Strontium Titanate Glass-Ceramic Composites via a Sol Coated Method

Qingyuan Hu<sup>1</sup>, Xiaoyong Wei<sup>1</sup>, Li Jin<sup>1</sup>

<sup>1</sup>Electronic Materials Research Laboratory, Key Laboratory of the Ministry of Education and International Center for Dielectric Research, Xi'an Jiaotong University, Xi'an 710049, China

Email: huqingyuan@stu.xjtu.edu.cn

The Ba<sub>0.6</sub>Sr<sub>0.4</sub>TiO<sub>3</sub> based glass-ceramics was successfully fabricated by a sol coated process. In this process, the nanosized Ba<sub>0.6</sub>Sr<sub>0.4</sub>TiO<sub>3</sub> (abbreviated as BST) powders prepared by sol-gel technology were dispersed into the MgO-SiO<sub>2</sub> glass-sol. The influence of the glass content on the microstructure, dielectric, and energy storage properties of this BST based glass-ceramics has been investigated. It is found that the grain size and dielectric constant of such glass-ceramics decreased with the increasing glass concentration. The average breakdown strength of samples with 4% by weight of glass additive increased dramatically, which was about 1.5 times higher than pure BST. The energy storage density was also studied, showing that the BST based glass-ceramics prepared by this sol coated method has a potential for pulse power applications.

## Fabrication and characterization of $\text{Pb}_{0.3}\text{Sr}_{0.7}\text{TiO}_3$ thin films on stainless steel by the Sol-gel method

Shengli Huang and Jinrong Cheng

School of Materials Science and Engineering, Shanghai University, Shanghai, 200072, China

Email: jrcheng@staff.shu.edu.cn

Abstract :

$\text{Pb}_{0.3}\text{Sr}_{0.7}\text{TiO}_3$  (PST) thin films were deposited on  $\text{La}_{0.5}\text{Sr}_{0.5}\text{CoO}_3$  (LSCO)-buffered stainless steel (SS) substrates. Both PST and LSCO thin films were prepared by the sol-gel method. X-ray diffraction and scanning electron microscopy analysis were used to investigate the crystallinity and surface morphology of PST thin films. It showed that the crack-free PST thin films presented pure perovskite phase. The introduction of LSCO had been found to facilitate the formation of (100) textured PST thin films. The dielectric loss and tunability of the PST thin films measured at 1MHz were 0.018 and 0.32 respectively. The figure of merit (FOM) of PST thin films reached a maximal value of 18.2. These measured properties indicate that the PST thin film is a promising candidate for tunability devices.

Keywords: PST thin films, Sol-gel method, Stainless Steel, dielectric properties, tunability



## Synthesis, Microstructural and Electrical Characterization of ZnO Nanorods Arrays Films with Different Diameter for Nanogenerators

Natiara V Madalossi<sup>1</sup>, Anderson V. Martins, Fernando A. Sigoli<sup>2</sup>, Ítalo O. Mazali<sup>2</sup>

<sup>1</sup>DMI, Centre for Information Technology Renato Archer - CTI, Campinas/Brazil

<sup>2</sup>Functional Materials Laboratory, Chemistry Institute / Universidade Estadual de Campinas, Campinas, SP/Brazil

Email: talita.mazon@cti.gov.br

Harvesting of unexploited mechanical energy to power and drive electronic or nanodevices is increasingly attracting scientific attention.<sup>1</sup> Nanoscale materials and nanotechnology could play important roles in the development of very small volume nanogenerators for self-powered electronics and nanodevices.<sup>2-5</sup> The 1 D ZnO nanostructures have been studied as nanogenerators due to excellent semiconducting and piezoelectric properties; little toxicity which makes it good for biosafe, biocompatible biomedical applications. In this work, ZnO nanorods were synthesized by chemical bath deposition (CBD).

Initially, a zinc citrate solution with viscosity range from 40 to 100 cP was deposited on Pt/Ti/SiO<sub>2</sub>/Si substrates by spin coating and heat treatment at 500 °C by 30 min, 550 °C by 4 h and 700 °C by 2 h to be used as nucleation layer.

After that, the nanorods were synthesized by CBD at 110°C by using zinc acetate and KOH with concentration 0.033 mol L<sup>-1</sup> as precursors. The ZnO nanorods were characterized by XRD and FE-SEM as structural and

microstructural properties. A series of oriented hexagonal wurtzite ZnO nanorods array films were grown on Pt/Ti/SiO<sub>2</sub>/Si substrates. The effect of the nucleation layer on the structure and diameter of ZnO nanorod array film was analyzed. It was found that the viscosity and heat treatment of the zinc citrate solution influenced on the diameter and length of the nanorods. A simple method was used for characterize the output voltage of the nanorods arrays films with different diameter. It was used a device with 8 mm<sup>2</sup> and Pt/Ti/SiO<sub>2</sub>/Si as counter electrode. It was observed that the device show a Schottky behavior from I vs V curves. The voltage measured ranged from 2 mV to 7 mV.

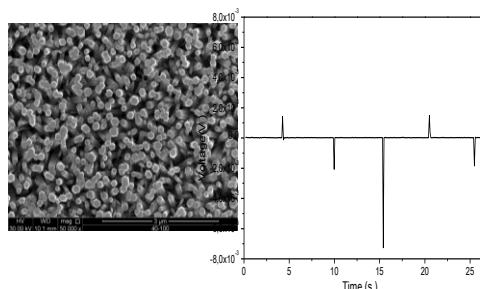


Fig. 48: ZnO nanorods array film and output voltage.

<sup>1</sup> R. S. Devan, R. A. Patil, J. Lin and Y. Ma, "One-dimensional Metal-Oxide Nanostructures: Recent Developments in Synthesis, Characterization and Applications", *Materials Views*, Vol. 22, pp. 3326-3370, 2012.

<sup>2</sup> P. X. Gao, J. H. Song and Z. L. Wang, *Advanced Materials*, Vol. 19, pp. 67-72, 2007.

<sup>3</sup> X. D. Wang, J. H. Song, J. Liu, Z. L. Wang, *Science*, Vol 316, pp. 102-105, 2007.

<sup>4</sup> M. P. Lu, J. Song, M. Y. Lu, M. T. Chen, Y. Gao, L. J. Chen, Z. L. Wang, *NanoLetteres*, Vol. 9, PP. 1223-1224, 2009.

<sup>5</sup> R. Yang, Y. Quin, C. Li, G. Zhu, Z. L. Wang, Nano Letters, Vol. 92, PP. 1201-1205, 2009.

## Multiferroic bismuth ferrite based thin films

G. Yesner, R. Rivera, L. Klein, A. Safari

Glenn Howatt Electroceramic Laboratory, Department of Materials Science and Engineering,  
Rutgers University, Piscataway, New Jersey

Email: gyesner@eden.rutgers.edu

BiFeO<sub>3</sub> (BFO) has stimulated a great interest in recent years for its multiferroic behavior and high remnant polarization at room temperature. However, high leakage current resulting from oxygen vacancies limits the practical applications of BFO films. Therefore, manganese doping is used in order to reduce leakage current. Mn-doped BFO thin films are deposited on Pt/TiO<sub>2</sub>/SiO<sub>2</sub>/Si substrate by a sol gel technique and compared with the un-doped BFO thin films.

A stoichiometric 0.2M BFO precursor solution was prepared followed by a modified sol gel and spin coating route. The nitrate raw materials were dissolved in a combination of ethylene glycol and citric acid followed by heating. Layers were deposited on the Pt/TiO<sub>2</sub>/SiO<sub>2</sub>/Si substrate and dried on a hot plate. Additional layers were deposited and dried to achieve the desired thickness of the film. Finally, the film was annealed using rapid thermal annealing (RTA). A similar process was carried out to fabricate Mn-doped BFO thin films.

The phase, microstructural, and electrical properties were investigated. The un-doped BFO sample (200nm) has unsaturated polarization with  $2P_s = 80.4 \mu\text{C}\cdot\text{cm}^{-2}$ ,  $2P_r = 33.0\mu\text{C}\cdot\text{cm}^{-2}$ , and  $2E_c = 400\text{kV}\cdot\text{cm}^{-1}$ . For the Mn-doped thin films, the leakage current is reduced by two orders of magnitude compared to un-doped samples. It is observed that the remnant polarization increases from 16.5 to  $40\mu\text{C}\cdot\text{cm}^{-2}$ . Processing will be further refined in order to improve electrical properties.

## **The effect of substitution on the synthesis and dielectric properties of lead-free KNN ceramics**

Ilze Smeltere, Maija Antonova, Anna Kalvane, Maris Livinsh

Institute of Solid State Physics University of Latvia

Email: [ilze.smeltere@cfi.lu.lv](mailto:ilze.smeltere@cfi.lu.lv)

Potassium sodium niobate (KNN) solid solutions are considered as possible alternative for the widely used PZT in some applications. However it is difficult to sinter fully dense KNN ceramic body what restricts the electrical properties. Therefore modification of ceramics has been performed:  $\text{MnO}_2$  was used as a sintering aid and partial B-site ion substitution was made. Obtained ceramics have a single phase of perovskite structure. The sintering process of alkaline niobates is characterized by forming a liquid phase which enhanced density of ceramics. For undoped KNN ceramic two sharp phase transitions are observed at  $190^\circ$  and about  $410^\circ\text{C}$ , corresponding to the phase transitions from orthorhombic to tetragonal ( $T_{O-T}$ ) and from ferroelectric tetragonal to paraelectric cubic ( $T_c$ ), respectively. After the partial substitution for  $\text{Nb}^{+5}$  both of these phase transitions are shifted to lower temperatures while increasing dielectric permittivity  $\epsilon$ .

## A piezoelectric MEMs process

J. Evans, N. Montross, G. Salazar

Radiant Technologies, Inc., Albuquerque, NM USA

Email: sframboss@ferrodevices.com

Fabricating piezoelectrically-driven micromachines (pMEMs) presents unique problems not faced by the traditional, silicon-based MEMs community. Specifically, the fabrication process for pMEMs devices requires the deposition of ceramic materials that must then be removed from certain areas of the substrate in order to complete the substrate etching and device release. When the bottom electrode is deposited globally followed by the piezoelectric or ferroelectric film, the ceramic material is prevented by the bottom electrode from reacting with the substrate surface, leaving a clean surface for deep etching by xenon difluoride or DRIE. The drawback is that this global stack of ceramic material and bottom electrode must be etched aggressively with RIE or ion-milling to remove the unnecessary materials and expose the substrate surface. A less expensive patterning approach is to use lift-off for the noble metal bottom electrode but this leaves the majority of the substrate surface exposed to the piezoelectric or ferroelectric ceramic material during high temperature annealing steps. Difficulty arises in removing the ceramic film from the surface trench areas and the scribe lanes for those devices that will self-disarticulate. Radiant uses a unique barrier layer in the field to mediate this issue. The barrier layer is deposited prior to the bottom electrode metal. Wells are etched in the barrier layer into which the bottom electrode is deposited. The barrier prevents the formation of unetchable layers under the piezoelectric or ferroelectric material where trenches or scribe lanes are to be placed. The entire stack of substrate oxide, barrier layer, and ceramic may be cleanly removed prior to surface DRIE steps. The authors will describe the technique and explain the benefits and difficulties that arise from the use of this approach in a pMEMs process flow.

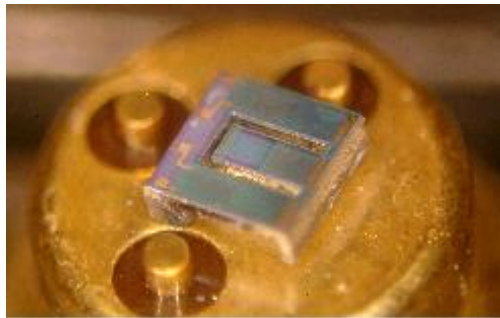


Fig. 49: ENHARVKAAL picowatt energy harvester prototype.

## Dielectric and Ferroelectric Properties of $Ba_{1-x}Sr_xTiO_3$ Ceramics Prepared by Multiple Stepped Microwave Sintering

Xusheng Wang, Yang Yu, Xi Yao

Functional Materials Research Laboratory, Tongji University, Shanghai, China

Email: xs-wang@tongji.edu.cn

Microwave sintering technique, compared with conventional sintering technique, has received considerable attention in ceramic preparation for its short time duration, uniform heating and low temperature in sintering process, in which the heat is generated internally within the material through microwave-material interaction instead of originating from external sources. Therefore, the material heated uniformly as the microwave-material interaction occurred from the inside to outside simultaneously rather than energy transfer from the outside to the inside. Here we report our result on dielectric and ferroelectric properties of  $Ba_{1-x}Sr_xTiO_3$  ceramics prepared by multiple stepped microwave sintering.

$BaTiO_3$  (99.9%, 100 nm) and  $SrTiO_3$  (99.9%, 100 nm) powders were used as raw materials.  $Ba_{1-x}Sr_xTiO_3$  powders were prepared by conventional ceramic technique, in which the powders were pre-fired at  $800^\circ C$  for 2 h. Then milled, mixed with PVA and pressed to pellet of 10 mm in diameter and 1 mm in thickness. The schematic diagram of the multiple stepped sintering is shown in Fig.1. The heating rate is about  $10^\circ C/min$  and the total sintering dwelling time kept to 60 min. The up temperature of the heating pulse is  $1200^\circ C$  and low temperature is  $800^\circ C$ . Multiple heating steps were chosen as 1\*60 min, 2\*30 min, 3\*20 min, 6\*10 min and 12\*5 min, respectively.

Figure 2 showed the dielectric comparison of the multiple stepped microwave sintering for a typical composition of  $Ba_{0.9}Sr_{0.1}TiO_3$  ceramics.

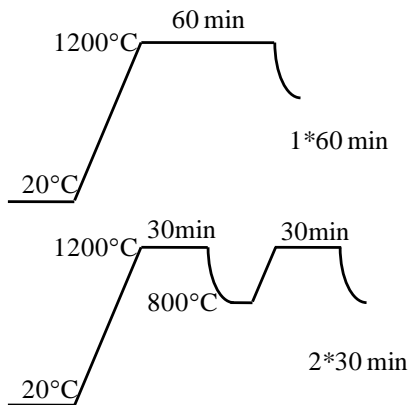


Figure 1 Schematic diagram of the multiple stepped microwave sintering

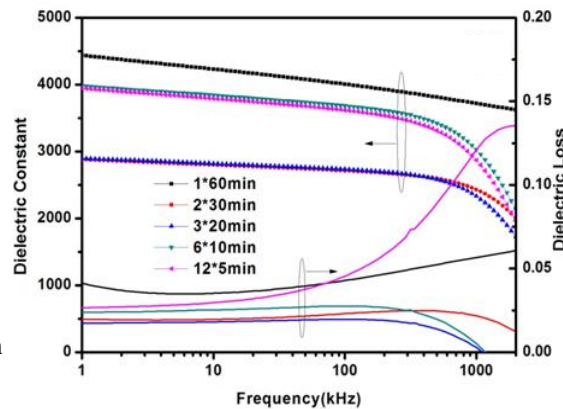


Figure 2 Frequency dependence of the dielectric properties for  $Ba_{0.9}Sr_{0.1}TiO_3$  ceramics prepared by different steps

## Growth of plate- and tube-shaped langasite-type $\text{Ca}_3\text{NbGa}_3\text{Si}_2\text{O}_{14}$ piezoelectric crystals and the properties

Yuui Yokota<sup>1</sup>, Shunsuke Kurosawa<sup>1,2</sup>, Andrey Medvedev<sup>1</sup>, Masato Sato<sup>3</sup>, Kazushige Tota<sup>3</sup>, Ko Onodera<sup>1,3</sup>, Akira Yoshikawa<sup>1,2,4</sup>

<sup>1</sup>Institute for Materials Research, Tohoku University, Sendai, Japan

<sup>2</sup>New industry creation hatchery center (NICHe), Tohoku University, Sendai, Japan

<sup>3</sup>TDK corporation, Nikaho, Japan

<sup>4</sup>C&A corporation, Sendai, Japan

Email: yokota@imr.tohoku.ac.jp

The langasite-type piezoelectric single crystals with no phase transition up to the melting points have been investigated for the applications which can be used at high temperature such as a combustion sensor. However, the manufacturing cost of the element in the combustion sensor is so high that the combustion sensor hasn't been spread in the market yet. Therefore, we have developed the growth technique of shape-controlled single crystals by the micro-pulling-down ( $\mu$ -PD) method to reduce the cost of cutting and polishing processes from the bulk crystal<sup>183</sup>. In addition, crystal growth and the physical properties of columnar-shaped langasite-type single crystals were investigated<sup>184</sup>. In this study, the plate- and tube-shaped  $\text{Ca}_3\text{NbGa}_3\text{Si}_2\text{O}_{14}$  [CNGS] single crystals were grown by the  $\mu$ -PD method and their physical properties were investigated.

Starting materials were mixed as a nominal composition,  $\text{Ca}_3\text{NbGa}_3\text{Si}_2\text{O}_{14}$ , and the mixed powder was sintered at 1200°C in air. Sintered powder was set in the Pt-Rh crucible with a special-shaped die at the bottom. For growths of shaped CNGS crystals, the crucibles with square- and tube-shape dies were used, respectively. The crucible was heated by the high-frequency induction coil.

After the crucible and sintered powder in the crucible reached the melting point of CNGS, the seed crystal with  $a$ -axis crystal orientation along to the growth direction was touched the bottom of the die (Fig.2(a)). The meniscus on the bottom of the die gradually expanded with pulling-down the seed crystal and finally the meniscus covered the full-area of the bottom of the die (Fig.2(b)). Then the tube-shaped CNGS crystal was grown continuously and the obtained tube-shaped CNGS crystal is shown in Fig.2(c). Crystal growth, crystallinity, chemical composition and piezoelectric properties of plate- and tube-shaped CNGS single crystals will be reported.

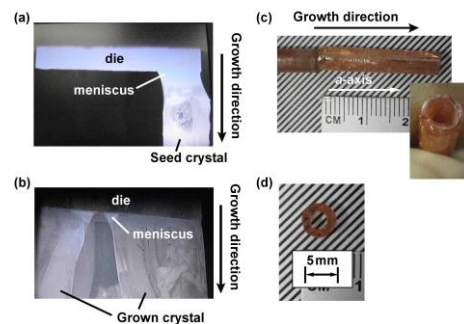


Fig. 50: Liquid-solid interface (a) when the seed crystal touched the bottom of die and (b) the grown crystal became tube-shape. (c) The as-grown and (d) polished tube-shaped CNGS crystals.

<sup>183</sup> Y. Yokota, A. Yoshikawa, *et.al.*, "Growth and crystallinity of shaped and multiple sapphire crystals by a micro-pulling-down method", *J. Cryst. Growth*, vol. 318, p. 983-986, 2011.

<sup>184</sup> Y. Yokota, A. Yoshikawa, *et.al.*, "Growth of Shape-Controlled  $\text{Ca}_3\text{NbGa}_3\text{Si}_2\text{O}_{14}$  and  $\text{Sr}_3\text{NbGa}_3\text{Si}_2\text{O}_{14}$  Single Crystals by Micro-Pulling-Down Method and Their Physical Properties", *Jpn. J. Appl. Phys.*, vol. 50, 09ND03, 2011.

## Growth and piezoelectric properties of PMN-PT crystal grown by micro-pulling-down method

Yuui Yokota<sup>1</sup>, Shunsuke Kurosawa<sup>1,2</sup>, Andrey Medvedev<sup>1</sup>, Akira Yoshikawa<sup>1,2,3</sup>

<sup>1</sup>Institute of Materials Research, Tohoku University, Sendai, Japan

<sup>2</sup>New industry creation hatchery center (NICHe), Tohoku University, Sendai, Japan

<sup>3</sup>C&A corporation, Sendai, Japan

Email: yokota@imr.tohoku.ac.jp

The  $(1-x)\text{PbMg}_{1/3}\text{Nb}_{2/3}\text{O}_3-x\text{PbTiO}_3$  [(1-x)PMN-xPT] and  $(1-x)\text{PbZn}_{1/3}\text{Nb}_{2/3}\text{O}_3-x\text{PbTiO}_3$  [(1-x)PZN-xPT] crystals with the greatly high dielectric and piezoelectric constants have been expected to be applied for some high-performance piezoelectric devices such as medical ultrasound imaging probes, Sonars for underwater communications, high-sensitivity sensors and actuators. However, it is difficult to grow the single crystals with high uniformity due to the strong segregation in the grown crystal and complex composition. Therefore, the PMN-PT crystal grown by Bridgmann method has the inhomogeneity of chemical compositions in the crystal and it decreases the yield ratio of bulk crystals<sup>185</sup>. On the other hand, we have developed the shape-controlled piezoelectric single crystals using the micro-pulling-down ( $\mu$ -PD) method<sup>186</sup>. The crystal growth of the shape-controlled single crystals by the  $\mu$ -PD method can reduce the cost of manufacturing for the langasite-type single crystals by the decrease of forming process. In this study, the shape-controlled PMN-PT crystals were grown by the  $\mu$ -PD method and the structural and piezoelectric properties of PMN-PT crystal were evaluated.

Starting materials, PbO, MgO, Nb<sub>2</sub>O<sub>5</sub>, TiO<sub>2</sub> powders (>3N purity) were mixed as the nominal composition,  $0.65\text{PbMg}_{1/3}\text{Nb}_{2/3}\text{O}_3-0.35\text{PbTiO}_3$  and mixed powder was set in the Pt-Rh crucible which had a 3 mm $\phi$  die at the bottom with 5 holes. The crucible was heated in air by the high-frequency induction coil up to the melting point of PMN-PT. After the powders were molten in the crucible, the melt came out to the bottom of crucible from the inside. The melt was pulled down by the Pt wire at 0.03 growth rate.

PMN-PT crystal grown by the  $\mu$ -PD method is shown in Fig.1(a). The crystal had the approximately 3 mm diameter and 10 mm length. The diameter of the crystal could be almost controlled by the 3 mm $\phi$  die of crucible. The crystal was cut perpendicular to the growth direction and cut planes were polished (Fig.1(b)). The center part of the crystal indicated transparency and the part are considered to be a single crystal of PMN-PT. On the other hand, the

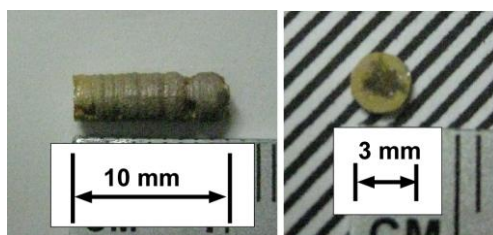


Fig. 51: (a) PMN-PT crystal grown by  $\mu$ -PD method. (b) Cut and polished PMN-PT crystal.

<sup>185</sup> G. Xu, *et al.*, "Growth and piezoelectric properties of  $\text{PbMg}_{1/3}\text{Nb}_{2/3}\text{O}_3\text{-PbTiO}_3$  crystals by the modified Bridgeman technique", *Solid State Commun.* vol. 120, p. 321-324, 2001.

<sup>186</sup> Y. Yokota, A. Yoshikawa, *et al.*, "Shaped crystal growth of langasite-type piezoelectric single crystals and their physical properties", *IEEE Trans. Ultrason. Ferroelectrics. Freq. Contr.*, vol. 59, p. 1868-1871, 2012.



periphery part had no transparency and the result is due to the evaporation of PbO during crystal growth. Other crystal growth and properties of grown crystals will be reported.

## **Electromechanical displacement of soft/hard PZT bi-layer composite actuator**

Piyalak Ngerchuklin<sup>1</sup>, C. Jeerapan<sup>1</sup>, C. Eamchotchawalit<sup>1</sup>

<sup>1</sup> Materials Innovation, Thailand institute of scientific and technological research (TISTR),  
Klong Luang, Pathum Thani, 12120, Thailand

Email: [piyalak@tistr.or.th](mailto:piyalak@tistr.or.th)

Lead Zirconate Titanate (PZT) is a well-known piezoelectric material which has been widely used for transducer, sensor and actuator applications. According to the compositional modifications near morphotropic phase boundary, PZTs can be classified into two types, soft PZT and hard PZT, which are distinguished by the piezoelectric properties. Therefore, the combination effect of the strain-E-field response of soft/hard PZT composite actuator has been much interested to be observed. In this study, soft and hard PZT powders were co-pressed into bi-layer disks with various ratios of soft PZT powder, ranging from 0-100 vol. % (with 10 % increments) and then co-sintering. Due to the shrinkage rate difference of the two layers, the bi-layer composites with various dome heights were obtained. Moreover, it was shown that the constrained layer either soft PZT or hard PZT affected to the dome geometry, the strain-E-field response and displacement hysteresis loop. The electromechanical properties and actuation performance of such bi-layer composite actuators have been investigated and compared to the soft and hard PZT single layer counterparts.

Keywords : soft PZT, hard PZT, bi-layer composite, actuator

## Polyol-based synthesis of high quality lead zirconate titanate nanostructured thin films

A.Nourmohammadi<sup>1</sup>, M. Khosravi<sup>2</sup>, E. Bahremandi<sup>3\*</sup>

<sup>1</sup> Department of Nanotechnology, Faculty of Advanced Science and Technologies, University of Isfahan, 81746-73441, Isfahan, I. R. Iran

<sup>2</sup> Department of Nanotechnology, Faculty of Advanced Science and Technologies, University of Isfahan, 81746-73441, Isfahan, I. R. Iran

<sup>3</sup> Department of Physics, Islamic Azad University, Central Tehran Branch, 14837-69444, Tehran, I.R. Iran  
Email: abolghasem.nourmohammadi@gmail.com

\*Email: e.bahremandi@yahoo.com

Nanostructured piezoelectric oxide thin films are suitable two-dimensional materials for the fabrication of many functional nanodevices such as nanosensors, nanoactuators and nano-electromechanical systems (NEMS). Lead zirconate titanate (PZT), with the perovskite structure, is a suitable ferroelectric and piezoelectric ceramic material for these applications because it has high spontaneous polarization, dielectric permittivity and piezoelectric coefficients. Therefore, much effort has already been devoted to improve the quality of PZT thin films.

PZT thin films have already been synthesized by the alkoxide based sol-gel technique using the hydrolysis and condensation of these precursors. However, alkoxide-based PZT sols are almost unstable because they contain water which lowers their storage time. This prevents longtime storage of the prepared PZT sols. Besides, successful crystallization of the perovskite phase from the annealed alkoxide-based PZT gels requires heat treatment above 650°C which alters the PbO stoichiometry of the film due to evaporation.

Here, high quality single phase PZT thin films were synthesized via a polyol-based sol-gel process. It was shown that single perovskite phase PZT thin films can be effectively produced using the polyol-based PZT sols at 590°C. Polyol-based process is a cost-effective synthesis method for the fabrication of PZT thin films because chloride precursors of titanium and zirconium are used. In addition, polyol-based sols are highly stable for a very long time of storage. However, this process is not extensively investigated, and only one report is available on the successful fabrication of PZT thin films using this method<sup>xxiii</sup>.

The prepared PZT thin films were deposited on Au/SiO<sub>2</sub> substrates to fabricate high quality PZT thin films. The films were built up with multiple spin-coating. Each coating step was followed by pyrolysis at 450°C, and the produced multilayered thin film was annealed at 590°C. X-ray diffraction, XRD, investigations confirmed formation of perovskite PZT thin films. Scanning electron microscopy, SEM, investigations indicated that high quality and crack free thin films have been obtained (Fig 1).

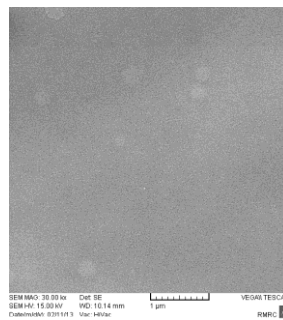


Fig1.SEM micrograph of a PZT thin film.

<sup>1</sup>Q.Zou" Novel polyol-derived sol route for fabrication of PZT thin ferroelectric films" Mat. Lett. 40(1999)240-245.

## UV laser-induced poling inhibition in proton exchanged optical waveguides in lithium niobate

G. Zisis<sup>1</sup>, M. Manzo<sup>2</sup>, K. Gallo<sup>2</sup>, T. Limböck<sup>3</sup>, E. Soergel<sup>3</sup>, S. Mailis<sup>1</sup>

<sup>1</sup>Optoelectronics Research Centre, University of Southampton, Southampton, SO17 1BJ, U.K.

<sup>2</sup>KTH, Applied Physics, SE-106 91 Stockholm, Sweden

<sup>3</sup>Institute of Physics, University of Bonn, Wegelerstrasse 8, 53115 Bonn, Germany

Email: soergel@uni-bonn.de

UV laser irradiation of the +z polar face of congruent and MgO doped lithium niobate crystals has been observed to inhibit ferroelectric domain inversion when the crystal subsequently undergoes uniform electric field poling at room temperature.<sup>187</sup> The UV laser-induced poling inhibition (PI) produces ferroelectric domain structures, which correspond to the UV laser-irradiated tracks and which have sufficient depth (a few  $\mu\text{m}$ ) to overlap with waveguide modes.<sup>188</sup> A common procedure for the fabrication of optical waveguides in lithium niobate is proton exchange followed by an annealing step.<sup>189</sup> Such waveguides are known as annealed proton exchanged (APE) waveguides.

Here we report preliminary results, which show that PI is applicable to APE wave-guides thus enabling the use of this method for the production of nonlinear optical waveguide devices. We therefore utilized a graded-index APE waveguide with a 1/e-depth of  $\sim 2.2 \mu\text{m}$ .

The existence of PI domains in the APE waveguides was given by piezoresponse force microscopy (PFM). Further evidence for the presence of PI domains in this material system were provided by wedge polishing at an oblique angle ( $\sim 5$  degrees) with respect to the surface, followed by brief etching in an HF acid solution. Wedge polishing offers in addition a detailed view of the depth profile because of a x10 stretching factor which corresponds to a slope of  $5^\circ$ .

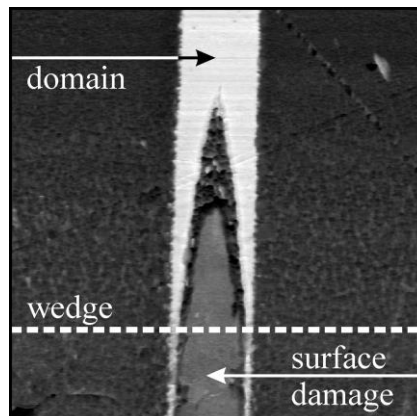


Fig. 52: PFM scan of a PI domain obtained on an APE waveguide. The sample was wedge-polished. Image size:  $30\mu\text{m} \times 30\mu\text{m}$

<sup>187</sup> C. L. Sones, A. C. Muir, Y. J. Ying, S. Mailis, R. W. Eason, T. Jungk, A. Hoffmann, E. Soergel, "Precision nanoscale domain engineering of lithium niobate via UV laser induced inhibition of poling" *Appl. Phys. Lett.*, vol. 92, 072905, 2008.

<sup>188</sup> H. Steigerwald, M. Lilienblum, F. von Cube, Y. J. Ying, R. W. Eason, S. Mailis, B. Sturman, E. Soergel, K. Buse, "Origin of UV-induced poling inhibition in lithium niobate crystals" *Phys. Rev. B*, vol. 82, p. 214105, 2010

<sup>189</sup> K. Gallo, C. B. E. Gawith, I. T. Wellington, S. Mailis, R. W. Eason, P. G. R. Smith, D. J. Richardson, and S. M. Kostritskii, "UV-written channel waveguides in proton-exchanged  $\text{LiNbO}_3$ ", *J. Appl. Phys.*, vol. 101, 14110, 2007

The ability to obtain PI domain structures in proton exchanged waveguides in lithium niobate opens the way for the utilization of this method for the fabrication of nonlinear, electro-optic and acousto-optic devices in lithium niobate.

## Adsorption Controlled MOCVD Growth of Bismuth Ferrite Thin Films

**Nitin Deepak<sup>1,2</sup>, Lynette Keeney<sup>1</sup>, Martyn E. Pemble<sup>1,2</sup> and Roger W. Whatmore<sup>1,2</sup>**

<sup>1</sup>*Tyndall National Institute, University College Cork, 'Lee Maltings', Dyke Parade, Cork, Ireland*

<sup>2</sup>*Department of Chemistry, University College Cork, Dyke Parade, Cork, Ireland*

*Email: [nitin.deepak@tyndall.ie](mailto:nitin.deepak@tyndall.ie)*

Bismuth ferrite (BiFeO<sub>3</sub>) is one of the most widely studied materials due to its interesting multiferroic properties<sup>1</sup>. The growth of BiFeO<sub>3</sub> by chemical vapour deposition (CVD) proves to be a unique challenge due to the interesting chemistry that happens during the growth. The growth window regarding temperature, pressure and precursor flow rates for pure BiFeO<sub>3</sub> phase is very small<sup>2</sup>, making the controlled growth of BiFeO<sub>3</sub> rather difficult.

In this present work we studied the metalorganic CVD (MOCVD) growth of epitaxial BiFeO<sub>3</sub> thin films on SrTiO<sub>3</sub> substrates and found that by carefully controlling the amount of the iron precursor, Fe(thd)<sub>3</sub>, where thd = 2,2,6,6 tetramethyl 3,5 heptanedionate, we were able to achieve adsorption controlled growth. Adsorption controlled growth of BiFeO<sub>3</sub> has been previously achieved using molecular beam epitaxy (MBE)<sup>3</sup> but to the best of our knowledge our work represents the first example of adsorption controlled growth of BiFeO<sub>3</sub> by MOCVD. The effect of the volume of the precursor injected on the growth of BiFeO<sub>3</sub> thin films is studied. Detailed x-ray diffraction (XRD) and transmission electron microscopy (TEM) studies are presented.

### References:

1. J. Wang, J. B. Neaton, H. Zheng, V. Nagarajan, S. B. Ogale, B. Liu, D. Viehland, V. Vaithyanathan, D. G. Schlom, U. V. Waghmare, N. A. Spaldin, K. M. Rabe, M. Wuttig and R. Ramesh, *Science* **299**, 1719 (2003).
2. S. Y. Yang, F. Zavaliche, L. Mohaddes-Ardabili, V. Vaithyanathan, D. G. Schlom, Y. J. Lee, Y. H. Chu, M. P. Cruz, Q. Zhan, T. Zhao and R. Ramesh, *Applied Physics Letters* **87**, 102903 (2005).
3. J. F. Ihlefeld, A. Kumar, V. Gopalan, D. G. Schlom, Y. B. Chen, X. Q. Pan, T. Heeg, J. Schubert, X. Ke, P. Schiffer, J. Orenstein, L. W. Martin, Y. H. Chu and R. Ramesh, *Applied Physics Letters* **91**, 071922 (2007).

## Functional properties of lead-free perovskite ( $\text{Na}_{0.5}\text{Bi}_{0.5}\text{TiO}_3$ ) $_{1-x}$ - ( $\text{BaTiO}_3$ ) $_x$ thin films

N. D. Scarisoreanu<sup>1</sup>, F. Craciun<sup>2</sup>, A. Andrei<sup>1</sup>, R. Birjega<sup>1</sup>, C. Galassi<sup>3</sup>, M. Dinescu<sup>1</sup>.

<sup>1</sup>NILPRP, Bucharest, Romania

<sup>2</sup>CNR-Istituto dei Sistemi Complessi, Rome, Italy

<sup>3</sup>CNR-ISTEC, Faenza, Italy

Email: dinescum@nipne.ro

The solid solution of ( $\text{Na}_{0.5}\text{Bi}_{0.5}\text{TiO}_3$ ) $_{1-x}$  - ( $\text{BaTiO}_3$ ) $_x$  is considered to be among the best candidate lead-free ferroelectric and piezoelectric material for applications as actuators and nonvolatile memory devices. The lead-free perovskite ( $\text{Na}_{0.5}\text{Bi}_{0.5}\text{TiO}_3$ ) $_{1-x}$  - ( $\text{BaTiO}_3$ ) $_x$  (NBT-BT) has a morphotropic phase boundary (MPB) between the rhombohedral and tetragonal phase ( $x = 0.06 - 0.07$ ), for which the dielectric, piezoelectric and ferroelectric properties of the material are considerably enhanced.

In this study, we have investigated the role of the BT amount on the crystalline structure, microstructure, dielectric properties, phase transition temperatures and stability limits of ferroelectric phases in NBT-BT thin films grown by pulsed laser deposition. Successful growth of NBT-BT films on platinumized silicon substrates has been achieved, the dielectric and piezoelectric properties of the films being comparable with bulk values. For example, the NBT-BT ( $x=0.06$ ) thin films show a classic switching behavior, the locally measured value of effective piezoelectric coefficient  $d_{33}^{\text{eff}}$  was 83 pm/V, which is higher than the previously reported values for pure NBT or several (more used) lead-based thin films. An enhanced stability of ferroelectric phase in thin films with respect to bulk has been observed and explained by their peculiar microstructure.

## Effects of TiO<sub>2</sub> addition on microstructure and dielectric properties of phase-mixed BST ceramics

Lixin Zhou, Dengren Jin, Jinrong Cheng, Hanting Dong, Chaojun Xie

(School of Materials Science and Engineering, Shanghai University, 200072)

**Abstract:** The effects of TiO<sub>2</sub> addition on dielectric temperature stability of the phase-mixed BST ceramics were investigated. These non-uniform phase-mixed BST ceramics were synthesized by a modified solid-state reaction. TiO<sub>2</sub> was introduced by the following ways: the TiO<sub>2</sub> powders were mixed with BT and ST powders (MixTi), and the TiO<sub>2</sub> were proportionally introduced during the calcining of BT and ST powders respectively (CalTi). The phase structures and microstructures of these ceramics were characterized by XRD and SEM, respectively. The compositional gradients were also examined by EDS and XRD. The Curie peak of MixTi is the lowest and widest, and MixTi has the best temperature stability, but the normal phase-mixed BST has much higher and more narrow Curie peak. MixTi also have high tunability more than 30% (1kV/mm, 100kHz). When TiO<sub>2</sub> was introduced during the calcination of ST, the BST has high and narrow Curie peak, and the temperature stability becomes worse. The surface SEM micrographs of these ceramics exhibit that, the grain size of MixTi is obviously smaller than the normal phase-mixed BST. In conclusion, the addition of TiO<sub>2</sub> can improve the thermal stability of BST, and sintering routine, such as sintering temperature and holding duration can change the properties of the Ti-excess BST. MixTi has better temperature stability, one reason probably is that TiO<sub>2</sub> can defer the diffusion of Ba<sup>2+</sup> and Sr<sup>2+</sup>, and their compositional gradients is maintained, and the grain size may be another cause. Different properties by various ways of TiO<sub>2</sub> addition may be mainly caused by the region of Ti-excess. Ti-excess region may exist at the grain boundary of BT, while most Ti-excess region may grow in the grain of ST. The mechanism of TiO<sub>2</sub> addition's effects on the temperatures stability and microstructures of the phase-mixed BST were investigated, respectively.

**Key words:** Ti-excess, (Ba,Sr)TiO<sub>3</sub>, phase-mixed, dielectric properties, temperature stability, microwave tunable



## RF Magnetron Sputtered $\text{Pb}(\text{Zr}_{0.52}\text{Ti}_{0.48})\text{O}_3$ (PZT) Thin Films on Flexible Copper Substrates

Joel Walenza-Slabe<sup>1</sup>, Troy Ansell<sup>1</sup>, David P. Cann<sup>1</sup>, and Brady J. Gibbons<sup>1</sup>

<sup>1</sup>Materials Science, School of Mechanical, Industrial, & Manufacturing Engineering, Oregon State University, Corvallis, OR 97331 (USA)

Email: brady.gibbons@oregonstate.edu

Lead zirconate titanate (PZT) thin films on copper foils were produced using RF magnetron sputtering and *ex situ* annealing in controlled atmospheres. The crystallization environment was best controlled by the combination of a forming gas atmosphere and use of a copper foil envelope, which buffered the oxygen partial pressure during heating and cooling. Films with low loss tangent (<5%) were produced with dielectric constants of  $\approx 500$ -700. No interfacial layer was detected in cross-sectional SEM imaging (see Fig. 1), however there was a second phase observed on the surface. Spin casting and annealing a PbO sol-gel layer on the surface was found to eliminate this second phase. The remanent polarization was 20-35  $\mu\text{C}/\text{cm}^2$ . The linear Rayleigh behavior, characterizing the sub-switching AC field response of the domain walls, was determined. An analysis of the hysteresis according to the Preisach formalism is also presented. The irreversible components of the dielectric constant and hysteresis are compared across films of varying thickness and processing conditions. Finally, cantilever energy harvesters were fabricated and tested. The device output as a function of frequency was compared with a model based on the Euler-Bernoulli beam equations. The resonant frequencies of the cantilevers, 20-40 Hz, were found to match the model well. Modeled peak-to-peak voltage was highly dependent on material parameters but typical values gave an expected output of 10-40 mV, which match the observed values well.

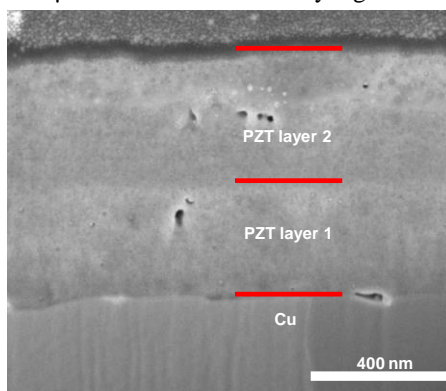


Figure 53: Cross-sectional image of a 2 layer PZT thin film deposited by rf magnetron sputtering on a flexible Cu foil substrate.

## Pulsed Laser Deposition of Epitaxial Piezoelectric Thin Films on Flexible Substrates

Ashley D. Mason<sup>1</sup>, Dylan R. Kearney<sup>1</sup>, and Brady J. Gibbons<sup>1</sup>

<sup>1</sup>Materials Science, School of Mechanical, Industrial, & Manufacturing Engineering,  
Oregon State University, Corvallis, OR 97331 (USA)

Email: masona@enr.orst.edu

Piezoelectrics transduce mechanical strain into a dielectric displacement as well as the converse, allowing these materials to be used as sensors, actuators, and transducers. Currently lead zirconate titanate (PZT) is the primary material used in these applications. The strong performance of PZT as a piezoelectric material can be associated with the existence of a morphotropic phase boundary (MPB).

In addition to maintaining compositions close to the MPB, the piezoelectric response of PZT can be improved by controlling the crystallographic texture of the film. Specifically, {100}-oriented films are known to exhibit a larger piezoelectric response than {111}-oriented films<sup>190</sup>. The nucleation and growth process of the film can be manipulated to achieve a desired orientation. On a single crystal substrate with appropriate lattice match, PZT almost inevitably grows in the same orientation as the template<sup>191</sup>. In this work, Ion Beam Assisted Deposition (IBAD) of biaxially textured MgO on a flexible substrate was utilized to integrate the enhanced piezoelectric properties of epitaxial PZT with a technically relevant, inexpensive, and flexible substrate. Pulsed laser deposition (PLD) was used to deposit the bottom electrode and PZT thin films; the complete device structure is shown in Fig. 1.

Additionally, development of an environmentally friendly, Pb-free, alternative material with properties comparable to that of PZT is also desirable. The same templating and device structure was used to study the properties of epitaxial Pb-free materials also deposited using PLD. The goal is to understand how crystallographic orientation impacts the piezoelectric properties of these thin films; based on  $(\text{Bi}_{0.5}\text{Na}_{0.5})\text{TiO}_3 - (\text{Bi}_{0.5}\text{K}_{0.5})\text{TiO}_3$  (BNT-BKT).

The structure and morphology of the deposited films were analyzed with x-ray diffraction (XRD) and atomic force microscopy (AFM). Piezoelectric properties are characterized at both the macro-

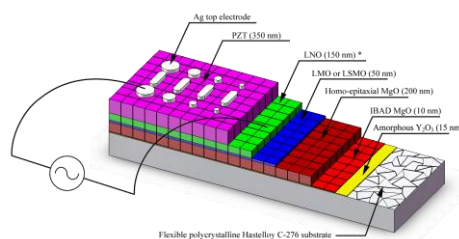


Fig. 54: Device structure. LNO is deposited on top of LSMO to increase the thickness of the bottom electrode prior to the addition of PZT. Evaporated Ag is used as a top electrode.

<sup>190</sup> X. Du, J. Zheng, U. Belegundu and K. Uchino, "Crystal orientation dependence of piezoelectric properties of lead zirconate titanate near the morphotropic phase boundary," *Applied Physics Letters*, vol. 72, pp. 2421-2423, 1998.

<sup>191</sup> P. Verardi, F. Craciun, M. Dinescu and C. Gerardi, "Epitaxial Piezoelectric PZT Thin Films Obtained by Pulsed Laser Deposition," *Thin Solid Films*, vol. 318, pp. 265-269, 1998.

and microscopic levels, using double beam laser interferometry and piezoresponse force microscopy (PFM). Ongoing work will be presented.

---

## THE STRUCTURE AND DIELECTRIC PROPERTIES OF BISMUTH-NICKEL-NIOBIUM OXIDE BASED CERAMICS

Xiukai Cai<sup>1</sup>, Mingying Lv<sup>1</sup>, Yun Su<sup>2</sup>

<sup>1</sup>School of Civil Engineering, Shandong Jianzhu University, Fengming Road, Lingang Development Zone, Ji'nan, 250100, China

<sup>2</sup>Department of Physics and Electronic Engineering, Hanshan Normal University, Eastern Bridge, Chaozhou 521041, China

Email: [xkcai@sdjzu.edu.cn](mailto:xkcai@sdjzu.edu.cn)

A large number of bismuth nickel niobate based dielectric ceramics have been prepared by conventional solid state reaction technique. The structure and dielectric properties of this ternary oxide system have been investigated by X-ray diffraction analysis and temperature dependences of dielectric constant and loss factor measured at a wide range of frequencies (100 Hz to 100 KHz). The structure of compounds around the batch of  $\text{Bi}_2\text{O}_3:\text{NiO}:\text{Nb}_2\text{O}_5=1:1:1$  is cubic pyrochlore, while departed from this composition there exist at least two phases, including cubic pyrochlore phase, impurities and some other phases. A low temperature dielectric relaxation peak in most compositions can be detected close to the liquid nitrogen temperatures, with the activation energy being of the order of 0.30 eV. Moreover, there also exists another high temperature dielectric loss peak for some samples, with the estimated activation energy of approximately 0.70 eV, which is attributed to the conduction process arisen from the impurities and/or the defect structure phases.

## ROLE OF TiO<sub>2</sub> AND WO<sub>3</sub> IN IMPROVING THE PROCESSING BEHAVIOURS OF BISMUTH-BASED CERAMICS

Yun Su<sup>1</sup>, Xiukai Cai<sup>2</sup>, Mingying Lv<sup>2</sup>

<sup>1</sup>Department of Physics and Electronic Engineering, Hanshan Normal University, Eastern Han River Bridge, Chaozhou 521041, China

<sup>2</sup>School of Civil Engineering, Shandong Jianzhu University, Fengming Road, Lingang Development Zone, Ji'nan, 250100, China

Email: syu@hstc.edu.cn

At least two compositions in the bismuth zinc niobate ternary oxide system, with different ratio of the amounts of pyrochlore structure phase in the finished ceramics, were chosen as base composition used for the TiO<sub>2</sub>, WO<sub>3</sub> adding trials. The processing behavior, especially the sinterability of the bismuth-based ceramics can be dramatically improved with the aids of the addition of both constitutions. The results of linear shrinkage and relative density measurements and the direct SEM observation make it clear that the densification process can be easily accomplished, with the sintering temperature lowered and the microstructure of the resultant ceramics finer and more uniform. At the same time the phase compositions for the TiO<sub>2</sub>, WO<sub>3</sub> doping compositions, i.e. the bismuth zinc niobate cubic pyrochlores, can be maintained. Further electron probe analyses demonstrate the distribution of Ti and W in the microstructures of ceramics, and a possible doping mechanism can be suggested.

## Synthesis and Characterization of Piezo-/Ferroelectric Bi(Zn<sub>1/2</sub>Ti<sub>1/2</sub>)O<sub>3</sub>-PbZrO<sub>3</sub>-PbTiO<sub>3</sub> Solid Solution

Bixia Wang, Yujuan Xie, Nan Zhang, Zuo-Guang Ye

Department of Chemistry and 4D LABS, Simon Fraser University,  
Burnaby, BC, V5A 1S6, Canada

Email: zye@sfu.ca

Pb(Zr,Ti)O<sub>3</sub> (PZT) ceramics are the most extensively used piezoelectric materials owing to its high Curie temperature ( $T_c \sim 350^\circ\text{C}$ ) and good piezoelectric and electromechanical properties near the morphotropic phase boundary (MPB). Recently, Bi-based perovskite solid solutions such as PbTiO<sub>3</sub>-BiFeO<sub>3</sub>, PbTiO<sub>3</sub>-BiScO<sub>3</sub> and PbTiO<sub>3</sub>-Bi(Mg,Ti)O<sub>3</sub> were investigated due to their large polarization and multiferroic properties. Bi<sup>3+</sup> ion possesses a similar electron configuration (6s<sup>2</sup> lone pair) to that of Pb<sup>2+</sup>, which can enhance polarization in the perovskite lattice. Among the Bi-based systems, (1-x)Bi(Zn<sub>1/2</sub>Ti<sub>1/2</sub>)O<sub>3</sub>-xPbTiO<sub>3</sub> (BZT-PT) with  $x \leq 0.4$  presents a significant increase in  $T_c$  ( $\approx 700^\circ\text{C}$ ) and tetragonality ( $c/a=1.11$ ) [1]. Our recent study [2] shows that adding BZT into PZT forms the ternary solid solution: Bi(Zn<sub>1/2</sub>Ti<sub>1/2</sub>)O<sub>3</sub>-PbZrO<sub>3</sub>-PbTiO<sub>3</sub> [BZT-PZ-PT], in which enhanced dielectric and ferroelectric and properties are found in the MPB compositions.

In this work, ternary ceramics of the BZT-PZ-PT ternary system are synthesized by solid state reactions and investigated by x-ray diffraction, dielectric spectroscopy, ferroelectric and piezoelectric measurements. Studies are focused on three series of compounds, 0.05BZT-0.095PZT, 0.1BZT-0.9PZT and 0.15BZT-0.85PZT, which have the compositions around the MPB with varying Zr/Ti ratio. It is found that the introduction of BZT into the PZT system makes the paraelectric to ferroelectric phase transition more diffuse, brings the MPB to a lower PT content and enlarges the binary MPB region of PZT. The maximum dielectric constant  $\epsilon' = 1490$  is found in the 0.1BZT-0.9PZT series. Enhanced ferroelectric and piezoelectric properties are found in the MPB region of the 0.15BZT-0.85PZT series, with  $P_r = 35 \mu\text{C}/\text{cm}^2$  and  $d_{33} = 275 \text{ pC}/\text{N}$ .

On the other hand, single crystals of BZT-PZ-PT have been grown by a high temperature solution method. The grown crystals exhibit a cubic morphology with light yellow colour. Structure analysis shows the coexistence of rhombohedral and tetragonal phases in the crystals, which is confirmed by the domain structure observed by polarized light microscopy, indicating that the composition of the crystals falls into the MPB region. The birefringence measurement of the rhombohedral phase indicates a phase transition from ferroelectric to paraelectric phase upon heating. The Curie temperature is found to be  $T_c = 300^\circ\text{C}$  by dielectric measurements. A remanent polarization  $P_r$  of  $24.6 \mu\text{C}/\text{cm}^2$  is displayed with a coercive field  $E_c$  of  $14.5 \text{ kV}/\text{cm}$ .

These results show that the BZT-PZ-PT system could be promising piezo-/ferroelectric materials for high-power electromechanical transducers that can operate in a wide temperature range.

*This work is supported by the Office of Naval Research (Grants No. N00014-11-1-0552 and N00014-12-1-1045) and the Natural Science and Engineering Research Council of Canada.*

<sup>1</sup> M. R. Suchomel and P. K. Davies, *Appl. Phys. Lett.* **86**, 262905:1-4 (2005).

<sup>2</sup> Y. Xie, L. Chen, W. Ren and Z.-G. Ye, *IEEE Trans. Ultrasonics, Ferroelectrics and Frequency Control* **58**, 1920 -

1927 (2011).

## Identification of $\text{LiNb}(\text{Ta})\text{O}_3$ , $\text{LiNb}(\text{Ta})_3\text{O}_8$ and $\text{Li}_3\text{Nb}(\text{Ta})\text{O}_4$ phases in thin films synthesized with different deposition techniques by means of XRD and Raman spectroscopy

Ausrine Bartasyte<sup>1</sup>, Valentina Plausinaitiene<sup>2</sup>, Adulfas Abrutis<sup>2</sup>, Sandra Stanionyte<sup>2</sup>, Samuel Margueron<sup>3</sup>, Pascal Boulet<sup>1</sup>, T. Kobata<sup>4</sup>, Yoshiaki Uesu<sup>4</sup>, Jerome Gleize<sup>5</sup>

<sup>1</sup>Department†Institute Jean Lamour, (UMR 7198) CNRS – Lorraine University, Nancy, France

<sup>2</sup>University of Vilnius, Dept. of General and Inorganic Chemistry, Vilnius, Lithuania

<sup>3</sup>Laboratoire Matériaux Optiques, Photonique et Systèmes, EA 4423, Lorraine University and Supelec, Metz, France

<sup>4</sup>Department of Physics, Faculty of Advanced Science and Engineering, Waseda University, Shinjuku, Tokyo 169-8555, Japan

<sup>5</sup>LCP-A2MC, Université de Lorraine (EA 4632), F-57078 Metz, France.

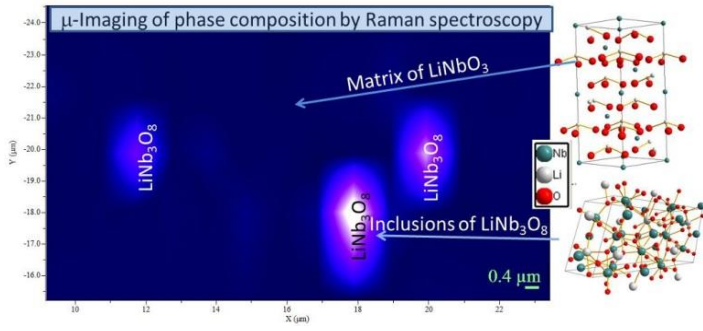
Email: ausrine.bartasyte@univ-lorraine.fr

Phase composition of epitaxial/textured  $\text{LiNb}(\text{Ta})\text{O}_3$  films on sapphire substrates, grown by pulsed laser deposition, atmospheric pressure metal organic chemical vapor deposition and pulsed injection metal organic chemical vapor deposition was studied by conventional X-ray diffraction techniques. Raman spectroscopy, being highly sensitive to the symmetry of materials, was used as a countercheck in the compositional analysis. The wavenumbers of Raman modes of  $\text{LiNb}(\text{Ta})_3\text{O}_8$  and  $\text{Li}_3\text{Nb}(\text{Ta})\text{O}_4$  phases were identified from Raman spectra of synthesized powders. It was found that standard XRD analysis of phase composition of textured  $\text{LiNbO}_3/\text{LiTaO}_3$  films might be not straightforward and confusing due to close reflection angles of  $\text{LiNbO}_3$  ( $\text{LiTaO}_3$ ) and  $\text{LiNb}_3\text{O}_8$  ( $\text{LiTa}_3\text{O}_8$ ) phases and different possible origins of asymmetric diffraction peak profiles. Asymmetry of profiles of X-ray diffraction reflections of  $\text{LiNb}(\text{Ta})\text{O}_3$  films was studied in details. This asymmetry may have different origins what consequently may result in misleading conclusions about phase composition of textured  $\text{LiNb}(\text{Ta})\text{O}_3$  films.

Raman spectroscopy, a fast, local and non-destructive probe, was applied for investigation and mapping of phase composition, Li stoichiometry and stresses in  $\text{LiNbO}_3$  ( $\text{LiTaO}_3$ ) films. The methodology of identification of different phases and extraction of residual stress and precise Li stoichiometry values from single Raman spectrum of  $\text{LiNb}(\text{Ta})\text{O}_3$  film will be presented. Moreover, this approach might be used for study of phase composition, stress and nonstoichiometry of other oxide films.

Fig. 55: 2D mapping of  $\text{LiNbO}_3$  and  $\text{LiNb}_3\text{O}_8$  phase distribution on the surface of film deposited on R-sapphire by means of Raman spectroscopy.





## Abnormally Large Dielectric Response in Textured PZT Thin Films

I.P. Pronin<sup>1,4</sup>, S.V. Senkevich<sup>1,4</sup>, E.Yu. Kaptelov<sup>1</sup>, O.N. Sergeeva<sup>2</sup>, A.A. Bogomolov<sup>2</sup>, D.A. Kiselev<sup>3</sup>,  
M.D. Malinkovich<sup>3</sup>, V.P. Pronin<sup>4</sup>

<sup>1</sup>Department of Dielectrics & Semiconductors, Ioffe Institute, Saint-Petersburg, Russia

<sup>2</sup>Department of Physics, Tver State University, Tver, Russia

<sup>3</sup>Department of the Material Science of Semiconductors and Dielectrics, National University of Science and Technology "MISIS", Moscow, Russia

<sup>4</sup>Department of Physics, Herzen State University, Saint-Petersburg, Russia

In the work, structural and ferroelectric properties of thin  $\text{PbZr}_{0.54}\text{Ti}_{0.46}\text{O}_3$  films grown by RF magnetron sputtering were studied. The films were fabricated in two stages. At first, films were deposited onto  $\text{Pt}/\text{TiO}_2/\text{SiO}_2/\text{Si}$  substrate at low temperature ( $\sim 150^\circ\text{C}$ ) and then, ones were thermally treated at  $530\text{--}580^\circ\text{C}$  in the conventional furnace to form single perovskite phase. Results of X-ray diffraction have shown a well-defined  $\langle 110 \rangle$ -texture film growth. Their microstructure was consisted of spherulite-type blocks of  $10\text{--}40\ \mu\text{m}$  in size, depending on annealing temperature ( $T_d$ ), Fig.1. The film thickness was varied from 300 to 500 nm. At increasing  $T_d$ , we have observed abnormally large dielectric permittivity ( $\epsilon_k$ ) reached of  $\sim 2000$  at room temperature.

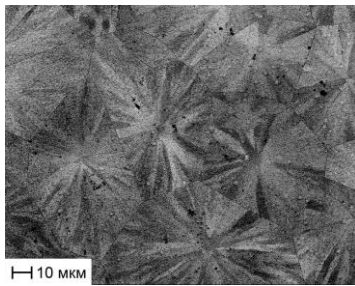


Fig. 56. Spherulite-type microstructure of 500 nm thick PZT film. Scanning electron microscopy, back-scattering electrons mode,  $E_p = 12\ \text{keV}$

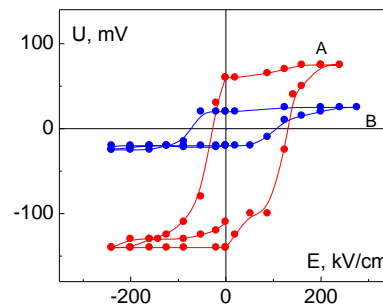


Fig. 2. Pyroelectric hysteresis loops measured in PZT samples having a high (A) and low (B) dielectric constant  $\epsilon_k$

An analysis of the results obtained has revealed the correlation between magnitude of  $\epsilon_k$  and size of spherulite blocks: the more were blocks dimensions, the more were magnitude of  $\epsilon_k$ . For more convincing were conducted pyroelectric and piezoelectric measurements on the samples differed by low and high magnitudes of  $\epsilon_k$  under applying strong electric fields. To a first approximation, pyroelectric response increased linear with  $\epsilon_k$ , Fig.2. Similar behavior was observed at piezoelectric contact mode measurements. The data obtained are discussed based on S.Wada approach to explain

giant piezoelectric response in ferroelectrics<sup>192</sup>.

---

<sup>1</sup> S. Wada, T. Muraishi, K. Yokoh, K. Yako, et.al. "Domain Wall Engineering in Lead-Free Ferroelectric Crystals", *Ferroelectrics*, vol. 355, p. 37-49, 2007

## Nanocomposite of magnetic nanoparticles in ferroelectric liquid crystalline host

Natalia Podoliak<sup>1</sup>, Vladimíra Novotná<sup>1</sup>, Jana Vejpravová<sup>1</sup>, Věra Hamplová<sup>1</sup>, Milada Glogarová<sup>1</sup>,  
Jan Prokleška<sup>2</sup>, Damian Pociecha<sup>3</sup>, Ewa Gorecka<sup>3</sup>

<sup>1</sup>Institute of Physics, Academy of Sciences of the Czech Republic, Na Slovance 2, 18221 Prague 8,  
Czech Republic

<sup>2</sup>Charles University, Faculty of Mathematics and Physics, Ke Karlovu 5, 121 16 Prague 2, Czech  
Republic

<sup>3</sup>Chemistry Department, Warsaw University, Al. Zwirki i Wigury 101, 02-089 Warsaw, Poland  
Email: podoliak@fzu.cz

Iron oxides nanoparticles (NPs) are a subject of numerous studies due to their unique superparamagnetic properties, controlled both by the phase composition and the particle size. When the magnetic NPs size is less than 50 nm, the single-domain state prevails. In such a case the surface and size effects become important, resulting in the increase in effective magnetic anisotropy. More attention is now paid to novel approaches for organizing NPs and different strategies are used for this purpose. Liquid crystals (LC) appear perfect candidates for new composites as they are able to self-organize on the molecular level. Additionally, nanocomposite of a ferroelectric liquid crystal and magnetic NPs can serve as a new type of multiferroic systems.

Herein we present a composite system of magnetic NPs in a ferroelectric LC compound denoted 9HL.<sup>193</sup> Monodisperse maghemite ( $\gamma$ -Fe<sub>2</sub>O<sub>3</sub>) NPs of size 5.0±0.5 nm have been prepared by thermal decomposition of iron acetylacetonate in organic media. Oleic acid coatings are chosen to keep the NPs apart, reducing mainly magnetic dipolar interactions, leading to agglomeration and surface spin effects. Studied LC compound 9HL, exhibiting the SmA\*-SmC\* phase sequence, has been mixed with NPs in concentration up to 8 weight % of Fe (11% Fe<sub>2</sub>O<sub>3</sub>). We have found the SmC\* phase disappears at concentration 5.6 % of NPs. For higher concentration the tendency of NPs to cluster together along the

smectic layers has been observed, which is addressed to the surface energy of the contact between nanoparticles being lower than the surface energy between the nanoparticles and liquid crystal. The strong magnetic field of 9 T influence on the temperature dependence of the permittivity has been studied for pure 9HL as well as for 1.4 % of NPs in 9HL host. The magnetic properties of NPs and its composite with 9HL have been studied and found typical for a system of superparamagnetic nanoparticles with inter-particle dipolar interactions and surface spin disorder. The magnetic response of the composite samples is somewhat modified due to the reduction of the dipolar interactions strength between the NPs.

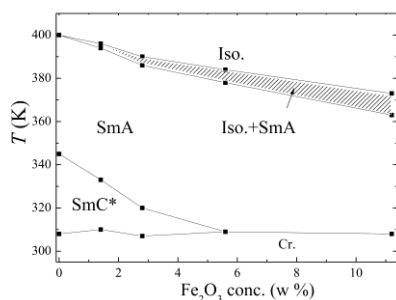


Fig. 1: Phase diagram of Fe<sub>2</sub>O<sub>3</sub> NPs in 9HL host. Concentration of Fe<sub>2</sub>O<sub>3</sub> is in weight %.

<sup>193</sup> F. Giesselmann P. Zugenmaier, I. Dierking, S. T. Lagerwall, B. Stebler, M. Kaspar, V. Hamplova, M. Glogarova, "Smectic-A\*-smectic-C\* transition in a ferroelectric liquid crystal without smectic layer shrinkage", Phys. Rev. E, vol. 60, p. 598-602, 1999.

This work is supported by the Czech Science Foundation, projects No P204/11/0723 and No 13-14133S.

## (Ag,Li)NbO<sub>3</sub> thin films fabricated on (001), (110), and (111)SrTiO<sub>3</sub> substrates by pulsed laser deposition

Yu Yamamoto\*, Ichiro Fujii and Takahiro Wada

Department of Materials Chemistry, Ryukoku University, Japan

E-mail address\*: [t12m093@mail.ryukoku.ac.jp](mailto:t12m093@mail.ryukoku.ac.jp)

AgNbO<sub>3</sub> (AN) has attracted attention as a lead-free material. We have successfully fabricated AN films on (001), (110), and (111)SrTiO<sub>3</sub> (STO) substrates by pulsed laser deposition (PLD)<sup>1</sup>. The films showed different dielectric and ferroelectric properties depending on the crystal orientation of STO substrates. In this work, we fabricated (Ag<sub>1-x</sub>Li<sub>x</sub>)NbO<sub>3</sub> (ALN) thin films with x=0.05(ALN05), 0.10(ALN10) and 0.15(ALN15) on (001), (110), and (111)STO substrates by PLD.

Before deposition of the ALN film, we deposited SrRuO<sub>3</sub> (SRO) film as a bottom electrode on (001), (110), and (111) STO substrates. Then, we deposited ALN films with a thickness of 1~4 μm. The fabrication conditions were as follows: laser repetition rate of 10 Hz, O<sub>2</sub> partial pressure of about 225 mTorr, substrate temperature of 700°C, and 750,000 laser shots. The crystalline structures of the ALN films were measured by  $\theta/2\theta$  X-ray diffraction analysis. The surface morphologies were observed by SEM. The relative dielectric constant  $\epsilon_r$  and dielectric loss  $\tan\delta$  were measured by an LCR meter, and  $P$ - $E$  hysteresis loops were observed using a ferroelectric tester.

X-ray diffraction (XRD) patterns showed that ALN(x=0,0.05,0.1,0.15) films were epitaxially grown on (001), (110), (111) STO substrates. The diffraction peaks of the ALN films shifted to a higher angle with increasing Li concentration. The ALN film on (001)STO had a smooth surface with several square holes. The film on (110)STO had a striped pattern, and that on (111)STO had trigonal pyramid-like structures. We reported similar microstructures for AN [1] and NaNbO<sub>3</sub> (NN) [2] films fabricated on the (001), (110), and (111) STO substrates. Figure 1 shows  $P$ - $E$  hysteresis of the ALN05, ALN10 and ALN15 films deposited on (001), (110), and (111) STO substrates. The ALN(x=0.1) film on (111) STO exhibits a ferroelectric behavior and has the largest remanent polarization ( $P_r$ ) of 40 μC/cm<sup>2</sup> of all the ALN films.

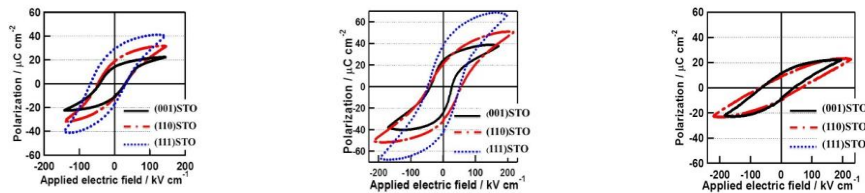


Fig. 1  $P$ - $E$  hysteresis of ALN (0.05,0.1,0.15) thin films deposited on (001), (110) and (111) SrTiO<sub>3</sub> substrates.

<sup>1</sup> H. Sakurai, S. Yamazoe, and T. Wada, Appl. Phys. Lett. 97, 042901 (2010).

## Influences of MgTiO<sub>3</sub> doping in Bi<sub>0.5</sub>Na<sub>0.5</sub>TiO<sub>3</sub> on microstructure and electrical parameters

Michael Naderer, Theresa Kainz, Klaus Reichmann

Christian Doppler Laboratory for Advanced Ferroic Oxides, Graz University of Technology, Graz, Austria

Email: Michael.naderer@tugraz.at

Bi<sub>0.5</sub>Na<sub>0.5</sub>TiO<sub>3</sub> or BNT is one of the most promising candidates to replace Pb(Ti,Zr)O<sub>3</sub> based materials in ferroelectric applications. It was discovered in the 1960 by Smolenskii<sup>1</sup> and receives increasing attention since the commencement of the RoHS guideline<sup>2</sup>. Structurally, BNT forms a complex rhombohedral perovskite with a 1 : 1 occupation of Bi<sup>3+</sup> and Na<sup>+</sup> on the 12-fold coordinated A-site and Ti<sup>4+</sup> on the 6-fold coordinated B-site.

The electrical and microstructural properties of BNT are highly modifiable. Doping of the system can occur using hetero- or isovalent elements (e.g. Li<sup>+</sup>, Sr<sup>2+</sup>, Nd<sup>3+</sup>, Nb<sup>5+</sup>) or by formation of solid solutions with other perovskites (e.g. Bi<sub>0.5</sub>K<sub>0.5</sub>TiO<sub>3</sub>, BaTiO<sub>3</sub>, K<sub>0.5</sub>Na<sub>0.5</sub>NbO<sub>3</sub>). The second possibility is the most common used, since it avoids high vacancy concentrations, which destabilizes the structure and therefore leads to decomposition.

This work describes the impact of alloying BNT with MgTiO<sub>3</sub> (MT) on the microstructure and electrical parameters. Unlike the heavier earth alkaline metals, Magnesium does not form a perovskite structure with Titanium. Despite the different structures of BNT and MT, solid solutions can be formed and Mg<sup>2+</sup> can be introduced into the BNT lattice, which acts as structural host.

The samples were prepared via a conventional mixed oxide route with Bi<sub>2</sub>O<sub>3</sub>, Na<sub>2</sub>CO<sub>3</sub>, MgO and TiO<sub>2</sub> as starting materials. The homogenization of the powder was carried out in a milling step using Tungsten Carbide milling balls and bowl on a planetary mill. The calcination reaction was performed at 800 °C to reduce the possibility of a Bi<sub>2</sub>O<sub>3</sub>-melt. The calcined powder was again ball milled with the equipment mentioned before. Before sintering, PEG20000 was added as a binding agent. The disc shaped samples, pressed with a diameter of 13 mm under a pressure of 150 MPa were debindered at 450°C and subsequently sintered at 1100 °C for 5 h.

The theoretical density and cell parameters were obtained by X-Ray diffraction, the apparent density was calculated using the Archimedes method. The microstructure was evaluated with SEM imaging in channeling contrast mode, instead of etching, in order to visualize grain size and domain structure. Secondary phase inclusions were also detected with SEM and EDX.

---

1. Smolenskii G, Isupov VA, Agranovskaya A, Krainik N. New ferroelectrics of complex composition. *Sov. Phys. Solid State*. 1961;2(11):2651–2654.

# Dopant effects on the phase diagram and piezoelectric properties of lead free piezoelectric niobate ceramics

Ruiping WANG<sup>1</sup>, Takuma ARIIZUMI<sup>2</sup>, Junta ZUSHI<sup>2</sup>, Seiji KOJIMA<sup>2</sup>, and Hiroshi BANDO<sup>1</sup>

<sup>1</sup>National Institute of Advanced Industrial Science and Technology, Tsukuba, Japan;

<sup>2</sup>University of Tsukuba, Tsukuba, Japan,

(Na<sub>0.5</sub>K<sub>0.5</sub>)NbO<sub>3</sub> shows orthorhombic structure at room temperature. Tetragonal is the high temperature and rhombohedral is the low temperature phases of it. When ATiO<sub>3</sub> (A = Ba, Sr, Ca, Bi<sub>0.5</sub>Na<sub>0.5</sub>, Bi<sub>0.5</sub>K<sub>0.5</sub>, Bi<sub>0.5</sub>Li<sub>0.5</sub>, ...) is mixed to it, the tetragonal phase could be tuned to room temperature. And when BZrO<sub>3</sub> (B = Ba, Sr, Ca, ...) is mixed to it, the rhombohedral phase could be tuned to room temperature. Therefore, tetragonal-rhombohedral MPB could be formed at room temperature by mixing (Na<sub>0.5</sub>K<sub>0.5</sub>)NbO<sub>3</sub>, ATiO<sub>3</sub> and BZrO<sub>3</sub> simultaneously.

It is reported that around the MPB, dielectric and piezoelectric properties were enhanced, similar to that of PZT. To investigate effects of element additive on the dielectric and piezoelectric properties of niobate ceramics, 0.92(Na<sub>0.5</sub>K<sub>0.5</sub>)NbO<sub>3</sub>-xBaZrO<sub>3</sub>-(0.08-x)(Bi<sub>0.5</sub>K<sub>0.5</sub>)TiO<sub>3</sub> (BBK) and 0.25 wt% MnO<sub>2</sub> added BBK samples were prepared; and their dielectric constant, electromechanical coupling coefficient  $k_p$ , piezoelectric  $d_{33}$  constant, mechanical quality factor  $Q_m$  and so on were studied.

Fig. 1 shows the composition dependence of  $k_p$ ,  $d_{33}$ , and  $Q_m$ , respectively.  $k_p$  is 15.16 % and  $d_{33}$  is 30 pC/N for  $x = 0.01$ . With increasing  $x$ , both  $k_p$  and  $d_{33}$  tend to increase. The highest  $k_p$  and  $d_{33}$  values, 43.38 % and 279 pC/N were obtained in  $x = 0.05$  for BBK, and 43.46 % in  $x = 0.05$  and 369 pC/N in  $x = 0.06$  for BBK+Mn, respectively. That is for both BBK and BBK+Mn, piezoelectric properties maximize around MPB. When  $x$  is beyond 0.05-0.06,  $k_p$  as well as  $d_{33}$  rapidly decrease. Composition dependence of dielectric constant at room temperature maximize at around MPB, too.

Comparing piezoelectric properties of BBK and those of BBK+Mn, it is clear that by adding Mn,  $k_p$ ,  $d_{33}$ , and  $Q_m$  are all increased. That is BBK could be both hardened and softened by adding Mn. The behaviors are attributed to the oxygen vacancy formation and grain size growing, respectively.

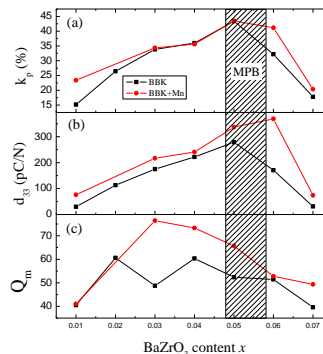


Fig. 1 Composition dependence of piezoelectric properties.



## **Influence of Germanium Substitution on Dielectric and Ferroelectric Properties of Ba(Fe<sub>0.5</sub>Nb<sub>0.5</sub>)O<sub>3</sub> Ceramics**

Puripat Kantha<sup>1</sup>, Nuttapon Pisitpipathsin<sup>1</sup>, Kamonpan Pengpat<sup>1,\*</sup>, Amar Bhalla<sup>2</sup>

<sup>1</sup>Department of Physics and Materials Science, Faculty of Science, Chiang Mai University, Chiang Mai 50200, Thailand

<sup>2</sup>Department of Electrical and Computer Engineering, College of Engineering, University of Texas at San Antonio, Texas 78256, USA

Email: [joonjanz\\_462@hotmail.com](mailto:joonjanz_462@hotmail.com), [kpengpat@gmail.com](mailto:kpengpat@gmail.com)\*

In this work, the influence of Ge<sup>4+</sup> substitution on dielectric and ferroelectric properties of high dielectric BaFe<sub>0.5</sub>Nb<sub>0.5</sub>O<sub>3</sub> ceramics was studied. The BGFN powders with a formula BaGe<sub>x</sub>(Fe<sub>0.5</sub>Nb<sub>0.5</sub>)<sub>1-x</sub>O<sub>3</sub> where x = 0.01, 0.015, 0.02 and 0.025 were produced via mixed-oxide method and subsequently calcined at 1100-1200°C for 4 h. To form the BGFN ceramics, the resulting powders were pressed into pellets and sintered at various temperatures from 1200 to 1350°C for 4 h in order to obtain the ceramic with maximum density under each condition. The phase formation, microstructure and electrical properties of these ceramics were investigated. It was found that the Ge<sup>4+</sup> substitution played an important role on the change of crystal structures and the phase formation of the BFN ceramics. The appearance of peak shift and peak split in XRD patterns confirmed the structural change from cubic to monoclinic in the ceramic samples at higher Ge<sup>4+</sup> content. The ceramics with x ≥ 0.015 contained three phases of BGFN, Ba<sub>3</sub>Fe<sub>2</sub>Ge<sub>4</sub>O<sub>14</sub> and BaGeO<sub>3</sub>. The amount of each phase was depended on the concentration of Ge<sup>4+</sup> where the Ba<sub>3</sub>Fe<sub>2</sub>Ge<sub>4</sub>O<sub>14</sub> and BaGeO<sub>3</sub> phases were found to increase with increasing x content. It was also found that the slightly lower densification, higher porosity and smaller grain sizes were found in the BGFN ceramics with higher level of Ge<sup>4+</sup> addition. This in turn affected their dielectric properties where dielectric constant was substantially decreased while the dielectric loss was greatly improved. The optimum composition for this system was found to be x = 0.015, where the maximum dielectric constant (~12282) with lower dielectric loss at room temperature were obtained.

## Tailored MPB BiScO<sub>3</sub>-PbTiO<sub>3</sub> piezoelectric ceramics for high temperature electromechanical transduction and magnetoelectric composites

Eider Beganza<sup>1</sup>, Harvey Amorín<sup>1</sup>, Pablo Ramos<sup>2</sup>, Alicia Castro<sup>1</sup>, Miguel Alguero<sup>1</sup>

<sup>1</sup>Instituto de Ciencia de Materiales de Madrid (ICMM), CSIC, Madrid, Spain

<sup>2</sup>Departamento de Electrónica, Universidad de Alcalá, Madrid, Spain

Email: malguero@icmm.csic.es

BiScO<sub>3</sub>-PbTiO<sub>3</sub> is the most studied system among general perovskite BiMO<sub>3</sub>-PbTiO<sub>3</sub> (M: cation in octahedral coordination) solid solutions with ferroelectric morphotropic phase boundaries (MPBs),<sup>195</sup> which are under extensive research for electromechanical transduction at temperatures between 200 and 400°C.<sup>196</sup> This is fostered by current industrial requirements for piezoelectric devices for operation in harsh environments, such as engines, deep oil drilling and space.

At ICMM, we have recently reported the functionality of MPB BiScO<sub>3</sub>-PbTiO<sub>3</sub> ceramics processed from nanocrystalline powders obtained by mechanosynthesis for intermediate temperature actuation (see Fig. 1). Low electric field high strain was obtained up to a temperature of 400 °C, with large extrinsic contributions from 300°C. High field strain could only be induced until 200°C, above which dielectric breakdown occurred.<sup>197</sup>

We report here the modification of MPB BiScO<sub>3</sub>-PbTiO<sub>3</sub> to tailor its functionality for a range of applications. Two approaches were addressed: (1) the introduction of Mn<sup>3+</sup> substituting for Sc<sup>3+</sup> in the perovskite B-site for reducing conductivity,<sup>198</sup> and (2) the formulation of A-site vacancies associated with an excess of Bi<sup>3+</sup> (in relation to charge compensated Pb<sup>2+</sup>) to enhance domain mobility. Functional measurements oriented to high temperature actuation, magnetoelectric composites and energy harvesting were carried out. Terfenol-based laminate cermets and unimorph structures were fabricated for the latter two characterizations.

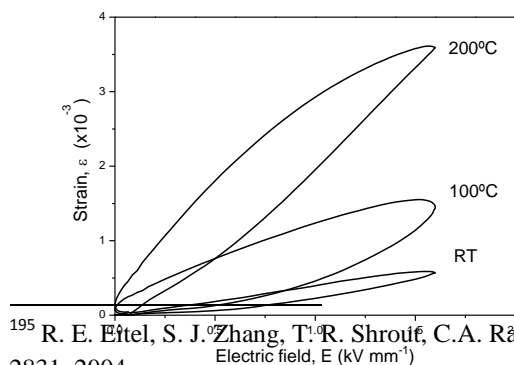


Fig. 1 Actuation characteristics of non-modified MPB BiScO<sub>3</sub>-PbTiO<sub>3</sub>

<sup>195</sup> R. E. Eitel, S. J. Zhang, T. R. Shroff, C.A. Randall, I. Levin, J. Appl. Phys., vol. 96, p. 2828-2831, 2004.

<sup>196</sup> A. Sehrioglu, A. Sayir, F. Dynys, J. Appl. Phys., vol. 106, art. n° 014102, 2009.

<sup>197</sup> M. Alguero, P. Ramos, R. Jiménez, H. Amorín, E. Vila, A. Castro, Acta Mater., vol. 60, p. 1174-1183, 2012.

<sup>198</sup> M. P. Drahos et al., Phys. Rev. B, vol. 86, art. n° 064113, 2011.

## Lead-free fibers with oriented structure

Bortolani Francesca<sup>1</sup>, Lusiola Tony<sup>1</sup>, Clemens Frank<sup>1</sup>

<sup>1</sup>Laboratory for High Performance Ceramics, Empa, Dübendorf, Switzerland

Email: Francesca.bortolani@empa.ch

In the past ten years, the use of lead in piezoelectric ceramics has been drastically reduced and the attention has moved to lead-free materials. KNN-based ceramics are good candidates as alternatives to PTZ, but their properties have to be improved in order to reach the PZT ones. A way to achieve this target is by grain orientation.

Platelet-like templates, with dimensions of  $\sim 20 \times 10 \times 3 \mu\text{m}$ , have been obtained by molten salt synthesis (MSS) and incorporated with anisotropic powder. By thermoplastic extrusion, the platelets have been oriented and KNN ceramic fibers were developed. The templates act as seeds during sintering and fibers with an oriented structure are eventually obtained. Microstructural characterisation of the ceramic fibers is shown. Ferroelectric behaviour of single fibers is also analysed by the use of a unique equipment in terms of hysteresis loop, butterfly loop (S-E) and piezoelectric coefficient ( $d_{33}$ ).

## Effect of Sn<sup>4+</sup> substitution on structure and properties in the PbSnO<sub>3</sub>–PbZrO<sub>3</sub>–PbTiO<sub>3</sub> ternary system

Zhuo Xing, Xiaoyong Wei, Li Jin

Electronic Materials Research Laboratory, Key Laboratory of the Ministry of Education & International Center for Dielectric Research, Xi'an Jiaotong University, Xi'an 710049, China

Email: xingzhuo@stu.xjtu.edu.cn

Piezoelectric materials have been extensively investigated in the last few decades for device applications, because of their multifunctional properties, which can be used in a broad range of applications. Piezoelectric properties are dependent on multiple variables, such as morphology, defect structure, grain size, domain size and density. Piezoelectric ceramics in the PbSnO<sub>3</sub>–PbZrO<sub>3</sub>–PbTiO<sub>3</sub> (PZST) ternary system with pure perovskite structure were synthesized by conventional solid state reaction method. Morphotropic phase boundary (MPB) compositions were confirmed by X-ray diffraction. The influence of Sn<sup>4+</sup> on dielectric, piezoelectric, and ferroelectric properties of PZST was investigated systematically. The experimental results showed that the perovskite structure changed from tetragonal to rhombohedral symmetry and the Curie temperature ( $T_C$ ) decreased gradually with increasing the content of PbSnO<sub>3</sub>. The composition with Zr:Sn=1:1 ceramics exhibited favorable properties of  $d_{33}$ ,  $d_{31}$ ,  $Q_m$ ,  $k_p$ ,  $T_C$ ,  $E_c$ .

## Novel series of temperature stable glass free LTCC $\text{Li}_2\text{BO}_4\text{-TiO}_2$ (B=Mo, W)

Jing Guo<sup>1</sup>, Di Zhou<sup>1</sup>, Gaoqun Zhang<sup>1</sup>, Hong Wang<sup>1</sup>

<sup>1</sup>Electronic Materials Research Laboratory, Key Laboratory of the Ministry of Education & International Center for Dielectric Research, Xi'an Jiaotong University, Xi'an 710049, China

Email: [j.gguo@stu.xjtu.edu.cn](mailto:j.gguo@stu.xjtu.edu.cn)

In this work, a new series of  $(1-x)\text{Li}_2\text{BO}_4\text{-}x\text{TiO}_2$  (B=Mo, W) ceramics were developed for microwave dielectric applications. They were prepared by solid state reaction method and the phase composition, microstructures, sintering behaviors, chemical compatibility with silver and microwave dielectric properties were investigated.  $\text{Li}_2\text{BO}_4$  (B=Mo, W) ceramics with ultra-low sintering temperatures ( $<650^\circ\text{C}$ ) exhibit good microwave dielectric properties (permittivity  $\epsilon_r=5.5$ ,  $Q \times f=46,000\sim 62,000$  GHz), but all of them have large negative temperature coefficient of resonant frequency ( $\tau_f = -146$  to  $-160$  ppm/ $^\circ\text{C}$ ). In order to compensate the negative  $\tau_f$  values of  $\text{Li}_2\text{BO}_4$  ceramics, rutile  $\text{TiO}_2$  was selected to form  $(1-x)\text{Li}_2\text{BO}_4\text{-}x\text{TiO}_2$  (B=Mo, W) mixtures. The X-ray diffraction pattern and scanning electron microscope analysis revealed that the  $\text{Li}_2\text{BO}_4$  did not react with rutile  $\text{TiO}_2$  and a stable two-phase composite system  $\text{Li}_2\text{BO}_4\text{-TiO}_2$  was formed. At  $x = 0.45 \sim 0.50$ , temperature stable microwave dielectric materials were obtained:  $\epsilon_r = 10.1\sim 12.2$ ,  $Qf = 29,300\sim 34,800$  GHz, and  $\text{TCF} \sim 0$  ppm/ $^\circ\text{C}$ .

# Investigating the effects of Ba-, Ca- and Sr-doping on the properties of PLZT

Mirjam Skof Theresa Kainz, Klaus Reichmann

Christian Doppler Laboratory for Advanced Ferroic Oxides, Graz University of Technology, Graz,  
Austria

E-Mail: [m.skof@student.tugraz.at](mailto:m.skof@student.tugraz.at)

Leadzirconate is an antiferroelectric material with interesting properties for storing charge at elevated electric fields. By replacing some of the Zr with Ti the antiferroelectric phase is destabilized in favor of a ferroelectric phase. Introducing  $\text{La}^{3+}$  as a substituent for  $\text{Pb}^{2+}$  generates A-site vacancies, thus stabilizing the antiferroelectric phase at higher Ti contents. Isovalent doping causes no changes in the vacancy concentration but leads to effects due to differences in mass and ionic radii.

Antiferroelectric to ferroelectric phase changes can be induced by applying a critical electric field causing a structural phase change resulting from the parallel alignment of anti-parallel dipoles. This enables a large increase in stored energy. Withdrawing the electrical field leads to a hysteretic recovery of the antiferroelectric phase.

In this study the influence of earth alkaline dopants on the properties of PLZT was investigated. Two basic compositions with differing Zr-/Ti-content were doped with Ba, Ca and Sr according to the formula  $(\text{Pb}_{0.89}\text{AE}_{0.02}\text{La}_{0.06})(\text{Zr}_{1-x}\text{Ti}_x)\text{O}_3$  (AE = Ca, Sr, Ba;  $x = 0,10$  &  $0,15$ ). The ceramic powders were processed via the mixed oxide route, calcined at  $925^\circ\text{C}$  and sintered at  $1250^\circ\text{C}$ . An excess of 2 % lead was added prior calcination.

After the preparation the samples were examined with XRD to control the formation of the perovskite structure and to observe changes in the volume of the unit cell. The sintering behavior of the ceramic was investigated with dilatometry.

To display the microstructure scanning electron microscopy was used in the channeling contrast mode instead of etching. The chemical composition of the samples was analyzed via EDX.

The dielectric properties were measured by determining the relative permittivity, the loss factor as well as their temperature dependence. Furthermore polarization curves were recorded leading to the switching field. The results were compared according to the chemical composition of the samples.

**Characterization and synthesis of Barium Titanate/Ni-nano metal composite by sol-gel process for high voltage capacitor**

**I S Kim<sup>1</sup>, Mohsin Saleem<sup>2</sup>, J S Song<sup>3</sup>, S J Jeong<sup>4</sup> and M S Kim<sup>5</sup>**

<sup>1,3,4,5</sup> Battery Research Center, KERI, Changwon, Republic of Korea, 641-120

<sup>2</sup> Department of Electrical Functionality Material engineering,  
University of Science and Technology, Daejeon, Republic of Korea 305-333

Email: kimis@keri.re.kr

A modified method has been applied to synthesize high purity Barium nickel titanate powder in nanometer range by sol-gel process. Conventionally, Barium titanate is synthesized by solid-state reaction between  $\text{BaCO}_3$  and  $\text{TiO}_2$ . The electrical behavior of barium titanate ceramics strongly depend on the composition and the microstructure. Because it is chemically and mechanically very stable, exhibits ferroelectric properties at and above room temperature, because it can be easily prepared and used in the form of ceramic polycrystalline samples. Due to its high dielectric constant and low dielectric loss characteristics barium titanate ( $\text{BaTiO}_3$ ) has been used in applications such as high voltage capacitors and energy storage devices.

In this paper,  $\text{BaTiO}_3$ -Ni composite is prepared by sol-gel technique with nickel content of different concentration for charge island in high voltage capacitors. It is thermally heated in anti-oxidation furnace. The electrical properties were characterized in term of relative permittivity, conductivity, C-V measurements. The electrical properties were affected by the conducting phase with increase in dielectric constant. The dielectric constant is increased from 5000 to 6000 by 10 to 15 % nickel paste which is high as compared to  $\text{BaTiO}_3$ -Ni synthesize by solid state process. Phase transformation and crystallite size of the powder were investigated by X-ray diffraction method; particle morphology and size were studied by scanning electron microscope. We suggested that a dielectric material is highly suitable for high voltage capacitors.

## Sintering and Dielectric Properties of $(1-x)$ BaTiO<sub>3</sub> – $x$ Sr<sub>3</sub>Ti<sub>2</sub>O<sub>7</sub> Composite Ceramics by a Coating Method

Chaojun Xie, Dengren Jin, Lixin Zhou, Hanting Dong, Jinrong Cheng

School of Materials Science and Engineering, Shanghai University, Shanghai, China

Email: [drjin@shu.edu.cn](mailto:drjin@shu.edu.cn)

Sintering and dielectric properties of  $(1-x)$  BaTiO<sub>3</sub>– $x$ Sr<sub>3</sub>Ti<sub>2</sub>O<sub>7</sub> composite ceramics fabricated by a coating method were investigated. In this research, the Ruddlesden-Popper(RP) Phase Sr<sub>3</sub>Ti<sub>2</sub>O<sub>7</sub> powders and BaTiO<sub>3</sub> powders were synthesized by the solid reaction, respectively, and then their mixed powders were coated with BaTiO<sub>3</sub> sol-gel by using ultrasonic irradiation. The structure evolution of the BaTiO<sub>3</sub> coating layer was investigated via transmission electron microscopy. Microstructure and phase variation, and ions inter-diffusion during the sintering were investigated by scanning electron microscopy and X-ray diffraction, respectively. Results show that the permittivity and dielectric loss were sharply decreased and temperature stability was improved effectively, due to the existence of ordered SrO-OSr stacking faults and the formation of an inhomogeneous micro-region nearby the grain boundary through the tuning of sintering schedules and the BaTiO<sub>3</sub> content.



## Processing and properties of BiFeO<sub>3</sub>-PbTiO<sub>3</sub>-Pb(Mn<sub>1/3</sub>Nb<sub>2/3</sub>)O<sub>3</sub> ternary system for high Curie temperature piezoceramics

Rui Dai, Shundong Bu, Dalei Wang, Dengren Jin and Jinrong Cheng<sup>\*199</sup>

<sup>1</sup> School of materials science and engineering, shanghai University, Shanghai 200072

BiFeO<sub>3</sub>-PbTiO<sub>3</sub>-Pb(Mn<sub>1/3</sub>Nb<sub>2/3</sub>)O<sub>3</sub> ternary solid solution system was investigated for the development of piezoelectric ceramics with high Curie temperature. (1-x)(0.7BiFeO<sub>3</sub>-0.3PbTiO<sub>3</sub>)-xPb(Mn<sub>1/3</sub>Nb<sub>2/3</sub>)O<sub>3</sub> (BFPT-PMN) for x=0.03, 0.04, 0.05, 0.06 and 0.1 ternary ceramics were fabricated by the conventional mixed oxide ceramic. XRD patterns reveal that all compositions possess perovskite structure with a rhombohedral symmetry and columbite disappears with the extension of dwell time. The surface morphology was examined by SEM. The dielectric property measurement on the ceramics confirmed the high Curie temperature and the improved loss tangent with the Pb(Mn<sub>1/3</sub>Nb<sub>2/3</sub>)O<sub>3</sub> doping. The values of dielectric constant, loss tangent and the Curie temperature were 314, 0.01 and 630 °C for x=0.03 at the sintering of 1040 °C and at the frequency of 10<sup>3</sup> Hz.

Keywords: BFPT-PMN ternary system; High Curie temperature; Dielectric properties;

---

\* Corresponding author: email: jrcheng@staff.shu.edu.cn

---

## **Integration and Tailored Micro/Nanostructures**

CLUB A

*Wednesday, July 24 2013, 10:30 am - 12:00 pm*

Chair: **Tadej Rojac**  
*Jozef Stefan Institute*

## Chemical Solution Processing of Ferroelectric Thin Films and Nanostructures

Nazanin Bassiri-Gharb<sup>1,2</sup>, Ashley Bernal<sup>1</sup>, Yaser Bastani<sup>1</sup>, Suenne Kim<sup>3</sup>, Elisa Riedo<sup>3</sup>, Haidong Lu<sup>4</sup>, Alexei Gruverman<sup>4</sup>, Amit Kumar<sup>5</sup>, Sergei Kalinin<sup>5</sup>

<sup>1</sup>G.W. Woodruff School of Mechanical Engineering, Georgia Institute of Technology, Atlanta, GA, USA

<sup>2</sup>School of Materials Science and Engineering, Georgia Institute of Technology, Atlanta, GA, USA

<sup>3</sup>School of Physics, Georgia Institute of Technology, Atlanta, GA, USA

<sup>4</sup>Department of Physics and Astronomy, University of Nebraska-Lincoln, Lincoln, NE, USA

<sup>5</sup>Center for Nanophase Materials Science, Oak Ridge National Laboratory, Oak Ridge, TN, USA

Email: nazanin.bassirigharb@me.gatech.edu

Ferroelectric (FE) thin films and nanostructures find a wide range of applications in capacitive elements, non-volatile memories, micro/nano-electromechanical system (MEMS/NEMS) sensors, actuators and transducers, as well as energy harvesting nano- and micro-generators. With the drive towards miniaturization, multiple intrinsic and extrinsic factors need to be leveraged in order to increase and/or maintain the high dielectric and piezoelectric response of ferroelectric materials and reduce size effects. However, the currently available processing methods, mostly based on pre-existing micromachining fabrication methods, suffer multiple limitations. Top-down approaches can damage surface layers due to the impact of high-energy particles (detrimental to the final electromechanical properties), or offer poor side-wall definition in wet-etch methods. Bottom-up approaches, while allowing creation of high quality ferroelectric materials, are mostly limited in patterning capability and compatibility for alignment with previous and subsequent layers. Chemical solution deposition provides a very flexible approach for processing of short and high-aspect ratio ferroelectric nanostructures, as well as thin and ultrathin ferroelectric films with controlled crystallographic orientation and enhanced dielectric and piezoelectric response on a variety of substrates.

This talk gives an overview of the processing methods developed in our group for such structures and thin films. Specifically, we report the results of a lift-mode AFM, employing a heated tip, used to locally crystallize sol-gel films of ferroelectric materials (e.g.  $\text{PbTiO}_3$  and  $\text{PbZr}_{1-x}\text{Ti}_x\text{O}_3$ ). Arbitrary shapes and periodic arrays of ferroelectric nanostructures are obtained on platinized soda-lime glass, silicon and polyimide substrates. The feature size ranged between  $\sim 10$  nm and  $2.5 \mu\text{m}$ . An alternative method for creation of ferroelectric microstructure is also explored by leveraging thermally decomposable, UV or e-beam patterned, sacrificial material. The photoresist or e-resist patterns are created via deep-UV lithography or e-beam patterning. A subsequent coating with the appropriate chemical solution precursor of the ferroelectric material, followed by heat treatment leads to crystallization of the ferroelectric and removal of the sacrificial patterns. Modification of the heat treatment profile and relative thicknesses of the resist/ferroelectric precursor result into creation of surface micro/nano-channels of ferroelectric material or alternatively patterned ferroelectric areas.

## Confinement Printing of Thin Film Lead Zirconate Titanate for MEMS Applications

A. J. Welsh<sup>1</sup>, D. Dezest<sup>2</sup>, L. Nicu<sup>2</sup>, M. A. Hickner<sup>1</sup>, and S. Trolier-McKinstry<sup>1</sup>

<sup>1</sup>The Pennsylvania State University, N-224 Millennium Science Complex, University Park, USA

<sup>2</sup>Laboratoire d'Analyse et d'Architecture des Systemes – Le Centre National de la Recherche Scientifique, University de Toulouse, Toulouse, France

Email: [ajw5000@psu.edu](mailto:ajw5000@psu.edu)

Thin film electroceramics used as sensors, capacitors, actuators, etc. are patterned into specific geometries, typically by either a wet or dry subtractive patterning approach. It is also interesting to consider additive patterning techniques for MEMS applications. Ceramic suspensions, pastes, and solutions have been additively patterned at the macro and meso-scale through the use of inkjet printing, screen printing, and embossing. Powder-free ceramic solutions have been patterned through soft lithographic techniques. Soft lithography utilizes elastomeric polymer stamps/molds to confine or deposit solutions onto a substrate. Printing of a ceramic solution from stamp protrusions directly onto a substrate, termed microcontact printing, has been used to deposit patterned lead zirconate titanate (PZT) thin films with comparable electrical properties to continuous PZT thin films. However, this technique deposits very thin layers of ceramic for every stamping cycle which is a concern for pattern registry. Elastomeric polymers have also been used as molds for ceramic solutions in order to deposit the film in a single processing step. These patterning techniques produce features that have large shape deformations or cracking of the final films.

This work explores the confinement printing of PZT liquid precursors from stamp wells (rather than stamp protrusions as is used in microcontact printing). The confinement printing of solutions uses an initial sacrificial printing step in order to remove solution from the protrusions of the stamp. The second stamping cycle deposits the solution from the wells of stamp. Printing from wells doubled the thickness (e.g. from 25 to 50 nm) of deposited solution per stamping cycle over microcontact printing. This work studies the printing characteristics of this patterning technique, including line edge resolution, feature thickness, side wall angles, and achievable lateral feature size. Arrays of PZT features were printed, characterized and compared to continuous PZT thin films of similar thickness. One micron thick printed PZT features exhibit a permittivity of 1030 and a loss tangent of 0.024. The hysteresis loops are well formed, without pinching of the loops. The patterned features showed remanent polarizations of  $29\mu\text{C}/\text{cm}^2$ , and coercive fields of  $52\text{kV}/\text{cm}$ . The piezoelectric response of the features produced an  $e_{31,f}$  of  $-7\text{ C}/\text{m}^2$ .

## Ferroelectric Order in Nanoscale Perovskites and its Control via Colloidal Processing

Gabriel Caruntu<sup>1,2</sup>, Amin Yourdkhani<sup>1,2</sup>, Mark J. Polking<sup>3,4</sup>, Daniela Caruntu<sup>1</sup>, Valeri Petkov<sup>5</sup>, Christian F. Kisielowski<sup>6</sup>, Vyacheslav V. Volkov<sup>7</sup>, Yimei Zhu<sup>6</sup>, A. Paul Alivisatos<sup>8</sup> and Ramamoorthy Ramesh<sup>9</sup>

<sup>1</sup>Advanced Materials Research Institute, University of New Orleans, New Orleans, Louisiana 70148, USA

<sup>2</sup>Department of Chemistry, University of New Orleans, New Orleans, LA 70148, USA

<sup>3</sup>Department of Materials Science and Engineering, University of California, Berkeley, Berkeley, CA 94720, USA

<sup>4</sup>Department of Chemistry, Harvard University, Boston, Massachusetts, USA

<sup>5</sup>Department of Physics, Central Michigan University, Mount Pleasant, MI 48859, USA

<sup>6</sup>National Center for Electron Microscopy, Lawrence Berkeley National Laboratory, Berkeley, CA 94720, USA

<sup>7</sup>Condensed Matter Physics and Materials Sciences Department, Brookhaven National Laboratory, Upton, NY 11973, USA

<sup>8</sup>Department of Chemistry, University of California, Berkeley, Berkeley, CA 94720, USA.

<sup>9</sup>Materials Sciences Division, Lawrence Berkeley National Laboratory, Berkeley, CA 94720, USA

In an attempt to address one of the fundamental questions related to the survival of ferroelectricity in technologically important perovskites, we present here an atomic-scale insight into the fundamental nature of ferroelectric order down to its ultimate size limit using. To this end we used monodisperse, aggregate-free BaTiO<sub>3</sub> colloidal nanocrystals as a model system.

Atomic resolution mapping of local ferroelectric distortions indicates a coherent, nearly linear, monodomain state accompanied by local structural distortions. The persistence of ferroelectric coherence in BaTiO<sub>3</sub> is further supported by single-particle studies with off-axis electron holography and PFM measurements of individual nanocubes demonstrating ferroelectric switching

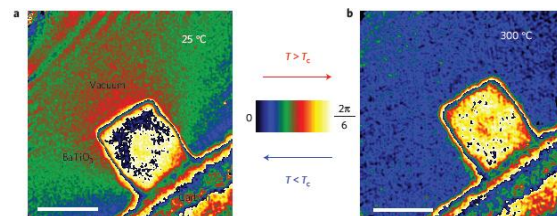


Fig. 1. Electron holography images of an individual 10 nm BaTiO<sub>3</sub> nanocube below (a) and above (b) the Curie temperature demonstrating the polarization structure in the ferroelectric state and its eradication above the phase transition

behaviour at room temperature. These PFM studies further demonstrate the ultimate stability limit of ferroelectric order. Careful atomic PDF studies point to the parallel roles played by surface-induced relaxation and depolarization effects in the dissolution of ferroelectric order at finite dimensions and indicate considerable structural disorder and dipole decoherence, even in conductive GeTe with strong polarization screening. These studies also demonstrate the utility of colloidal morphology control

as a means of stabilizing the polar state at nanoscale dimensions. These experiments reveal the ultimate limit of the ferroelectric state and provide a pathway to unravelling the fundamental physics of nanoscale ferroelectricity at the smallest possible size scales.

## Structural and Electric Properties of $\text{Ca}_2\text{Nb}_3\text{O}_{10}$ Thin Films grown by Electrophoretic Method

Sang Hyo Kweon<sup>1</sup>, Mir Im<sup>1</sup>, Sahn Nahm<sup>1</sup>

<sup>1</sup>Department of Material Science and Engineering, Korea University, Seoul, South Korea

Email: petitzel1223@korea.ac.kr

$\text{KCa}_2\text{Nb}_3\text{O}_{10}$  ceramics, Dion-Jacobson layered perovskite materials, have been widely investigated because they can be easily exfoliated to the nano-sized sheets which can be used to the future multilayer capacitors with a small size and high performance. A  $\text{KCa}_2\text{Nb}_3\text{O}_{10}$  phase was formed at  $900^\circ\text{C}$  and a dense ceramics were obtained after sintering at  $1375^\circ\text{C}$  for 10 h. A proton exchange process was carried out to produce the intermediate phase of  $\text{HCa}_2\text{Nb}_3\text{O}_{10}$  and the stable  $(\text{Ca}_2\text{Nb}_3\text{O}_{10})^-$  nanosheet colloids were formed using the mixture of the  $\text{HCa}_2\text{Nb}_3\text{O}_{10}$  powders, tetrabutylammonium hydroxide (TBAOH) solution and water having the same  $\text{TBA}^+/\text{H}^+$  ratio. The exfoliated  $(\text{Ca}_2\text{Nb}_3\text{O}_{10})^-$  nanosheets were dispersed into the acetone intermediate, which was used to form the thin film by the electrophoretic method under 100 V electric source. The electrophoretic thin films were then annealed at various temperatures for 30 min under air condition and all the films have the  $\text{Ca}_2\text{Nb}_3\text{O}_{10}$  phase. In particular, a high dielectric constant of 65 with a loss of 2.1% at 100 kHz was obtained from the film annealed at  $600^\circ\text{C}$  and this film also showed the low the leakage current density of  $1 \times 10^{-7}$  A/cm<sup>2</sup> at 0.1 MV/cm.

## Multiferroic Properties of Bismuth Ferrite Porous Thin Films

Stella Skiadopoulou, Eliana Carvalho, Alichandra Castro, Paula Ferreira, Paula M. Vilarinho

Department of Materials and Ceramic Engineering, CICECO, University of Aveiro, Aveiro,  
Portugal

Email: styliani@ua.pt

Magnetolectric multiferroics' ability of magnetic field manipulation via electric fields or vice versa can be extremely promising for information storage applications, leading to thinner, as well as flexible devices, with significantly high energetic efficiencies and huge capacities<sup>200</sup>. Bismuth ferrite ( $\text{BiFeO}_3$ ), being the only single-phase multiferroic at room temperature, is considered the model multiferroic<sup>201</sup>. Porous matrices, apart from providing lighter devices, have a great importance for a large range of applications, since novel architectures can be achieved by the incorporation of diverse materials in the pores, producing multifunctional films<sup>202</sup>.

For that purpose,  $\text{BiFeO}_3$  porous thin films were prepared by combination of simple processes: modified sol-gel (with a block copolymer), Evaporation Induced Self-Assembly (EISA) method and dip-coating deposition on  $\text{Pt/TiO}_2/\text{SiO}_2/\text{Si}$  substrates. Different copolymer concentrations were used in the as-prepared solutions, in order to study the effect of porosity on the multiferroic properties. Additionally, film deposition was conducted at increasing deposition velocities, aiming at the characterization of films with varying thicknesses. Ferroelectric and ferromagnetic properties were studied at the nanoscale via Piezoresponse Force Microscopy (PFM) and Magnetic Force Microscopy (MFM) respectively. Dense films with similar characteristics were prepared for comparison purposes.

The variations in the piezoresponse signal of porous films with increasing porosity and decreasing thickness is discussed and related with the microstructure of the films, domain configuration and substrate interaction.

### Acknowledgment

The authors are grateful to FCT and FEDER (QREN - COMPETE) for financial support PTDC/CTM/098130/2008).

---

<sup>200</sup>Spaldin, N.A., S.W. Cheong, and R. Ramesh, *Multiferroics: Past, present, and future*. Physics Today, vol. 63, p. 38-43, 2010.

<sup>201</sup>Martin, L.W. and R. Ramesh, *Overview No. 151 Multiferroic and magnetolectric heterostructures*. Acta Materialia, vol. 60, p. 2449-2470, 2012.

<sup>202</sup>Ferreira, P., et al., *Nanoporous Piezo- and Ferroelectric Thin Films*. Langmuir, vol. 28, p. 2944-2949, 2012.

---

## **Pb-Free Piezoelectrics**

CLUB B

*Wednesday, July 24 2013, 10:30 am - 12:00 pm*

Chair: **Clive Randall**  
*Pennsylvania State University*



## Texturation of lead-free BaTiO<sub>3</sub>-based piezoelectric ceramics

A. Nguetou-Kamlo<sup>1</sup>, F. Levassort<sup>2</sup>, M. Pham Thi<sup>3</sup>, P. Marchet<sup>1</sup>

<sup>1</sup> Laboratoire de Science des Procédés Céramiques et de Traitements de Surface, UMR 7315 CNRS, Université de Limoges, Centre Européen de la Céramique, 12, rue Atlantis, F-87068 Limoges Cedex, France.

<sup>2</sup> Université François Rabelais de Tours, GREMAN CNRS 734, 10 Boulevard Tonnellé, BP 3223, F-37032 TOURS Cedex 1, France

<sup>3</sup> THALES Research & Technology France, Campus Polytechnique, 1, Av. Augustin Fresnel, F-91767 Palaiseau Cedex - France

Email: pascal.marchet@unilim.fr

Nowadays, piezoelectric ceramics are integrated in a wide range of devices, in particular in ultrasonic applications (underwater sonar systems, medical imaging, non-destructive testing...). Most of them use Pb(Zr,Ti)O<sub>3</sub> (PZT). However, due to health care and environmental problems, lead content must be reduced in such applications<sup>203</sup>. Recent reviews demonstrated that few lead-free materials families can be considered: the alkaline-niobates (K<sub>0.5</sub>Na<sub>0.5</sub>NbO<sub>3</sub>), the alkaline-bismuth-titanates (Na<sub>0.5</sub>Bi<sub>0.5</sub>TiO<sub>3</sub>, K<sub>0.5</sub>Bi<sub>0.5</sub>TiO<sub>3</sub>), the bismuth layered compounds (Bi<sub>4</sub>Ti<sub>3</sub>O<sub>12</sub>) and barium titanate based materials (BaTiO<sub>3</sub>)<sup>204,205</sup>.

One of the limitations of ceramic materials is their isotropic nature. This is the reason why texturation process has been developed in order to improve their properties in particular electromechanical parameters. The aim of the present study is thus to obtain textured BaTiO<sub>3</sub> based materials by using the templated grain growth process (TGG) and to measure their piezoelectric properties. Nanosized BaTiO<sub>3</sub> powders were prepared by classical solid state route at relatively low temperature. BaTiO<sub>3</sub> templates of different morphologies were elaborated by a molten salts process. Dispersing agent, binder and plasticizer, the mixture of the templates and matrix particles was then dispersed in the appropriated solvent using non-aqueous formulation. The slurry was then tape-casted on plastic film. After drying, the green sheet was cut, stacked, thermo compressed and then sintered at the appropriated temperature. This process allowed obtaining highly-oriented materials with a texturation degree around 95% (fig. 1), presenting K<sub>t</sub> values around 35-40%, higher than for non-textured BaTiO<sub>3</sub> ceramics.

**Acknowledgements:** The authors kindly acknowledge financial support from the French Research National Agency (ANR), project

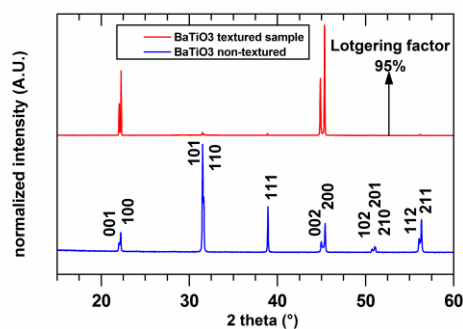


Fig. 57: X-ray diffraction diagram of (tetragonal) textured sample BaTiO<sub>3</sub> and (tetragonal) non-textured BaTiO<sub>3</sub> ceramic as reference.

<sup>203</sup> Directive 2002/95/EC, Official Journal of the European Union, 13.2.2003

<sup>204</sup> J. Rodel, W. Jo, T.P. Seidert, E-M. Anton, T. Granzow, D. Damjanovic, J. Am. Ceram. Soc. 92, 1153-1177, 2009

<sup>205</sup> P.K. Panda, J. Mater. Sci. 44, 5049-5062, 2009

HYPERCAMPUS

## Electric-Field-Induced phase switching in textured Ba-doped bismuth ferrite-lead titanate

Meghdad Palizdar<sup>1,5</sup>, Tim P. Comyn<sup>1</sup>, Tim J. Stevenson<sup>1</sup>, Stephen F. Poterala<sup>2</sup>, Gary L. Messing<sup>2</sup>, Ender Suvaci<sup>3</sup>, Annette P. Kleppe<sup>4</sup>, Andrew J. Jephcoat<sup>4</sup> and Andrew J Bell<sup>1</sup>

<sup>1</sup>Institute for Materials Research, University of Leeds, LS2 9JT, Leeds, UK

<sup>2</sup>Department of Materials Science and Engineering, Pennsylvania State University, University Park, USA

<sup>3</sup>Department of Materials Science and Engineering, Anadolu University, Eskisehir, Turkey

<sup>4</sup>Diamond Light Source Ltd, Diamond House, Harwell Science and Innovation Campus, Didcot, Oxfordshire, UK

<sup>5</sup>Institute for Materials Research, Iran University of Science and Technology, Tehran, Iran

e-mail: ml07m2p@leeds.ac.uk

The solid solution between bismuth ferrite and lead titanate ( $x\text{BiFeO}_3-(1-x)\text{PbTiO}_3$  or BFPT) possesses a morphotropic phase boundary (MPB) between the rhombohedral and tetragonal forms at  $x=0.7$ . It is of interest to investigate the influence of field-driven rhombohedral-tetragonal phase transitions across the MPB, to determine whether correctly oriented BFPT can provide both giant piezoelectric properties and significant magnetoelectric coupling.

Here, we used the reactive templated grain growth (RTGG) technique to prepare crystallographically textured BFPT ceramics, by using  $\text{BaTiO}_3$  as templates. It was found that conventional XRD is not sufficient for evaluating texture development in partially oriented 60:40BFPT ceramics. Hence, synchrotron radiation experiments were used in two different directions, perpendicular and parallel to the cast direction. These experiments highlighted significant differences in crystallographic orientation between perpendicular and parallel directions. Also, vibrating sample magnetometry (VSM) data, measured with both cast direction normal and parallel to the magnetic field, clearly showed orientation of magnetic response as a result of crystallographically textured structure. The coercive field of 177 Oe and maximum magnetization of 1.43 emu/g was obtained when magnetic field applied normal to the cast direction. By applying the magnetic field along to the cast direction, a far higher coercive field of 908 Oe, and lower maximum magnetization of 0.29 emu/g was realized. VSM data suggested the existence of ferromagnetic textured BFPT at room temperature. However, EDX data showed that  $\text{BaTiO}_3$  templates dissolved in the matrix and resulted in  $\text{Ba}^{+2}$ -doped BFPT with the formula of  $\text{Bi}_{0.57}\text{Fe}_{0.55}\text{Pb}_{0.34}\text{Ba}_{0.08}\text{Ti}_{0.44}\text{O}_x$ .

A ferroelectric Curie temperature of  $\sim 570$  °C and remanent polarization of  $2\text{Pr} = 60$   $\mu\text{C}/\text{cm}^2$  at 7.5 kV/mm were recorded.

Finally, in situ synchrotron diffraction shown that by applying external electric field on mixed rhombohedral and tetragonal  $\text{Ba}^{+2}$ -doped BFPT phases along [001] direction, single phase tetragonal was obtained.

To summaries,  $\text{BaTiO}_3$  has succeeding in generating a textured, ferromagnetic system.

## **Fabrication of Barium Titanate Grain-oriented Ceramics using Barium Titanate Particles with Different Crystal Structure by Electrophoresis Deposition Method under High Magnetic field and Their Dielectric and Piezoelectric Properties**

Satoshi Wada<sup>1</sup>, Eigo Kobayashi<sup>1</sup>, Shintarou Ueno<sup>1</sup>, Kouichi Nakashima<sup>1</sup>, Takahiro Takei<sup>1</sup>, Nobuhiro Kumada<sup>1</sup>, Thoru Suzuki<sup>2</sup>, Tetsuro Uchikoshi<sup>2</sup>, Yoshio Sakka<sup>2</sup>, Eisuke Magome<sup>3</sup>, Chikako Moriyoshi<sup>3</sup>, Yoshihiro Kuroiwa<sup>3</sup>, Yasuo Miwa<sup>4</sup>, Shinichiro Kawada<sup>4</sup>, Suetake Omiya<sup>4</sup>, and Noriyuki Kubodera<sup>4</sup>

<sup>1</sup>Material Science and Technology, Interdisciplinary Graduate School of Medical and Engineering, University of Yamanashi, 4-4-37 Takeda, Kofu, Yamanashi 400-8510, Japan

<sup>2</sup>National Institute for Materials Science, 1-2-1 Sengen, Tsukuba, Ibaraki 305-0047, Japan

<sup>3</sup>Murata Manufacturing Co., Ltd. 2288 Ooshinohara, Yasu, Shiga 520-2393, Japan

<sup>4</sup>Department of Physical Science, Hiroshima University, 1-3-1 Kagamiyama, Higashi-Hiroshima, Hiroshima 739-8526, Japan

Email: [swada@yamanashi.ac.jp](mailto:swada@yamanashi.ac.jp)

Barium titanate (BaTiO<sub>3</sub>, BT) grain-oriented ceramics were prepared by electrophoresis deposition (EPD) method under high magnetic field (HM-EPD) of 12 T. For this objective, two kinds of BT particles, i.e., the tetragonal BT single-domain nanoparticles with *c/a* ratio of 1.009 and size of 99 nm and hexagonal BT nanoparticles with high *c/a* ratio of 2.55 and size of about 300 nm, were used in this study. Using these BT nanoparticle slurry, BT nanoparticle accumulations were prepared by EPD with/without high magnetic field. As the results, from X-ray diffraction (XRD) measurements, the accumulation of tetragonal BT nanoparticles was assigned to randomly oriented one while the accumulation of hexagonal BT nanoparticles was assigned to <001> oriented one with a degree of orientation of almost 40 %. After binder burnout, these accumulations were sintered at 1250 °C to inhibit abnormal grain growth, and from XRD measurements, it was revealed that the BT ceramics prepared using tetragonal BT nanoparticles exhibited completely randomly-oriented one, while the BT ceramics prepared using hexagonal BT nanoparticles showed <111> oriented one with a degree of orientation of almost 79 %. These results revealed that the magnetic field of 12 T was insufficient for magnetic alignment of tetragonal BT nanoparticles because of its low diamagnetic anisotropy. Moreover, the microstructure of the <111> oriented BT ceramics was observed using a scanning electron microscope (SEM) with EBSD, and its grain size was estimated at almost 1 μm. Therefore, using hexagonal BT nanoparticles, fine-grained BT ceramics along <111> orientation of almost 80 %.

## Anisotropy of piezo- and ferroelectricity in textured $K_{0.5}Na_{0.5}NbO_3$ -based materials from novel texturing method

Astri Bjørnetun Haugen<sup>1</sup>, Gerhard Henning Olsen<sup>1</sup>, Francesco Madaro<sup>1</sup>, Maxim Morozov<sup>1</sup>, Goknur Tutuncu<sup>2</sup>, Jacob L. Jones<sup>2</sup>, Tor Grande<sup>1</sup> and Mari-Ann Einarsrud<sup>1</sup>

<sup>1</sup>Department of Materials Science and Engineering, Norwegian University of Science and Technology (NTNU), Trondheim, Norway

<sup>2</sup>Department of Materials Science and Engineering, University of Florida, Gainesville, Florida, USA

Email: [astri.b.haugen@ntnu.no](mailto:astri.b.haugen@ntnu.no)

Lead-free piezoelectrics have been shown to exhibit properties similar to  $Pb(Zr,Ti)O_3$  through doping and introduction of preferential grain orientation (texture) in  $(K,Na)NbO_3$  (KNN). Textured KNN is normally obtained from templated grain growth (TGG) with plate-like  $NaNbO_3$  templates in a KNN matrix.

In this work,  $\langle 001 \rangle_{pc}$  (pc for pseudo-cubic indices) textured KNN and KNN doped with Mn and Mn, Li and Ta were produced by TGG with needle-like KNN templates. Tape casting with a gated doctor blade was used to align the templates. Characterization of the sintered compacts revealed weak  $\langle 001 \rangle_{pc}$  texture and some non-beneficial  $\langle 110 \rangle_{pc}$  texture in the tape cast plane resulting in lower piezoelectric performance than corresponding non-textured materials. This is attributed to rotation of the templates around their long axis. Alignment of the templates' long axes did, however, introduce a larger degree of  $\langle 100 \rangle_{pc}$  texture along the tape cast direction.

Synchrotron X-ray diffraction using a 2D detector confirmed the texture as described above and allowed *in situ* measurement of domain switching during electric field loading. The largest relative intensity changes within sets of  $\{hkl\}$ s vs. electric field magnitude were observed for field applied parallel to the direction of highest texture (tape cast direction) as shown in Fig.1. This is attributed to better accommodation of the strain from domain switching in the direction of high texture. Piezoelectric constant ( $d_{33}$ ) measured after the *in situ* study was also highest in this direction due to high  $\langle 100 \rangle_{pc}$  texture. These results are therefore consistent with the polarization rotation mechanism of piezoelectric enhancement for orthorhombic symmetry.<sup>206</sup>

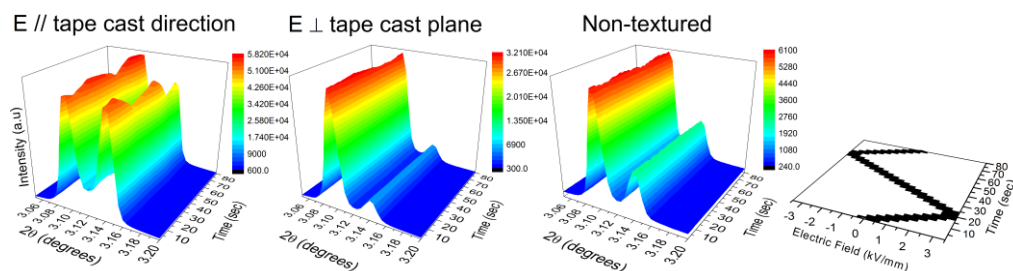


Fig. 58: Surface plots of the diffracted  $\{200\}_{pc}$  of KNN during *in situ* electric field loading.

<sup>206</sup> M. Davis *et al.*, J. Appl.Phys., vol. 101, p.054112, 2007.

## The electric property of textured lead-free piezoelectric thick films

Jiwei Zhai\*, Bo Shen, and Fang Fu,

Functional Materials Research Laboratory, Tongji University, Shanghai 200092, China  
apzhai@tongji.edu.cn

(h00)-textured lead free piezoelectric thick films were fabricated by tape casting and screen printing method, respectively. Main family members of lead free piezoelectric materials such as BT, NBT, and KNN-based thick film are all investigated. The textured  $(\text{Ba}_{0.85}\text{Ca}_{0.15})(\text{Zr}_{0.1}\text{Ti}_{0.9})\text{O}_3$  (BCZT) thick films were fabricated via screen printing using anisotropically shaped  $\text{BaTiO}_3$  templates on platinum substrate. The textured BCZT thick film exhibited excellent electric properties with the piezoelectric constant  $d_{33}^* = 427$  pm/V and remnant polarization  $P_r = 15.8$   $\mu\text{C}/\text{cm}^2$  sintered at 1300 °C for 4 h with 81% of Lotgering's factor.

High-stain textured thick film with the composition of NBT-BT-KNN was also fabricated. The grain orientation degree reached to 75%. The large signal  $d_{33}$  reached to 349 pm/V, which is comparable to the value of PZT thick films. Furthermore, the temperature stability of the textured NBT-BT-KNN thick film was also evaluated. A ferroelectric-antiferroelectric phase transition was started at 70 °C and both ferroelectric and antiferroelectric phase were co-existed in the thick film.

Tape casting method was also applied on KNN-based textured thick films. The grain orientation degree of KNN textured thick film was 61%. The piezoelectric constant  $d_{33}$  improved from 38 to 61 pm/V. The grain orientation degree increased to 82% with adding 6 mol%  $\text{LiSbO}_3$ . The piezoelectric constant  $d_{33}$  was enhanced to 173 pm/V due to the addition of  $\text{LiSbO}_3$ .

## Fabrication of Random and Textured Lead-free (K,Na)NbO<sub>3</sub> in Fiber, Ribbon and Ceramic Form

Sedat Alkoy<sup>1,2</sup>, Ebru Mensur Alkoy<sup>3</sup>, Ayse Berksoy Yavuz<sup>1,2</sup>,

<sup>1</sup>Dept. Materials Sci. & Eng., Gebze Institute of Technology, Gebze, Kocaeli, Turkey

<sup>2</sup>ENS Piezodevices Ltd., Gebze, Kocaeli, Turkey

<sup>3</sup>Faculty of Engineering and Natural Sciences, Maltepe University, Maltepe, Istanbul, Turkey

Email: sedal@gyte.edu.tr

To achieve high electroacoustic performance on the piezoelectric ceramics, there are various approaches. Piezoelectric ceramics in the bulk form have poor electroacoustic properties due to high acoustic impedance. Flexible piezoelectric transducers can be one of the approaches to get better properties. The main design proposed for the problem is the piezocomposite where piezoelectric fibers or particles are embedded in a passive polymer matrix.

In this study, lead-free potassium sodium niobate (KNN) piezoelectric fibers were fabricated using sodium alginate gelation method. The thickness of the sintered fibers could be adjusted depending on the drawing nozzle and 300  $\mu\text{m}$  thick fibers were used in this study. First of all, fibers were obtained with random crystallographic orientation. These fibers were embedded into the polymer matrix and 1-3 piezocomposites were prepared. Capacitance and tan loss measurements were taken at from 1 kHz to 1 MHz frequency range. Dielectric constant and loss of the composite samples were calculated as 81 and 1%, respectively.

Besides fabricating piezocomposites with random oriented fibers, to obtain better properties, the study was done to fabricate textured KNN ceramic fibers. Anisometric template particles, i.e. microscale single crystal particles with non-equax morphology are used in the fabrication of crystallographically textured ceramics as templates. Sodium niobate – NN [NaNbO<sub>3</sub>] templates were synthesized in plate-like morphology by the molten salt synthesis method and in needle-like morphology by the hydrothermal synthesis method. Alginate gelation was used together with the templated grain growth (TGG) method for the first time to fabricate textured (K,Na)NbO<sub>3</sub> based lead-free piezoceramics. KNN with plate-like NN templates was fabricated continuously in ribbon form and KNN with needle-like NN templates was fabricated in fiber form. The micrograph of plate-like NN templates, the textured microstructure of KNN ribbons are given in Figure 1 along with the XRD patterns taken from the surface and the cross-section of the ribbon, demonstrating the crystallographic texture in <001> direction.

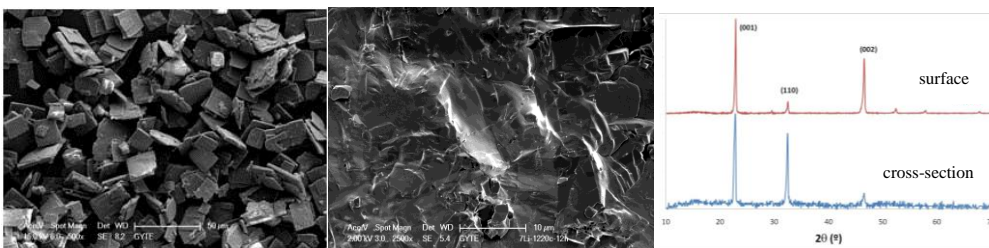


Fig. 59: (a) Plate-like NN templates, (b) Microstructure and (c) XRD patterns of textured KNN ribbons.

---

## **Pb-based ceramics: Domains**

CLUB C

*Wednesday, July 24 2013, 10:30 am - 12:00 pm*

Chair: **Celine Lichtensteiger**  
*DPMC - University of Geneva*



## Study of Domain Structure and Phase Transitions in $\text{Pb}(\text{Zr}_{1-x}\text{Ti}_x)\text{O}_3$ Single Crystals

Zuo-Guang Ye, Yujuan Xie, Alexei A. Bokov and Xifa Long

Department of Chemistry and 4D LABS, Simon Fraser University,  
Burnaby, BC, V5A 1S6, Canada

Email: zye@sfu.ca

$\text{PbZr}_{1-x}\text{Ti}_x\text{O}_3$  (PZT) system has been extensively studied over the past decades for both industrial applications and fundamental research. Recently,  $\text{PbZr}_{1-x}\text{Ti}_x\text{O}_3$  single crystals with compositions ( $0.2 \leq x \leq 0.65$ ) across the morphotropic phase boundary (MPB) region have been grown in our laboratory by a top-seeded solution growth (TSSG) technique. The availability of PZT single crystals makes it possible to systematically investigate the correlation between structural evolution and electrical properties in PZT system.

In this work, the domain structure and phase transitions of PZT single crystals with compositions  $x=0.32$ ,  $x=0.42$ ,  $x=0.46$  and  $x=0.62$  are studied by polarized light microscopy (PLM), piezoresponse force microscopy and dielectric measurements. PLM observation shows an increase of extinction angle in the two rhombohedral crystals:  $x=0.32$  at  $340^\circ\text{C}$ , and  $x=0.42$  at  $250^\circ\text{C}$ , indicating a thermally induced polarization rotation accompanied with the rhombohedral (R) to monoclinic (M) phase transition. The ferroelectric to paraelectric phase transition in  $x=0.32$  is of first order with a discontinuous change of birefringence around  $T_C=351^\circ\text{C}$ . The dielectric measurements show anomalies below  $T_C$ , confirming the R-M phase transitions in both crystals. For the MPB composition  $x=0.46$ , PLM shows a monoclinic symmetry with complicated domain at room temperature, which upon heating changes to a tetragonal phase at about  $286^\circ\text{C}$  and then to a cubic phase at  $T_C=394^\circ\text{C}$ . Crystals of composition  $x=0.46$  exhibit the best piezoelectric properties, with a piezoelectric constant  $d_{33}=1223$  pC/N and an electromechanical coupling factor  $k_{33}=80\%$ . The (100) plate of the tetragonal crystal with composition  $x=0.62$  is optically isotropic, but the (011) plate shows a small birefringence at  $45^\circ$  (angle between polarizer and  $\langle 100 \rangle$  direction). This is because of the formation of nano-sized tetragonal domains due to the instability of the ferroelectric phase. A total compensation is achieved in the (100) plate, but in the (011) plate the compensation is only partial. By applying an electric field, macroscopic domains can be induced in a (100) plate at a field of  $25\text{kV/cm}$  and the crystal becomes anisotropic. Birefringence becomes larger with increasing field and shows a maximum value  $\Delta n=0.012$  at the field of  $30\text{kV/cm}$ . After the electric field is removed, the crystal changes back to isotropic, indicating the field induced macroscopic domain is metastable. We discuss the mechanisms for the formation of domain structures and phase transitions in PZT single crystals and compared them with the behaviour and mechanisms of relaxor ferroelectrics.

*This work is supported by the Office of Naval Research (Grants No. N00014-11-1-0552 and N00014-12-1-1045) and the Natural Science and Engineering Research Council of Canada.*

## Morphotropic interfaces in $\text{Pb}(\text{Mg}_{1/3}\text{Nb}_{2/3})\text{O}_3\text{-PbTiO}_3$ single crystals

I. Rafalovskyi<sup>1</sup>, M. Guennou<sup>1</sup>, I. Gregora<sup>1</sup>, and J. Hlinka<sup>1</sup>

<sup>1</sup>Institute of Physics, Academy of Sciences of the Czech Republic  
Na Slovance 2, 182 21 Prague 8, Czech Republic

Email: [hlinka@fzu.cz](mailto:hlinka@fzu.cz)

Large electromechanical coupling constant, piezoelectric coefficient and strain level of poled  $(1-x)\text{Pb}(\text{Mg}_{1/3}\text{Nb}_{2/3})\text{O}_3\text{-}x\text{PbTiO}_3$  (PMN- $x$ PT) single crystals have attracted considerable interest because of their excellent performance in various solid state electromechanical sensors and actuators.<sup>207,208,209</sup> It is well understood that the piezoelectricity results from the ferroelectric ordering and that the best piezoelectric figures of merit are found in materials with the composition corresponding to the so-called morphotropic phase boundary.<sup>3</sup> This phase boundary is only very weakly temperature dependent, but in a narrow concentration region around  $x \approx .33$  (which precisely comprises in the materials of technological interest), one may typically pass from the rhombohedral-like phase to the tetragonal-like phase at a certain<sup>210</sup> temperature  $T_{\text{RT}}$ , i.e. one may cross the MPB also upon heating.

Here we have investigated passage across the  $T_{\text{RT}}$  temperature in 0.68PMN-0.32PT single crystal and in the course of our studies we have observed formation of macroscopic planar interfaces between the rhombohedral-like and tetragonal-like phase, or, in other words, interfaces that could be denoted as "real-space morphotropic phase boundaries". The optical observation has been complemented by Raman spectroscopy investigations what allowed to establish several interesting links to the previous observations.

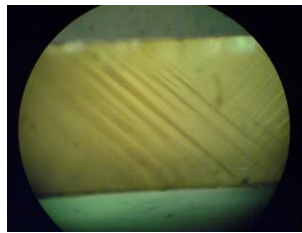


Fig. 60: Mesoscopic stripe pattern formed in a PMN-PT crystal by heating after a field-cooling process.

<sup>207</sup> S. E. Park and T. R. Shrout, "Ultra-high strain and piezoelectric behavior in relaxor based ferroelectric single crystals", *J. Appl. Phys.*, vol. 82, p. 1804, 1997.

<sup>208</sup> D. Damjanovic, M. Budimir, M. Davis and N. Setter, "Monodomain versus polydomain piezoelectric response of  $0.67\text{Pb}(\text{Mg}_{1/3}\text{Nb}_{2/3})\text{O}_3\text{-}0.33\text{PbTiO}_3$  single crystals along nonpolar directions", *Appl. Phys. Lett.*, vol. 83, p. 527, 2003.

<sup>209</sup> S. Zhang and F. Li, "High performance ferroelectric relaxor- $\text{PbTiO}_3$  single crystals: Status and perspective", *J. Appl. Phys.*, vol. 111, p. 031301, 2012.

<sup>210</sup> Z. Feng, X. Zhao, and H. Luo, "Bias field effects on the dielectric properties of  $0.67\text{Pb}(\text{Mg}_{1/3}\text{Nb}_{2/3})\text{O}_3\text{-}0.33\text{PbTiO}_3$  single crystals with different orientations", *Solid State Commun.*, vol. 130, p. 591, 2004.

## ***In situ* TEM on Phase Transitions in Perovskite Ceramics**

Xiaoli Tan, Hanzheng Guo, Cheng Ma

Department of Materials Science and Engineering, Iowa State University, Ames, Iowa/USA

Email: xtan@iastate.edu

Perovskite oxides are rich in electric field-induced phase transitions, such as the relaxor-to-ferroelectric and antiferroelectric-to-ferroelectric ones. In this study, electric field *in-situ* TEM technique is used to investigate the seemingly unlikely ferroelectric-to-relaxor and ferroelectric-to-antiferroelectric transitions at room temperature. Specifically, antiferroelectric  $\text{Pb}_{0.99}\text{Nb}_{0.02}[(\text{Zr}_{0.57}\text{Sn}_{0.43})_{0.92}\text{Ti}_{0.08}]_{0.98}\text{O}_3$  (PNZST43/8/2) and relaxor  $\text{Pb}_{0.92}\text{La}_{0.08}(\text{Zr}_{0.65}\text{Sn}_{0.35})\text{O}_3$  (PLZT8/65/35) ceramics are focused in this study.

During the application of the very first cycle of electric field to these ceramics, the electric field in the first quarter cycle transforms the antiferroelectric PNZST43/8/2 or the relaxor PLZT8/65/35 phase into a ferroelectric phase. The “induced ferroelectric phase” is metastable and its polarization is largely preserved during the second quarter cycle. The remanent polarization is switched to the reversed direction in the third quarter cycle when the electric field with reversed polarity increases. The coercive field,  $E_C$ , is at the intercept of the polarization curve with the electric field axis in the third quarter cycle. Presumably, the induced metastable ferroelectric phase behaves as a normal ferroelectric and switches its polarization through a normal domain nucleation and growth process. However, there have been indications that this polarization reversal is quite unusual and unique because it takes place through seemingly unlikely phase transitions at close vicinity of  $E_C$ . These reverse phase transitions produce “transient antiferroelectric” and “transient relaxor” phases during the polarization switching process of the induced ferroelectric phase. These transient phases are directly visualized in real time at nanometer resolution with the electric field *in-situ* TEM technique.

In addition, electric field-induced phase transitions in  $(\text{K}_{0.5}\text{Na}_{0.5})\text{NbO}_3$ -based ceramics were also investigated with the *in situ* TEM technique.

## Heat treatment effects on domain configuration and strain behavior under electric field in undoped $\text{Pb}[\text{Zr}_x\text{Ti}_{1-x}]\text{O}_3$ ferroelectrics

Ljubomira Ana Schmitt<sup>1</sup>, Hans Kungl<sup>2</sup>, Manuel Hinterstein<sup>3</sup>, Hans-Joachim Kleebe<sup>1</sup>,  
Michael J. Hoffmann<sup>2</sup>, Hartmut Fuess<sup>1</sup>

<sup>1</sup>Institute of Materials and Geo-Sciences, Technische Universität Darmstadt,  
64287 Darmstadt, Germany

<sup>2</sup>Institute for Ceramics and Mechanical Engineering, Karlsruhe Institute of Technology,  
76131 Karlsruhe, Germany

<sup>3</sup>Institut für Werkstoffwissenschaften, Technische Universität Dresden,  
01062 Dresden, Germany

Email: [Ljuba@st.tu-darmstadt.de](mailto:Ljuba@st.tu-darmstadt.de)

Undoped  $\text{Pb}[\text{Zr}_x\text{Ti}_{1-x}]\text{O}_3$  (PZT) ceramics with Zr/Ti ratios 52/48, 52.5/47.5, 56/44 and 57.5/42.5 from the tetragonal and the rhombohedral side of the morphotropic phase boundary were examined. Effects of heat treatments below and slightly above Curie temperature on domain configuration and strain behavior were investigated.

Changes in domain configuration during the heating cycles were observed by *in situ* hot-stage transmission electron microscopy<sup>1</sup>. After cooling down, the domain configurations do not immediately return to their initial shape. However, after exposure at ambient temperature conditions for 96 h, they redevelop to a state largely similar to the initial configuration. During the transient post annealing state, changes in the strain behavior under electric field were found, when comparing the strain behavior of non-heat treated and heat treated ceramics right after cooling. The enhanced response to 4 kV/mm electric fields results in qualitatively different effects for PZT from the tetragonal side and from the rhombohedral side of the morphotropic phase boundary.

Overall the experiments show that after annealing the domain configuration is reversible, but time is required to return to the initial patterns. During the transient non equilibrium state, enhanced influence of electric field was detected, which may show up in different forms, depending on the material and the level of the electric fields applied.

<sup>1</sup> L. A. Schmitt, R. Theissmann, J. Kling, H. Kungl, M. J. Hoffmann and H. Fuess “*In situ* hot-stage transmission electron microscopy of  $\text{Pb}(\text{Zr}_{0.52}\text{Ti}_{0.48})\text{O}_3$ ”, *Phase Transitions*, vol. 81, p. 323-329, 2008.

## Field-induced phase transitions in soft $\text{Pb}(\text{Zr}_{1-x}\text{Ti}_x)\text{O}_3$ at the morphotropic phase boundary

Yo-Han Seo<sup>1</sup>, Daniel J. Franzbach<sup>1,2</sup>, Jurij Koruza<sup>3</sup>, Andreja Benčan<sup>3</sup>, Barbara Malič<sup>3</sup>, Marija Kosec<sup>3</sup>, Jacob L. Jones<sup>4</sup>, Kyle G. Webber<sup>1</sup>

<sup>1</sup>Institute of Materials Science, Technische Universität Darmstadt, 64287, Darmstadt, Germany

<sup>2</sup>Graduate School of Computational Engineering, Technische Universität Darmstadt, 64287, Darmstadt, Germany

<sup>3</sup>Jožef Stefan Institute, Jamova c. 39, Si-1000, Ljubljana, Slovenia

<sup>4</sup>Department of Materials Science and Engineering, University of Florida, 32611, Gainesville, FL, USA

Email: [webber@ceramics.tu-darmstadt.de](mailto:webber@ceramics.tu-darmstadt.de)

Ferroelectric lead zirconate titanate,  $\text{Pb}(\text{Zr}_{1-x}\text{Ti}_x)\text{O}_3$  (PZT), displays well-known nonlinear ferroelectric and ferroelastic behavior during electrical and mechanical loading resulting in hysteretic behavior. It has been demonstrated that both the ferroelectric and ferroelastic behavior of PZT are influenced by the composition, where enhanced ferroelectricity and ferroelasticity are observed at the morphotropic phase boundary (MPB), which separates the ferroelectric rhombohedral and ferroelectric tetragonal phases in the composition-temperature phase diagram. Some investigators have attributed the enhanced properties at the MPB to the coexistence of the tetragonal and rhombohedral phases, the presence of an additional monoclinic  $Cm$  phase, or the existence of nanopolar regions in the MPB region of PZT. These works, however, have not addressed the influence of an external electrical or mechanical field on the stable phase in PZT.

Recent ferroelectric and ferroelastic measurements of various PZT compositions ( $\text{Pb}_{0.98}\text{Ba}_{0.01}(\text{Zr}_{1-x}\text{Ti}_x)_{0.98}\text{Nb}_{0.02}\text{O}_3$ ,  $0.40 < x < 0.60$ ) in the vicinity of the MPB have shown exceptionally large remanent strain-to-switching strain ratios, in some compositions above the theoretical values allowed by domain switching alone (Fig. 1). This strongly indicates the presence of hysteretic processes in addition to ferroelectricity and ferroelasticity during the application of an external field. To further investigate this observed behavior, a phenomenological free energy analysis was used to predict the effects of electric field and stress on the stable phase in ferroelectrics and predict the susceptibility of the rhombohedral and tetragonal structure to a field-induced phase transition. Modeling results were in very good agreement with experimental observations and indicate the relative importance of such phase transitions on

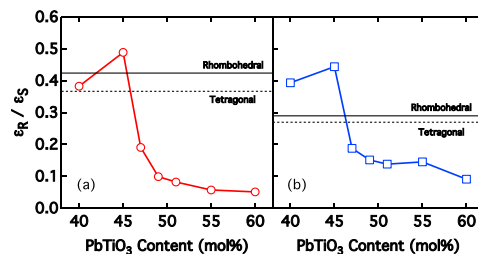


Fig. 61: The measured ratio of remanent strain produced during electrical (a) and mechanical (b) loading to the switching strain is shown for various PZT compositions. The theoretical maximum ratio values allowed by ferroelectricity and ferroelasticity in a polycrystalline are also shown for the rhombohedral (solid line) and tetragonal (dotted line) phases. The maximum applied electric field and stress were 6 kV/mm and -400 MPa.

macroscopic behavior, giving an indirect method to observe field-induced phase transitions in polycrystalline ferroelectrics.

## Depolarization of High Temperature $x\text{PbTiO}_3 - y\text{BiScO}_3 - z\text{Bi}(\text{Ni}_{1/2}\text{Ti}_{1/2})\text{O}_3$ Ternary Perovskite Piezoelectric System

Troy Ansell<sup>1</sup>, David Cann<sup>1</sup>

<sup>1</sup>School of Mechanical, Industrial, and Manufacturing Engineering, Oregon State University, Corvallis, OR/USA

Email: [ansellt@onid.orst.edu](mailto:ansellt@onid.orst.edu)

Most common piezoelectric systems that incorporate lead titanate (PT)<sup>211</sup> experience a degradation in the poled state upon heating at temperatures below the Curie temperature ( $T_C$ ). This phenomenon, known as the depolarization temperature ( $T_D$ ), is observed in poled materials through five different methods<sup>212</sup>: *in-situ* X-ray diffraction, dielectric loss measurements, *in-situ*  $d_{33}$ , temperature-stimulated current (TSC), and the piezoelectric resonance method. All of these measurements were applied to the high temperature piezoelectric system  $x\text{PbTiO}_3 - y\text{BiScO}_3 - z\text{Bi}(\text{Ni}_{1/2}, \text{Ti}_{1/2})\text{O}_3$  (PT-BS-BNiT). For different compositions, the value of  $T_D$  ranged between 275 °C – 375°C. It has also been observed that the values of the piezoelectric coefficient increased as the temperature is raised in *in-situ*  $d_{33}$  [pm/V].

Fig. 1 displays an example of the depolarization via an *in-situ*  $d_{33}$  measurement for the composition  $x = 50, y = 30, z = 20$ . The depolarization of soft PZT is included for comparison. This ternary PT-BS-BNiT system includes two binary systems PT-BS and PT-BNiT and this research demonstrates that both  $d_{33}$  and  $T_D$  increase as the composition moves from PT-BNiT to PT-BS.

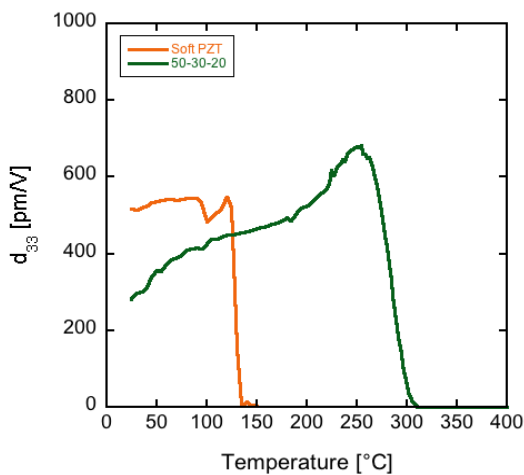


Figure 1. The depolarization of the composition 50PT-30BS-20BNiT is shown as compared to soft PZT. The temperature of depolarization is the temperature at which the value of  $d_{33}$  begins to drop off.

<sup>211</sup> A. Sehirlioglu, A. Sayir, F. Dynys, "Doping of BiScO<sub>3</sub>-PbTiO<sub>3</sub> Ceramics for Enhanced Properties," J. Am. Ceram. Soc., vol. 93, p 1718-1724, 2010.

<sup>212</sup> E. A. Anton, W. Jo, D. Damjanovic, J. Rödel, "Determination of depolarization temperature of (Bi<sub>1/2</sub>Na<sub>1/2</sub>)TiO<sub>3</sub>-based lead-free piezoceramics," J. Appl. Phys., vol. 110, p. 094108 1-14, 2011.



---

## **Pb-free film processing**

CLUB A

*Wednesday, July 24 2013, 02:00 pm - 03:30 pm*

Chair: **Jon Ihlefeld**  
*Sandia National Laboratories*

## Growth and size control of $\text{Bi}_4\text{Ti}_3\text{O}_{12}$ nanowalls and their piezoelectric property

Tomoaki Yamada<sup>1,2</sup>, Takaaki Shibata<sup>1</sup>, Koji Ishii<sup>3</sup>, Masahito Yoshino,<sup>1</sup> Junichi Kimura<sup>4</sup>, Hiroshi Funakubo<sup>4</sup>, and Takanori Nagasaki<sup>1</sup>

<sup>1</sup>Department of Materials, Physics and Energy Engineering, Nagoya University, Nagoya, Japan

<sup>2</sup>PRESTO, Japan Science and Technology Agency, Tokyo, Japan

<sup>3</sup>Asylum Technology Co., LTD., Tokyo, Japan

<sup>4</sup>Department of Innovative and Engineered Material, Tokyo Institute of Technology, Yokohama, Japan

Email: [t-yamada@nucl.nagoya-u.ac.jp](mailto:t-yamada@nucl.nagoya-u.ac.jp)

Large piezoelectricity in ferroelectric materials attracts attentions for developing small energy conversion devices such as micro actuators and energy harvesters. It has been theoretically and experimentally shown that the piezoelectric response in the ferroelectric film is strongly suppressed as the film is mechanically clamped by the substrate. On the contrary, the nanostructure with large aspect ratio (for instance, nanorod) can offer exceeding properties as such a clamping effect can be ignored. So far, the fabrication of  $\text{Pb}(\text{Zr},\text{Ti})\text{O}_3$  nanorods by FIB<sup>213</sup> and by self-assembled growth<sup>214</sup> having enhanced piezoelectric property has been demonstrated; however, such nanostructures of other ferroelectrics –especially, *lead-free ferroelectrics*– have been rarely reported. In this presentation, we demonstrate the growth of size controlled  $\text{Bi}_4\text{Ti}_3\text{O}_{12}$  (BIT) nanowall structure by utilizing its growth anisotropy, and investigate their piezoelectric property.

BIT was epitaxially grown on  $\text{TiO}_2(101)$  substrate<sup>215</sup> with  $a(b)$ -axis orientation at different temperatures and oxygen pressures by pulsed laser deposition. It was found that, by depositing BIT at temperatures below 700 °C, the nanowall-like structure was formed. As shown in Fig. 1, BIT grew fast with  $a$ - and  $b$ -axes and slow with  $c$ -axis. Therefore, it can be said that the formation of the BIT nanowalls is driven by the strong anisotropy of the growth rate of BIT. In addition, the width of nanowalls decreased with decreasing the deposition temperature (Fig. 2), which implies that the surface diffusivity of PLD species plays a role in changing the width of nanowalls. It was also found that the density of nanowalls can be effectively controlled by the oxygen pressures during the deposition.

The PFM phase (Fig.3) and amplitude (not shown here) of a BIT nanowall show evident ferroelectric and piezoelectric nature. The detailed piezoelectric property and the

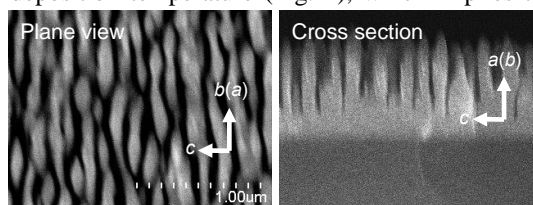


Fig.1 SEM images of  $a(b)$ -axis oriented BIT deposited at 600 °C and 200 mTorr  $\text{O}_2$ .

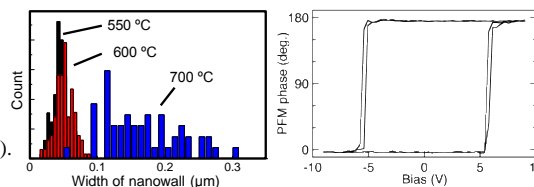


Fig.2 Width of BIT nanowall deposited at 550, 600 and 700 °C under 200 mTorr  $\text{O}_2$ .

Fig.3 PFM phase of BIT nanowall deposited at 600 °C and 200 mTorr  $\text{O}_2$ .

<sup>213</sup> J.-H. Li *et al.*, Appl. Phys. Lett. **84**, 2626 (2004).

<sup>214</sup> T. Yamada *et al.*, ISAF-PFM-2011, July 2011.

<sup>215</sup> T. Watanabe *et al.*, Appl. Phys. Lett. **81**, 1660 (2002).

comparison with the different size of nanowalls are presented.

**Processing and Ferroelectric Properties of undoped and Mn-doped  $x[\text{Bi}_{0.5}\text{Na}_{0.5}\text{TiO}_3]-(1-x)[\text{Bi}_{0.5}\text{K}_{0.5}\text{TiO}_3]-(0.04)[\text{Bi}_{0.5}\text{Li}_{0.5}\text{TiO}_3]$  Thin films**

M. Hejazi, A. Safari  
Glenn Howatt Electroceramics Laboratory  
Department of Materials Science and Engineering, Rutgers University  
607 Taylor Rd, Piscataway, NJ 08854

Lead free thin films with different compositions  $\text{Bi}_{0.5}(\text{Na}_{0.76}\text{K}_{0.2}\text{Li}_{0.04})_{0.5}\text{TiO}_3$  (BNKLT76) and  $\text{Bi}_{0.5}(\text{Na}_{0.88}\text{K}_{0.08}\text{Li}_{0.04})_{0.5}\text{TiO}_3$  (BNKLT88) were deposited on  $\text{SrRuO}_3$  coated (001)- $\text{SrTiO}_3$  substrates by pulsed laser deposition technique. The effects of oxygen pressure and Mn-doping on the leakage current, ferroelectric and dielectric properties were investigated. It was found that polarization and permittivity of BNKLT76 composition is higher than those of BNKLT88 thin films. However, it suffers from high dielectric loss and leakage current. To improve the insulating properties, ceramic targets were doped with 2 mol.% Mn. The remnant polarization and dielectric constant (at 10 kHz) of Mn-doped BNKLT76 film deposited at 400 mtorr were measured to be  $23 \mu\text{C}\cdot\text{cm}^{-2}$  and 660, respectively. The leakage current density of Mn-doped films was suppressed by more than two orders of magnitude and the polarization was considerably enhanced. It was also demonstrated that Mn doping decreases the dielectric loss without any adverse effect on permittivity. The XPS results showed coexistence of  $\text{Mn}^{2+}$ ,  $\text{Mn}^{3+}$ , and  $\text{Mn}^{4+}$  in doped-films. Oxidation of  $\text{Mn}^{2+}$  to higher valence states by absorbing holes along with occupation of A-site vacancies might be possible reasons for a reduced leakage current and dielectric loss in Mn-doped films.

## Bi-based Piezoelectric Thin Films via Chemical Solution Deposition

Yu Hong Jeon<sup>1</sup>, Eric Patterson<sup>2</sup>, David P. Cann<sup>1</sup>, Peter Mardilovich<sup>3</sup>, William Stickle<sup>3</sup>, and Brady J. Gibbons<sup>1</sup>

<sup>1</sup>Materials Science, School of Mechanical, Industrial, & Manufacturing Engineering, Oregon State University, Corvallis, OR 97331 (USA)

<sup>2</sup>Institute of Materials Science, Technische Universität Darmstadt, Darmstadt, 64287, Hesse, Germany

<sup>3</sup>Hewlett-Packard Corporation, Corvallis, OR 97330 (USA)

Email: brady.gibbons@oregonstate.edu

The highest performing piezoelectric materials include lead as a major constituent. Worldwide, increased restrictions on the use of lead have resulted in a search for candidates to replace these lead-based piezoelectric materials. One promising material is the solid solution of  $(\text{Bi}_{0.5}\text{Na}_{0.5})\text{TiO}_3 - (\text{Bi}_{0.5}\text{K}_{0.5})\text{TiO}_3$  (BNT-BKT). Although promising behavior has been observed in bulk materials, similar results have been elusive for BNT-BKT thin films. In this work, 0.8 BNT – 0.2 BKT thin films (near morphotropic phase boundary composition) were synthesized on platinumized silicon substrates via chemical solution deposition. Well-crystallized BNT – BKT thin films were grown at varying processing conditions. Phase purity was confirmed by X-ray diffraction. As Bi, Na, and K are volatile elements, overdoping of these cations (addition of excess cation precursors) was introduced to compensate for volatilization during synthesis. Quantitative compositional analysis of films was performed with electron probe microanalysis and compositional depth profiling to confirm atomic ratios via X-ray photoelectron spectroscopy. The composition data from both measurements were consistent and indicated stoichiometric films were achieved. Dependent on the overdoping and annealing conditions, dense, smooth, crack-free films were achieved with relative dielectric constants from 390 to 730 and low dielectric loss of 2 - 5% at 1 kHz. Additionally, maximum and remanent polarizations of 45 and 16  $\mu\text{C}/\text{cm}^2$ , respectively, were recorded at 200 Hz. The addition of  $\text{Bi}(\text{Mg}_{0.5}\text{Ti}_{0.5})\text{O}_3$  (BMgT) was also explored, as promising piezoelectric response (high field  $d_{33}$  up to 600 pm/V) in bulk compositions has been observed. BNT-BKT-BMgT thin films were prepared, showing very promising piezoelectric response with  $d_{33,f}$  up to 75 pm/V and strain values up to 0.35%, as measured by double beam interferometry (see Fig. 1, with values compared to typical Pb-based thin films).<sup>216</sup> Finally, Rayleigh analysis was completed on several Bi-based thin film compositions

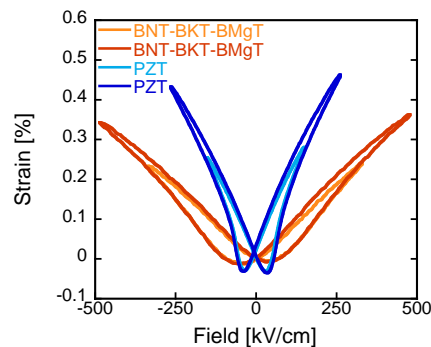


Figure 62: Strain measurements of BNT-BKT-BMgT thin films compared to typical lead zirconate titanate (52/48) solution derived thin films.

<sup>216</sup> Y-H. Jeon, *et al.* "Large piezoresponse and ferroelectric properties of  $(\text{Bi}_{0.5}\text{Na}_{0.5})\text{TiO}_3 - (\text{Bi}_{0.5}\text{K}_{0.5})\text{TiO}_3 - \text{Bi}(\text{Mg}_{0.5}\text{Ti}_{0.5})\text{O}_3$  thin films prepared by chemical solution deposition," *J. Am. Ceram. Soc.*, in press.

to extract the intrinsic and extrinsic contributions to the dielectric properties.

## Realization and characterization of manganese-doped BST thin films for reflect array applications

Hartmut W. Gundel<sup>1</sup>, Kevin Nadaud<sup>1</sup>, Caroline Borderon<sup>1</sup>, Sabrina Pavy<sup>1</sup>, Raphaël Gillard<sup>2</sup>

<sup>1</sup>IETR, University of Nantes, Nantes, France

<sup>2</sup>IETR, INSA of Rennes, Rennes, France

E-mail: Hartmut.gundel@univ-nantes.fr

Ferroelectric thin films are attractive materials for tunable microwave devices such as electrically tunable filters, reflect arrays, resonators or phase shifters. For this type of application, the ferroelectric material should have an important tunability of the dielectric permittivity and low dielectric losses. It is well known that the dielectric properties strongly depend on the material's microstructure and that they are particularly sensitive to existing defects. In perovskite type ferroelectric thin films, oxygen vacancies play an important role as these defects create conduction in the film and losses may be important; hence it becomes necessary to dope the film in order to reduce the influence of the defects.

Mn-doped  $\text{Ba}_{(1-x)}\text{Sr}_x\text{TiO}_3$  (BST) thin films already have been realized by Chemical Solution Deposition (CSD) on stainless steel substrates<sup>217</sup> and the influence of its morphology on the dielectric properties has been shown<sup>218</sup>.  $\text{Ba}_{(1-x)}\text{Sr}_x\text{TiO}_3$  is a mixed compound of  $\text{BaTiO}_3$  and  $\text{SrTiO}_3$  which is widely studied because its Curie temperature depends on the ratio between barium and strontium in the material. This allows tailoring the material for a use at room temperature either in the ferroelectric or in the paraelectric phase.

In the present work, Mn-doped  $\text{Ba}_{0.80}\text{Sr}_{0.20}\text{TiO}_3$  (BST) thin films were realized by Chemical Solution Deposition (CSD) on alumina as the foreseen application for a reflect array needs integration of the ferroelectric on an insulating substrate. This allows utilization of the tunable dielectric permittivity in a CoPlanar Waveguide (CPW) technology.

In order to compensate the electrons released by the oxygen vacancies, we have studied manganese doping which acts as an electron acceptor, substituting the titanium ions. As the optimum dopant rate to be inserted depends on the material's defect density, we have investigated BST doping with a manganese content ranging from 0% to 2%. The dielectric and electrical characteristics were investigated as a function of Mn content in the frequency range of 100 Hz to 10 GHz. Depending on the expected application, a compromise between high tunability and low dielectric losses thus can be established by using the appropriate amount of the dopant. .

<sup>217</sup> C. Borderon, D. Averty, R. Seveno, H.W. Gundel, "Preparation and characterization of barium strontium titanate thin films by chemical solution deposition", *Ferroelectrics* **362** (2008) 1-7

<sup>218</sup> C. Borderon, D. Averty, R. Seveno, H.W. Gundel, "Influence of the morphology of Barium Strontium Titanate thin films on the ferroelectric and dielectric properties", *Integrated Ferroelectrics* **97** (2008) 12-19

## Ferroelectric properties of ultrathin SrTiO<sub>3</sub> films epitaxially grown on graphene

Peter K Petrov<sup>1</sup>, Bin Zou<sup>1</sup>, Clementine Walker<sup>1</sup>, Ling Hao<sup>2</sup>, Edward Romans<sup>3</sup>, Arnaud Blois<sup>3</sup>, Sergiy Rozhko<sup>3</sup>, Norbert Klein<sup>1</sup>, Olena Shaforost<sup>1</sup>, Cecilia Mattevi<sup>1</sup>, Neil Alford<sup>1</sup>

<sup>1</sup>Department of Materials, Imperial College London, London SW7 2AZ, UK

<sup>2</sup>National Physical Laboratory, Teddington, TW11 0LW, UK

<sup>3</sup>University College London, London WC1E 7JE, UK

Email: p.petrov@imperial.ac.uk

Graphene is attracting enormous scientific attention due to its unique properties e.g. electrical conductivity and optical transparency. It is considered as the successor of the costly ITO in large scale and flexible displays.

In this study we investigated the properties of SrTiO<sub>3</sub> (STO) thin films epitaxially grown on graphene layers. Graphene layers were CVD grown on Cu foil and transferred to TiO<sub>2</sub>-terminated STO substrates.

SrTiO<sub>3</sub> layers with thicknesses varying from 10nm to 100 nm were deposited at a temperature of 850 °C, and oxygen pressure ranging from 0.01 mTorr to 300 mTorr using pulsed laser deposition (PLD). The two-dimensional growth of the STO layer was monitored in-situ by RHEED. To measure its electrical properties, the STO film was covered with a 50 nm Au layer using dc magnetron sputtering; and MIM capacitor structures were formed with photolithography followed by ion-milling.

The surface of the STO film was analyzed using AFM, while its crystal structure was examined by x-ray, SEM and TEM. Results of the electrical measurements carried out within a temperature range of 77K up to 100°C will be presented.

The feasibility of detecting the change of magnetisation in such samples with a technique such as SQUID-based microscopy will also be discussed.

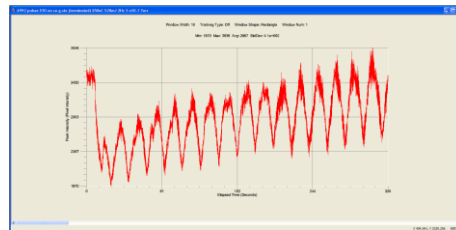


Fig. 63: RHEED oscillations observed during the growth of the STO film on graphene layer. Each maximum represents a complete STO monolayer.

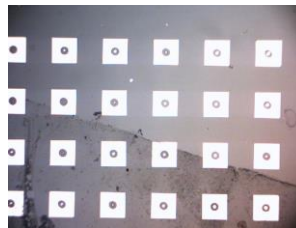


Fig. 2: Optical image of the MIM capacitor structures formed on the top of the graphene/STO/Au multilayer.



## Solgel Hydrothermal Synthesis of BaTiO<sub>3</sub>/MWCNTs for Microelectronic Applications

Amit Mahajan<sup>1</sup>, [Paula M. Vilarinho](mailto:paula.vilarinho@ua.pt)<sup>1</sup>, Angus Kingon<sup>2</sup> and Ákos Kukovecz<sup>3,4</sup>

<sup>1</sup>Department of Materials and Ceramic Engineering, CICECO, University of Aveiro, 3810-193 Aveiro, Portugal

<sup>2</sup>Division of Engineering, Brown University, Providence, Rhode Island 02912, USA

<sup>3</sup>Department of Applied and Environmental Chemistry, Faculty of Sciences, University of Szeged, H-6720 Szeged, Hungary

and

<sup>4</sup>MTA-SZTE “Lendület” Porous Nanocomposites Research Group, 6720 Szeged, Rerrich Béla tér 1.

Email: [paula.vilarinho@ua.pt](mailto:paula.vilarinho@ua.pt)

CNTs have a unique set of mechanical, chemical and electrical properties which make them very promising for the development of nanostructures and nanocomposites. In particular the ballistic electron transport and a huge current - carrying capacity, are of interest for the many future microelectronics applications such as super capacitors, FET and memory cells<sup>1</sup>. Therefore, carbon nanotubes (CNTs) is an interesting option under consideration to be used as templates or bottom electrodes for 3D structures and used as metal filler in polymer and/or Ferroelectric (FE) in order to improve the electrical properties<sup>2</sup>. In the last decades, efforts have been carried out in order to cover MWCNTs with various FE by physical vapor deposition and chemical methods to fabricate 3D capacitor structures<sup>2-4</sup>. Covering CNTs with FE is not a trivial task and many aspects are still unexploited and unclear. Therefore, in this work systematic studies were carried out for the fabrication by a sol gel hydrothermal method of BT/MWCNTs composites and measurement of electrical properties.

Functionalized MWCNTs with HNO<sub>3</sub> were used, having diameter and length around 10-35 nm and ~10 μm, respectively. Barium titanate solution was prepared from barium acetate and titanium isopropoxide precursor. In the BT solution, MWCNTs were dispersed for five minutes using ultra high -sonication followed by 2 h stirring. Potassium hydroxide solution was added in to BT-MWCNTs solution, in order to precipitate BT. The precipitated slurry was transfer to the autoclave and the hydrothermal reaction was carried out from 2 to 24 h and temperatures ranging from 100 to 250 °C to obtained BT-MWCNTs composites. Pure BT powder was also synthesis using similar process for comparison. The composite were characterized by XRD, FTIR, Raman and Electron Microscopy for phase formation and morphology of the composites. The electrical properties were measured using Piezo Force Microscope (PFM) and Impedance spectroscopy.

---

## **Novel Ferroelectric Devices**

CLUB B

*Wednesday, July 24 2013, 02:00 pm - 03:30 pm*

Chair: **Glen Fox**  
*Fox Materials Consulting*

# Planar Laser-Micro Machined Bulk PZT Bimorph For In-Plane Actuation

Sachin Nadig<sup>1</sup>, Serhan Ardanuç<sup>2</sup>, Victor Haas<sup>3</sup>, Amit Lal<sup>4</sup>

<sup>1</sup>Electrical And Computing Engineering, Cornell University, Ithaca, NY 14853,USA

Email: spn36@cornell.edu

In this work, we demonstrate a PZT bimorph technology for high level chip-scale nano-motion actuator integration. Precision piezoelectric stages for linear and rotary motion have proven to be of great value in areas that require accurate positioning and calibration. Ultrasonic motors and piezoelectric actuators such as bimorphs, unimorphs and shear tubes are key elements of these systems. Bimorphs are the most commonly used actuators to maximize displacement. Most bimorphs are macro scale, millimeters in thickness and centimeters in width and length, making it unsuitable for integration in microsystems. Manual assembly of many of these large devices is required for large displacements and this does not lead to small systems. Alternatively, thin film MEMS unimorphs and bimorphs use microns of piezoelectric material (PZT, AlN, ZnO) that generally produce out of plane motion. A miniature bimorph technology that enables many bimorphs to be placed in precision and provide lateral in-plane motion, with single direction of polarization is not available. In this work, we present experimental results on a bimorph fabricated from bulk PZT 4H by laser cutting of PZT plates.

The actuators were fabricated using a commercial laser cutting tool to define beams by cutting entirely through the PZT plate. The laser cutting tool is also used to define arbitrary two-dimensional electrode patterns on the PZT beam. A 10mm long, 0.45mm wide and 0.5mm thick PZT 4H actuator was tested with actuation capabilities of  $\sim 0.08\mu\text{m}/\text{V}$  for single side and  $\sim 0.18\mu\text{m}/\text{V}$  for double sided electrode patterns. Figure 1 shows the process flow and the fabricated bimorph.

Our demonstrated actuator can be useful in low-cost miniature precision nano-motion stages for manipulating MEMS devices. The laser cutting enables a repeatable, high-throughput fabrication process, which creates devices that are capable of larger displacements than conventional bimorphs. While we demonstrate the process on a planar bimorph structure, this also allows fabrication of 3D piezoelectric actuators with arbitrary electrode patterns, allowing engineering of complex displacement profiles.

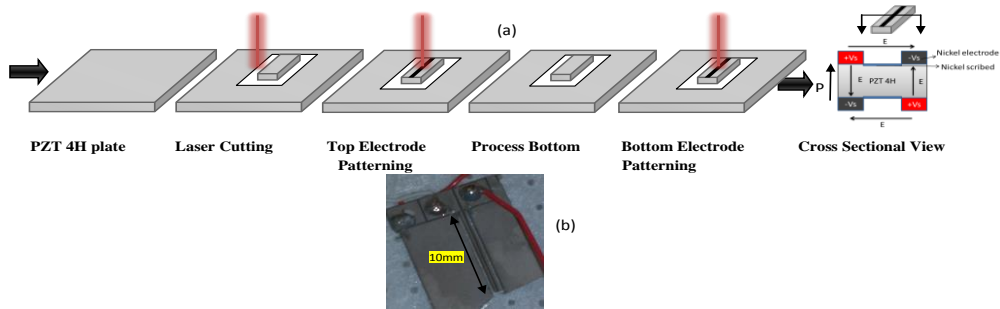


Fig 1 (a) Shows the process flow used for fabricating the Bulk PZT bimorphs. Fig 1 (b) shows the image of the fabricated 10mm long 0.45mm wide and 0.5mm thick bulk PZT bimorph for in-plane actuation.

## Improvement of the Stability of X-ray Emission by the Thermal Excitation of Pyroelectric Crystals

Fumihiko Naruse<sup>1</sup>, Hiroyuki Honda<sup>1</sup>, Yoshikazu Nakanishi<sup>1</sup>,  
Shinji Fukao<sup>1</sup>, Yoshiaki Ito<sup>2</sup>, Yuuki Sato<sup>1</sup>, Shinzo Yoshikado<sup>1</sup>

<sup>1</sup>Graduate School of Science and Engineering, Doshisha University, Kyotanabe, Kyoto, Japan

<sup>2</sup>Institute of Chemical Researches, Kyoto University, Uji, Kyoto, Japan

Email: syoshika@mail.doshisha.ac.jp

A miniaturized X-ray source based on a pyroelectric crystal can be used in portable analytical instruments such as portable X-ray fluorescence spectrometers. The X-ray emission for a long time requires the crystal temperature to be periodically changed to form intense electric fields. Therefore, X-ray is emitted discontinuously. Continuous emission can be achieved by using multiple crystals and changing their temperatures with appropriate phase differences<sup>219</sup>, however, the X-ray intensity is still unstable. When the net amount of charge exceeds a certain threshold, electrostatic creeping discharge occurs along the crystal surface and the X-ray emission suddenly ceases. To avoid such discharge, the initial amount of electric charge on a crystal for each temperature cycle must be equal. It is suggested that the amount of accumulated charges on the surface is dependent on the pressure of ambient gas, amount of electrons supplied, and period of the temperature cycle. In this study, the stability of the X-ray emission using one or six crystal(s) was investigated by changing the temperature cycle period. Furthermore, in order to investigate the contribution of the electrons to the stabilization, electrons were supplied to the space between a crystal and a target using the photoelectric effect using a conventional tube-type X-ray source.

Nonstoichiometric LiTaO<sub>3</sub> single crystals were used. In the case of one crystal, a round copper foil of 20 μm thickness as a target was placed at 15 mm above the negatively charged surface ( $-z$  surface) of the crystal in a chamber made from stainless steel. In order to supply electrons, a conventional tube-type X-ray source (Amptek Mini-X) was attached to the chamber and aluminium plate of 10 mm square and 2 mm thickness as an electron source was placed near the crystal. The tube voltage was 30 kV. The crystal temperature was controlled by the application of triangular voltages to the Peltier device. The temperature range  $\Delta T$ , was fixed at approximately 30 or 40°C. The temperature change period  $L$ , and the tube current  $I$ , were varied. The ambient gas was air and the pressure in the chamber was approximately 10<sup>-4</sup> Pa. X-ray emission was measured using a Si-PIN X-ray detector.

Fig. 1 shows the energy spectra of X-rays per period with one crystal for  $L = 1000$  s. Fig. 2 shows the average count rate of photons of Cu K<sub>α</sub> X-rays with six crystals for  $L =$

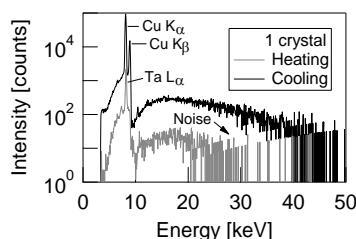


Fig. 1: Energy spectra of X-rays per period for  $L = 1000$  s.

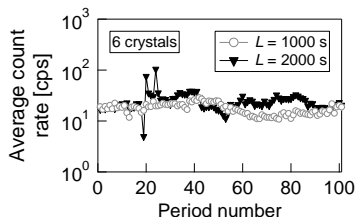


Fig. 2: Average count rate of photons of Cu K<sub>α</sub> X-rays for  $L = 1000$  and  $2000$  s

<sup>219</sup> H. Honda et al., "Evaluation of Compact X-ray Source Using Multiple LiTaO<sub>3</sub> Single Crystals", Key Eng. Mater., vol. 485, p. 295-298, 2011.

1000 and 2000 s. The long-term stability of the X-ray emission was significantly changed when  $L$  was varied.

## New Cooling Technologies based on the Electrocalorics

Brigita Rožič<sup>1,2</sup>, Zdravko Kutnjak<sup>1,2,3</sup>, George Cordoyiannis<sup>1,2,4</sup>, Maja Trček<sup>1</sup>, Hana Uršič<sup>1,2</sup>, Jurij Koruza<sup>1,2,3</sup>, Marko Vrabelj<sup>1,3</sup>, Barbara Malič<sup>1,2,3</sup>, Raša Pirc<sup>1</sup>, S.-G. Lu<sup>5</sup>, Qiming M. Zhang<sup>5</sup>

<sup>1</sup> Jožef Stefan Institute, Jamova cesta 39, 1001 Ljubljana, Slovenia

<sup>2</sup> Centre of Excellence Namaste, Jamova cesta 39, 1001 Ljubljana, Slovenia

<sup>3</sup> Jožef Stefan International Postgraduate School, Jamova cesta 39, 1001 Ljubljana, Slovenia

<sup>4</sup> Department of Physics, University of Athens, 15784 Athens, Greece

<sup>5</sup> Material Research Institute, the Pennsylvania State University, University Park, PA 16802, USA

Email: brigita.rozic@ijs.si

Electrocalorics, materials that exhibit a temperature change under the adiabatically applied/removed electric field, i.e., the electrocaloric effect (ECE), are very important for more energy efficient and environmentally acceptable technologies. An increasing interest in the research of these materials has been revived recently by the predictions of the giant electrocaloric response in some inorganic and organic materials<sup>2,20,2</sup>.

The electrocaloric materials are, in comparison to thermoelectric or magnetocaloric materials, good insulators and because of miniaturization possibilities they are very promising for different applications including household refrigerators, sensors, actuators, heat pumps, devices for cooling microelectronic components, applications in microrobotics, etc.

In this presentation a review of our direct measurements of the ECE in various inorganic and organic bulk, thick and thin films such as relaxor ferroelectric ceramics including PMN, PMN-PT, PLZT, KNN-STO, and thin films of normal ferroelectric and relaxor ferroelectric polymers, i.e., P(VDF-TrFE)-based terpolymers, copolymers and various blends<sup>3,4</sup> will be given. Observed magnitudes of the ECE confirm existence of the large electrocaloric effect in these systems and it was also shown that in bulk relaxor ferroelectrics the ECE behaviour determined from the direct measurements is in a good agreement in the vicinity of the critical point with the theoretical predictions<sup>5</sup>.

### Acknowledgment:

The contribution of Prof. Marija Kosec who passed away in December 2012 is gratefully acknowledged.

<sup>20</sup> A. S. Mischenko et al., "Giant electrocaloric effect in thin-film  $\text{Pb}_{0.95}\text{Ti}_{0.05}\text{O}_3$ ", *Science*, vol. 311, p. 1270-1271, 2006.

<sup>2</sup> B. Neese et al., "Large electrocaloric effect in ferroelectric polymers near room temperature", *Science*, vol. 321, p. 821-823, 2008.

<sup>3</sup> S.-G. Lu et al., "Organic and inorganic relaxor ferroelectrics with giant electrocaloric effect", *Appl. Lett. Phys.*, vol. 97, 162904, 2010.

<sup>4</sup> B. Rožič et al., "Influence of the critical point on the electrocaloric response of relaxor ferroelectrics", *J. Appl. Phys.*, vol. 110, 064118, 2011.

<sup>5</sup> R. Pirc et al., "Electrocaloric effect in relaxor ferroelectrics", *J. Appl. Phys.*, vol. 110, 074113, 2011.

## Photopyroelectric breakdown in Mg-doped LiTaO<sub>3</sub> crystal at second harmonic generation

Kenji Kitamura<sup>1,2</sup>, Hideki Hatano<sup>1,2</sup>, Oleg A. Louchev<sup>3</sup> and Satoshi Wada<sup>3</sup>

<sup>1</sup> National Institute for Materials Science (NIMS), Tsukuba, Ibaraki 305-0044, Japan

<sup>2</sup> SWING Ltd. Tsukuba, Ibaraki 305-0033, Japan

<sup>3</sup> RIKEN, 2-1 Hirosawa, Wako, Saitama, 351-0198, Japan

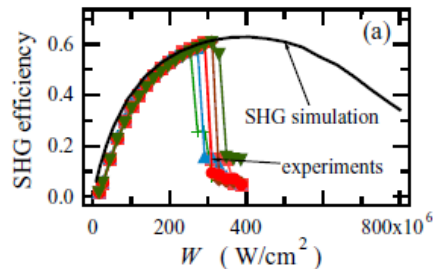
Email:KITAMURA.Kenji@nims.go.jp

Periodically poled ferroelectric crystals such as LiNbO<sub>3</sub> (LN) and LiTaO<sub>3</sub> (LT) are widely used for a variety of laser frequency conversion processes. The theory of nonlinear optical conversion allows reliable efficiency prediction under low intensities. Under high intensities additional effects are involved inhibiting non-linear conversion: two-photon absorption and multi-photon absorption resulting in electron generation into conduction band, heating, harmonics wave vectors mismatch, lensing, and defects generation many of which can be taken into account by performing rigorous computer simulations. However, the theory of optical discharge and consequent damage in dielectrics is often disagrees with the numerous empirical observations and continues to remain in the focus nonlinear optics research closely cooperating with the actively explored fields of laser-matter interactions, laser ablation, laser optical properties modification and recording in dielectrics.

It is generally accepted that in laser-matter interaction the electrons absorbing energy from the radiation dissipate this energy to the lattice and the equilibrium is established for laser pulses extending longer than the electron-to-lattice energy transfer time. We show that additionally to this process an opposite lattice-to-electron energy transfer takes place in nonlinear crystals providing an effective kinetic pathway for discharge during laser frequency conversion.

In particular, we conclude that in the experiments for SHG of 532 nm radiation using a periodically poled SLT crystal the

discharge and damage are due to the following mechanism: (i) the photo-absorption increase during SHG<sup>1</sup> at the back side of the crystal induces (ii) an initial temperature increase of  $\approx 1-1.5$  K in non-symmetric crystal lattice leading to (iii) a high gradient of the spontaneous polarization across the irradiated zone and (iv) to the onset of high electric field,  $\approx 10^4$  V/cm, enabling (v) acceleration of free electrons generated by resonant two-photon absorption to the energy,  $\approx 10-20$  eV (the critical value corresponding to the impact generation of electrons from the valence band in LT is  $\approx 1.5E_g \approx 6.9$  eV), followed by (vi) the impact ionization and structural damage of operating crystal.



SHG efficiency vs  $W$  in PPS LT showing material damage at the input FH pulse power density,  $W=300$  MW/cm<sup>2</sup>



Fig. 2: Structural damage close to the output face of SLT SHG device left by 5 series of experiments.

<sup>1</sup>LO.A.Louchev, N-E, Yu, S. Kurimura, K.Kitamura, Appl. Phys. Lett. **87** 131101 (2005).



**Photoconductivity from Electrospun Bismuth Ferrite Nanofibers**

R. Rivera, R. Kappera, M. Chhowalla and A. Safari

Department of Materials Science and Engineering

Rutgers, The State University of New Jersey, New Jersey, USA

Email: [rutri10@eden.rutgers.edu](mailto:rutri10@eden.rutgers.edu)

Bismuth ferrite (BFO) has attracted great attention not only because of its potential applications as a multiferroic material in the spintronics, and micro-electromechanical area but also because of its photo-electronic behavior in energy harvesting fields. Regardless of the great interest in BFO for ferroelectric applications, there are only a few studies on the photoconductivity of this material. In this investigation, we report the observation of photoconductivity from multiferroic BFO nanofibers whose photo response varies with the diameter of the nanofiber. Bismuth ferrite nanofibers were deposited on oxidized silicon and quartz substrates using a sol-gel based electrospinning technique. The thickness of the fibers was well controlled by varying the molar ratio of the precursor solution. X-ray photoelectron spectroscopy (XPS) results showed a combination of Fe<sup>3+</sup> and Fe<sup>2+</sup> valence states in the fibers. Rutherford backscattering spectroscopy (RBS) results showed a stoichiometric composition after heat treatment. Both scanning electron microscopy (SEM) and atomic force microscopy (AFM) images revealed that the fiber structure is uniform in diameter, ranging from 15 to 100 nm and several microns in length as well. Photoconductivity measurements show a considerable increase in the current flowing through the fibers when measured under illumination. This photoresponse behavior is almost 100 times higher for a fiber of 50 nm diameter than for a fiber of 15 nm. This effect is described by a size-dependent surface recombination mechanism.

## Application of PIN-PMN-PT:Mn in High-Performance Flame Detectors

A. Movchikova<sup>1</sup>, N. Neumann<sup>1</sup>

<sup>1</sup>InfraTec GmbH, Gostritzer Str. 61-63, 01217 Dresden, Germany

Email: a.movchikova@infratec.de

Ferroelectric relaxor-PbTiO<sub>3</sub> single crystals were reported to be the most promising candidates for pyroelectric applications, because of their ultra-high pyroelectric coefficient and relatively low dielectric loss<sup>221</sup>. In our previous works was shown that PMN-0.26PT:Mn and PMN-0.29PT:Mn crystals, outperforms LiTaO<sub>3</sub> (LTO) crystals in pyroelectric detectors by a 3 times higher specific detectivity<sup>222</sup>. Unfortunately, rhombohedral PMNT single crystals exhibit low phase transition temperatures ( $T_{RT} \approx 100^\circ\text{C}$ ), which limit the processing temperature during fabrication and also the operating temperature range. Therefore, more attention is focused on the ternary solid solution system  $x\text{PIN}-y\text{PMN}-(1-x-y)\text{PT}$ , PIMNT which is distinguished by a higher Curie temperature<sup>223</sup>. In this work the suitability of Mn-doped 0.26PIN-0.42PMN-0.32PT single crystals in single and quad channel flame detectors was evaluated and compared with standard LTO.

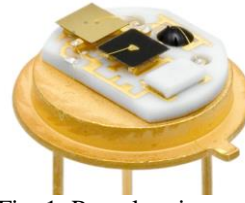


Fig. 1: Pyroelectric detector based on PIMNT

The phase transitions, dielectric and pyroelectric properties of rhombohedral phase [111] oriented 0.26PIN-0.42PMN-0.32PT single crystals were investigated. InfraTec's detector design PIE-205 operating in current mode were used for the evaluation. In addition detectors based on LiTaO<sub>3</sub> were prepared for an easier comparison. Responsivity and noise of both detectors were measured in the frequency range 0.1 Hz – 10 kHz at room temperature. The specific detectivity was calculated from signal and noise measurements (Table 1).

The evaluation shows that also Mn doped PIN-PMN-PT based detectors outperform the standard LiTaO<sub>3</sub> based detectors especially in the low frequency range of 1-10 Hz. Based on this basic design a new generation of high-performance long-range flame detectors will be established.

Table 1: Material properties and detector performance of PIN-PMN-PT, LiTaO<sub>3</sub> single crystals

Pyroelectric material	Detector Type	Element Size	Thickness	p	$\epsilon_r$	$\tan\delta$	$T_{RT}$	$T_C$	$D^*$ (500 K, 10 Hz, BW 1Hz, 25°C) cmHz <sup>1/2</sup> /W
		mm <sup>2</sup>	$\mu\text{m}$	$\mu\text{C}/\text{m}^2/\text{K}$	(1 kHz)	(1 kHz)	°C	°C	
PIMNT	PIE-205	2.0 x 2.0	33	730	525	0.0003	125	181	$9.5 \times 10^8$
LT	LIE-205	2.0 x 2.0	24	175	43.5	0.0001	-	603	$3.6 \times 10^8$

<sup>221</sup> Y. Tang. "Large pyroelectric response in relaxor-based ferroelectric  $(1-x)\text{Pb}(\text{Mg}_{1/3}\text{Nb}_{2/3})\text{O}_3-x\text{PbTiO}_3$  single crystals", J. Appl. Phys., vol. 98, 084104, 2005

<sup>222</sup> N. Neumann, M. Es-Souni, H. Luo. "Application of PMN-PT in pyroelectric detectors", Proc ISAF-IMF-2009, August 23-29, 2009, Xi'an, China.

<sup>223</sup> N. Yasuda. "Crystal growth and electrical properties of lead indium niobate-lead titanate binary single crystal", J. Cryst. Growth, vol. 229, p.299-304, 2001.

---

## Capacitors

CLUB C

*Wednesday, July 24 2013, 02:00 pm - 03:30 pm*

Chair: **Satoshi Wada**  
*University of Yamanashi*

## The effects of Sn<sup>2+</sup> ion doping on perovskite titanates

Shoichiro Suzuki<sup>1</sup>, Atsushi Honda,<sup>1</sup> Naoki Iwaji,<sup>1</sup> Shin'ichi Higai,<sup>1</sup> Akira Ando<sup>1</sup>

<sup>1</sup>Murata Manufacturing Co., Ltd. 1-10-1 Higashikotari, Nagaokakyo, Kyoto 617-8555, Japan

Email: shoichiro\_suzuki@murata.co.jp

It is well known that ferroelectric perovskite titanates (ATiO<sub>3</sub>) are important materials for applied electronics industries. The substitution of Sn<sup>2+</sup> ions into the A sites of the perovskite lattice has recently been a subject of intensive research, because this is a promising approach for the fabrication of Pb-free ferroelectric materials.<sup>1</sup> However, the synthesis of ferroelectric ATiO<sub>3</sub> of which A sites are substituted with Sn<sup>2+</sup> ions has been found to be difficult from several studies.<sup>2</sup>

In recent studies, we have fabricated Sn<sup>2+</sup> and Ca<sup>2+</sup> codoped BaTiO<sub>3</sub> (BT) ferroelectric ceramics and examined their thermal and dielectric properties. As a result, the Sn<sup>2+</sup> and Ca<sup>2+</sup> codoped BT ceramics exhibited a higher  $T_c$  than Sn non-doped and Sn<sup>4+</sup> doped ceramics.<sup>3-4</sup> We also found that decreasing the perovskite lattice size by Ca<sup>2+</sup> doping is effective for Sn<sup>2+</sup> substituting into Ba site of BT with an aid of first principle theoretical calculations.<sup>5</sup> Moreover, a spherical aberration corrected scanning transmission electron microscope observation revealed that Sn ions exist at Ba sites.<sup>6</sup> From these results, we concluded that Sn<sup>2+</sup> ions substitution into Ba sites enhanced the ferroelectricity of BT. On the other hand, we have studied the effects of Sn<sup>2+</sup> ion doping on the properties of another perovskite material

SrTiO<sub>3</sub> (ST). Here, we compare the effects of Sn<sup>2+</sup> ion doping on ST with other element such as Pb. The relationship between  $T_{\epsilon_{\max}}$  and doping concentration  $x$  is shown Figure.1 where  $T_{\epsilon_{\max}}$  is a temperature which gives maximum dielectric permittivity. Circles represent the Sn doping of our study and solid line represents Pb doping reported by Lemanov et al.<sup>7</sup>  $T_{\epsilon_{\max}}$  is increasing with increasing for both the cases of Sn and Pb. Interestingly,  $T_{\epsilon_{\max}}$  of Sn doped ST is much higher than the Pb doped one. We consider that the difference of increasing  $T_{\epsilon_{\max}}$  originates from the ion size difference between Sn<sup>2+</sup> and Pb<sup>2+</sup>. Smaller Sn<sup>2+</sup> ion prefers to locate the off-center position rather than remaining center position, thus it introduce a stronger local dipolar distortion around Sr site than that caused by Pb doping. The cooperation forces between the stronger local dipoles by Sn<sup>2+</sup> doping keeps ferroelectricity at high temperatures.

<sup>1</sup> Y.Uratani, T.Shishidou and T.Oguchi, Jpn. J. Appl. Phys. 47, 7735 (2008).

<sup>2</sup> S.Matar, I.Baraille and M.Subramanian, Chem. Phys. 355, 43 (2009).

<sup>3</sup> S.Suzuki, T.Takeda, A.Ando and H.Takagi, Appl. Phys. Lett. 96, 132903 (2010).

<sup>4</sup> S.Suzuki, T.Takeda, A.Ando, T.Oyama, N.Wada, H.Niimi and H.Takagi, Jpn. J. Appl. Phys. 49, 09MC04 (2010).

<sup>5</sup> S.Suzuki, A.Honda, S.Higai, A.Ando, N.Wada, and H.Takagi, Jpn. J. Appl. Phys. 50, 09NC11 (2011).

<sup>6</sup> S.Suzuki, N.Iwaji, A.Honda, S.Higai, N.Wada, A.Ando and H.Takagi, Jpn. J. Appl. Phys. 51 (2012) 09LC08.

<sup>7</sup> V.V.Lemanov, E.P.Smirnova and E. A.Tarakanov, Phys. Solid State 39, 628 (1997).

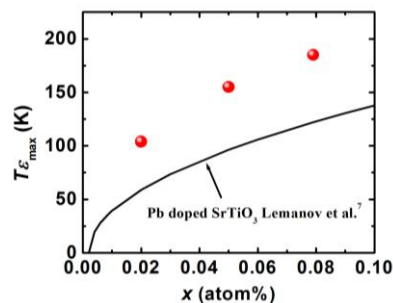


Fig. 64:  $T_{\epsilon_{\max}}$  for SrTiO<sub>3</sub> ceramics as a function of doping concentration  $x$ .

## Lead free LTCC/PZT modules (LPM)

Markus Flössel<sup>1,2</sup>, Sylvia Gebhardt<sup>2</sup>, Andreas Schönecker<sup>2</sup>, Alexander Michaelis<sup>1,2</sup>

<sup>1</sup>TU Dresden, Institute of Material Science, Chair of Inorganic Non-Metallic Materials, 01062  
Dresden, Germany

<sup>2</sup>Fraunhofer IKTS, Winterbergstraße 28, 01277 Dresden, Germany

e-mail: markus.floessel@ikts.fraunhofer.de

The combination of multilayer- and piezo-technology by laminating fired lead zirconate titanate (PZT) ceramic discs with low temperature cofired ceramics (LTCC) green layers and subsequently sintering of the package yields to the so-called LTCC/PZT modules (LPM), which were first published in 2010<sup>224</sup>.

The design of the LPM can be modified and it can so be used in two different cases of application. On one side it is used as sensor/actuator module which is metal die casted in an aluminum component and it controls the dynamic properties (vibration damping) of thin walled devices. Besides with this metal die casting step, batch production by combining fabrication of mechanical components and integration of LPM in one production chain is possible. Then again it can also be used as an ultrasonic transducer for Structural Health Monitoring (SHM) which permanently monitors the health and condition of components used in rotorcraft, aircraft, pipelines, automobiles et cetera.

This presentation will give an overview on technological challenges and their solution of producing LPM and have a look of material properties and interactions especially chemical reactions in the phase boundary of LTCC and PZT which is necessary to fabricate functional microsystems.

Regarding to the directive of the European Union 2002/95/EG and 2011/65/EU which means restriction of the use of certain hazardous substances (RoHS) conform components, we first developed lead free LPM and show properties of low-level signals and ferroelectric hysteresis loops.

---

<sup>224</sup> Flössel, M.; Gebhardt, S.; Schönecker, A.; Michaelis, A.: Development of a Novel Sensor-Actuator-Module with Ceramic Multilayer Technology, In: Journal of Ceram. Sci. Tech., 01[01]55-58, 2010

## Pulsed discharge behavior of $(\text{Bi}_{0.2}, \text{Ba}_{0.8})(\text{Zn}_{0.1}, \text{Ti}_{0.9})\text{O}_3$ -based relaxor multilayer ceramic capacitors

Harlan J. Brown-Shaklee, John J. Borchardt, Mia A. Blea and Geoff L. Brenneka

Material Science and Engineering Center, Sandia National Laboratories,  
Albuquerque, New Mexico, USA

Email: [hjbrown@sandia.gov](mailto:hjbrown@sandia.gov)

Reduction of permittivity with increased electric field is a phenomenon known as voltage tuning and limits the energy density that many commercial ceramic capacitors can achieve. Using DC fields up to 3kV, small signal permittivity was determined from impedance data and compared to large signal permittivity derived from P-E loops. The  $\text{Bi}(\text{Zn}_{1/2}\text{Ti}_{1/2})\text{O}_3$ -0.8BaTiO<sub>3</sub> (BZT-BT) dielectrics maintained high permittivities ( $k > 1000$ ) at fields greater than 100 kV/cm in contrast to commercial dielectrics that fell to  $k \sim 600$  at half the field. This combination of high permittivity and breakdown strength resulted in energy densities of  $> 1.3 \text{ J/cm}^3$  and makes the BZT-BT family of dielectrics attractive for high-energy density multilayer capacitors. We will present the electrical properties of 220nF BZT-BT multilayer ceramic capacitors (MLCC) designed to withstand  $> 1500$  volts. Until recently, the time domain response of this new relaxor system was not evaluated. Here, we developed low inductance circuits to evaluate the time domain response of our 220nF multilayer ceramic capacitors (MLCCs) comprised of BZT-BT dielectrics. These circuits were able to discharge the 220nF MLCCs with  $< 80\text{ns}$  rise times while providing the means to evaluate the time dependent current. The nano-second time domain signal collected during pulsed discharge was used to determine capacitance of the MLCCs as a function of temperature and charge voltage. We will show that capacitance values calculated from the time domain signals using RLC circuit models agree well with high frequency capacitance values derived from frequency domain impedance data.

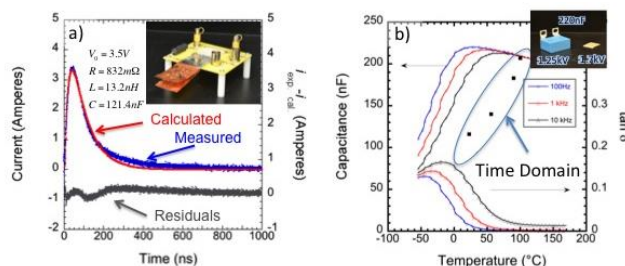


Figure 65. a) Pulsed discharge data collected from a 220nF BZT-BT MLCC. The inset shows the circuit board used to measure the time domain response. b) Capacitance measured in the frequency and time domains with the time domain response having a characteristic circuit frequency of 2.8 MHz and exhibiting the same temperature dependent frequency response that is characteristic for relaxor dielectrics.

This work was supported through the Energy Storage Program managed by Dr. Imre Gyuk of the Department of Energy's Office of Electricity Delivery and Energy Reliability. Sandia National Laboratories is a multi-program laboratory managed and operated by Sandia Corporation, a wholly owned subsidiary of Lockheed Martin Corporation, for the U.S. Department of Energy's National Nuclear Security Administration under contract DE-AC04-94AL85000.

## Free-Electron Gas at Charged Domain Walls in Ferroelectrics

Sluka Tomas<sup>1</sup>, Tagantsev Alexander<sup>1</sup>, Bednyakov Petr<sup>1</sup>, Setter Nava<sup>1</sup>

<sup>1</sup>Ceramics Laboratory, EPFL Swiss Federal Institute of Technology, Lausanne, CH-1015 Switzerland

Email: Tomas.Sluka@epfl.ch

Solid interfaces between two distinct materials or material states are quasi two-dimensional objects with uniquely distorted electronic structures and ionic displacements. Properties of such interfaces may therefore be entirely different from those of the parent materials. Indeed, technologically enticing phenomena were found at hetero-interfaces between metal oxides<sup>225,226</sup> and at compositionally homogeneous interfaces such as ferroic domain walls<sup>227</sup>. The latter are especially attractive for their naturally guaranteed high quality and mutability of their positions, shapes and intrinsic properties which could be utilized inside a ready device<sup>228</sup>.

Unique properties are theoretically predicted at ferroelectric domain walls which form head-to-head and tail-to-tail polarization divergences<sup>229,230</sup> (Fig. 1). The stabilization of these “strongly” charged domain walls (sCDW) depends vitally upon almost perfect compensation of bound charge by free carriers (if not by charged defects) and on ferroelastic clamping. The compensation, in theory, leads to formation of quasi-two-dimensional free-electron (or hole) gas analogously to the polar catastrophe known at hetero-interfaces.

Here we show this phenomenon experimentally in sCDW of the prototypical ferroelectric BaTiO<sub>3</sub>. Their giant steady metallic-type conductivity evidence the presence of stable degenerate electron gas.

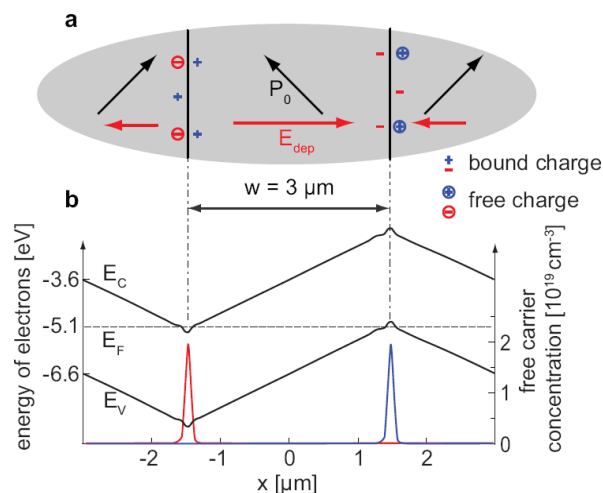


Fig. 66: Free carrier concentration and band bending at sCDW. (a) A periodic structure of 90° sCDW where bound polarization charge (+, -) is almost perfectly compensated by free carriers. (c) The band bending induced by bound charge causes that the edges of the conduction  $E_C$  or valence  $E_V$  bands (solid black lines) approach the Fermi level  $E_F$  (dashed black line) where high concentration of free electrons (red line) or holes (blue line) are generated.

<sup>225</sup> A. Tsukazaki et al., “Quantum Hall effect in polar oxide heterostructures”, *Science*, 315, 2007.

<sup>226</sup> J. Mannhart et al., “Oxide Interfaces-An Opportunity for Electronics”, *Science*, 327, 2010.

<sup>227</sup> J. Seidel et al., “Conduction at domain walls in oxide multiferroics”, *Nat. Mater.*, 8:229, 2009.

<sup>228</sup> G. Catalan et al., “Domain wall nanoelectronics” *Rev. Mod. Phys.*, 84:119, 2012.

<sup>229</sup> B. M. Vul et al., “II. Encountering domains in ferroelectrics”, *Ferroelectrics*, 6:29, 1973.

<sup>230</sup> M. Y. Gureev et al. “Head-to-head and tail-to-tail 180 degrees domain walls in an isolated ferroelectric”. *Phys. Rev. B*, 83, 2011.

## Electrical and Thermal Properties of Polymer Systems With Coexisting Ferroelectric and Relaxor States

Goran Casar<sup>1</sup>, Xinyu Li<sup>2</sup>, Jurij Koruza<sup>1</sup>, Qiming Zhang<sup>2</sup>, and Vid Bobnar<sup>1</sup>

<sup>1</sup>Jožef Stefan Institute and Jožef Stefan International Postgraduate School, Jamova 39, SI-1000 Ljubljana, Slovenia

<sup>2</sup>Department of Electrical Engineering and Materials Research Institute, The Pennsylvania State University, University Park, Pennsylvania 16802, USA

Email: goran.casar@ijs.si

Electroactive ferroelectric and, particularly, relaxor polymers based on poly(vinylidene fluoride-trifluoroethylene) copolymer, P(VDF-TrFE), are of great interest for a broad range of applications as they exhibit giant electrostriction<sup>231</sup>, fast response speeds, high dielectric constant and high electric energy density<sup>232</sup>, and large electrocaloric effect<sup>233</sup>. Up to now, however, most of the investigations have focused on either normal ferroelectric polymers or polymers that are completely transformed into a relaxor, i.e., (i) terpolymers where the long-range ordering of polymer chains is broken by introduction of additional monomers that contain large chlorine atoms or (ii) P(VDF-TrFE), irradiated with high-energy electrons using relatively high doses<sup>234</sup>.

Here we report dielectric, calorimetric, and electrocaloric investigations of P(VDF-TrFE) copolymer, irradiated also with low and moderate doses of high-energy electrons. While the ferroelectric copolymer is completely transformed into a relaxor system at high irradiation doses, dielectric investigations, particularly nonlinear dielectric experiments, i.e., the temperature dependences of the second and the third harmonic dielectric response, clearly evidence that at lower doses ferroelectric and relaxor states coexist in the P(VDF-TrFE) system<sup>235</sup>. This coexistence is confirmed by the differential scanning calorimetry, which further reveals the influence of irradiation on the copolymer crystallinity and melting point. Finally, it is shown and explained that large electrocaloric response of VDF-TrFE-based polymers is further enhanced in systems with coexisting relaxor and normal ferroelectric states.

<sup>231</sup> Q. M. Zhang *et al.*, "Giant electrostriction and relaxor ferroelectric behavior in electron-irradiated poly(vinylidene fluoride-trifluoroethylene) copolymer", *Science*, vol. 280, p. 2101-2103, 1998.

<sup>232</sup> B. Chu *et al.*, "A dielectric polymer with high electric energy density and fast discharge speed", *Science*, vol. 313, p. 334-336, 2006.

<sup>233</sup> B. Nasse *et al.*, "Large electrocaloric effect in ferroelectric polymers near room temperature", *Science*, vol. 321, p. 821-823, 2008.

<sup>234</sup> V. Bobnar *et al.*, "Dielectric properties of relaxor-like vinylidene fluoride-trifluoroethylene-based electroactive polymers", *Macromolecules*, vol. 36, p. 4436-4442, 2003.

<sup>235</sup> G. Casar *et al.*, "Electrical and thermal properties of vinylidene fluoride-trifluoroethylene-based polymer system with coexisting ferroelectric and relaxor states", submitted.



---

## **ISAF3G: Pb-based materials: Films**

CLUB A

*Wednesday, July 24 2013, 04:30 pm - 06:00 pm*

Chair: **Brady Gibbons**  
*Oregon State University*

## Flexoelectric Effects in Compositionally Graded Ferroelectric Thin Films – Towards Strain 2.0

Lane W. Martin<sup>1</sup>

<sup>1</sup>Department of Materials Science and Engineering and Materials Research Laboratory, University of Illinois, Urbana-Champaign, Urbana, IL, USA

Email: lwmartin@illinois.edu

In ferroelectric thin films, the utilization of epitaxial strain has enabled researchers to exact dramatic control over the structure and properties of ferroelectrics. Modern manifestations of ferroelectric thin films, including bilayer and superlattice heterostructures, have also provided access to exotic structures and properties. In this presentation, we explore an alternative method by which we can tune the ferroelectric properties, namely compositionally graded hetero-structures, and how these structures can push the edge of strain control of materials.

Compositionally graded thin films possess a smooth variation in the composition throughout the thickness of the film. We will discuss the evolution of crystal and ferroelectric domain structure as well as the dielectric, piezoelectric, pyroelectric, and ferroelectric properties of compositionally graded versions of  $\text{PbZr}_x\text{Ti}_{1-x}\text{O}_3$  (PZT),  $\text{Ba}_{1-x}\text{Sr}_x\text{TiO}_3$  (BSTO), and other common ferroelectric systems. In the PZT system, for example, we will focus on compositions between the two end-members  $\text{PbZr}_{0.2}\text{Ti}_{0.8}\text{O}_3$  (tetragonal, lattice parameters  $a = 3.94 \text{ \AA}$  and  $c = 4.12 \text{ \AA}$ ) and  $\text{PbZr}_{0.8}\text{Ti}_{0.2}\text{O}_3$  (rhombohedral, lattice parameter  $a = 4.118 \text{ \AA}$  and  $\alpha = 89.73^\circ$ ). Using pulsed-laser deposition, we have synthesized various thicknesses of films on a range of substrates and have explored a number of sample variants including: single-layer, bilayer, and compositionally graded heterostructures.

Extensive X-ray diffraction and piezoresponse force microscopy studies have been completed on all sample variants. Among the most surprising results are the fact certain versions of bilayer and compositionally graded heterostructures are found to be nearly coherently strained to the substrate (despite nearly 4% lattice mismatch) and that these films exhibit unexpected crystal and domain structures (e.g., tetragonal versions of  $\text{PbZr}_{0.8}\text{Ti}_{0.2}\text{O}_3$ ) [Fig. 1]. Subsequent studies of the properties of these films reveal dramatically reduced permittivity (as low as 90 for certain compositionally graded films), large remnant polarizations, and horizontally shifted hysteresis loops (indicating the presence of a built-in electric field as large as 200 kV/cm). These effects are the result of the coupling between the polarization and strain gradients in the film (or flexoelectricity). We will highlight how we can generate strains as large as  $\sim 4.5 \times 10^{-5} \text{ m}^{-1}$ , produce exotic properties and susceptibilities, and the potential of compositionally graded films as a powerful new tool to tune the properties of ferroelectric thin films towards Strain 2.0.

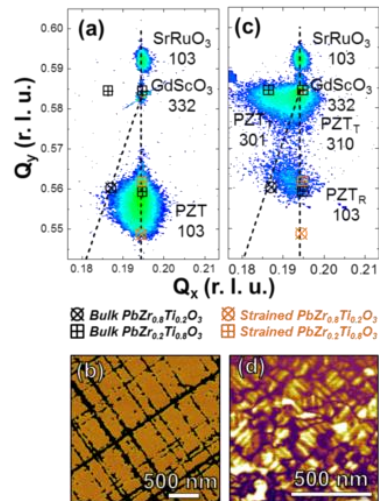


Fig. 1: Reciprocal space mapping about the 103 and 332-diffraction conditions and Piezoresponse force microscopy images of (a) compositionally up-graded, and (b) down-graded heterostructure.



## Ferroelastic Domain Wall Motion in PZT Thin Films

Raegan L. Johnson-Wilke<sup>1</sup>, Rudeger H.T. Wilke<sup>1</sup>, Margeaux Wallace<sup>1</sup>, Giovanni Esteves<sup>2</sup>, Jacob Jones<sup>2</sup>, Susan Trolier-McKinstry<sup>1</sup>

<sup>1</sup> The Pennsylvania State University, Department of Materials Science and Engineering, University Park, PA, USA

<sup>2</sup> University of Florida, Department of Materials Science and Engineering, Gainesville, FL, USA

Email: rlj12@psu.edu

Lead zirconate titanate (PZT) thin films are used in microelectromechanical systems (MEMS) due to their large piezoelectric response. The electromechanical response in PZT is a result of both the intrinsic (lattice) piezoelectric effect as well as the motion of ferroelectric and ferroelastic domain walls (extrinsic effect). The work presented will describe an *in-situ* technique used to directly measure the extent of ferroelastic domain wall motion as well as lattice strain in 2  $\mu\text{m}$  thick PZT (30/70) films with different crystallographic textures. Synchrotron X-ray diffraction was used to monitor the main Bragg peaks while subjecting the film to an applied electric field. Relative changes in intensity between 200 and 002 peaks were measured. It was found that both the {001} oriented and randomly oriented films exhibited a significant amount of ferroelastic domain wall motion during applied voltages above and below the coercive field. The effect is illustrated in the figures below showing an increase in intensity in the 002 peak and a corresponding decrease in intensity in the 200 peak as the applied electric field is increased. This indicates that the volume fraction of 002 domains increased under the application of an electric field. The piezoelectric coefficient,  $d_{33}$ , was calculated using X-ray diffraction by measuring peak shifts in primary Bragg reflections. Upon examination of the shift in the 111 Bragg peak, the intrinsic component of  $d_{33}$  was calculated to be  $\sim 50$  pm/V for the {001} oriented 30/70 film. This value will be compared to values measured using a double beam interferometer.

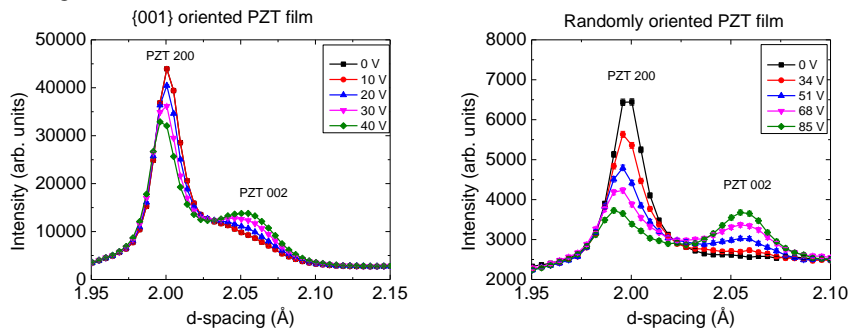


Figure: X-ray diffraction pattern near the 002 and 200 peaks in a PZT {001} oriented film (left) and a randomly oriented PZT film (right). The fact that the 002 peak shows an increase in intensity as a function of applied voltage indicates that the volume of 002 domains is increasing in the films as a function of electric field.

# Characterization of GHz electromechanical properties of PZT single crystalline thin films without removing substrate

Takahiko Yanagitani<sup>1</sup>, Masashi Suzuki<sup>1</sup>, Kiyotaka Wasa<sup>2</sup>

<sup>1</sup> Graduate School of Engineering, Nagoya Institute of Technology, Nagoya, Japan

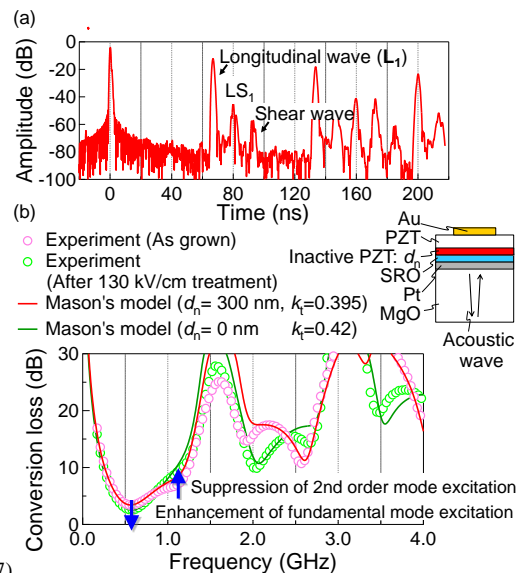
<sup>2</sup> Micro-Engineering, Kyoto University, Kyoto, Japan

Email: yana@nitech.ac.jp

Single crystalline (SC) PZT has attracted interest for high Q resonator and tunable filters. However, bulk SC-PZT near MPB can not be grown, and therefore the most common approach to obtain SC-PZT is epitaxial growth technique. General epitaxial substrate: SrTiO<sub>3</sub> or MgO is difficult to etch away. Therefore, FBAR resonance-antiresonance method which is the most accurate method to obtain electromechanical coupling coefficient  $k_t$  in the GHz range cannot be used.

In this study, GHz  $k_t$  value of SC-PZT films was extracted from HBAR (High-overtone bulk acoustic resonator) structure including substrate. We fabricated the HBAR consisting of Pb(Zr<sub>0.53</sub>Ti<sub>0.47</sub>)O<sub>3</sub> thin films near MPB with 2.8  $\mu\text{m}$  grown on (101)SRO/(001)Pt: total 100 nm / (001)MgO: 0.3 mm substrate by using RF magnetron sputtering. First, impulse response of HBAR is obtained by an inverse Fourier transform of  $S_{11}$  measured by a network analyzer. As shown in Fig. 1 (a), acoustic waves excited from PZT film propagate in MgO substrate, reflect at substrate bottom, and is detected again by PZT film. Energy conversion efficiency so-called conversion loss (CL) including 1)electromechanical coupling of the film, 2)mismatch between capacitive impedance of the film and 50  $\Omega$  measurement system, 3)transmission loss at boundary of each layer and substrate, 4)propagation and diffraction losses in the substrate (which is negligible in high  $k$ ) can be obtained by Fourier transform of  $L_1$ . 2) and 3) can be simulated by Mason's equivalent circuit model including each layer. Therefore,  $k$  value can be extracted from the CL<sup>236</sup>

Figure 1 (b) shows the experimental and simulated CL curves. 2nd-order thickness extensional mode excitation observed at 1.2 GHz in experimental CL indicates the existence of piezoelectric inactive layer at initial stage of PZT growth. Simulated curve in which the inactive layer is taken into account showed good agreement in detail with the experimental curve.  $k_t$  value is determined to be 0.395. Next, 130 kV/cm was applied to the film to polarize the inactive layer. As a result, fundamental mode was enhanced and 2nd order mode was suppressed. In contrast to the previous result, simulated curve excluding the inactive layer agreed well with the experimental curve.  $k_t$  value increased to 0.42 after the polarization treatment. This method is an effective tool to investigate



<sup>236</sup> T. Yanagitani, et al., *J. Appl. Phys.*, 102, 024110, (2007).

Fig. 1 (a) Impulse response of the PZT HBAR and (b) conversion loss obtained from Fourier transform of  $L_1$ .  $d_n$  is the thickness of piezoelectric inactive PZT layer.

polarization state and  $k_t$  value in the single crystalline PZT films.

## ***In-situ* XRD observation of (100)/(001)-oriented Pb(Zr,Ti)O<sub>3</sub> films under applied electric field**

Hiroshi Funakubo<sup>1</sup>, Ayumi Wada<sup>1</sup>, Yoshitaka Ehara<sup>1</sup>, Shintaro Yasui<sup>1</sup>, Mitsumasa Nakajima<sup>1</sup>, Takahiro Oikawa<sup>1</sup>, Hitoshi Morioka<sup>2</sup>, and Takeshi Kobayashi<sup>3</sup>

<sup>1</sup>Tokyo Institute of Technology, Yokohama, Japan

<sup>2</sup>Bruker AXS K.K., Yokohama, Japan

<sup>3</sup>National Institute of Advanced Industrial Science and Technology (AIST), Tsukuba, Japan

Email: funakubo.h.aa@m.titech.ac.jp

Pb(Zr,Ti)O<sub>3</sub> thick films prepared on Si substrates have been widely investigated for MEMS applications. Piezoelectric response of the polydomain films consists of not only the lattice strain but also other contributions, such as domain switching, phase transition and so on. To understand these contributions individually, *in-situ* observation of the crystal structure under an applied electric field is the most effective way. However, these investigation has been limited for Pb(Zr,Ti)O<sub>3</sub> thick films<sup>1,2</sup>. In the present study, we measured *in-situ* XRD analysis under an applied electric field as well as before and after the applied electric field.

(100)/(001)-oriented Pb(Zr<sub>0.3</sub>Ti<sub>0.7</sub>)O<sub>3</sub> and Pb(Zr<sub>0.52</sub>Ti<sub>0.48</sub>)O<sub>3</sub> films with 1 μm-thick were prepared at 600 °C on (111)Pt/Ti/SiO<sub>2</sub>/(100)Si substrates by chemical solution deposition method<sup>3</sup>. Capacitor structure of Pt/Pb(Zr,Ti)O<sub>3</sub>/Pt was used to measure the electrical properties. XRD measurements were used to evaluate the crystal structure of the films on the Pt top electrodes using concentrated X-ray source with the space resolution of about 50 μm combined with two dimensional detector (Bruker, D8).

Figure 1 shows the XRD patterns before, under, and after applied electric field of 150 kV/cm For Pb(Zr<sub>0.3</sub>Ti<sub>0.7</sub>)O<sub>3</sub> films after 10<sup>0</sup> and 10<sup>7</sup> bipolar switching cycles Piezoelectric fatigue was observed after 10<sup>7</sup> cycles as well as the polarization fatigue. However, the change in the XRD patterns with the switching cycles was relatively small (see Fig. 1). On the other hand, the XRD patterns change under applied electric field for the films after 10<sup>0</sup> cycles was smaller than that after 10<sup>7</sup> cycles. This shows that the domain switching from (100) to (001) was diminished after 10<sup>7</sup> switching cycles. Crystal structure change of Pb(Zr<sub>0.52</sub>Ti<sub>0.48</sub>)O<sub>3</sub> thick films is also presented as well as the piezoelectric property.

<sup>1</sup> Osone *et al.*, Appl. Phys. Lett., **90**, 262905, 2005.

<sup>2</sup> Morioka *et al.*, Jpn. J. Appl. Phys., **48**, 09KA03, 2009.

<sup>3</sup> Kobayashi *et al.*, Thin Solid Films, **489**, 74, 2005.

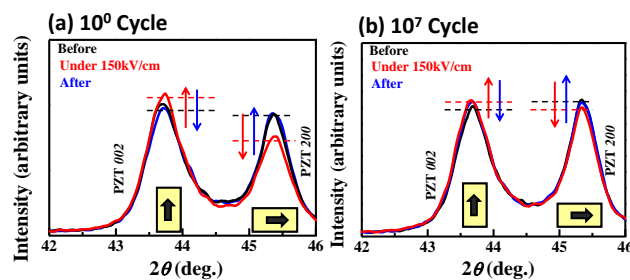


Fig.1 XRD patterns before, under and after applied electric fields of 150 kV/cm for Pb(Zr<sub>0.3</sub>Ti<sub>0.7</sub>)O<sub>3</sub> films after 10<sup>0</sup> and 10<sup>7</sup> bipolar switching cycles.

## Piezoelectric responses of epitaxial PZT film-based membrane in $d_{31}$ and $d_{33}$ actuation mode

Minh Nguyen<sup>1,2,3</sup>, Matthijn Dekkers<sup>1,2</sup>, Dave Blank<sup>1</sup>, Guus Rijnders<sup>1</sup>

<sup>1</sup>Inorganic Materials Science (IMS), MESA+ Institute for Nanotechnology, University of Twente, P.O. Box 217, 7500AE Enschede, The Netherlands

<sup>2</sup>SolMateS B.V., Drienerlolaan 5, Building 6, 7522NB Enschede, The Netherlands

<sup>3</sup>International Training Institute for Materials Science (ITIMS), Hanoi University of Science and Technology, No. 1 Dai Co Viet road, Hanoi, Vietnam

Email: d.m.nguyen@utwente.nl

The magnitude of the  $d_{33}$  coefficient is 2.0 to 2.5 times higher than the  $d_{31}$  coefficient. Therefore, the generated open-circuit voltage of a  $d_{33}$ -mode device will be much higher (20 times or greater) than that of the  $d_{31}$ -mode generator of similar dimensions, resulting in a potentially higher energy conversion factor. Hence, the  $d_{33}$ -mode is the key to make the thin-film PZT device for power generation<sup>237</sup>.

In this report,  $d_{31}$  and  $d_{33}$  actuation mode micromechanical systems piezoelectric actuators and sensors were fabricated and compared to investigate their displacements and quality factors. For  $d_{31}$ -mode membrane, an epitaxial  $\text{Pb}(\text{Zr}_{0.52}\text{Ti}_{0.48})\text{O}_3$  (PZT) thin film was deposited on  $\text{SrRuO}_3$ -buffered YSZ/Si substrate; whereas, the deposition of the epitaxial PZT thin film was done on YSZ/Si substrate for  $d_{33}$ -mode membrane. All layers of PZT film (500 nm),  $\text{SrRuO}_3$  electrode (100 nm) and yttria-stabilized zirconia (YSZ, 50 nm) buffered-layer were deposited using pulsed laser deposition (PLD). Diameter and thickness of the membranes were 300-1000  $\mu\text{m}$  and 10  $\mu\text{m}$ , respectively.

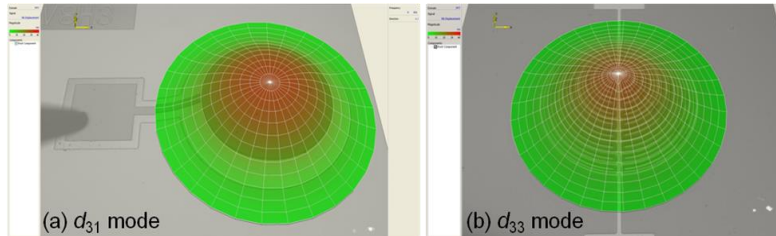


Fig. 67: Piezoelectric displacements of (a)  $d_{31}$ -mode and (b)  $d_{33}$ -mode membranes. The diameter of membranes is 500  $\mu\text{m}$ . All measurements are performed at an *ac*-voltage of 3 V and 8 kHz frequency.

The piezoelectric responses, including piezoelectric displacement and quality factor, were performed using a laser Doppler vibrometer (LDV). The piezoelectric displacement and quality factor of the  $d_{31}$  and  $d_{33}$ -mode were 22.4 nm/V and 102, and 10.2 nm/V and 128, respectively, with 500- $\mu\text{m}$  in membrane diameter. In this study, the center displacements of membranes were measured at an *ac*-voltage of 3 V and 8 kHz frequency (*off-resonance*); while the quality factors were calculated from resonance peaks which were measured at an *ac*-voltage of 1 V and in the frequency range from 0 to 2

<sup>237</sup> Y. B. Jeon, R. Sood, J. -h. Jeong, S. -G. Kim, "MEMS power generator with transverse mode thin film PZT", *Sens. Actuators A*, vol. 122, p. 16-22, 2005; W. J. Choi, Y. Jeon, J. H. Jeong, R. Sood, S. G. Kim, "Energy harvesting MEMS device based on thin film piezoelectric cantilevers", *J. Electroceram.*, vol. 17, p. 543-548, 2006.



MHz. The effects of diameter membrane on the piezoelectric responses of the  $d_{31}$  and  $d_{33}$  mode have been also investigated.

## Piezoelectric Energy Harvesting

CLUB B

*Wednesday, July 24 2013, 04:30 pm - 06:00 pm*

Chair: **Paula Vilarinho**  
*Universoty of Aveiro*

## Energy Harvesting with Piezoelectric MEMS

Paul Muralt, Andrea Mazzalai, Ramin Matloub

Ceramics Laboratory, EPFL, Lausanne, Switzerland

Email: paul.muralt@epfl.ch

During recent years, energy harvesting from vibration and motion sources has attracted much interest. Electrical power generators based on piezoelectric materials were investigated, first as flexible piezoelectric bulk composite materials containing PZT ceramics, and later also as MEMS devices based on thin films, or even nanowires. In case of micro power devices, the main target applications are wireless communication, sensors, and specifically wireless sensors. Average supply powers of  $100 \mu\text{W}$  are sufficient to operate wireless nodes with low duty cycles. There is general agreement on the fact that motions and vibrations constitute the most versatile and ubiquitous ambient energy sources available, if light harvesting is excluded by the application. The progress in piezoelectric thin films and MEMS technology has led to the development of demonstration devices that show sufficiently large power outputs and voltage levels, i.e. more than several  $100 \mu\text{W}/\text{cm}^2$  at over one volt. The standard configuration is to use parallel plate capacitor geometry exploiting the transverse piezoelectric coefficient. It looks evident that  $\text{Pb}(\text{ZrTi})\text{O}_3$  and related ferroelectric materials should be the best choice. However, ferroelectric thin films exhibit high dielectric constants – meaning low voltage output - and usually suffer from limited remanent polarization. Remedies can be found in using interdigitated electrode systems, or imprinted films. Another solution, however, could be to use  $\text{AlScN}$  thin films. Substituting Al in part by Sc leads to higher  $e_{31,f}$  coefficients with only a moderate increase of the dielectric constant.

In this talk, the principles of piezoelectric energy harvesting will be introduced and illustrated with achieved results. Direct strain coupling to moving parts is compared to acceleration coupling by means of inertial masses. Specific thin films issues will be addressed such as material's choice, and electrode configurations. The interdigitated electrode system will be discussed in more detail, including growth on insulators, poling, domain issues and performance. The energy figure of merit  $e^*h$  as derived from measurements is introduced to compare materials and electrode systems. Experimental results will be compared to numerical simulations.

## Curled PZT Cantilever Based MEMS Harvester

Hyeonsu Park, Jongcheol Park, Jaeyeong Park\*

Department of Electronic Engineering, Kwangwoon University, Seoul, Korea

\*Email: jaepark@kw.ac.kr

In this paper, a micro-fabricated PZT cantilever based energy harvester was newly developed to generate high output voltages from two dimensional ambient vibrations. A curled PZT cantilever was proposed to scavenge both vertical and longitudinal vibrations, which was comprised of a polyimide, PZT, and electrode layers formed on a low stress silicon nitride film. The inter-digitally shaped electrodes were employed for the  $d_{33}$  piezoelectric mode operation and high output voltage. The polyimide was utilized as an elastic layer to decrease the resonant frequency of the harvester. The harvester generated an output voltage of 0.5 V and 1.08 V at its resonant frequency of 114.7 Hz under a vertically and longitudinally induced vibration with an acceleration of  $2.3 \text{ m/s}^2$ . Most of MEMS vibration harvesters employing a flat cantilever can only be operated under vertically induced vibration<sup>1)</sup>. Therefore, they must be installed on the perpendicular plane to vibration in order to achieve its maximum output power. However, the proposed device can generate electricity from both vertically and longitudinally induced vibrations. Since the arbitrary vibration induced on the curled cantilever leads the proof mass at the free end of cantilever to oscillate.

The proposed cantilever structure was realized by using intrinsic bending deformation of a multi-layered cantilever. The polyimide layer was utilized as an elastic layer for lowering the resonant frequency of the cantilever due to its low elastic modulus. The fabricated piezoelectric cantilever has a volume of  $4000 \times 2000 \times 18$  (height)  $\mu\text{m}^3$ . The silicon proof mass has a volume of  $2000 \times 2000 \times 500$  (height)  $\mu\text{m}^3$ . As shown in Fig. 1, the fabricated curled PZT cantilever has a radius curvature of 1.5 mm. The fabricated PZT thin film has a remnant polarization and coercive field of approximately  $2P_r = 49.3 \mu\text{C/cm}^2$  and  $2E_c = 67.6 \text{ kV/cm}$ .

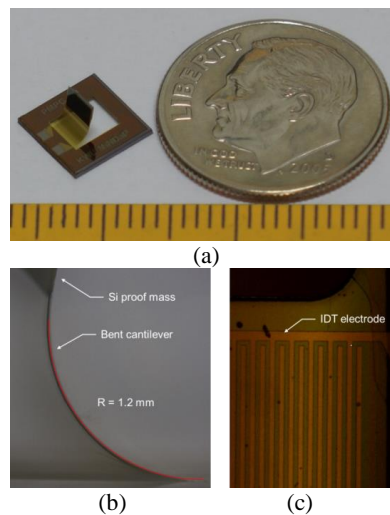


Fig. 68: Photographs of top view (a), side view (b), and inter-digitally shaped electrodes of fabricated curled PZT cantilever based energy harvester with  $d_{33}$ -mode operation (c).

<sup>1)</sup> R. Elfrink, T. Kamel, M. Geodbloed, S. Matova, D. Hohlfeld, Y. Andel, R. Schaijk, Vibration Energy Harvesting with Aluminum Nitride-based Piezoelectric Devices, J. Micromech. Microeng. Vol. 19, no.1, p. 251 ~ 265, 2009



# A Tunable Vibrating Piezoelectric Cantilever for Energy Harvesting

Ahmed Seddik Bouhadjar, Despesse Ghislain, Defay Emmanuel

<sup>1</sup>CEA, LETI, Minatec Campus, Grenoble, France

Email: [emmanuel.defay@cea.fr](mailto:emmanuel.defay@cea.fr)

This paper describes how an adjustable electrical load can be used to achieve a wideband mechanical vibration energy harvester based on piezoelectric material. We discuss the design optimization of the developed structure in terms of coupling mode and cantilever shape. The developed device is based on the longitudinal piezoelectric mode of a cantilever in the centimeter range. This last exhibits a resonance frequency at 208 Hz and 294 Hz respectively in short and open circuit conditions. The key element of the tunability process is an adjustable electrical load, namely a variable capacitor, coupled with the piezoelectric material which allows a controllable shift of the resonant frequency between these two frequencies. This device yields a frequency variation as high as 41%.

Fig. 1 sketches the cross section of the device performed throughout this study. Piezoelectric cuboids have been glued to a steel substrate. PZN-5.5%PT single crystals have been chosen thanks to their outstanding electromechanical coupling  $k_{33}^2$ , namely 80%. Reaching such a high coupling requires using the longitudinal configuration, which induces a peculiar pattern of PZN-PT subparts, as displayed in Fig.1. The reversed polarization of adjacent subparts prevents the compensation of the generated charges. Note that the subparts are connected in parallel electrically in order to reach a high capacitance and connected in series mechanically in order to reduce the mechanical stiffness.

Fig.2 shows the measured resonance frequency of the cantilever once one makes vary the capacitive load in parallel (see Fig. 1). Two orders of magnitudes of capacitance load induce a frequency variation as high as 41%. This device is intended to harvest vibrating energy exhibiting a variable frequency.

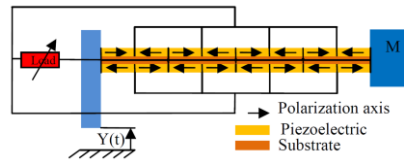


Fig. 69: Sketch of the cross section of the tunable harvester. Pre-poled piezoelectric cuboids in the mm range have been arranged face to face and in parallel in order to avoid charge compensation. They are connected to a variable load made of a capacitors bank.

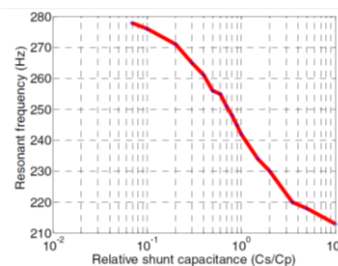


Fig. 2: Frequency variation exhibited by the loaded cantilever versus the capacitive shunt load.



# Piezoelectric MEMS Vibrational Energy Harvester

## Using BiFeO<sub>3</sub> Films

T. Yoshimura<sup>1</sup>, S. Murakami<sup>2</sup>, K. Wakazono<sup>1</sup>, K. Kariya<sup>1</sup>, N. Fujimura<sup>1</sup>

<sup>1</sup>Department of Physics and Electronics/Osaka Prefecture University, Sakai, Osaka/Japan

<sup>2</sup>Technology Research Institute of Osaka Prefecture, Izumi, Osaka/Japan

Email: tyoshi@pe.osakafu-u.ac.jp

Recently, vibration energy harvester (VEH) is receiving a considerable amount of interest, because the vibration energy exists in many environments. Although several methods are useful for obtaining electrical energy from vibration energy, piezoelectric materials are the most suitable because of their capability of converting applied strain energy into useful electric energy directly and the ease with which they can be integrated into a system.

Various types of piezoelectric MEMS VEHs based on the mass-spring design have been reported. Pb(Zr,Ti)O<sub>3</sub> and AlN films are the most commonly used piezoelectric materials for VEHs. For VEH applications, it can be expected that a piezoelectric film with a large piezoelectric coefficient and low dielectric permittivity will exhibit a high figure of merits (FOM). We have proposed that BiFeO<sub>3</sub> films are suitable for piezoelectric VEH applications, because BiFeO<sub>3</sub> has high spontaneous polarization and low dielectric permittivity.<sup>1)</sup> We have also improved the piezoelectric properties of BiFeO<sub>3</sub> films by domain engineering and by using strain-induced morphotropic phase boundaries (MPB). The highest FOM of a domain-engineered BiFeO<sub>3</sub> film to date is 20.8 GPa, which is comparable to the best-performing PZT films.

In this study, piezoelectric MEMS VEHs using BiFeO<sub>3</sub> films were fabricated and its energy harvesting performance was characterized. SOI wafers were used as substrates. The substrate was oxidized, and then Pt/Ti bottom electrodes were deposited on the substrate by a sputtering method. BiFeO<sub>3</sub> films were deposited on the substrate by a sol-gel method. Micro-cantilevers were then fabricated by a conventional MEMS process.

A VEH with a resonant frequency near 200 Hz was designed. While the VEH was strongly affected by nonlinear resonance, the VEH exhibited a relatively high output voltage of about 1 V·G<sup>-1</sup> (G: 9.8m/s<sup>2</sup>). Fig. 1 shows the average output power of the VEH measured at the resonant frequency. The highest power at an acceleration of 0.014 Grms is 3.3 μW·mm<sup>-3</sup>·G<sup>-2</sup>. This harvesting performance is comparable to piezoelectric MEMS VEHs using other piezoelectric films.

Acknowledgement: This study was supported by Industrial Technology Research Grant Program in 2011 from New Energy and Industrial Technology Development Organization (NEDO) of Japan.

1) K. Ujimoto, T. Yoshimura, A. Ashida and N. Fujimura, Appl. Phys. Lett., 100 (2012) 102901.

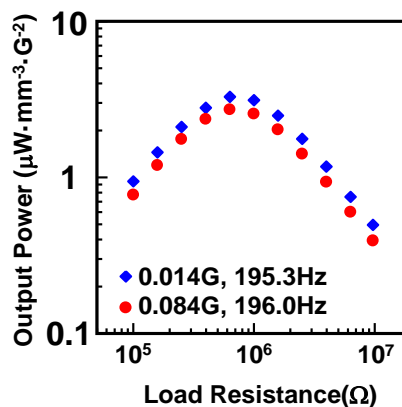


Fig. 1 Average output power of the harvester using BiFeO<sub>3</sub> films.





## Efficient flexible nanogenerator made of organic ferroelectric dabcoHReO<sub>4</sub>

Dmitry Isakov<sup>1</sup>, Etelvina de Matos Gomes<sup>1</sup>, Bernardo Almeida<sup>1</sup>, Igor Bdikin<sup>2</sup> and Andrei Kholkin<sup>3</sup>.

<sup>1</sup> University of Minho, Center of Physics, Campus de Gualtar, 4710-059 Braga, Portugal

<sup>2</sup> University of Aveiro, Department of Mechanical Engineering and TEMA, 3810-193 Aveiro, Portugal

<sup>3</sup>Department of Ceramics and Glass Engineering & Center for Research in Ceramic and Composite Materias (CICECO), University of Aveiro, 3810-193 Aveiro, Portugal

Email: [dmitry@fisica.uminho.pt](mailto:dmitry@fisica.uminho.pt)

In the last years, one-dimensional nanostructures have gathered significant scientific, technological and industrial interest, for application in fields such as drug delivery and regenerative medicine, sensing and chemical catalysis, nanophotonics and nanoelectronics. In this regard special attention has been paid to organic materials due to their low cost and structural flexibility. However, while organic 1D nanostructures can be produced by a variety of laboratory methods (polymerization against porous templates, self-assembly, soft lithographies etc.), electrospinning is one of the few technologies which can be adequately scaled-up to an industrial level. The electrospinning process is based on the uniaxial elongation of a jet, ejected from the surface of a charged polymer solution possessing sufficient molecular entanglements, in the presence of an intense electric field. The plastic stretching of the electrified jet and concomitant solvent evaporation results in the formation of continuous nanofibers with significant cross-section reduction of up to six orders of magnitude.

The important feature of electrospun nanofibers is that the strong shear and electrostatic forces experienced during the process cause the alignment of dopants, molecules and chains within the principal fiber axis. This is an especially attractive phenomenon for polar materials, since promoting such internal molecular orientation (self-assembling) of the organic molecules can also result in achieving polarized emission or enhanced polar properties and an anisotropic alignment of active components is expected to bring in new features and applications. Recent interest on electrospun nanofibers for piezoelectric applications reveals a big potential of this low-cost nanomanufacturing process for the development of fiber-based energy harvesting elements. However, up to date, among the various organic polar materials, only nanofibers of PVDF have been used in piezoelectric actuators. In this work, we present a production of nanofibers of a room temperature hybrid organic-inorganic ferroelectric 1,4-diazabicyclo[2.2.2]-octane perrhenate (dabcoHReO<sub>4</sub>).

The nanofibers have preferentially oriented dabcoHReO<sub>4</sub> nanocrystals with their polarized hydrogen bonds along the fiber axis displaying enhanced piezoelectricity and second harmonic generation response. An efficient strain-electricity flexible nanogenerator based on parallel array dabcoHReO<sub>4</sub> nanofibers reveal above 100 mV output voltage and can be used as a sensitive biocompatible strain sensor and implantable voltage generator.

---

## **Bulk Piezoelectric Materials**

CLUB C

*Wednesday, July 24 2013, 04:30 pm - 05:45 pm*

Chair: **Pavel Mokry**  
*Technical University of Liberec*

**Ian Reaney**<sup>1</sup>

<sup>1</sup>*Materials Science and Engineering, University of Sheffield, Sheffield, South Yorkshire, United Kingdom*

## **From Materials Discovery to Prototype Devices**

**Ian M. Reaney**

**Functional Materials Group**

**Materials Science and Engineering**

**University of Sheffield, UK**

The main goals of the Functional Materials Group (FMG) at Sheffield are to develop new materials, characterise their structure and functional properties and develop prototype devices to demonstrate their commercial potential. The remit of the FMG is broad with a wide range of projects that focus on ionic conduction for Li-battery applications, magnetic memories and sensors, piezoelectrics, MW and *rf* dielectrics and thermoelectrics. This presentation will review recent advances at Sheffield in the development of i) Pb-niobate thin films for tunable filters, ii) high  $T_C$  piezoelectric ceramics and iii) dielectrically loaded MW antennas. An overview of the key driving forces in the science and technology of these topics will be presented followed by detailed descriptions of the key advances made.

## Phase Transition Toughening in Antiferroelectric Ceramics

Xiaoli Tan<sup>1</sup>, S. Eli Young<sup>1</sup>, Yohan Seo<sup>2</sup>, Kyle G. Webber,<sup>2</sup> Jürgen Rödel<sup>2</sup>

<sup>1</sup>Department of Materials Science and Engineering, Iowa State University, Ames, Iowa/USA

<sup>2</sup>Institute of Materials Science, Technische Universität Darmstadt, Darmstadt/ Germany

Email: xtan@iastate.edu

In antiferroelectric solid crystals, the antiparallel electrical dipoles are originated from cation displacements in the unit cell. Aligning these originally antiparallel electric dipoles to the direction of the applied electric field requires cooperative adjustment of the crystal lattice in many unit cells and corresponds to a first order displacive phase transition. The vast majority of antiferroelectric ceramics are based on the prototype compound  $\text{PbZrO}_3$  with the perovskite structure. In these oxides, the antiferroelectric-to-ferroelectric phase transition manifests itself in the development of a large polarization and is generally accompanied by a significant volume expansion when the applied field exceeds a critical magnitude  $E_F$ . The developed macroscopic polarization results from the antiparallel dipoles being forced parallel at the transition. The associated volume expansion at the phase transition implies that there might be a toughening effect.

In this study, a series of  $\text{Pb}_{0.99}\text{Nb}_{0.02}[(\text{Zr}_{0.57}\text{Sn}_{0.43})_{1-y}\text{Ti}_y]_{0.98}\text{O}_3$  (PNZST43/100y/2) solid solution ceramics were investigated for their antiferroelectric  $\leftrightarrow$  ferroelectric phase transitions. It was found that the induced ferroelectric phase is metastable in compositions with  $0.07 \leq y \leq 0.08$  at room temperature. Strain measurements and X-ray diffraction analysis confirmed that the ferroelectric phase has a larger volume than the antiferroelectric phase. Crack growth resistance tests were carried out at room temperature on compact tension specimens with dimensions of  $24 \text{ mm} \times 25 \text{ mm} \times 3 \text{ mm}$  in PNZST43/6.1/2, 43/6.4/2, 43/6.7/2, 43/8/2, 43/10/2 ceramics. The results indicate the fracture toughness in PNZST43/8/2 is much higher than other compositions, verifying the antiferroelectric-to-ferroelectric phase transition toughening effect. The localized phase transition zone was directly mapped with microRaman spectroscopy.

## High Power Piezoelectric Properties of Some Bismuth Layer-Structured Ferroelectric Ceramics and their Applications to Ultrasonic Motors

Hajime Nagata<sup>1</sup>, Shun Endo<sup>1</sup>, Tadashi Takenaka<sup>1</sup>

<sup>1</sup>Department of Electrical Engineering, Faculty of Science and Technology,  
Tokyo University of Science/Japan

Email: h-nagata@rs.noda.tus.ac.jp

Recently, many high-power piezoelectric ceramic devices, such as ultrasonic motors and piezoelectric transducers, have been developed so far. Hard  $\text{Pb}(\text{Zr,Ti})\text{O}_3$  (PZT) ceramics with a high piezoelectric strain constant  $d_{ij}$  and a high mechanical quality factor  $Q_m$  are often used in high-power piezoelectric applications. Normally, hard PZT-based ceramics are driven at a vibration velocity of 1 m/s owing to a resonance frequency change, heat generation and  $Q_m$  reduction. Additionally, PZT ceramics contain a large amount of PbO. Therefore, lead-free piezoelectric materials for replacing PZT have recently been demanded from the viewpoint of environmental protection. The family of bismuth layer structured ferroelectrics (BLSFs) has been attracting attention as a lead-free piezoelectric material for resonators and filters because they have large  $Q_m$  values. Thus, they seem to be good candidates for high-power ceramic devices realizing a large-amplitude and a linear stability against vibration velocity<sup>238,239</sup>. So, in this study, high-power piezoelectric characteristics under continuous driving were studied on some bismuth layer-structured ferroelectric ceramics, i.e.,  $\text{Sr}_{0.25}\text{Bi}_{1.75}\text{Ti}_{0.75}\text{Ta}_{1.25}\text{O}_9$  (SBTT,  $m=2$ ),  $\text{Bi}_4\text{Ti}_{2.98}\text{V}_{0.02}\text{O}_{12}$  (BITV,  $m=3$ ),  $\text{Bi}_4\text{Ti}_3\text{O}_{12}\text{-SrBi}_4\text{Ti}_4\text{O}_{15} + \text{MnCO}_3$  0.2 wt% (BIT-SBTi,  $m=3, 4$ ), and  $(\text{Sr}_{0.7}\text{Ca}_{0.3})_2\text{Bi}_4\text{Ti}_5\text{O}_{18} + \text{MnCO}_3$  0.2 wt% (SCBT,  $m=5$ ).

The vibration velocities,  $v_{0-p}$ , of SBTT, BIT-SBTi, and SCBT ceramics were above 2.0 m/s at 5 V/mm. Also, we observed that the resonance frequency changes and temperatures on the sample surfaces for SBTT, BIT-SBTi, and SCBT ceramics were less than 1.0% and 50 °C at a  $v_{0-p}$  of 2.0 m/s, respectively. The high-power characteristics of the ceramics were superior to those of BITV and hard PZT at a vibration velocity  $v_{0-p} > 0.6$  m/s. Therefore, SBTT, BIT-SBTi and SCBT ceramics are promising candidates for lead-free high-power applications requiring high vibration velocity and frequency stability.

As an example of the high-power piezoelectric application, we tried to demonstrate an ultrasonic motor using some BLSF ceramics. The ultrasonic motor we fabricated by some BLSF ceramics successfully rotated under the large amplitude driving around the resonance frequency. The maximum rotation-speed was over 600 rpm on the ultrasonic motor fabricated by BIT-SBTi, and SCBT ceramics. This rotation-speed was much higher than that in the motors by hard PZT ceramics. Additionally, the resonance frequency of BLSF motor was almost constant under the large amplitude driving. In fact, the ultrasonic motor by SCBT ceramic was continuously rotated for more than 5 min without any control of the resonance frequency. This means that the ultrasonic

<sup>238</sup> S. Kawada, H. Ogawa, M. Kimura, K. Shiratsuyu, and H. Niimi: Jpn. J. Appl. Phys., 45 (2006) 7455.

<sup>239</sup> H. Ogawa, S. Kawada, M. Kimura, K. Shiratsuyu, and Y. Sakabe: IEEE Trans. UFFC, 54 (2007) 2500.

motor using BLSF ceramics can eliminate the additional circuit for pursuing the resonance frequency.

## Using A New Design of Piezoelectric Device for Micro UEDM Application

Yung Ting, Chia-An Wei, Chin-Chih Yeh, Chih-Hsuan Yu and Hsiang-Hung Huang

Department of Mechanical Engineering, Chung Yuan Christian University, 200, Chung Pei Rd. Chung Li, Taiwan 32023, ROC

Email: [yung@cycu.edu.tw](mailto:yung@cycu.edu.tw)

**Keywords :** Micro UEDM, Piezoelectric Actuator, energy harvester

### Abstract

Using two pieces of piezoelectric ceramics a two-stage energy harvester for an application of micro Ultrasonic Electrical Discharge Machining (UEDM) is developed in this article. Ceramics in the first stage (PZT#1) plays the role of actuator driven with oscillation of high frequency and amplitude. In the second stage (PZT#2), the ceramics receives part of the power transmitted from the actuator in the first stage and generates electricity of satisfactory voltage and current for the application requirement.

In the case study of micro UEDM, the entire system is designed and presented in Figure 1. Fundamental components include an actuator, a generator, a compliant mechanism, and a proof mass and so on. A selected example of electric power of about 0.4~3 watts for electrical discharge and oscillation in the range of 150~500kHz for removing dregs is preserved in the second stage for the application of micro UEDM. Design of the external power includes the oscillation frequency and amplitude in the first ceramic actuator as well as the transmission mechanism to transfer the energy from the first stage to the second stage. Modeling and analysis as well as experiment are carried out. The analytical results are nearly approximate to the experiment results, and the outcomes verify the proposed design can reach the target of generating both electricity and oscillation for the application of UEDM. Figure 2 is UEDM mechanism and Measurement data.

With power input to the first actuator to oscillate, the connected second one makes use of the transmitted mechanical vibration energy to generate electricity, which has the meaning of renewable energy. In case the energy expense is less as compared to the general use for both applications, the developed device has the advantage of energy saving. Moreover, this device builds with both functions in one set that is compact and economic. Also, a micro structure is designed to control electric power output with better function for micro UEDM.

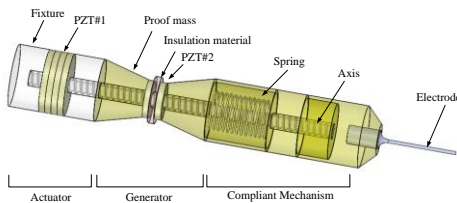


Fig. 1: Configuration of Micro UEDM using Piezoelectric Ceramics

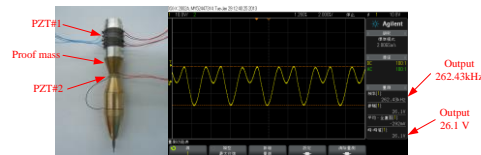


Fig. 2: UEDM mechanism and Measurement data



## Efficient Compensation of Nonlinear Transfer Characteristics for Piezoceramic Actuators

Felix Wolf<sup>1</sup>, Hartmut Hirsch<sup>1</sup>, Alexander Sutor<sup>1</sup>, Stefan J. Rupitsch<sup>1</sup>, Reinhard Lerch<sup>1</sup>

<sup>1</sup>Chair of Sensor Technology, Friedrich-Alexander-University, Erlangen, Germany

Email: felix.wolf@lse.e-technik.uni-erlangen.de

The hysteretic, nonlinear transfer characteristics is one of the main drawbacks when using piezoceramic materials in actuator applications. Multiple effects on various length scales contribute to this difficult material behavior, making precise positioning and manipulation tasks erroneous. Two solutions are commonly used to overcome these tracking errors:

1. The use of amplifiers with charge output
2. Open- and closed-loop control strategies

The second solution is more favorable, since the charge-strain relation is only linear in a limited operational range and circuitry of charge amplifiers has some disadvantages. However, efficient models describing the nonlinear material behavior are necessary for control strategies. The Preisach hysteresis operator is such an efficient model, but it allows only for the calculation of the transfer characteristics in forward direction, i.e.,

$u(t) \rightarrow f_{\text{sim}}(t)$ . An analytic inversion of this model for calculating the input  $u_{\text{inv}}(t)$  required for a given output  $f_{\text{target}}(t)$  does not exist.

In our previous work, we proposed a generalized Preisach model with an analytic weight function. The model was extended to cover the influence of additional mechanical stress<sup>240</sup> on the transfer characteristics as well as of creep effects utilizing an additional creep operator<sup>241</sup>.

The scope of the present contribution is to introduce a novel algorithm allowing for an efficient iterative inversion of the Preisach operator. The algorithm is based on a sophisticated two-step search procedure in the Preisach plane representing the “memory” of the material. The computing time depends on the discretization  $M$  of the Preisach plane. As our investigations reveal, a discretization level of  $M=200$  is sufficient for precise inversion and prediction results (see Fig.1). For this discretization level, a maximum sampling frequency of 3.45 kHz is allowed for the signals to be inverted.

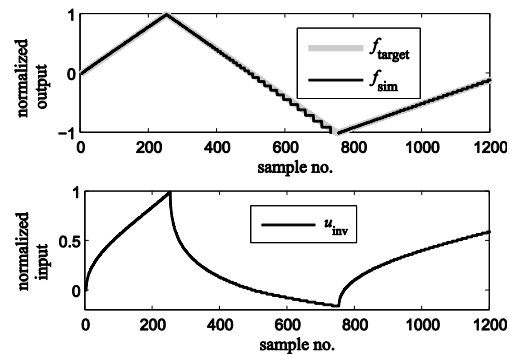


Fig. 70: Desired target quantity  $f_{\text{target}}$ , inverted input-signal  $u_{\text{inv}}(f_{\text{target}})$  for discretization level  $M = 200$  as well as simulated model output  $f_{\text{sim}}(u_{\text{inv}})$ .

<sup>240</sup> F. Wolf, A. Sutor, S. J. Rupitsch and R. Lerch, A generalized Preisach approach for piezoceramic materials incorporating uniaxial compressive stress, J. Sen. Act. A, 2012, 186, 223-229

<sup>241</sup> F. Wolf, A. Sutor, S. J. Rupitsch and R. Lerch, Modeling and measurement of creep- and rate-dependent hysteresis in ferroelectric actuators, J. Sen. Act. A, 2011, 172, 245-252

The model inversion is further verified via open-loop control of the strain output of soft PZT bulk ceramics as well as of trimorph bending actuators. The model inversion we introduce shows to be an efficient tool for compensating the nonlinearities in piezoceramic actuator applications.

## ISAF Group 3 Posters

Forum Hall

*Wednesday, July 24 2013, 01:00 pm - 04:30 pm*

## Properties of Hafnium/Zirconium doped ( $\text{Na}_{1/2}\text{Bi}_{1/2}\text{TiO}_3$ ) Relaxor-Ferroelectric Ceramics Under Bias Electrical Field

DERYA KIRSEVER<sup>1</sup> and HUSEYIN YILMAZ<sup>2</sup>

<sup>1</sup> Sakarya University, Department of Metallurgical and Materials Engineering, TURKEY

<sup>2</sup> Gebze Institute of Technology, Department of Material Science and Engineering, TURKEY

[dkirsever@sakarya.edu.tr](mailto:dkirsever@sakarya.edu.tr), [h.yilmaz@gyte.edu.tr](mailto:h.yilmaz@gyte.edu.tr)

**Abstract** Lead-free piezoelectric materials are intensely studied due to being environmentally friendly. Among them, sodium bismuth titanate ( $\text{Na}_{1/2}\text{Bi}_{1/2}\text{TiO}_3$ , or NBT) and its various solid solutions have been drawing special attention as a new candidate for their lead based counterparts. There is a great demand for reducing the adverse effect of lead. In this study, Hafnium or Zirconium doped grain oriented ( $\text{Na}_{1/2}\text{Bi}_{1/2}\text{TiO}_3$ ) (NBT) ceramics with  $\langle 001 \rangle$  orientation were fabricated by Templated Grain Growth (TGG) method using anisotropically shaped  $\text{SrTiO}_3$  template particles. These molten salt synthesized  $\text{SrTiO}_3$  platelets were tape cast with calcined NBT powder, and sintered at  $1200^\circ\text{C}$  for 6 h. Texture fractions up to 70% have been obtained.  $\text{Hf}^{+4}$  or  $\text{Zr}^{+4}$  doped NBT ceramics were characterized by using X-Ray diffraction (XRD), scanning electron microscopy (SEM), polarization and electromechanical measurements. Electromechanical properties of  $\text{Hf}^{+4}$  and  $\text{Zr}^{+4}$  doped NBT ceramics were studied under electrical bias. Unipolar strains up to  $> 0.25\%$  was measured. Electrostrictive coefficient of  $\text{Hf}^{+4}$  doped NBT ceramics were determined to be  $0.032 \text{ m}^4/\text{C}^2$ , which is much larger than that of PMN-based electrostrictive materials.

## Simulation of the Locally Measured $d_{33}$ of Piezoelectric 1-3-Composites

Christoph Pientschke<sup>1</sup>, Sabine Kern<sup>1</sup>, Hartmut S. Leipner<sup>1</sup>

<sup>1</sup>Martin-Luther-University, Interdisciplinary Center of Materials Science (CMAT),  
06099 Halle (Saale), Germany

Email: christoph.pientschke@physik.uni-halle.de

Piezoelectric 1-3-composites consist of aligned piezoelectric fibers or rods that are surrounded by a polymer matrix. The effective piezoelectric coefficient  $d_{33,\text{eff}}$  of the composite can be calculated with analytic approximation formulas. The inputs of these formulas are the piezoelectric coefficient  $d_{33}$  of the piezoelectric fibers or rods, their volume content and some mechanical properties of the constituents. These formulas presume among others an uniform displacement of the composite surface. However, the displacement of the surface is nonuniform. In addition to that the displacement is measured with a local method that is sensitive to a certain area of the surface. So the questions arises: How does the measurement process influence the measured mean  $d_{33}$  of the composites and to what amount does it deviate from the prediction of the approximation formulas? To answer these questions, the experimental situation was simulated using the finite-element-method (FEM) and a subsequent analysis.

In the simulated experiment, the  $d_{33}$  is quasi-statically measured. For this purpose, the local displacement is translated to a capacitive distance detector using a tappet touching the sample surface within a measuring spot. The tappet is moved by the largest displacement within that spot. The  $d_{33,\text{eff}}$  of the 1-3-composites is determined by averaging the local measured piezoelectric coefficients of several tappet positions. For the simulations, the local displacements of 1-3-composites were calculated with FEM. 1-3-composites with periodically and randomly arranged piezoelectric rods were investigated. The resulting data were displayed as a contour plot with pixel values related to the local displacement. The measuring spot was represented by a circle. It was randomly placed on the contour plot. The largest pixel value within that circle was regarded as representation of the measured local  $d_{33}$ . This procedures were repeated several hundred times. The resulting values were statistically analyzed.

According to the simulations, the measured mean  $d_{33}$  and the effective  $d_{33,\text{eff}}$  calculated by the approximation formulas differ significantly. This deviation is not only affected by the measuring spot diameter but also by the volume content of the piezoelectric rods and the thickness of the composite. The approximation formulas overestimate the actual mean  $d_{33}$  of the composites. The difference of the calculated  $d_{33,\text{eff}}$  and the measured mean  $d_{33}$  is smaller than this because increasing spot diameters result in an increase in the measured mean  $d_{33}$ . In addition to that the distribution of the measured  $d_{33}$  changes significantly with increasing spot diameters. For small spot diameters, the distribution of the measured mean  $d_{33}$  and the actual value of the whole surface are similar. The inner structure of the 1-3-composites influences the distribution of the measured  $d_{33}$ . The standard deviation of the measured  $d_{33}$  is a function of the spot diameter. It decreases with increasing spot diameters. For small volume contents, it reaches a maximum before decreasing.

Summarizing, the simulations provide a new access to the understanding of the distribution of locally measured  $d_{33}$  of piezoelectric 1-3-composites and to its relation to approximation formulas.



# Structure and Ferroelectric Properties of Multiferroic BiFeO<sub>3</sub>/SrTiO<sub>3</sub> Superlattices Prepared by RF Sputtering

Hsin-Yi Lee<sup>1</sup>, Shang-Jui Chiu<sup>1</sup>, Ge-Ping Yu<sup>2</sup>

<sup>1</sup>National Synchrotron Radiation Research Center, Hsinchu, Taiwan

<sup>2</sup>Institute of Nuclear Engineering and Science, National Tsing Hua University, Hsinchu, Taiwan

Email: hylee@nsrrc.org.tw

Asymmetric superlattice structures consisting of multiferroic BiFeO<sub>3</sub> (BFO) and paraelectric SrTiO<sub>3</sub> (STO) sublayers were grown on a Nb-doped STO substrate with rf magnetron sputtering at temperatures in a range 500 - 800 °C. For a substrate temperature less than 500 and at 800 °C only poorly crystalline films resulted, whereas a BFO/STO superlattice structure film of great crystalline quality was obtained for a substrate temperature in a range 550 - 750 °C. To characterize the structure of the buried interface and the surface morphology of these films, we measure the x-ray reflectivity and diffraction pattern. The fitted result from x-ray reflectivity curves shows that the density of the BFO film is slightly less than that of the bulk phase. The formation of a superlattice structure was confirmed through both the appearance of Bragg lines separated by Kiessig fringes in x-ray reflectivity curves and the satellite features of a (002) diffraction pattern. The clearly discernible main feature and satellite features on both sides of the substrate around the (002) STO Bragg peak of superlattice films indicate the high quality of the BFO/STO artificial superlattice structure as shown in Fig. 1(a). For BFO/STO superlattice films deposited at 600-750 °C, an increased crystalline quality with smaller interface roughness correlates with larger lattice strain and remanent polarization of the film. The measurement of hysteresis loops shows that the largest remanent polarization ( $P_r$ ) occurs at deposition temperature 600°C as shown in Fig. 1 (b). These measurements of the hysteresis loops show that the ferroelectric properties of BFO/STO superlattice films are highly correlated with lattice strain, interface roughness and crystalline quality of the films.

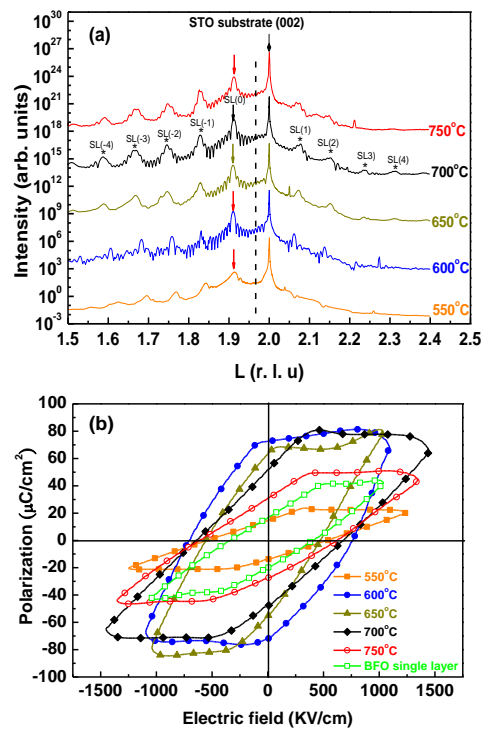


Fig. 71: (a) Intensity distribution of a (002) radial scan of BFO/STO superlattice films deposited at varied substrate temperatures. An arrow marks the position of the superlattice main peak and a dashed line denotes the position of the mean value of the superlattice. (b) Electric hysteresis loops of superlattice films deposited at varied substrate temperatures. For a single-layer film of BFO (thickness 40 nm) deposited at 600 °C and prepared under the same sputtering conditions,  $2Pr \sim 40 \mu\text{C cm}^{-2}$ .

<sup>1</sup> S. J. Chiu, Y. T. Liu, H. Y. Lee, G. P. Yu and J. H. Huang, *J. Crystal Growth* **334**, 90-95 (2011).



## Inverse Scheme to Identify the Temperature Dependence of Electromechanical Coupling Factors for Piezoceramics

Stefan J. Rupitsch, Jürgen Ilg, Reinhard Lerch

Chair of Sensor Technology, Friedrich-Alexander-University Erlangen-Nuremberg

Email: stefan.rupitsch@lse.eei.uni-erlangen.de

Finite element (FE) simulations are oftentimes utilized to predict the electrical as well as mechanical behavior of devices incorporating piezoceramic materials. Apart from the setup of the devices, precise material parameters of the piezoceramics are indispensable to obtain reliable simulation results. These material parameters determine the electromechanical coupling factors which are decisive quantities for applications of piezoceramic materials. As devices usually operate in a certain temperature range, the temperature-dependent behavior of the material parameters has also to be considered within FE simulations.

Common approaches to identify material parameters of piezoceramic materials are based on the IEEE/ANSI standard<sup>1</sup>. Thereby, the frequency resolved electrical impedance of several samples exhibiting different geometries is acquired and analyzed. By means of simple analytical relations, 10 independent material parameters can be computed which entirely characterize the piezoceramic material. However, the IEEE/ANSI standard presumes monomodal mechanical vibrations of the investigated samples that cannot be fulfilled in practice. As a result, the determined material parameters do not yield reliable simulations for piezoceramics. On account of this fact, we developed an alternative approach for the identification of accurate material parameters<sup>2</sup>. The approach is based on an adjustment of FE simulations to measurements. In particular, the electrical behavior of two block-shaped piezoceramic samples featuring different directions of polarization is investigated. With the aid of an Inverse Scheme, the material parameters serving as input quantity of the FE simulation are adjusted in a convenient way. Since this approach utilizes FE simulations, the identification procedure is not based on the assumption of monomodal mechanical vibrations.

In order to study the variation of material parameters as well as coupling factors with respect to the ambient temperature, the piezoceramic samples were placed in a climatic chamber providing the temperature range -35 °C to 145 °C. Figure 1a shows temperature-dependent variations of selected material parameters for the piezoceramic material PIC255 which were identified by means of the Inverse Scheme. As can be seen, the dielectric coefficient  $\epsilon_{11}^S$  strongly relies on temperature. In contrast, the elastic stiffness modulus  $c_{12}^E$  remains nearly constant. Although the dielectric coefficients are altered up to 50%, the electromechanical coupling factors decrease only slightly with increasing temperature (see Fig. 1b). Hence, we can state that the performance of the piezoceramic material PIC255 stays almost constant in the investigated temperature range.

<sup>1</sup> IEEE Standard on Piezoelectricity, ANSI-IEEE Std 176-1987.

<sup>2</sup> S.J. Rupitsch, R. Lerch, Applied Physics A, vol. 97(4), p. 735-740, 2009.

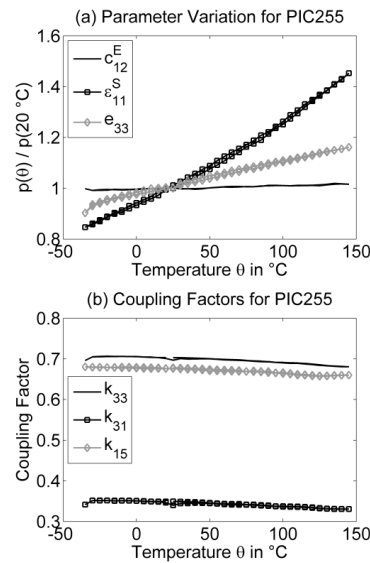


Figure 1: (a) Variation of selected material parameters with respect to temperature for PIC255. (b) Resulting electromechanical coupling factors.

## Short pulse characterization of nanosecond-range dielectric degradation in ferroelectric thin-film capacitors

A.Q. Jiang, T.A. Tang

State Key Laboratory of ASIC & System, Department of Microelectronics, Fudan University, Shanghai 200433, People's Republic of China

Email: aqjiang@fudan.edu.cn

Generally, the ferroelectric capacitance under a dc voltage stressing drops continuously with time over a few days and months, and the capacitance-voltage ( $C$ - $V$ ) loop looks like a butterfly shape. The slow dielectric degradation is considered to originate from oxygen-vacancy motion and/or defect-dipole alignments along the field<sup>242</sup>. The large nonlinear capacitance can be applied to high-density dynamic random access memories, tunable microwave filters, and phased array antennas<sup>2</sup>. If the  $C$ - $V$  sweeping time is short enough, the mechanisms beyond the defect-related slow processes should be protruded. With modern techniques, domain switching speed can be characterized from a series of voltage pulses with widths as short as a few nanoseconds.<sup>14</sup> It is curious what happens in  $C$ - $V$  loops as the voltage sweeping time is shortened into the nanosecond order. Obviously, the present commercial electrical bridges cannot realize so high a voltage sweeping speed.

With the improved short-pulse measurements, we estimated the differential capacitance of ferroelectric Au/BiFeO<sub>3</sub>/LaNiO<sub>3</sub>/SrTiO<sub>3</sub> and Pt/IrO<sub>2</sub>/(Pb(Zr,Ti)O<sub>3</sub>/IrO<sub>2</sub>/Pt thin-film capacitors from nanosecond discharging currents induced by a delta voltage overlapping each stressing voltage pulse with widths of 500 ns – 1 s. With the shortening of this pulse width, we clearly observed two capacitance maxima from each branch of capacitance-voltage loops ( $C$ - $V$ ) in Fig. 1, reminiscent of an antiferroelectric behavior. This finding provides the evidence of the nonlinear dielectric contribution of reversible domain motion. The reversible domains can align along the field under the voltage, but reverses back immediately into their previous directions under a reduced field strength to release their polarization charge, just like an antiferroelectric. As the voltage stressing time is long enough, the internal field to drive the reversible domain motion is temporally screened by the near-electrode charge injection. Finally, we evidenced the charge injection from the imprint profile and reversible domain freezing into irreversible domains upon cooling.

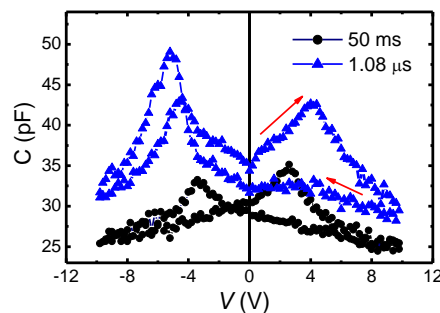


Fig. 72:  $C$ - $V$  loops for 300 nm thick BiFeO<sub>3</sub> thin films under different voltage sweeping times with electrode area of  $7.85 \times 10^{-5} \text{ cm}^2$ .

1. Y.A. Boikov, B.M. Goltsman, V.K. Yarmarkin and V.V. Lemanov, "Slow capacitance relaxation in (BaSr)TiO<sub>3</sub> thin films due to the oxygen vacancy redistribution", *Appl. Phys. Lett.*, vol. 78, p. 3866-3868, 2001.
2. F. DeFlaviis, N.G. Alexopoulos and O.M. Stafsudd, "Planar microwave integrated phase-shifter design with high purity ferroelectric material", *IEEE Trans. Microwave Theory Tech.* vol. 45, p. 963-969, 1997.



## Characteristics and structure of Mn-doped (0.6-x)PMT-0.4PT-xPZ ternary system near morphotropic phase boundary

Hua Hao, Hanxing Liu, Wenhua Sun, Zhonghua Yao, Minghe Cao, Zhiyong Yu

School of Material Science and Engineering; State Key Laboratory of Advanced Technology for Materials Synthesis and Processing, Wuhan University of Technology, Wuhan, P.R.China 430070  
Email: [haohua@whut.edu.cn](mailto:haohua@whut.edu.cn)

The excellent electrical properties and potential applications of  $\text{Pb}(\text{B}'_{1/3}\text{B}''_{2/3})\text{O}_3$  lead-based perovskite relaxor ferroelectrics have attracted considerable research interest. Comparing to the large number of papers on the niobate perovskite relaxors and their solid solution, very few investigations on the  $\text{Pb}(\text{Mg}_{1/3}\text{Ta}_{2/3})\text{O}_3$  (PMT) and related solid solution were reported till now. As observed in other systems such as  $\text{Pb}(\text{Mg}_{1/3}\text{Nb}_{2/3})\text{O}_3$ - $\text{PbZrO}_3$  (PZ)- $\text{PbTiO}_3$  (PT), anomalously good dielectrical properties were observed for compositions lying near the morphotropic phase boundary (MPB). Therefore, improved dielectric properties with increasing transition temperature can be expected in PMT-PZ-PT system, due to the relatively high Curie temperature of end members of PZ ( $T_C = 230^\circ\text{C}$ ) and PT ( $T_C = 492^\circ\text{C}$ ).

In this work, the tetragonal intensity ratio TP(%) of (0.6-x)PMT-0.4PT-xPZ(x=0.2) samples doped with various  $\text{MnO}_2$  values(0~1.0%(wt)) was calculated by Raman spectra. TP(%) values increase with  $\text{MnO}_2$  doping content from 67.6% to 78.3%, then decrease sharply at the doping limit. XRD testing of Mn 0.2% (wt) doped (0.6-x) PMT-0.4PT-xPZ(x=0.25) sample indicates more tetragonal phase at room temperature and XRD peak tested at 90-160°C become broader, induced by the rhombohedral to tetragonal phase transition. The remnant polarization ( $P_r$ ) was found to be increased while the coercive field was decreased with increasing Mn doped level. Due to the hardening effect caused by the Mn addition, the dielectric constant and loss of 0.35PMT-0.25PZ-0.4PT ceramics decreased, while the mechanical quality factors were found to increase up to 790. Meanwhile, the piezoelectric coefficient ( $d_{33} \sim 435\text{pC/N}$ ) and electromechanical coupling factors ( $k_p = 59\%$ ) were found to increase showing a “soft” effect.

Table 1 Dielectric and piezoelectric properties of Mn-doped 0.35PMT-0.25PZ-0.4PT

Samples	$\epsilon_r$	loss	$d_{33}$ (pC/N)	$k_p$ (%)	$Q_m$	$T_c$ ( $^\circ\text{C}$ )	$P_r$ ( $\mu\text{C}/\text{cm}^2$ )	$E_c$ (kV/cm)
0.35PMT-0.25PZ-0.4PT	2000	0.035	215	26	110	185	17.3	8.7
$\text{MnO}_2$ 0.2%(wt)	1530	0.005	435	59	790	197	29.9	6.2
$\text{MnO}_2$ 0.5%(wt)	1085	0.005	300	42	605	194	23.9	8.1

## Domain Size Effects on the Local $d_{33}$ of Tetragonal $(\text{Na}_{0.53}\text{K}_{0.45}\text{Li}_{0.02})(\text{Nb}_{0.8}\text{Ta}_{0.2})\text{O}_3$ Ceramics

Jeong-Ho Cho, Duc-Thang Le, Young-Hun Jeong, Joong Hee Nam, Ji-Sun Yun, Jong-Hoo Paik, and Byung-Ik Kim

Intelligent Electronic Component Team, Korea Institute of Ceramic Engineering and Technology, Seoul 153-023, South Korea

Email: [goedc@kicet.re.kr](mailto:goedc@kicet.re.kr)

Lead-free  $(\text{Na}_{0.53}\text{K}_{0.45}\text{Li}_{0.02})(\text{Nb}_{0.8}\text{Ta}_{0.2})\text{O}_3$  (NKLNT) was prepared using a conventional cold-pressing method. A commercial Piezoresponse Force Microscope (PFM) was applied to observe the domain structures of NKLNT ceramics. The typical configuration of the ferroelectric domain was analyzed in abnormal grains with grain sizes that exceeded  $40\ \mu\text{m}$ , where tetragonal  $90^\circ$  domains are predominant.

In this study, ferroelectric domains and the local piezoresponse were investigated in tetragonal Li- and Ta-modified NKN (NKLNT) ceramic materials. PFM observations revealed a typical tetragonal domain structure with  $90^\circ$  lamella domains predominating. Measurements of the local piezoresponse indicated that the equilibrium domain size greatly influences the coercive field and local longitudinal piezoelectric coefficient. The coercive field ( $V_c$ ) decreased and the measured value of longitudinal piezoelectric coefficient ( $d_{33}$ ) increased significantly with a decrease in the domain size ( $dw$ ). These changes confirm that the domain size should be considered as a very important parameter which contributes to the piezoelectric properties of ceramics. Finally, the most interesting aspect here is the possibility that the piezoelectric performance of the lead-free NKLNT ceramics can be improved due to the investigation of the optimum domain size. Therefore, the introduction of microwave sintering to NKLNT ceramics may be proposed in this case.

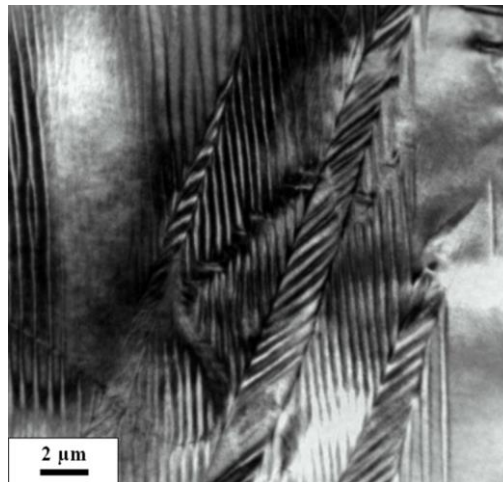


Fig. 73: Transmission electron microscopy (TEM) image of NKLNT ceramics shows lamella and herringbone-shaped domains existing simultaneously. The domain size is evaluated  $<1\ \text{nm}$ .

## Resistive Hysteresis of MOD-made BaTiO<sub>3</sub> Ferroelectric Thin Film Dependent on Film Thickness

Syu Ou, Hideaki Kawahara, Kaoru Yamashita, Minoru Noda

Grad. Sch. Sci. & Tech., Kyoto Institute of Technology, Kyoto, Kyoto/Japan

Email: noda@kit.ac.jp

A perovskite BaTiO<sub>3</sub> (BT) thin film has been so far much investigated as a successful ferroelectric material. Moreover, a recent epitaxially grown BT ultrathin film as thin as 1-3 nm realized definite ferroelectricity (as piezoelectricity) [1]. While, BT family of perovskite ferroelectric film has generally showed considerable ‘size effect’ that means either ferroelectricity or high permittivity is lost when the film becomes thinner than a critical thickness. On the other hand, as one of a promising candidate material for Resistive RAM (ReRAM), the BT film has been also investigated for its resistive hysteresis and mechanism [2,3]. For the latter researches, however, the focus is mainly on properties of charge transfer mechanism in the oxide film as a conventional paraelectric metal oxide but not much on those of intrinsic ferroelectric behavior in the BT film. In this work, we formed MOD(Metal-Organic-Decomposition)-made BT thin film with chemical stoichiometry then investigate the relation between the film thickness dependence of its ferroelectricity and the resistive hysteresis.

An MOD solution of BT was spin-coated on a sputtered Pt(111)/Ti/SiO<sub>2</sub>/Si substrate with condition of 500 rpm-3 s/3000 rpm-30 s, thereafter dried on a hot plate at 200 °C for 10 min. These processes were repeated once or twice to the thickness of about 60 or 110 nm, and RTA final-annealed at 600 °C for 20 min in ambient atmosphere. XRD(2θ-θ) revealed that the prepared film was polycrystalline and (110) and (101) preferentially oriented. A BT film by two MOD layers with around 110 nm-thickness revealed remanent polarization ( $P_r$ ) of about 5 μC/cm<sup>2</sup> and coercive force ( $E_c$ ) of about 1-2 MV/cm at room temperature. Figure 1 shows absolute value of current density vs. electric field, meaning resistive hysteresis of the 110 nm-BT film when applying 3rd triangle electric field scan (0--> Max.(+4500kV/cm)-->0-->Min.(-4500kV/cm)-->0). It is clear from Fig. 1 that the leakage level keeps different throughout the electric field and the ratio is around 1-2 order of magnitude between scans of + and - direction of electric field(blue and red, respectively), whereas the leakage curve is dependent on polarization reversal at near  $E_c$ . Next, we made one MOD layered BT film with around 60 nm thickness, which showed little  $P_r$  and  $E_c$ , respectively, meaning its ferroelectricity is almost lost. A resistive hysteresis of the 60 nm-BT film(Fig. 2) when applying the same scans above shows no relation with the polarization reversal but some ‘set’ and ‘reset’ events of current are observed similar to [2,3] at higher electric field (2.5 to 3.0 MV/cm) than  $E_c$ , which is maybe unipolar switching [2]. Current on/off ratio between the ‘set’ and ‘reset’ seems small to be about 3.

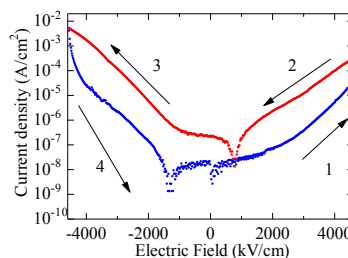


Fig. 74: Resistive hysteresis of 110 nm-thickness BaTiO<sub>3</sub> 2-MOD layer film.

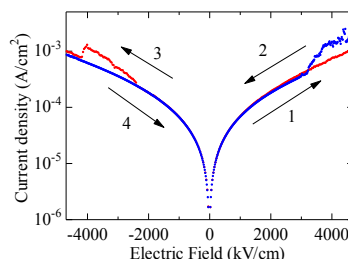


Fig. 2: Resistive hysteresis of 60 nm-thickness BaTiO<sub>3</sub> 1-MOD layer film.

Therefore, it is thought from the results that the current on/off ratio is much larger for 110 nm-BT than for 60 nm-BT. This indicates a possibility that the existence of ferroelectricity relates to the on/off ratio in the resistive hysteresis phenomena of BT thin film.

## Effect of polarization switching on the electron emission of PZST antiferroelectric ceramic

Yang Liu,<sup>1,2</sup> Yujun Feng,<sup>1</sup> Hongliang He,<sup>2</sup> and Zhuo Xu<sup>1</sup>

<sup>1</sup>*Electronic Materials Research Laboratory, Key Laboratory of the Ministry of Education & International Center for Dielectric Research, Xi'an Jiaotong University, Xi'an 710049, China*

<sup>2</sup>*National Key Laboratory of Shock Wave and Detonation Physics, Institute of Fluid Physics, CAEP, Mianyang 621900, People's Republic of China*

Email: [sakulaly@gmail.com](mailto:sakulaly@gmail.com)

### Abstract

Stable pulse electric-field-induced electron emissions from antiferroelectric cathode material lead zirconate stannate titanate (PZST) have been investigated. According to the same composition, we analyzed the results of three different pulse-loading types. For antiferroelectric, the polarization change could be written as  $\Delta P = \partial_A \bullet P_S$ , where  $\partial_A$  and  $P_S$  defined, respectively, the polarization switching factor and the saturated polarization. For ferroelectric (the orientation of polarization was codirectional with the positive pulse), the polarization change  $\Delta P = \partial_B \bullet (P_S - P_r)$ , where  $P_r$  referred remnant polarization. For ferroelectric (the orientation of polarization was reverse with the same pulse), the polarization change  $\Delta P = \partial_C \bullet (P_S + P_r)$ . It was found that the emission charges which were gotten from the emission current waveforms were increasing with the polarization switching factor  $\partial_i$  decreasing. The results may give an insight into the physical mechanism underlying the emission process.



## Evaluation of the Polarization State of Piezofiber Composites

Agnes Eydam<sup>1</sup>, Gunnar Suchanek<sup>1</sup>, Kai Hohlfeld<sup>2</sup>, Sylvia Gebhardt<sup>3</sup>, Alexander Michaelis<sup>2,3</sup>, Gerald Gerlach<sup>1</sup>

<sup>1</sup>TU Dresden, Solid State Electronics Lab, Dresden, Germany

<sup>2</sup>TU Dresden, Institute of Materials Science, Dresden, Germany

<sup>3</sup>Fraunhofer Institute for Ceramic Technologies and Systems, Dresden, Germany

Email: Agnes.Eydam@tu-dresden.de

Integrated piezoelectric sensors and actuators find applications for health-monitoring, for reducing noise emission, for vibration control and damping, etc. The polarization distribution of piezoelectric materials is usually determined by means of thermal waves recording the time or frequency dependencies of the pyroelectric current. In the so-called Laser Intensity Modulation Method (LIMM) an intensity-modulated laser beam is absorbed in the sample and generates thermal waves with a modulation-frequency-dependent penetration depth. The average pyroelectric coefficient  $p_{av}$  can be additionally measured by heating the whole sample harmonically at low modulation frequencies by means of a Peltier element and determining the pyroelectric current.

In this work, we evaluate the polarization state of PZT fibers embedded in epoxy resin. The investigated samples could be described as 1-3 piezocomposites. Irregularly arranged PZT fibers with about 330  $\mu\text{m}$  in diameter represent the active phase which is continuous in only one direction.

An analytical solution of the 1-D thermal problem was derived for an embedded piezoelectric plate. The homogeneously poled, harmonically heated plate exhibits heat losses to the environment characterized by a continuous distribution of relaxation times  $\tau$ . This model was then applied to fiber composites as illustrated in Fig. 1. The average pyroelectric coefficient of the PZT fibers is in the range of  $10^{-11}$  to  $10^{-10}$  C/cm<sup>2</sup>K. We have evaluated the influence of fiber processing parameters on the polarization state by comparing the values of  $p_{av}$  and also the amplitudes of the pyroelectric current. The value of the spontaneous polarization  $P_s$  was derived from the  $P$ - $E$  hysteresis loop.

The penetration depth of the thermal wave is determined by the thermal diffusivity of the material and the circular frequency of heat modulation. The thermal diffusivity of the piezofiber composite was estimated (i) by the laser flash method and (ii) by means of the frequency dependence of the pyroelectric coefficient determined under conditions of sufficient heat losses to the environment from the top electrode. Here, the threshold frequency of thermal wave confinement in the piezoceramic layer was evaluated.

We demonstrated that the thermal wave method is a promising non-destructive tool to evaluate the polarization state of piezofiber composites. By this way, the influence of thermal and mechanical loads during the fabrication process can be evaluated.

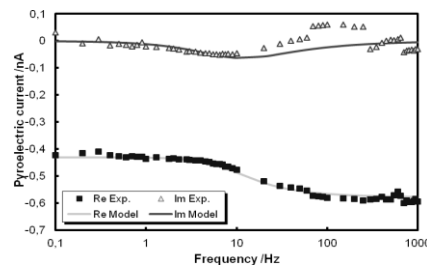


Fig. 75: Pyroelectric current spectrum of a fiber composite sensor in comparison with a fit to an analytical model. The real part of the pyroelectric current is denoted as Re and the imaginary part as Im.

## MPB in $x(\text{BaZrO}_3)$ - $y(\text{Bi}(\text{Mg}_{0.5}\text{Ti}_{0.5})\text{O}_3)$ - $z(\text{K}_{0.45}\text{Na}_{0.5}\text{Li}_{0.05})\text{NbO}_3$ lead-free piezoelectric ceramics

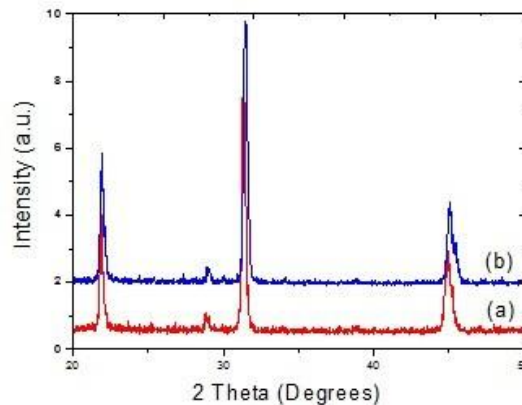
Ruilin Wu<sup>1</sup>, Guorong Li<sup>1</sup>, Jiangtao Zeng<sup>1</sup>, Liaoying Zheng<sup>1</sup>

<sup>1</sup>Shanghai Institute of Ceramics, Chinese Academy of Science, Shanghai, China

Email: zhengly@mail.sic.ac.cn

During the last years, with the increase of awareness for environmental topics<sup>243</sup>, lead-free piezoelectric draw much attention. The lead-free alkali niobate ceramics based on  $(\text{K}, \text{Na})\text{NbO}_3$  (KNN) are the most promising one because of its high  $T_c$  and good piezoelectric properties<sup>244</sup>. From low temperature to high temperature, KNN undergoes successive phase transitions which can be adjusted by adding some dopants to improve its temperature stability<sup>245</sup>.

The  $x(\text{BaZrO}_3)$ - $y(\text{Bi}(\text{Mg}_{0.5}\text{Ti}_{0.5})\text{O}_3)$ - $z((\text{K}_{0.45}\text{Na}_{0.5}\text{Li}_{0.05})\text{NbO}_3)$  lead-free piezoelectric ceramics has been prepared by solid-state reaction method. The dielectric properties, ferroelectric properties and piezoelectric properties have been investigated. The  $\text{Zr}^{4+}$  occupied the B site of KNN lattice which caused the structure transforming from orthorhombic to tetragonal, while the  $\text{Ba}^{2+}$  occupied the A site caused transforming from orthorhombic to rhombohedral. A morphotropic phase boundary (MPB) between a rhombohedral phase and a tetragonal phase was found. The addition of BMT made the ceramics relaxation. The BZ-BMT-KNLN ceramics is a potential lead-free piezoelectric ceramics.



KNLN8/1/91(b) BZ-BMT-KNLN//1/92

<sup>243</sup> Alain Brice Kounga, "Morphotropic phase boundary in  $(1-x)\text{Bi}_{0.5}\text{Na}_{0.5}\text{TiO}_3$ - $x\text{K}_{0.5}\text{Na}_{0.5}\text{NbO}_3$  lead-free piezoceramics", *Appl. Phys. Lett.*, 92, 222902, 2008.

<sup>244</sup> Pei Zhao, "High piezoelectric  $d_{33}$  coefficient in Li-modified lead-free  $(\text{Na}, \text{K})\text{NbO}_3$  ceramics sintered at optimal temperature", *Appl. Phys. Lett.*, 90, 242909, 2007.

<sup>245</sup> Laijun Liu, "Oxygen-vacancy-related high-temperature dielectric relaxation and electrical conduction in  $0.9\text{K}_{0.5}\text{Na}_{0.5}\text{NbO}_3$ - $0.05\text{BaZrO}_3$  ceramics", *Physica B*, 407, 136-139, 2012.

## Photo-optical Properties of Functional Chiral Photochromic Liquid Crystalline Polyacrylates

Natalia Podoliak<sup>1</sup>, Alexey Bobrovsky<sup>2</sup>, Alexej Bubnov<sup>1</sup>, Věra Hamplová<sup>1</sup>, Miroslav Kašpar<sup>1</sup>, Valery Shibaev<sup>2</sup>

<sup>1</sup> Institute of Physics, Academy of Sciences of the Czech Rep., 182 21 Prague, Czech Republic

<sup>2</sup> Faculty of Chemistry, Moscow State University, Leninskie gory, 119992 Moscow, Russia

Email: podoliak@fzu.cz

Due to photosensitivity, low molar mass liquid crystalline (LC) materials and LC polymer systems containing azobenzene groups are very promising materials for optical data recording and optoelectronics. Recently, several series of photosensitive materials have been synthesized<sup>246</sup> and the respective liquid crystalline polyacrylates (LCP) have been prepared and studied.

Comparative study of chiro- and photo-optical properties of three new chiral photochromic azobenzene-containing comb-shaped LCP has been performed. These LCP contain the same polyacrylate backbones, but have different structure of azobenzene-containing mesogenic groups with chiral chain. Depending on the chemical structure, they exhibit cholesteric N\*, paraelectric SmA\* and ferroelectric SmC\* phases. Lateral chlorine substituent in the mesogen fragment leads to an extreme decrease of isotropisation temperature and causes a disappearance of N\* phase. Circular dichroism (CD) spectra demonstrate a formation of helical order elements even in the amorphoused spin-coated polymer films. Possibility of manipulation of CD values and degree of a helical order by light and annealing was studied. UV-irradiation of all polymers induces E-Z isomerization of azobenzene groups, disrupting LC-order. On the other hand, the irradiation of LCP films by polarized light leads to a photoorientation process due to the cycles of E-Z-E isomerization (see Fig. 1). As a result, an appearance of significant linear dichroism, dependent on the relative position of azobenzene moiety, was observed. The observed photo-optical phenomena are of considerable interest for possible application of chiral photo-chromic polyacrylates in photonics and optoelectronics. For example, the synthesized LCP could be used as photoactive media for optical data storage with the possibility of non-destructive data reading. Optical recording could be realized by the photo-induced local change of birefringence or optical activity modulation. In both the cases the reading of recorded information could be performed by light with the wavelength outside the azobenzene chromophores absorbance band, ensuring the absence of erasing during the reading.

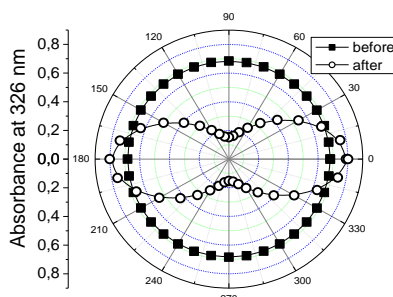


Fig. 77: Polar diagram of polarized absorbance before and after (220 s) the polarized light irradiation (457 nm,  $\sim 0.5 \text{ W/cm}^2$ ) of LC polymer amorphoused film.

<sup>246</sup>M. Kašpar, et. al., *Liq. Cryst.* 2004, 31, 821; A. Bubnov, et. al., *Mol. Cryst. Liq. Cryst.* 2007, 465, 93; M. Kašpar, et. al., *Eur. Pol. J.* 2008, 44, 233; V. Novotná, et. al., *J. Mater. Chem.* 2009, 19, 3992; A. Bobrovsky, et. al., *Liq. Cryst.* 2009, 36, 989; A. Bubnov, et. al., *Phase Transitions* 2010, 83, 16.

This work is supported by projects: ASCR M100101204 & M100101211, CSF P204/11/0723 & CSF 13-14133S.

## High-frequency dielectric properties of $\text{Pb}(\text{Fe}_{1/2}\text{Nb}_{1/2})\text{O}_3$ ceramics and single crystal

R. Mackevičiūtė<sup>1</sup>, J. Banys<sup>1</sup>, A. Kania<sup>2</sup>, V. Goian<sup>3</sup>, D. Nuzhnyy,<sup>3</sup> S. Kamba<sup>3</sup>

<sup>1</sup> Vilnius University, Faculty of Physics, Vilnius, Lithuania

<sup>2</sup> A. Chelkowski Institute of Physics, University of Silesia, Katowice, Poland

<sup>3</sup> Institute of Physics, Academy of Sciences of the Czech Republic, Prague, Czech Republic

Email: Ruta.Mackeviciute@ff.vu.lt

Multiferroic materials, like bismuth ferrite (BFO), lead iron niobate (PFN) and others draw a lot of scientific attention in recent years, as the possibility to control magnetization with electric field, or polarization with magnetic field. It opens the route to a wide variety of new applications. However, despite the fact that PFN ceramic was studied more than 50 years<sup>247</sup>, a dispersion of dielectric permittivity is still not investigated in a wide frequency range.

Dielectric measurements were performed between 300 and 500 K in the frequency range from 20 Hz to 0.8 THz. PFN ceramics are known to undergo a single diffuse phase transition between 370 K and 380 K<sup>1</sup>. This is characterized by a broad peak in  $\epsilon'(T)$ , whose position does not move with frequency. Our experimental data exhibit relaxor ferroelectric behavior, because the peak of  $\epsilon'(T)$  moves to higher T with increasing frequency (see Fig. 1). Detail frequency analysis of dielectric dispersion revealed two anomalous dielectric relaxations; one in sub-THz region and the second in microwave and radio-frequency region. In contradiction to ceramics, we observed two dielectric anomalies in PFN single crystal<sup>248</sup>, one at  $\sim 370\text{K}$ , and additional one, coming from structural phase transition, at  $\sim 355\text{K}$ . The rise of the dielectric permittivity near the temperature of phase transitions is much sharper in single crystal than in ceramics, and the temperatures of maxima of the dielectric permittivity do not depend on frequency, i.e. no relaxor or diffuse phase transition behavior was observed.

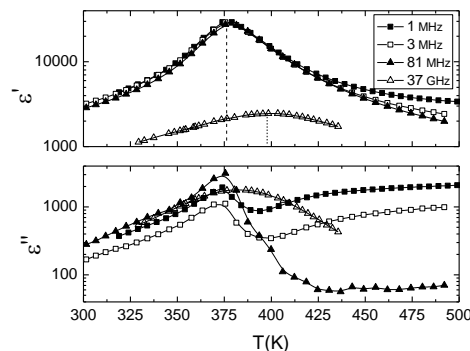


Fig. 78: Temperature dependence of the real and imaginary parts of dielectric permittivity of PFN ceramics.

<sup>247</sup> V. A. Bokov, I. E. Mylnikova, and G. A. Smolenskii, "Ferroelectric antiferromagnetics", *Sov Phys-JETP*, vol. 15, p. 447–449, 1962

<sup>248</sup> A.Kania, E.Talik, and M.Kruczek, "X-Ray Photoelectron Spectroscopy, Magnetic and Dielectric Studies of  $\text{PbFe}_{1/2}\text{Nb}_{1/2}\text{O}_3$  Single Crystals", *Ferroelectrics*, vol. 391, p. 114-121, 2009

## Microwave Dielectric Properties of DyScO<sub>3</sub> and TbScO<sub>3</sub> Substrates Measured by Thin Dielectric Resonator

Martin Kempa<sup>1</sup>, Valeriy Pashkov<sup>2</sup>, Viktor Bovtun<sup>1</sup>, Vitaliy Molchanov<sup>2</sup>, Stanislav Kamba<sup>1</sup>, Yuriy Poplavko<sup>2</sup>, Yuriy Yakymenko<sup>2</sup>

<sup>1</sup> Department of Dielectrics, Institute of Physics ASCR, Prague, Czech Republic

<sup>2</sup> Department of Microelectronics, NTUU "Kyiv Polytechnic Institute", Kyiv, Ukraine

Email: kempa@fzu.cz

Single-crystalline scandate substrates are widely used for deposition of the in-plane strained epitaxial thin films with increased ferromagnetic and ferroelectric transition temperatures or coexisting ferromagnetism and ferroelectricity<sup>2,49,2</sup>. Tentative applications of such films and heterostructures in electronics and telecommunication require knowledge of microwave dielectric properties of both films and substrates. Recently we proposed the thin dielectric resonator (DR) consisting only of the dielectric substrate (or substrate and deposited film) for the non-destructive electrode-free microwave characterization of thin films and substrates<sup>3</sup>. Their in-plane averaged dielectric permittivity and losses can be measured using the TE<sub>01δ</sub> mode<sup>4,5</sup>. The HE<sub>11δ</sub> modes are proposed for the in-plane dielectric anisotropy characterization. Here we report new developments and applications of the thin DR method for the anisotropic substrate characterization.

In-plane components of anisotropic microwave dielectric parameters of the (110) DyScO<sub>3</sub> and (110) TbScO<sub>3</sub> substrates were measured from 10 K to 400 K. Their values and temperature dependences are well consistent with the THz and infra-red parameters<sup>6</sup>, as well as with the permittivity components along crystallographic axes measured at low frequencies<sup>7</sup>. Essential anisotropy of microwave dielectric losses revealed at low temperatures is similar to that in THz range. A pronounced maximum of dielectric losses is observed at 120-150 K.

DyScO<sub>3</sub> and TbScO<sub>3</sub> substrates do not satisfy fully to the strict requirements usual for microwave applications: they are characterized by higher losses, strong anisotropy and pronounced temperature dependence of their dielectric parameters. Nevertheless, the level of losses is still acceptable and allows use of unique properties of the strained films deposited on them.

<sup>249</sup> D. Nuzhnyy, J. Petzelt, S. Kamba, P. Kužel, et al., "Soft mode behavior in SrTiO<sub>3</sub>/DyScO<sub>3</sub> thin films: Evidence of ferroelectric and antiferrodistortive phase transitions", *Appl. Phys. Lett.*, vol. 95, 232902, p. 1-3, 2009.

<sup>2</sup> J.H. Lee, L. Fang, E. Vlahos, X. Ke, Y.W. Jung, et al., "A strong ferroelectric ferromagnet created by means of spin-lattice coupling", *Nature*, vol. 466, p. 954-958, 2010.

<sup>3</sup> V. Bovtun, V. Pashkov, M. Kempa, S. Kamba, et al., "An electrode-free method of characterizing the microwave dielectric properties of high-permittivity thin films", *J. Appl. Phys.*, vol. 109, 024106, p. 1-6, 2011.

<sup>4</sup> V. Skoromets, S. Glinšek, V. Bovtun, M. Kempa, J. Petzelt, et al., "Ferroelectric phase transition in polycrystalline KTaO<sub>3</sub> thin film revealed by terahertz spectroscopy", *Appl. Phys. Lett.*, vol. 99, No. 5, 052908, p. 1-3, 2011.

<sup>5</sup> S. Kamba, V. Goian, M. Orlita, D. Nuzhnyy, J. H. Lee, et al., "Magnetodielectric effect and phonon properties of compressively strained EuTiO<sub>3</sub> thin films deposited on (001) LSAT", *Phys. Rev. B*, vol.85, 094435, p. 1-10, 2012.

<sup>6</sup> S Kamba, V Goian, D. Nuzhnyy, V Bovtun, M. Kempa, J. Prokleska, M. Bernhagen, R. Uecker, D.G. Schlom, "Polar phonon anomalies in single-crystalline TbScO<sub>3</sub>" - Phase Transitions, vol. 86, p. 206-216, 2013.

<sup>7</sup> S. Coh, T. Heeg, J.H. Haeni, M.D. Biegalski, J. Lettieri, L. F. Edge, et al., "Si-compatible candidates for high-k dielectrics with the Pbnm perovskite structure", *Phys. Rev. B*, vol. 82, 064101, p. 1-16, 2010.

## Lattice distortions and Raman spectra of multiferroic heterostructures

Yuzyuk Yury<sup>1</sup>, Khabiri Gomaa<sup>1,4</sup>, Anokhin Andrey<sup>1,2</sup>, Bunina Olga<sup>3</sup>, Stryukov Daniil<sup>1,3</sup>, Golovko Yury<sup>2</sup>, Mukhortov Vladimir<sup>2</sup>, Shirokov Vladimir<sup>2</sup>

<sup>1</sup>Faculty of Physics, Southern Federal University, Rostov-on-Don, Russia

<sup>2</sup>Southern Scientific Centre, Russian Academy of Sciences, Rostov-on-Don, Russia

<sup>3</sup>Research Institute of Physics, Southern Federal University, Rostov-on-Don, Russia

<sup>4</sup>Faculty of Science, Fayoum University, Fayoum, Egypt

Email: yuzyuk@rumbler.ru

Multilayer films and superlattices (SLs) consisting of ferroelectric and multiferroic layers offer a very efficient way of strain engineering to design materials with enhanced magnetoelectric responses. We report on synthesis, x-ray diffraction (XRD) and Raman scattering characterization of epitaxial heterostructures containing alternating  $(\text{Bi}_{0.98}\text{Nd}_{0.02})\text{FeO}_3$  (BNFO) and  $(\text{Ba}_{0.8}\text{Sr}_{0.2}\text{TiO}_3)$  (BST) layers deposited onto (100) MgO substrates. Both layer thickness and number of deposited layers were varied with the aim to investigate the lattice strains as a function of layers thickness.

XRD and Raman examinations were performed after deposition of each layer with aim to clarify transformation of the lattice distortions at each step of growth. XRD patterns of multilayer BNFO/BST heterostructures containing five relatively thick (80 nm) layers showed slightly shifted diffraction peaks of both parent materials due to their distortion. BST layers were found to be under compressive stress, while BNFO sandwiched between two BST layers is under tensile stress. Significant shift of the E(TO) soft mode corresponding to BST layers and partial depolarization in the Raman spectra of multilayer heterostructures were observed due to lattice distortions imposed by epitaxial strains.

For heterostructures with the modulation periods smaller than 30 nm XRD patterns contain one central peak (00l) located midway between respective BNFO and BST peaks and so-called satellite peaks typical for modulated structures – SLs. Detailed XRD examination revealed parallel “cube-on-cube” relationship between each layer and substrate, both BST and BNFO layers are highly strained. In contrast to single BST and BNFO films and heterostructures with relatively thick BNFO/BST layers, hardening of the soft mode and significant tilts and deformation of the  $\text{FeO}_6$  octahedra occurs in SLs and the symmetric-stretching mode of  $\text{FeO}_6$  octahedra about  $705\text{ cm}^{-1}$  appears in the Raman spectra. We propose that distortion in  $\text{FeO}_6$  octahedra is enforced by the epitaxial strains and induces enhanced magnetic properties recently observed<sup>250</sup> in BNFO/BST SLs with a few-nanometers modulation periods.

---

<sup>250</sup> M. S. Ivanov, N. E. Sherstyuk, E. D. Mishina, A. S. Sigov, V. M. Mukhortov, and V. T. Moshnyaga, “Enhanced magnetization and ferroelectric switching in multiferroic BST/BNFO superstructures,” *Ferroelectrics* vol. 433, p. 158-163, 2012.

## Fundamental Understanding of Structural Contributions to Macroscopic Strain in Barium Titanate

Qinghua Cao<sup>1</sup>, John Daniels<sup>1</sup>

<sup>1</sup>The School of Materials Science and Engineering, University of New South Wales, NSW, 2052 Australia

Email: [z3300841@student.unsw.edu.au](mailto:z3300841@student.unsw.edu.au)

The observation of enhanced strain obtained when fields are applied along non-polar directions in many material compositions has led to the renewed study of classical ferroelectrics. In single crystals, the piezoelectric properties at low fields can be attributed to the contribution of lattice strain (intrinsic strain) and field-induced domain wall motion (extrinsic strain). Both intrinsic and extrinsic mechanisms are highly anisotropic with crystallographic orientation. At higher fields, crystallographic phase transformations may be induced which are proposed to generate the enhanced response. For future materials development it is necessary to understand the coupling of anisotropic lattice strain and domain wall motion with the field induced phase transformations. Strain mechanisms in Barium Titanate (BT) single crystals have been studied by several methods (i.e. PFM, SEM, and XRD). Here, we use neutron diffraction methods to allow us to probe the intrinsic, extrinsic and phase stability of BT, in-situ, from the bulk, with application of electric fields. The goal of this research is to characterize the anisotropy of both the intrinsic and extrinsic contributions to macroscopic strain in Barium Titanate single crystals and directly measure the crystallographic phase symmetry at each field step. This initially will lead to a more general understanding of ultrahigh strains observed along non-polar directions, for which there is very little structural experimental evidence.

[100], [110], [111] oriented BT crystals have been cut into 1\*1\*1 mm cubes. Macroscopic properties, including strain and polarization have been measured. The electric field applied on the samples is 2 kV/mm, 2.5 kV/mm, 3 kV/mm, respectively, in order to excite all strain mechanisms including intrinsic, extrinsic, and phase transformations. Neutron diffraction measurements were conducted at the High-Intensity Powder Diffractometer at the Australian Nuclear Science and Technology Organisation. Multiple reflections from each crystal were monitored at a sequence of increasing electric fields.

Macroscopic strain obtained on [100], [110], [111] oriented BT crystals, which is under unipolar electric field, exhibits an increase trend. Intrinsic strain has been observed by the variation of lattice spacing along the field direction (Fig. 1). Extrinsic domain wall motion is observed by variations of the intensity ratios of ferroelastic twin peaks. Phase transformations were observed in [110], and [111] BT crystals at the fields of 1.5 kV/mm and 2 kV/mm, respectively. The results show that the extrinsic domains switching strain is dominant in [100], and [110], orientations at low fields, while intrinsic effects are dominant in the [111] orientation. The crystallographic structure of the field induced phases in [110] and [111] crystals will be discussed.

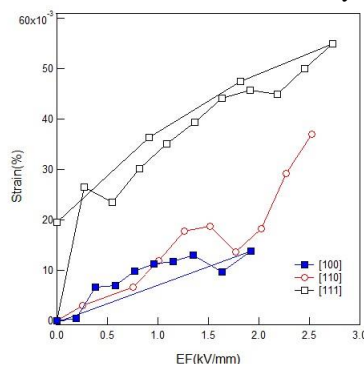


Fig. 1 Intrinsic lattice strain of [100], [110], [111] oriented BT crystals





## Formation Mechanism and Dielectric Properties of the $\text{KTiNbO}_5$ and $\text{K}_3\text{Ti}_5\text{NbO}_{14}$ Ceramics

Mir Im<sup>1</sup>, Sang-Hyo Kweon<sup>1</sup>, Guifang Han<sup>1</sup>, Sahn Nahm<sup>a,1</sup>, Ji-Won Choi<sup>2</sup> and Seong-Ju Hwang<sup>3</sup>

<sup>1</sup>Department of Materials Science and Engineering, Korea University, Seoul 136-701, South Korea

<sup>2</sup>Electronic Materials Center, KIST 39-1 Hawolkkok-dong, Seongbuk-gu, Seoul 137-791, South Korea

<sup>3</sup>Center for Intelligent Nano-Bio Materials (CINBM), Department of Chemistry and Nano Sciences, Ewha Womans University, Seoul 120-750, South Korea

Email: [mirueex@korea.ac.kr](mailto:mirueex@korea.ac.kr)

$\text{TiNbO}_5$  and  $\text{Ti}_5\text{NbO}_{14}$  nano-films synthesized by  $\text{KTiNbO}_5$  and  $\text{K}_3\text{Ti}_5\text{NbO}_{14}$ -layered compounds, respectively, have been reported to exhibit a high  $\epsilon_r$  with a low leakage current density.[1] Although their dielectric properties have been reported, their structural and dielectric properties have not been clearly investigated.[2] In order to fabricate a nano-film having good dielectric properties, it is necessary to understand the microstructure and dielectric properties of the bulk layered perovskite compounds. In this work, therefore, the formation process, the microstructure and dielectric properties of the  $\text{KTiNbO}_5$  and the  $\text{K}_3\text{Ti}_5\text{NbO}_{14}$  oxides are systematically studied. A homogeneous  $\text{KTiNbO}_5$  and  $\text{K}_3\text{Ti}_5\text{NbO}_{14}$  phases were formed at 900°C and the dense  $\text{KTiNbO}_5$  and  $\text{K}_3\text{Ti}_5\text{NbO}_{14}$  ceramics were obtained from the specimen sintered at 1150°C and 1125°C, respectively. Liquid-phase-assisted abnormal grain growth occurred in both specimens along the directions perpendicular to  $\langle 002 \rangle$  during the sintering. Moreover, the secondary phases were developed in the specimens sintered at high temperatures due to the evaporation of  $\text{K}_2\text{O}$ . The  $\text{KTiNbO}_5$  and  $\text{K}_3\text{Ti}_5\text{NbO}_{14}$  ceramics oxides sintered at 1150°C and 1125 °C, respectively, showed the highest relative density of 96.0 % and 96.9% of the theoretical density. The detailed formation processes of the  $\text{KTiNbO}_5$  and  $\text{K}_3\text{Ti}_5\text{NbO}_{14}$  ceramics and their dielectric properties will be also discussed in this work.

## Infrared and terahertz study of lattice dynamics in $\text{PbTiO}_3$

Tetyana Ostapchuk<sup>1</sup>, Christelle Kadlec<sup>1</sup>, Petr Kužel<sup>1</sup>, Jiří Hlinka<sup>1</sup>, and Antoni Kania<sup>2</sup>

<sup>1</sup>Department of Dielectrics, Institute of Physics, Academy of Sciences of the Czech Republic,  
18221 Prague 8, Czech Republic

<sup>2</sup>Institute of Physics, University of Silesia, Uniwersytecka 4, 40007 Katowice, Poland

Email: ostapcuk@fzu.cz

Recent success in understanding of the dynamics of the ferroelectric transition in  $\text{PbTiO}_3$ <sup>xxiv,xxv</sup> still requires a straightforward interconnection of the lattice modes behavior with the macroscopic dielectric characteristics. Here we present high-frequency dielectric spectra evaluated from the far infrared reflectivity and time-domain terahertz transmission measurements. Their analysis enabled us not only to get a full set of the polar mode parameters from the center of the Brillouin zone but also to estimate the contribution of the lattice vibrations in the dielectric anomaly of  $\text{PbTiO}_3$  quantitatively.

## A Study of Properties of Ferrite - Ferroelectric Structures for tunable electronic devices

A.V. Es'kov<sup>1</sup>, A.A. Semenov<sup>2</sup>, A.I. Dedyk<sup>2</sup>, P. Yu. Beliavskiy<sup>2</sup>, Yu.V. Bogachev<sup>2</sup>, M.N. Knjazev<sup>2</sup>, I.L. Mylnikov<sup>2</sup>, O.V. Pakhomov<sup>1</sup>

<sup>1</sup>*Department of Cryogenic/ National Research University of Information Technologies, Mechanics and Optics, St. Petersburg/ Russia*

<sup>2</sup>*Physical Electronics & Technology Department/ St. Petersburg Electrotechnical University LETI (ETU), St. Petersburg/ Russia*

Email: aeskow@gmail.com

Multiferroics are of great practical interest for modern microelectronics. In this study, we analyzed two ways to obtain materials with multiferroic properties: 1) formation of multilayer structures containing ferroelectric and ferromagnetic films<sup>251</sup> and 2) introduction of magnetic elements into ferroelectric materials in concentrations sufficient for magnetic properties to appear in a composite material<sup>252</sup>.

This work presents the results of multilayer structures study such as Cu-Cr/BSTO/YIG/GGG and the results of the investigation of influence of Mn-ions concentration (0–20 wt.%) on dielectric properties of Cu-Cr/BSTO/ $\alpha$ -Al<sub>2</sub>O<sub>3</sub> and Cu-Cr/BSTO/GGG film structures. The structure and composition of the samples were studied by means of XRD and by analysis of XPS spectra. For the detection of paramagnetic ions in the samples used EPR spectroscopy. The measurements of dielectrics characteristics of the planar capacitors were carried out at the frequencies 1 MHz and 6.44 GHz.

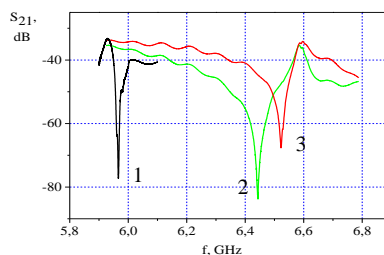


Fig. 1: Experimental frequency characteristics of a ferrite-ferroelectric resonator.

The optimal content of the Mn additive, as regards the dielectric properties (values of  $\epsilon$ ,  $\tan\delta$ , tunability, and resistance), is 15 wt %. At this concentration of Mn in the film BST observed the greatest change in the C-V characteristics of the structures Cu-Cr/BSTO/ $\alpha$ -Al<sub>2</sub>O<sub>3</sub> and Cu-Cr/BSTO/GGG in a magnetic field  $H = 1570$  Oe.

Figure 1 shows the tunability by changing of the magnetic field of the multi-layer ferrite-ferroelectric resonator based on the structure Cu-Cr/BST/YIG/GGG is about 75 MHz at a frequency of 6.44 GHz. Curve 1 corresponds to zero strength of the control electric field and a magnetic field strength of 1420 Oe; curves 2 and 3 were measured at a magnetic field strength of 1570 Oe, with the electric field strength being zero for curve 2 and 5V/ $\mu$ m for curve 3. Influence of magnetic field

<sup>251</sup> G. Srinivasan, S Dong, D Viehland, M Bichurin, C Nan, "Multiferroic magnetoelectric composites", J. Appl. Phys., vol. 103, pp. 031101-35, 2008.

<sup>252</sup> G.A. Smolenskiy, V.A. Bokov, V.A. Isupov, N.N. Krainik, R.E. Pasinkov, N.S. Shur, "Ferroelectrics and antiferroelectrics", Nauka, L., 1971.

on the C-V characteristics of investigated structures and on the tunability of the resonator associated with magnetoelectric effect.

## Structure and Multifunctionality of Strontium-Barium Niobate

Dec Jan<sup>1</sup>, Miga Seweryn<sup>1</sup>, Wokulska Krystyna<sup>1</sup>, Paszkowski Robert<sup>1</sup>, Świrkowicz Marek<sup>2</sup>,  
Łukasiewicz Tadeusz<sup>2</sup>, Kleemann Wolfgang<sup>3</sup>

<sup>1</sup>Institute of Materials Science, University of Silesia, Katowice, Poland

<sup>2</sup>Institute of Electronic Materials Technology, Warsaw, Poland

<sup>3</sup>Angewandte Physik, Universität Duisburg-Essen, Duisburg, Germany

Email: jan.dec@us.edu.pl

Solid solutions of the strontium-barium niobate  $\text{Sr}_x\text{Ba}_{1-x}\text{Nb}_2\text{O}_6$  where  $0.25 < x < 0.8$  (SBN) are environmental friendly (lead free) polar materials of oxygen octahedral family. This type of materials is recognized as very prolific due to its five different cationic crystallographic sites. Consequently, physical characteristics of SBN are strongly correlated to composition and chemical bonding. As a result of the compositional flexibility, SBN is recognized to exhibit diverse properties. Correspondingly, its potential applications are based on very attractive pyroelectric, electromechanical, electro-optic, photorefractive, and nonlinear optical and dielectric properties.

Structurally strontium-barium niobate is distinguished by its open tungsten bronze structure, i.e. the compound contains five  $\text{AB}_2\text{O}_6$  formula units per tetragonal unit cell in which six A sites are occupied by five divalent metal ions A. As a result the empty sites give rise to quenched electric random fields even in the stoichiometric compound. Consequently, by changing the ratio between strontium and barium components one may tune the system from ferroelectric ( $x < 0.5$ ) to a generic relaxor ( $x > 0.6$ ) behavior while maintaining the structure unchanged<sup>253</sup>.

Using the Czochralski method eleven single crystalline compounds with nominal  $x = 0.26, 0.35, 0.40, 0.45, 0.50, 0.55, 0.61, 0.65, 0.70, 0.75,$  and  $0.80$  designated hereafter as SBN26, ..., SBN80 have been grown. The crystals, grown along the [001] tetragonal direction, were up to 22 mm in diameter and 40 mm in length with characteristic 24 faces, free from striations and other extended defects. Density of etch pits was found to be of the order of  $10^2 - 10^3 \text{ cm}^{-2}$ .

Investigations of the linear dielectric response measured within  $10^0 \leq f \leq 10^5 \text{ Hz}$  along the polar c-axis of the obtained single crystals reveal a gradual crossover from ferroelectric (SBN26) to utmost relaxor-like (SBN80) behavior with a strong spatial anisotropy in the response. Complementary, temperature dependences of the lattice parameters confirm existence of structural phase transitions in all the investigated systems and conoscopic observations disclose an optical biaxiality for the crystals with  $0.75 \leq x$ .

Financial support by MNiSW under grant N N507 455034 is gratefully acknowledged.

<sup>253</sup> A. M. Glass, "Investigation of the Electric Properties...", J. Appl. Phys., vol. 40, p. 4699-4713, 1969.

## Structural changes in the $Y_{1-x}Ca_xMnO_3$ solid solutions

Razumnaya A., Rudskaya A., Vlasenko M., Kupriyanov M.

Department of Physics, Southern Federal University, Rostov-on-Don, Russia

Email: razumnaya1@gmail.com

Solid solutions are usually used with the aim to modify properties of functional material based on Mn-containing oxides. A well-known multiferroic  $YMnO_3$  are widely used as one of the basic components of these solid solutions. Although in recent years  $Y_{1-x}Ca_xMnO_3$  solid solutions system were studied in a number of articles<sup>254,255</sup>, the peculiarities of their structures is not yet understood. The main feature of these solid solutions is the occurrence of the reconstructive transition from the hexagonal, typical for  $YMnO_3$ , to orthorhombic structure at room temperature when the Ca concentration increases.

The purpose of this work was to investigate in details the structural changes in the  $Y_{1-x}Ca_xMnO_3$  solid solutions as a function of Ca concentration in order to determine symmetry of phases, ranges of their concentration stability and variation of interatomic bond distances.

It is found that  $YMnO_3$  is characterized by hexagonal phase  $P6_3cm$ , as expected. It is shown that at room temperature the concentration boundary between hexagonal  $P6_3cm$  and  $P6_3/mmc$  phases in  $Y_{1-x}Ca_xMnO_3$  solid solutions is located around  $x = 0.15$ . A reconstructive transition from hexagonal  $P6_3/mmc$  phase to orthorhombic perovskite  $Pnma$  phase occurs in the concentration range  $0.17 \leq x \leq 0.25$ . The compounds with  $x = 0.3; 0.5$  belong to the orthorhombic perovskite  $Pnma$  structure. In addition to the orthorhombic perovskite phase the cubic phase  $Pm3m$  coexists in the sample with  $x = 0.7$ .

As known,  $YMnO_3$  can be synthesized with the perovskite type structure only at high pressure<sup>256</sup>. Alternatively, the formation of the perovskite phase in the  $Y_{1-x}Ca_xMnO_3$  solid solutions with  $x \geq 0.15$  occurs at normal pressure. The observed at room temperature concentration phase transition in the  $Y_{1-x}Ca_xMnO_3$  solid solutions at  $x \sim 0.17$  from the polar  $P6_3cm$  to nonpolar  $P6_3/mmc$  phase with the emergence of the orthorhombic perovskite  $Pnma$  phase is an evidence of complicated structural changes.

A comparative analysis of the interatomic bond distances in the oxygen polyhedra of hexagonal and orthorhombic perovskite structures shows that the Mn-O bond distances are close in both structures. Thus, reconstruction does not affect the interatomic distances in oxygen polyhedra considerably.

The results of preliminary measurements of the magnetic properties of the  $Y_{1-x}Ca_xMnO_3$  solid solutions are presented. The evidences of magnetic ordering at temperatures of about 50 K have been found.

<sup>254</sup> M. N. Iliev, B. Lorenz, A. P. Litvinchuk, Y. Q. Wang, Y. Y. Sun, C. W. Chu, "Structural, transport, magnetic properties and Raman spectroscopy of orthorhombic  $Y_{1-x}Ca_xMnO_3$  ( $0 \leq x \leq 0.5$ )", J. Phys.: Condens. Matter., vol. 17, p. 3333, 2005.

<sup>255</sup> J. R. Sahu, C. R. Serrao, A. Ghost, A. Sundaresan, C. N. R. Rao, "Charge-order-driven multiferroic properties of  $Y_{1-x}Ca_xMnO_3$ ", Solid State Commun., vol. 149, p. 49-51, 2009.

<sup>256</sup> V. E. Wood, A. E. Austin, E. W. Collings, "Magnetic properties of heavy-rare-earth orthomanganites", Phys. Chem. Solids., vol. 34, p. 859-868, 1973.

## Raman spectroscopy of Sodium Bismuth Titanate ceramics

Marco Deluca<sup>1,2</sup>, Denis Schütz<sup>3</sup>, Elena Aksel<sup>4</sup>, Gunnar Picht<sup>5,6</sup>, Humberto M. Foronda<sup>4</sup>, Antonio Feteira<sup>7</sup>, Klaus Reichmann<sup>3</sup>, Kyle Webber<sup>8</sup> and Jacob L. Jones<sup>4</sup>

<sup>1</sup>Materials Center Leoben Forschung GmbH, Leoben, Austria

<sup>2</sup>Institut für Struktur- und Funktionskeramik, Montanuniversität Leoben, Leoben, Austria

<sup>3</sup>Technische Universität Graz, Graz, Austria

<sup>4</sup>Department of Materials Science and Engineering, University of Florida, Gainesville, FL, USA

<sup>5</sup>Robert Bosch GmbH, Stuttgart, Germany

<sup>6</sup>Institute of Applied Materials, Karlsruhe Institute of Technology, Karlsruhe, Germany

<sup>7</sup>Sheffield Hallam University, Sheffield, UK

<sup>8</sup>Technische Universität Darmstadt, Darmstadt, Germany

Email: marco.deluca@mcl.at

Sodium Bismuth Titanate (NBT) is a room-temperature ferroelectric perovskite currently being considered as the basis for possible lead-free substitutes for Lead Zirconate Titanate (PZT) piezoelectrics in actuators. This interest is motivated by the discovery of a large field-induced strain in NBT-based compositions, surpassing that of commercial PZT<sup>257</sup>. These properties, however, persist above the depolarization temperature  $T_d$ , where the material is in a long-range non-ferroelectric state. The obvious differences with PZT have triggered a large amount of structural studies on NBT and its modifications, mostly by x-ray diffraction (XRD), transmission electron microscopy (TEM) and Raman spectroscopy. XRD studies generally revealed a pseudocubic structure above  $T_d$ , whereas the Raman signal points to the presence of local disorder<sup>258</sup>. TEM observations further confirmed the presence of nanostructured phases within the same grain in NBT<sup>259</sup>.

In this work, temperature- and field-dependent Raman spectroscopy measurements on several NBT compositions substituted with Fe, Barium Titanate (BT) and Potassium Bismuth Titanate (KBT) will be presented and discussed together with the results of dielectric, electro-mechanical and synchrotron XRD measurements. Raman spectroscopy offers the unique advantage of being a non-destructive, laboratory-scale technique that reveals short-range information,

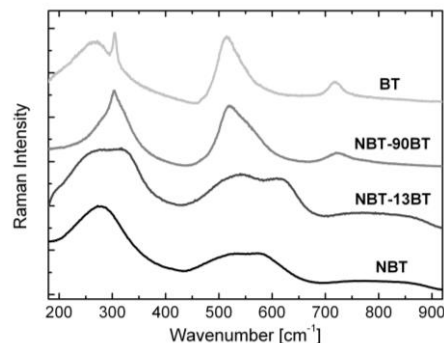


Fig. 79: Room-temperature Raman spectra of pure, undoped NBT, NBT with 13% and 90% BT (NBT-13BT and NBT-90BT, respectively), and pure BT.

<sup>257</sup> S.-T. Zhang, A. B. Kounga, W. Jo, C. Jamin, K. Seifert, T. Granzow, J. Rödel, D. Damjanovic, "High-strain lead-free antiferroelectric electrostrictors", *Adv. Mater.*, vol. 21, p. 4716-4720, 2009.

<sup>258</sup> E. Aksel, J. S. Forrester, B. Kowalski, M. Deluca, D. Damjanovic, J. L. Jones, "Structure and properties of Fe-modified  $\text{Na}_{0.5}\text{Bi}_{0.5}\text{TiO}_3$  at ambient and elevated temperatures", *Phys. Rev. B*, vol. 85, p. 024121-1-11, 2012.

<sup>259</sup> L. A. Schmitt, H.-J. Kleebe, "Single grains hosting two space groups – a transmission electron microscopy study of a lead-free ferroelectric", *Funct. Mat. Lett.*, vol. 3, p. 55-58, 2010.



complementary to the aforementioned techniques.

## Broadband Dielectric Spectroscopy and the Application of Lichtenecker Mixing Formula for Barium Titanate and Nickel-Zinc Ferrite Composite Ceramics

Aurimas Sakanas<sup>1</sup>, Robertas Grigalaitis<sup>1</sup>, Jūras Banys<sup>1</sup>, Liliana Mitoseriu<sup>2</sup>, Vincenzo Buscaglia<sup>3</sup>, Paolo Nanni<sup>4</sup>

<sup>1</sup>Faculty of Physics, Vilnius University, Vilnius, Lithuania

<sup>2</sup>Physics Department, University “Alexandru Ioan Cuza”, Iasi, Romania

<sup>3</sup>Institute of Energetics & Interphases, IENI-CNR, Genoa, Italy

<sup>4</sup>Department Chemical & Process Engineering, University Genoa, Genoa, Italy

Email: aurimas.sakanas@ff.vu.lt

Many theoretical approaches exist to describe properties of composite materials, according to the volume fraction of the component phases. The effective medium approximation (EMA) models are the most suitable for such analysis and one of the approximations are Lichtenecker mixing formulae<sup>260</sup>, allowing to calculate the effective macroscopic response of the composite mixture according to its constituents.

Multiferroic barium titanate and nickel-zinc ferrite composite ceramics, having chemical formula  $x\text{BaTiO}_3-(1-x)\text{Ni}_{0.5}\text{Zn}_{0.5}\text{Fe}_2\text{O}_4$  with the volume fractions  $x=0.466, 0.567$  and  $0.67$ , were investigated adapting the broadband dielectric spectroscopy methods in 20 Hz to 50 GHz frequency range and in 100 K to 500 K temperature range. The results obtained indicate the preserved properties of pure barium titanate with the noticeable conductivity contribution, caused by the ferrite phase of the composite.

In the present contribution, the approximation of the experimental effective permittivity data of the composite ceramics using Lichtenecker mixing formula will be proposed. Computed dielectric permittivity values for barium titanate and nickel-zinc ferrite at 100 MHz frequency (Fig. 1) manifest the presence of three peaks corresponding to phase transitions of barium titanate at approximately the same temperatures known from the classical experimental results with the values of dielectric permittivity being realistic for barium titanate ceramic materials. Nickel-zinc ferrite exhibits much lower dielectric permittivity values showing almost no dependency on the temperature.

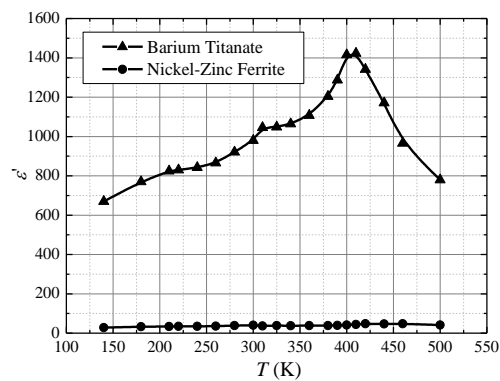


Fig. 80: The real part of dielectric permittivity of barium titanate and nickel-zinc ferrite at 100 MHz frequency, calculated from the experimental results using Lichtenecker mixing formula

<sup>260</sup> T. Zakri, J. P. Laurent, M. Vauclin, “Theoretical evidence for ‘Lichtenecker’s mixture formulae’ based on the effective medium theory”, J. Phys. D: Appl. Phys., vol. 31, p. 1589-1594, 1998.



**LiNbO<sub>3</sub>-LiTaO<sub>3</sub> mixed crystals:  
A joint theoretical and Raman investigation**

S. Neufeld<sup>1</sup>, S. Sanna<sup>1</sup>, A. Riefer<sup>1</sup>, M. Grothe<sup>1</sup>, G. Berth<sup>1</sup>, A. Zrenner<sup>2,1</sup>,  
H. Zhang<sup>3</sup> and W. G. Schmidt<sup>1</sup>

<sup>1</sup>Universität Paderborn, 33098 Paderborn, Germany

<sup>2</sup>Center for Optoelectronics and Photonics Paderborn (CeOPP), 33098 Paderborn, Germany

<sup>3</sup>State Key Lab of Crystal Materials, Shandong University, Jinan 250100, China

e-mail: [simone.sanna@uni-paderborn.de](mailto:simone.sanna@uni-paderborn.de)

Mixed crystals have recently attracted the attention of the scientific community, as they offer the possibility to tune the physical properties by varying the composition. Lithium niobate-tantalate (LNT) is one of the simplest ferroelectric mixed crystals, which shows quite unusual physical properties. In particular, the existence of a composition with zero birefringence at room temperature is unique in ferroelectric nonlinear-optical materials. Indeed within this composition the crystal is optical isotropic and yet electrically polar [1,2].

Despite the huge potential in electro-optic and acousto-optic devices and the extensive use of the end-compounds LN and LT, relatively few is known about the mixed crystals [3,4]. In this contribution, we characterize LiNb<sub>1-x</sub>Ta<sub>x</sub>O<sub>3</sub> over a wide composition range by the combined approach of *first-principles* simulations in the framework of the density functional theory and Raman spectroscopy.

Structural parameters (such as volumes and lattice constants) show a Vegard-like behaviour between the end-compounds LN and LT, while the electronic band gap shows pronounced deviations from the linearity. Measured Raman spectra and frequencies predicted from the theoretical models are compared. In particular, the frequency and intensity dependence of the four A<sub>1</sub>-TO modes on the crystal composition is discussed and explained on the basis of the phonon eigenvectors calculated within the density functional theory. Based on our result, we show that the LNT composition can be quite accurately estimated by its vibrational properties.

- [1] I. G. Wood, P. Daniels, R. H. Brown and A. M. Glazer, J. Phys.: Cond. Mat. **20**, 235237 (2008).
- [2] A. Bartaszyte, A. M. Glazer, F. Wondre, D. Prabhakaran, P. A. Thomas, S. Huband, D. S. Keeble, S. Margueron, Mat. Chem. Phys., **134**, 728 (2012).
- [3] S. Margueron, A. Bartaszyte, A. M. Glazer, E. Simon, J. Hlinka, I. Gregora, and J. Gleize, J. App. Phys. **111**, 104105 (2012).
- [4] D. Xue, K. Betzler, H. Hesse, Solid State Communications **115**, 581(2000).

# High-Temperature X-ray Diffraction of $\text{Ca}_3\text{TaGa}_3\text{Si}_2\text{O}_{14}$ and $\text{La}_3\text{Ga}_5\text{SiO}_{14}$ Piezoelectric Crystals Excited by Surface Acoustic Waves

Luc Ortega<sup>1</sup>, Dmitry Roshchupkin<sup>2</sup>, Dmitry Irzhak<sup>2</sup>, Ivo Zizak<sup>3</sup>

<sup>1</sup>Laboratoire de Physique des Solides, Univ. Paris-Sud, CNRS, F-91405 Orsay, France

<sup>2</sup>Institute of Microelectronics Technology and High-Purity Materials,  
Russian Academy of Sciences, 142432 Chernogolovka, Russia

<sup>3</sup>BESSY GmbH, Albert-Einstein Str. 15, D-12349 Berlin, Germany

Email: ortega@lps.u-psud.fr

$\text{Ca}_3\text{TaGa}_3\text{Si}_2\text{O}_{14}$  (CTGS) and  $\text{La}_3\text{Ga}_5\text{SiO}_{14}$  (langasite: LGS) crystals are promising piezoelectric materials for acoustooptics, acoustoelectronics and optoelectronics. They can be used to produce electroacoustic devices at high temperature due to their high thermal stability; for example LGS exhibits no phase transition up to 1470°C. The process of Surface Acoustic Wave propagation in these crystals is investigated using diffraction techniques since x-ray radiation is sensitive to the crystal lattice distortions. The SAW propagation at the surface crystal produces the sinusoidal modulation of the crystal lattice, which leads to the appearance of diffraction satellites around a Bragg peak (figure 1). SAW amplitudes and wavelengths can be deduced from the satellites intensities and their angular positions<sup>261</sup>.

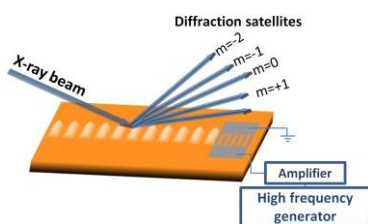


Fig. 81: Experimental principle of a surface acoustic wave device for x-ray diffraction.

X-ray diffraction rocking curves of acoustically modulated crystals were studied at x-ray energy of 11 keV (near Ga K-edge and Ta L-edge) in the kinematical diffraction conditions (x-ray penetration depth is smaller than the SAW penetration depth). Experiments were performed at the KMC2 beamline of the synchrotron source BESSY II in Berlin.

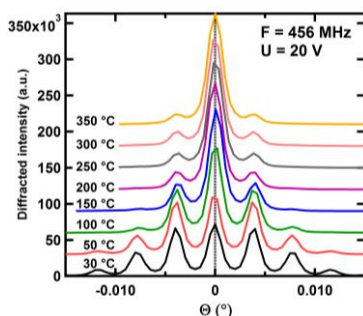


Fig. 2: X-ray rocking curves of CTGS from RT to 350°C with fixed excitation conditions;

<sup>261</sup> E=11 keV;  $\Lambda=6 \mu\text{m}$ ; (110) reflection.

We report, for the first time, temperature characteristics of surface acoustic wave propagation using x-ray diffraction method. To follow the change of the diffraction profiles in situ during heat treatments, the samples with iridium made transducers were placed on a heater inside a hemispherical Be window under high-vacuum conditions. Measurements were carried out at temperatures that gradually increased from room temperature up to 400°C. Rocking curves in figure 2 show the change of SAW propagation with temperature for a fixed excitation. We analyzed the frequency response at each temperature for CTGS and LGS single crystals.

oulou, O.A. Buzanov, "X-ray Bragg diffraction from langasite crystal  
I. Phys., vol. 94 p. 6692-6696, 2003.

Other SAW and piezoelectric characteristics such as the power flow angle can be determined using this method.

## Effects of $\gamma$ -ray irradiation on ferroelectric properties of Pr and Mn co-substituted BiFeO<sub>3</sub> thin films

Zheng Wen<sup>1,2,3</sup>, Chunyan Zheng<sup>3</sup>, Jin Li<sup>3</sup>, Lijun He<sup>3</sup>, Jiating Zhu<sup>4</sup>, Di Wu<sup>1,2</sup>, Aidong Li<sup>1,2</sup>

<sup>1</sup>National Laboratory of Solid State Microstructures, Nanjing University, Nanjing 210093, China

<sup>2</sup>Department of Materials Science and Engineering, College of Engineering and Applied Sciences, Nanjing University, Nanjing 210093, China

<sup>3</sup>Key Laboratory of Ningxia for Photovoltaic Materials, Ningxia University, Yinchuan 750021, China

<sup>4</sup>Agricultural Application of Nuclear-Radiation-Research Team, Jiangsu Academy of Agriculture Science, Nanjing 210014, China

Email: [diwu@nju.edu.cn](mailto:diwu@nju.edu.cn)

Polycrystalline Pr and Mn co-substituted BiFeO<sub>3</sub> (BPFMO) thin films are deposited on Pt/TiO<sub>2</sub>/SiO<sub>2</sub>/Si substrates by chemical solution deposition. Pt/BPFMO/Pt capacitors were subjected to 1.33-MeV  $\gamma$ -ray irradiation from a <sup>60</sup>Co source for 24 hours, which results in total dose of 5.0 Mrad.  $\gamma$ -ray irradiation effects on ferroelectric properties of BPFMO thin films are investigated by polarization-voltage hysteresis measurements and piezoresponse force microscopy. The irradiated BPFMO capacitors get imprinted and show reduced switchable polarizations. The shift of hysteresis loops (imprint) depends on the direction of polarization prior to irradiation. And the loss of switchable polarization increases with decreasing polarization value prior to irradiation. These are discussed in terms of separation of  $\gamma$ -ray-excited electron-hole pairs and subsequent charge trapping and aggregation on electrode/film interfaces and domain walls. Charge aggregation on electrode/film interfaces gives rise to an extra internal electric field to stabilize the polarization and results in a shift of hysteresis loops along the horizontal axis, while charge trapping on domain walls blocks domain switching and results in the observed polarization degradation.

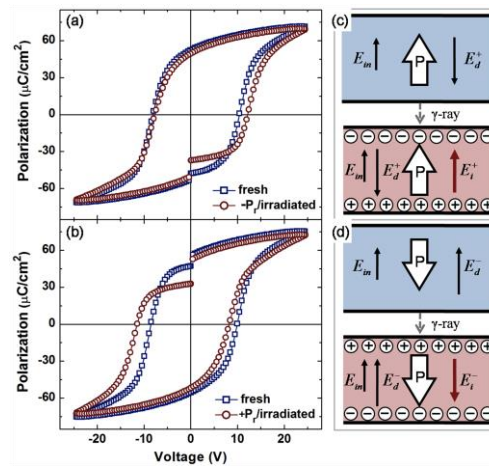


Fig. 82: Hysteresis loops recorded before and after irradiation for Pt/BPFMO/Pt thin-film capacitors poled to positive (a) and negative (b) polarizations. Corresponding internal electric field components are illustrated schematically in (d) and (e) for the positively and negatively poled capacitors, where ⊕/⊖ symbols represent  $\gamma$ -ray-excited holes and electrons, respectively.

## Resonance Line Shape Behavior of 2-2 Magnetoelectric Sensors on Cantilever Substrates

Jascha Lukas Gugat<sup>1</sup>, Matthias C. Krantz<sup>1</sup>, Martina Gerken<sup>1</sup>

<sup>1</sup>Institute of Electrical and Information Engineering,  
Christian-Albrechts-Universität zu Kiel, Germany

Email: jlg@tf.uni-kiel.de

We investigate theoretically the influence of substrate thickness on the resonance line shape of bilayer magnetoelectric (ME) sensors calculated using the finite element method (FEM).

Recent research on magnetoelectric sensors based on multiferroic composites described pico-Tesla AC magnetic field sensitivity<sup>262</sup> and nano-Tesla DC magnetic field sensitivity.<sup>263</sup> Further enhancements in sensitivity are achieved for sensors consisting of a magnetostrictive (MS) and a piezoelectric (PE) phase by operation at mechanical resonance.<sup>264</sup> Due to their potential small scale, inexpensive wafer-based manufacturing process, and operation at room temperature such thin-film based ME sensors are of particular interest for biomagnetic applications. The MS layer is frequency dependently deformed by a magnetic field. Due to elastic coupling the deformation is transferred to a strain in the PE layer inducing a voltage signal.

The small signal behavior of layered cantilever ME sensors is simulated using 2D FEM with a linear material model. Cantilevers consisting of a 2.5  $\mu\text{m}$  high Terfenol-D (MS) layer on top of a 2.5  $\mu\text{m}$  high PZT (PE) layer on top of a silicon substrate with a total length of 300  $\mu\text{m}$  and varying thickness are considered. These are typical dimensions for micro-electro-mechanical systems (MEMS) sensors.<sup>265</sup> Fig. 1 shows the induced electric potential across the PE layer as a function of frequency in the range of the first bending mode for different substrate thicknesses. The resonance line shapes are asymmetric and dependent on the substrate thickness. A zero response frequency is observed either below or above

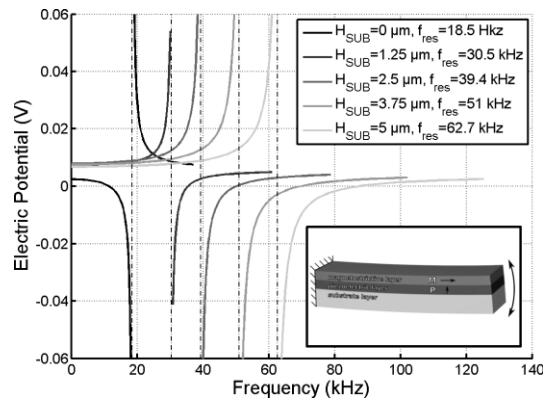


Fig. 83: Induced electric potential across the PE layer as a function of frequency for different cantilever substrate thicknesses. Inset: Schematic of investigated magnetoelectric sensor structure.

<sup>262</sup> S. X. Dong, J. Y. Zhai, F. Bai, J. F. Li, and D. Viehland, "Push-pull mode magnetostrictive/piezoelectric laminate composite with an enhanced magnetolectric coefficient," *Appl. Phys. Lett.* 87, 062502 (2005)

<sup>263</sup> S. X. Dong, J. Y. Zhai, J. F. Li, and D. Viehland, "Small DC magnetic field response of magnetolectric laminate composites," *Appl. Phys. Lett.* 88, 082907 (2006)

<sup>264</sup> H. Greve, E. Woltermann, R. Jahns, S. Marauska, B. Wagner, R. Knöchel, M. Wuttig, and E. Quandt, "Low damping resonant magnetolectric sensors," *Appl. Phys. Lett.* 97, 152503 (2010)

<sup>265</sup> S. Marauska, R. Jahns, H. Greve, E. Quandt, R. Knöchel, and B. Wagner, "MEMS magnetic field sensor based on magnetolectric composites," *J. Microelectromech. Syst.* 22, 065024 (2012)



the resonance frequency. These results may be explained by considering the mechanical stress and strain distributions in the cantilever structure.

## Infrared and Terahertz Spectroscopy of Epitaxial BaTiO<sub>3</sub>/SrTiO<sub>3</sub> Superlattices

V. Železný<sup>1</sup>, Ch. Kadlec<sup>1</sup>, A. Soukiassian<sup>2</sup>, X.X. Xi<sup>3</sup>, D.G. Schlom<sup>2</sup>

<sup>1</sup>Institute of Physics, ASCR, Na Slovance 2, 182 21 Praha 8, Czech Republic

<sup>2</sup>Department of Materials Science and Engineering, Cornell University, Ithaca, New York, 14853-1501, USA

<sup>3</sup>Department of Physics, Temple University, Philadelphia, Pennsylvania 19122, USA

Email: zelezny@fzu.cz

Crystal lattice dynamics brings fundamental information for understanding the physical properties of ferroelectrics. Infrared spectroscopy is a very effective tool for studying and understanding the behavior of ferroelectrics because the incident radiation couples directly to the order parameter (polarization). This can be used for the direct extraction of the dielectric function and determination of the parameters important for lattice dynamics. Thin films and superlattices are more suitable for device application, but they show difference in their behaviour compared bulk materials. Varying temperature enables us to study nanoscale ferroelectric heterostructures in the vicinity of the phase transition.

The infrared reflectivity and terahertz transmission measurements were performed on fully commensurate [(BaTiO<sub>3</sub>)<sub>8</sub>(SrTiO<sub>3</sub>)<sub>4</sub>]<sub>40</sub> superlattices grown by molecular-beam epitaxy on scandate substrates. The experimental spectra were measured in two polarizations along the *c* axis and perpendicular to it on the (110) cut of SmScO<sub>3</sub> substrate. The Drude-Lorentz form of the dielectric function was used for both substrate and superlattice. First we fit the spectrum of the bare substrate then we fixed all of its parameters. Adding the top layer to the model and fitting the total system (substrate + superlattice), we could determine the effective parameters of the superlattice. A further refinement of the dielectric function was done using a variational dielectric function procedure, which provides the dielectric function in a non-parametrized form. The resulting dielectric function is of perovskite-like character with three dominating vibration modes. Combining these approaches enabled us to observe the soft mode and extract its parameters. The temperature behavior of the modes and their parameters were also studied. The obtained results demonstrate that the softening of the soft mode is much smaller than for the bulk materials of the superlattice components.

This work was partially supported by Grant Agency of the Czech Republic under Contract No. 204/11/1011.

## Measurement of the indirect piezoelectric coefficient of thin films using interferometry

Mark Stewart<sup>1</sup> and Markys G Cain<sup>1</sup>

<sup>1</sup>National Physical Laboratory, Teddington, Middlesex, UK

Email: mark.stewart@npl.co.uk

Piezoelectric thin films are a promising high force actuation technology for MEMS devices. At present materials are still at the research stage, with very few Fab plants offering piezoelectric materials as a standard option. Users and manufacturers of these films want to assess the quality of the films at an early stage in production, so there is a requirement to be able to measure the piezoelectric coefficient of films as produced on a substrate.

In the late 90's Kholkin et al<sup>266</sup> showed that many measurements of the piezoelectric output of thin films suffered from bending effects, resulting in inflated values. To overcome this they proposed the double beam interferometer method which became the de facto 'standard'. More recently the availability of microscope based laser Doppler vibrometers have led workers to re-evaluate the use of single sided measurements, where the sample bending is eliminated by adhesive bonding to a rigid substrate.

This work will compare both experimental methods and with the aid of FEA examine the effects of various realistic boundary conditions on observed and predicted output.

---

<sup>266</sup> A. L. Kholkin, Ch. Wüthrich, D. V. Taylor, and N. Setter, "Interferometric measurements of electric field-induced displacements in piezoelectric thin films", *Rev. Sci. Instrum.* **67**, 1935, 1996.

## Hybrid improper ferroelectric phase transition in $\text{Ca}_3\text{Mn}_2\text{O}_7$

S. Kamba<sup>1</sup>, V. Goian<sup>1</sup>, C. Adamo<sup>2</sup>, P. Vaněk<sup>1</sup>, J. Drahokoupil<sup>1</sup>, A. Mould<sup>3</sup>, H. Seiner<sup>4</sup>,  
L. Palatinus<sup>1</sup>, M. Klementová<sup>1</sup>, M. Svatuška<sup>1</sup>, N.A. Benedek<sup>5</sup>, and D.G. Schlom<sup>2,6</sup>

<sup>1</sup>Institute of Physics, Academy of Sciences of the Czech Republic, Prague, Czech Republic

<sup>2</sup>Department of Materials Science and Engineering, Cornell University, Ithaca, New York, USA

<sup>3</sup>Department of Materials Science and Engineering, University of Sheffield, Sheffield, UK

<sup>4</sup>Institute of Thermomechanics, ASCR, Prague, Czech Republic

<sup>5</sup>Materials Science and Engineering Program, The University of Texas at Austin, Texas, USA

<sup>6</sup>Kavli Institute at Cornell for Nanoscale Science, Ithaca, New York, USA

Email: goian@fzu.cz

Based on *ab initio* calculations, a new type of ferroelectric phase transition was recently proposed in  $\text{Ca}_3\text{Mn}_2\text{O}_7$ , which crystallizes in Ruddlesden-Popper structure.<sup>267</sup> The ferroelectricity in such system should be induced by freezing of two nonpolar phonons from Brillouin zone boundary. If the modes of  $X_2^+$  and  $X_3^-$  symmetries will freeze simultaneously,  $I4/mmm$  phase will transform directly to  $A2_1am$  orthorhombic structure and the phase transition is called the hybrid improper ferroelectric phase transition. If the modes will freeze gradually, paraelectric  $I4/mmm$  phase should transform to intermediate  $Cmcm$  ( $X_3^-$  mode freezes first) or  $Cmca$  phase ( $X_2^+$  mode freezes first) and after freezing of the second parameters, the ferroelectric  $A2_1am$  orthorhombic structure will finally appear. The same calculations have shown that in biaxially strained  $\text{Ca}_3\text{Mn}_2\text{O}_7$  films, the switching of polarization by electric field should cause  $180^\circ$  flip of magnetic moments by reversing the octahedral tilt.<sup>267</sup>

The aim of this contribution is to determine whether  $\text{Ca}_3\text{Mn}_2\text{O}_7$  undergoes one hybrid or two successive phase transitions. We have combined X-ray and electron diffraction with measurements of thermal expansion, resonant ultrasound and infrared (IR) spectroscopy. We investigated both bulk ceramics and strained  $\text{Ca}_3\text{Mn}_2\text{O}_7$  thin films deposited using reactive molecular beam epitaxy on (110)LuAlO<sub>3</sub> and (110)YAlO<sub>3</sub> substrates (compressive strain up to 1.5 %).

Our room temperature electron and X-ray diffraction studies confirm  $A2_1am$  crystal structure, which could be ferroelectric, but rather high conductivity of the ceramics did not allow us to perform measurements of ferroelectric hysteresis loops or temperature dependence of radio-frequency permittivity. X-ray diffraction reveal abrupt change near 670 K, thermal expansion coefficient exhibits the structural phase transition at 690 K IR spectra of ceramics and thin films support improper-ferroelectric character of the phase transition near the same temperature. However, resonant ultrasound spectra of ceramics revealed two phase transitions; first one near 650 K and second one near 770 K. Details high-temperature structural studies, which should determine the intermediate and high-temperature structure symmetries, are in progress.

<sup>267</sup> N. Benedek N. and C.J. Fennie, Hybrid improper ferroelectricity: A mechanism for controllable polarization-magnetization coupling, Phys. Rev. Lett., vol. 106, p. 107204, 2011.

## Microwave Characterization of Tunable Interdigitated Capacitors on BTS Thin Films deposited by sol-gel

Waldhoff Nicolas<sup>1</sup>, Fasquelle Didier<sup>1</sup>, Blary Karine<sup>2</sup> et Carru Jean-Claude<sup>1</sup>

<sup>1</sup>UDSMM Laboratory, ULCO, 50 rue F. Buisson, BP717 - 62228 Calais

<sup>2</sup>IEMN, Université de Lille1, avenue H. Poincaré, 59652 Villeneuve d'Ascq

Email: nicolas.waldhoff@eilco-ulco.fr

The strong dependence of the dielectric permittivity of ferroelectric materials under electric field ensures that they are particularly attractive for microwave applications. Moreover, by using interdigitated capacitors, which allow the extraction of different characteristics such as the tunability or the dielectric loss, they also offer the opportunity to deposit ferroelectric films on insulating substrates like sapphire, and owning excellent High Frequencies (HF) properties. Nowadays, many developments are migrating to BaTiO<sub>3</sub> (BT) materials. However, their use in HF applications is limited by their losses. To overcome this problem, without affecting the electrical performance, the BT material can be doped with strontium or tin<sup>268</sup>.

The BaTi<sub>0.98</sub>Sn<sub>0.02</sub>O<sub>3</sub> (BTS) solutions were prepared by a sol-gel method using barium acetate, tin acetate and titanium isopropoxide as starting materials. BTS films were then deposited onto sapphire substrates by spin coating. Two samples were realized. Crystallization was achieved via post deposition annealing at 750°C (named BTS750) during 1 hour for the first sample and at 950°C (named BTS950) during 15 min for the second. Interdigitated electrodes were then deposited on the film surface by a lift-off process and gold sputtering.

The interdigitated structures were measured in reflection with coplanar accesses and quasi-TEM transmission line. Based on a de-embedding (D-E) method derived from the extraction technique of silicon transistors<sup>2</sup>, OPEN and SHORT structures were realized to perform D-E on the capacitances.

Two samples were characterized using S parameters measurements up to 67 GHz. The Figure 1 compares the same capacitance on both samples with and without OPEN-SHORT D-E. At 67 GHz, after D-E, the tunability is similar (26 and 28%). At 250 MHz (not presented here), the tunability reaches 50%. Other structures were

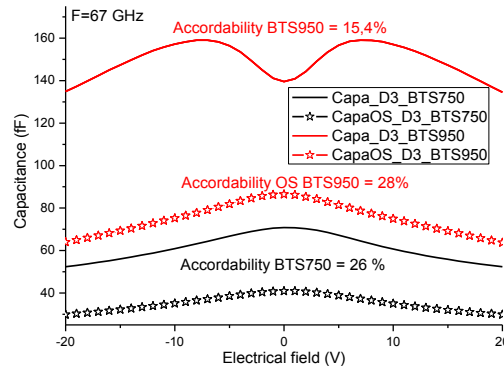


Fig. 84: Interdigitated capacitances (BTS750 and BTS950) evolutions at 67 GHz with and without OPEN-SHORT structure versus electrical field.

<sup>268</sup> J. – C. Carru et al, “Electrical Characterization of lead free Sr and Sn doped BaTiO<sub>3</sub> ferroelectric films deposited by sol-gel”, FERROELECTRICS book by INTECH (Rijeka, Croatia), chapter 3, pp. 49-72, June 2011.

<sup>2</sup> N. Waldhoff, et al, « Improved Characterization Methodology for MOSFETs up to 220 GHz », Microwave Theory and Techniques, IEEE Transactions on, vol. 57, no 5, p. 1237 - 1243, may 2009.

analyzed. The variation of their planar electrodes dimensions was investigated along with various characteristics which will be presented.

## Far-infrared and THz spectroscopy in thick PZT films

Elena Buixaderas<sup>1</sup>, Christelle Kadlec<sup>1</sup>, Volodymyr Skoromets<sup>1</sup>, Dmitry Nuzhnyy<sup>1</sup>, Jan Petzelt<sup>1</sup>,  
Hana Ursic<sup>2</sup>, Barbara Malic<sup>2</sup>

<sup>1</sup>Department of Dielectrics, Institute of Physics, ASCR, Prague, Czech Republic

<sup>2</sup>Department of Electronic Ceramics, Jožef Stefan Institute, Ljubljana, Slovenia

Email: buixader@fzu.cz

Pure and dense highly tetragonal ceramics of  $\text{Pb}(\text{Zr}_{1-x}\text{Ti}_x)\text{O}_3$  (PZT 100x/100(1-x)) are quite hard to grow, which is a problem for the study of the real PZT system. The great strain anisotropy between the polar axis and the plane perpendicular to it creates high stresses within domains and grains in samples with  $x > 0.60$  and these ceramics tend to break apart. Usually, to obtain dense tetragonal PZT ceramics some extra components have to be added during the fabrication process at least in a small amount.

To overcome this problem without adding any extra atom to the lattice, which could affect the dielectric behaviour of the samples and/or their phonons, pure PZT films can be deposited on suitable substrates. In this work, thick PZT films were deposited by screen printing on sapphire substrates (c-cut) for two compositions (36/64 and 38/62) and subsequent sintering at different temperatures for two hours. The resulting films had thicknesses between 23 and 30  $\mu\text{m}$ .

In order to analyze the homogeneity of the films Raman maps were taken at room temperature and compared with spectra on dense ceramics of similar compositions.

The flatness and porosity together with the overall phonon response of the films were tested measuring the far-infrared (FIR) reflectivity spectra. Dielectric response below phonons was measured using transmission time-domain terahertz spectroscopy.

Results are compared with dielectric data already measured on bulk tetragonal PZT 42/58.<sup>269</sup> The effect of porosity has been evaluated using the Bruggeman effective medium approach.

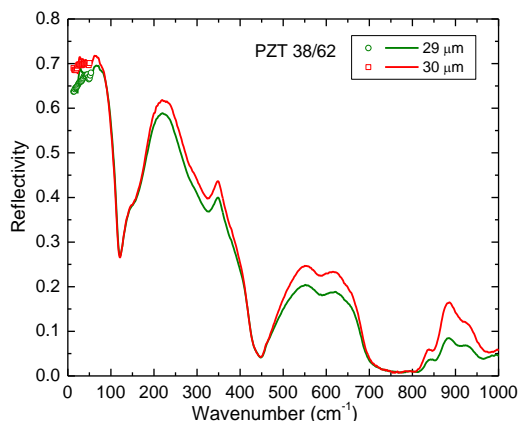


Fig. 85: FIR and THz reflectivity of the PZT 38/62 films on sapphire at room temperature.

Authors would like to thank Silvo Drnovšek and Kostja Makarovič for help during the processing of the samples.

<sup>269</sup> E. Buixaderas et al, "Lattice dynamics and dielectric response of undoped, soft and hard  $\text{PbZr}_{0.42}\text{Ti}_{0.58}\text{O}_3$ ", Phase Transitions, vol. 83, p. 917-930, 2010.





## Anisotropic electrical properties of BNT based textured lead-free piezoceramics

Haibo Zhang, Wook Jo, Jürgen Rödel

*Institute of Materials Science, Technische Universität Darmstadt, 64287 Darmstadt, Germany*

Lead-free piezoelectric materials have been the subject of ongoing experimental and theoretical investigations due to their fundamental scientific interest and their importance in technological applications. Various lead-free piezoceramics have been considered as candidates for replacing Pb-based piezoceramics during the past decades. Bismuth sodium titanate,  $(\text{Bi}_{1/2}\text{Na}_{1/2})\text{TiO}_3$  (BNT), is considered to be an excellent candidate as a key lead-free piezoelectric material, because it forms a solid solution with  $\text{BaTiO}_3$  (BT) or  $\text{Bi}_{1/2}\text{K}_{1/2}\text{TiO}_3$  (BKT) showing improved dielectric and piezoelectric properties at the rhombohedral-tetragonal morphotropic phase boundary (MPB). Recently, a giant strain of 0.45% was observed in BNT-BT-2KNN (with 2 mol% KNN) ceramic at room temperature, which is higher than the strain of a commercial soft PZT ceramic (PIC151, PI Ceramics). However, the giant strain can only be realized at very high electric fields ( $>6$  kV/mm), which should be reduced before it can be considered for industrial applications. It is well known that physical properties of piezoelectric ceramics strongly depend on the microstructure. Piezoelectric single crystals show enhanced performance as compared to polycrystalline ceramics. As a consequence, textured piezoceramics are expected to possess improved piezoelectric properties due to cooperating domains with uniformly aligned polarizations. Most recently we found the poling field in textured BNT based piezoceramics is much lower than that in random piezoceramics. In the present work, the BNT based piezoceramics were prepared by the templated grain growth (TGG) technique. The processing route is to be improved to get highly textured piezoceramics with various phase structures. The high degree of orientation (Lotgering factor  $f > 90\%$ ) was achieved. The dielectric properties, ferroelectric properties and the bipolar and unipolar strain of the textured piezoceramics were measured, analyzed and compared with those of common bulk materials. Moreover, a special attention will be paid to the anisotropic electrical properties using textured samples cut at different angles.

**Reference:**

1. Zhang, S. T., Kounga, A. B., Aulbach, E., Granzow, T., Jo, W., Kleebe, H. J., and Rödel, J. Lead-free piezoceramics with giant strain in the system  $\text{Bi}_{0.5}\text{Na}_{0.5}\text{TiO}_3\text{-BaTiO}_3\text{-K}_{0.5}\text{Na}_{0.5}\text{NbO}_3$  I. Structure and room temperature properties. *J. Appl. Phys.*, 2008, 103, 034107.
2. Seifert, K. T. P., Jo, W., and Rödel, J. Temperature-insensitive large strain of  $(\text{Bi}_{1/2}\text{Na}_{1/2})\text{TiO}_3\text{-}(\text{Bi}_{1/2}\text{K}_{1/2})\text{TiO}_3\text{-}(\text{K}_{0.5}\text{Na}_{0.5})\text{NbO}_3$  lead-free piezoceramics. *J. Am. Ceram. Soc.*, 2010, 93, 1392-1396.
3. Jo, W., Dittmer, R., Acosta, M., Zang, J., Groh, C., Sapper, E., Wang, K., and Rödel, J. Giant electric-field-induced strains in lead-free ceramics for actuator applications—status and perspective. *J. Electroceram.*, 2012, 1-23.

## The frequency and temperature dependence of hysteresis loop in P(VDF-TrFE) copolymer films

Manfang Mai<sup>1</sup>, Andreas Leschhorn<sup>1</sup>, Herbert Kliem<sup>1</sup>

<sup>1</sup>Institute of Electrical Engineering Physics, Saarland University, Saarbruecken, Germany

Email: manfangmai@mx.uni-saarland.de

The experimental hysteresis loop of ferroelectric poly(vinylidene fluoride-trifluoroethylene) [P(VDF-TrFE)] copolymer films is measured in a wide frequency and temperature range. For extrinsic switching, ferroelectrics in general do not exhibit well-defined coercive fields. There are three regions in the frequency dependence of coercive field. Below 1 Hz, the coercive field gets to a saturation. In the lower frequency region from 1 Hz to 5 kHz, the hysteresis loop widens and the coercive field increases with increasing frequency while the remanent polarization is almost constant. As frequency increases, the excitation field changes faster than the dipole switching. The dipoles become more difficult to catch up with the external signal and a higher coercive field is expected. A linear fit of the frequency dependence of  $E_c$  in the log-log scale plot gives an exponent value of 0.04. In the higher frequency region from 5 kHz to 1 MHz where the switching time is longer than half of the external signal period, switching is suppressed and the amount of the switchable polarization depends on the frequency. The hysteresis loop starts to shrink and the coercive field decreases with increasing frequency. For a constant frequency, the hysteresis loop measured at different temperature exhibits a linear decrease of coercive field with increasing temperature. A double hysteresis loop is observed close to the Curie point and a sharp jump of the remanent polarization is obtained in samples as thick as 600nm indicating a first order phase transition. For samples as thin as 90nm, the double hysteresis loop of the polarization is absent and the change of remanent polarization on temperature is smoother.

The above experimental results can be explained and simulated in the Weiss mean field model. It is essentially a feedback model where the polarization evokes a field that in turn stimulates the polarization. The model assumes that the electrostatic interaction between the dipoles leads to a field  $\alpha P$  proportional to the polarization of the system. The superposition of the external field and the field due to the polarization yields the local field. At the dipole sites we find

$$E_{loc} = E_a + \alpha P \quad (1)$$

Assuming that the dipoles with dipole moment  $p$  and density  $n$  fluctuate thermally activated in double well potentials, the transient polarization is described by a first-order differential equation ( $\tau$  relaxation time),

$$\tau \frac{dP}{dt} + P = np \tanh\left(\frac{p}{kT} E_{loc}\right) \quad (2)$$

Combining (1) and (2) with  $E_a = E_0 \sin(\omega t)$  the dynamic hysteresis loop can be obtained. To get the double hysteresis loop, the piezoeffect in the ferroelectric is introduced to the model. Due to the piezoeffect the volume  $V$  of the sample changes with the polarization ( $\nu$  piezo coefficient),

$$V = V_0(1 + \nu P) \quad (3)$$

This causes the dipole density, the dipole moment and/or the coupling constant varying with the polarization. Eqns. (1)-(3) can yield a second order or first order phase transition depending on the piezo coefficients of the system. The simulation results show good coincidence with the experiments.

## Unexpected Domains Structure in BaTiO<sub>3</sub> Single-Crystal revealed by Confocal Raman Microscopy

F. Rubio-Marcos<sup>1</sup>, A. Del Campo<sup>1</sup>, P. Marchet<sup>2</sup>, and J. F. Fernández<sup>1</sup>.

<sup>1</sup> Electroceramic Department, Instituto de Cerámica y Vidrio, CSIC, Kelsen 5, 28049, Madrid, Spain.

<sup>2</sup> Laboratoire de Science des Procédés Céramiques et de Traitements de Surface, UMR 7315 CNRS, Université de Limoges, Centre Européen de la Céramique, 12, rue Atlantis, 87068, Limoges Cedex, France.

Email: jfernandez@icv.csic.es

Confocal Raman Microscopy, CRM, is used to in situ resolve the domain structure in BaTiO<sub>3</sub> single-crystals. Two different BaTiO<sub>3</sub> single crystals, BTO, are studied: (i) "c"-plane or  $\langle 001 \rangle$ -plane, and (ii) "a"-plane or  $\langle 100 \rangle$ -plane. These two orientation degrees provide different scenarios to study the domain structure in single crystal samples. Obviously, the structure of the ferroelectric domain is related to the crystallographic orientation. However, in both orientations, the structure of "a-c" stripe domains has been directly observed and resolved by CRM mapping. As a relevant result, unexpected needle-like "a-c"-domains bundle (represented by green color) with the reverse "a"- (and "c") subdomain orientation spontaneously nucleated, along the domain wall which is formed by two single "a-c"-domains (in red and blue colors on Fig. 1, respectively). It subsequently propagated forward until it reached the "a"-domains (red) and alternating between "c"-domains (blue).

This unexpected configuration is clearly reflected in the formation of perpendicular domain boundaries in the depth scan of single-crystal BTO sample (Fig. 1c). The needlelike domains appear as consequence of the surface stress in the BTO due the overlapping of "a" and "c" domain orientation.

The implications of the present findings introduce a fruitful discussion to the 3D understanding of ferroelectric domain structure and represent the key point to design new domains that allow engineering the piezoelectric response.

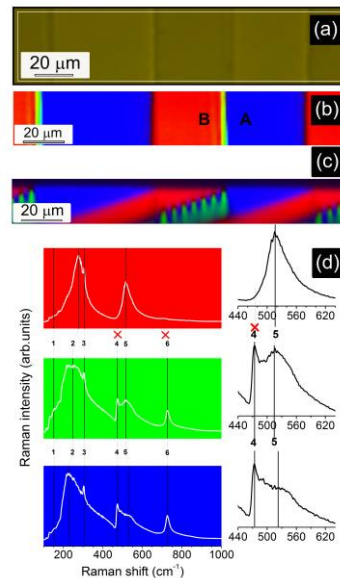


Fig. 86: *Characterization in the a-plane of the BTO single crystal through Confocal Raman Microscopy*: (a) optical image. (b & c) Raman color maps showing the distribution of the different ferroelectric domains: (b) in the *a*-plane of the planar-section and (c) of the depth scan or cross section. (d) Raman spectrum of selected BTO regions (represented by its color code) indicating the characteristic Raman modes of each BTO ferroelectric domain.

## Precise determination of piezoelectric $d_{33}$ -coefficients of piezoelectric thin films assisted by finite element modeling

Chris Stöckel<sup>1</sup>, Christian Kaufmann<sup>1</sup>, Robert Schulze<sup>1</sup>, Detlef Billep<sup>2</sup>, Thomas Gessner<sup>1,2</sup>

<sup>1</sup>Center for Microtechnologies (ZfM), Chemnitz University of Technology, Chemnitz, Germany

<sup>2</sup>Multi Device Integration, Fraunhofer (ENAS), Chemnitz, Germany

Email: [chris.stoeckel@zfm.tu-chemnitz.de](mailto:chris.stoeckel@zfm.tu-chemnitz.de)

For the design of piezoelectric microsystems, the determination of the piezoelectric coefficients is essential to predict the behavior and to optimize them. The paper presents an approach to determine the  $d_{33}$ -coefficient of piezoelectric thin films utilizing Finite Element (FE) simulations and Laser Doppler Vibrometry (LDV). A detailed description of the interaction between the piezoelectric thin film and substrate is presented. The influence of the substrate properties and geometry is discussed.

For determining the  $d_{33}$  of piezoelectric thin films, equation (1) can be used [1,2]. It is shown that for thin films the influence of the piezoelectric transverse mode cannot be neglected. In equation (1)  $\xi$  is the deflection in consequence of an excitation with electrical voltage  $U$  and the  $s_{11}^E$ ,  $s_{12}^E$  and  $s_{13}^E$  are the elastic coefficients of the piezoelectric material.

$$d_{33} = d_{33,f} + d_{31} \cdot \frac{2s_{13}^E}{s_{11}^E + s_{12}^E} = \frac{\xi}{U} + d_{31} \cdot \frac{2s_{13}^E}{s_{11}^E + s_{12}^E} \quad (1)$$

In [2] an infinitely stiff substrate is assumed, but an elastic constant of the substrate, e.g. silicon, which is not infinite causes deviations in the determination of the  $d_{33}$  [3]. Therefore an investigation of this phenomenon and limitations of equation (1) were done using FE simulations.

For the verification of the FE simulation results PZT thin films on silicon substrate were analyzed with Laser Doppler Vibrometry. It can be noticed that there is congruence of the measured and simulated deflections of the substrate nearby the edge of the piezoelectric material.

A high influence of electrode area and substrate thickness has been determined in simulations and measurements, Fig. 1. The present results will be discussed extensively in the article.

[1] P. Murali: Piezoelectric thin films for MEMS. In: *Integrated Ferroelectrics*, 17 (1-4), pp. 297-307, 1997.

[2] K. Lefki and G. J. M. Dormans: Measurement of piezoelectric coefficients of ferroelectric thin films. In: *Journal of Applied Physics*, 76(3), pp. 1764-1767, 1994.

[3] G. J. T. Leighton, et al.: Accurate measurement of the piezoelectric coefficient of thin films by eliminating the substrate bending effect using spatial scanning laser vibrometry. In: *Smart Materials and Structures* 19(6), pp. 065011, 2010.

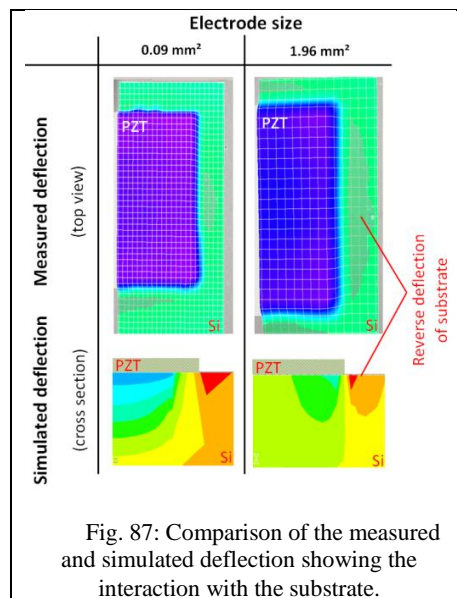


Fig. 87: Comparison of the measured and simulated deflection showing the interaction with the substrate.

## Linear and Nonlinear Dielectric Properties of Ternary Solid Solutions $0.4\text{Na}_{0.5}\text{Bi}_{0.5}\text{TiO}_3-(0.6-x)\text{SrTiO}_3-x\text{PbTiO}_3$

Šarūnas Svirskas<sup>1</sup>, Maksim Ivanov<sup>1</sup>, Šarūnas Bagdzevičius<sup>1</sup>, Jūras Banys<sup>1</sup>, Jan Dec<sup>2</sup>, Seweryn Miga<sup>2</sup>, Marija Duncė<sup>3</sup>, Eriks Birks<sup>3</sup>, Maija Antonova<sup>3</sup>, Andris Sternbergs<sup>3</sup>

<sup>1</sup>Vilnius University, Faculty of physics, Saulėtekio av. 9, III b., LT-10222 Vilnius, Lithuania

<sup>2</sup>University of Silesia, Institute of Materials Science, Katowice, Poland

<sup>3</sup>Institute of Solid State Physics, University of Latvia, Kengaraga street 8, LV-1063 Riga, Latvia

Email: sarunas.svirskas@ff.vu.lt

Sodium bismuth titanate (NBT) along with lead magnesium niobate (PMN) is one of the oldest relaxor systems known. NBT attracts attention due to its promising electromechanical properties and the absence of lead which is environmentally hazardous. Despite thorough studies which already last for about 50 years there are still unanswered questions about this material. Recently, a lot of interest in complex solid solutions containing NBT as primary material is shown<sup>270</sup>. Such materials as strontium titanate, lead titanate or barium titanate were mixed with sodium bismuth titanate in order to enhance dielectric, piezoelectric properties or to get knowledge how A-site ions influence phase transitions of NBT.

Temperature dependences of the linear and the first order and second order nonlinear dielectric susceptibilities give useful information on the formation of polar nano-regions. On the other hand, broadband linear dielectric spectroscopy allows to evaluate the dynamics of polar nano regions (or dipolar entities in general). Distribution of relaxation times can be calculated from dielectric spectra. On the other hand, nonlinear dielectric measurements help to identify the order of phase transition precisely and the nonlinear scaling factor  $a_3$  shows the fundamental differences between classical ferroelectrics and relaxors or dipolar glasses<sup>271</sup>.

In this work we present our measurements of  $0.4\text{NBT}-(0.6-x)\text{ST}-x\text{PT}$  ( $x = 0, 0.05, 0.1, 0.15, 0.2$ ). The exchange of strontium with lead changes dielectric properties dramatically. The system in low lead side of phase diagram exhibits relaxor-like properties and when the content of PT increases the phase transition from relaxor to ferroelectric state occurs.

<sup>270</sup> Jung-Kun Lee et. al. J. Appl. Phys. 91, 4538 (2002)

<sup>271</sup> Seweryn Miga, Jan Dec and Wolfgang Kleemann “*Non-Linear Dielectric Response of Ferroelectrics, Relaxors and Dipolar Glasses*”, Ferroelectrics - Characterization and Modeling, ISBN: 978-953-307-455-9 (2011)

## Nano-domain engineering in ultrashort-period ferroelectric superlattices

Jaichan Lee<sup>1</sup>, Taekjib Choi<sup>2</sup>, Hyungjung Shin<sup>3</sup>, Bae Ho Park<sup>4</sup>

<sup>1</sup>School of Advanced Materials Science and Engineering, Sungkyunkwan University (SKKU), Suwon, Korea

<sup>2</sup>Faculty/Institute of Nanotechnology and Advanced Materials Engineering, Sejong University, Seoul, Korea

<sup>3</sup>Department of Energy Science, Sungkyunkwan University (SKKU), Suwon, Korea

Email: jclee@skku.edu

Ultrashort-period  $\text{PbZrO}_3$  (PZO)/ $\text{PbTiO}_3$  (PTO) ferroelectric/antiferroelectric superlattices are proposed for nano-domain engineering.<sup>1</sup> The ultrashort-period PZO/PTO superlattices behaved like single ferroelectric metamaterials with monodomain-like excluding  $90^\circ$  domain boundary, irrespective of total thicknesses. Further, nanosized  $180^\circ$  domains, as small as  $\sim 12$  nm, were achieved by applying short pulse voltage. Such domain structures of superlattices result from lowering the symmetry of supercell by specific atomic stacking in superlattices, contrary to domain structures of ferroelectric thin films developed by the strain-induced ferroelectric instability, as shown in Fig. 1. Domain size increases linearly with the pulse voltage, while domain size is linearly dependent on logarithmic value of the pulse duration. Domain wall motion can be explained by an activated process following Merz's law. The electric field ( $E$ ) dependence of the domain wall velocity ( $v$ ) satisfied  $v \sim \exp(-\delta/E)$ , where the activation field ( $\delta$ ) was found to be  $\sim 2.7$  MV/cm. It is noted that domain wall motion with a relatively high activation field implies a strong stability of domain. In practice, the domain pattern shows a long-term retention behavior up to over one month.

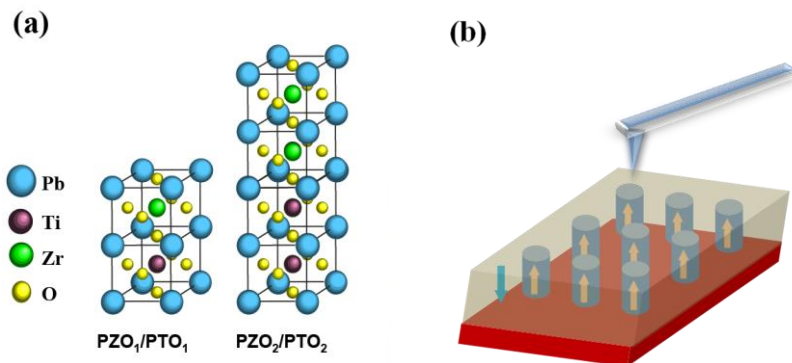


Figure 1. (a) Supercell of the PTO/PZO artificial superlattice with various stacking periods, and (b) schematic of local polarization switching in the PTO/PZO superlattice using a scanning probe tip in data storage media applications.

1. T. Choi, B.H. Park, H. Shin, and J. Lee, "Nano-domain engineering in ultra-short-period ferroelectric superlattices", *Appl. Phys. Lett.* 100, 222906, 2012.

## Influence of spin-phonon coupling in SrMnO<sub>3</sub> and CaMnO<sub>3</sub> on their dielectric properties and phonon spectra

V. Goian<sup>1</sup>, M. Savinov<sup>1</sup>, V. Skoromets, J. Hejtmánek<sup>1</sup>, V. Bovtun<sup>1</sup>, M. Kempa<sup>1</sup>, F. Borodavka<sup>1</sup>, P. Vaněk<sup>1</sup>, D. Nuzhnyy<sup>1</sup>, A.A. Belik<sup>2</sup>, J.H. Lee<sup>3</sup>, K.M. Rabe<sup>3</sup>, S. Kamba<sup>1</sup>

<sup>1</sup>Institute of Physics, Academy of Sciences of the Czech Republic, Prague, Czech Republic

<sup>2</sup>WPI-MANA, National Institute for Materials Science, Tsukuba, Ibaraki, Japan

<sup>3</sup>Department of Physics and Astronomy, Rutgers University, Piscataway, New Jersey, USA

Email: savinov@fzu.cz

Investigated SrMnO<sub>3</sub> and CaMnO<sub>3</sub> ceramics crystallize in perovskite cubic *Pm3m* and orthorhombic *Pnma* crystal structure, respectively and exhibit magnetic phase transition to antiferromagnetic G-type phase near 230 K and 120 K, respectively. Although both materials are paraelectric down to liquid He temperatures, recent first principles calculations predicted that both systems can become ferroelectric and even ferromagnetic under a biaxial strain.<sup>272,273</sup> The strain effect was not yet confirmed experimentally, but Sakai et al.<sup>274</sup> expanded SrMnO<sub>3</sub> lattice by Ba doping and successfully induced ferroelectricity in Sr<sub>1-x</sub>Ba<sub>x</sub>MnO<sub>3</sub> ( $x \geq 0.45$ ) with  $T_c \approx 400$  K and canted ferromagnetism with  $T_N \approx 200$  K. Important fact is that in this case the strong ferroelectricity ( $P_S = 13 \mu\text{C}/\text{cm}^2$ ) is driven by displacement of magnetic Mn<sup>4+</sup> cations and the magnetoelectric coupling is therefore the largest yet attained.<sup>274</sup>

Infrared reflectivity spectra of SrMnO<sub>3</sub> ceramics reveal 25 cm<sup>-1</sup> stiffening of the lowest-frequency phonon below Néel temperature. The temperature change of polar phonon frequency is extraordinarily high and we explain it by the exceptionally strong spin-phonon coupling. The same phonon shift with temperature was obtained from the first principles calculations. Polar phonons become Raman active below  $T_N$ , although they are forbidden in the cubic crystal structure. It gives evidence that the cubic symmetry is locally broken due to the strong magnetoelectric coupling. Multiphonon and multimagnon scattering is also seen in Raman spectra. Microwave and THz permittivity is strongly influenced by hopping electronic conductivity, which is caused by a small non-stoichiometry of the sample. THz conductivity unusually increases on cooling, while the DC conductivity markedly decreases. Thermoelectric measurements gave the room-temperature free carriers concentration of  $n_e = 3.16 \cdot 10^{20} \text{ cm}^{-3}$  and the sample composition was determined as Sr<sup>2+</sup>Mn<sup>4+</sup><sub>0.98</sub>Mn<sup>3+</sup><sub>0.02</sub>O<sup>2-</sup><sub>2.99</sub>.

Our radio-frequency dielectric, THz and infrared studies of CaMnO<sub>3</sub> ceramics reveal metal insulator phase transition at  $T_N$  and splitting of some polar phonons below  $T_N$ . Both effects give evidence on the strong spin-phonon coupling, which reduces crystal symmetry in this material.

<sup>272</sup> J.-H. Lee and K.M. Rabe, Epitaxial-strain-induced multiferroicity in SrMnO<sub>3</sub> from first principles, Phys. Rev. Lett. vol. 104, p. 207204, 2010.

<sup>273</sup> S. Bhattacharjee, E. Bousquet, and P. Ghosez, Engineering multiferroism in CaMnO<sub>3</sub>, Phys. Rev. Lett. vol. 102, p. 117602, 2009

<sup>274</sup> H. Sakai et al. Displacement-type ferroelectricity with off-center magnetic ions in perovskite Sr<sub>1-x</sub>Ba<sub>x</sub>MnO<sub>3</sub>, Phys. Rev. Lett. vol. 107, p. 137601, 2011



## The nature of the defect structure of solid solutions based on lead zirconate titanate (PZT) (by ESR and NMR method)

I.P.Bykov<sup>1</sup>, Yu.A. Zagorodniy<sup>2</sup>, L.P.Yurchenko<sup>1</sup>, V. V.Trachevsky<sup>3</sup>,  
V.Dimza<sup>4</sup>, K.Nejezchleb<sup>5</sup>, L.Jastrabik<sup>6</sup>, A.Dejneka<sup>6</sup>

<sup>1</sup>Frantcevych Institute for Problems of Materials Science, National academy of Sciences of Ukraine, Kiev, 03680,Ukraine

<sup>2</sup>G.V. Kurdumov Institute for Metal Physics, National Academy of Sciences of Ukraine, Kiev 03680, Ukraine

<sup>3</sup>Technical Centre, National Academy of Sciences of Ukraine, 04070 Kiev,Ukraine

<sup>4</sup>Institute of Solid State Physics,University of Latvia, 226063Riga,Latvia

<sup>5</sup>Noliac Ceramics s.r.o.Školní 86, Libřice, CZ-503 44, Czech Republic

<sup>6</sup>Institute of Physics ASCR, v. v. i., 182 21 Prague, Czech Republic

The nature of intrinsic and impurity defects in lead zirconate titanate and lead (PZT, PLZT) ceramics of various compositions prepared by solution chemistry has been explored. Using electron paramagnetic resonance (EPR) and nuclear magnetic resonance (NMR), several defects sites have been identified in the as-received materials, which include  $\text{Fe}^{3+}$ -oxygen vacancy ( $V_O$ ) complex and isolated  $\text{Cu}^{2+}$  ions. Both of these ions are incorporated into the lattice by replacing the Ti (Zr) ion. A  $\text{Fe}^{3+}$ - $V_O$  complex serves as a sensitive probe of the local crystalline field environment of the ceramic. The symmetry of this defects is roughly correlated with its phase diagram as the composition PZT. The paramagnetic center  $\text{Fe}^{3+}$ - $V_O$  experiences tetragonal, rhombic and orthorhombic symmetry in varied PZT and PLZT. Paramagnetic center of the  $\text{Cu}^{2+}$  is different, it appears as though the addition of Zr and not a change in phase, is largely responsible in determining the local environment of this acceptor impurity. The  $\text{Cu}^{2+}$  EPR weakly reflect the Ti-O or Zr-O bond covalency in the perovskite lattice.

Two different lead ion positions with tetragonal and orthorhombic local symmetry were revealed in PZT and PLZT ceramics on the base of  $^{207}\text{Pb}$  NMR spectra measurements at room temperature. The obtained data and their analysis on the base of the spectra shape calculations are in agreement with experiment. The comparison of observed spectra in PZT and PLZT with calculated spectra allowing for resonance frequency chemical shift and spin-spin interaction show that the displacements of lead and oxygen ions are not random quantities in the investigated PZT and PLZT ceramic samples.

## WEAK FERROMAGNETISM IN DYSPROSIUM SUBSTITUTED BISMUTH FERRITE CERAMICS

V. Koval<sup>1</sup>, I. Skorvanek<sup>2</sup>, H. Yan<sup>3</sup>, L. Mitoseriu<sup>4</sup> and M. Reece<sup>3</sup>

<sup>1</sup>Institute of Materials Research, Slovak Academy of Sciences, Kosice, Slovak Republic

<sup>2</sup>Institute of Experimental Physics, Slovak Academy of Sciences, Kosice, Slovak Republic

<sup>3</sup>Nanoforce Technology Ltd & Materials Department, Queen Mary University of London, UK

<sup>4</sup>Faculty of Physics, "Al.I. Cuza" University, Iasi, Romania

E-mail: vkoval@imr.saske.sk

Dysprosium-substituted bismuth ferrite ( $\text{Bi}_{1-x}\text{Dy}_x\text{FeO}_3$ ,  $x = 0, 0.1$  and  $0.2$ ) polycrystalline samples were prepared by a modified solid-state reaction method, adopting the SPS powder precursors consolidation followed by the rapid sintering and quenching process. By optimizing the annealing conditions, a bulk density value up to 96% of the theoretical density was achieved for the doped ceramics. The effect of the partial replacement of smaller  $\text{Dy}^{3+}$  ions for bigger  $\text{Bi}^{3+}$  ions on the crystal structure, morphology, dielectric and magnetic properties was investigated. Room-temperature X-ray diffraction investigations revealed the structural transformation of the initially rhombohedral  $R3c$  phase ( $x = 0$ ) into a mixture of the  $R3c$  and  $Pnma$  phases with a final phase ratio of about 1:3 for the  $x = 0.2$  compound (Figure 1). It was found that the substitution inhibits the grain growth and eliminates the appearance of secondary phases. The average grain size decreased almost by one order of magnitude to  $\approx 1.5 \mu\text{m}$  as the concentration of dysprosium increased from 0 to 20%. A strong dielectric dispersion and anomalous dielectric behavior at elevated temperatures were suggested to result from the interfacial polarization and hopping conduction mechanism of oxygen vacancies. Magnetization measurements in a wide temperature and field range showed that the introduction of magnetic  $\text{Dy}^{3+}$  ions results in a weakly ferromagnetic state at room temperature, and the spontaneous magnetization can be further enhanced by decreasing the temperature down to 5 K. At room temperature, the maximum remanent magnetization ( $M_r = 0.34 \text{ emu/g}$ ) was achieved for the  $\text{Bi}_{0.8}\text{Dy}_{0.2}\text{FeO}_3$  samples (Figure 2).

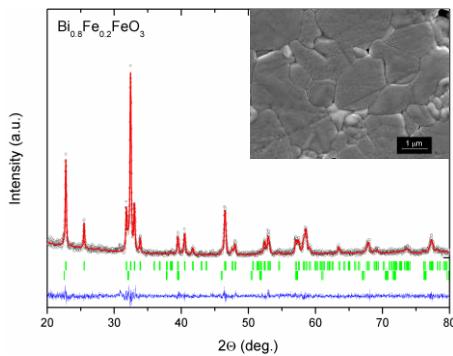


Figure 1. Refined XRD pattern of  $\text{Bi}_{0.8}\text{Dy}_{0.2}\text{FeO}_3$  ceramics

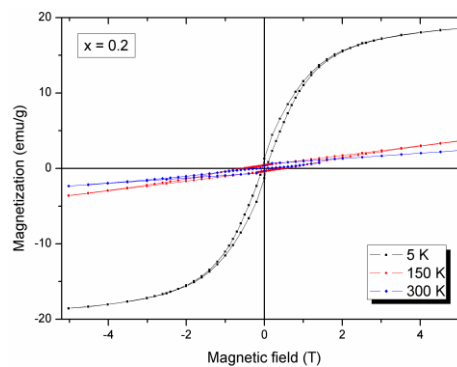


Figure 2. M-H loops for  $\text{Bi}_{0.8}\text{Dy}_{0.2}\text{FeO}_3$  ceramics



## Structure, dielectric, and piezoelectric properties of (0.95-x) BiFeO<sub>3</sub>-x PbTiO<sub>3</sub>-0.05 Pb(Zn<sub>1/3</sub>Nb<sub>2/3</sub>)O<sub>3</sub> ternary high Curie temperature piezoelectric ceramics

Jiajia Jiang<sup>1</sup>, Jianguo Chen<sup>1</sup>, Jinrong Cheng<sup>1</sup>

<sup>1</sup> Electronic Information Material Department, Material Institute, Shanghai, China

Email: jrcheng@staff.shu.edu.cn

A series of solid solutions (0.95-x) BiFeO<sub>3</sub>-x PbTiO<sub>3</sub>-0.05 Pb(Zn<sub>1/3</sub>Nb<sub>2/3</sub>)O<sub>3</sub> (BF-PT-PZN) (x= 0.30, 0.31, 0.33, 0.35, 0.37, 0.40) have been fabricated by solid state reaction method. X-ray diffraction analysis revealed that phase transition from rhombohedral to tetragonal was observed at PT content of 0.35. Values of the dielectric constant  $\epsilon_r$ , dielectric loss tangent  $\tan\theta$ , Curie temperature  $T_c$  and piezoelectric constant  $d_{33}$  for the composition x=0.35 were of 250, 0.02, 550 °C and 70 C/N, respectively. Temperature-dependent piezoelectric constant and electromechanical coupling coefficient were stable from room temperature up to 450 °C, about 300 °C higher than that of conventional Pb(Zr,Ti)O<sub>3</sub> (PZT) piezoelectric ceramics. All these results together with the good thermal stabilities made the BF-PT-PZN ceramics promising candidates for high temperature piezoelectric applications.

Key words: High Curie Temperature, piezoelectric properties, ternary system

## Search for Polar LiNbO<sub>3</sub>-Type Compounds

Alexei A. Belik<sup>1</sup>, Takao Furubayashi<sup>2</sup>, Hitoshi Yusa<sup>2</sup>, Eiji Takayama-Muromachi<sup>2</sup>

<sup>1</sup> International Center for Materials Nanoarchitectonics (WPI-MANA), National Institute for Materials Science (NIMS), 1-1 Namiki, Tsukuba, Ibaraki 305-0044, Japan

<sup>2</sup> NIMS, Tsukuba, Ibaraki 305-0047, Japan

Email: Alexei.Belik@nims.go.jp

ABO<sub>3</sub> compounds crystallize in a number of structure types, e.g., perovskite, LiNbO<sub>3</sub>, hexagonal LuMnO<sub>3</sub>-type, hexagonal BaMnO<sub>3</sub>-type, pyroxene, corundum, ilmenite (ordered corundum), rare earth sesquioxide structures (A, B, and C (bixbyite)), PbReO<sub>3</sub>, KSbO<sub>3</sub>, AlFeO<sub>3</sub>, CaIrO<sub>3</sub>, and others. The LiNbO<sub>3</sub> structure in principle can be described as a highly distorted perovskite structure, to which it can be related by a displacive transformation. The LiNbO<sub>3</sub> structure is polar (space group *R3c*). Therefore, LiNbO<sub>3</sub>-type compounds should exhibit ferroelectric and piezoelectric properties footnotes<sup>275</sup>.

Most of the ABO<sub>3</sub> compounds crystallize in the perovskite-type structure. However, when the size of the A-type compounds is decreased the LiNbO<sub>3</sub>-type structure can be stabilized.

In this work, we investigated ABO<sub>3</sub> compounds with A = Sc and In<sup>2,3</sup>. We will discuss a new class of multiferroic materials: In-based perovskites. We show that In<sub>1-x</sub>M<sub>x</sub>MO<sub>3</sub> with x = 0.112–0.176 and M = Fe<sub>0.5</sub>Mn<sub>0.5</sub> has the LiNbO<sub>3</sub>-type structure (Fig. 1) and high Curie temperature; In<sub>1-x</sub>M<sub>x</sub>MO<sub>3</sub> is a canted antiferromagnet with the Néel temperature close to RT<sup>2</sup>. In<sub>1-x</sub>M<sub>x</sub>MO<sub>3</sub> presents a new class of perovskite materials (with In<sup>3+</sup> in the A site of a perovskite ABO<sub>3</sub>) that is almost completely unexplored. This class of materials is unique because (1) long-range magnetic ordering survives near room temperature (RT) despite of significant disordering in the A and B sites, (2) the same transition metals are located in both A and B sites, and (3) a polar distortion is realized without presence of ions with the lone electron pair. Our results give a significant contribution to the development of RT multiferroics and open wide possibilities for thin-film research and future improvement of In-based perovskites. Our results also show new ways for the preparation of perovskite-type materials.

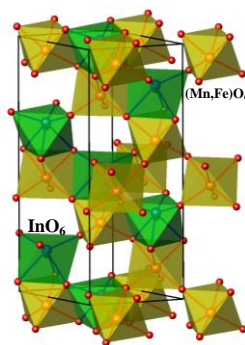


Fig. 88: Crystal Structure of In<sub>1-x</sub>M<sub>x</sub>MO<sub>3</sub> with x = 0.112–0.176 and M = Fe<sub>0.5</sub>Mn<sub>0.5</sub>.

<sup>275</sup> A. A. Belik, T. Furubayashi, H. Yusa, E. Takayama-Muromachi, *J. Am. Chem. Soc.* **133**, 9405 (2011).

<sup>2</sup> A. A. Belik, T. Furubayashi, Y. Matsushita, M. Tanaka, S. Hishita, E. Takayama-Muromachi, *Angew. Chem. Int. Ed.* **48**, 6117 (2009).

<sup>3</sup> A. A. Belik, Y. Matsushita, M. Tanaka, E. Takayama-Muromachi, *Angew. Chem. Int. Ed.* **49**, 7723 (2010).



## Dielectric properties of *modified* BiFeO<sub>3</sub> ceramics

Kachaporn Sanjoom<sup>1,3</sup>, Duangpon Laksawat<sup>1</sup>, Kamonpan Pengpat<sup>1,2</sup>, Sukum Eitssayeam<sup>1,2</sup> and Gobwute Rujijanagul<sup>1,2,3,\*</sup>

<sup>1</sup>Department of Physics and Materials science, Faculty of Science, Chiang Mai University, Chiang Mai, 50200, Thailand

<sup>2</sup>Materials Science Research Center, Faculty of Science, Chiang Mai University, Chiang Mai, 50200, Thailand

<sup>3</sup>Thailand Center of Excellence in Physics, Commission on Higher Education, 328 Sri Ayutthaya Road, Bangkok, 10400, Thailand

Email: rujijanagul@yahoo.com

The modified BiFeO<sub>3</sub> (BFO) ceramics (BFO doped with Sb and Dy) were prepared by a solid-state reaction method. Excess Bi<sub>2</sub>O<sub>3</sub> (3 wt%) was introduced prior to powder calcination to compensate for any Bi<sub>2</sub>O<sub>3</sub> that may have been lost from the samples due to volatilization during heat treatments. X-ray diffraction analysis revealed that pure phase perovskite was observed for the samples calcined at a low heating rate. Dielectric behavior of undoped ceramic exhibited high dielectric constant over a wide temperature region. However, the doping shifted this region to a higher temperature. The doping affected the peak of dielectric loss of the samples. Activation energy of dielectric relaxation also shifted with increasing the additive concentration. In addition, complex impedance analysis was applied to determine the behavior of grain boundary and grain after doping.

**Acknowledgements** This work was supported by National Research University (NRU), Office of Higher Education Commission (OHEC), Thailand center of excellence in Physics (Thep) and Faculty of Science and Graduate School Chiang Mai University.

## Electrical properties of PbLaZrTiOx capacitors with conductive oxide buffer layer on Pt electrodes

Takeyasu Saito, Yoko Takada, Toru Tsuji, Naoki Okamoto, Kazuo Kondo, Takeshi Yoshimura<sup>a</sup>, Norifumi Fujimura<sup>a</sup>, Koji Higuchi<sup>b</sup>, Akira Kitajima<sup>b</sup>, and Akihiro Oshima<sup>b</sup>

Dept. of Chem. Eng., Osaka Prefecture University, Sakai, Osaka 599-8531, JAPAN

<sup>a</sup> Dept. of Phys. Electro., Osaka Prefecture University, Sakai, Osaka 599-8531, JAPAN

<sup>b</sup> Inst. of Sci. and Ind. Res., Osaka University, Ibaraki, Osaka 567-0047, JAPAN

Email: [tsaito@chemeng.osakafu-u.ac.jp](mailto:tsaito@chemeng.osakafu-u.ac.jp)

Ferroelectric Random Access Memory (FeRAM) has attracted much attention and it is believed to be next generation non-volatile memory for its high operation (read/write) speed and low power consumption<sup>1)</sup>. To achieve higher density integration, ferroelectric capacitors requires higher switching charge and better fatigue and imprint properties. It was reported that the introduction of a buffer layer is one of effective methods to improve fatigue characteristics of ferroelectric thin films<sup>2)</sup>. A buffer layer was also used to control the orientation of ferroelectric thin films<sup>3)</sup>. In this study, we used conductive Al-doped ZnO (AZO) and Sn doped In<sub>2</sub>O<sub>3</sub> (ITO) as buffer layer on Pt bottom electrodes.

The substrates were highly (111)-oriented sputtered Pt as lower electrodes. PLZT (Pb:La:Zr:Ti=113:3:30:70) films (500 nm) were prepared by the sol-gel method. The films were deposited on Pt substrate by spin coating, at 3000 rpm for 20 s. Then, the gel-films were dried at 200°C for 2 min in order to eliminate the solvent, and pyrolyzed at 300°C for 10 min, in air for organic components removal. The films were prepared by repeating (3 times) the deposition and pyrolysis cycle. The prepared thickness was 500 nm. The coated films were finally calcined in air at 750°C, 10 min, in air for achieving crystallization. AZO buffer layers and top electrodes were deposited by PLD (Pulsed Laser Deposition). This deposition was performed with a metal through mask having 50 μm ~ 500 μm diameter. The composition of AZO and ITO targets were ZnO:Al<sub>2</sub>O<sub>3</sub>=98.5:1.5 wt.% and In<sub>2</sub>O<sub>3</sub>:SnO<sub>2</sub>=95.0:5.0 wt.%, respectively.

Fig. 1 shows the polarization values of PLZT capacitors with AZO top electrodes and with or without AZO buffer layer from 10 nm ~ 120 nm. Polarization value of PLZT capacitors with 10 nm buffer layer and without buffer layer were 21.6 μC/cm<sup>2</sup> and 18.2 μC/cm<sup>2</sup>, respectively at 15 V. The polarization ratio of PLZT capacitors with 10 nm buffer layer and without buffer layer after 10<sup>7</sup> 10 V, 100 μs width and 1 ms interval cycles were 0.60 and 0.39, respectively. PLZT capacitors with AZO buffer layer were also confirmed to be promising in terms of hydrogen endurance.

### References

- 1) M.M. Zhang *et al*, Solid-State Electronics, Vol. 53, p. 473 (2009).
- 2) H. Peng *et al.*, Progress in Natural Science: Materials International, Vol. 22, p. 219 (2012)
- 3) X.S. Wang *et al*, Scripta Materialia, Vol. 46, p. 783 (2002)

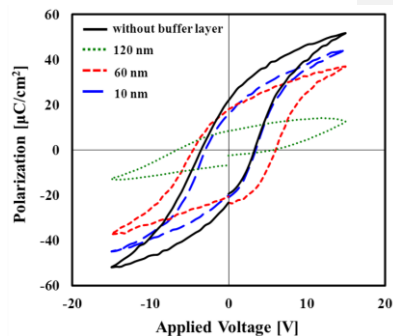


Fig. 1 Hysteresis loops of PLZT capacitors with or without buffer



## Polarization Reversal in Crystals of Congruent Lithium Tantalate at Elevated Temperatures

Chezganov Dmitry<sup>1</sup>, Shur Vladimir<sup>1,2</sup>, Baturin Ivan<sup>1,2</sup>, Akhmatkhanov Andrey<sup>1,2</sup>

<sup>1</sup>Ferroelectric laboratory, Ural Federal University, Ekaterinburg, Russia

<sup>2</sup>Labfer Ltd., Ekaterinburg, Russia

Email: dmit.chezganov@gmail.com

The polarization reversal and domain structure evolution under application of linear increasing field has been studied in single crystalline congruent lithium tantalate (LiTaO<sub>3</sub>) in range from room temperature to 250°C. The fitting of the switching current data by modification of Kolmogorov-Avrami formula for switching in linear increasing field has been used for characterization polarization reversal process<sup>276,277</sup>. The static domain patterns revealed by selective chemical etching have been visualized by optical microscopy at both polar surfaces.

The analysis of the switching current data obtained at low temperatures (below 200°C) allowed us to separate the polarization reversal process in three stages. The first stage starting at low field was fitted by  $\beta$  (2D) model corresponding to growth of domains existing in the initial state. The beginning of appearance of new domains at the second stage allowed us to fit the current in terms of  $(\beta+\alpha)$  (2D) model. The termination of nucleation at the final stage leads to return to domain kinetics according to  $\beta$  (2D) process.

The current shape changes essentially for the temperatures above 200°C. In this case the role of the initial domain growth is negligible. Thus from the very beginning the switching current has been fitted successively in terms of  $\alpha$  (2D) model. The final stage of the switching process has been fitted by exponential decay with additional switching current component corresponding to bulk conductivity.

The proposed fitting allowed us to extract the value of the threshold field at which the nucleation of new domains begins. The threshold field two times decrease was revealed in the studied temperature range. The temperature dependence of the domain kinetics and shape of isolated domains at both polar surfaces was observed. The shape of isolated domains changes from triangular to circular at temperatures above 200°C. Moreover it was shown that the growth of non-through domains observed at low temperatures changed by formation of through truncated conical domains at elevated.

The observed experimental facts have been attributed to effective bulk screening due to increase of the bulk conductivity at elevated temperatures.

The equipment of the UCSU "Modern Nanotechnology", Institute of Natural Sciences, UrFU has been used. The research was made possible in part by RFBR (Grants 13-02-01391-a, 11-02-91066-CNRS-a), by Ministry of Education and Science (Contract 14.513.12.0006), by OPTEC LLC.

<sup>276</sup> V. Ya. Shur, E. L. Rumyantsev, S. D. Makarov, Kinetics of phase transformations in real finite systems: Application to switching in ferroelectrics. *J. Appl. Phys.*, vol. 84, p. 445–451, 1998.

<sup>277</sup> V. Ya. Shur, E. L. Rumyantsev, S. D. Makarov, A. L. Subbotin, and V. V. Volegov, Transient current during switching in increasing electric field as a basis for a new testing method. *Integr. Ferroelectr.*, vol. 10, p. 223–230, 1995.



**ELECTRICAL AND MAGNETIC PROPERTIES OF A NEW AURIVILLIUS PHASE** **$\text{Bi}_{14}\text{ThFe}_4\text{Ti}_8\text{O}_{45}$** V. G. Vlasenko<sup>a</sup>, V.A. Shuvaeva<sup>a</sup>, S.Zubkov<sup>a</sup>, S. Levchenkov<sup>b</sup><sup>a</sup> *Southern Federal University, Research Institute of Physics, Stachki Ave. 194, Rostov-on-Don, 344090, Russia*<sup>b</sup> *Southern Federal University, Department of Chemistry, Zorge str. 7, Rostov-on-Don, 344090, Russia*

Recently Aurivillius phases, containing magnetic cations, such as  $\text{Bi}_5\text{Ti}_3\text{FeO}_{15}$ , have drawn special attention as they have potential to display both ferroelectric and ferromagnetic properties simultaneously

A new layered perovskite-like oxide  $\text{Bi}_{14}\text{ThFe}_4\text{Ti}_8\text{O}_{45}$ , has been prepared, and the temperature dependence of the dielectric and magnetic properties of the material has been investigated. The composition and structure of the material is close to that of multiferroic material  $\text{Bi}_5\text{Ti}_3\text{FeO}_{15}$  but it has a higher content of magnetoactive  $\text{Fe}^{3+}$  due to partial substitution of Bi by Th in B perovskite positions. The dielectric properties of  $\text{Bi}_{14}\text{ThFe}_4\text{Ti}_8\text{O}_{45}$  were studied in a temperature range from 295 K to 1200 K at fixed frequencies of 100, 200, 500 and 1000 kHz. The temperature dependence of the dielectric constant  $\varepsilon/\varepsilon_0(T)$  reveal a broad peak at about 970 K, which is typical of a ferroelectric material with a high conductivity, undergoing a diffuse phase transition.

The magnetic susceptibility of the sample has been measured by the Faraday method in the temperature range from 77.4 K to 300 K. The values of magnetic susceptibility of the sample at 295 and 77 K were found to be  $5.88 \cdot 10^{-6}$  и  $14.16 \cdot 10^{-6} \text{ cm}^3/\text{g}$  respectively and the corresponding magnetic moments per formula unit were calculated to be 7.91 и 6.28 mB. The temperature dependence of the  $1/\chi_g$  is typical for paramagnetic compounds with short range antiferromagnetic exchange. The extrapolation of the part of the curve, measured at temperatures above 150 K, to the low temperature region yields a Weiss constant of -200 K, which is lower than that of  $\text{Bi}_5\text{Ti}_3\text{FeO}_{15}$ . This shows that higher Fe concentration results in enhancing of antiferromagnetic coupling.

## A New Criterion regarding the Flack parameter

J. Fábry<sup>1</sup>, M. Dušek<sup>2</sup>

<sup>1</sup> Department of Dielectrics, Institute of Physics AS CR, Prague, Czech Republic

<sup>2</sup> Department of Structure Analysis, Institute of Physics AS CR, Prague, Czech Republic

Email: fabry@fzu.cz

Existence of ferroelectric crystal structures is limited to the point groups 1, 2, 3, 4, 6, *m*, *2mm*, *3m*, *4mm*, *6mm*. All these point groups and the respective space groups are non-centrosymmetric. In practice, non-centrosymmetric crystals structures, determined by single crystal X-ray diffraction, are nowadays refined with inclusion of the Flack parameter<sup>278</sup>. Flack and his collaborators published a series of articles (e.g.<sup>279</sup>) in which they investigated behaviour of this parameter and assessment of its reliability in dependence of various conditions such as prominence of the resonant scattering, presence of pseudocentrosymmetric substructure in the structure and quality of the measurement. Here, another criterion for the reliability of the Flack parameter is suggested. It takes into account the contribution of the resonant scattering to intensity of each diffraction *hkl* and compares this contribution to the standard uncertainty of the observed intensity. The advantage of these criteria follows from the fact they are independent of the measurement of the Bijvoet pairs.

---

<sup>278</sup> H. D. Flack, Acta Cryst. A39, 876-881 (1983).

<sup>279</sup> H. D. Flack & G. Bernardinelli, Acta Cryst. A64, 484-493 (2008).

## Optical and electrical properties of $(\text{Ba}_{1-x}\text{Ca}_x)(\text{Zr}_y\text{Ti}_{1-y})\text{O}_3$ thin films obtained by pulsed laser deposition assisted by radio-frequency discharge.

N. D. Scarisoreanu<sup>1</sup>, F. Craciun<sup>2</sup>, A. Andrei<sup>1</sup>, V. Ion<sup>1</sup>, R. Birjega<sup>1</sup>, L. Nedelcu<sup>3</sup>, M.G. Banciu<sup>3</sup> and M. Dinescu<sup>1</sup>.

<sup>1</sup>NILPRP, P.O. Box MG-16, RO-77125, Bucharest, Romania

<sup>2</sup>CNR-Istituto dei Sistemi Complessi, Area della Ricerca Roma-Tor Vergata, Via del Fosso del Cavaliere 100, I-00133, Rome, Italy

<sup>3</sup>NIMP-National Institute of Materials Physics, 077125 Bucharest-Magurele, Romania

Email: snae@nipne.ro

The dielectric and piezoelectric characteristics of  $(\text{Ba}_{1-x}\text{Ca}_x)(\text{Zr}_y\text{Ti}_{1-y})\text{O}_3$  ceramic system have been reported for bulk form, but its properties in form of thin films are still unexplored. We report on the growth of lead-free perovskite  $(\text{Ba}_{0.85}\text{Ca}_{0.15})(\text{Zr}_{0.1}\text{Ti}_{0.9})\text{O}_3$  thin films using pulsed laser deposition assisted by radio-frequency discharge (RF-PLD) for MEMS applications.

A parametric study on the influence of substrate temperature and gas pressure on the dielectric and piezoelectric properties of thin layer was carried out.

Dielectric function of  $(\text{Ba}_{0.85}\text{Ca}_{0.15})(\text{Zr}_{0.1}\text{Ti}_{0.9})\text{O}_3$  was determined in low range of frequencies (1KHz-100 MHz) and in the optical domain (250-1700 nm) using dielectric spectroscopy and ellipsometry techniques. Topography of surface was evaluated by atomic force microscopy (AFM) techniques, while the piezoelectric response was measured by PFM technique. In the measured frequency domain, the films exhibit moderate dielectric constant ( $\approx 450$ ) and relatively low dielectric losses ( $\approx 1.5\%$ ). In order to extract the dielectric function (refractive indices and extinction coefficients), the ellipsometric analyses were carried out. The final values of refractive indices, absorption and optical band-gap were calculated with Lorentz oscillator model.

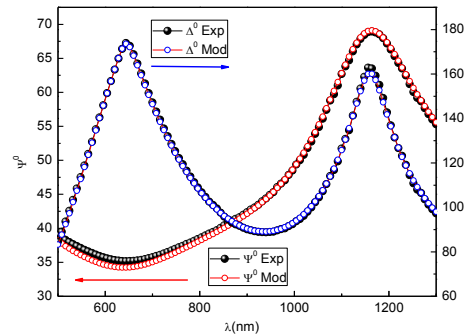


Fig. 89: Ellipsometry spectrum for BCTZ thin film growth on platinized silicon (i.a.  $70^\circ$ ). The black dots represent the experimental data, while the open circles result from the fitting procedure using a Cauchy dispersion formula.

## Ultrasonic Investigation of Phase Transition Temperature Hysteresis in $\text{Ba}_2\text{Nd}_{(1-x)}\text{Pr}_x\text{FeNb}_4\text{O}_{15}$ solid solutions

Martynas Kinka<sup>1</sup>, Vytautas Samulionis<sup>1</sup>, Michael Josse<sup>2</sup>, Dainius Gabrielaitis<sup>1</sup>, Robertas Grigalaitis<sup>1</sup> and Mario Maglione<sup>2</sup>

<sup>1</sup> Faculty of Physics, Vilnius University, Vilnius, Lithuania

<sup>2</sup> ICIMCB-CNRS, Universite de Bordeaux, Bordeaux, France

Email: martynas.kinka@delfi.lt

$\text{Ba}_2\text{Nd}_{(1-x)}\text{Pr}_x\text{FeNb}_4\text{O}_{15}$  solid solutions under investigation here belong to the Tetragonal Tungsten Bronze (TTB) structural family, which is one of the largest oxygen octahedral ferroelectric families next to the ferroelectric perovskites. Three types of open channels that develop within TTB structure allows solid state chemists to perform a wide range of substitutions triggering various ferroic properties. Recently, dielectric investigations of  $\text{Ba}_2\text{Nd}_{(1-x)}\text{Pr}_x\text{FeNb}_4\text{O}_{15}$  ceramics suggested the continuous transformation from the ferroelectric behavior of  $\text{Ba}_2\text{NdFeNb}_4\text{O}_{15}$  to the pure relaxor response of  $\text{Ba}_2\text{PrFeNb}_4\text{O}_{15}$  with increasing  $x$ <sup>280</sup>. For intermediate  $x$  values, coexisting ferroelectric transition and relaxor dielectric signatures were observed, corresponding to two different phenomena in the framework of these materials. Ferroelectric transition is accompanied by a 50 K wide cooling–heating hysteresis, which origin is still under discussion.

In order to define the phase diagram (Fig. 1) more precisely we have decided to investigate elastic properties of these materials by ultrasonic spectroscopy, because this non-destructive technique is very useful for identification of phase transitions. In this way, we have studied the temperature dependence of the longitudinal ultrasonic velocity and ultrasonic attenuation in  $\text{Ba}_2\text{Nd}_{(1-x)}\text{Pr}_x\text{FeNb}_4\text{O}_{15}$  solid solution family. In addition our ultrasonic method allowed us to investigate piezoelectric sensitivity of these TTB samples. The experiments showed small anomalies of ultrasonic velocity and attenuation, which depend on the thermal history of samples. The piezoelectric sensitivity which was observed in low temperature phase confirmed the existence of the polar phase e.g. the ferroelectric phase transition in  $\text{Ba}_2\text{NdFeNb}_4\text{O}_{15}$  material and their solid solutions with  $\text{Ba}_2\text{PrFeNb}_4\text{O}_{15}$ .

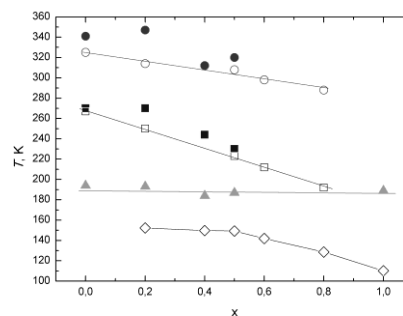


Fig. 90:  $\text{Ba}_2\text{Nd}_{(1-x)}\text{Pr}_x\text{FeNb}_4\text{O}_{15}$  phase diagram, where  $\square, \circ$  – ferroelectric phase transition temperatures on cooling and heating determined from dielectric data;  $\blacksquare, \bullet$  – ferroelectric phase transition temperatures on cooling and heating determined from ultrasonic measurements;  $\blacktriangle$  – temperatures of ultrasonic anomalies probably caused by relaxor state;  $\diamond$  – calculated  $T_{VF}$  values.

<sup>280</sup> M. Kinka, “Coexistence of Ferroelectric and Relaxor States in  $\text{Ba}_2\text{Pr}_x\text{Nd}_{1-x}\text{FeNb}_4\text{O}_{15}$  Ceramics”, IEEE Trans. Ultrason., Ferroelectr., Freq. Control, vol. 59, p. 1879-1882, 2012

## Pyroelectric and electrocaloric properties of PZT- and BaTiO<sub>3</sub>-based ceramics

Hiroshi Maiwa<sup>1</sup>

<sup>1</sup>Department of Materials and Human Environmental Sciences, Shonan Institute of Technology,  
Fujisawa, Japan

Email: maiwa@mate.shonan-it.ac.jp

Thermal energy harvesting using non-linear pyroelectric effects in PZT with different  $T_c$ , PLZT, Ba(Zr<sub>0.2</sub>Ti<sub>0.8</sub>)O<sub>3</sub> and (Ba<sub>0.8</sub>Sr<sub>0.2</sub>)TiO<sub>3</sub> ceramics, and PMN-PT crystals were investigated. Commercial bulk Ba(Zr,Ti)O<sub>3</sub> (BZT), (Ba,Sr)TiO<sub>3</sub> (BST) and PLZT(7/65/35) powders (Hayashi Chemical) were used as starting materials. The powders were fired at 1350°C for Ba(Zr,Ti)O<sub>3</sub>, 1400°C for (Ba,Sr)TiO<sub>3</sub>, 1225°C for PLZT ceramics. 0.2mol%Mn-doped BZT (BZT-Mn) were prepared using the same procedure. To characterize the non-linear pyroelectric response, polarizations of the samples at various temperatures were measured using a combination of a programmable signal generator and a charge-amplifier. The samples were cut into 3-5 mm squares, and the temperatures of the samples were changed by immersing them in a heated oil bath. PLZT ceramics (3x3x4mm) rod were used for the ECE measurement. The temperatures were measured using radiation temperature sensor.

Measurements of the polarization in ceramics were performed using a charge-amplifier circuit. An alternating electric field of 0.1 Hz was used in these measurements. The relationship between high temperature and stored energies is show in Fig. 5. Generally, stored energies increased with temperature, due to the expanding of the difference of the polarization at room temperature and high temperature. PLZT ceramics with  $T_c$  of 140°C exhibited large energy generation of 54.8 J/L/cycle with temperature variations from 30°C to 200°C and field variations from 0 to 20kV/cm. Ba(Zr<sub>0.2</sub>Ti<sub>0.8</sub>)O<sub>3</sub> ceramics with  $T_c$  of 40°C exhibited energy generation of 58.6 J/L/cycle with temperature variations from 30°C to 125°C and field variations from 0 to 20kV/cm.

The electrocaloric temperature changes  $\Delta T$  due to applied  $\Delta E$  were measured. PLZT(7/65/35) ceramics exhibited  $\Delta T$  of 0.2K at room temperature under a bipolar switching field of 20kV/cm.

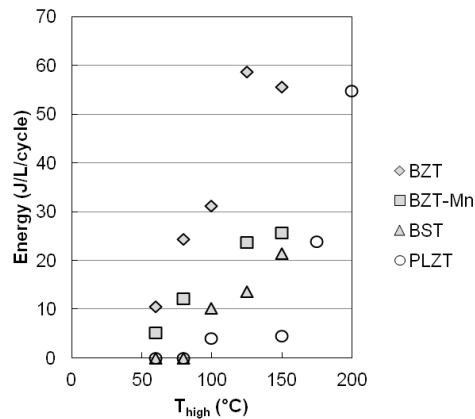


Fig. 91: Relationship between high temperature and stored energies for Ba(Zr,Ti)O<sub>3</sub>, Ba(Zr,Ti)O<sub>3</sub>-Mn, (Ba,Sr)TiO<sub>3</sub>, and PLZT(7/65/35) ceramics.

This study was supported in part by a grant in aid (C, No.22560671) and GRENE (Green network of excellence) project from the ministry of education, culture, sports, science, and technology, Japan.



## Temperature Dependence of Electric Field Induced Changes in Raman Spectrum of Lithium Niobate Single Crystals

Zelenovskiy Pavel<sup>1</sup>, Shur Vladimir<sup>1</sup>, Mingaliev Eugene<sup>1</sup>, Bourson Patrice<sup>2</sup>, Fontana Marc<sup>2</sup>

<sup>1</sup>Ferroelectric Laboratory, Ural Federal University, Ekaterinburg, Russia

<sup>2</sup>Laboratory of optical and photonic materials and systems, University of Lorraine, Metz, France

Email: zelenovskiy@labfer.usu.ru

The temperature dependence of Raman spectrum changes induced by residual depolarization field in the vicinity of the domain walls has been studied in periodically poled lithium niobate single crystals. It was demonstrated that the changes of measured integrated intensity and frequency shift of specified Raman lines disappeared at temperatures above 120°C.

It has been shown experimentally that the parameters of specified Raman lines, being very sensitive to lattice distortion, change remarkably in the vicinity of the domain walls produced at room temperature in lithium niobate (LiNbO<sub>3</sub>, LN) single crystals<sup>281</sup>. This effect is used for visualization of the micro- and nanodomain structures in LN both at the surface and in the bulk using Raman confocal microscopy<sup>282</sup>. While the effect is absent for domain structure produced at elevated temperatures. The changes of the Raman spectrum have been attributed to distortion of the crystal lattice induced by the residual depolarization field existing in the vicinity of the domain walls near the crystal surface<sup>1</sup>.

The changes of integrated intensity and frequency of E(TO<sub>8</sub>) and A<sub>1</sub>(LO<sub>4</sub>) Raman lines were measured in  $Z(xx)\bar{Z}$  configuration in the vicinity of neutral domain walls LN surface at different steady-stated temperatures ranged from 25 to 120°C. The mapping of Raman spectra across the domain walls has been done at constant temperature.

It has been revealed that the absolute values of the integrated intensity changes gradually decreased with temperature increasing and disappeared at 120°C. Frequency shift of E(TO<sub>8</sub>) line possesses strong variations while the shift of A<sub>1</sub>(LO<sub>4</sub>) line remains approximately constant during the whole temperature range. At temperature 120°C frequency shift rapidly goes to zero for both spectral lines.

The additional experimental measurement of the temperature dependence of the pyroelectric field during heating with the constant rate about 7°C/min demonstrates the field maximum just at 120°C. This fact has been attributed to increase of the bulk conductivity leading to more effective screening of the depolarization field and decreasing of pyroelectric field<sup>283</sup>. It is clear that effective bulk screening at elevated temperature must diminish the residual depolarization field in the vicinity of the domain wall thus leading to disappearance of the changes of Raman spectrum.

The research was made possible in part by RFBR (Grants 13-02-01391-a, 12-02-31377-mol-a, 11-02-91066-CNRS-a); by Ministry of Education and Science (Contracts 14.513.12.0006 and

<sup>281</sup> P.S. Zelenovskiy, V.Y. Shur, P. Bourson, M.D. Fontana, D.K. Kuznetsov, and E.A. Mingaliev, *Ferroelectrics* **398**, 34 (2010).

<sup>282</sup> P.S. Zelenovskiy, M.D. Fontana, V.Ya. Shur, P. Bourson, and D.K. Kuznetsov, *Appl. Phys. A* **99**, 741 (2010).

<sup>283</sup> V.Ya. Shur, D.K. Kuznetsov, E.A. Mingaliev et al., *Appl. Phys. Lett.* **99**, 082901 (2011).

16.740.11.0585), by OPTEC LLC and in terms of Ural Federal University development program with the financial support of young scientists.

## Retention of Thin Ferroelectric VDF-TrFE Copolymer Films Evaluated from Dielectric Non-Linearities

Danny von Nordheim<sup>1</sup>, Sebastian Koch<sup>1</sup>, Soichiro Okamura<sup>2</sup>, Bernd Ploss<sup>1</sup>

<sup>1</sup>Department of SciTec, University of Applied Sciences Jena, Jena, Germany

<sup>2</sup>Department of Applied Physics, Tokyo University of Science, Shinjuku, Tokyo 162-8601, Japan

Email: danny.von.nordheim@fh-jena.de

Polarisation retention of a ferroelectric is an important feature for most of its applications, especially for memories but also for pyroelectrics or piezoelectrics. On the other hand, a reduction or loss of remanent polarisation might be favourable when the ferroelectric is used as the dielectric in a capacitor to store energy.

In the common procedure to investigate retention the ferroelectric sample is first polarised by the application of an appropriate voltage pulse. After a specified time a further voltage pulse is applied while the charge response is recorded. The limitation of this technique is that the sample is polarised again by the second ‘read’ pulse and a continuous recording of polarization loss is not possible. Therefore we propose an alternative procedure which is based on the continuous measurement of the small signal linear and second order non-linear dielectric permittivity as a function of time after the sample has been polarized by a ‘write’ pulse. As the polarisation of the ferroelectric is not influenced by the small signal measurement, this non-destructive method gives an accurate measure of the temporal development of polarisation.

Thin VDF-TrFE copolymer films of molar ratio 70/30 and thickness below 200 nm have been deposited by spin coating on a glass substrate covered with aluminium electrodes. After annealing at a temperature appropriate for films with this thickness and deposition of the top electrodes, the sample has been poled with a series of positive triangular pulses. Directly after the last poling pulse a small sinusoidal voltage has been applied to the sample while the current response has been recorded and analysed in terms of first and second order permittivities. The quotient  $\epsilon_0 \epsilon_2' / (\epsilon_0 \epsilon_1')$  is proportional to the remanent polarisation. At 30 °C we observed an initial decrease of polarisation with a time constant of about 1 hour which finally settled at about 80 per cent of the initial value. This reduction after poling is essentially attributed to the rearrangement of charges injected into the ferroelectric film by the poling pulses.

The same non-destructive method can be used to read out the polarisation state of a ferroelectric memory cell making a rewrite of the initial polarisation dispensable. Thus, the readout speed and the cell’s lifetime could be improved.

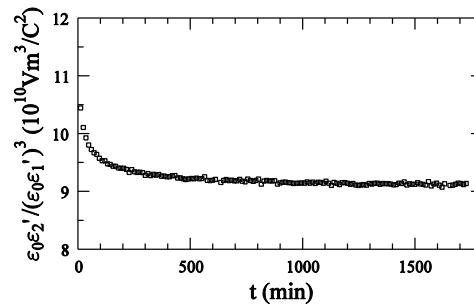


Fig. 92: Polarisation versus time for a 90 nm thin P(VDF-TrFE) sample at 30 °C.



## Composition and Morphology Effects on the Thermal Conductivity of PZT Thin Films

Jon F. Ihlefeld,<sup>1</sup> Brian M. Foley,<sup>2</sup> John C. Duda,<sup>2</sup> Harlan Brown-Shaklee,<sup>1</sup> Douglas Medlin,<sup>3</sup> Bryan D. Huey,<sup>4</sup> Bonnie B. McKenzie,<sup>1</sup> Brady J. Gibbons<sup>5</sup> and Patrick E. Hopkins<sup>2</sup>

<sup>1</sup>Sandia National Laboratories, Albuquerque, New Mexico/USA

<sup>2</sup>Department of Mechanical and Aerospace Engineering, University of Virginia, Charlottesville, Virginia/USA

<sup>3</sup>Sandia National Laboratories, Livermore, California/USA

<sup>4</sup>Institute of Materials Science, University of Connecticut, Storrs, Connecticut/USA

<sup>5</sup>Materials Science, School of Mechanical, Industrial, and Manufacturing Engineering, Corvallis, Oregon/USA

Email: jihlefe@sandia.gov

In this presentation we explore the effects of composition, phase, and morphology on the thermal conductivity of lead zirconate titanate thin films. Epitaxial and polycrystalline films with compositions ranging from  $\text{PbZr}_{0.2}\text{Ti}_{0.8}\text{O}_3$  to  $\text{PbZr}_{0.8}\text{Ti}_{0.2}\text{O}_3$  have been prepared by chemical solution deposition on (001)-oriented  $\text{SrTiO}_3$  and  $\text{Pt/ZnO/SiO}_2/\text{Si}$  substrates. Thermal conductivities were measured using time-domain thermoreflectance at room temperature. For single-crystalline films, the composition dependent thermal conductivity trend will be shown to be consistent with that expected for alloy scattering from the mixed *B*-site. For polycrystalline films, it will be shown that grain boundary scattering dominates the measured thermal conductivities and decreases the composition dependence. For specific compositions in both epitaxial and polycrystalline films, however, a decreased thermal conductivity is observed that is consistent with scattering from finer-scale features. These results will be discussed in the context of phonon scattering from domain walls. This presentation represents one of the first studies of the composition and morphology dependence of thermal conductivity in a ferroelectric thin film. Sandia National Laboratories is a multi-program laboratory managed and operated by Sandia Corporation, a wholly owned subsidiary of Lockheed Martin Corporation, for the U.S. Department of Energy's National Nuclear Security Administration under contract DE-AC04-94AL85000.

## Comparable Measurements and Modeling of Piezoelectric Thin Films for MEMS application

Thorsten Schmitz-Kempen<sup>1</sup>, Stephan Tiedke<sup>1</sup>, Peter Mardilovich<sup>2</sup>, Subramanian Sivaramakrishnan<sup>2</sup>,  
Thomas Lisec<sup>3</sup>, Fabian Stoppel<sup>3</sup>

<sup>1</sup>aixACCT Systems GmbH, Aachen, Germany

<sup>2</sup>Hewlett-Packard, Corvallis, USA

<sup>3</sup>Fraunhofer Institute for Silicon Technology, Itzehoe, Germany

Email: [schmitz@aixacct.com](mailto:schmitz@aixacct.com)

Accurate and reliable measurements of piezoelectric coefficients on thin films are required to perform thin film process development and compare different manufacturing techniques and quality especially in MEMS applications.

State of the art measurements are performed by double-beam laser interferometry since many years, however the variety of parameter ranges and test conditions make it difficult to compare measurement results. Films on a substrate exhibit effective piezoelectric coefficients due to substrate clamping and the coefficient also depends on feature size and substrate thickness. This was shown by FEM simulations for the case of  $d_{33,f}$  measurements by DBLI (K. Prume et al, Proc. IEEE ISAF 2004) and latest simulation and measurement results show that a considerable reduction of the measured  $d_{33,f}$  was obtained for small electrodes and an increase for large electrodes. The measured  $d_{33,f}$  value at large electrodes is even larger than the true  $d_{33,f}$  of the film and for small feature sizes it is lower. A feature size chosen equivalent to the substrate thickness exhibits the most exact number for the effective coefficient  $d_{33,f}$  (S. Sivaramakrishnan et al, presentation on 3rd PiezoMEMS Workshop 2013).

Furthermore nonlinearity and hysteresis of ferroelectric films requires the definition of measurement parameters to obtain comparable procedures regarding hysteresis, poling conditions, and other property nonlinearities, voltage and frequency dependency of coefficients, and large and small signal responses. For easier comparison of films a large signal coefficient ( $d_{33,ls}$ ) is introduced as the average slope of a displacement vs. voltage measurement over the full operating voltage range. For thin film measurements it reflects the potential displacement in typical actuator applications in comparison to small-signal coefficients and allows better comparison of materials for actuation.

## Investigation of the dielectric, piezoelectric and elastic properties of BaTiO<sub>3</sub> by means the thermal noise method

I. Shnidshtein<sup>1</sup>, P. Bednyakov<sup>2</sup>, B. Strukov<sup>1</sup>

<sup>1</sup>Lomonosov Moscow State University, Moscow, Russia

<sup>2</sup>École Polytechnique Fédérale de Lausanne, Lausanne, Suisse

Email: shnidshtein@physics.msu.ru

Crystals of barium titanate BaTiO<sub>3</sub> (BT) belong to classical model ferroelectrics which have been extensively investigated by various methods since the discovery of their ferroelectric properties. However the role of the fluctuation effects at the ferroelectric phase transition in BT crystals is so far not clear<sup>284</sup>. This is due both to the fact that the ferroelectric phase transition in BT is a phase transition of the first order and with the difficulty to differ the behavior related with the fluctuations and other similar factors such as defects or the experiment conditions.

The thermal noise method allows to controlling the experimental conditions due to the absence of the measuring voltage. Moreover, that in BT crystals noise voltage level is high and as it was shown earlier by Brophy and Webb<sup>285</sup> it can be changed by changing the thermal conditions of the experiment. By this way we can separate the different contributions responsible for the noise voltage, such as thermal Barkhausen noise, white noise and the noise caused by the piezoelectric effect.

This approach has been used in our previous work<sup>286</sup>. In addition to the results obtained there, we discuss new data on the impact of the bias electric field for different types of noise near the ferroelectric phase transition. These data are directly related to the observation of the piezoelectric effect in the cubic phase of BT crystals. Also for the first time the possibility of determining of the elastic properties of the crystal by the noise measurements are discussed.

This work is supported by Russian Foundation for Basic Research (project of №11-02-01317).

---

<sup>284</sup> Y.L. Wang, A.K. Tagantsev, D. Damjanovic, N. Setter, V.K. Yarmarkin, A.I. Sokolov, Anharmonicity of BaTiO<sub>3</sub> single crystals, *Phys. Rev B*, vol. 73, 132103, 2006.

<sup>285</sup> J.J. Brophy, S.L. Webb, Critical fluctuation in triglecene sulphate, *Phys. Rev*, vol. 128, 584, 1962.

<sup>286</sup> P.S. Bednyakov, I.V. Shnidshtein, B.A. Strukov, Investigation of the dielectric properties of BaTiO<sub>3</sub> single crystals of different qualities by the thermal noise method, *Physics of the Solid State*, vol. 53, 350, 2011.

## Band gap asymmetry and local segregation in barium zirconate titanate epitaxial thin films

Jofre Ventura<sup>1</sup>, Sergio Hernández<sup>2</sup>, Adolf Canilas<sup>1</sup>, Jordi Sancho-Parramón<sup>3</sup>, Luis Emerson Coy<sup>1</sup>, Cèsar Ferrater<sup>1</sup>, María del Carmen Polo<sup>1</sup>, María Victoria García-Cuenca<sup>1</sup>, Manuel Varela<sup>1</sup>

<sup>1</sup>Department de Física Aplicada I Òptica, Universitat de Barcelona, Barcelona, Spain

<sup>2</sup>Department d'Electrònica, Universitat de Barcelona, Barcelona, Spain

<sup>3</sup>Ruder Bošković Institute, Bijenička 54, Zagreb 10000, Croatia

Email: jofre.ventura@ub.edu

The substitution of  $\text{Ti}^{4+}$  by  $\text{Zr}^{4+}$  in  $\text{BaZr}_x\text{Ti}_{1-x}\text{O}_3$  (BZT) changes its dielectric character from proper ferroelectric to ferroelectric with pinched phase transition, second-order-like diffuse phase transition, relaxor behavior, polar cluster and then simple paraelectric<sup>287</sup>. The dynamic coupling between  $\text{BaTiO}_3$  polar nanoregions and  $\text{BaZrO}_3$  nonpolar ones is thought to be the mechanism behind such a rich phase diagram. However, these short-range composition variations are not detectable with X-ray diffraction, which relies on the coherent scattering from many unit cells, and this topic is thus rarely addressed.

We have grown thin films of BZT on (001)-oriented  $\text{Nb:SrTiO}_3$  substrates by pulsed laser deposition. Structural characterization by X-ray diffractometry showed that a solid solution with single cube-on-cube epitaxial domain is formed across the entire compositional range. Excluding tetragonal  $\text{BaTiO}_3$ , the unit cell of BZT is cubic and its volume increases linearly with Zr content, suggesting proper intermixing of Zr and Ti into an average BZT lattice.

However, two-mode behavior of the  $A_{1g}$  breathing mode of the oxygen octahedron was detected in the Raman inelastic scattering spectra of BZT, which might be attributed to a heterogeneous distribution of B-site cations with different Ti-O and Zr-O bond distances (or local clustering) rather than long-range ordering<sup>288</sup>.

Furthermore, the dependence of band gap energy with composition determined from spectroscopic ellipsometry measurements (Fig. 1) does not follow a *bowing* parabolic dependence as one could expect from local lattice relaxations alone. Instead, an asymmetric trend suggests the tendency to the enrichment of one chemical species over another, as expected from a nonideal solid solution behavior<sup>289</sup>. An empirical modified Vegard's equation with an asymmetry weighted function was successfully fitted to the experimental data.

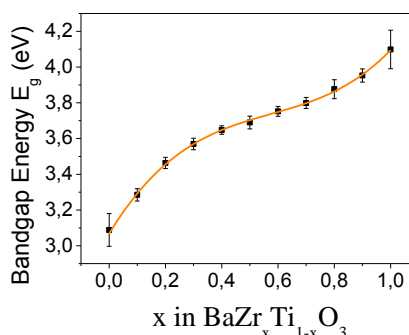


Fig. 93: Dependence of band gap energy on Zr content as obtained from spectroscopic ellipsometry (black points) and asymmetric empirical model (orange line).

<sup>287</sup> T. Maiti *et al.*, J. Am. Ceram. Soc., vol. 91, p. 1769-1780, 2008.

<sup>288</sup> I. Levin *et al.*, Chem. Mater., vol. 18, p. 854-860, 2006.

<sup>289</sup> S. Lee *et al.*, J. Appl. Phys., vol. 107, p. 023523, 2010.





## Determination of the vibrational properties of potassium titanyl phosphate and identification of domain structure sensitive phonon modes

M. Rüsing<sup>1</sup>, C. Buchholz<sup>1</sup>, G. Berth<sup>1,2</sup> and A. Zrenner<sup>1,2</sup>

<sup>1</sup>Department Physik, Universität Paderborn, 33098 Paderborn, Germany

<sup>2</sup>Center for Optoelectronics and Photonics Paderborn (CeOPP), 33098 Paderborn, Germany

Email: mruesing@mail.upb.de

Ferroelectric materials are commonly used for a wide range of applications in the field of integrated optics. Their special characteristics such as permanent polarization and nonlinear properties make them an ideal material for nonlinear devices. Especially the opportunity for quasi-phase-matching via periodically poled structures is a central topic for the application of this material class. One of these ferroelectrics is potassium titanyl phosphate (KTP) which has attracted particular attention due to its large electro-optical coefficients, high nonlinear coefficients and high damage threshold<sup>290</sup>. For advancement in application of periodically poled devices often smaller periods of alternating domains with opposing polarity are needed. In previous work it has been shown, that second harmonic generation can be used for imaging of ferroelectric domain walls in KTP<sup>291</sup>. Due to complex domain engineering a deep understanding of the material properties is inevitable. Here Raman spectroscopy represents a widely used method for elemental analysis of crystal structures.

In this work confocal Raman spectroscopy was applied on KTP. The confocal application enriches Raman spectroscopy with the power of high spatial resolution enabling the characterization of the transferred ferroelectric domain structure. With this combined technology a detailed analysis of additional information becomes possible. Raman spectroscopy has already been successfully used to examine the ferroelectric domain structure in other ferroelectric materials<sup>292</sup>.

Confocal Raman spectroscopy was applied for studying the vibrational properties of KTP in its entirety. Therefore polarization-dependent measurements in various scattering configurations were performed. Our measurements are in good agreement with previous work on KTP<sup>293</sup>. Furthermore we have characterized periodically poled potassium titanyl phosphate in terms of polarity- and structure-sensitive phonon modes. Here we found vibrations which are linked to the ferroelectric domain structure. This might be due to changes in the polarizability originated from both the domain boundaries and the inner field distribution. Hence a direct visualization based on the spatial Raman intensity variation of specific phonon modes becomes possible.

---

<sup>290</sup> M. E. Hagerman, K. R. Poeppelmeier, "Review of the Structure and Processing-Defect-Property Relationships of Potassium Titanyl Phosphate: A Strategy for Novel Thin-Film Photonic Devices", *Chem. Mater.*, vol. 7, p. 602-621, 1995.

<sup>291</sup> S. I. Bozhevlnyi et al., "Second-harmonic imaging of ferroelectric domain walls", *Appl. Phys. Lett.*, vol. 73, p. 1814-1817, 1998.

<sup>292</sup> G. Berth et al., "Imaging of the Ferroelectric Domain Structures by Confocal Raman Spectroscopy", *Ferroelectrics.*, vol. 420, p. 44-48, 2011.

<sup>293</sup> G. E. Kugel et. al., "The vibrational spectrum of  $\text{KTiOPO}_4$  single crystal studied by Raman and infrared reflectivity spectroscopy", *J. Phys C: Solid State Phys.*, Vol. 21, p. 5565-5583, 1988.



## Novel Electromechanical Analysis to Investigate Small Signal Properties of Single Fibers

Frank Jörg Clemens<sup>1</sup>, Francesca Bortolani<sup>1</sup>

<sup>1</sup>Laboratory for High Performance Ceramics, Empa, Dübendorf, Switzerland

Email: frank.clemens@empa.ch

Ferroelectric fibers are interesting for application in ultrasonic, micro-electronic, structure health monitoring and energy harvesting systems. For such applications the fibers are embedded into a polymeric matrix to design either AFCs (Active Fiber Composites) or so-called 1-3 composite structures. Their properties strongly depend on fiber content, fiber diameter and material composition. In comparison to piezoelectric bulk materials, the characterization method of fibers is undersized. For the characterization of piezoelectric fibers, 1-3 composites with a high fiber content (> 60vol%) are often used. The fibers are aligned in a single direction and the effective ferroelectric, dielectric and elastic properties of the composite can be determined by conventional dynamic or quasistatic methods.

With the new equipment ("FerroFib"), properties like small and large signal behavior  $S(E)$ , dielectric and piezoelectric charge constant as well as polarization on single fibers can be now evaluated. With the new FerroFib, characterization can be done at different frequencies and temperatures. Additionally the so-called blocking force can be investigated. The results achieved with the use of the FerroFib are comparable with the data already published by the group in collaboration with national and international partners. First evaluation was done on Single PZT-based ceramic fibers sintered at 1100, 1150 and 1200°C in a lead enriched atmosphere (PbZrO<sub>3</sub>+ZrO<sub>2</sub>). The results were linked with the microstructure and compared with data which were measured with other equipment. The piezoelectric coefficient  $d_{33}$  for fibers sintered at 1200°C is comparable with the one reported in the data sheet of the powder (Fig. 1).

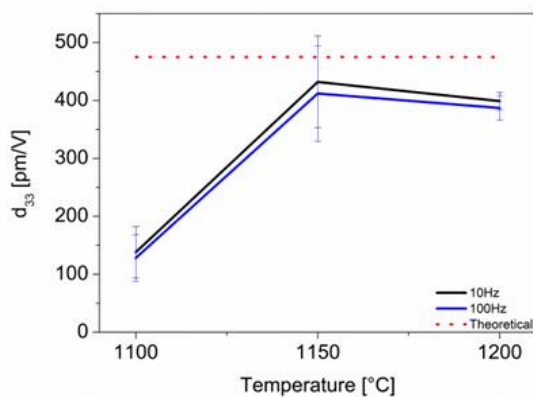


**Fig. 1:** Piezoelectric coefficient ( $d_{33}$ ) evolution as a function of sintering temperature.

## Magnetoelectric coupling in $\text{Bi}_{1-x}\text{A}_x\text{FeO}_3$ (A=La, Nd) solid solutions

A.A. Amirov<sup>1</sup>, I.K. Kamilov<sup>1</sup>, L.A. Reznichenko<sup>2</sup>, O.N. Razumovskaya<sup>2</sup>, I.A. Verbenko<sup>2</sup>

<sup>1</sup> Institute of Physics, Dagestan Scientific Center of Russian Academy of Sciences, 94 Yaragskogo Street, Makhachkala, Russia

<sup>2</sup> Institutes of Physics, South Federal University, 194 Stachki Street, Russia  
e-mail: [amiroff\\_a@mail.ru](mailto:amiroff_a@mail.ru)

The investigation of systems with strongly coupled magnetic and electronic degrees of freedom has drawn significant interest in recent years due to both challenges for many-body theory as well as for potential technical applications [1–2]. In connection with the compounds on base of  $\text{BiFeO}_3$  are very perspective multiferroic materials due to high temperature of magnetic and ferroelectric phase transitions, bad conductivity and simple chemical structure [1-2].

High quality ceramics were synthesized on the basic of  $\text{Bi}_{1-x}\text{A}_x\text{FeO}_3$  (A=La, Nd;  $x=0-0.2$ ) solid solutions. Their crystal and grain structure, Mossbauer spectra, dielectric, magnetic, thermal characteristics were studied. The ac-susceptibility vs. temperature curve of  $\text{BiFeO}_3$  has a sharp peak at 646 K which corresponds to the antiferromagnetic phase transition and it is confirmed by literature data [3]. The anomalies of dielectric permeability, spacing parameter, thermal conductivity and heat capacity near temperature of antiferromagnetic order  $T_N$  were observed in all samples and it is related with correlation between magnetic and ferroelectric subsystem which is typical for multiferroics. The magnetization curves also have been studied at the room temperature for the samples. The magnetization of pure  $\text{BiFeO}_3$  is small and grows linearly with magnetic field. Such type of magnetization curve is typical for antiferromagnetic materials. La and Nd substitutions lead to increase magnetic properties of  $\text{BiFeO}_3$ . The substitution Bi by La or Nd changes the temperature of the antiferromagnetic order and increases the magnetization of pure  $\text{BiFeO}_3$ . The magnetic properties change occurs not only on account of magnetic moment and ionic radiuses (lanthanum atom has no its magnetic moment), but also because of La and Nd ions magnetic moments anisotropy.

The samples were also studied for the presence of the magnetodielectric effect (magnetocapacitance), which is a change in the permittivity of the sample caused by the application of a magnetic field

$$\frac{\Delta\varepsilon(H)}{\varepsilon(0)} = \frac{\varepsilon(H) - \varepsilon(0)}{\varepsilon(0)},$$

where  $\varepsilon(H)$  and  $\varepsilon(0)$  are the permittivities in a magnetic field and in the absence of it, respectively. The measurement results showed an increase in magnetodielectric effect is associated with an increase in the degree of interaction between the dipole and magnetic subsystems. The slower increase of magnetocapacitance in the range  $0.05 \leq x \leq 0.1$  associated with the change of predominant mechanism in the solid solutions, as in  $0.15 \leq x \leq 0.2$  - with the existence of invar effect due to the appearance of a new monoclinic phase.

<sup>1</sup>J. Wang et al., *Science* 299, 1719 (2003)

<sup>2</sup>A.K. Zvezdin and A.P. Pyatakov, *Sov. Phys. Usp.* 47, 8 (2004).

<sup>3</sup>Sosnowska and A. K. Zvezdin, *J. Magn. Magn. Mater* 140–44, 167 (1995)

## Measurement of Vibration Mode Structure for Adaptive Vibration Suppression System by Digital Holography

Pavel Psota<sup>1,2</sup>, Vít Lédl<sup>1,2</sup>, Roman Doleček<sup>1,2</sup>, Pavel Mokry<sup>1,2</sup>

<sup>1</sup>TOPTEC Centre, Turnov, Czech Republic

<sup>2</sup>Technical University of Liberec, Liberec, Czech Republic

Email: psota@ipp.cas.cz

The frequency-shifted digital holographic interferometry (FSDHI) for measurements of vibration amplitudes in the range of nanometers has been recently introduced and demonstrated<sup>294,295</sup>. The FSDHI method addressed some of the drawbacks of conventional methods and was mainly used for measurements of piezoelectric transformer vibration amplitudes and mode structures<sup>296</sup>. The limiting factor for the application of this method is the maximal measured value of the vibration amplitude without the risk of an ambiguity. The value is approximately 80nm for the frequency doubled Nd: YAG line.

Since FSDHI enables us to precisely measure vibration amplitudes over the whole inspected area with a very high lateral resolution, it could also be a very useful tool for measurements of vibration amplitudes and mode structures in the research and development of adaptive noise suppression systems. Such measurements would provide a necessary feedback about the system behavior.

The aforementioned issues have motivated the work where we put an effort to the modification of the FSDHI method with the aim of increasing its dynamic range while keeping its precision. The essential breakthrough in this paper is an innovative data processing technique based on recurrence relationship of the first kind Bessel functions. Finally, a measurement method called high dynamic range - frequency shifted digital holographic interferometry (HDR-FSDHI) was developed. The method has the ability to measure in a nearly arbitrary range of vibration amplitudes.

The HDR-FSDHI method was applied on a vibration amplitudes measurement of a window. The window was a vibration system model where the vibrations were suppressed by attached piezoelectric macro fiber composite (MFC) actuators shunted by active circuits with a negative capacitance<sup>297</sup>. The paper presents the basic principle of the method, the experimental setup and some results of measurements.

---

<sup>294</sup> V. Lédl, J. Vaclavik, R. Dolecek, and V. Kopecky, "Frequency Shifted Digital Holography for the Measurement of Vibration with Very Small Amplitudes," in American Institute of Physics Conference Series, 2010.

<sup>295</sup> V.Lédl, P.Psota, R.Dolecek, T.Vit, J.Vaclavik, "Testing of recently developed digital holographic method for very small amplitude measurement" in "Optical Measurement Techniques for Systems and Structures," Shaker Publishing BV, 2013.

<sup>296</sup> P. Psota, V. Lédl, R. Dolecek, J. Erhart, and V. Kopecky, "Measurement of piezoelectric transformer vibrations by digital holography," IEEE Transactions on Ultrasonics, Ferroelectrics and Frequency Control, 59, 1962 –1968, 2012.

<sup>297</sup> M. Kodejska, P. Mokry, V. Linhart, J. Vaclavik, T. Sluka. "An adaptive vibration suppression system: An alternative control law for a negative capacitor shunt of a piezoelectric actuator," IEEE transactions on ultrasonics, ferroelectrics, and frequency control, 12/2012.

## Nonlinear signatures of periodically poled waveguide structures in X- and Y-cut lithium niobate

T. Steinrück<sup>1</sup>, A. Widhalm<sup>1</sup>, G. Berth<sup>1,2</sup> and A. Zrenner<sup>1,2</sup>

<sup>1</sup>Department Physik, Universität Paderborn, 33098 Paderborn, Germany

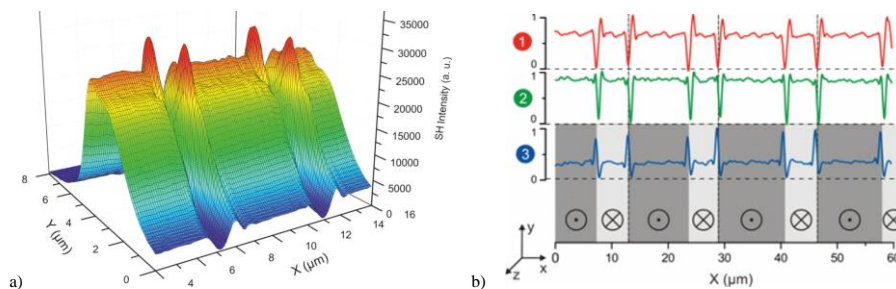
<sup>2</sup>Center for Optoelectronics and Photonics Paderborn (CeOPP), 33098 Paderborn, Germany

Email: tobiasst@mail.uni-paderborn.de

Essential topic for the efficiency of nonlinear processes is the quality of the transferred ferroelectric domain structure enabling quasi-phase-matching. In this context periodically poled lithium niobate (PPLN) represents a well-established material system due to its unique combination of properties. For the noninvasive visualization of such domain structures nonlinear confocal laser scanning microscopy is an established tool<sup>298</sup>. Here, the observed nonlinear signatures mainly depend on the poling method/fabrication parameters and the crystallographic orientation/area. Up to now the occurring basic contrast mechanisms are not understood.

Within this work we focus on nonlinear signatures originated from waveguides in X- and Y-cut PPLN prepared in planar and ridge geometry. Besides the visualization of the periodic domain structure a depth-resolved analysis of the specific second harmonic (SH) response in the mapped area of transition has been performed systematically. In fact, second harmonic generation is particularly a boundary surface effect, therefore specific changes can especially be observed there.

For recorded SH maps of surface-near micro domains in planar and ridge waveguides a similar nonlinear signature can be found. In the area of polarity reversal domain fragments become visible linked to the applied electric field. Furthermore a detailed nonlinear analysis of the transition area of contrarily poled domains reveals specific signal sequences subject to the period and polarity. A direct correlation with the nonlinear susceptibility tensor can be expected. In addition, these sequences exhibit a functional dependence on depth. This might be due to the influence of surface charge and the inner electric field distribution. Overall a complex interaction of a multitude of parameters is existent.



<sup>298</sup> M. Flörshheimer et al., "Second-harmonic imaging of ferroelectric domains in LiNbO<sub>3</sub> with micron resolution in lateral and axial directions", Appl. Phys. B, vol. 67, p. 593-599, 1998.

Fig. 1: (a) SH intensity as a function of the depth in Y-cut PPLN (period: 16 $\mu\text{m}$ , scan increment: 100 nm).  
(b) Signal sequences perpendicular to the domain structure in XZ area for three different depths (red: Y = 0  $\mu\text{m}$ , green: Y = -2.2  $\mu\text{m}$ , blue: Y = -4.5  $\mu\text{m}$ ).



## Piezoelectric Properties of High Energy Density Pb(Zr,Ti)O<sub>3</sub>-Pb[(Zn,Ni)<sub>1/3</sub>Nb<sub>2/3</sub>]O<sub>3</sub> Thick Films for Energy Harvesting Device Application

Younghun Jeong, Jisun Yun, Junghee Nam, Jeongho Cho, Jonghoo Paik

Electronic Materials Convergence Division, Korea Institute of Ceramic Engineering and Technology, Seoul, Republic of Korea

Email: yhjeong@kicet.re.kr

Pb(Zr,Ti)O<sub>3</sub>-Pb[(Zn,Ni)<sub>1/3</sub>Nb<sub>2/3</sub>]O<sub>3</sub>-based piezoelectric ceramics have been intensively studied for energy harvesting device application<sup>299</sup>. The piezoelectric transducer material is advantageous for converting vibration energy into electrical energy, with the mixture of hard and soft characteristics, on a basis of the criterion for material selection in design of bulk piezoelectric energy harvesters. In particular, the 0.7Pb(Zr,Ti)O<sub>3</sub>-0.3Pb[(Zn,Ni)<sub>1/3</sub>Nb<sub>2/3</sub>]O<sub>3</sub> bulk ceramic sintered at the relatively low temperature of 950°C exhibited an extremely high transduction coefficient ( $d_{33} \cdot g_{33}$ ), where  $d_{33}$  and  $g_{33}$  values are the piezoelectric charge and voltage constant, respectively. In the Pb(Zr,Ti)O<sub>3</sub>-Pb[(Zn,Ni)<sub>1/3</sub>Nb<sub>2/3</sub>]O<sub>3</sub> solid solution, the magnitude of transduction coefficient is dependent on the composition; thus, high energy density material for energy harvesting devices can be achieved by selecting the best composition with superior transduction coefficient.

In this work, high energy density 0.72Pb(Zr<sub>0.47</sub>Ti<sub>0.53</sub>)O<sub>3</sub>-0.28Pb[(Zn<sub>0.45</sub>Ni<sub>0.55</sub>)<sub>1/3</sub>Nb<sub>2/3</sub>]O<sub>3</sub> (PZT-PZNN) thick films by a tape casting method were developed for energy harvesting device application. The PZT-PZNN thick films were sintered at various temperatures from 900°C to 1200°C. When sintered at 1050°C, the 190 μm-thick PZT-PZNN film with a dense and homogeneous microstructure revealed superior piezoelectric properties while the films sintered above 1050°C exhibited deteriorated electrical characteristics due to the formation of a non-ferroelectric pyrochlore phase of lead zinc niobate. In particular, the film sintered at 1050°C revealed an excellent transduction coefficient ( $d_{33} \cdot g_{33}$ ) of  $20,340 \times 10^{-15} \text{ m}^2/\text{N}$ , which is comparable to that of bulk ceramic.

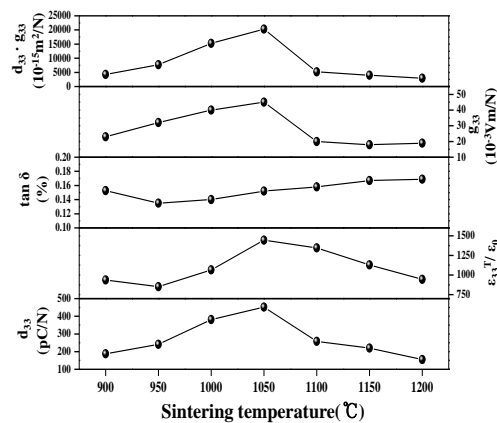


Fig. 94: Variation of  $d_{33}$ ,  $\epsilon_{33}^T / \epsilon_0$ ,  $k_p$ ,  $g_{33}$ , and  $d_{33} \cdot g_{33}$  for 0.72Pb(Zr<sub>0.47</sub>Ti<sub>0.53</sub>)O<sub>3</sub>-0.28Pb[(Zn<sub>0.45</sub>Ni<sub>0.55</sub>)<sub>1/3</sub>Nb<sub>2/3</sub>]O<sub>3</sub> thick films sintered at various temperatures.

<sup>299</sup> Y.-J. Cha, I.-T. Seo, I.-Y. Kang, S.-B. Shin, J.-H. Choi, S. Phys., vol. 110, p. 084111, 2011.

## Resolved E-symmetry zone-centre phonons in LiTaO<sub>3</sub> and LiNbO<sub>3</sub>

S. Margueron<sup>1</sup>, A. Bartaszyte<sup>2</sup>, A.M. Glazer<sup>3</sup>, E. Simon<sup>4</sup>, J. Hlinka<sup>4</sup>, I. Gregora<sup>4</sup>

<sup>1</sup>Laboratoire Matériaux Optiques, Photonique et Systèmes, EA 4423, Lorraine University and Supelec, Metz, France

<sup>2</sup>Institute Jean Lamour, (UMR 7198) CNRS – Lorraine University, Nancy, France

<sup>3</sup>Department of Physics, Oxford University, Parks Road, Oxford OX1 3PU, UK

<sup>4</sup>Institute of Physics AS CR, Prague 8, Czech Republic

Email: [samuel.margueron@univ-lorraine.fr](mailto:samuel.margueron@univ-lorraine.fr)

Lithium niobate and lithium tantalate have been the subject of intense studies because of their applications in electro-optic, nonlinear-optic, photo-refractive and acoustical devices. The optical phonon frequencies, damping parameters and intensities are used for the studies of phase transitions, symmetry, effect of pressure, stress, composition and heterogeneities in thin films, integrated structures, nano- and bulk materials. It is essential to know the frequencies of all zone-centre optical phonons in calculations of dielectric constant, oblique modes and electro-optic coefficients. There is good agreement in the reported frequencies of A<sub>1</sub>-symmetry phonons of LiNbO<sub>3</sub> and LiTaO<sub>3</sub>. Nevertheless, over the last fifty years there has been much discussion in the literature concerning the E-symmetry phonons in these materials. To date, this discussion on the E-mode assignment is still open.

In this study, all E-symmetry optical phonons at the  $\Gamma$  point of LiNbO<sub>3</sub> and LiTaO<sub>3</sub> were experimentally resolved in the spectra measured by infrared and Raman spectroscopy<sup>300</sup>. For this purpose, congruent and nearly stoichiometric crystals of LiNbO<sub>3</sub> and LiTaO<sub>3</sub>, and mixed LiNb<sub>1-x</sub>Ta<sub>x</sub>O<sub>3</sub> crystals were studied. The results show that some of the E modes have weak intensities in Raman or infrared spectra. Thus, the complete assignment of E-symmetry modes has been achieved by comparing Raman and infrared data. The wavenumbers of the E-modes, estimated experimentally, were close to those calculated theoretically for LN. The clamped relative ordinary and extraordinary permittivities of LN and LT were calculated using LST relation with good agreement with Terahertz Time Domain spectroscopy.

---

<sup>300</sup> S. Margueron, A. Bartaszyte, A.M. Glazer, E. Simon, J. Hlinka, I. Gregora, and J. Gleize, J. Appl. Phys. 111, 104105, 2012.

## Infrared Photoluminescence in Er Doped Bismuth Layered Ferroelectrics

Dengfeng Peng, Hua Zou, Xusheng Wang<sup>301</sup>, and Xi Yao

(Functional Materials Research Laboratory, Tongji University, 1239 Siping Road, Shanghai 200092, China)

**Abstract:** For ferroelectric materials, doping is usually applied to modify electronic properties, such as dielectric, ferroelectric, and piezoelectric properties. Recently, multifunctionality has renewed the interest in ferroelectrics, such as ferroelectric-photo, ferroelectric-elastic, ferroelectric-elastic-magnetic, ferroelectric-mechanical, integration and/or coupling, which can lead to a remarkable progress with numerous new materials and devices for photovoltaic, spintronic and optical-electrical-mechanical actuator and sensor applications. Here we examine the Er<sup>3+</sup> doped CaBi<sub>4</sub>Ti<sub>4</sub>O<sub>15</sub> bismuth layered structured ferroelectrics (BLSF) and demonstrate that a certain amount of Er<sup>3+</sup> doped ceramic sample shows an infrared photoluminescence while simultaneously keeping ferroelectric characteristics. Photoluminescence excitation spectra show that the samples have broad excitations from ultraviolet to green regions. The ultraviolet excitation is associated with the electronic transition within the host solid and the green excitation corresponds to the f-f transitions of Er<sup>3+</sup>, respectively. Upon these excitations, the doped samples show a strong infrared emission at room temperature, corresponding to <sup>4</sup>I<sub>13/2</sub>→<sup>4</sup>I<sub>15/2</sub> transition of Er<sup>3+</sup>. The infrared photoluminescence of Er<sup>3+</sup> reported here has also been discovered in a variety of BLSF oxides such as BaBi<sub>4</sub>Ti<sub>4</sub>O<sub>15</sub>, SrBi<sub>4</sub>Ti<sub>4</sub>O<sub>15</sub> and CaBi<sub>2</sub>Ta<sub>2</sub>O<sub>9</sub> et al., and as series of multifunctional ferroelectrics, Er<sup>3+</sup> doped BLSF materials would be of great importance for the fundamental study of optical-electrical-mechanical couplings and multifunctional design of future optical-electrical integrated devices.

---

<sup>301</sup> Corresponding author. Tel.: +86 21 65980544; fax: +86 2165985179;  
E-mail: [xs-wang@tongji.edu.cn](mailto:xs-wang@tongji.edu.cn); pengdengfeng1984@163.com.

## Dielectric Characterization of PLZST

Theresa Kainz<sup>1</sup>, Michael Naderer<sup>1</sup>, Denis Schütz<sup>1</sup>, Klaus Reichmann<sup>1</sup>

<sup>1</sup> CD-Laboratory for Advanced Ferroic Oxides, University of Technology, Graz, Austria

Email: [theresa.kainz@tugraz.at](mailto:theresa.kainz@tugraz.at)

Lead zirconate – lead titanate, in short PZT, is a well-known and widespread ferroelectric material for many applications such as actuators, sensors, transducers and further more.

In the zirconium rich region of the solid solution its structural properties are changing causing a distortion of the unit cell and opposed neighboring electric dipoles inside the cell resulting in a zero net spontaneous polarization transforming a ferroelectric material to an antiferroelectric one. The substitution of lead by aliovalent lanthanum stabilizes the antiferroelectric phase. Applying an electric field higher than a critical switching field converts the anti-parallel to a parallel dipole alignment inducing a ferroelectric state. Removing the field reverses the alignment to the antiferroelectric phase releasing the stored polarization and producing a current. The change in the structure enables to store charge and energy respectively at higher electric fields where conventional ferroelectric materials deteriorate in permittivity.

In this work the electric field induced antiferroelectric-to-ferroelectric phase transition of lanthanum modified lead zirconate titanate stannate ceramics was investigated in order to clarify the role of tin. The compositions varied in the tin content replacing the zirconium ( $\text{Pb}_{0,91}\text{La}_{0,06}\text{V}_{\text{Pb}'}_{0,03})(\text{Zr}_{0,90-x}\text{Ti}_{0,1}\text{Sn}_x)\text{O}_3$  ( $x = 0,01-0,24$ ) were located in the antiferroelectric phase region.

The ceramic was prepared by the conventionally mixed oxide route with an excess of lead added before calcination. The mixture was calcined at 850°C and sintering was performed at 1250°C for 3 hours.

Dielectric behavior was investigated by measuring the low signal permittivity, capacitance and the piezoelectric coefficient  $d_{33}$  as well as recording the polarization curves. To display the microstructure scanning electron microscopy was used in the channeling contrast mode instead of etching. Furthermore the chemical composition of the as-prepared ceramic could be identified with energy dispersive x-ray spectroscopy.

## Dielectric relaxations and polarons in $\text{Sn}_2\text{P}_2\text{S}_6$ ferroelectrics

A. Dziaugys<sup>1</sup>, J. Banys<sup>1</sup>, M. Medulych<sup>2</sup>, A. Molnar<sup>2</sup>, Yu. Vysochanskii<sup>2</sup>

<sup>1</sup> Faculty of Physics, Vilnius University, Lithuania

<sup>2</sup> Institute of Physics and Chemistry of Solid State, Uzhgorod University, Ukraine

Email: andrius.dziaugys@ff.vu.lt

For  $\text{Sn}_2\text{P}_2\text{S}_6$  ferroelectrics the second order phase transition at  $T_0 \approx 337$  K is related with nonlinear interaction of the fully symmetrical and soft polar optic modes. The stereoactivity of tin cations lone pair electrons determines the chemical bonds changes and charge transfer at transition into the ferroelectric phase [1,2]. Semiconductive properties of these crystals are determined by sulfur vacancies deep donor states and tin vacancies shallow acceptor states in the energy gap. The deep energy level of small electron polarons, which are selftrapped at  $\text{Sn}^+$  cations, and shallow energy levels of small hole polarons that are trapped at  $\text{S}^-$  anions also induce the local states in the gap [3]. The dielectric spectroscopy for the temperature interval 20 – 380 K have been applied for studying of slow dynamics of the polaronic particles in by vapor transport and Bridgmann methods grown  $\text{Sn}_2\text{P}_2\text{S}_6$  crystals. The dielectric relaxation anomaly was found with dielectric losses maximum near 60 K at low frequencies. Also two losses peaks were observed in 160 – 260 K temperature range. Observed dielectric relaxation anomalies are explained by small hole polarons dynamics with donor-acceptor compensation processes in lattice with tin and sulfur vacancies.

1. Yu. M. Vysochanskii, T. Janssen, R. Currat, R. Folk, J. Banys, J. Grigas, V. Samulionis (Vilnius University Publishing House, Vilnius, 2006).
2. K. Rushchanskii, Yu. Vysochanskii, D. Strauch, Phys. Rev. Letters, 99, 207601 (2007).
3. Yu. Vysochanskii, A. Molnar, R. Yevych, K. Glukhov, M. Medulych, Ferroelectrics, 438, 55 (2012).

### Acknowledgment

We wish to acknowledge the support of the Research Council of Lithuania funding this work according to the project “Postdoctoral Fellowship Implementation in Lithuania”.

## Magnetostriction and magnetoelectric effect in intermetallic/relaxor/PVDF composites

Guzdek Piotr<sup>1</sup>

<sup>1</sup>Department of Microelectronics, Institute of Electron Technology, Cracow Division, Zablocie St. 39, 30-701 Cracow, Poland

Email: pguzdek@ite.waw.pl

Magnetostrictive and magnetoelectric materials, a class of smart materials, are drawing much attention due to their practical applications. Magnetostriction has been defined as an elastic strain causing a change in shape of material during magnetization. In the magnetic field magnetostrictive material reorientates its magnetic domains, so it causes physical length change in the material. Magnetoelectric effect is defined as an induced dielectric polarization under an applied magnetic field. In the past decade, smart materials have attracted increasing interest because of their practical applications in sensors, actuators, memory devices, transducers, filters, waveguides, switches, phase invertors

Magnetoelectric effect in bulk and multilayer structures consisting of intermetallic compounds as magnetostrictive phase and ferroelectric relaxors and PVDF as piezoelectric phase was investigated. This paper describes the synthesis and tape casting process for ferrimagnetic  $Tb_{0.27-x}Dy_{0.73-y}A_{x+y}Fe_2$  compounds ( $A = Y, Tb, Yb$ ) and ferroelectric  $Pb(Fe_{0.5}Ta_{0.5})O_3$ ,  $Pb(Fe_{0.5}Nb_{0.5})O_3$  relaxors. All the composites were characterized by scanning electron microscope observations and complex impedance analysis. Magnetostrictive and ferroelectric grains were distributed homogeneously in a PVDF matrix. Complex impedance and dielectric permittivity of bulk and layered composites were studied in a temperature range from  $-40$  to  $150^\circ\text{C}$  and frequency range  $10\text{ Hz} - 2\text{ MHz}$ . Magnetic hysteresis and magnetization were measured by a vibrating sample magnetometer (VSM) in an applied magnetic field up to  $85\text{ kOe}$  at temperature range from  $4\text{ K}$  to  $400\text{ K}$ . The magnetic hysteresis determined for composites are typical of a mixture of the soft magnetic material with a significant amount of the paramagnet. The bifurcation of ZFC-FC magnetizations observed for both composites implies spin-glass behavior. Magnetostriction measurements at room temperature were carried out using Strain Gauge Technique in range of static magnetic field ( $300\text{--}7200\text{ Oe}$ ). Magnetoelectric effect at room temperature was investigated as a function of static magnetic field ( $300\text{--}7200\text{ Oe}$ ) and frequency ( $10\text{ Hz}\text{--}10\text{ kHz}$ ) of sinusoidal modulation magnetic field ( $5\text{--}20\text{ Oe}$ ). Both types of composites exhibit a distinct magnetoelectric effect.

## High-Temperature Structural Transitions in $\text{YMn}_{1-x}\text{Ti}_x\text{O}_3$

M. Tomczyk<sup>1</sup>, P.M. Vilarinho<sup>1</sup>, V.V. Laguta<sup>2</sup>, I. Levin<sup>3</sup>

<sup>1</sup> Department of Ceramics and Glass Engineering, University of Aveiro, 3810-193 Aveiro, Portugal

<sup>2</sup> Institute of Physics AS CR, Cukrovarnicka 10, 162 53 Prague, Czech Republic

<sup>3</sup> Materials Measurement Science Division, NIST, Gaithersburg, MD 20899, USA

Email: paula.vilarinho@ua.pt.

$\text{YMnO}_3$ , which at ambient pressure crystallizes with a layered hexagonal structure, has attracted much interest because of its multiferroic properties<sup>302</sup>.  $\text{YMnO}_3$  undergoes two phase transitions: a non-polar to polar ( $P6_3/mmc$  to  $P6_3cm$ ) transition at 1273 K<sup>303</sup>, which is accompanied by tripling of the unit-cell volume, and a subtle, isosymmetric, ( $P6_3cm$  to  $P6_3cm$ ) transition at 920 K<sup>304</sup>. This lower temperature phase transition, the nature of which still remains uncertain, has been associated with the Curie temperature ( $T_C$ ) of  $\text{YMnO}_3$ . However, recent neutron diffraction studies of  $\text{YMnO}_3$ <sup>305</sup> suggested that the macroscopic polarization is non-zero even above  $T_C$  and drops abruptly below  $T_C$ . These results, which remained unmentioned in the literature, question our understanding of the ferroelectric transition in  $\text{YMnO}_3$ .

In the present study, we used variable-temperature X-ray and neutron diffraction to examine the effects of Ti substitutions in  $\text{YMn}_{1-x}\text{Ti}_x\text{O}_3$  ( $0 < x < 0.15$ ) solid solutions on the phase transitions in this system. The temperature of the high-temperature transition  $P6_3/mmc$ - $P6_3/cm$  decreases continuously as  $x$  increases. At lower temperatures (from 650 K to 800 K, depending on  $x$ ), we observed an anomalous behavior of the  $c$ -lattice parameter, which appears to be connected to an isosymmetric transition of the type seen in  $\text{YMnO}_3$ . In  $\text{YMnO}_3$ , structural parameters are independent of the sample atmosphere. By contrast, in  $\text{YMn}_{1-x}\text{Ti}_x\text{O}_3$ , the structural anomalies vary markedly with the atmosphere, suggesting strong effects of point defects induced by the substitution of Ti on the supposed structural transition. Apparently, the presence of point defects enhances the structural changes associated with this transition. In the talk, we will discuss our findings that provide new insights into the nature of structural transitions in  $\text{YMnO}_3$  and  $\text{Y}(\text{Mn,Ti})\text{O}_3$  solid solutions.

<sup>302</sup> W. Prellier, M.P. Singh, P. Murugvel, J. Phys.: Condens. Matter, vol.17, R803, 2005.

<sup>303</sup> K. Lukaszewicz, J. Karut-Kalicinska, Ferroelectrics, vol. 7, 81, 1974.

<sup>304</sup> I.G. Ismailzade, S.A. Kizhaev, Sov. Phys. Solid. State, vol.7, 236, 1965.

<sup>305</sup> A.S. Gibbs, K.S. Knight, P. Lightfoot, Phys. Rev. B, vol. 83, 184418, 2005.

---

## **Piezoelectric MEMS**

CLUB A

*Thursday, July 25 2013, 08:30 am - 10:00 am*

Chair: **Paul Muralt**  
*EPFL*



## 3D MEMS Piezoelectric Ultrasound Transducer Technology

Arman Hajati, Dimitre Latev, Deane Gardner

FUJIFILM Dimatix, Inc., Santa Clara, CA 95050 USA

Email: ahajati@fujifilm.com

Here we present a novel ultrasound transducer technology called Clarinet™<sup>306</sup> based on a combination of micromachined 3D dome-shaped piezoelectric resonators arranged in a unique flexible architecture.

As an alternative to bulk piezoelectric transducers, MEMS-based ultrasound transducers have recently emerged aiming to offer advantages such as increased bandwidth, flexible geometries, natural acoustic match with water, reduced voltage requirements, mixing of different resonant frequencies, and potential for integration with supporting electronic circuits. However, difficulties in fabricating reliable MEMS structures combined with various technical issues have prevented PMUT and CMUT technologies from becoming a viable and practical solution up to now.

In this paper we present CLARINET™ which can be seen as a monolithic integrated ultrasonic circuit manufactured by lithography with four main advantages over bulk piezoelectric transducers: cost, performance, customization, and miniaturization capability. Our proprietary high performance PZNT film is implemented in 3D dome-shaped structures which form the basic resonating cells. In a process similar to designing RFIC filters, adjustable frequency response is realized by mixing these basic cells and modifying the dimensions by lithography.

Exploiting a 5<sup>th</sup> order filter design, a 5MHz linear array designed, fabricated and tested and unique features such as high sensitivity (more than 100kPa/V), adjustable wide-bandwidth frequency response (greater than 55%), CMOS-compatible low transmit voltage (2V-20V), low electrical impedance (less than 50 Ohms), efficient electromechanical coupling (greater than 45%), and reliable monolithic fabrication are demonstrated. Updated testing results including the receiving sensitivity and the two-way pulse echo response will be presented for the first time. We envision that this technology can be

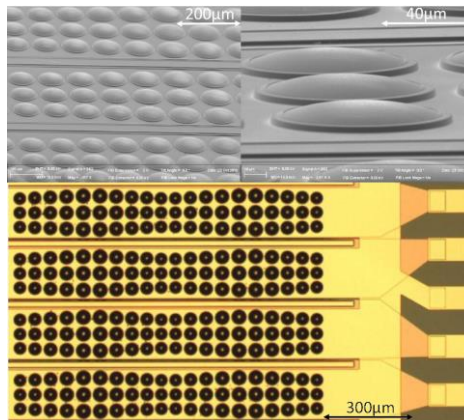


Fig. 95: Optical and SEM image of the device

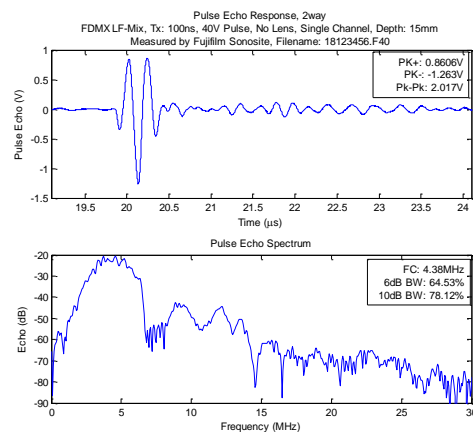


Fig. 2: Single channel pulse echo response

<sup>306</sup> A. Hajati et al, "Three-dimensional micro electromechanical system piezoelectric ultrasound transducer", Appl. Phys. Lett., vol. 101, 253101, 2012.

implemented as a desirable solution in high performance 3D/4D, low-power portable and in-vivo imaging systems.

## Ferroelectric Film Bulk Acoustic Wave Resonators for Liquid Viscosity Sensing

Andrei Vorobiev and Spartak Gevorgian

Department of Microtechnology and Nanoscience, Chalmers University of Technology,  
Gothenburg, Sweden

Email: andrei.vorobiev@chalmers.se

The piezoelectric film bulk acoustic wave (BAW) resonators have proven to be suitable for application as high accuracy and CMOS-compatible liquid viscosity sensors. However, the non-ferroelectric BAW sensors, usually operating in thickness shear mode, always have a longitudinal wave component generated as by-product due to inclination of polarization. The longitudinal contribution leads to a fluid turbulence at the device surface, which disturbs the conditions of the shear viscosity measurements. In the proposed paper we present, for the first time, the concept of the liquid viscosity sensing with the ferroelectric BAW resonators allowing for realization of truly shear displacement. The advantage of the ferroelectric based sensors is associated with the nature of the dc field induced piezoelectric effect. The induced polarization strictly coincides with the electric field. This allows for exclusively shear displacement and, hence, laminar shear of fluid at the resonator vertical side walls.

The sensors have been fabricated as the BAW solidly mounted resonators, based on the  $0.67\text{BiFeO}_3\text{-}0.33\text{BaTiO}_3$  multiferroic films<sup>307</sup>, operating at 4.2 GHz resonant frequency and 10 V dc bias. In the experiments the resonators have been covered by layers of liquids with different viscosity and thickness controlled to be about 250  $\mu\text{m}$ .

The measured resonator response has been analyzed using the proposed model of a harmonic oscillator damped by a viscous force in the form of the Stokes' law. It can be seen from Fig. 1 that the hyperbolic dependence of the resonator  $Q$ -factor, predicted by the model, agrees well with the measurements. The sensitivity of the resonator with the  $Q=200$  is ca  $10\text{ (mPa s)}^{-1}$ , which is high enough for the accurate characterization of water and other low viscosity liquids. Analysis indicates that the resonator effective mass is much larger than the added mass of the liquids, which explains the observed insensitivity of the  $Q$ -factor and resonance frequency to the liquid layer thickness. This makes the measurements simpler and more accurate since does not involve the liquid layer thickness and mass density.

Another advantage of the proposed sensors is possibility of simultaneous monitoring of the liquid temperature using inherent temperature dependence of the ferroelectric permittivity. This is a very useful feature, since the viscosity of many liquids is strongly temperature dependent. Estimates show that the temperature can be monitored with accuracy of ca 0.01 K.

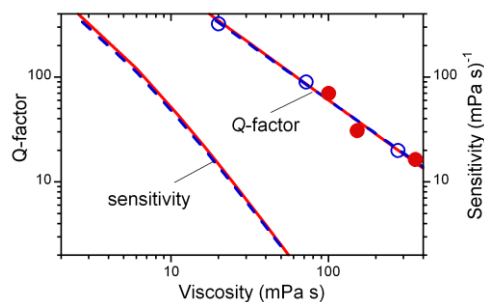


Fig. 96:  $Q$ -factors and sensitivity of the ferroelectric BAW vs. viscosity. The  $Q$ -factor dependence lines are hyperbolic fitting curves.

<sup>307</sup> A. Vorobiev, S. Gevorgian, N. Martirisyanyan, M. Löffler, and E. Olsson "Intrinsically tunable  $0.67\text{BiFeO}_3\text{-}0.33\text{BaTiO}_3$  thin film bulk acoustic wave resonators", Appl. Phys. Lett., vol. 101, p. 232903-5, 2012.



## New Human Machine Interface Devices Using a Piezoelectric Poly(L-lactic acid) Film

Masamichi Ando<sup>1,2</sup>, Hideki Kawamura<sup>1</sup>, Hiroaki .Kitada<sup>1</sup>, Takafumi .Inoue<sup>1</sup>, Yoshiro Tajitsu<sup>2</sup>

<sup>1</sup>Organic Film Devices Project/Murata Manufacturing Co. ,Ltd., Nagaokakyo-shi, Kyoto/Japan

<sup>2</sup>Graduate School of Engineering/Kansai University, Suita-shi, Osaka/Japan

Email: andoh@murata.co.jp

Poly(lactic acid) (PLA) has become widely known as an ecofriendly biomass polymer. The lactic acid monomer has an asymmetric carbon; thus, it has chirality. If the L-lactide is polymerized, then the PLA polymer is called an L-type PLA or a poly(L-lactic acid) (PLLA). If the polymer undergoes drawing or elongation, then they exhibit shear piezoelectricity<sup>308</sup>. In collaboration with Mitsui Chemicals, we have produced a stable PLLA film with a sufficient piezoelectric constant to be used for sensing applications<sup>309</sup>. The piezoelectric PLLA film does not have pyroelectricity, because it does not have intrinsic polarization. Therefore, even if the PLLA film is used for a human-machine interface (HMI), which operates by direct operation by hand, there is no incorrect detection due to heat.

It has been recognized that a capacitive-type touch panel (CTP) is a very useful HMI for a smart phone and a tablet type personal computer. The touch panel with a pressure recognition function has been desired for more often these days. The PLLA film is very suitable for a CTP as a pressure sensing film. Pressure due to the slight bending of the glass during touch screen applications can be detected accurately. Furthermore, because the PLLA has very high transparency, it is suitable for touch panel pressure sensing, in which transparency is required. Figure 1 shows the relationship between the load on the glass and the generated electric charge. The PLLA film is attached on the glass. The glass size is 110(L)×60(W)×0.5(T) mm. The PLLA film forming the electrode on both principal surfaces is 0.07 mm in thickness and has a piezoelectricity,  $d_{14} = 6.0 \text{ pC N}^{-1}$ . The four sides of the glass are attached to a case, approximately the size of a smart phone. Although there is some difference in the sensitivity due to the position of the applied pressure, the sensitivity can be equalized and linearized by combining it with position detection information. Figure 2 shows an example of multiple electrodes formed on the PLLA film, which consists of a pressure detection electrode and an electrode for the CTP. Additional electrode layers are not required with such a composition; thus, the resulting pressure detection touch panel is highly transparent.

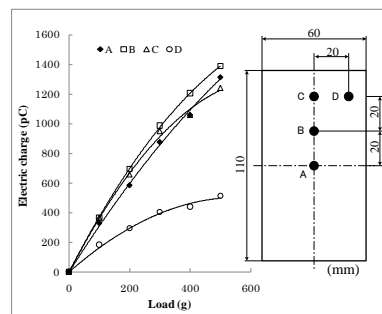


Fig.1: Relationship between the applied load and generated electric charge.

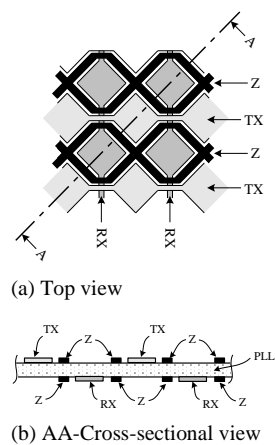


Fig.2: Multiple electrodes.

<sup>1</sup> E. Fukada: IEEE Trans. Dielectr. Electr. Insul. **13** (2006) 1110.

<sup>2</sup> M. Ando, H. Kawamura, K. Kageyama, and Y. Tajitsu: Jpn. J. Appl. Phys. **51** (2012) 09LD14



## Piezoelectric Microelectromechanical Systems (MEMS) Across Length Scales

R. Johnson, D. Wilke, C. Yeager, T. N. Jackson, and S. Trolier-McKinstry: Penn State  
P. Reid, V. Cotroneo, and D. Schwartz: SAO  
D. Newns, G. Martyna, T. Shaw, M. Copel, T. Theis: IBM

### *Abstract*

Piezoelectric thin films are of increasing interest in low voltage microelectromechanical systems (MEMS) for sensing, actuation, and energy harvesting. They also serve as model systems to study fundamental behavior in piezoelectrics. Piezoelectric MEMS devices range over a wide range of length scales. On the extreme upper end are large area devices for applications such as adaptive optics. In this case, the piezoelectric film can be used to produce local deformation of a mirror surface, in order to correct figure errors associated with fabrication of the component or to correct for atmospheric distortion. For example, should a mission such as Gen-X be flown, it would require up to 10,000 m<sup>2</sup> of actuatable optics in order to correct the figures of the nested hyperboloid reflecting segments. In this case, the “micro” in “microelectromechanical systems” is clearly a misnomer, although the fabrication techniques would involve conventional micromachining for patterning of the electrodes. Many piezoelectric MEMS devices are fabricated at intermediate length scales (tens of microns to 1 cm). Here, examples will be given of piezoelectric energy harvesting devices. We have recently demonstrated improvements in the energy harvesting figure of merit for the piezoelectric layer by factors of 4 – 10. Finally, piezoelectric MEMS are also attracting attention at a substantially smaller size scale (tens of nm) as a potential replacement for CMOS electronics. Examples of the materials choice as well as specific devices at all three of these length scales will also be discussed.

## A MEMS AlN transducer array for use as a cochlear implant

Katherine Knisely and Karl Grosh

Mechanical Engineering, University of Michigan, Ann Arbor, MI

Email: kknisely@umich.edu

Aluminum nitride (AlN) has emerged as an excellent material for a variety of MEMS applications because of its high electrical resistance, low dielectric loss, and high sound velocity. Recently, MEMS sensors using AlN in a bimorph cantilever configuration have been demonstrated with low noise floors and good sensitivity<sup>310</sup>. Because of its very low dielectric loss factor and relatively simple deposition process as a thin film, AlN is an excellent material for microphones. The cantilever configuration has many benefits, including a more linear response, control of the frequency response using simple changes to the beam geometry, and simple adaptation from microphone to hydrophone.

We present an array of AlN bimorph cantilevers, fabricated using MEMS batch processing techniques, with applications both as a hydrophone array and as a completely implantable cochlear implant (CI). A silicon backbone supports five 400 $\mu\text{m}$  wide, 5 $\mu\text{m}$  thick bimorph (Platinum/aluminum nitride (AlN) stack) cantilevers, each of which is designed to have a resonance, in water, that corresponds to its tonotopic location in the guinea pig cochlea (20-40kHz). A 1mm wide, 10 $\mu\text{m}$  thick parylene and gold ribbon cable extends 3cm from the probe to an electrode bay, where electrical connections to each cantilever are accessed. The frequency response of a cantilever in a viscous fluid is predicted using a modified Euler-Bernoulli equation that includes fluid loading and viscous damping<sup>311</sup>, and is measured in air using a laser vibrometer and in water using a calibrated underwater transducer pair.

Unlike traditional CIs, this probe is designed to transduce mechanical vibrations of the cochlear fluid into electrical signals that stimulate the auditory nerves without the use of an external sound processing unit. Vibrations in the cochlear fluid deflect the cantilevers, resulting in a potential forming on the outer electrode layers of the cantilever. The outer electrodes are in electrical contact with the ionic fluid of the cochlea, producing a current in the cochlear fluid that is passed to the auditory nerves. In this design the energy is locally sensed and converted into stimulation within the cochlea, therefore our design does not require the traditional signal processing unit, microphone, and transceiver that current CIs employ. Benefits of this design include lower power, smaller size, and lower latency when compared with current commercial CIs.

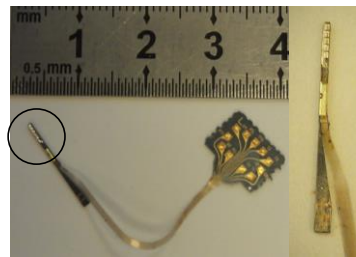


Fig. 97: The fabricated device. The cantilever array (left, circled, with a closeup on the right ) is connected to an electrode bay for external electrical monitoring by a flexible parylene-gold ribbon cable.

<sup>310</sup> R. Littrell and K. Grosh, *Journal of Microelectromechanical Systems* 21(2), 406 (2012).

<sup>311</sup> JE Sader. *Journal of Applied Physics*, 84:64–76, 1998.





---

## **Modeling: multiscale, first-principles,...**

CLUB B

*Thursday, July 25 2013, 08:30 am - 10:00 am*

Chair: **George Rossetti**  
*University of Connecticut*

## Point defects in $\text{LiNbO}_3$ from density functional theory using local and hybrid electron XC functionals

Yanlu Li, Simone Sanna, Wolf Gero Schmidt

Lehrstuhl für Theoretische Physik, Universität Paderborn, 33095 Paderborn, Germany

Email: liyanlu.cs@gmail.com

Lithium Niobate ( $\text{LiNbO}_3$ , LN) is a versatile material of great technological importance with many practical applications. Numerous experimental investigations suggest that defects, caused by its non-stoichiometry, critically affect many physical properties of LN. However, the precise defect structures and energetics are still under debate. This is due to the wealth of possible defects formed in a ternary compound and the charge compensation mechanisms required to achieve charge neutrality. Here, the defect species related to  $\text{Li}_2\text{O}$  deficiency are determined by density functional theory (DFT) in the framework of both generalized gradient approximation (GGA) and hybrid functionals (HSE06) to describe the electron exchange and correlation (XC).

The calculated electronic band gap of bulk LN is 5.21eV and 3.36eV within HSE06 and GGA, respectively. The HSE06 result agrees closely with earlier GW calculations<sup>312</sup>. Also the lattice parameters determined within HSE06 describe the experiment better than GGA results. Marked differences between local and hybrid XC functionals are found as well for the defect energies: HSE06 increases the Li and Nb vacancy ( $V_{\text{Li}}$  and  $V_{\text{Nb}}$ ) formation energies and decreases the Nb antisite ( $\text{Nb}_{\text{Li}}$ ) energy with respect to the GGA. Transition levels not detected in previous GGA calculations are observed, e.g., for  $V_{\text{Li}}$ . The charge state of  $V_{\text{Nb}}$  changes from 0 to -5 directly in both calculation schemes, showing a so-called *negative-U* effect. This behavior is quite different from previous reports<sup>313,314</sup>, however. Additionally,  $\text{Nb}_{\text{Li}}$  is less strongly bonded to  $V_{\text{Nb}}$  than  $V_{\text{Li}}$ . The  $\text{Nb}_{\text{Li}}-V_{\text{Nb}}$  binding energy increases by decreasing the magnitude of the defect pair charge. The present findings provide new insight into the energetics and microscopic structures of LN point defects, vital for its macroscopic properties.

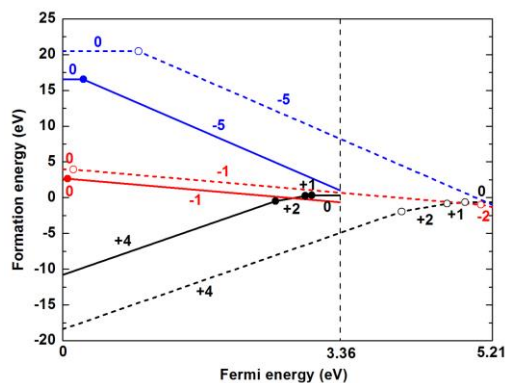


Fig. 98: Defect formation energies of  $\text{Nb}_{\text{Li}}$  (black lines),  $V_{\text{Li}}$  (red lines) and  $V_{\text{Nb}}$  (blue lines) as a function of Fermi energy calculated by DFT-GGA (solid lines) and HSE06 (dash lines). The Fermi energies range from 0 to 3.36eV by DFT and 0 to 5.21eV by HSE06.

<sup>312</sup> W. G. Schmidt, M. Albrecht, S. Wippermann, S. Blankenburg, E. Rauls, “ $\text{LiNbO}_3$  ground- and excited-state properties from first-principles calculations”, Phys. Rev. B, vol. 77, p. 035106, 2008.

<sup>313</sup> H. X. Xu, D. Lee, J. He, S. B. Sinnott, V. Gopalan, V. Dierolf, S. R. Phillpot, “Stability of intrinsic defects and defect clusters in  $\text{LiNbO}_3$  from density functional theory calculations”, Phys. Rev. B, vol. 78, p. 174103, 2008.

<sup>314</sup> Q. K. Li, B. Wang, C. H. Woo, H. Wang, R. Wang, “First-principles study on the formation energies of intrinsic defects in  $\text{LiNbO}_3$ ”, J. Phys. Chem. Solid, vol. 68, p. 1336-1340, 2007.

## First-principles study of defect and domain wall interactions in $\text{PbTiO}_3$

Anand Chandrasekaran<sup>1,2</sup>, Dragan Damjanovic<sup>2</sup>, Nava Setter<sup>2</sup> and Nicola Marzari<sup>1</sup>

<sup>1</sup>Laboratory of Theory and Simulation of Materials, EPFL, Lausanne, Switzerland

<sup>2</sup>Ceramic Laboratory, EPFL, Lausanne, Switzerland

Email: anand.chandrasekaran@epfl.ch

The properties of ferroelectric materials such as Lead Zirconate Titanate (PZT) are heavily influenced by the addition of dopants. These dopants lead to the formation of defects and defect associates which then interact with domain walls. In the case of iron doped materials, first principles calculations show the formation of defect associates involving the acceptor substitutional defect

and a charged oxygen vacancy. This defect associate shows a strong tendency to align in the direction of the bulk polarization (Fig. 1). Nudged elastic band calculations are used to determine the barrier energy for the hopping of oxygen vacancies around the acceptor dopant. It is shown that defect alignment is likely responsible for ageing phenomena in acceptor doped PZT. Calculations also reveal that lead and oxygen divacancies are capable of forming polar defect complexes which align with the bulk polarization. However, calculations on donor doped materials do not indicate the formation of polar defect complexes involving donor substitutional defects. The interaction of defects with 180 degree domain walls is also studied. It is observed that both isolated defects and defect associates are more stable at 180 degree domain wall. However, polar defect complexes show a highly asymmetric potential at the domain wall due to the interaction of the defect polarization with the bulk polarization. Fig. 2 depicts the movement of the domain wall across a defect. The relative pinning characteristics of different defects are then compared to develop an understanding of defect-domain wall interactions in both pure and doped  $\text{PbTiO}_3$ .

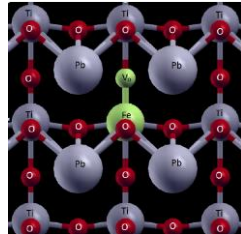


Fig. 1 Defect associate between iron and oxygen vacancy.

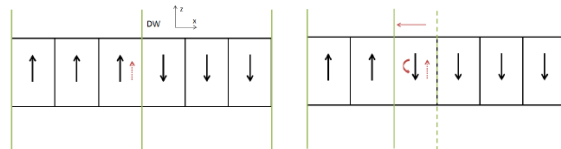


Fig. 2 Schematic of the movement of the domain wall in the presence of the defect. (a) Initial state of supercell with defect oriented in the direction of the bulk. (b) Final state with defect oriented in

the opposite direction of the bulk. This temporary disalignment is the driving force for ageing and loop pinching

# Self-Consistent Modeling of the Depolarization Field Evolution during Polarization Switching in Polycrystalline Ferroelectrics

Yuri A. Genenko, Jens Wehner, Heinz von Seggern

Institute of Materials Science/Technische Universität Darmstadt, Darmstadt, Germany

Email: genenko@mm.tu-darmstadt.de

The development of polarization during switching in thin ferroelectric films<sup>315,316</sup> as well as in bulk polycrystalline ferroelectrics<sup>317</sup> exhibits a slowing down at long poling times in contrast to the predictions of the classical Kolmogorov-Avrami-Ishibashi model with a single switching time  $\tau$ . This phenomenon is often interpreted as a dispersive polarization reversal characterized by a wide spectrum of switching times<sup>1-3</sup>. On the other hand, such interpretations typically ignore the feed-back effect of the depolarization field changing during polarization switching. Recently an attempt to account for this effect in a thin ferroelectric film was made by Lou in a self-consistent one-dimensional model<sup>318</sup>, which resulted in switching curves similar to those of the experiment<sup>2</sup>.

In the current communication it will be shown that identical results can be obtained by solving a single first-order differential equation which self-consistently describes the polarization switching<sup>319</sup> instead of using a system of 100 coupled differential equations<sup>4</sup>. Furthermore, by combining this equation with two-dimensional finite-element calculations of the depolarization field a model for the self-consistent analysis of the polarization response in bulk disordered ferroelectrics accounting for both the statistical distribution of switching times and the feed-back effect of the depolarization fields was developed for the first time. The results are compared with previous statistical descriptions of disordered ferroelectric systems.

---

<sup>315</sup> A.K. Tagantsev, I. Stolichnov, N. Setter, J. S. Cross, M. Tsukada, "Non-Kolmogorov-Avrami switching kinetics in ferroelectric thin films", *Phys. Rev. B*, vol. 66, 214109, 2002.

<sup>316</sup> J.Y. Jo, H.S. Han, J.-G. Yoon, T.K. Song, S.-H. Kim, and T.W. Noh, "Domain switching kinetics in disordered ferroelectric thin films", *Phys. Rev. Lett.*, vol. 99, 267602, 2007.

<sup>317</sup> Y.A. Genenko, S. Zhukov, S.V. Yampolskii, J. Schüttrumpf, R. Dittmer, W. Jo, H. Kungl, M.J. Hoffmann, and H. von Seggern, "Universal polarization switching behavior of disordered ferroelectrics", *Adv. Funct. Mater.* vol. 22, p. 2058-2066, 2012.

<sup>318</sup> X.J. Lou, "Statistical switching kinetics of ferroelectrics", *J. Phys.: Condens. Matter*, vol. 21, 012207, 2009.

<sup>319</sup> H. von Seggern and G.F. Leal Ferreira, "Switching dynamics in poly(vinylidene fluoride) and copolymers", *Appl. Phys. Lett.*, vol. 83, p. 3353-3355, 2003.

## FBAR tuning from first principles and high-order electrostriction

Alexander Kvasov<sup>1</sup>, Alexander Tagantsev<sup>1</sup>

<sup>1</sup>Ceramics Laboratory, École Polytechnique Fédérale de Lausanne, Lausanne, Switzerland

Email: alexander.kvasov@epfl.ch

Tunable thin film bulk acoustic wave resonators (TFBARs) based on  $\text{Ba}_x\text{Sr}_{1-x}\text{TiO}_3$  (BST) thin films are considered for frequency agile applications due to the DC bias dependent parameters of the resonator. TFBARs seem to be a very attractive component for microwave applications since they offer possibilities to increase the functionality of telecommunication systems. At the same time, for practical application as tunable microwave filters simultaneous tuning of resonance and antiresonance frequencies is highly desired.

In [1] it was demonstrated that, for TFBAR antiresonance frequency  $f_{AR}$  tuning, it is important to take into account nonlinear electrostriction  $m_{111}$  ( $F = \dots - \frac{m_{111}}{2} P_1^2 u_1^2 + \dots$ ) which being traditionally neglected [2] is unknown experimentally.

In this work  $m_{111}$  was calculated for the first time using *ab initio* methods for BST (Table I). To improve the reliability of the obtained results we used two different packages: Vienna Ab-initio Simulation Package (VASP) and Quantum ESPRESSO (QE).

$m_{111}, 10^{11} \frac{m}{F}$	VASP	QE
SrTiO <sub>3</sub> ( $x = 0$ )	-2.2±0.4	-3.0±0.4
BaTiO <sub>3</sub> ( $x = 1$ )	-2.8±0.4	-2.8±0.4

Table 1. Data obtained with the first principles calculations.  $m_{111}$  - nonlinear electrostriction coefficient.

It was established that for BST based TFBARs the antiresonance tuning is smaller than previously made estimations. Our calculations demonstrate the importance of taking into account both nonlinear electrostriction  $m_{111}$  and background permittivity  $\epsilon_b$  which are equally responsible for the tuning (Fig. 1).

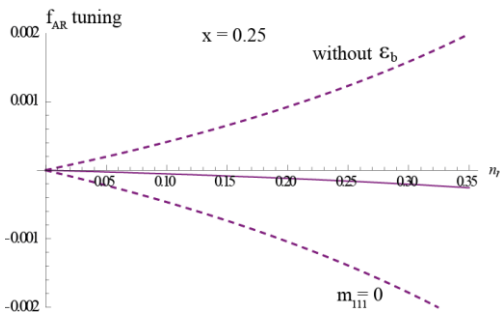


Figure 1. Modelled dependences of antiresonance frequency  $f_{AR}$  tuning on relative tunability  $n_r$  for the TFBAR using the [001]-oriented thin film of BST with  $x=0.25$ . Dashed lines show the antiresonance behaviour without taking into account background permittivity  $\epsilon_b$  or high-order electrostriction  $m_{111}$ . Relative tunability  $n_r$  is defined as:

$$n_r = \frac{\epsilon(0) - \epsilon(E^{DC})}{\epsilon(0)}$$

**Precursor dynamics, incipient ferroelectricity and huge anharmonicity in antiferroelectric lead zirconate  $\text{PbZrO}_3$**

Annette Bussmann-Holder<sup>1</sup>, Jae-Hyeon Ko<sup>2</sup>, Andrzej Majchrowski<sup>3</sup> and Krystian Roleder<sup>4</sup>

<sup>1</sup>Max Planck Institut für Festkörperforschung, Heisenbergstr. 1, 70569 Stuttgart, Germany

<sup>2</sup>Department of Physics, Hallym University, Hallymdaehakgil, Chuncheon, Gangwondo 200-702, Korea

<sup>3</sup>Military University of Technology, Warsaw, Poland and

<sup>4</sup>Institute of Physics, University of Silesia, ul. Uniwersytecka 4, 40-007 Katowice, Poland

To understand better the phase transition mechanism of  $\text{PbZrO}_3$  (PZO) the lattice dynamics of this antiferroelectric compound are investigated within the polarizability model, with emphasis on the cubic to orthorhombic phase transition. Similarly to ferroelectric transitions in  $\text{ABO}_3$  perovskites, polar dynamical ferroelectric type clusters develop and grow in size upon approaching  $T_c$  from the high temperature side and never form a homogeneous state. Simultaneously, elastic anomalies set in and compete with polar cluster dynamics. These unusual dynamics are responsible for precursor effects that drive the PZO lattice towards an incipient ferroelectric state. Comparison of the model calculations with temperature dependencies of elastic coefficients measured on PZO single crystals reveals striking similarity.



## Gauge Theory for Relaxor Ferroelectrics

Yousra Nahas, Igor Kornev

Laboratoire Propriétés et Modélisations des Solides, Ecole Centrale Paris, France

Email: [yousra.nahas@ecp.fr](mailto:yousra.nahas@ecp.fr), [igor.kornev@ecp.fr](mailto:igor.kornev@ecp.fr)

When examining the occurrence of the relaxor behavior, one of the main requirements appears to be lattice disorder<sup>320,321</sup>. Due to their heterovalency and their size mismatch, substitutional impurities and accompanying vacancies can act as sources of both random electric and strain fields. These defects can introduce substantial disorder, therefore destroying translational and rotational symmetries and hampering the onset of long-range order. Furthermore, the presence of an impurity on a given site can induce dipoles in its vicinity, resulting in correlated orientational degrees of freedom that cause symmetry breaking at the local scale<sup>1</sup>. A corollary feature of disorder in relaxors is thus the dualism between their local and average structures. The coexistence of locally preferred structures and an absent macroscopical phase change<sup>1,2</sup>, gives local symmetry back its preeminence.

We argue that these two features, namely the lattice disorder and the local vs global twofoldness, can be described within the *local gauge theory*<sup>322</sup>. This surmise stands on the belief that the effects of random local environments stemming from lattice disorder can be probed within local gauge transformations involving *local symmetry*, i.e. an extended symmetry allowing independent transformations at different points in space.

Starting with the first-principles-based effective Hamiltonian approach<sup>323</sup>, we formulate our model in a manifestly gauge-invariant manner, based upon continuous local symmetry and lattice gauge theory<sup>4</sup>. Technically, we focus on disordered ( $Pb_{1-x}La_x$ ) ( $Zr_{60}Ti_{40}$ )  $O_3$  solid solutions. The B-site disorder alone leads to the well known ferroelectric *PZT*, whereas the A-site disorder can lead to the relaxor behavior<sup>1</sup>. This latter disorder is seen as a source of a partially quenched random gauge field. The presented approach incorporates ferroelectric and elastic degrees of freedom, as well as gauge fields taking values in a Lie group and reproduces the main static features of *PLZT* systems (e.g. Fig.1).

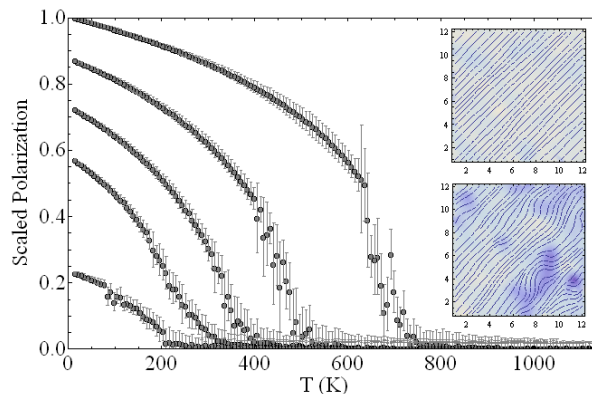


Fig. 99: Temperature dependence of the scaled polarization for (from up to down) the pure system *PZT* and for *PLZT* with 5%, 10%, 15% and 20% of  $La^{3+}$ . Upper and lower inserts show the streamlines associated to the dipole moments vector field at 50K in the cases of *PZT* and *PLZT* with 10% of  $La^{3+}$ , respectively.

<sup>320</sup> G. A. Samara, *Solid State Physics* **56** (2001) 239

<sup>321</sup> W. Kleeman, *Journal of materials science* **41** (2006) 129-136

<sup>322</sup> K. Moriyasu, *An elementary primer for gauge theory*, World Scientific, Singapore, 1983

<sup>323</sup> W. Zhong, D. Vanderbilt, K. Rabe, *Phys. Rev. Lett.* **73** (1994) 1861 ; *Phys. Rev. B* **52** (1995) 6301

This work is partially supported by the ERA. Net RUS grant, STProjects-133, NANO-C.

---

## **Local Phenomena**

CLUB C

*Thursday, July 25 2013, 08:30 am - 10:00 am*

Chair: **Yasuo Cho**  
*Tohoku University*

## Multiple bias-induced transitions and multiferroic states in half-doped $\text{La}_{0.5}\text{Ca}_{0.5}\text{MnO}_3$ manganite

Fábio. Figueiras<sup>1,2,3</sup>, Igor. K. Bdikin<sup>4</sup>, Vitor. S. Amaral<sup>1,2</sup>, Andrei. L. Kholkin<sup>2,5</sup>

<sup>1</sup> Physics' Department, University of Aveiro, 3810-193 Aveiro, Portugal

<sup>2</sup> CICECO, University of Aveiro, 3810-193 Aveiro, Portugal

<sup>3</sup> IFIMUP & IN, Physics & Astronomy Dep., Science Fac., Porto Univ., 4196-007 Porto, Portugal

<sup>4</sup> Mechanics' Eng. Department & TEMA, University of Aveiro, 3810-193 Aveiro, Portugal

<sup>5</sup> Materials' Eng. & Ceramics Department, University of Aveiro, 3810-193 Aveiro, Portugal

Email: ffigueiras@ua.pt

Phase separation, competition and nanoscale coexistence are ubiquitous characteristics of strongly correlated electronic complex oxides, such as mixed valence manganites. In  $\text{La}_{1-x}\text{Ca}_x\text{MnO}_{3+\delta}$  system phase diagram<sup>324</sup>, a delicate balance occurs near half doping ( $x \sim 0.5$ ) with a metallic ferromagnetic state for  $\text{Mn}^{4+}/\text{Mn}^{3+} \leq 1$ , whereas for  $\text{Mn}^{4+}/\text{Mn}^{3+} \geq 1$  brings an antiferromagnetic/charge-ordered insulator state. The nanoscopic electronic phase coexistence and inhomogeneity turns this material highly sensitive to external factors namely, ionic doping, temperature, electric/magnetic external fields and pressure. Further, the possibility of simultaneous presence of site- and bond-centered orbital ordering, can lead to a break of structural inversion symmetry allowing the conditions to the appearance of ferroelectricity<sup>325</sup>. This potentiates the emergence of at least three distinct electronic transport states mechanisms, by suitable stimulus. The propensity of manganites to tolerate local chemical/structural/charge inhomogeneities constitutes therefore a paradigmatic category of self-composite multiferroic system where metastable phases coexist in nearby nanoscale volumes. Previous works show clear bias-induced piezocontrast and local hysteresis loops could be investigated provided evidence of the existence of a local polar state with ferroelectric response at room temperature, even above charge order transition temperature<sup>326,327</sup>. In this framework we studied polycrystalline  $\text{La}_{0.5}\text{Ca}_{0.5}\text{MnO}_{3+\delta}$  combining Force Microscopy techniques (PFM, MFM, KFM, IV) to study the effects of nano-indentation and bias lithography leading to local modifications of electrochemical or electromechanical properties at the surface of these manganite systems<sup>328</sup>. The bias steering of phase transitions and lithographically setting single domain (~500 nm) electronic metastable phases was demonstrated at room temperature (poling voltages up to 30 V), inducing either enhance conductivity or insulating-ferroelectric behaviors. The enlarged possibilities near multiphase competition and nano coexistence (such as in half-doped manganite) opens a new pathway to achieve spatially localized multiferroic effects and artificial functionalities from a single base material having large potential for technology applications as data storage and processing.

<sup>324</sup> E. Dagotto, et al Physics Reports vol.344, p. 1-153, 2001.

<sup>325</sup> D. Efremov et al, Nature materials, 3, 853-856, 2004

<sup>326</sup> Ch. Jooss, et al, PNAS vol. 104, no. 34 ,p. 13597-13602, 2007 and

<sup>327</sup> R. F. Mamin, et al, App. Phys. Lett. Vol. 94, p. 222901, 2009.

<sup>328</sup> S. V. Kalilin et al., Mat. Today Vol. 11, no. 11, p. 16-27, 2008.

The work was partially supported by FCT grant SFRH/BPD/80663/2011, project PTDC/FIS/105416/2008 and PEst-C/CTM/LA0011/2011

## Peptide nanotubes as building blocks for nanosize transducers and sensors

Shima Dayarian<sup>1</sup>, Alisa Rudnitskaya<sup>2</sup>, Maciej Wojtas<sup>1</sup>, Svitlana Kopyl<sup>3</sup>, E. Bosne<sup>1</sup>, Ivonne

Delgadillo<sup>4</sup>, Andrei Kholkin<sup>1</sup>

<sup>1</sup> Department of Materials and Ceramic Eng. & CICECO, University of Aveiro, Aveiro, Portugal

<sup>2</sup> Chemistry Department & CESAM, University of Aveiro, Aveiro, Portugal

<sup>3</sup> Department of Mechanical Engineering & TEMA, University of Aveiro, Aveiro, Portugal

<sup>4</sup> Chemistry Department & QOPNA, University of Aveiro, Aveiro, Portugal

Email: kholkin@ua.com

Peptide nanotubes (PNT) based on the self-organization of the dipeptide diphenylalanine have received much attention as a promising nanostructure. Self-organizing nanotubes based on these particular dipeptides display unique biological and physical properties such as inherent biocompatibility, extraordinary thermal stability and organic solvent stability, high Young's modulus and bending stiffness. Recently, a strong piezoelectric activity was discovered in aromatic PNTs<sup>329</sup>. This functional property is very important as based on it a new generation of nanosize acoustic transducers including biosensors and sensors for biomedical ultrasound applications can be developed. For biosensing application, grafting of the receptor molecules on the PNT's is necessary to confer them sensitivity and selectivity to the particular analytes. Scaling down to nanosize i.e. by using single nanotube as acoustic resonator, can dramatically improve analytical performance of the sensors. Straightforward synthesis self-assembling and easy modification procedures due to the presence of the functional groups makes PNTs an interesting alternative to the inorganic nanostructures such as CNTs for chemical and biosensor fabrication. Moreover, a chip based on peptide nanotubes allows different types of electrical measures to be made such as impedance or piezoresonance, which could improve its analytical performance. Despite growing interest in PNT application, their integration into the microdevices and eventually  $\mu$ TAS remains a largely unresolved issue.

In this work we applied a new technology of PNT manipulation in an ac electric field. Using this method PNTs can be oriented to lay on the substrate between two gold electrodes. Morphology and resonance behaviour of the nanotubes deposited on the dielectrophoresis microchip were characterized using SEM, AFM and PFM. Further, the performance of peptide nanotubes for piezoelectric devices is analyzed in terms of their figures of merit for various applications.

---

<sup>329</sup> A.L.Kholkin et al, "Strong piezoelectricity in bioinspired peptide nanotubes". ACS Nano 4, 610, 2010

---

**PROBING COUPLED METAL-INSULATOR AND FERROIC TRANSITIONS FROM THE  
ATOMISTIC TO MESOSCOPIC SCALES: IN-SITU PLD-STM STUDY**

S.V. Kalinin, A. Tselev, Z. Gai, P. Maksymovych, M. Pan, and A.P. Baddorf

sergei2@ornl.gov

Oak Ridge National Laboratory, Oak Ridge, TN 37831

The coupling between electronic and ferroic behaviors has emerged as one of the most intriguing aspects of condensed matter physics, with examples including phase separation in complex oxides, metal-insulator transitions in ferroelastic oxides, and complex electronic ordering patterns in superconducting and charge-density wave materials. Both structural and electronic aspects of these behaviors are currently of interest for energy generation and storage applications, and are uniquely accessible through high-resolution probe-based studies. In this presentation, I will discuss several examples of high-resolution studies of the mechanisms of coupled electronic (metal-insulator, superconductive) and ferroic (ferro- and antiferroelastic, ferro and antiferroelectric) transitions from atomistic to mesoscopic scales enabled by combination of the *in-situ* Pulsed Laser Deposition growth with atomic resolution Scanning Tunneling Microscopy and Spectroscopy. Notably, for oxide these studies should explicitly address the possibility of vacancy dynamics and vacancy coupling to measured physical phenomena. On the mesoscopic level, we explored experimental signatures of the bias- and strain induced vacancy dynamics in simple oxides including NiO through the high-dimensional scanning probe microscopy measurements, and developed associated Ginzburg-Landau based theoretical description. On the atomistic level, we extended the applicability of local crystallographic mapping to scanning tunneling microscopy data, allowing for mapping surface electrochemistry and order parameter fields on the atomic level in manganites, ruthenates, and high-temperature superconductors.

This work was supported by the U.S. Department of Energy, Office of Basic Energy Sciences (BES), Materials Sciences and Engineering Division (SVK, PM, AT). ZG, MP and AB are supported by the Center for Nanophase Materials Sciences which is sponsored by the Scientific User Facilities Division, Office of Basic Energy Sciences, U.S. Department of Energy

## SKIN LAYERS ON MULTIFERROIC AND RELAXOR SINGLE CRYSTALS

Neus Domingo,<sup>1</sup> Jose Santiso,<sup>1</sup> Gustau Catalan<sup>2,3</sup>

<sup>1</sup> Oxide Nanoelectronics Group, Centre d'Investigació en Nanociència i Nanotecnologia, CIN2 (CSIC-ICN), Bellaterra, Spain

<sup>2</sup> Oxide Nanoelectronics Group, Institut Català de Nanociència (ICN), Bellaterra, Spain

<sup>3</sup> Institut Català de Recerca i Estudis Avançats, (ICREA) Catalunya, Spain.

Email: neus.domingo@cin2.es

Skin effects are commonly observed in different types of single crystals: in regions close to the surface, structural and functional properties different from that of the bulk can be observed. In this presentation we want to overview the main features that characterize skin layers observed in different types of ferroelectric single crystals, from multiferroic materials such as BiFeO<sub>3</sub> to different examples of relaxors such as PZN-PT.

Skin layer of BiFeO<sub>3</sub> has been analyzed with different techniques from surface impedance and grazing incidence X-ray diffraction to atomic force based techniques such as Piezoresponse Force Microscopy (PFM). It has been demonstrated that the skin shows a specific phase transition at  $T^* \sim 275$  °C below the bulk transition temperature, characteristic dielectric properties and a complex distribution of near-surface ferroelectric nanodomains that organize in a hierarchical metastructure on top of the existing bulk domains.

On the other hand, morphotropic phase boundary relaxors have been intensely studied for the last 15 years, on account of their giant electromechanical performance. The relaxation dynamics have traditionally been linked to the existence of both chemical and structural heterogeneity on a nanoscopic scale, with random bonds and random fields disrupting a true long-range ferroelectric ordering. For reasons that are as yet not understood, relaxor ferroelectrics display fairly thick surface layers (“skin layers”) with different symmetry compared to bulk. Thus, in morphotropic phase boundary materials such as PMN-PT, X-ray diffraction indicates that the symmetry of the surface layer is instead rhombohedral, and investigations by piezoresponse force microscopy show a labyrinthine 180 degree domain structure with out-of-plane polarization. In this presentation, we will show in closer detail the surface layer of these materials, and in particular the temperature dependence of its properties. Using a combination of temperature-dependent Piezoresponse force microscopy (PFM) and grazing incidence X-ray (XRD) we confirmed that the skin layer indeed has different symmetry and different domain structure as compared to the bulk, surviving to temperatures hundreds of degrees above the bulk, corroborating that skin layers have their own phase diagram quite independent from that of bulk.

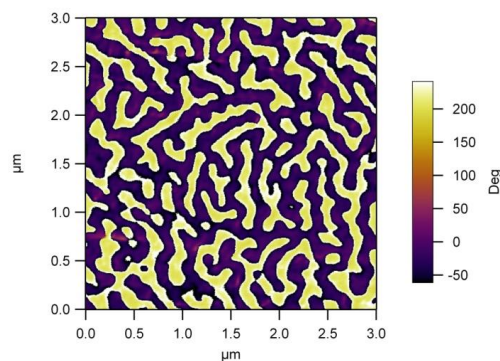


Fig. 100: Phase PFM image of the skin layer of PZN-PT measured at room temperature.



## Experimental and theoretical methods of accessing local correlations in modern ferroelectric materials

Marek Paściak<sup>1</sup>, T. Richard Welberry<sup>2</sup>, Jiri Hlinka<sup>1</sup>

<sup>1</sup>Institute of Physics, The Academy of Sciences of the Czech Republic, Prague, Czech Republic

<sup>2</sup>Research School of Chemistry, Australian National University, Canberra, Australia

Email: pasciak@fzu.cz

Modern ferroelectric materials are often based on chemically disordered compounds in which local strain and charge imbalance are used to enhance dielectric properties. Proper understanding of the atomic-scale phenomena is essential for material engineering and it constitutes a necessary first step of any multi-scale modelling.

In our work we explore theoretical and experimental methods of accessing local structure of modern ferroelectric materials. A lot of attention is paid to lead-based compounds such as  $\text{PbMg}_{1/3}\text{Nb}_{2/3}\text{O}_3$  (PMN) or  $\text{PbZr}_x\text{Ti}_{1-x}\text{O}_3$  (PZT) but we also include  $\text{BaTiO}_3$ -related relaxor materials. As far as the experiment is concerned we concentrate on diffraction methods which are unique in giving opportunity of getting into nanoscale structural correlations. These methods include xray and neutron diffuse scattering measurements for single crystal materials and pair distribution function studies for ceramic/powder samples. However, interpretation of these diffraction experiments is very rarely straightforward. Traditionally atomistic simulations (mostly using the Monte Carlo method) are helpful here. Therein, tuning of effective interactions between atoms allows assessing correlation mechanisms. With ever-growing computational power more sophisticated models, e.g. ab-initio based inter-atomic potentials, can be used for direct interpretation of diffuse scattering<sup>330</sup>. Working in a real space with trustworthy potentials has also an advantage of providing a direct access into mechanisms that drive the relationship between chemical disorder/short-range order and polar correlations.

The other important issue is related to distinguishing dynamic and static phenomena. While neutron inelastic scattering can give some insight into the time-scale of short-range ordered clusters (nanoregions), molecular dynamics method (either classical or first principles) is suitable for

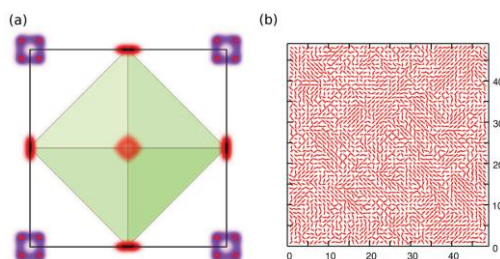


Fig. 101: Local structure of  $\text{PbMg}_{1/3}\text{Nb}_{2/3}\text{O}_3$  (PMN) – results of a molecular dynamics simulation at 10 K. (a) arrangements of atoms in a B-site centered perovskite unit cell with a characteristic disordered distribution of lead positions, (b) dipole arrangement on the  $xy$  plane of the simulated crystal.

<sup>330</sup> M. Paściak, T. R. Welberry, J. Kulda, M. Kempa and J. Hlinka, “Polar nanoregions and diffuse scattering in the relaxor ferroelectric  $\text{PbMg}_{1/3}\text{Nb}_{2/3}\text{O}_3$ ”, Phys. Rev. B, vol. 85, p. 224109, 2012.

interpretation of these results. Simulations at varied temperatures can help understanding development of correlations and slowing down processes across (usually diffuse) phase transitions.

## Spin-Phonon Coupling Role towards Ferroelectricity Rise in Magnetolectric Y-Substituted GdMnO<sub>3</sub>

R. Vilarinho<sup>1</sup>, A. Almeida<sup>1</sup>, P. B. Tavares<sup>2</sup> and J. Agostinho Moreira<sup>1</sup>

<sup>1</sup>IFIMUP and IN-Institute of Nanoscience and Nanotechnology, and Departamento de Física e Astronomia, Faculdade de Ciências da Universidade do Porto, Porto, Portugal.

<sup>2</sup>Centro de Química, Universidade de Trás-os-Montes e Alto Douro, Vila Real, Portugal.

Email: ruivilarinhosilva@gmail.com

Magnetolectric multiferroics are very interesting materials, as they exhibit ferromagnetism and ferroelectricity coupled together, opening the possibility of new technological devices. However, these kinds of materials are very scarce. Among the magnetolectric compounds, some orthorhombic rare-earth manganites, with distorted perovskite structures, and general formula  $RMnO_3$ , with  $R = \text{Eu to Dy}$ , are the most studied<sup>xxvi</sup>. In these compounds, ferroelectricity has been comprehended on the ground of the inverse Dzyaloshinskii-Moriya model, where the modulated spin ordering induces lattice deformations, yielding electric polarization. In this scope, the interplay between the magnetic and polar degrees of freedom involves spin-lattice and thus spin-phonon coupling. Spin-phonon coupling has been studied in several magnetolectric materials by using both Raman and infrared spectroscopies and have confirmed the significant role played by the Dzyaloshinskii-Moriya mechanism in determining their phase diagrams<sup>xxvii</sup>. Although an extensive study, the origin of magnetically induced ferroelectricity is not yet fully understood.

In this work, we present a detailed characterization of magnetic, dielectric and thermodynamic properties, as well as the study of lattice dynamics at low temperatures of the system  $Gd_{1-x}Y_xMnO_3$ , with  $x = 0$  to  $0.4$ . The substitution of the  $Gd^{3+}$  ion by the smaller  $Y^{3+}$  ion enables us to control the unit cell distortion, involving a complex set of geometrical changes, where two of them stand-up: Jahn-Teller and tilt of  $MnO_6$  octahedra, occurring alternately in opposite directions along the crystallographic  $c$ -direction, if  $Pbnm$  notation is used. These distortions, characterized by the bonds connecting  $Mn^{3+}$  and octahedral oxygen ions, highly depend on the effective size of the  $R$  ion ( $r_R$ ). The great advantage of this solid solution is that by increasing the substitution ratio only the effect of geometrical mechanisms, and thus the magnetic exchange integrals, is expected to influence its phase diagram, enabling to establish the role of spin-phonon coupling in tailoring the nature and number of different phases<sup>xxviii</sup>.

The magnetolectric effect is evidenced by the anomalous behavior of the dielectric constant through the magnetic phase transition. Inversion polarization measurements are in favor for non-linear polar effects, which yields the emergence of ferroelectricity induced by A-site substitution and magnetic field. The temperature dependence of the Raman active modes of the  $MnO_6$  units has revealed either a positive or negative shift regarding the pure anharmonic temperature dependence of the phonon frequency, which can be understood in terms of competitive ferromagnetic and antiferromagnetic interactions, strongly dependent on Y concentration. The relation between spin-spin correlation function and anomalous Raman mode frequency behavior is evidenced enabling the determination of the spin-phonon coupling parameter.

---

## **Electrocaloric Materials and Devices**

CLUB A

*Thursday, July 25 2013, 10:30 am - 12:00 pm*

Chair: **Stanislav Kamba**  
*Institute of Physics, Academy of Sciences of the Czech Republic*

## Influence of Electrical and Mechanical Boundary Conditions on the Electrocaloric Properties of Ferroelectric Thin Films

George A. Rossetti Jr.<sup>1</sup>, S. Pamir Alpay<sup>1</sup>

<sup>1</sup>Materials Science and Engineering, University of Connecticut, Storrs, CT, USA

Email: rossetti@ims.uconn.edu

The electrothermal (electrocaloric and pyroelectric) properties of ferroelectric thin films have many applications in active solid-state cooling and infrared sensing devices. The electrocaloric and pyroelectric responses describe converse effects, wherein an adiabatic change in temperature occurs in response to a change in applied electric field, or a change in the dielectric displacement occurs in response to a change in temperature. It has been demonstrated that some thin-film ferroelectrics can produce much larger electrothermal responses than their bulk counterparts. For on-chip applications, thin film ferroelectrics must be deposited on IC compatible substrates. The growth of ferroelectric films typically employs sputtering or metal-organic solution deposition techniques and the resultant ferroelectric film is usually polycrystalline. For such films, in-plane strains arise from thermal stresses due to the thermal expansion mismatch between the film and the substrate, and also from the self-strain of the paraelectric-ferroelectric phase transformation. A thermodynamic methodology is described and used to investigate the electrocaloric response of ferroelectric thin films under the influence of differing electrical and mechanical boundary conditions including bias and driving field, lateral clamping and misfit strain, and thermal stresses. The calculations are performed on perovskite ferroelectric materials including BaTiO<sub>3</sub>, PbTiO<sub>3</sub>, and the incipient ferroelectric SrTiO<sub>3</sub>. The results show how electrical and mechanical boundary conditions modify the electrocaloric properties for a given material composition. It is further shown that thermal stresses that develop during processing can have a significant influence on the electrothermal properties of polycrystalline ferroelectric films on IC-friendly substrates. Therefore, appropriate choices of the ferroelectric material, substrate, growth or annealing temperature, and electrode configuration can be used to control the electrocaloric response.

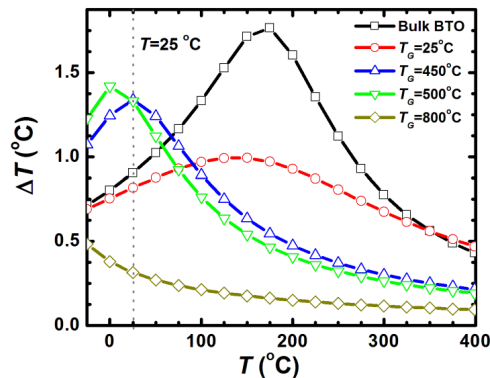


Fig. 102. Adiabatic temperature change,  $\Delta T$ , in bulk single crystal and (001) textured polycrystalline BaTiO<sub>3</sub> on Si as a function of temperature at different growth temperatures,  $T_G$ , under a bias field  $E_a=50$  kV/cm and field

## The electrocaloric efficiency of ceramic and polymer films

E. Defay<sup>1,2</sup>, S. Crossley<sup>2</sup>, S. Kar-Narayan<sup>2</sup>, X. Moya<sup>2</sup> and N. D. Mathur<sup>2</sup>

<sup>1</sup>CEA, LETI, Minatec Campus, Grenoble, France

<sup>2</sup>Department of Materials Science, University of Cambridge, Cambridge, UK

Email: [emmanuel.defay@cea.fr](mailto:emmanuel.defay@cea.fr); [ndm12@cam.ac.uk](mailto:ndm12@cam.ac.uk)

Voltage-driven thermal changes known as electrocaloric (EC) effects are large in ferroelectric thin films near the Curie temperature, where entropic electrical phase transitions may be reversibly driven by electric fields  $\Delta E$  that approach the high breakdown fields generically associated with thin films. The thermal changes in a single film are small, but macroscopic assemblies of ferroelectric films in the multilayer capacitor geometry have been proposed for cheap, environmentally friendly and energy efficient cooling applications. However, candidate EC materials have hitherto only been analysed in terms of EC performance, i.e. the change in isothermal entropy  $\Delta S$ , the isothermal heat  $Q$ , and the change in adiabatic temperature  $\Delta T$ . Surprisingly, the corresponding electrical work  $W$  that is done when charging and discharging the host EC capacitors has been neglected. Therefore we introduce here electrocaloric efficiency  $\eta$  to describe the ratio of reversible electrocaloric heat to reversible electrical work under isothermal conditions<sup>1</sup>. This figure of merit permits a comparison of EC materials that does not depend on details of any refrigeration cycle, i.e. the type of cycle, the hot and cold temperatures of the EC material, and the sink and load temperatures. We investigate in detail 350 nm thick films of the prototypical electrocaloric ceramic  $\text{PbZr}_{0.95}\text{Ti}_{0.05}\text{O}_3$  (PZT) with Pt electrodes<sup>2</sup>, and 0.4 - 2.0  $\mu\text{m}$ -thick films of the prototypical electrocaloric polymer poly(vinylidene fluoride-trifluoroethylene) (55/45 mol %) [P(VDF TrFE)] with Al electrodes<sup>3</sup>. For these films near their respective Curie temperatures, the electrical data that were used to predict large and nominally reversible EC effects, are used here to calculate the nominally reversible electrical work, yielding  $\eta = 3.0$  for the ceramic and  $\eta = 7.5$  for the polymer. We subsequently use the Landau theory of phase transitions to reveal the presence of non electrocaloric edge layers that increase the work, and to reveal the role of a previously observed complexity in the polymer phase transition of ref. 3. In a wider study, we find that ceramic and polymer films possess overlapping efficiencies, and therefore both classes of material may be attractive for applications despite previous indications. More generally, optimising  $\eta$  should in future guide the selection of electrocaloric, elastocaloric and magnetocaloric materials for novel cooling devices that are energy efficient.

<sup>1</sup> E. Defay, S. Crossley, S. Kar-Narayan, X. Moya and N. D. Mathur, *Adv. Mat.*, 2013

<sup>2</sup> A. S. Mischenko, Q. Zhang, J. F. Scott, R. W. Whatmore and N. D. Mathur, *Science*, 2006, 311, 1270.

<sup>3</sup> B. Neese, B. Chu, S.-G. Lu, Y. Wang, E. Furman and Q. M. Zhang, *Science*, 2008, 321, 821.

## High Temperature Piezoelectric and Electrocaloric Metrology

P. M. Weaver<sup>1</sup>, P. Woolliams<sup>1</sup>, T. Correia<sup>1</sup>, G. Bartl<sup>3</sup>, T. Quast<sup>3</sup>, T. Stevenson<sup>4</sup>, J. Hameury<sup>5</sup>, P. Klapetek<sup>6</sup>, M. Shpak<sup>7</sup>, T. Schmitz-Kempen<sup>8</sup>

<sup>1</sup>National Physical Laboratory, Teddington, UK

<sup>2</sup>Department, Institution/Company, City, State/Country

<sup>3</sup>Physikalisch-Technische Bundesanstalt (PTB), Braunschweig, Germany

<sup>4</sup>Institute for Materials Research, University of Leeds, Leeds, UK

<sup>5</sup>Laboratoire National de Métrologie et d'Essais (LNE), Trappes / France

<sup>6</sup>Department, Institution/Company, City, State/Country

<sup>7</sup>Thermal and Mass Metrology, Centre for Metrology and Accreditation, Espoo, Finland

<sup>8</sup>aixACCT Systems GmbH, Aachen, Germany

Email: paul.weaver@npl.co.uk

New piezoelectric materials capable of operating at elevated temperatures, are being developed to reduce energy consumption and improve efficiency and reliability in automotive, energy, process, electronics and medical industries. Degradation of material and electrical properties at high temperature means that these applications are typically limited to operating below 200 °C. The electrocaloric effect in ferroelectrics has strong potential as an efficient cooler for computer chips and domestic and industrial refrigeration. The ferroelectric materials used in these applications exhibit strong coupling between electrical, thermal and mechanical properties. Direct coupling provides the technological useful properties of piezoelectric and electrocaloric effects, but cross-coupling also needs to be taken into account. Examples include the dependence of thermal expansion (thermoelastic effect) on electrical conditions, and stress effects on electrocaloric cooling.

This presentation describes a pan-European effort to develop new metrological approaches to the challenges of measuring multifunctional coupling at temperatures up to 1000 °C. Non-contact approaches to measuring coupled piezoelectric and thermoelastic strain and direct electrocaloric measurements are described. To unravel the thermoelastic and electromechanical couplings, PTB conducts high-accuracy piezoelectric strain measurements within a temperature range from room temperature to 200°C. This is achieved by full-optical-field multi-wavelength interferometry. To extend the capabilities of the current setup, a heatable sample environment with high-voltage functionality is being developed. For aixACCT Systems as an industry partner within this project, extending the test capabilities of their commercial piezoelectric test systems to high temperatures is a main focus as well as standardization of piezoelectric testing under temperature and creating stable reference materials and samples for metrology. Initial results on high  $T_C$  materials of current technological interest, based on bismuth ferrite perovskite systems, are described.

This work has been performed in the framework of the joint research project “Metrology of electro-thermal coupling for new functional materials technology”, which is supported by the European Metrology Research Programme (EMRP), jointly funded by the EMRP participating countries within EURAMET and the European Union.

## Requirements to (Ba,Ca)(Zr,Ti)O<sub>3</sub> electrocaloric materials

Gunnar Suchaneck, Gerald Gerlach

Solid State Electronics Lab, TU Dresden, 01062 Dresden, Germany

Email: Gunnar.Suchaneck@tu-dresden.de

Heating and cooling are major power consumption technologies. For instance, the demand for heating and cooling is about half of the total energy demand in Europe, most of which is needed at low to medium temperatures (up to 250°C). Lead-free (Ba,Ca)(Zr,Ti)O<sub>3</sub> electrocaloric (EC) devices based on a reverse Brayton cycle (adiabatic polarization heating the sample, heat rejection to the thermal bath, adiabatic depolarization cooling the sample and heat absorption from the device) are expected to provide cooling power densities of 30 to 300 W/cm<sup>2</sup>.

The adiabatic temperature change above the Curie temperature  $T_C$  is determined mainly by the applied electric field which hence is a key parameter of an EC device. An approach to reach high breakdown field strengths of films in a bulk material is to use a multilayer capacitor structure with interdigitated metallic electrodes. They do not require a substrate, provide an efficient heat transfer between the EC elements and avoid arcing as a frequent failure mechanism. The main requirements to the EC layers are: (i) a maximum temperature coefficient  $d\epsilon/dT$  of dielectric permittivity ( $> 100 \text{ K}^{-1}$ ) (ii)  $T_C$  just below the operation temperature range, (iii) large dielectric strength ( $> 100 \text{ V}/\mu\text{m}$ ) and low electrical aging, (iv) low dielectric losses ( $< 2\%$ ), (v) sufficient thermal conductivity and large heat capacity of one EC element, and (vi), a positive slope of  $d\epsilon/dT$ , i.e.,  $d^2\epsilon/dT^2 > 0$ , in order to prevent EC element heating during the successive thermodynamic cycles.

The ternary BaTiO<sub>3</sub>-BaZrO<sub>3</sub>-CaTiO<sub>3</sub> phase diagram shows different regions of dielectric behavior (Fig. 1). The maximum  $d\epsilon/dT$  above  $T_C$  appears when the three phase transitions of BaTiO<sub>3</sub> (rhombohedral  $\Rightarrow$  orthorhombic  $\Rightarrow$  tetragonal  $\Rightarrow$  cubic) occur simultaneously at the same temperature. This coincides also with the known tricritical triple points of the cubic paraelectric phase, the ferroelectric rhombohedral and tetragonal phases in pseudobinary Ba(Ti<sub>1-x</sub>Zr<sub>x</sub>)O<sub>3</sub>-(Ba<sub>1-y</sub>Ca<sub>y</sub>)TiO<sub>3</sub> solid solutions.

This paper discusses the electric field dependence of the EC effect, the influence of the ferroelectric-paraelectric phase transition diffuseness on EC device operation as well as the influence of film composition, stoichiometry and acceptor doping on materials aging.

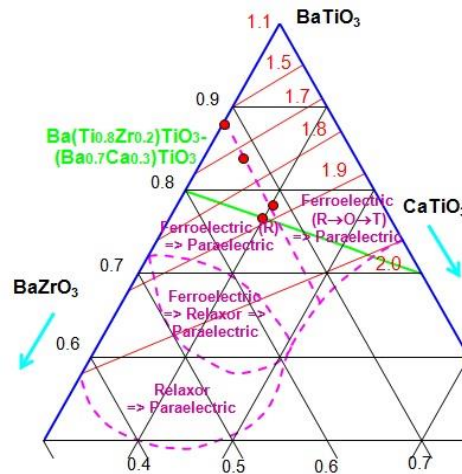


Fig. 103: BaTiO<sub>3</sub>-BaZrO<sub>3</sub>-CaTiO<sub>3</sub> ternary phase diagram, zones of different dielectric behavior<sup>331</sup>, tricritical points of Ba(Ti<sub>1-x</sub>Zr<sub>x</sub>)O<sub>3</sub>-(Ba<sub>1-y</sub>Ca<sub>y</sub>)TiO<sub>3</sub> solid solutions and diffuseness coefficient of the phase transition to the paraelectric state.

<sup>331</sup> J. Ravez, A. Simon, "Spontaneous transition from r to t", Ferroelectrics, vol. 240, p. 1579-1586, 2000.





## Scaling Laws for the Electrocaloric Effect in Alkaline Earth Titanates

A. Berenov<sup>1</sup>, F. Le Goupil<sup>1</sup>, N. Alford<sup>1</sup>

<sup>1</sup>Department of Materials, Imperial College London, London, UK

Email: a.berenov@imperial.ac.uk

Recently, solid state refrigeration based on the electrocaloric effect, EC, has attracted a great deal of attention due to the easy generation of large electric fields, high efficiency and relatively low cation variance<sup>332</sup>) in the perovskite structure on the EC behavior was evaluated.

A series of perovskites with the general formula  $Ba_{1-x-y}Sr_xCa_yTiO_3$  ( $0 \leq x \leq 0.35$ ,  $0 \leq y \leq 0.22$ ) were prepared. The dependence of  $T_C$  on both the average ionic radii and the cation variance was established. The studied specimens showed typical ferroelectric behavior with low leakage current.

Molar entropy change,  $\Delta S_{mol}$ , during the EC response was measured both directly by the modified DSC technique and indirectly from the P-E loops. A very good agreement between the values of  $\Delta S_{mol}$  measured by both techniques was obtained. The EC performance of the studied ceramics was evaluated as a function of temperature,  $T$ , and applied electric field,  $E$ . The maximum  $\Delta S_{mol}$  was observed close to the  $T_C$  and increased with the  $T_C$ . The EC response depended on the applied electric field as  $\Delta S_{mol} \sim E^n$ . The temperature dependence of  $n$  was similar to the one observed in magnetocaloric materials. Universal curves of the temperature dependence of  $\Delta S_{mol}$  (Fig 1) and  $n$  were constructed by analogy with magnetocaloric materials<sup>333</sup>. The parameters of the universal curves depended on the values of  $T_C$  and allowed complete description of the EC effect in (Ba,Sr,Ca)TiO<sub>3</sub> perovskites. The temperature changes observed in the studied alkaline earth titanates (e.g. 0.92 K at 20 °C and 44 kV/cm for Ba<sub>0.65</sub>Sr<sub>0.35</sub>TiO<sub>3</sub>) suggested that they are very promising EC materials which are environmentally friendly alternatives to current lead containing EC compounds (e.g. PMN-PT<sup>334</sup>).

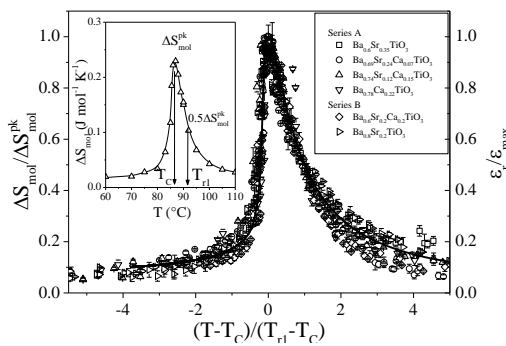


Fig. 104: Universal curves of the temperature dependence of  $\Delta S_{mol}$  for studied (Ba,Sr,Ca)TiO<sub>3</sub> samples when plotted on reduced axis. Inset shows EC data for Ba<sub>0.74</sub>Sr<sub>0.12</sub>Ca<sub>0.15</sub>TiO<sub>3</sub> at 10 kV/cm.

<sup>332</sup> L.M. Rodriguez-Martinez et al., "Cation disorder and size effects in magnetoresistive manganese oxide perovskites", Phys. Rev. B, Vol. 54, p. R15622-R 15625, 1996.

<sup>333</sup> V. Franco et al., "Scaling laws for the magnetocaloric effect in second order phase transitions: From physics to applications for the characterization of materials", Int. J. Refrig., Vol. 33, p. 465- 473, 2010.

<sup>334</sup> G. Sebald et al., "Electrocaloric and pyroelectric properties of 0.75Pb(Mg<sub>1/3</sub>Nb<sub>2/3</sub>)O<sub>3</sub>-0.25PbTiO<sub>3</sub> single crystals", J. Appl. Phys., Vol. 12, p. 124112, 2006

---

## **Modeling: LGD, Phase-Field,...**

CLUB B

*Thursday, July 25 2013, 10:30 am - 12:00 pm*

Chair: **To Be Announced**

## Thermodynamic Theory and Phase Field Model of Domain Structures in Ferroelectric Thin Layers and Bi-Layers

Andrei Artemev<sup>1</sup> and Alexander Roytburd<sup>2</sup>

<sup>1</sup>Department of Mechanical and Aerospace Engineering, Carleton University, Ottawa, Canada

<sup>2</sup>Department of Materials Science and Engineering, University of Maryland, College Park, USA

Email: aartemev@connect.carleton.ca

The domain structure in ferroelectric thin layers and bi-layer films formed by weak and strong ferroelectrics or by a ferroelectric and a dielectric was studied using the homogenized thermodynamics model and phase field simulations. The thermodynamic analysis predicted that the increase in the weak ferroelectric or dielectric layer thickness would result in the changes in the critical field of the single-domain (SD) to polydomain (PD) transition from negative to positive, and the hysteresis loop shape from simple rectangular to composite, consisting of two offset triangular loops describing the PD $\leftrightarrow$ SD transition hysteresis and a central loop describing the hysteresis of the PD state switching, with the central loop reduced to a zero-hysteresis  $P(E)$  curve in dielectric-ferroelectric bilayers, and in the reduction in the remnant polarization and coercive field.

The phase field simulations were performed for the a) bilayers consisting of either strong ferroelectric  $BaTiO_3$  and weak ferroelectric  $Ba_{0.3}Sr_{(1-0.3)}TiO_3$  or strong ferroelectric  $BaTiO_3$  and dielectric  $Ba_{0.2}Sr_{(1-0.2)}TiO_3$  with a high dielectric constant ( $\epsilon=950$ ), and b) thin layers of  $BaTiO_3$  with a low dielectric constant ( $\epsilon=8$ ) deadlayers. In all simulations the clamping effect of the  $SrTiO_3$  substrate was introduced using the renormalization of the Landau-Ginsburg-Devonshire free energy density function. The simulations were performed for the bilayers with different a) ratios of the layer thickness and b) absolute thickness of the  $BaTiO_3$  ferroelectric layer. In all simulations the clamping effect of the substrate resulted in the  $180^\circ$  domain structure formation. 1D and 3D ferroelectric models produced significantly different results; hence, it is important to use a full 3D ferroelectric model even for the simulation of films containing only  $180^\circ c$  domains due to clamping or poling effects.

The phase field simulations demonstrated that the stripe (or labyrinth) domain structure is produced in all films by the transformation from a paraelectric state at zero applied field conditions. The domain structure completely penetrates a weak ferroelectric or dielectric layer with a high dielectric constant; however, there is almost no penetration into low dielectric constant deadlayers. This domain structure transforms into columnar domains during poling, after which the PD state changes into the SD state. The  $P(E)$  loops obtained by the phase field modeling for strong ferroelectric-weak ferroelectric bilayers were similar to those predicted by the thermodynamic model. However, the loops obtained for strong ferroelectric - dielectric bilayers differed from the thermodynamic predictions. As a result of a specific behavior of the columnar domain structure produced by the SD to PD transition in the reversing applied field, they had a central loop with a large hysteresis effect instead of a zero-hysteresis curve connecting two offset triangular loops. Phase field modeling demonstrated the possibility of the hysteresis effect of the stripe to columnar domain morphology transition appearing as a result of a repulsive interaction between columnar domains. The simulation results and thermodynamic analysis demonstrate that in thin films the SD to PD

transition can go through the spinodal decomposition of the SD state, while in thick films it should develop by the nucleation and growth mechanism.

## Tracking the origin of dielectric response of simple domain patterns in BaTiO<sub>3</sub>

P. Marton, I. Rychetský, A. Klíč, and J. Hlinka

Department of dielectrics, Institute of Physics, Acad. Sci. Czech Rep., Praha, Czech Republic

Email: marton@fzu.cz

Domain walls in ferroelectric materials are known to have significant impact on the electromechanical response to an external loading. The exact role of domain walls in dielectric response is, nevertheless, complex and not yet fully understood. A domain wall can sweep macroscopically through the crystal, allowing polarization reversal at moderate electric-field amplitudes well below the coercive field of a monodomain sample. In reality, however, the mobility of walls is usually strongly limited, e.g. due to different types of pinning.

Even if macroscopically immobile, walls can still significantly alter the dielectric response. The effect may originate e.g. in domain-wall deflection from its original position, broadening, and other recently suggested mechanisms<sup>335336337338</sup>. There are as well simple situations where a domain wall only acts as an interface between the surrounding domains, and the domain geometry itself and its relation to the acting field are dominant.

In this contribution we provide analysis of a frequency-dependent dielectric response of several important domain patterns appearing in the tetragonal phase of prototype ferroelectric material BaTiO<sub>3</sub>. We make distinction between the response from a domain wall, and response from domain structure as such. Combination of the analytical algebraic derivations and numerical simulations within the Ginzburg-Landau-Devonshire phenomenological theory, complemented with the Finite-element-method<sup>339</sup> simulations of domain configuration with zero-thickness domain walls is employed.

---

<sup>335</sup> Rao and Wang, "Domain wall broadening mechanism for domain size effect of enhanced piezoelectricity in crystallographically engineered ferroelectric single crystals" *Appl. Phys. Lett.*, vol. 90, p. 041915, 2007.

<sup>336</sup> J. Hlinka, P. Ondrejko, and P. Marton, "The piezoelectric response of nanotwinned BaTiO<sub>3</sub>", *Nanotechnology*, vol. 20, p. 105709, 2009.

<sup>337</sup> V. Stepkova, P. Marton, and J. Hlinka, "Stress-induced phase transition in ferroelectric domain walls of BaTiO<sub>3</sub>", *J. Phys.: Condens. Matter*, vol. 24, p. 212201, 2013.

<sup>338</sup> T. Sluka, A. K. Taganstev, D. Damjanovic, M. Gureev, and N. Setter, "Enhanced electromechanical response of ferroelectrics due to charged domain walls", *Nature Communications*, vol. 3, p. 748, 2012.

<sup>339</sup> A. Klic and I. Rychetsky, "Dielectric Response of Arbitrary-Shaped Clusters Studied by the Finite Element Method", *Ferroelectrics*, vol. 427, p. 143, 2012.

## Nonlinear Extrinsic Permittivity and Piezoelectricity in Lead Titanate due to Domain Walls Pinning

Pavel Mokry<sup>1</sup>, Tomáš Sluka<sup>2</sup>, Alexander K. Tagantsev<sup>2</sup>

<sup>1</sup> Institute of Mechatronics and Computer Engineering, Technical University of Liberec  
Studentská 2, Liberec, Czech Republic, CZ-46117

<sup>2</sup> Ceramics Laboratory, Swiss Federal Institute of Technology (EPFL) Lausanne  
CH-1015 Lausanne, Switzerland

Email: pavel.mokry@tul.cz

It is known that the restoring force acting on a disequibrated domain wall is the key factor which controls macroscopic values of the extrinsic (i.e. domain wall) contributions to permittivity and piezoelectricity. Considering the bulk properties of perovskites, the main contribution to the restoring force comes from the interaction of domain walls with so called pinning centers (PCs) such as crystal lattice point defects or dislocations. It is clear that the number of PCs can be essentially controlled by composition of the material and the processing technology. In addition, there exist two types of domain wall movement between PCs: First, the planar wall passes through the PC and, second, the domain wall bends between PCs. It has been shown by analytical modeling<sup>340</sup> that each physical phenomenon that controls the restoring force on the domain wall introduces qualitatively different macroscopic features to the nonlinear dielectric and piezoelectric response. These features can be identified in experimental data.

The aforementioned issue has motivated the work presented in this paper. We have developed a thermodynamic Phase-Field-Model of 180° and 90° domain walls interacting with a PC (see Fig. 1) in lead titanate. We have performed a series of massive numerical computations, which resulted in macroscopic values of piezoelectric coefficients. The results of our computations indicated that both the extrinsic permittivity and piezoelectricity are generally nonlinear. We computed the linear and nonlinear contribution to the extrinsic permittivity and piezoelectricity as a function of PCs concentration. The results indicated a cubic relationship between linear and nonlinear permittivity for this type of extrinsic contribution, which is quite different from that of the lattice contribution derived from Landau theory. These results are in a good agreement with a simple but rather general thermodynamic model. We propose that such results can be used for the analysis of experimental data and for the characterization of lead-free ceramics and single crystals.

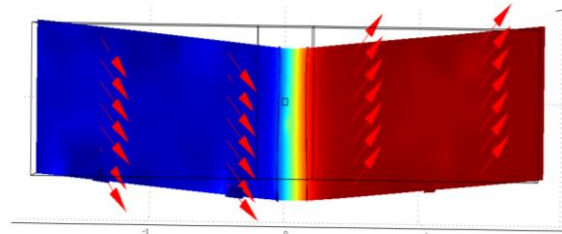


Fig. 105: Visualization of the 90° domain wall in lead titanate using Phase-Field-Model. When an external electric field is applied in the vertical direction, the domain wall is shifted. The domain wall shift contributes to the piezoelectricity.

<sup>340</sup> P. Mokry, "A method to study ageing of polydomain ferroelectrics using measurements of nonlinear permittivity", *Ferroelectrics*, vol. 375, p. 40-55, 2008.





## Influence of uniaxial stress on the ferroelectric-to-paraelectric phase transition in barium titanate

Florian Schader<sup>1</sup>, Emil Aulbach<sup>1</sup>, George A. Rossetti, Jr.<sup>2</sup>, and Kyle G. Webber<sup>1</sup>

<sup>1</sup>Institute of Materials Science, Technische Universität Darmstadt, 64287, Darmstadt, Germany

<sup>2</sup>Department of Materials Science and Engineering and Institute of Materials Science, University of Connecticut, Storrs, Connecticut 06269, USA

Email: schader@ceramics.tu-darmstadt.de

The perovskite compound barium titanate ( $\text{BaTiO}_3$ ) is an important material for discrete and multilayer capacitors because of its high relative dielectric permittivity. As an end member in lead-free ferroelectrics solutions, such as  $(1-x-y)(\text{Bi}_{1/2}\text{Na}_{1/2})\text{TiO}_3-x\text{BaTiO}_3-y(\text{K}_{0.5}\text{Na}_{0.5})\text{NbO}_3$ ,  $\text{BaTiO}_3$  has received renewed interest. These lead-free compositions can display large unipolar strains, attractive for actuator applications. In the mechanically unloaded state,  $\text{BaTiO}_3$  undergoes three well-known first order polymorphic phase transitions on cooling from high temperature, cubic (C)  $\rightarrow$  tetragonal (T)  $\rightarrow$  orthorhombic (O)  $\rightarrow$  rhombohedral (R). The ferroelectric-to-paraelectric (FE-PE) and inter-ferroelectric transition temperatures have been shown to depend on a number of extrinsic factors, including grain size, dopants, and the quality and form (single crystal, polycrystalline) of the specimen investigated, in addition to the electrical and mechanical boundary conditions.

In order to better understand the influence of mechanical boundary conditions on phase transitions in perovskite ferroelectrics, the effect of uniaxial compressive stress on unpoled  $\langle 001 \rangle_{\text{C}}$ -oriented single crystal and polycrystalline  $\text{BaTiO}_3$  has been investigated. Attention is restricted to the dielectric behavior near the C-T phase transition where the Landau theory is asymptotically accurate. The influence of uniaxial mechanical stress on the Curie point, Curie-Weiss temperature, and Curie constant were experimentally measured (Fig. 1). The results are analyzed using a 6<sup>th</sup> order Landau polynomial, where the dependence of the expansion coefficients on stress was determined. It is found that even at stresses below the coercive stress ( $< 30$  MPa), the quartic term in the Landau potential must display a linear dependence on stress in order to describe the experimental observations. The results are expected to be of particular importance in modeling the behavior of ferroelectric thin films, where in-plane strains are large enough to generate new phases and induce ferroelectricity, and for sensors, transducers, and actuators, where substantial mechanical preloads are often applied.

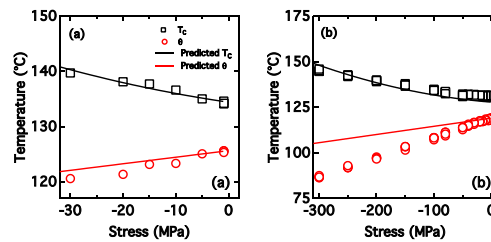


Fig. 106: Measured Curie point (square symbols) and Curie-Weiss temperature (circular symbols) for  $\langle 001 \rangle_{\text{C}}$ -oriented single crystal (a) and polycrystalline (b)  $\text{BaTiO}_3$  samples compared to predicted values as a function of applied uniaxial

## Finite Element based Phase Field Simulation on Interaction of Point Defects with Domain Structure in Ferroelectrics

Baixiang Xu, Yinan Zuo

Department of Materials and Earth Science, TU Darmstadt, Darmstadt, Germany

Email: xu@mfm.tu-darmstadt.de

Widely used in actuator and sensor technologies, piezoelectric ceramics are known to experience the performance degradation problem, which includes e.g. aging and fatigue phenomena. It has been well recognized that the interaction of point defects with domain structure plays significant role in aging and fatigue<sup>341</sup>. However, there are various theories regarding the exact interacting mechanisms. In this work numerical simulations based on a phase field model<sup>342</sup> are conducted to investigate the influence of point defects from two different aspects.

First of all, the free space charge may be available by considering that ferroelectrics can be semiconducting material particularly in the presence of defects. Simulation results, based on the phase field model and the semiconducting theory, will be shown for ferroelectric single crystal, for instance, BaTiO<sub>3</sub>, to demonstrate the influences of these space charges on the domain structures and the stability of charged domain walls. In particular, the stability of the charged domain wall will be demonstrated by using the calculated driving forces.

On the other hand, the defect dipoles, formed for instance by the oxygen vacancies with the cations, may play a very different role, as it is less mobile than the spontaneous polarization<sup>343</sup>. Phase field simulations by handling the defect dipole as additional eigenpolarization can enclose the effects of the defect dipoles on the domain structure and the hysteresis, see Fig.1.

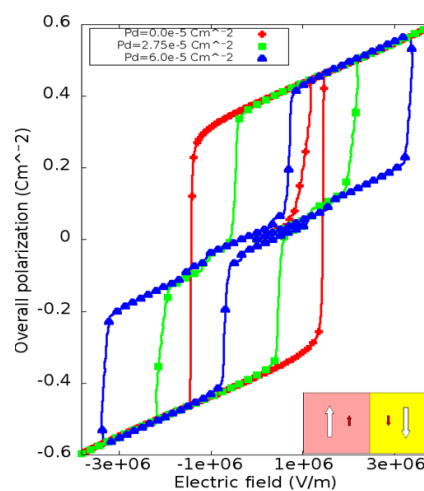


Fig. 107: The calculated double loop dielectric hysteresis, which is introduced by the defect dipole. The larger the magnitude of the defect dipole is, the wider the two loops are separated. As the electric field returns to zero, the spontaneous polarization tends to follow the direction of the defect polarization in favor of a minimization of total energy of the depolarization field (domain memory effect). Thus the overall polarization again becomes nearly zero. That may provide an explanation to the double loop effect.

<sup>341</sup> G. Arlt, H. Neumann, "Internal bias in ferroelectric ceramics: Origin and time dependence", *Ferroelectrics*, vol. 87, p. 109-120, 1988.

<sup>342</sup> B.X. Xu, D. Schrade, R. Müller, D. Gross, T. Granzow, J. Rödel. Phase field simulation and experimental investigation on electromechanical behavior of ferroelectrics. *ZAMM* 90 (7-8), 623- 632, 2010.

<sup>343</sup> X. Ren, "Large electric-field-induced strain in ferroelectric crystals by point mediated reversible domain switching", *Nature Materials*, 3 (2), 91-94, (2004).



## Piezoelectric response of twinned BaTiO<sub>3</sub>

P. Ondrejko<sup>1</sup>, J. Hlinka<sup>1</sup>, P. Marton<sup>1</sup>, M. Guennou<sup>1</sup>, A. Tagantsev<sup>2</sup>, N. Setter<sup>2</sup>

<sup>1</sup>Department of Dielectrics, Institute of Physics ASCR, Prague, Czech Republic

<sup>2</sup>Ceramics Laboratory, Swiss Federal Institute of Technology, Lausanne, Switzerland

Email: [ondrejko@fzu.cz](mailto:ondrejko@fzu.cz)

In the past decade, the high piezoelectric performance of single crystal perovskites was achieved by the procedure called domain-engineering. For example, Wada and Tsurumi<sup>344</sup> discovered that the both longitudinal and transverse piezoelectric coefficients are enhanced in engineered tetragonal BaTiO<sub>3</sub> with a high density of 90° domain walls. This discovery was an inspiration for many phase-field simulation studies, but the mechanism is still unclear. Nowadays, the role of charged 90° domain walls on piezoelectric properties is widely discussed<sup>345,3</sup>. However these studies require incorporation of compensation mechanisms in phase-field models, e.g. free charges and charged point defects.

In this contribution, longitudinal piezoelectric coefficient of a twinned ferroelectric perovskite material with an array of partially compensated head-to-head and tail-to-tail 90° domain walls has been studied by phase-field simulations in the framework of the Ginzburg-Landau-Devonshire model of BaTiO<sub>3</sub>. Our results extend the recent phase-field simulations of Li et al<sup>346</sup>, but also elucidate the mechanism responsible for the reported enhancement of the macroscopic piezoelectric coefficient.

In particular, we would like to show that the magnitude of the compensating charge at the domain wall and the decreasing domain wall distance are both promoting rotation of the static polarization vector within the body of adjacent domains. This polarization rotation drives the domain closer towards transition to an orthorhombic state. The proximity to this phase transition is in fact directly related to the enhancement of the properties. Our simulations and the theory also suggest that the same system with overcompensated charged walls may show a negative effective longitudinal coefficient (see Fig. 1). Obtained results can be used for quantitative estimates of piezoelectric properties of domain-engineered crystals.

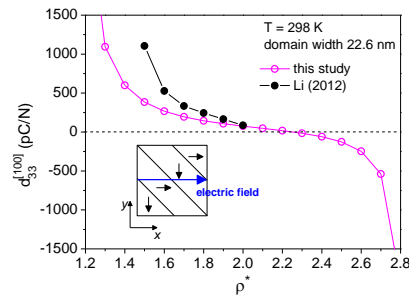


Fig. 108: Effective longitudinal piezoelectric coefficient along the [100] direction as a function of dimensionless compensation bound charge ( $\rho^*=2$  stands for the full compensation) in charged 90° domain walls. The inset shows the orientation of the applied electric field with respect to studied domain structure.

<sup>344</sup> S. Wada and T. Tsurumi, "Enhanced piezoelectricity of barium titanate single crystals with engineered domain configuration", *Br. Ceram. Trans.*, vol. 103, p. 93-96, 2004.

<sup>345</sup> T. Sluka, A. Tagantsev, D. Damjanovic, M. Gureev, and N. Setter, "Enhanced electromechanical response of ferroelectrics due to charged domain walls", *Nature Communications*, vol. 3, p. 748, 2012.

<sup>346</sup> Z. Li, H. Wu, and W. Cao, "Piezoelectric response of charged non-180° domain walls in ferroelectric ceramics", *J. Appl. Phys.*, vol. 111, p. 024106, 2012.

---

## **Les Bowen Memorial Session on Transducer Materials and Devices**

CLUB C

*Thursday, July 25 2013, 10:30 am - 12:00 pm*

Chair: **Ahmad Safari**  
*Rutgers University*

## Advanced, Broadband High Performance Piezocomposite Transducers

Brian Pazol, Timothy Mudarri, Joseph Aghia and Constance Ursch

Materials Systems Inc., Littleton, Massachusetts, USA 01460

Email: bpazol@matsysinc.com

Piezocomposites are a widely known form of piezoelectric material with proven advantages over conventional monolithic piezoelectric ceramics. Transducers made with piezocomposite (a two phased material consisting of piezoceramic and polymer) are naturally broadband (up to 80% fractional bandwidth), have high sensitivity (up to 10 dB more than solid ceramic transducers) and can be made in cost effective large sheets.

Materials Systems Inc. (MSI) utilizes a low cost injection molding technique<sup>1</sup> that allows large areas to be made by tiling ceramic preforms (Fig. 1) into large areas at a reasonable cost. Because a significant amount (60% to 85%) of the material is polymer, piezocomposite transducers can be much lighter in weight. There is a large design space that allows better transducer optimization by adjusting the matrix material, active material (PZT in most cases) and the ratio of active to inactive material (volume fraction). The material is conformable and can be shaped to match the curvature of a small vehicle. Piezocomposites have the added benefit of being extremely durable and have demonstrated survivability against explosive shock.

A brief overview and history of MSI's injection molding process will be presented. Several practical transducer examples that exploit the unique properties of piezocomposite will be discussed along with measured results. These include its ability to be curved into unusual shapes to tailor the beam pattern for special applications, broadband response for clutter rejection and lightweight designs for unmanned vehicles. In addition, the incorporation of second generation single crystal materials into piezocomposites and their potential in future sonar systems will be discussed.

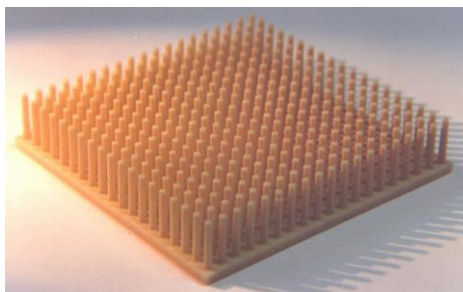


Fig. 1: Photograph of a 50 mm x 50 mm injection molded ceramic preform used to make 1-3 piezocomposite.

<sup>1</sup> L. J. Bowen and K. W. French, "Fabrication of Piezocomposite Ceramic/Polymer Composites by Injection Molding," Proceedings of the 8<sup>th</sup> IEEE International Symposium on Applications of Ferroelectrics, pp. 160-163, 1992.

## Effect of Electric Bias Field and Pressure on PMN-PT Piezoelectric Single Crystals in Tonpilz transducers.

C. Granger<sup>1</sup>, J.C. Debus<sup>1</sup>, A.C. Hladky-Hennion<sup>1</sup>, T. Pastureaud<sup>2</sup>, M. Doisy<sup>2</sup>, M. Pham Thi<sup>3</sup>

<sup>1</sup>IEMN, UMR CNRS 8520, ISEN, 41 Boulevard Vauban, 59046 Lille, France

<sup>2</sup>THALES UNDERWATER SYSTEMS, 525 Route de Dolines, Sophia Antipolis, France

<sup>3</sup>THALES Research & Technology-France, RD 128, F-91767, Palaiseau cedex, France

Email: mai.phamthi@thalesgroup.com

PMN-PT single crystals in free standing mode exhibit high electric/piezoelectric constants and high coupling efficiency ( $k_{33} = 0.9$ ) but their physical constants depend strongly on temperature, stress and in particular their coercive electric field is low, about 200V/mm.

The properties of PMN PT single crystals are reversible up to 70°C before the first rhombohedral-tetragonal ferroelectric transition. The depolarized field, measured from resonance spectra versus electric bias field near 200V/mm, is consistent with the electric coercive field. Under axial pressure of 35MPa, the depolarized field is observed near 35V/mm.

Tonpilz acoustic transducers were built with PMN-PT single crystals ring stack in a standard 33 mode. Several prototypes of transducers with different numbers of rings, head- mass materials and mechanical bias were investigated. Application of a mechanical stress or an electrical bias to single crystal rings induces reversible phase transitions leading to better stability in the range of mechanical stress used in Tonpilz transducer. In water, the Tonpilz projector exhibits high sensitivity ( $S_v=137\text{dB}$ ) and large bandwidth between 10 and 29 kHz. With the application of an electric bias field (135V/mm) the sensitivity increases up to 145 dB and the maximum of bandwidth shifts toward low frequency (9kHz).

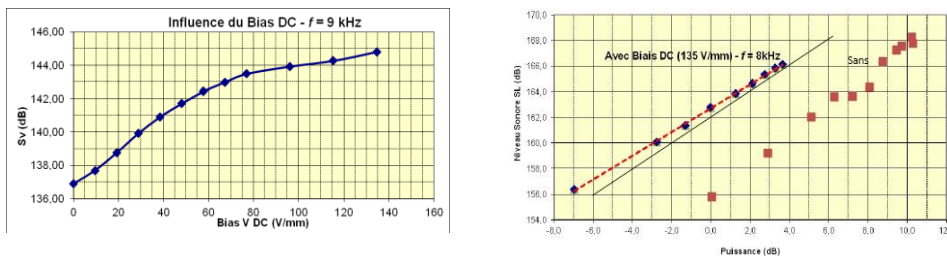


Figure: Sensitivity of Tonpilz transducer versus electric bias field (left) and power (right).

## Flexensional Composite Structure with PZN-PZT Crystals for Energy Harvesting Applications

Emre Tufekcioglu<sup>1</sup>, Aydin Dogan<sup>1</sup>

<sup>1</sup>Department of Materials Science and Engineering  
Faculty of Engineering  
Anadolu University, 26555, Eskisehir, TURKEY

Email: emretufekcioglu@gmail.com

The majority of piezoelectric energy harvesting research is based on structures operating in 31 (transverse) mode. For obtaining the highest level of energy from 31 mode, energy harvesters are constructed to produce the maximum strain on the transducer material, i.e. the bimorph transducers or monomorph patches adhered on beams. The high level of cyclic tensile stresses applied on the piezoelectric ceramic materials cause microcracks to form inside the material and eventually failure occurs.

In this study, the power harvesting capability of a flexensional piezo-composite structure with PZN-PZT relaxor-ferroelectric crystals as electro-active materials was evaluated. The flexensional piezo-composite is constantly kept under pre-stress so that the life-time of the ceramic is extended. The energy harvesting (EH) structure consists of a cymbal electromechanical transducer and an attached proof mass, all pre-stressed inside a rigid frame (Fig. 1). The power harvested was evaluated by vibrating the whole structure sinusoidally with varying frequencies and measuring the electrical outputs like voltage, current and power depending on the frequency, pre-stress, proof mass and resistive load. The results obtained from the PZN-PZT crystals were compared with the results obtained from soft PZT crystals.

Results show that the PH structure with PZN-PZT crystals is capable of producing 700  $\mu$ W of power at 4300 Hz and with a 5N of prestress which was measured across an electrical resistance of 100 k $\Omega$ . The measured power is more than two times the power generated by the structure with soft PZT crystals.

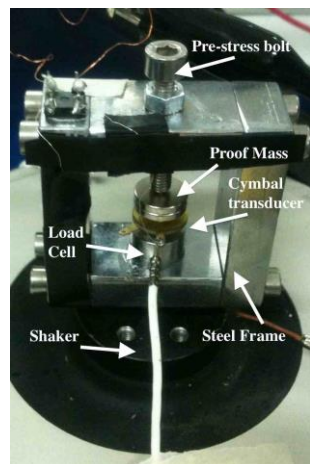




Fig. 1. The Energy Harvesting Structure

## Effect of Growth Conditions on Performance of 0.67BiFeO<sub>3</sub>-0.33BaTiO<sub>3</sub> Bulk Acoustic Wave Resonators

Andrei Vorobiev<sup>1</sup>, Spartak Gevorgian<sup>1</sup>, Markus Löffler<sup>2</sup>, Eva Olsson<sup>2</sup>

<sup>1</sup>Department of Microtechnology and Nanoscience, Chalmers University of Technology, Gothenburg, Sweden

<sup>2</sup>Department Applied Physics, Chalmers University of Technology, Gothenburg, Sweden

Email: andrei.vorobiev@chalmers.se

Intrinsically tunable 0.67BiFeO<sub>3</sub>-0.33BaTiO<sub>3</sub> (BF-BT) thin film bulk acoustic wave resonators with record high tunability of 4.4%, electromechanical coupling coefficient of 10% and rather high  $Q$ -factor of 200, at 4 GHz, have been demonstrated recently<sup>347</sup>. In the proposed contribution we disclose, for the first time, results of comprehensive studies of correlations between the growth conditions, microstructure and acoustic performance of the resonators, which allowed for optimization of the growth condition and achieving the device high performance. Particularly, it is shown that the pulsed laser deposition results in a *strong asymmetric distribution* of the BF-BT film grain size, surface roughness and texturing. The rms surface roughness decreases, from 30 nm to 12 nm in the beam-plume plane, leading to significant increase in the  $Q$ -factor, from 20 up to 200 (Fig. 1), due to reduction of loss associated with wave scattering at reflection from rough interface. We explain the phenomenon by an asymmetric angular energy distribution of the plume species caused by the laser beam-plume interaction.

The BF-BT film microstructure and surface morphology are analyzed by means of XRD, SEM, TEM and AFM. The observed distribution of the surface roughness is associated with variations in the lateral grain size and shape of the grain faceted tips due to the BF-BT film texturing. The films grown in the area affected by the beam-plume interaction are more (100) oriented in comparison with the on-axis films revealing more (110) grains.

The tunable performance of the BF-BT resonators is analyzed using the theory of dc field induced piezoelectric effect. The increase in the electromechanical coupling coefficient, from 6% to 10%, for the (100) oriented films, is associated with anisotropy of the linear electrostriction coefficient. Analysis of tunability of the parallel resonance frequency indicates also anisotropy of the nonlinear electrostriction coefficient. The higher and negative nonlinear electrostriction coefficient of the (100) oriented films limits the tunability of the series resonance frequency.

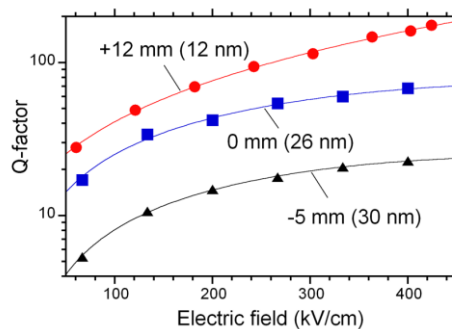


Fig. 109:  $Q$ -factors of the resonators with BF-BT films grown in different positions relative to the laser plume axis. Corresponding rms surface roughness is given in brackets.

<sup>347</sup> A. Vorobiev, S. Gevorgian, N. Martirisyanyan, M. Löffler, and E. Olsson "Intrinsically tunable 0.67BiFeO<sub>3</sub>-0.33BaTiO<sub>3</sub> thin film bulk acoustic wave resonators", Appl. Phys. Lett., vol. 101, p. 232903-5, 2012.

We assume that the observed effect of the laser beam-plume interaction is general and should be taken into account for any type of perovskite films grown by the pulsed laser deposition.

## Hysteresis-Free High-Temperature Bimorph Lithium Niobate Actuators Produced by Direct Bonding

Zorikhin Dmitry<sup>1,2</sup>, Baturin Ivan<sup>1,2</sup>, Mingaliev Eugene<sup>1,2</sup>, Udalov Artur<sup>1</sup>,  
Akhmatkhanov Andrey<sup>1,2</sup>, Zelenovskiy Pavel<sup>1</sup>, Shur Vladimir<sup>1,2</sup>

<sup>1</sup>Ferroelectric Laboratory, Ural Federal University, Ekaterinburg, Russia

<sup>2</sup>Labfer Ltd., Ekaterinburg, Russia

Email: [dmitry.zorikhin@labfer.usu.ru](mailto:dmitry.zorikhin@labfer.usu.ru)

Piezoelectric materials are widely used for precise positioning systems. Conventional piezoelectric materials such as PZT and lead-free ceramics have high piezoelectric coefficients but lack the temperature stability due to low Curie temperature ( $T_c$ ) and are prone to hysteresis and nonlinear behavior. The manufacturing of linear hysteresis-free piezoelectric actuators operable in a wide temperature range (from 77 to 900K) presents an actual technical challenge. Lithium niobate  $\text{LiNbO}_3$  (LN) single crystals can be used in a wide temperature range ( $T_c = 1200^\circ\text{C}$ ). Bimorph bending actuators based on bidomain LN crystals were realized by annealing close to  $T_c$  which leads to formation of domain wall in the middle of the wafer<sup>xxix,xxx</sup>. Present work is focused on the fabrication of bimorph LN actuators using wafer-scale direct bonding.

Based on the angular dependence of the piezoelectric coefficients the optimal wafer orientations for bimorph layers were selected. Commercially available wafers with  $Y+128^\circ$  and  $Y+41^\circ$  (rotation of  $Y+$  axis towards  $Z+$ ) cuts characterized by high absolute values of transverse piezoelectric coefficients (27.3 and 17 pC/N) and low shear coefficient (7.4 and 3.8 pC/N) were used.

Direct wafer bonding with the mirrored  $Y$  and  $Z$  axes was realized by wafer cleaning, surface activation and pre-bonding followed by annealing. To achieve particle and contamination free surfaces mechanical cleaning with lint-free tissues followed by ultrasonic clean in DI-water for 5 min was used. Activation of bonding surfaces was achieved by rinse in RCA-1 solution ( $\text{NH}_4\text{OH} : \text{H}_2\text{O}_2 : \text{H}_2\text{O}$ , 1:1:5) at  $80^\circ\text{C}$  for 20 minutes followed by DI-water spin-cleaning for 5 minutes and spin-drying by  $\text{N}_2$ . Such treatment resulted in reasonably clean surfaces with low contact angle which necessary for the hydrophilic bonding. Wafers were aligned and brought into contact. Slight pressure applied to the center had led to the spreading of the bonded area over the whole wafer. Subsequent annealing at  $300^\circ\text{C}$  for 6 hours resulted in the bond strength sufficient for the mechanical processing and actuator operation.

Actuators (10-20 mm in length and 0.5-1 mm thick) were fabricated by diamond blade cutting, polishing and sputter deposition of Ta electrodes. The displacement of the actuator during application of driving voltage was measured by the optical interferometry and atomic force microscopy. Linear hysteresis-free operation was demonstrated. Measured displacement values were close to the calculated ones. Temperature stability study of the actuator performance shows no degradation after treatment from 77 K up to 900 K. Measurements of the actuator characteristics in wide temperature range will be performed.

The equipment of the UCSU "Modern Nanotechnology", Institute of Natural Sciences, UrFU has been used. The research was made possible in part by RFBR (Grants 13-02-01391-a, 11-02-91066-CNRS-a), by Ministry of Education and Science (Contract 14.513.12.0006) and with the financial support of young scientists in terms of Ural Federal University development program.

---

## **LiTaO<sub>3</sub> and LiNbO<sub>3</sub>**

CLUB A

*Thursday, July 25 2013, 02:00 pm - 03:30 pm*

Chair: **Hong Wang**  
*Xi'an Jiaotong University*

# Nano-Domains and Their Related Phenomena in LiTaO<sub>3</sub> Single Crystal Studied by Using Scanning Nonlinear Dielectric Microscopy

Yasuo Cho<sup>1</sup>

<sup>1</sup>Reserach Institute of Electrical Communication, Tohoku University, Sendai, Japan

Email: yasuocho@riec.tohoku.ac.jp

Scanning nonlinear dielectric microscopy is a powerful technique for measuring nano-scale domain structure of ferroelectrics. In this paper, we present two topics, i.e. super higher order nonlinear dielectric spectroscopy studies on congruent LiTaO<sub>3</sub> (CLT) single crystal and conductions around nano-sized domain dots in CLT.

Recently, we have developed new method to measure a higher-order (second order) or super-higher-order (higher than second order) nonlinear dielectric response. Nonlinear dielectric constants  $\varepsilon(n)$ , with  $n=3, 4, 5, 6, \dots$  (in particular, we call  $\varepsilon(5)$ ,  $\varepsilon(6)$ ,  $\dots$ , super-higher-order nonlinear dielectric constants) are measured for high-resolution imaging of ferroelectrics<sup>1</sup>. Using this method, we found the marked enhancement of nonlinear dielectric “constants” when the applied tip-sample voltage exceeded a particular threshold value. This is due to domain nucleation activated by a huge electric field under the tip. Moreover, low frequencies (less than a few hundred Hz) did not enhance the nonlinearity. An effectively lower electric field caused by ion conduction in the sample under the tip is a possible reason for the frequency-dependent characteristics of the enhanced nonlinearity for the applied voltage. Next, we measured conduction current flowing around the nano-sized domain dots. When the size of nano-domain dots were relatively large ( $\sim 100$  nm in diameter. (Fig.2.(a))), a flowing current was detected at the domain wall just like reported in BFO and PZT (But, the width of current pass is much larger than that of domain wall.) However, surprisingly, when the domain size gets smaller than about 25nm (Fig.2(b)), the current flows on the whole area of the nano domain dot (not at the domain wall). Schottky-like rectifying behavior of current flow was observed even in nanometer sized domain dot. Precise experimental results will be presented in the meeting.

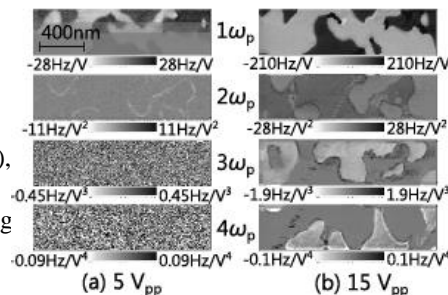


Fig. 110: Examples of acquired images of multidomain CLT. The amplitude of applied alternating voltage  $V_p$ s were (a)  $V_p = 5V_{pp}$  and (b)  $V_p = 15V_{pp}$ . In all images, the dark and bright contrasts represent the positive and negative signals, respectively. In the measurement of each  $V_p$ , the  $1\omega_p$ – $4\omega_p$  images were obtained by successively switching the order of demodulated signal, i.e., the

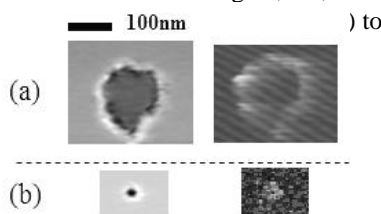


Fig.2: SNDM polarization images of nano-domain dots (Left) and conduction current images on the same dots (Right). (a) Large nano-domain dot, (b) Small nano-domain dot

---

<sup>1</sup> N. Chinone et al. "Lateral resolution improvement in scanning nonlinear dielectric microscopy by measuring super-higher-order nonlinear dielectric constants", *Appl. Phys.Lett.*, vol. 101,213112, 2012.

## Stabilizing mechanisms of strongly polar oxide surfaces: The LiNbO<sub>3</sub> Z-cut

S. Sanna,<sup>1</sup> S. Rode,<sup>2</sup> R. Hölscher,<sup>1</sup> S. Klassen,<sup>2</sup> K. Kobayashi,<sup>3</sup> H. Yamada,<sup>3</sup> W.G. Schmidt,<sup>1</sup> and A. Kühnle<sup>2,\*</sup>

(1) Lehrstuhl für Theoretische Physik, Universität Paderborn, Paderborn, Germany.

(2) Institut für Physikalische Chemie, Johannes Gutenberg-Universität Mainz, Mainz, Germany.

(3) Department of Electronic Science and Engineering, Kyoto University, Katsura, Nishikyo, Japan

e-mail: [simone.sanna@uni-paderborn.de](mailto:simone.sanna@uni-paderborn.de)

Atomic-resolution frequency modulation atomic force microscopy (FM-AFM) [1] and first-principles calculations [2] are employed to elucidate the mechanisms that stabilize strongly polar oxide surfaces [3]. Using lithium niobate Z-cut as a prototypical example [4,5], it is found that different scenarios occur at different temperatures. At room temperature and for slight annealing, an adsorbate layers remains on the surface and shields the polarization surface charge. At moderate temperatures (annealing between around 500 - 1000 K), the adsorbates desorb and an adatom-induced ( $\sqrt{7}\times\sqrt{7}$ ) R19.1° surface reconstruction forms. The adatoms provide extra surface charge that compensates the internal electric dipole moment. Finally, annealing at higher temperatures leads to an atomically smooth surface with a  $1\times 1$  translational periodicity.

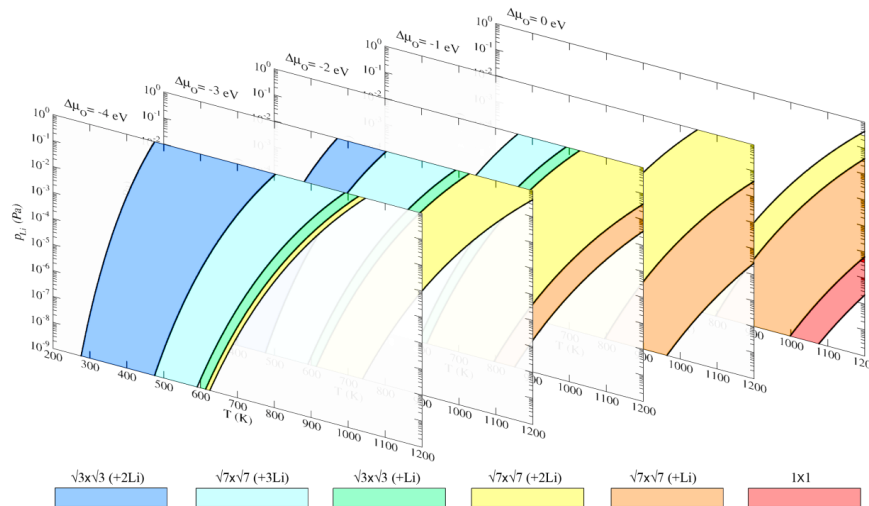


**Fig. 1:** Calculated phase diagram of the LN(0001) surface as a function of temperature and pressure

- [1] S. Rode, R. Hölscher, S. Sanna, S. Klassen, K. Kobayashi, H. Yamada, W.G. Schmidt and A. Kühnle, Phys. Rev. B **86**, 075468 (2012).
- [2] S. Sanna, R. Hölscher and W. G. Schmidt, Phys. Rev. B **86**, 205407 (2012).
- [3] Goniakowski, F. Finocchi, and C. Noguera, Rep. Prog. Phys. **71**, 016501 (2008).
- [4] S. Sanna and W. G. Schmidt, Phys Rev B **81**, 214116 (2010).



[5] S. V. Levchenko and A. M. Rappe, Phys. Rev. Lett. **100** (2008).

## Strain and chemical engineering in LiNbO<sub>3</sub> and LiTaO<sub>3</sub> thin films

A. Bartasyte<sup>1</sup>, V. Plausinaitiene<sup>2</sup>, A. Abrutis<sup>2</sup>, S. Margueron<sup>3</sup>, T. Murauskas<sup>2</sup>, P. Boulet<sup>1</sup>, V. Kubilius<sup>2</sup>, Z. Saltyte<sup>2</sup>

<sup>1</sup>Institute Jean Lamour, (UMR 7198) CNRS – Lorraine University, Nancy, France

<sup>2</sup>University of Vilnius, Dept. of General and Inorganic Chemistry, Vilnius, Lithuania

<sup>3</sup>Laboratoire Matériaux Optiques, Photonique et Systèmes, EA 4423, Lorraine University and Supelec, Metz, France

Email: [ausrine.bartasyte@univ-lorraine.fr](mailto:ausrine.bartasyte@univ-lorraine.fr)

LiNbO<sub>3</sub> and LiTaO<sub>3</sub> are the two of the most important crystals, being the equivalent in the field of optics, nonlinear optics and optoelectronics to silicon in electronics. Optically isotropic ferroelectric materials (for thermal sensing) or piezoelectric materials with reduced temperature coefficient of frequency (for acoustic delays lines/resonators) were obtained by chemical engineering of LiNbO<sub>3</sub> and LiTaO<sub>3</sub><sup>348,349</sup>. Thus, the studies about epitaxial ferroelectric LiNbO<sub>3</sub> and LiTaO<sub>3</sub> thin films are of great interest because of their potential application as miniaturized and integrated elements in static random access memories, high dielectric constant capacitors, acoustic delay lines, resonators, pyroelectric sensors, and optical waveguides. Although LiNbO<sub>3</sub> and LiTaO<sub>3</sub> films have been fabricated by different techniques, many electrical and electro-optical properties reported are not comparable for those of LiNbO<sub>3</sub> and LiTaO<sub>3</sub> single-crystals. The growth of high quality LiNbO<sub>3</sub>/LiTaO<sub>3</sub> films is far from being a routine due to a difficulty to estimate the phase composition and Li stoichiometry. Thus, the deposited films are hardly reproducible, often contain undesirable phases (for example, LiNb<sub>3</sub>O<sub>8</sub> or Li<sub>3</sub>NbO<sub>4</sub>) or are stoichiometrically inhomogeneous. This inhibits the applications of the materials in the thin film form.

In this work, the physical and structural properties of LiTaO<sub>3</sub> and LiNbO<sub>3</sub> thin films were tuned by changing their chemical composition and strain state. The possibility to change by several times the thermal expansion of LiNbO<sub>3</sub>/LiTaO<sub>3</sub> thin films by applying biaxial strain was observed. This opens new avenues for temperature compensated devices<sup>350</sup>. Moreover, the indirect methods, used to estimate Li concentration in the single crystals, cannot be applied directly due to the presence of strain, size effects or other defects in the films, which influences also the structural, optical and other physical properties. Thus, the indirect method for estimation of nonstoichiometry of LiNbO<sub>3</sub> and LiTaO<sub>3</sub> films, based on Curie temperature and dampings of Raman modes and taking into account secondary effects, was developed.

<sup>348</sup> A.M. Glazer, P.A. Thomas, N. Zhang, A. Bartasyte, D.S. Keeble, Patent WO/2011/158022, 2011.

<sup>349</sup> A. Bartasyte and O. Elmazria, Patent F12 52410, 2012.

<sup>350</sup> A. Bartasyte, V. Plausinaitiene, A. Abrutis, T. Murauskas, P. Boulet, S. Margueron, J. Gleize, S. Robert, V. Kubilius, and Z. Saltyte, Appl. Phys. Lett., 101, 122902, 2012.

## Study of $\text{LiNb}_{1-x}\text{Ta}_x\text{O}_3$ mixed crystals by Raman and IR spectroscopy

A. BartasYTE<sup>1,2</sup>, S. Margueron<sup>3</sup>, A.M. Glazer<sup>2</sup>, E. Simon<sup>4</sup>, J. Hlinka<sup>4</sup>, I. Gregora<sup>4</sup>, P.A. Thomas<sup>5</sup>

<sup>1</sup>Institute Jean Lamour, (UMR 7198) CNRS – Lorraine University, Nancy, France

<sup>2</sup>Department of Physics, Oxford University, Parks Road, Oxford OX1 3PU, UK

<sup>3</sup>Laboratoire Matériaux Optiques, Photonique et Systèmes, EA 4423, Lorraine University and Supelec, Metz, France

<sup>4</sup>Institute of Physics AS CR, Prague 8, Czech Republic

<sup>5</sup>Department of Physics, University of Warwick, Coventry, UK

Email: ausrine.bartasYTE@univ-lorraine.fr

Lithium niobate (LN) and lithium tantalate (LT) have been subject of intense studies because of their optical applications in industry. At room temperature LN and LT are isomorphous and ferroelectric, crystallizing in the space group R3c. The ferroelectric LN and LT crystal structure can be described in terms of polar displacements of the cations along the [0001] direction, with corner-linked oxygen octahedra tilted according to the system  $a\bar{a}a$ . Despite LT and LN structural similarity, these materials have different physical properties. Therefore,  $\text{LiNb}_{1-x}\text{Ta}_x\text{O}_3$  (LNTx) materials are of special interest because their properties can be tuned between those of LN and LT<sup>351</sup>. However, the fundamental properties of LNTx solid solutions have not yet been investigated sufficiently to date.

The dynamical properties of LN and LT have been intensively studied. The optical phonon frequencies, damping parameters, and intensities are of special interest in studies of phase transitions, symmetry, effect of pressure, stress, composition and heterogeneities in thin films, integrated structures, nano and bulk materials. It is essential to know the frequencies in calculations of dielectric constant, oblique modes, and electro-optic coefficients. There are numerous reports concerning optical phonons in LT and LN, studied by Raman and infrared spectroscopies<sup>352</sup>, neutron inelastic scattering and theoretically. Generally speaking, dynamical properties of different type of solid solutions have been extensively studied in literature. Nevertheless, there is only one report on the study of LNT solid-solution zone-centre phonons.<sup>353</sup> The authors studied only LNT0.9, and claimed that the Raman mode assignment is similar to that of LT. LNTx with other compositions of solid solutions and the change of zone-centre phonons with Ta/Nb ratio have never been studied.

In this work, all 26 optical phonons at  $\Gamma$  point of LNTx single crystals were identified in polarized spectra measured by IR and Raman spectroscopies. The effect of Nb replacement by Ta on the

<sup>351</sup> A. BartasYTE, A.M. Glazer, F. Wondre, D. Prabhakaran, P.A. Thomas, S. Huband, D.S. Keeble, and S. Margueron, *Mater. Chem. Phys.* 134, 728-735, 2012.

<sup>352</sup> S. Margueron, A. BartasYTE, A.M. Glazer, E. Simon, J. Hlinka, I. Gregora, and J. Gleize, *J. Appl. Phys.* 111, 104105, 2012.

<sup>353</sup> Ge, Y.-C. and C.-Z. Zhao. *J. Raman Spectroscopy*, **26**, 975-979, 1995.

wavenumbers, Raman efficiency coefficients, oblique mode dispersion and overlap matrix of zone-centre phonons over the whole composition range  $0 \leq x \leq 1$  was described.

## Charged Domain Wall Conductivity in Lithium Niobate and Lithium Tantalate Single Crystals

Baturin Ivan<sup>1,2</sup>, Chezganov Dmitry<sup>1</sup>, Esin Alexander<sup>1</sup>, Shur Vladimir<sup>1,2</sup>,  
Akhmatkhanov Andrey<sup>1,2</sup>, Ksenofontov Danila<sup>1</sup>

<sup>1</sup>Ferroelectric Laboratory, Ural Federal University, Ekaterinburg, Russia

<sup>2</sup>Labfer Ltd., Ekaterinburg, Russia

Email: [ivan@labfer.usu.ru](mailto:ivan@labfer.usu.ru)

Charged domain wall conductivity in lithium niobate (LN) and lithium tantalate (LT) single crystals and its relaxation after polarization reversal have been studied. Strong increase of the conductivity along the charged domain walls (CDW) was shown for the first time for head-to-head domain structure in ferroelectric semiconductor SbSI<sup>xxxix</sup>. Recently conduction properties of domain walls have attract a great attention with the progress in AFM characterization techniques. Electronic conductivity along ferroelectric domain walls in multiferroic BiFeO<sub>3</sub><sup>xxxii</sup> was observed using c-AFM measurements. Moreover, the reversible resistance transition caused by the polarization reversal<sup>xxxiii</sup> was found in ferroelectric MgO doped LN crystals, which is extensively used for domain-engineered QPM nonlinear optical applications. Recently, the domain wall conductivity in LN was studied by c-AFM in the presence of UV illumination<sup>xxxiv</sup>. The observed resistive change behavior is believed to be useful for memory applications<sup>2,3</sup>.

Z-cut LN and LT crystals with congruent and near stoichiometric composition as well as with MgO doping have been used for the present study. CDW were fabricated by polarization reversal by application of the electric field at elevated temperature (100-250°C) using metal electrodes deposited on both sides of z-cut samples<sup>xxxv</sup>. Strong increase of the conductivity current was observed during polarization reversal in all studied LN and LT crystals due to CDW formation. This strongly affects the domain patterning in MgO doped LN leading to decrease of applied field and sample fracture due to local heating. Absence of significant conductivity during polarization reversal using liquid electrodes was attributed to formation of the neutral walls only.

Partial switching with different fraction of the switched area followed by immediate current measurement was used to study the domain wall conductivity in details. It was shown that the domain wall conductivity essentially relaxes after partial polarization reversal following exponential decay behavior with the characteristics time of about tens of seconds. It was found that maximum value of conductivity current is proportional to the switched area, which determines the total length of CDW. The maximum value of the effective conductivity was found to be several orders of magnitude higher than for single domain sample.

The equipment of the UCSU “Modern Nanotechnology”, Institute of Natural Sciences, Urfu has been used. The research was made possible in part by RFBR (Grants 13-02-01391-a, 11-02-91066-CNRS-a), by Ministry of Education and Science (Contract 14.513.12.0006) and with the financial support of young scientists in terms of Ural Federal University development program.

---

## **Piezoelectrics**

CLUB B

*Thursday, July 25 2013, 02:00 pm - 03:30 pm*

Chair: **To Be Aannounced**

## Dielectric & Piezoelectric Enhancement of Potassium Niobate/Barium Titanate Nano-complex Ceramics with Parallel Configuration of Structure-gradient Regions

Satoshi Wada<sup>1</sup>, Hideto Kawashima<sup>1</sup>, Shintarou Ueno<sup>1</sup>, Kouichi Nakashima<sup>1</sup>, and

Nobuhiro Kumada<sup>1</sup>

<sup>1</sup>Material Science and Technology, Interdisciplinary Graduate School of Medical and Engineering, University of Yamanashi, 4-4-37 Takeda, Kofu, Yamanashi 400-8510, Japan

Email: [swada@yamanashi.ac.jp](mailto:swada@yamanashi.ac.jp)

Barium titanate (BaTiO<sub>3</sub>, BT) and potassium niobate (KNbO<sub>3</sub>, KN) (BT-KN) nano-structured ceramics with artificial morphotropic phase boundary (MPB) structure were successfully prepared by solvothermal method at temperatures below 230 °C. Especially, structure-gradient region (SGR) can be expected to enhance piezoelectric and dielectric properties, and then, to induce parallel configuration of SGR, new preparation method was proposed and developed in this study. As the results, KN epitaxial layer was successfully deposited on BT nanoparticle accumulation with necking structure between neighbored BT nanoparticles. Various characterizations confirmed that the BT-KN nano-structured ceramics exhibited BT/KN molar ratio of 1, a porosity of around 30 % and heteroepitaxial interface between BT and KN. Their apparent piezoelectric constant  $d_{33}^*$  was estimated at 300 pC/N, and was eight times larger value than that of the 0.5BT-0.5KN dense ceramics, while dielectric constant was estimated at 1600 at room temperature. The concept proposed in this study can be a new way to create piezoelectric ceramics with artificial MPB region. Moreover, this method is very universal and applied into various functional materials such as magnetic, conductive, semi-conductive, and optical materials in addition to dielectric, piezoelectric and ferroelectric materials. In the future, we will develop various new materials with heteroepitaxial interfaces on the basis of the concept.

## Chemically Modified Solution-Derived $\text{Na}_{0.5}\text{K}_{0.5}\text{NbO}_3$ Thin Films: From Macro- to Nanoscale Response

Sebastjan Glinšek<sup>1</sup>, Seung-Hyun Kim<sup>1</sup>, Lindsay Kuhn<sup>1</sup>, Alice Leung<sup>1</sup> and Angus Kingon<sup>1</sup>

<sup>1</sup>School of Engineering, Brown University, Providence, USA

Email: [sebastjan\\_glinsek@brown.edu](mailto:sebastjan_glinsek@brown.edu)

A great potential for applications in micro- and nanoscale devices is a driving force for the still-growing interest in thin-film piezoelectric materials. Among huge amount of applications, micro-electro-mechanical system (MEMS) piezoelectric vibration energy harvesters could be used for powering medical implants.<sup>354</sup> For this purpose both thin-film and substrate materials have to be non-toxic. For the substrates, stainless steel foils are good candidates since they are bio-compatible, flexible and enable high-temperature processing, as well as ease of microfabrication.

The (Na,K)NbO<sub>3</sub>-based materials (NKN) are among the most promising lead-free piezoelectrics.<sup>355</sup> However, in the thin-film form their properties are regularly deteriorated compared to the bulk counterparts. It is believed that the problem arises mainly from high and differential volatility of alkali compounds during heating. Therefore their functional properties are still not well understood, in particular, there is a strong need to link the measured macroscopic properties to the nanoscale domain structure and local switching behavior.

With the aim of improving functional response NKN is often chemically modified. Our group recently reported on strong enhancement of functional properties of the solution-derived NKN-based thin films by the addition of small amounts of BiFeO<sub>3</sub> (BFO). The films with 5 % BFO have room-temperature value of the kHz-dielectric permittivity ~600, leakage current density ~10<sup>-7</sup> A/cm<sup>2</sup> and piezoelectric coefficient d<sub>33</sub> ~57 pm/V.<sup>356</sup>

In this paper our recent advances on NKN, NKN-LN (LiNbO<sub>3</sub>) and NKN-BFO solution-derived films will be presented. The phase-pure perovskite films were prepared either on standard platinized silicon or flexible stainless steel substrates. In addition to the macroscale functional characterization, piezoresponse force microscopy was employed to study domain structure and local polarization switching behavior. Influence of different dopants, substrates and relationships between the macroscopic performance and nanoscale properties will be addressed.

<sup>354</sup> S.-G. Kim, S. Priya, I. Kanno, "Piezoelectric MEMS for Energy Harvesting", MRS Bulletin, vol. 37, p. 1039-50, 2012

<sup>355</sup> J. Rodel, W. Jo, T. P. Seifert et al., "Perspective on the Development of Lead-Free Piezoceramics", J. Am. Ceram. Soc., vol. 92, p. 1153-77, 2009

<sup>356</sup> S.-H. Kim, A. Leung, C. Y. Koo et al., "Lead-Free (Na<sub>0.5</sub>K<sub>0.5</sub>)(Nb<sub>0.95</sub>Ta<sub>0.05</sub>)O<sub>3</sub>-BiFeO<sub>3</sub> Thin Films for MEMS Piezoelectric Vibration Energy Harvesting Devices", Mater. Lett., vol. 69, p. 24-26, 2012



## CaBi<sub>4</sub>Ti<sub>4</sub>O<sub>15</sub>/PZT Sol-Gel Composite for High Temperature Ultrasonic Transducers

Makiko Kobayashi<sup>1</sup>, Takuo Inoue<sup>2</sup>, Hajime Nagata<sup>3</sup>, Tadashi Takenaka<sup>3</sup>

<sup>1</sup>Graduate School of Science and Technology/Kumamoto University, Kumamoto/Japan

<sup>2</sup>Faculty of Engineering/Kumamoto University, Kumamoto/Japan

<sup>3</sup>Faculty of Science and Technology/Tokyo University of Science, Chiba/Japan

Email: kobayashi@cs.kumamoto-u.ac.jp

In these days, high temperature ultrasonic transducers becomes in high demand. Especially in Japan, old fuel plants are working in full load, and it is preferable to monitor minor problem points on-line which are found during periodical off-line monitoring. However, the operation temperature of cooling pipes is above 500°C so that it is very severe conditions for ultrasonic transducers.

Sol-gel composite materials could be good candidates for those applications because of high temperature durability and curved surface suitability. However, the composites with Bi<sub>4</sub>Ti<sub>3</sub>O<sub>12</sub> (BIT) piezoelectric powder phase have difficulty for long term usage above 500°C. The temperature stability of the composites with LiNbO<sub>3</sub> is excellent, though the signal strength is not so high and its poling is relatively difficult.

Therefore the sol-gel composite, between CaBi<sub>4</sub>Ti<sub>4</sub>O<sub>15</sub> (CBT) piezoelectric powder and lead zirconate titanate (PZT) sol-gel was investigated for high temperature ultrasonic transducer applications. CBT was chosen because of relatively high Curie temperature, ~800°C. PZT sol-gel was chosen because of high dielectric constant. CBT powder and PZT sol-gel was mixed together, then the mixture were sprayed onto a steel substrate with 4.2mm thick, ~50mm length, ~50mm width, respectively. Spray coating process and thermal process was repeated several times. After poling, clear reflected echoes from the back surface of the substrate at room temperature.

In order to investigate high temperature performance of CBT/PZT, reflected echoes were monitored from room temperature up to 550°C. The signal strength was compared with BIT/PZT and PZT/PZT. As a result, CBT/PZT showed the best temperature stability and it showed the almost same signal strength as that of BIT/PZT. It is noted that no signal was obtained from PZT/PZT at 550°C. Further research will be presented regarding long-term high temperature durability test.

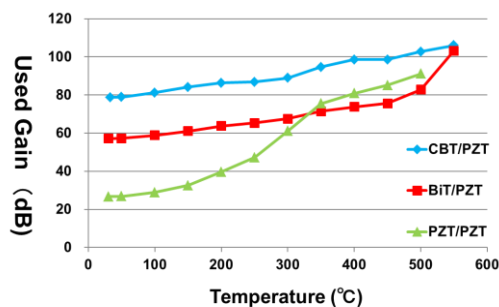


Fig. 111: Temperature dependence of used gain for 4Vp-p of 3<sup>rd</sup> reflected echoes.

## Effect of the Powder Processing on Dielectric and Leakage Current

### Properties of Flux Grown 94NBT-6BT Single Crystals

Mevlüt Gürbüz<sup>1,2</sup> and Aydın Doğan<sup>1</sup>

<sup>1</sup>Department of Materials Science and Engineering, Faculty of Engineering,  
Anadolu University, 26555, Eskisehir, Turkey

<sup>2</sup>Department of Mechanical Engineering, Faculty of Engineering,  
Ondokuz Mayıs University, Samsun 55139, Turkey  
[mevlutg@anadolu.edu.tr](mailto:mevlutg@anadolu.edu.tr) [adogan@anadolu.edu.tr](mailto:adogan@anadolu.edu.tr)

#### Abstract

Lead zirconate titanate based (PZT) ceramics have been used for years because of their excellent electrical properties. However, the use of lead based piezoelectric materials cause to environmental problems during processing due to toxic nature of lead. Therefore, use of lead based ceramics will be prohibited by environmental regulations in near future<sup>1</sup>. In recently, the researchers have focused on to alternative lead free materials.  $94\text{Na}_{0.5}\text{Bi}_{0.5}\text{TiO}_3\text{-}6\text{BaTiO}_3$  (94NBT-6BT) based lead free ceramics are alternative materials instead of lead containing ceramics. NBT based materials and their variations are intensively investigated to enhance piezoelectric properties<sup>2</sup>. Recently, considerable research efforts have been devoted to the growth of NBT based single crystals by various crystal growth methods, such as flux growth, top seeded solution growth and solid state solution growth<sup>3</sup>. In this study, 94NBT-6BT single crystals were grown by flux growth method using uncalcined and calcined 94NBT-6BT powder. Influences of the powder processing type on dielectric and leakage current properties of the grown 94NBT-6BT crystals were analyzed by impedance/gain phase analyzer, LCR meter, AIXACT (aixPES/CMA) piezoelectric and ferroelectric analyzer. The results showed that, single crystals which were produced by heat-treated powders gave better dielectric and leakage current properties than uncalcined single crystals (Figure 1).

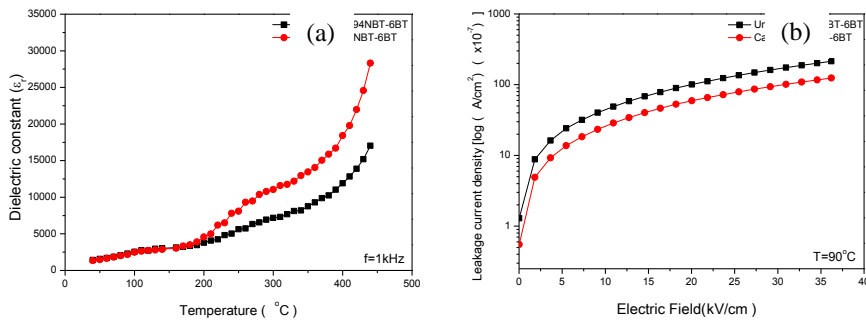


**Figure 1.** Dielectric (a) and leakage current density (b) of the grown 94NBT-6BT crystals

<sup>1</sup> Xu G., Duan Z., Wang X., Yang D. "Growth and some electrical properties of lead-free piezoelectric crystals  $(\text{Na}_{1/2}\text{Bi}_{1/2})\text{TiO}_3$  and  $(\text{Na}_{1/2}\text{Bi}_{1/2})\text{TiO}_3\text{-BaTiO}_3$  prepared by a Bridgman method", J.Cryst. Growth., 275, 113–119, 2005

<sup>2</sup> Ge W., Liu H., Zhao X., Pan X., He T., Lin D., Xu H., Luo H., "Growth and characterization of  $\text{Na}_{0.5}\text{Bi}_{0.5}\text{TiO}_3\text{-BaTiO}_3$  lead-free piezoelectric crystal by the TSSG

method", *J. Alloy. Compd.*, 456, 503–507, 2008

<sup>3</sup>Moon K.S., Rout D., Lee H.Yong., Kang S.J. L., "Solid state growth of  $\text{Na}_{1/2}\text{Bi}_{1/2}\text{TiO}_3$ - $\text{BaTiO}_3$  single crystals and their enhanced piezoelectric properties", *J. Cryst. Growth.*, 317, 28-31, 2011

## Growth, Properties and Structure of High Performance PIN-PMN-PT Single Crystals

Zhuo Xu, Zhenrong Li, Fei Li, Shiji Fan and Xi Yao

Electronic Materials Research Laboratory, Key Laboratory of the Ministry of Education & International Center for Dielectric Research, Xi'an Jiaotong University, Xi'an 710049, China

Ternary  $\text{Pb}(\text{In}_{1/2}\text{Nb}_{1/2})\text{O}_3\text{-Pb}(\text{Mg}_{1/3}\text{Nb}_{2/3})\text{O}_3\text{-PbTiO}_3$  (PIN-PMN-PT) crystals with morphotropic phase boundary (MPB) composition have attracted much interest due to the higher ferroelectric-ferroelectric transition temperature  $T_{R-T}$  ( $>120^\circ\text{C}$ ), improved  $E_C$  ( $\sim 5\text{kV/cm}$ ), and similar piezoelectric properties ( $d_{33}>1500$  pC/N,  $k_{33}>90\%$ ), when compared to binary  $\text{Pb}(\text{Mg}_{1/3}\text{Nb}_{2/3})\text{O}_3\text{-PbTiO}_3$  (PMN-PT) crystals. These properties make PIN-PMN-PT crystals good candidates for various transducer applications.

The paper reviews the recent progress of research on growth, piezoelectric/dielectric properties and structure of PIN-PMN-PT single crystal in Xi'an Jiaotong University. (1) PIN-PMN-PT single crystals of 2' diameter and 3' diameter were grown by the modified Bridgman technique. Variations of composition of PIN-PMN-PT single crystal along growth direction were presented. The homogeneity of PIN-PMN-PT single crystals is needed to be improved in the future. (2) Variations of piezoelectric/dielectric properties of PIN-PMN-PT single crystal along growth direction were measured in detailed. Phase transition characteristics of PIN-PMN-PT single crystals with different composition were investigated. The phase diagram of PIN-PMN-PT was built. (3) The high shear piezoelectric response with improved thermal stability ( $d_{24}\sim 2000$  pC/N) was obtained in orthorhombic crystals. Meanwhile, the high electromechanical couplings  $k_{33}$  ( $>84\%$ ) and mechanical quality factors  $Q$  ( $>2000$ ) were concurrently obtained in tetragonal crystals with broadened temperature usage range. (4) Domain size effect in PIN-PMN-PT single crystal was studied. The piezoelectric constant  $d_{33}$  is improved with decreasing domain size. The fitting curve of the relationship between the domain size and  $d_{33}$  was obtained.

## Dielectric Relaxation in Lead-Free $(1-x)\text{Bi}_{0.5}\text{K}_{0.5}\text{TiO}_3 - x\text{BiFeO}_3$ Ceramics with High Electromechanical Properties

Maxim Morozov, Mari-Ann Einarsrud, Tor Grande,

Department of Material Science and Engineering,  
Norwegian University of Science and Technology, Trondheim, Norway

Email: maxim.morozov@ntnu.no

Perovskite  $\text{ABO}_3$  compounds with mixed bismuth and alkaline cations on the A-site are among the leading candidates for lead-free piezoelectric ceramics. In particular, the system of  $(1-x)\text{Bi}_{0.5}\text{K}_{0.5}\text{TiO}_3 - x\text{BiFeO}_3$  (BKT-BFO) solid solutions includes the regions with appreciably high and thermally stable electromechanical properties, in both sensor (at  $x \approx 0.6$ )<sup>357</sup> and actuator (at  $x \approx 0.25$ )<sup>358</sup> regimes. However, relatively high conductivity observed in the system, especially in the region with high BFO content, is a challenge for practical application.

In this contribution we investigate the dielectric response of BKT-BFO ceramics in broad frequency (1 mHz – 1 MHz) and temperature (25 – 700 °C) ranges, as well as in various atmospheres (natural and synthetic air,  $\text{N}_2$ ,  $\text{O}_2$ ). The dielectric relaxation in ceramics with high BFO content has been analyzed in terms of a traditional model of two parallel equivalent resistance-capacitance circuits in series, which represents the “bulk” and “barrier” contributions by two semi-circles in the complex impedance plane. Our results demonstrate that the “barrier” contribution becomes more significant as the BFO content increases. The same trend characterizes the conductivity of the “bulk” contribution. The “barrier” contribution can be eliminated by heat treatment in dry synthetic air, while the resistivity of “bulk” contribution can be affected by heat treatment in presence of an inert gas (Fig. 1). These results suggest that the “barrier”-type relaxation may originate from interaction with moisture, when ceramics is fabricated. The “bulk” conductivity at ambient conditions is electronic in nature, and is likely associated with the valence state of Fe, which is controlled by the oxygen partial pressure during thermal annealing.

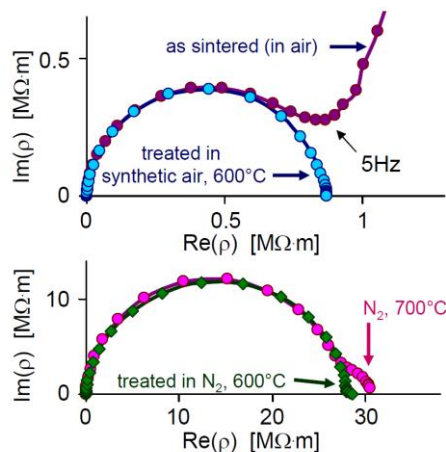


Fig. 112: Complex impedivity plot for 30BKT-70BFO ceramics after treatment in different atmospheres.

<sup>357</sup> H. Matsuo *et al.*, “Structural and piezoelectric properties of high-density  $(\text{Bi}_{0.5}\text{K}_{0.5})\text{TiO}_3 - \text{BiFeO}_3$  ceramics”, J. Appl. Phys., vol. 108, 104103, 2010.

<sup>358</sup> M. I. Morozov *et al.*, “Polarization and strain response in  $\text{Bi}_{0.5}\text{K}_{0.5}\text{TiO}_3 - \text{BiFeO}_3$  ceramics”, Appl. Phys. Lett., vol. 101, 252904, 2012.

Thus, our study demonstrates the way to improve electric resistivity in BKT-BFO ceramics.

## Smart Materials and Devices

CLUB C

*Thursday, July 25 2013, 02:00 pm - 03:30 pm*

Chair: **To Be Announced**

## Ferroelectric Tunnel Junctions Based on Pseudotetragonal $\text{BiFeO}_3$

F.Y. Bruno<sup>1</sup>, V. Garcia<sup>1</sup>, S. Fusil<sup>1</sup>, C. Carretero<sup>1</sup>, C. Deranlot<sup>1</sup>, E. Jacquet<sup>1</sup>, K. Bouzehouane<sup>1</sup>, S. Xavier<sup>1</sup>, M. Bibes<sup>1</sup>, and A. Barthélémy<sup>1</sup>.

<sup>1</sup>Unité Mixte de Physique CNRS/Thales, Palaiseau, France and Université Paris-Sud, Orsay, France

Email: flavio.bruno@thalesgroup.com

The concept of a ferroelectric tunnel junction (FTJ) was formulated in the early 70s by Esaki et al. It took more than 30 years to realize this idea experimentally in a reliable and reproducible manner<sup>1</sup>. FTJs have shown to be versatile devices and the possibility to use them as memories<sup>2</sup> and memristors<sup>3</sup> have been recently demonstrated on  $\text{BaTiO}_3$  based junctions. With the aim of expanding its functionalities we have realized FTJ with multiferroic pseudotetragonal  $\text{BiFeO}_3$  (T-BFO) tunnel barriers. This polytype of BFO has a large predicted polarization ( $>100 \mu\text{C cm}^{-2}$ ). We will show by piezoresonance force microscopy (PFM) that thin films of BFO grown on and  $\text{LaAlO}_3$  substrates are ferroelectric down to a 2.5 nm thickness. In order to fabricate junctions we deposited fully epitaxial bilayers consisting of a  $\text{LaNiO}_3$  bottom electrodes and the T-BFO tunnel barrier. On top of this bilayers, Co/Au electrodes as small as 200 nm in diameter were defined by e-beam lithography and lift-off. We have measured ON/OFF ratios as large as 1000 on these junctions, much larger than that observed in FTJs with  $\text{BaTiO}_3$  tunnel barriers. In Figure 1 we show typical hysteresis curve of resistance vs write voltage pulses on a 300 nm capacitor. We will show that the resistance of the FTJ in its high, low and intermediate states is related with the polarization state of the barrier as observed by PFM. We acknowledge financial support from the European Union Research Council (ERC Advanced Grant Femmes, No. 267579).

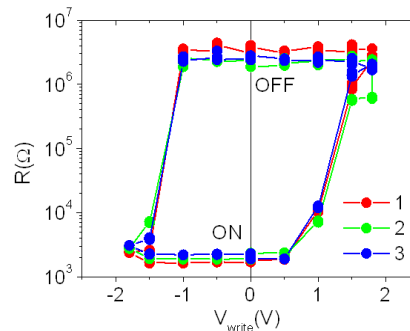


Figure 1 Typical hysteresis of resistance with write voltage pulses of a 300 nm wide Pt/Co/BFO/LNO capacitor showing reproducibility of the ON to OFF switching.



## Performance Investigation and Optimization of Si:HfO<sub>2</sub>-FeFETs on a 28 nm Bulk Technology

Stefan Mueller<sup>1</sup>, Johannes Müller<sup>2</sup>, Alban Zaka<sup>3</sup>, Tom Herrmann<sup>3</sup>, Ekaterina Yurchuk<sup>1</sup>,  
Uwe Schröder<sup>1</sup>, and Thomas Mikolajick<sup>1</sup>

<sup>1</sup> NaMLab gGmbH / Dresden University of Technology, Dresden, Germany

<sup>2</sup> Fraunhofer Center for Nanoelectronic Technologies, Dresden, Germany

<sup>3</sup> GLOBALFOUNDRIES Dresden Module One LLC & Co. KG, Dresden, Germany

Email: Stefan.Mueller@namlab.com

Ferroelectric field effect transistors (FeFET) have long been envisioned as low-power, non-volatile memory solution<sup>359</sup>. However, mass storage based on these devices has never reached maturity due to limited scalability, low retention and CMOS incompatibility<sup>360</sup>. Only recently, these obstacles seem to have been resolved by the discovery of ferroelectric properties in silicon doped hafnium dioxide (Si:HfO<sub>2</sub>)<sup>361</sup>. 28 nm FeFET devices making use of this novel ferroelectric material could finally close the gap to the logic technology roadmap and possess the potential of realizing highly-scaled ultra low-power memory cells<sup>362</sup>.

In our present study we show that for different Si:HfO<sub>2</sub> thicknesses, the experimentally observed ferroelectric hysteresis can well be reproduced by a Preisach-based TCAD modeling approach (Fig. 1)<sup>363</sup>. It was possible to verify that simulated sub-loop characteristics coincide with polarization measurements and further support the assumption of true ferroelectricity in HfO<sub>2</sub>. The ferroelectric model was furthermore used for simulation of FeFET transistors and their respective memory characteristics (Fig. 2). As shown by experiments, the ferroelectric properties change depending on the thickness of the functional layer and indicate that FeFET properties can be tailored by various parameters i.a. film thickness, dopant concentration and annealing conditions. 30 nm layers possess an increased  $P_r / P_s$  ratio, reduced permittivity and smaller remanent polarization in general. It is shown by simulation that the

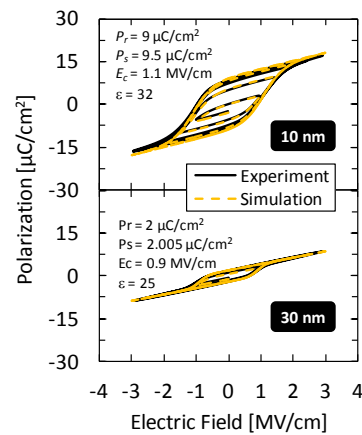


Fig. 1. Measured and simulated polarization hysteresis for 10 nm and 30 nm Si:HfO<sub>2</sub> MFM capacitors.

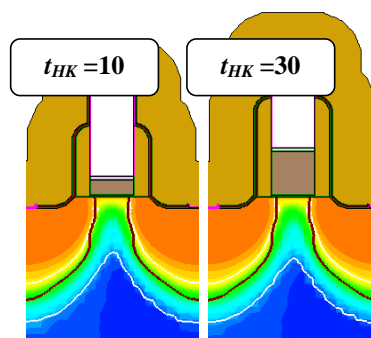


Fig. 2. Simulated electron density at  $V_C = 0V$  after  $E_{HK} \sim 2.5$

<sup>359</sup> J. L. Moll, *IEEE Trans. Electron Dev.*, vol. ED-10, p. 338, 1963.

<sup>360</sup> T. P. Ma, *IEEE Electron. Dev. Lett.*, vol. 23, pp. 386-388, 2002.

<sup>361</sup> T. S. Börscke, *Appl. Phys. Lett.*, vol. 99, p. 102903, 2011.

<sup>362</sup> J. Müller, *IEEE Symp. on VLSI Tech.*, pp. 25-26, 2012.

<sup>363</sup> B. Jiang, *IEEE Symp. on VLSI Tech.*, pp. 141-142, 1997.

interfacial field stress can be reduced using thicker Si:HfO<sub>2</sub> layers which might contribute to FeFET endurance optimization in the future.

## A 3.8 GHz tunable filter based on Ferroelectric Interdigitated Capacitors

Areski GHALEM, Freddy Ponchel, Denis Remiens, Tuami Lasri

Email: Denis.Remiens@univ-valenciennes.fr

In recent years, ferroelectric materials especially  $Ba_xSr_{(1-x)}TiO_x$  have shown interesting properties for telecommunication applications. Actually, the combination of the good tunability and the relatively low losses [1] offered by this kind of material makes it a very interesting candidate for the development of reconfigurable devices. Another advantage brought by the ferroelectric based thin film technology is the suitability for highly integrated microwave devices compatible with planar circuits. The dielectric characterization at 3.8 GHz using a specific coplanar waveguides has shown a tunability of 44% (applied electric field  $E_{max} = 300$  kV/cm) and a loss factor ( $\tan \delta$ ) of 2%. The measurement of the ferroelectric interdigitated capacitors (IDC), conceived and realized, has shown a tunability of 35% under a low electric field (150 kV/cm). Finally, the realization of a tunable hairpin filter using these IDCs (figure 1) has been achieved. The results of the microwave characterization of this device are given in figure 2.

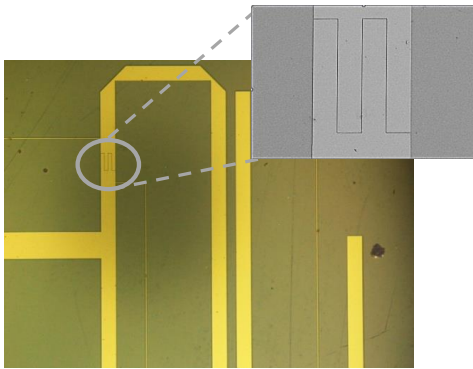


Fig. 1: Photograph of tunable hairpin filter

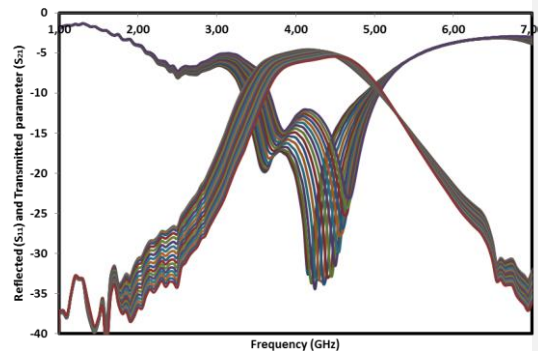


Fig. 2: Frequency evolution of  $S_{11}$  and  $S_{21}$  parameter for different polarization conditions

The measurement of  $S_{11}$  and  $S_{21}$  parameters has been done for different bias voltage ([0; 30 V] range by 2V step). The experimental results clearly show that the variation of permittivity of BST film through the bias voltage modification gives rise to a frequency shift of reflection and transmission parameters. The effect of polarization is translated by a modification of the material permittivity. The measurement exhibits a frequency shift from 3.5 GHz at 0V to 3.9 GHz at 30V. The filter has a tuning frequency of 11.4 % (under 300 kV/cm).

<sup>1</sup> F. Ponchel, J. Midy, J. F. Legier, C. Soyer, D. Rèmes, T. Lasri, and G. Guégan. "Dielectric microwave characterizations of  $(Ba,Sr)TiO_3$  film deposited on high resistivity silicon substrate: Analysis by two-dimensional tangential finite element method". Journal of Applied Physics, [107], 054112, 2010.

## Fabrication of Bimorph with Double Pb[Zr,Ti]O<sub>3</sub> Thick Films

Jun-ichi Inoue<sup>1</sup>, Kensuke Kanda<sup>1</sup>, Takayuki Fujita<sup>1</sup>, Kazusuke Maenaka<sup>1</sup>

<sup>1</sup>Graduate School of Engineering, University of Hyogo, Himeji, Hyogo/ Japan

Email: kanda@eng.u-hyogo.ac.jp

Piezoelectric Pb[Zr,Ti]O<sub>3</sub> (PZT) bimorph structures with the total thickness of 5.4 μm are fabricated and characterized. Optimizations of the sputtering conditions for PZT and metals result in good piezoelectric characteristics of the PZT/PZT thick films.

Bimorph structures are useful for enlarging actuation displacement and generative force. Challenges to fabricate thin-film PZT/PZT bimorphs have been reported for the device application and miniaturization. Since conventional PZT/PZT bimorphs have been quite thin (typically less than 1 μm)<sup>364,365,366</sup>, it has been difficult to apply to specific devices, *e.g.* bimorph beam vibrating and supporting proof mass in MEMS gyroscopes. The thickness of the fabricated PZT/PZT bimorph is enough thick to adapt the bimorph to MEMS structures. The performed bimorph is made by complete batch process without troublesome bonding between bulk PZT material and Si wafer.

Fig. 1 shows the cross sectional SEM (scanning electron microscopy) image of the sputtered PZT/PZT layers. Both PZT layers are dense and columnar crystalline structures without cracks and pores. The *P-E* (polarization and electric field) curves demonstrate that the PZT layers have preferable ferroelectric characteristics (Fig. 2). In addition, other electrical properties of the two PZT layers are well matched with each other. Test cantilevers are fabricated by using dry etching processes to evaluate the characteristics. The relationship between the applied voltage and tip displacement of a 1-mm-long cantilever for unimorph and bimorph actuation (parallel drive) is shown in Fig. 3. The bimorph actuation doubled in the tip displacement compared to the unimorph actuations. The estimated piezoelectric  $d_{31}$  value about -40 pm/V is larger than our previous work for thin PZT/PZT bimorph<sup>3</sup>.

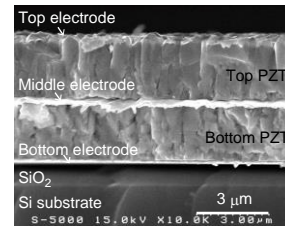


Fig. 113: Cross-sectional SEM image of PZT/PZT layers.

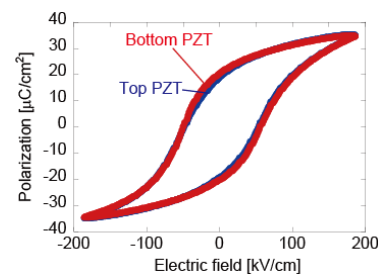


Fig. 2: P-E hysteresis loop for top and bottom PZT layers.

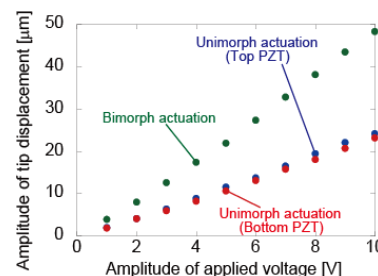


Fig. 3: Applied voltage vs. tip displacement of the cantilever. (@500Hz, resonant frequency: 2.86 kHz)

<sup>364</sup> J. Tsaur et al., "Design and Fabrication of 1D and 2D Micro Scanners Actuated by Double Layered Lead Zirconate Titanate (PZT) Bimorph Beams", *Jpn. J. Appl. Phys.*, vol. 41, p. 4321-4326, 2002.

<sup>365</sup> D. F. L. Jenkins, et al., "PZT Thin Film Bilayer Devices for Phase Controlled Actuation in MEMS", *J. Electroceram.*, vol. 7, p. 5-11, 2001.

<sup>366</sup> K. Kanda, et al., "Fabrication and Characterization of Double-Layer Pb(Zr,Ti)O<sub>3</sub> Thin Films for Micro-Electromechanical Systems", *Jpn. J. Appl. Phys.*, vol. 51, 09LD12, 2012

## PZT PIEZOELECTRIC FILMS ON GLASS FOR ADJUSTABLE X-RAY OPTICS

Rudeger H.T. Wilke<sup>1</sup>, Raegan L. Johnson-Wilke<sup>1</sup>, Susan Trolier-McKinstry<sup>1</sup>, Vincenzo Cotroneo<sup>2</sup>, Stuart McMuldroch<sup>2</sup>, Paul B. Reid<sup>2</sup> and Daniel A. Schwartz<sup>2</sup>

<sup>1</sup>Materials Research Institute, The Pennsylvania State University, University Park, USA

<sup>2</sup>Harvard-Smithsonian Center for Astrophysics, Cambridge, USA

Email: rhw11@psu.edu

Adjustable X-ray optics, using piezoelectric lead zirconate titanate (PZT) films deposited on slumped, thin glass substrates, are a candidate for the Square Meter Arc Second X-ray Telescope (SMART-X) mission concept. The mirror pieces are shaped in the form of paraboloids and hyperboloids with an iridium mirror deposited on the concave surface of the glass and a PZT film deposited on the convex surface. The geometrical constraints make processing of the PZT films by chemical solution deposition quite complex. As a result, an RF magnetron sputtering approach has been adopted. PZT films were deposited on Corning Eagle glass substrates. Two different shaped substrates were used; one in the form of flat 100 mm rounds and the second in cylinders slumped along an axial direction with a radius of curvature of 220 mm. Crystallization into the perovskite phase was performed at 550 °C, approximately 100 °C below the strain point of the glass substrates. Films deposited on flat round substrates demonstrate the feasibility of using PZT thin films to provide high precision control of the surface figure of the mirror. Influence function measurements of the 1.5 µm thick films indicate 2.5 µm out of plane deflection for 1 cm<sup>2</sup> actuators at a drive level of +10 V, in good agreement with finite element analysis models. Depositions onto curved substrates were carried out using multiple sputter guns to ensure optimal film thickness uniformity across the two axes of the cylinder. The electrical and electromechanical properties of the PZT films on curved glass were comparable to those of films deposited on flat pieces. The permittivity of the films was 1500 at 100 Hz, with a loss tangent of 0.04. The hysteresis loops were square with remanent hysteresis values approximately 21 µC/cm<sup>2</sup> and coercive field values near 30 kV/cm. Initial results for influence functions on the curved substrates (measured along the axial direction) show a 0.4 µm deflection for an actuator driven at 4 V (40 kV/cm). The deflection profile about the actuator matches finite element model predictions.

## Giant Piezoelectric Response in Nanostructured Ferroelectric Thin Film Membranes

Nazanin Bassiri-Gharb<sup>1,2</sup>, Yaser Bastani<sup>1</sup>, Amit Kumar<sup>3</sup>, Sergei Kalinin<sup>3</sup>

<sup>1</sup>G.W. Woodruff School of Mechanical Engineering, Georgia Institute of Technology, Atlanta, GA, USA

<sup>2</sup>School of Materials Science and Engineering, Georgia Institute of Technology, Atlanta, GA, USA

<sup>3</sup>Center for Nanophase Materials Science, Oak Ridge National Laboratory, Oak Ridge, TN, USA

Email: nazanin.bassirigharb@me.gatech.edu

PZT and relaxor-ferroelectric solid solutions with polymorphic phase boundaries have been to the date the industry standard for many piezoelectric applications (such as underwater sonars, medical ultrasounds, acoustic transducers, as well as MEMS sensors and actuators, environmental energy harvesters, microfluidic and inkjet printer pumps, ...), owing to their very large piezoelectric response, with respect to the non-ferroelectric compositions, such as ZnO and AlN. However, while the presence of phase boundaries usually corresponds to an enhancement of the electromechanical response by factors of 4x to 10x, the piezoelectric responses of PZT and other ferroelectric solid solution ceramics at the MPB are still relatively small with respect to the intrinsic lattice strains. In fact, in comparison, many other phase-separated systems (such as giant magnetoresistive manganites) demonstrate enhancement of response by many orders of magnitude. Here, we argue that the long-range elastic interactions that give rise to the mesoscopic clustering in disordered ferroelectrics are the predominant reason for suppressed enhancement factors in these systems.

(100)-textured PZT thin films were processed on platinized Si substrates, and their dielectric and piezoelectric response was monitored at reduction of the Si thickness over a large area ( $\sim 1 \text{ cm}^2$ ). The reduction of the Si thicknesses below  $\sim 200 \text{ }\mu\text{m}$  is accompanied with a continuous and large enhancement of the effective piezoelectric response,  $d_{33,f}$ , as measured by a double beam laser interferometer. At a residual Si thickness of  $\sim 10\text{-}20 \text{ }\mu\text{m}$ ,  $d_{33,f}$  values up to 10 nm/V are observed in the membrane-like PZT films. Band-excitation piezoresponse force microscopy (BE-PFM) was used to characterize the local response of the samples. Virgin PZT capacitors showed a typical cluster-like response previously observed in many ferroelectric ceramics and thin films. Conversely, the piezoresponse amplitude of the membrane capacitors showed huge enhancement, more than an order of magnitude with respect to the clamped sample, no long-range interactions were present, and switching happened in a one by one paradigm of grains. A combination of the dielectric and piezoelectric macroscopic measurements, X-ray maps, and PFM data are presented to illustrate that long-range elastic interactions in the clamped ferroelectric films are the primary factor that limits the giant electromechanical responses, even at the MPB compositions, in such systems.

---

## **ISAF Group 4 Posters**

Forum Hall

*Thursday, July 25 2013, 01:00 pm - 04:30 pm*

**Jonathan Bock**<sup>1</sup>, Soonil Lee<sup>2</sup>, Susan Trolier-McKinstry<sup>3</sup>, Clive Randall<sup>3</sup>

<sup>1</sup>Materials Science and Engineering, The Pennsylvania State University, University Park, PA, USA, <sup>2</sup>Materials Research Institute, The Pennsylvania State University, University Park, PA, USA, <sup>3</sup>Materials Science and Engineering, The Pennsylvania State University, University Park, PA, USA

### Electrical Conductivity in Heavily Reduced Ferroelectrics near the Mott Metal-Insulator Transition

Heavy reduction of ferroelectrics can lead to carrier concentrations above the Mott metal-insulator transition and, therefore, metallic conductivity. Some of these materials show promising properties for their use in thermoelectric applications due to their low thermal conductivities (Figure of Merits  $>1$ ). Recent data shows that the paraelectric-ferroelectric transition in materials such as  $(\text{Ba,Sr})\text{TiO}_{3-\delta}$  and  $(\text{Sr,Ba})\text{Nb}_2\text{O}_{6-\delta}$  show a transition from metallic conduction in their paraelectric states to semiconducting behavior in their ferroelectric states. The nature of this metal-insulator transition is currently unknown but is suspected to be caused by shifts in carrier concentrations due to the need for screening of the polarization within the domains that form during the paraelectric-ferroelectric transition. Electrical conduction mechanisms within different temperature regimes as well as evidence for a polarization induced metal-insulator transition will be discussed.



## Photochemical Deposited Metal Nanoparticles on Polarized LiNbO<sub>3</sub> Surface for SERS Applications

Xiaoyan Liu<sup>1</sup>, Kenji Kitamura<sup>2</sup>, Minoru Osada<sup>2</sup>, and Guozhong Cao<sup>1</sup>

<sup>1</sup>Dept. of Materials Sci. & Eng., University of Washington, Seattle, USA,

<sup>2</sup>National Institute for Materials Science, Tsukuba, Japan

Email:xyliu@uw.edu

By applying an alternating external electric field, ferroelectric domains with patterned-polar surfaces ranging from micro- to nano-meters under precise control and rational design can be fabricated in LiNbO<sub>3</sub> single crystal.<sup>1</sup> Domains with different polarization present surfaces with different properties including surface charges and surface potential. The use of ferroelectric LiNbO<sub>3</sub> as templates for growth of patterns of metal nanoparticles via photochemical reaction related to surface charge properties has found potential applications in surface enhanced Raman scattering (SERS) sensors.

As an example, when polarized surface of LiNbO<sub>3</sub> contacts to a metal ion solution and exposes to an above-band-gap irradiation, metal nanoparticle patterns associate with ferroelectric domains can be formed due to a large photogalvanic effect of LiNbO<sub>3</sub>.<sup>2</sup>

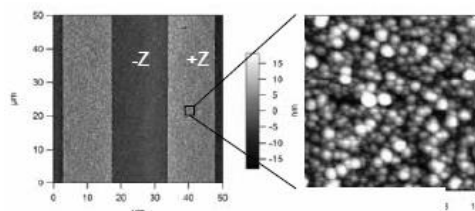


Fig.1: Ag nanoparticles deposited selectively on positively-poled domain surfaces of

LiNbO<sub>3</sub>. Fig.1 is an AFM topographic image showing the high contrast Ag nanoparticle pattern fabricated on the positively-poled domain surfaces of LiNbO<sub>3</sub>. Zoom-in image (right) shows the uniformity of Ag nanoparticles at an average diameter of 30 nm. A variety of metal nanoparticles including Au, Ni and Co can be fabricated using the same method.

The success of SERS is highly dependent on the interaction between adsorbed molecules and the surface of plasmonic nanostructures, often the classic SERS substrates of Au and Ag. Although, SERS effect is known for nearly four decades, search for the suitable substrate is still under active area of research. An ideal SERS substrate should be uniform, reproducible, and robust while exhibit high SERS enhancement over large active area. Fig.2 shows the SERS spectra of porphyrin molecules adsorbed on Au nanoparticles photochemical deposited on LiNbO<sub>3</sub> that present a large enhancement factor more than  $10^8$  (red line). The SERS signals also show a high reproducibility cross the Au nanoparticle regions. The results demonstrate the photochemical deposited Ag and Au nanoparticles on LiNbO<sub>3</sub> can be used for an improved SERS substrate. Besides the application to SERS substrate, we report here new applications of LiNbO<sub>3</sub> templates for molecular manipulations.

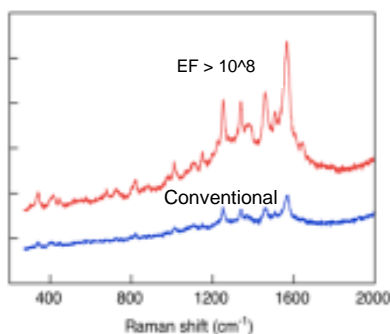


Fig.2: Raman enhancement from our substrate and a conventional SERS substrate with Au nanoparticles.

2. X. Liu et al. *Appl. Phys. Lett.* 2007, 91, 044101.

## Microwave Dielectric Constant Measurements of Strontium Titanate Using Five Mixture Equations

Jyh Sheen\* and Yong-Lin Wang

Department of Electronic Engineering, National Formosa University,  
Hu-Wei, Yun-Lin 632, Taiwan.

\*E-mail: jsheen@nfu.edu.tw

This research dedicates to find a different measurement procedure of microwave dielectric properties for ceramic materials with high dielectric constants.

For the composite of ceramic dispersed in the polymer matrix, one major development is to calculate the permittivity of ceramic from measurements on composite based on the mixture rules<sup>367-2</sup>. It has shown that both the physical curve matching with experimental results and low potential theory error are important to promote the calculation accuracy<sup>3</sup>. The study of mixture equation with high dielectric constant ceramics at microwave frequency has also been presented for strontium titanate ( $\text{SrTiO}_3$ )<sup>4</sup>, which has a dielectric constant 300. The accuracy on the report of high dielectric constant measurements is can still be improved. There are still some important and well known mixture rules require adequate investigation to the application for measurements of high dielectric constant ceramics. Therefore, five more well known mixing rules are selected to understand their application to high dielectric constant ceramic. Their theoretical error equations are derived and investigated.

Strontium titanate is an interesting ceramic for microwave applications. In this research, its powder is adopted as the filler material and polyethylene powder is as the matrix material. The dielectric constants of those ceramic-polyethylene composites with various compositions were measured at 10 GHz. The theoretical curves of the five published mixture equations are shown together with the measured results in Fig. 1 to understand the curve matching condition of each rule. Finally, based on the experimental observation and theoretical analysis, one of the five rules was selected and modified to a new powder mixture equation (Fig. 1). This modified rule has shown very good curve matching with the measurement data and low theoretical error. We can then calculate the dielectric constant of pure filler medium (strontium titanate) by those mixing equations from the measured dielectric constants of composites. The accuracy for estimating dielectric constant of pure ceramic by various mixture rules was compared. The modified mixture rule has also shown good measurement accuracy on the dielectric constant of strontium titanate ceramic. This studied can be applied to the microwave dielectric properties measurement of other high dielectric constant ceramic materials in the future.

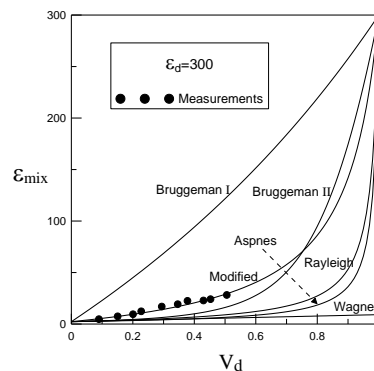


Figure 1 Comparisons of experimental data and mixture rules.

<sup>367</sup> F. Xiang, H. Wang, and X. Yao, J. Eur. Ceram. Soc., vol. 26, pp. 1999-2002, 2006.

<sup>2</sup> W. Z. Yang and J. P. Huang, J. Appl. Phys., vol. 101, p. 064903, 2007.

<sup>3</sup> J. Sheen and Z. W. Hong, European Polymer Journal, vol. 45, pp. 1316-1321, 2009.

<sup>4</sup> J. Sheen and Y. L. Wang, To be published.



## UV direct-write domain inversion on 128° YX-cut LiNbO<sub>3</sub>: towards novel SAW applications

Andreas Boes<sup>1,2</sup>, Didit Yudistira<sup>1</sup>, Amgad Rezk<sup>1</sup>, Tristan Crasto<sup>1,2</sup>, Hendrik Steigerwald<sup>1,2</sup>,  
Elisabeth Soergel<sup>3</sup>, Scott Wade<sup>4</sup>, James Friend<sup>1</sup>, Arnan Mitchell<sup>1,2</sup>

<sup>1</sup>Electrical and Computer Engineering, RMIT University, VIC 3001, Melbourne, Australia

<sup>2</sup>Center for Ultra-high Bandwidth Devices for Optical Systems (CUDOS)

<sup>3</sup>Institute of Physics, University of Bonn, Wegelerstr. 8, 53115 Bonn, Germany

<sup>4</sup>Engineering and Industrial Science, Swinburne University of Technology, VIC 3122, Australia

Email: andreas.boes@rmit.edu.au

Applications of domain engineered lithium niobate crystals (LiNbO<sub>3</sub>), in particular the periodic domain inversion for surface acoustic wave (SAW) generation, has been reported recently<sup>368</sup>. Domain inversion was achieved by means of electric field poling on Z-cut LiNbO<sub>3</sub> crystals. However, utilizing a 128° YX-cut LiNbO<sub>3</sub> for SAW is preferable because of its higher electromechanical coupling constant (5.3%) as compared to Z-cut crystals (0.53%)<sup>1</sup>. Domain engineering has so far not been reported for 128° YX-cut LiNbO<sub>3</sub> crystals because of its inclined polarization axis, which makes it difficult to use standard electric field poling<sup>369</sup>. In this contribution we report for the first time to our knowledge of periodic domain inversion on 128° YX-cut LiNbO<sub>3</sub> whereby domain inversion is achieved using UV direct domain writing<sup>370</sup>.

For domain formation, tightly focused, continuous wave UV laser light ( $\lambda = 244$  nm,  $I = 3.2 \times 10^5$  W/cm<sup>2</sup>,  $d = 6$  μm) was scanned across the crystal's surface. Laser tracks were written perpendicular to the crystallographic  $x$ -axis with a velocity of 0.1 mm/s by the use of a computer-controlled translation stage. The written domain pattern was investigated using piezoresponse force microscopy (PFM).

The four bright stripes in the PFM picture (Fig. 1) show UV-written domains on a 128° YX-cut LiNbO<sub>3</sub> crystal. In the picture is also evidence of surface damage and cracks, which are a common feature of UV written domains.

We have successfully demonstrated that the UV domain writing technique is capable of achieving periodic domain inversion on 128° YX-cut LiNbO<sub>3</sub> in the micrometer regime. Promising methods for the suppression of the observed surface damage are also under investigation. The suitability of these structures for the generation of SAW has been analyzed theoretically and is the topic of a distinct submission to this conference. We hope to experimentally observe the use of these structures for SAW transduction shortly and will report our progress towards this goal at the conference.

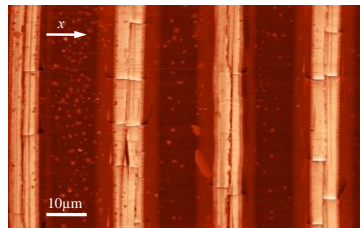


Fig. 114: PFM picture of the UV-written domains on a 128° YX-cut LiNbO<sub>3</sub> crystal. Small cracks and surface damage are visible.

<sup>368</sup> D. Yudistira, S. Benchabane, D. Janner, and V. Pruneri, "Surface acoustic wave generation in ZX-cut LiNbO<sub>3</sub> superlattices using coplanar electrodes," *Applied Physics Letters*, **95**, 052901 (2009).

<sup>369</sup> S. Sonoda, I. Tsuruma, and M. Hatori, "Second harmonic generation in a domain-inverted MgO-doped LiNbO<sub>3</sub> waveguide by using a polarization axis inclined substrate," *Applied Physics Letters*, **71**, 3048 (1997).

<sup>370</sup> H. Steigerwald, Y. J. Ying, R. W. Eason, K. Buse, S. Mailis, and E. Soergel, "Direct writing of ferroelectric domains on the  $x$ - and  $y$ -faces of lithium niobate using a continuous wave ultraviolet laser," *Applied Physics Letters*, **98**, 062902 (2011).

## PLD Elaboration of Piezoelectric ZnO Thin Film for 540 MHz Al/ZnO/Pt Bulk Acoustic Wave Resonator

Serhane Rafik<sup>1</sup>, Abdelli-Messaci Samira<sup>1</sup>, Lafane Slimane<sup>1</sup>, Khales Hammouche<sup>1</sup>, Aouimeur Walid<sup>1</sup>, Hassein-Bey Abdelkadder<sup>1,2</sup>, Boutkedjirt Tarek<sup>3</sup>

<sup>1</sup> Centre for Development of Advanced Technologies (CDTA). Cité 20 Août 1956, Baba Hassen, BP: 17, DZ-16303, Algiers, Algeria.

<sup>2</sup> Micro & Nano Physics Group, Faculty of Sciences, University Saad Dahlab of Blida (USDB), BP. 270, DZ-09000 Blida. Algeria

<sup>3</sup> Equipe de Recherche Physique des Ultrasons, Faculté de physique, Université des Sciences et de la Technologie Houari Boumediene (USTHB), BP 32, DZ-16111, El-Alia, Bab-Ezzouar, Algiers. Algeria.

Email: [rafik\\_serhane@hotmail.com](mailto:rafik_serhane@hotmail.com), [rserhane@cda.dz](mailto:rserhane@cda.dz)

ZnO thin films in Al/ZnO/Pt/Ti/SiO<sub>2</sub>/Si Bulk Acoustic Wave (BAW) resonators are realized by reactive Pulsed Laser Deposition (PLD) technique. It is of most interest to improve their piezoelectric characteristics. These later are intimately linked to the texture, the microstructure and growth conditions. In this work, piezoelectric characteristics of ZnO thin films have been investigated. The Wurtzite ZnO thin films were prepared on Pt(111) at different substrate temperatures (100-500 °C) by a reactive PLD technique. The 200 nm of Pt on 20 nm Ti were prepared by Electron Beam Deposition (EBD) technique at room temperature on 2 μm SiO<sub>2</sub> substrate. This SiO<sub>2</sub> film has been realized by Silicon wet thermal oxidation step, under (H<sub>2</sub>+O<sub>2</sub>)(5 slm+3.5 slm) gas flows at 1100 °C for 9h 10min. The top electrode of the BAW was made by thermal evaporation of Aluminum; the piezoelectric film was confined in a circle of 1.8 mm radius.

The X-Ray diffraction (XRD) characterization showed that the deposited Pt (bottom electrode) has (111) preferential orientation. It also showed that the ZnO films were *c*-axis (002) oriented. The Scanning Electron Microscopy (SEM) of the realized ZnO thin film showed evidence of compact grains with honeycomb-like structure on surface and evidence of columnar structure on cross-section. The measurements indicate that all substrate temperatures are suitable to obtain a good quality of ZnO, but  $T_s=300$  °C is the optimized one. In order to evaluate the piezoelectric properties of the BAW, measurements of the electrical input impedance and admittance have been performed. They showed evidence of piezoelectric response. The resonance frequency was obtained at 524.5 MHz and the anti-resonance frequency at 540.9 MHz. The values of quality factors were respectively;  $Q_r=1125.6$  and  $Q_a=856.51$ . The electromechanical coupling coefficient was evaluated at  $K_{eff}^2=7.26$  %, which is an indicator of a good piezoelectric response. From this measured values, the thickness and wave velocity in the ZnO slab were deduced to be ( $d = 6.15$  μm and  $V_p = 6451.35$  m/s) and the piezoelectric constant  $e_{33}$  was found to be equal to 1.21 C/m<sup>2</sup>.

# Ferroelectric Liquid Crystals for Display and Photonics

## Applications

Vladimir Chigrinov

Hong Kong University of Science and Technology,  
Clear Water Bay, Kowloon, Hong Kong

Email: eechigr@ust.hk

Ferroelectric liquid crystals (FLC) is a good candidate for the new generation display and photonics devices with advanced performance in comparison with usually used nematic LC. Several electrooptical modes can be used for for the new generation of FLC devices for displays and photonics [1]: (i) deformed helix ferroelectric (DHF) effect; (ii) electrically suppressed helix ferroelectric liquid crystals (ESHFLC); (iii) modulation of light in diffraction FLC grating; and (iv) orientational electro-optic Kerr effect.

The novel FLC devices may include field sequential color (FSC) FLC with a high resolution, low power consumption and extended color gamut, which can be used in the screens of portable PCs, mobile phones, PDAs and micro and pico-projectors.

FLC photonics devices have found applications for the generation of digital holograms, adaptive beam steering systems, sensors and polarization gratings. Additionally, high-speed communication systems, producing elements (such as switches, attenuators, polarization rotators) demand FLC devices with extremely fast response, stable, low loss, operable over a wide temperature range, and that require small operating voltages and extremely low power consumption.

[1] Vladimir Chigrinov, Eugene Pozhidaev, Abhishek Srivastava, Guo Qi, Ma Ying, Hoi Sing Kwok, Fast Ferroelectric Liquid Crystal Modes Based on Photoaligning Technology, SID 2013, Vancouver, Canada, May 2013.

## Piezoelectric Transducer Applications on Basis of Free-formed PZT Components

Kai Hohlfeld<sup>1</sup>, Sylvia Gebhardt<sup>2</sup>, Alexander Michaelis<sup>1,2</sup>

<sup>1</sup>Chair of Inorganic Non-Metallic Materials, Institute of Materials Science / TU Dresden, Dresden, Germany

<sup>2</sup>Fraunhofer Institute for Ceramic Technologies and Systems (IKTS), Dresden, Germany

Email: kai.hohlfeld@ikts.fraunhofer.de

Adaptive structures are the future trend in several fields of mechanical engineering, automotive and aerospace industries. Since lightweight materials and composite structures are used more extensively in these fields there is an increasing demand of systems for vibration/noise damping, shape control and structural health monitoring. Usually adaptive structures are created from passive structural parts with subsequent application/integration of sensor/actuator modules and electronics. We investigate volume fabrication of piezoceramic components with regard to cost-effectiveness and direct integration into lightweight materials within Collaborative Research Centre/Transregio 39 PT-PIESA supported by the Deutsche Forschungsgemeinschaft (DFG)<sup>1</sup>. Our focus is on the development of free-formed lead zirconate titanate (PZT) components and resulting PZT/polymer composites as basis for sensor, actuator and ultrasonic transducer applications.

So far sintered PZT fibers (SP505, CeramTec, Germany) of 100-800  $\mu\text{m}$  in diameter and up to 150 mm length were generated by a quasi-continuous spinning process and a modified phase inversion technique. Furthermore nearly spherical PZT elements – so called pearls – in a diameter range of 0.8-1.6 mm were manufactured. The paper reports on low and high signal properties of piezocomposites made of free-formed PZT elements. 1-3 fiber composites fabricated from PZT/polymer blocks with dense fiber packing (approx. 75 vol% PZT fibers) reached values of dielectric constant  $\epsilon_{33}^T/\epsilon_0 = 800-1000$  and electromechanical coupling  $k_t = 0.56-0.63$ . Remnant polarization  $P_{\text{rem}} = 20-28 \mu\text{C}/\text{cm}^2$  and relative strain response  $S_{\text{rel}} = 1-1.2 \times 10^{-3}$  were measured at  $E = 2 \text{ kV}/\text{mm}$ . Composites based on PZT pearls showed  $\epsilon_{33}^T/\epsilon_0 = 200-600$ ,  $P_{\text{rem}} = 6 \mu\text{C}/\text{cm}^2$  and  $S_{\text{rel}} = 0.6-0.9 \times 10^{-3}$ . Coercive field strength  $E_c = 1.3 \text{ kV}/\text{mm}$  and dielectric loss factor  $\tan \delta = 0.2$  were determined for both composite types.

Due to high values in ferroelectric coupling and strain response fibers or fiber composites respectively are seen as suitable for a variety of actuator and ultrasonic transducer applications. Composites based on spherical PZT elements offer advantages in manufacturing and handling. According to their properties they could be introduced as basis material for cost-effective sensors. Applications of integrated free-formed PZT components and composites in glass fiber reinforced polyurethane-, thermoplastic polymer- (e.g. polyamide) as well as aluminum sheet-structures to develop adaptive structures compatible for high volume production will be shown.

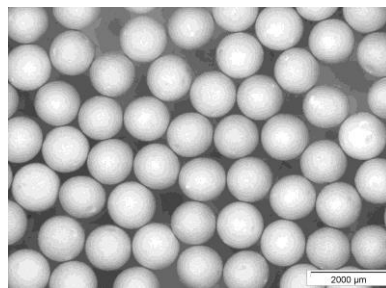


Fig. 115: Novel PZT elements: pearls, with approx. diameter of 1.2 mm.

<sup>1</sup> [www.pt-piesa.tu-chemnitz.de](http://www.pt-piesa.tu-chemnitz.de)





## Enhanced Electrocaloric Effect in Novel Lead-Free Relaxor Ferroelectrics.

Florian Le Goupil<sup>1</sup>, Andrey Berenov<sup>1</sup>, Anna-Karin Axelsson<sup>1</sup>, Matjaz Valant<sup>2</sup> and Neil McN. Alford<sup>1</sup>

<sup>1</sup>Department of Materials, Imperial College London, London, United Kingdom

<sup>2</sup>Materials Research Laboratory, University of Nova Gorica, Nova Gorica, Slovenia

Email: [f.le-goupil09@imperial.ac.uk](mailto:f.le-goupil09@imperial.ac.uk)

In polar crystals the spontaneous polarization increases with application of an external electric field. Under adiabatic conditions, the system compensates this alignment of dipoles with an increase in temperature, in order to keep the overall entropy of the system constant. This phenomenon is called the electrocaloric effect (ECE). The need for more efficient and environmentally-friendly materials in the refrigeration industry has led to a significant effort towards the discovery of materials that exhibit a pronounced EC effect.

We have constructed a direct ECE measurement system, based on a modified-Differential Scanning Calorimeter (DSC), allowing the acquisition of both thermal (ECE, heat capacity) and electrical (P-E loops, leakage current) information simultaneously. The ECE of several novel lead-free relaxor ferroelectric have been measured, including perovskites (substituted BaTiO<sub>3</sub>), Aurivillius phases (substituted SrBi<sub>2</sub>Ta<sub>2</sub>O<sub>9</sub>) and tungsten bronzes (Sr<sub>x</sub>Ba<sub>(1-x)</sub>Nb<sub>2</sub>O<sub>6</sub>). For most of these systems, the direct ECE measurements presented here are the first ever reported. It is shown that, most definitely due to their polar nano-regions, relaxor ferroelectrics experience a second ECE peak, sometimes far above the temperature of the ferroelectric phase transition, which could provide the wide temperature range that is required to establish a solid-state electrocaloric cooling cycle.

Comparisons between direct and indirect measurements, obtained from dielectric polarization measurements versus electric field and temperature, have also been performed on these systems. Contrary to what we reported for normal ferroelectrics<sup>371</sup>, we found large discrepancies between both methods above the ferroelectric phase transition, in both trend and absolute values. This result highlights the significant limitations of the indirect ECE method, especially in the case of relaxor ferroelectrics.

---

<sup>371</sup> F. Le Goupil, A. Berenov, A. Axelsson, M. Valant, and N. M. Alford "Direct and indirect electrocaloric measurements on <001>-PbMg1/3Nb2/3O3-30PbTiO3 single crystals", J. Appl. Phys., vol. 111, p. 124109, 2012.

# Enhanced dielectric properties of BaTiO<sub>3</sub>/poly(vinylidene fluoride) nanocomposites for energy storage applications

Ke Yu<sup>1</sup>, Hong Wang<sup>1</sup>, Yongcun Zhou<sup>1</sup>, Yuanyuan Bai<sup>1</sup>, Yujuan Niu<sup>1</sup>

<sup>1</sup>Electronic Materials Research Laboratory, Key Laboratory of Ministry of Education, Xi'an Jiaotong University, Xi'an 710049, China

Email: ke.yu.ke@stu.xjtu.edu.cn

In our present work<sup>372</sup>, homogeneous ceramics-polymer nanocomposites consisting of surface treated BaTiO<sub>3</sub> (BT) particles as fillers and poly(vinylidene fluoride) (PVDF) polymer as matrix have been prepared using a solution casting process.

The nanocomposites exhibit enhanced dielectric permittivity and reduced loss tangent. The frequency and temperature dependencies of the dielectric permittivity and loss tangent of the nanocomposites suggest that the introduced BT phase and interface areas contribute to the improvement of the dielectric responses.

Meanwhile, the X-ray diffraction patterns and Differential Scanning Calorimetry (DSC) curves indicate that the incorporation of ceramic particles contributes to the decrease of the crystallite size, the increase of the crystallinity, and the shift of the crystallization temperature of the polymer matrix.

Furthermore, the dielectric displacement and energy density of the nanocomposites are significantly enhanced and an energy density of 3.54 J/cm<sup>3</sup> was obtained under an electric field of 200 MV/m with the BT concentration of 20 vol. %.

The results indicate that the introduced ceramic fillers and interface areas have positive influences on the structure of the polymer matrix and contribute to the enhancement of the dielectric responses and energy storage properties of the nanocomposites.

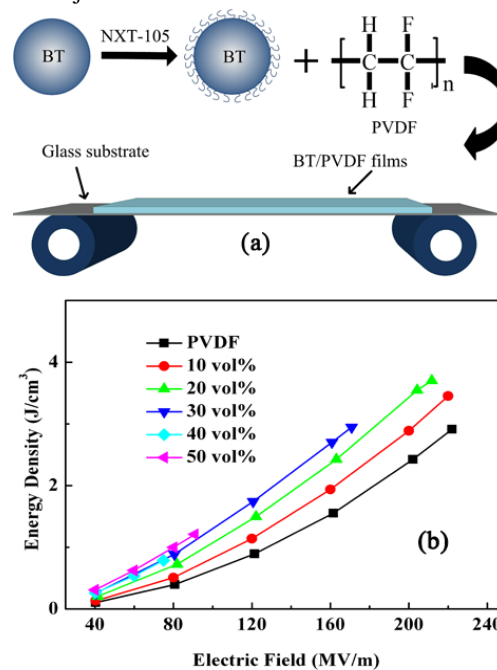


Fig. 1: Schematic of the fabrication of the BT/PVDF nanocomposites (a) and energy density of the pure polymer and the nanocomposites as a function of the volume fraction of BT (b).

<sup>372</sup> K. Yu, H. Wang, Y. Zhou, Y. Bai, and Y. Niu, "Enhanced dielectric properties of BaTiO<sub>3</sub>/poly(vinylidene fluoride) nanocomposites for energy storage applications", J. Appl. Phys., 113, 034105 (2013).

## New microfabrication method to reverse micrometric ferroelectric domains on lithium niobate wafers for RF applications

Florent Bassignot<sup>1</sup>, Emilie Courjon<sup>1</sup>, Fabien Henrot<sup>1</sup>, Thomas Baron<sup>1</sup>, Sylvain Ballandras<sup>2</sup>

<sup>1</sup>FEMTO-ST Institute, 32 avenue de l'observatoire, 25000 Besançon cedex, FRANCE

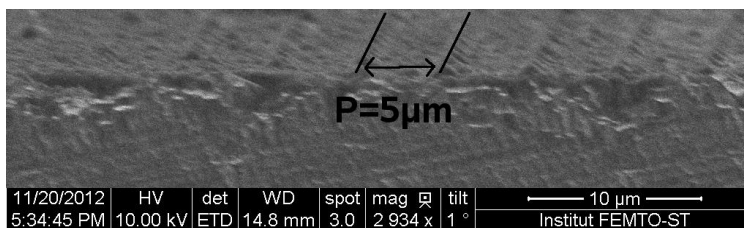
<sup>2</sup>FreC'N'Sys SAS, 18 rue Alain Savary, 25000 Besançon cedex, FRANCE

Email: florent.bassignot@femto-st.fr

The demand of acoustic wave devices in telecom as resonators or filters has generated a strong innovative activity. These components are usually based on surface or bulk acoustic wave technologie. Recently, we have investigated the interest of periodically poled transducers (PPTs) on single crystal 500  $\mu\text{m}$ -thick  $\text{LiNbO}_3$  Z-cut plates through a new acoustic resonator<sup>373</sup>. The PPT consists of two electrically conductive medias embracing a periodically poled ferroelectric layer. Its fabrication is based on a poling bench which mainly consists of a high voltage amplifier used to submit the patterned ferroelectric wafer to an electric field strong enough to invert its native polarization. The resonance frequency of the new resonator is fixed by the PPT period. In order to answer to the need of high frequencies sources (RF until X band domain), the PPT period must be lower to ten microns. For this specification, the PPT fabrication using the classical method by electric field application is difficult due to the enlargement of the reverse ferroelectric domains under the electrical insulating layer.

In this work, we present a new microfabrication method allowing to reverse micrometric ferroelectric domains by electric field application. As the enlargement of the reverse ferroelectric domains under the electrical insulating layer depends of the applied electric field value, a technology based on wafer-bonding and plate thinning techniques has been developed. The method firstly consists of bonding a 500  $\mu\text{m}$ -thick lithium niobate Z-cut single crystal plate onto a doped silicon wafer, the ferroelectric wafer is then thinned down to a few tens of microns by lapping and polishing techniques. The resulting composite wafer is finally poled by applying a low electric field.

The fabrication of PPTs exhibiting a poling period of 5  $\mu\text{m}$  has been successfully achieved by means of this new microfabrication method on a 50  $\mu\text{m}$ -thick lithium niobate layer bonded on a doped silicon wafer (Fig. 1). It has been successfully implemented on the new acoustic resonator<sup>1</sup> and tested allowing the excitation of elastic waves at frequencies up to 1 GHz ( $V_\phi=6500 \text{ m.s}^{-1}$ ).



<sup>373</sup> F. Bassignot et al., "Acoustic resonator based on periodically poled transducers: Concept and analysis", J. Appl. Phys., vol. **111**, 064106, 2012.

Fig. 116: SEM view of a 5  $\mu\text{m}$  period device based on a doped silicon plate bonded on a 50  $\mu\text{m}$ -thick lithium niobate layer. The structure has been etched in a hydrogen fluoride solution in order to observe the domain alternation.

## **BZN Thin-Film Multilayer Capacitors Fabricated at Low Temperature by Radio Frequency Magnetron Sputtering**

Fan He, Saeed Khan, Wei Ren\*, Peng Shi, and Xiaoqing Wu

Electronic Materials Research Laboratory, Key Laboratory of the Ministry of Education & International Center for Dielectric Research, Xi'an Jiaotong University, Xi'an 710049, China

\* Email: wren@mail.xjtu.edu.cn

In this study, thin film multilayered capacitors (MLCs) composed of amorphous  $\text{Bi}_{1.5}\text{Zn}_{1.0}\text{Nb}_{1.5}\text{O}_7$  (BZN) dielectric layers with internal electrodes were fabricated by radio-frequency (RF) sputtering at a temperature below 150 °C. All BZN thin films were deposited through a set of steel shadow masks at room temperature and post-annealed at 150 °C. XRD pattern and SEM images confirmed that the BZN dielectric layers used in these MLCs are amorphous and the thickness for each BZN layer is approximately 200 nm. Metallic Pt and Cu with about 50 nm thick were studied as internal electrodes, respectively. We fabricated BZN thin film MLCs with different layers. The thin film MLCs with 5 BZN layers exhibit promising dielectric properties: the relative permittivity of around 60, the dielectric loss of 13% at 10 kHz and a leakage current of  $10^{-4}$  A at a dc bias electric field of 150 kV/cm. The capacitance density for each dielectric layer is around 300 nF/cm<sup>2</sup>. The BZN thin film MLCs have a potential application on embedded PCBs.

### Piezoelectric thick film sensors: Fabrication and characterization

Florian VERY<sup>1</sup>, Philippe COMBETTE<sup>1</sup>, Denis COUDOUEL<sup>1</sup>, Alain GIANI<sup>1</sup>, Jean-Yves FERRANDIS<sup>1</sup>, Eric ROSENKRANTZ<sup>1</sup>, Damien FOURMENTEL<sup>2</sup>

<sup>1</sup>IES, Institut d'Electronique du Sud, Université Montpellier2, FRANCE

<sup>2</sup>CEA Cadarache, DEN/DER/SPEX/LDCI, St Paul lez Durance, FRANCE

The screen printing of piezoelectric offers a wide range of possible applications for the development of acoustic sensors and the measurement of small size deformations. Material properties characterizations of these thick-film PZT resonators are essential for device design and applications. We measured the electrical properties for different ranges of frequencies and temperature –from 1 $\mu$ Hz up to 13MHz between 30 and 400 ° C-. The piezoelectric coefficients  $d_{33}$ ,  $d_{31}$  and pyroelectric coefficient are also investigated. With this aim, we made various thicknesses of Lead Zirconate Titanate (PZT) thick films, up to 60  $\mu$ m by screen printing process. The deposit has been obtained by superposition of several layers thick of 20 microns. We implement different screen printing processes –firing and co-firing duration, controlled temperature rate to bring the best piezoelectric coefficients and acoustic impedance values. We will highlight the use of these thick films in order to characterize both the liquid acoustic properties and the mass determination.

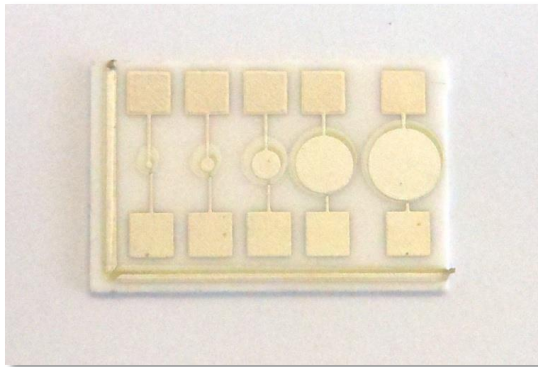


Figure 117 : Screen printed piezo sensor

## **Multi-physical numerical modeling of a piezoelectric loudspeaker for hearing aid applications and experimental validation**

Gustavo C. Martins<sup>1</sup>, Leonardo Seki<sup>1</sup>, Júlio A. Cordioli<sup>1</sup>

<sup>1</sup>Department of Mechanical Engineering, Federal University of Santa Catarina, Florianópolis, Brazil

Email: [gustavo.martins@lva.ufsc.br](mailto:gustavo.martins@lva.ufsc.br)

Piezoelectric materials are widely used in applications involving miniaturized components. The application of these materials in hearing aid receivers presents technical and economic advantages such as reducing the number of parts of the system and its manufacturing cost. The modeling of a miniaturized piezoelectric loudspeaker for hearing aids involves multi-physical models with strong coupling between the involved physics. In the literature, analytical models of these components can be found. However, these analytical models usually involve very simple geometries and boundary conditions. These characteristics restrict the use of such models as a design tool for miniaturized piezoelectric loudspeaker analysis. This work presents multi-physical numerical models of miniaturized loudspeaker prototypes. The numerical models were constructed using the Finite Element Method (FEM). The loudspeakers are composed of a piezoelectric diaphragm coupled to small cavities with different depths, and the multi-physical model includes the coupled piezoelectric, structural and acoustic behaviors of the systems. For the cavity with reduced depth, thermal and viscous effects on the acoustic propagation are taken in account in the FEM model. Finally, experimental tests of the piezoelectric diaphragm alone and coupled with the acoustic cavities are used to validate the multi-physical model.



## Barium-Strontium-Titanate Thin Film Varactors Integrated on Low-resistivity Silicon and Sapphire Substrates

Hailing Yue<sup>1</sup>, Dustin Brown<sup>1</sup>, Guru Subramanyam<sup>1</sup>, Kevin Leedy<sup>2</sup>, Charles Cemy<sup>2</sup>

<sup>1</sup>Department of Electrical Engineering, University of Dayton, Dayton, Ohio/The United States

<sup>2</sup>Air Force Research Laboratory, Wright Patterson AFB, Dayton, OH/The United States

Email: yueh01@udayton.edu

Barium-Strontium-Titanate(BST) thin film based ferroelectric varactors are designed for specific capacitance values at 0V dc bias on CMOS compatible low-resistivity silicon substrates and sapphire substrates. The BST varactor device operation is based on the nonlinear dielectric tunability of BST thin film sandwiched between two metal layers in an optimized conductor-backed coplanar waveguide(CBCPW) transmission line configuration(Fig. 1). The effective varactor capacitance at 0V dc bias is determined by the overlap area between the CPW signal line in the top metal electrode and a shunt line in the bottom electrode.

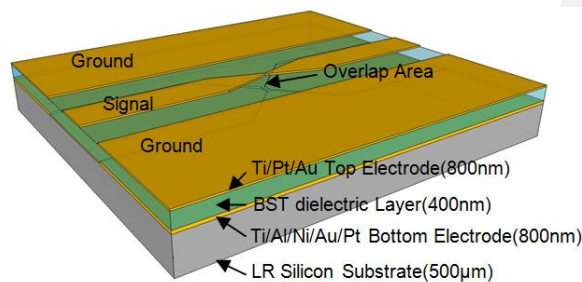


Fig. 118: 3D view of the standard BST varactor device.

Devices with 0V bias effective capacitances ranging from 0.8pF to 4.8pF were designed and fabricated by changing their corresponding overlap areas calculated from the generic parallel-plate capacitance equation. A schematic model was also utilized to extract the designed and measured capacitances. The relationship between the sizes of the overlap areas and the extracted capacitances from both electromagnetic and matched schematic models is demonstrated by a reasonable agreement with the experimental measurements from the fabricated devices on low-resistivity silicon substrates. Following the same procedure, devices with higher 0V capacitances ranging from 5 pF to 50pF were also designed and fabricated on sapphire substrate with three variations from standard configuration aiming to reduce the parasitic resistance. The experimental results from these highly capacitive device and their variations also agrees with the simulation results.

## High Energy Density composites Based on Poly (vinylidene fluoride-chlorotrifluoroethylene) and lanthanum doped lead zirconate titanate stannate antiferroelectric ceramic

Fei Wen, Weimin Xia, Xiaoyong Wei, Zhuo Xu

Electronic Materials Research Laboratory, Key Laboratory of the Ministry of Education & International Center for Dielectric Research, Xi'an Jiaotong University, Xi'an 710049. P. R. China

Email: wen.1205@stu.xjtu.edu.cn

### Abstract

Recently, the investigation of dielectric materials with high energy density for high pulse capacitors application have attracted considerable attention, especially since the poly(vinylidene fluoride) (PVDF) based ferroelectric elastomers were reported.<sup>374</sup> In an effort to further enhance the energy storage properties of the fluoro-polymers, several inorganic fillers were introduced into these fluoro-elastomers as well. At present, the inorganic fillers are most focused on antiferroelectrics, ferroelectrics, and linear dielectrics. The antiferroelectrics is favorable candidate because it can be released the total stored charges due to the absence of any remnant polarization.

The lanthanum doped lead zirconate titanate stannate antiferroelectric ceramic ( $\text{Pb}_{0.97}\text{La}_{0.02}$ )( $\text{Zr}_{0.65}\text{Sn}_{0.25}\text{Ti}_{0.10}$ ) $\text{O}_3$  (PLZST) was used for inorganic fillers. Three series of (PLZST)/P(VDF-CTFE) composites with varied compositions were fabricated via solution cast process followed by thermally treated in different ways. Quenching the composite samples at lower temperature could effectively enhance their dielectric constant, breakdown strength as well as the energy density. The highest energy density ( $12.1\text{J}/\text{cm}^3$ ) is observed in quenched from  $200^\circ\text{C}$  to  $-195^\circ\text{C}$  with 5 vol% PLZST as shown in table 1, which is much higher than that reported in the current literature. As the PLZST content increasing, the dielectric permittivity and energy density measured under the same electric field increases. However, the dielectric breakdown strength and the energy density measured at breakdown strength of the resultant composites decrease as PLZST content increasing.

TABLE I. Discharged energy density ( $U_e$ ) of PLZST/P(VDF-CTFE) composites under varied electric field.

PLZST content vol%	$U_e$ ( $\text{J}/\text{cm}^3$ ) of $Q_{100}$ at various $E$ (MV/m)			$U_e$ ( $\text{J}/\text{cm}^3$ ) of $Q_{94}$ at various $E$ (MV/m)			$U_e$ ( $\text{J}/\text{cm}^3$ ) of $Q_{-195}$ at various $E$ (MV/m)		
	100	200	$E_b$	100	200	$E_b$	100	200	$E_b$
0	0.30	1.17	4.82	0.51	2.06	12.4	0.40	1.69	11.3
5%	0.37	1.38	4.10	0.61	2.42	10.5	0.70	2.77	12.1
10%	0.46	1.81	4.84	0.58	2.32	7.56	0.62	2.47	5.73
15%	0.55	2.26	5.07	0.81	3.11	7.15	0.71	2.58	5.40
20%	0.56	2.22	2.96	0.93	3.11	6.22	0.67	2.80	3.42
25%	0.69	2.47	2.67	0.71	3.26	3.26	1.06	3.60	4.25
30%	0.71	-	2.18	1.20	-	2.94	1.09	-	2.84
40%	0.74	-	1.41	1.46	-	2.46	1.35	-	2.72

“-”denotes the sample is broken under the corresponding electric field.

<sup>374</sup> B. Chu, X. Zhou, K. Ren, B. Neese, M. Lin, Q. Wang, F. Bauer, and Q. M. Zhang, “A Dielectric Polymer with High Electric Energy Density and Fast Discharge Speed”, *Science*, vol.313, p.334-336, 2006.

## Flexible Piezoelectric Energy Harvesters Fabricated by $\text{KNbO}_3$ Nanowires

Mi-Ri Joung<sup>1</sup>, Haibo Xu<sup>1</sup>, Jin-Seong Kim<sup>1</sup>, In-Tae Seo<sup>1</sup>, Sahn Nahm<sup>1,2</sup>, Seok-Jin Yoon<sup>3</sup>, Chong-Yun Kang<sup>2,3</sup>

<sup>1</sup>Department of Materials Science and Engineering, Korea University, Seoul, Korea

<sup>2</sup>Department of Information Technology-Nano Science, Korea University-Korea Institute of Science and Technology School, Korea University, Seoul, Korea

<sup>3</sup>Electronic Materials Center, Korea Institute of Science and Technology, Seoul, Korea

Email: miri0805@korea.ac.kr

Tetragonal  $\text{KNbO}_3$  (KN) nanowires were formed when the synthesis was carried out at  $120^\circ\text{C}$  for 48 h. However, when the fabrication was conducted at high temperatures ( $\geq 150^\circ\text{C}$ ) or at  $120^\circ\text{C}$  for a long period of time ( $\geq 72$  h), orthorhombic KN nanowires were obtained. Moreover, the KN nanowires synthesized at  $120^\circ\text{C}$  for 60 h showed a morphotropic phase boundary (MPB) structure in which both tetragonal and orthorhombic structures coexisted. A tetragonal KN nanowire exhibited a  $d_{33}$  value of 137.1 pm/V, which is larger than that of the orthorhombic KN nanowire (104.5 pm/V), probably because of the softening effect of the metal vacancies. The MPB KN nanowires exhibited a larger  $d_{33}$  value of 146.0 pm/V. Three types of the KN nanowires were mixed with Polydimethylsiloxane (PDMS) and these mixtures (PDMS-KN) were deposited on the Au-coated Polyimide (PI) substrate. Finally, the Au-coated PI was covered on the PI/Au/PDMS-KN device to fabricate the piezoelectric energy harvester. In these work, three types of KN piezoelectric energy harvesters were fabricated and the output power of these harvesters were investigated. Moreover, the magnitude of their output power was explained based on the structural and piezoelectric properties of the KN nanowires.

## Polymer Matrix-Based Piezoelectric Composite for Structural Health Monitoring

Walter Katsumi Sakamoto<sup>1</sup>, Ricardo Tokio Higuti<sup>2</sup>, Evelyn Brazoloto Crivelini<sup>1</sup>, Haroldo Naoyuki Nagashima<sup>1</sup>.

<sup>1</sup>Departamento de Física e Química, Universidade Estadual Paulista - UNESP, Ilha Solteira, São Paulo, Brazil.

<sup>2</sup>Departamento de Engenharia Elétrica, Universidade Estadual Paulista - UNESP, Ilha Solteira, São Paulo, Brazil.

Email: sakamoto@dfq.feis.unesp.br

Structural health monitoring (SHM) refers to the procedure of assessing the structure conditions continuously so it is an alternative to conventional nondestructive evaluation (NDE) techniques<sup>375</sup>. With the growing developments in sensor technology acoustic emission (AE) technology has been attracting attention in SHM applications. AE are characterized by waves produced by the sudden internal stress redistribution caused by the changes in the internal structure, such as fatigue, crack growth, corrosion, etc. Piezoelectric materials such as Lead Zirconate Titanate (PZT) ceramic have been widely used as sensor due to its high electromechanical coupling factor and piezoelectric  $d$  coefficients. Because of the poor mechanical characteristic and the lack in the formability of the ceramic, polymer matrix-based piezoelectric composites have been studied in the last decade in order to obtain better properties in comparison with a single phase material. In this study a composite film made of polyurethane (PU) and PZT ceramic particles partially recovered with polyaniline (PAni) was characterized and used as sensor for AE detection. Figure 1 shows the photo of the experiment and the response of the sensor to a pencil lead break simulated AE source recorded by an oscilloscope. Preliminary results indicate that the presence of a semiconductor polymer (PAni) recovering the ceramic particles, make the poling process easier and less time consuming. Also, it is possible to observe that there is a great potential to use such type of composite as sensor for structure health monitoring.

---

<sup>375</sup> H-S. Yoon; D. Jung; J-H. Kim, "Lamb wave generation and detection using piezoceramic stack transducers for structural health monitoring applications, Smart Mater. Struct., 21, 055019 (2012).

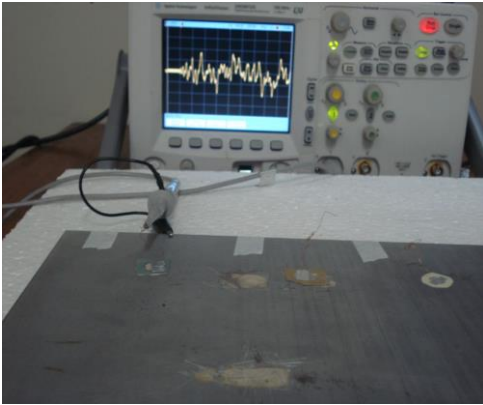


Fig. 1. – PZT-PAni/PU composite surface mounted on aluminum plate. Pencil lead break was used as simulated AE source.

## Piezoelectricity of New Peptide-Based Materials

Maciej Wojtaś<sup>1,2</sup>, Andrei Kholkin<sup>2</sup>

<sup>1</sup>Faculty of Chemistry, University of Wrocław, Wrocław, Poland

<sup>2</sup>CICECO, University of Aveiro, Aveiro, Portugal

Email: m.wojtas@ua.pt

Piezoelectricity is the ability of noncentrosymmetric crystals to produce mechanical stress/strain under electric field or charge under mechanical stress. This property has long been used in acoustic transducers, sensors/actuators, piezomotors, and more. Pushed by the technology progress, superior energy density, and low energy consumption, piezoelectrics have recently experienced a drastic miniaturization giving rise to a new direction commonly abbreviated as piezoMEMS (for MicroElectroMechanical Systems).

The new organic and bioorganic materials having significant piezoactivity are indispensable to revolutionize the piezoMEMS. However, as for today, only weak piezoelectric effects in bioorganic materials have been observed. Therefore, the search for micro- and nanoscale piezoelectric materials has drawn much attention in the last decades.

We present the new peptide-based materials of interesting physicochemical properties (including piezoelectricity). These materials are characterized by the wide variety of structures created giving opportunity to design and develop new nanoscale devices, to name only a few: biosensors, piezoMEMS or in drug transport/carrier applications.

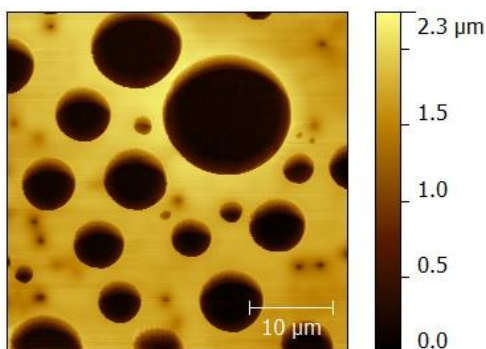


Figure 119 The example of the peptide-based nanostructure.

## Evaluation of the performance of a piezoelectric nanowire-based composite microgenerator

Olivier Graton<sup>1</sup>, Guylaine Poulin-Vittrant<sup>2</sup>, Louis-Pascal Tran Huu Hue<sup>2,3</sup> and Marc Lethiecq<sup>2</sup>

<sup>1</sup>GREMAN UMR 7347, 16 rue Pierre et Marie Curie, Tours Cedex2 37071, France

<sup>2</sup>GREMAN UMR 7347, Rue de Chocolaterie, BP 3410, Blois Cedex 41034, France

<sup>3</sup>ENIVL, Rue de Chocolaterie, BP 3410, Blois Cedex 41034, France

Email: olivier.graton@univ-tours.fr

Recently, a new generation of piezoelectric micro-harvester based on ZnO nanowires (NWs) has been developed with promising results<sup>1</sup>. This kind of generators is made up of arrays of vertically or laterally aligned NWs wrapped in a polymer matrix. It works in quasi-static regime and thus seems to be well-adapted to harvest mechanical energy from low frequency natural sources.

In order to estimate the performance of such devices, we have developed a new model of NW-based microgenerator. If a single ZnO NW can be seen as a one-dimensional piezoelectric nanotransducer, an array of NWs in a passive polymer matrix is rather comparable to a 1-3 piezocomposite. Thus, the polymer phase must be taken into account when simulating the mechanical and electrical behavior of the generator. Since the microgenerator works in quasi-static regime, we consider the composite as an effective homogeneous medium whose physical properties are expressed in terms of the volume fraction of ZnO. The equivalent circuit of the microgenerator is then established. As an application, we have modeled the microgenerator based on a vertical array of NWs presented in<sup>1</sup>.

Numerical results showed a good agreement with experimental results given in the cited paper, both in terms of open-circuit voltage and short-circuit current. We have also studied the impact of the composite material parameters on the microgenerator performance. It has been found that its power density is proportional to the square of the volume fraction of ZnO (Fig. 1).

This model seems to be well adapted to NW-polymer based micro-harvesters and should be extended to lateral NWs array configurations. Finally, by performing an exhaustive parametric study, this equivalent circuit could be a valuable tool for both design and performance prediction of NWs based microgenerators.

1. S. Xu. et al., "Self-powered nanowire devices", Nat. Nanotechnol., vol. 5, p. 366-373, 2010.

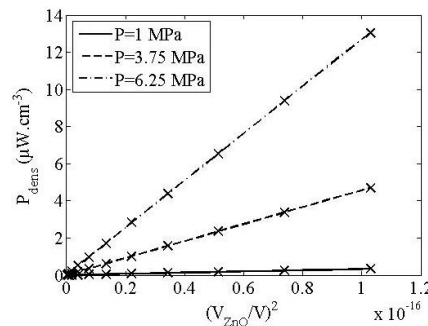


Fig. 120: Computed power density of the microgenerator excited by a low frequency (5 Hz) compressive stress.

## Piezoelectric PZT Fiber Composite as a Low Frequency Vibration Sensor

Qian Chen<sup>1</sup>, Yingying Sun<sup>1</sup>, Lifeng Qin<sup>2</sup>, Hao Hue<sup>2</sup>, and Qing-Ming Wang<sup>1</sup>

<sup>1</sup>Department of Mechanical Engineering and Materials Science, University of Pittsburgh, Pittsburgh, PA, USA. Email: qiw4@pitt.edu

<sup>2</sup>Xiamen University, Xiamen 361005, P. R. China

The recently developed macro fiber composites (MFCs) with in-plane aligned PZT fibers embedded in polymeric thick films combine the excellent piezoelectric property of PZT fibers and the flexibility of polymer, which are suitable for many sensor and actuator applications<sup>376,2</sup>. In this paper, we present both theoretical and experimental studies of a low frequency vibration sensor using the PZT fiber composite in a simple cantilever structure.

The constitutive relations for the in-plane aligned PZT fiber composite with interdigitated transducer (IDT) electrodes were derived and an analytical model for calculating the material effective parameters was obtained. The global properties of PZT fiber composite were then calculated and validated with results obtained by mixing rule and data from literatures. These global parameters of the PZT fiber composite were then substituted into the lumped and distributed parameter models for cantilevered piezoelectric unimorph vibration sensors to predict the voltage output sensitivity and frequency response. Finally, experimental studies were carried out and the predicted performance of the low frequency vibration sensor agrees well with the experimental results. Shown in Fig. 1 is the experimentally schematic of the PZT fiber composite cantilever tested as a low frequency vibration sensor; and Fig. 2 is the experimental and calculation results of the frequency response of output voltage per unit vibration amplitude for a MFCs unimorph. With excellent flexibility, tailorable elastic, dielectric and piezoelectric properties, and large time constant, the PZT fiber composite works well as vibration sensor that has very low resonant frequency.

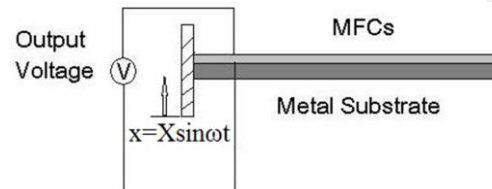


Fig. 121: The schematic of the MFCs unimorph vibration sensor.

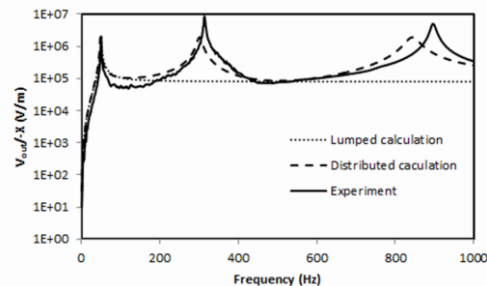


Fig. 122: Experimental and calculation results of the frequency response of output voltage per unit vibration amplitude for a PZT MFCs unimorph

<sup>376</sup> A. Bent, and N. W. Hagood, "Piezoelectric fiber composites with interdigitated electrodes," *J. Intell. Mater. Syst. Struct.*, vol. 8, no. 11, pp. 903-919, 1997.

<sup>2</sup> Deraemaeker, H. Nasser, A. Benjeddou, and A. Preumont, "Mixing rules for the piezoelectric properties of macro fiber composites," *J. Intell. Mater. Syst. Struct.*, vol. 20, no. 12, pp. 1475-1482, 2009.



## 3D Sensor Based on Polyvinylidene Fluoride (PVDF)

Yung Ting, Hariyanto Gunawan, Jain-Zhi Zhong and Kai-Jian Zheng

Department of Mechanical Engineering, Chung Yuan Christian University, Chung Li, Taiwan

Email: yung@cycu.edu.tw

Polyvinylidene Fluoride (PVDF) material is one of electroactive material which has high sensitivity and good response. In this study, it is attempted to build a 3D sensor based on polyvinylidene fluoride (PVDF) material. For existing 3D sensors, they are usually constructed with three layers. Each layer is in charge of the response of one axis individually. Distinguish from these sensors, a new developed 3D sensor is designed with only one layer that can measure the response of all three axis simultaneously. Thin, flexible, and high sensitivity are the advantages of this 3D sensor. An example of 40x40x0.01mm of stretched PVDF is built. Combination of polarization in thickness and planar direction are applied in order to produce 3D sensor. The piezoelectric constant of PVDF is measured by using FTIR and DSC characterization and voltage response of PVDF is measured using oscilloscope. Fig. 1 shows the designed 3D sensor. As shown,  $(X_1, X_2)$ ,  $(Y_1, Y_2)$ ,  $(Z)$  represent the measure along the X, Y, and Z axis respectively. To measure the voltage response of 3D sensor, vertical and horizontal force of about 1.96 N is applied to the sample respectively as shown in Fig. 2. Voltage response of 3D sensor is measured and shown in Fig 3a and Fig 3b for the case of applied vertical and horizontal force respectively. As seen in Fig 3, voltage response in X, Y, Z-axis can be measured simultaneously while a force is applied. Regarding some other important characteristics, measurement data and discussion will also be presented and addressed later.

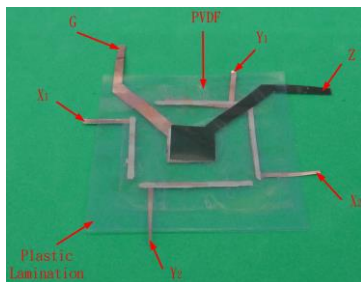
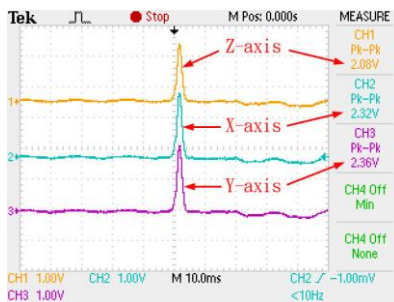


Fig. 1. Design of 3D Sensor.



(a)

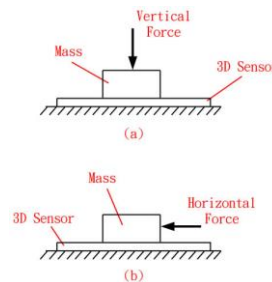
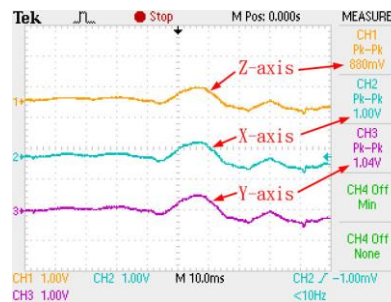


Fig. 2. Scheme of Applying Force



(b)

Fig. 3 Voltage response of 3D sensor when applying: (a) Vertical force, (b) Horizontal force

## **Bi<sub>2</sub>(Zn<sub>2/3</sub>Nb<sub>4/3</sub>)O<sub>7</sub>/Epoxy composites with enhanced dielectric properties for embedded capacitor applications**

Yuanyuan Bai<sup>1</sup>, Hong Wang<sup>1</sup>, Feng Xiang<sup>1</sup>, Yu Ke<sup>1</sup>, Yujuan Niu<sup>1</sup>

<sup>1</sup>Electronic Materials Research Laboratory, Key Laboratory of Ministry of Education,  
Xi'an Jiaotong University, Xi'an 710049, China  
Email: bai.yuanyuan@stu.xjtu.edu.cn

In the present work, Bi<sub>2</sub>(Zn<sub>2/3</sub>Nb<sub>4/3</sub>)O<sub>7</sub> (BZN) ceramic filled epoxy based composites were prepared using ball-milling mixing followed by solution casting process. The BZN/Epoxy composite exhibits enhanced dielectric permittivity and reduced loss tangent in the microwave frequency range from 5 GHz to 20 GHz.

The dielectric permittivity and loss tangent of the BZN/Epoxy composites were investigated as a function of the volume fraction of BZN powders. The dielectric permittivity and loss tangent of the composite with 40% volume fraction of filler loading was 11.6 and 0.02, respectively, at 5 GHz. The results indicated that the incorporation of pyrochlore BZN ceramic powders could greatly enhance the dielectric permittivity and decrease the loss tangent of the BZN/Epoxy composite, making the BZN/Epoxy composite a desirable candidate for embedded capacitor applications. In addition, the measured dielectric constant and loss factor were in well consistence with the effective medium theory and the parallel formula, respectively.

Furthermore, the comparison of the dielectric properties between the composite with BZN particles milled by regular ball-milling and that with BZN particles milled by high-energy ball-milling indicated that high-energy ball-milling contributed to enhance the dielectric permittivity of the composite at low frequency range.

## Electrocaloric properties of $0.7\text{Pb}(\text{Mg}_{1/3}\text{Nb}_{2/3})\text{O}_3-0.3\text{PbTiO}_3$ ceramics

Marko Vrabelj<sup>1,2</sup>, Hana Uršič<sup>1,3</sup>, Brigita Rožič<sup>1,3</sup>, Zdravko Kutnjak<sup>2,4</sup>, Silvo Drnovšek<sup>1,3</sup>, Barbara Malič<sup>1,2</sup>

<sup>1</sup>Electronic Ceramics Department, Jožef Stefan Institute, Ljubljana, Slovenia

<sup>2</sup>Jožef Stefan International Postgraduate School, Ljubljana, Slovenia

<sup>3</sup>Centre of Excellence NAMASTE, Ljubljana, Slovenia

<sup>4</sup>Condensed Matter Physics Department, Jožef Stefan Institute, Ljubljana, Slovenia

Email: marko.vrabelj@ijs.si

The electrocaloric (EC) effect is a conversion of electrical energy to heat and may be defined as an adiabatic and reversible temperature change that occurs in a polar material upon external electric field. The aim of our work was to prepare  $0.7\text{Pb}(\text{Mg}_{1/3}\text{Nb}_{2/3})\text{O}_3-0.3\text{PbTiO}_3$  (0.7PMN–0.3PT) ceramics and to study the EC temperature change ( $\Delta T$ ) vs. applied electric field and temperature.

For the synthesis of the 0.7PMN–0.3PT bulk ceramics, PbO, MgO, TiO<sub>2</sub> and Nb<sub>2</sub>O<sub>5</sub> were used. The homogenized, stoichiometric powder mixtures were mechanochemically activated in a high-energy planetary mill. The synthesized powders were milled in an attrition mill in isopropanol. The powder compacts were sintered at 1200 °C for 2 h in a double alumina crucible in the packing powder. The ceramics had relative density 97 % and the grain size of  $(1 \pm 0.5)$  μm.

In order to study EC effect by direct approach, a high resolution calorimeter was used. The observed magnitudes of the EC effect confirm the existence of the large effect in this material. A characteristic peak of  $\Delta T$  as a function of the electric field is observed near the critical point as shown in Fig. 1, where  $\Delta T$  is 2.7 K at 90 kV/cm and 430 °C.<sup>377</sup>

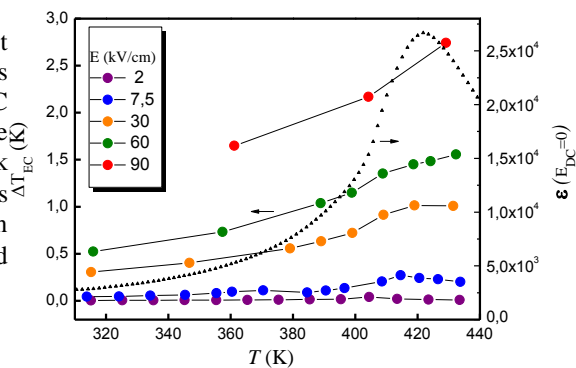


Fig. 123: EC temperature change  $\Delta T$  of 0.7PMN–0.3PT ceramics as a function of temperature for several amplitudes of the electric field. Triangles denote the dielectric constant.<sup>1</sup>

Acknowledgments:

The contribution of Prof. Marija Kosec who passed away in December 2012 is gratefully acknowledged. The authors would like thank Jena Cilenšek, Brigita Kmet and David Žehelj for

<sup>377</sup> B. Rožič, M. Kosec, H. Uršič, J. Holc, B. Malič, Q. M. Zhang, R. Blinc, R. Pirc, Z. Kutnjak, Influence of the critical point on the electrocaloric response of relaxor ferroelectrics, *J. Appl. Phys.*, vol. 110, p. 064118 1-5, 2011.

their help with the experimental work and the Slovenian Research Agency for financial support (research program P2-0105 and doctoral program PR-05025).

## Experimental and numerical characterization of a hearing aid prototype microphone with piezoelectric membrane

Israel Pereira<sup>1</sup>, Gustavo Martins<sup>1</sup>, Júlio A. Cordioli<sup>1</sup>,

<sup>1</sup>Mechanical Engineer Department, Federal University of Santa Catarina, Florianópolis, SC/Brazil

Email: israel.pereira@live.com

The microphone is an important component of hearing aids. They are responsible for converting acoustic energy into electrical energy and a proper design of this component is critical to obtain good results in everyday life of hearing aids users. Electret microphones are the current first choice in this kind of application but alternative designs of microphones are also been considered.

Piezoelectric microphones have numerous advantages over electret microphones, like the reduced number of components, very flat frequency response and high resistance to mechanical shocks. Furthermore, piezoelectric microphones can have very simple constructions, ensuring reduced manufacturing costs. The main difficulty of using this type of microphone in hearing aids is its typical lower sensitivity when comparing to electret ones. Many efforts are in progress to increase the sensitivity of piezoelectric microphones and one of the most important tools to achieve that is a proper numerical modeling of these transducers.

This paper presents the numerical modeling of a piezoelectric prototype used as a microphone. The transducer is modeled with different variations of the Finite Element Method (FEM), including the traditional coupled Acoustic-Structure FEM and a modified formulation that includes the effects of viscothermal losses in the model. Also, an analysis of the load applied to the piezoelectric model is performed in order to obtain realistic results.

The model is validated with experimental results and its sensitivity level is compared with commercial microphones. After the validation, the numerical model can be used to optimize the piezoelectric microphone properties in order to fulfill the requirements for hearing aids.

# A Flexible Piezoelectric Power Generator Based on Self-assembled, Highly <001> Oriented BaTiO<sub>3</sub> Micro Platelet Thin Layer by an Interfacial Strategy

Hao Xue<sup>†</sup>, Donghua Fan<sup>†</sup>, Zhaoxian Xiong<sup>†</sup>, Qing-Ming, Wang,<sup>\*\*‡</sup>

<sup>†</sup>Department of Materials Science and Engineering, College of Materials, Xiamen University, Xiamen 361005, P. R. China. Email: qiw4@pitt.edu

<sup>‡</sup>Department of Mechanical Engineering and Materials Science, University of Pittsburgh, Pittsburgh, PA, 15261, USA

Energy harvesting technologies that convert existing sources of energies, such as mechanical energy from the natural sources of wind, ocean waves, vibration of structure, and human or animal movements into electrical energy, is attracting tremendous interest in the scientific community<sup>378,2</sup>. In this paper, we present a flexible piezoelectric generator based on self-assembled, highly <001> oriented BaTiO<sub>3</sub> micro platelet like thin film layer embedded in soft polymer matrix. Perovskite ferroelectric materials often exhibit evidently anisotropic characteristics on piezoelectricity. We successfully controlled the morphology and orientations of BaTiO<sub>3</sub> micro platelet like crystals through a chemical processing, and subsequently obtained the highly <001> oriented BaTiO<sub>3</sub> by a facile interfacial self-assembled approach. The assembled BaTiO<sub>3</sub> was packaged with PDMS and coated with top and bottom electrodes. The composite films were poled by an electric field at room temperature, and then attached on a flexible substrate to form a piezoelectric generator. Fig.1 shows the obtained BaTiO<sub>3</sub> micro platelets. By comparison with random oriented BaTiO<sub>3</sub> based piezoelectric generator, this <001> oriented BaTiO<sub>3</sub> film based piezoelectric produced evidently higher output voltage and current under dynamic periodic load by applying a harmonic force. The <001> oriented BaTiO<sub>3</sub> film based piezoelectric generator were using to harvest the energy of human body movement and the generator fixed on finger provided the highest open circuit output voltage of 0.53v and Short-circuit current of 70nA, respectively.

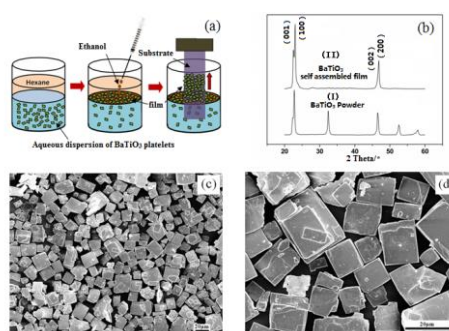


Fig. 124: a) Illustration of the self-assembly of the BaTiO<sub>3</sub> micro-platelets at the hexane/water interface and the transfer procedure. b)The XRD pattern of samples: (i) BaTiO<sub>3</sub> plate-like particles, (iv) BaTiO<sub>3</sub> self assembled film by an interfacial strategy; c) and d)SEM images of the highly oriented BaTiO<sub>3</sub> film transferred onto plastic substrate.

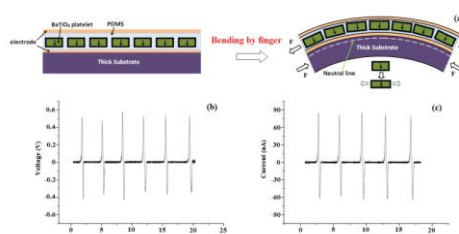


Fig. 125: (a) Schematics of the cross-sectional structure of <001> oriented BaTiO<sub>3</sub> film based piezoelectric generator bended by finger movement; (b) The open circuit output voltage generated from <001> oriented BaTiO<sub>3</sub> film based piezoelectric generator bended by finger movement; (c) The short circuit output current generated from <001> oriented BaTiO<sub>3</sub> film based piezoelectric generator bended by finger movement.

<sup>378</sup> Yang, R. S., Qin, Y., Dai, L. M. & Wang, Z. L. Power generation with randomly oriented piezoelectric ferroelectric

<sup>2</sup> Choi, D. et al. Fully Rollable Transparent Nanogenerators Based on Graphene Electrodes. Adv Mater 22, 2187 (2010).

# Photocurrent Characteristics of PbTiO<sub>3</sub>/TiO<sub>2</sub> Heterostructure Nanotubes using Anodic TiO<sub>2</sub> Nanotubes

Sung Sik Won<sup>\*</sup>, Chang Won Ahn and Ill Won Kim

Department of Physics and Energy Harvest-Storage Research Center,  
University of Ulsan, Ulsan 680-749, South Korea

When electrically poled ferroelectric materials are illuminated by light beam, photo-voltage and photo-current can be generated due to the separation of photoinduced electrons and holes by its internal electric field. Such photovoltaic phenomena in the ferroelectric thin films exhibit potential applications for realizing remote control and wireless energy transfer in microelectromechanical system (MEMS) devices. In this study, we have grown TiO<sub>2</sub> nanotube layers on sputter-deposited Ti thin films by glycerol/NH<sub>4</sub>F electrolytes. PbTiO<sub>3</sub>/TiO<sub>2</sub> heterostructure nanotube was obtained by deposited Pb into the highly ordered TiO<sub>2</sub> nanotube layers and thermally annealed in the oxygen ambient. The crystalline structure and surface morphology of PbTiO<sub>3</sub>/TiO<sub>2</sub> heterostructure nanotubes were investigated by XRD and FE-SEM studies. Compared with pure TiO<sub>2</sub> nanotube array, the PbTiO<sub>3</sub>/TiO<sub>2</sub> heterostructures exhibited enhanced photocurrent under UV light irradiation.



## Planar acoustic metamaterials with the active control of acoustic impedance using a piezoelectric composite actuator

K. Nováková<sup>1</sup>, P. Mokřý<sup>2</sup>, J. Václavík<sup>2</sup>, P. Márton<sup>2</sup>, M. Černík<sup>2</sup>, P. Psota<sup>1</sup>, R. Doleček<sup>1</sup>, V. Lédl<sup>1</sup>

<sup>1</sup>Regional Centre for Special Optics and Optoelectronic Systems (TOPTEC),  
Sobotecká 1660, CZ-51101 Turnov, Czech Republic

<sup>2</sup>Institute of Mechatronics and Computer Engineering, Technical University of Liberec  
Studentská 2, Liberec I, CZ-46117 Czech Republic

Email: novakova@ipp.cas.cz

Noise and vibrations affect our lives and the intensity of generated noise and vibrations has become an important parameter indicating the quality of the environment. One of the major noise sources in our homes and offices are vibrations of windows and glazed facades. Propagation of acoustic energy in an acoustic medium and the reflection of noise at interfaces of two different media are controlled by a physical property called the acoustic impedance  $Z$ . By specified tuning the acoustic impedance of the planar structure at the interface of acoustic media one can achieve devices such as perfectly absorbing surfaces or perfect sound shields. It is clear that realization of two aforementioned devices usually requires such values of the acoustic impedance that are not observed in nature. Such systems are generally called acoustic metamaterials.

In the Paper, there are presented methods for a precise active control of the acoustic impedance of large planar structures, e.g glass plates or shells, by means of distributed flexible piezoelectric composite actuators which are connected to passive or active electronic shunt circuits. Design of tunable acoustic metamaterials is realized using Finite Element Method simulations and their acoustic properties are evaluated using acoustic transmission loss measurements (Fig. 1). Static and dynamic displacements of the metamaterials produced by electric voltage are measured using Digital Holographic Interferometry. We believe that deep understanding of presented systems should result in future applications that improve the quality of everyday life. This work was supported by Czech Science Foundation Project No.: GACR 13-10365S.

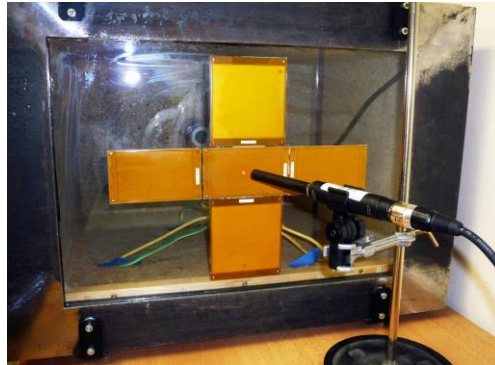


Fig. 126: Acoustic transmission loss measurement setup. Electronically tunable acoustic metamaterial vibrates due to the incident acoustic wave and transmits one part of the wave to the other side. Both acoustic pressures and vibration amplitude are measured and the acoustic transmission loss is computed.

## Stress and Temperature Dependent Properties of Single Crystal Piezoelectric Materials and Devices

D.C. Markley<sup>1</sup>, R.J. Meyer, Jr.<sup>1</sup>, Z. G. Lowe<sup>1</sup>, N.P. Sherlock<sup>1</sup>, and P. Mosbah<sup>2</sup>

<sup>1</sup>Applied Research Laboratory, The Pennsylvania State University, State College, PA USA

<sup>2</sup>Department of Acoustics, Institut Supérieur d'Electronique et du Numérique, Lille, France

Email: rmeyer@psu.edu

Work has been done to understand the stress and temperature dependent properties of the active materials used in SONAR transducers. Increased power and duty cycle demands push these devices closer to their stress and thermal limits. Demanding environmental conditions make predicting performance difficult due to changes in material properties. New single crystal piezo-electrics have larger degrees of non-linearity in both stress and temperature than typical ceramics, such as PZT-8. This presentation addresses measurement results obtained in experiments at the Applied Research Laboratory to determine the effects of the dynamic and static stress, elevated temperatures, and high electric fields on material properties and device behavior to provide feedback and validation of the new fully non-linear solution procedure in the ATILA finite element program. Dynamic stress and strain measurements were made on unconstrained 33-mode bar samples for PZT 8 and PZT 4 ceramics and single crystals of PMNT, PIMNT and Mn doped PIMNT. Mechanical prestress and thermal effects were determined using symmetrically loaded “dumbbell” transducers. An Agilent 4294A Impedance Analyzer was used for small signal measurements of complex impedance and capacitance to calculate mechanical and dielectric losses. The LDV was used to obtain the effective  $d_{33}$  of the entire device by measuring displacement at the face of the end mass. A status of the ATILA++ finite element code will also be provided.

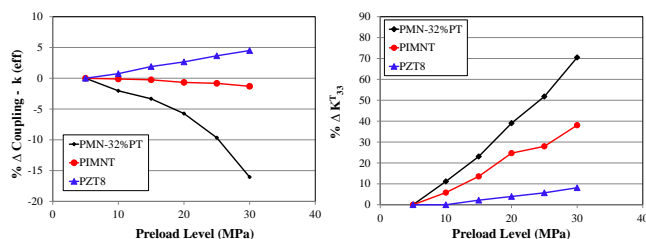


Fig.1 Measured small signal changes in effective coupling coefficient and dielectric constant plotted as a function of increasing static preload on dumbbell style transducers samples.

## Piezoelectric polymer multilayers on flexible substrate for energy harvesting

Lei Zhang, Sharon Su Yin Oh, Ting Chong Wong, Chin Yaw Tan and Kui Yao  
Institute of Materials Research and Engineering, A\*STAR (Agency for Science, Technology and Research), 3 Research Link, Singapore 117602

Email: [k-yao@imre.a-star.edu.sg](mailto:k-yao@imre.a-star.edu.sg)

Piezoelectric materials possess inherent functions of converting mechanical energy into electrical energy and they are competitive candidates for harvesting mechanical energy from ambient environments. One of major disadvantages of piezoelectric materials, particularly piezoelectric polymers, for energy harvesting is the low current output with high voltage magnitude due to the high impedance of piezoelectric materials. The high impedance of piezoelectric materials also affects the energy output to a typical external load as a result of impedance mismatch. Adoption of piezoelectric multilayer structure is an effective method to overcome this issue, particularly for piezoelectric polymer materials, by providing reduced impedance, increased current output and adjustable impedance for matching the external load impedance.

In this work, piezoelectric polymer multilayer structure is fabricated on flexible substrate and operates in bending mode for energy harvesting. Analytical and numerical models are developed to understand the effect of material parameters which are critical to the energy harvesting performance of the piezoelectric multilayer structure on flexible substrate. The relationship among the maximum output power of the piezoelectric multilayer on flexible substrate, the piezoelectric coefficient and the dielectric permittivity is established. It is also found that the thickness of the internal electrodes of piezoelectric multilayer significantly affects the electric energy generation in the bending mode. The effect of impedance matching is clearly illustrated with comparison between a piezoelectric multilayer and a piezoelectric single layer on the same flexible substrate for bending-mode energy harvesting. Dramatic improvement on energy output is shown for a 22-layer P(VDF-TrFE) multilayer structure on flexible substrate compared to that of a single-layer of the similar configuration with the load resistance range of 25  $\Omega$  to 25 k $\Omega$ . A 10-layer P(VDF-TrFE)-based multilayer structure is fabricated by solution coating process on flexible aluminum substrate with multiple thin layer of internal metal electrodes prepared by physical vapor deposition method. The experimental results of energy output is evaluated with electrical loading, which indicates that the energy generated is adequate for many low power electronics.

**Photovoltaic effect of Bi-layered  $(\text{Na}_{0.82}\text{K}_{0.18})_{0.5}\text{Bi}_{4.5}\text{Ti}_4\text{O}_{15}$  thin films  
with different Pt and ITO top electrodes**

Won Seok Woo, Sung Sik Won, Chang Won Ahn, Song A Chae, and Ill Won Kim\*

Department of Physics and Energy Harvest-Storage Research Center,

University of Ulsan, Ulsan 680-749, S. Korea

\*E-mail: [kimiw@mail.ulsan.ac.kr](mailto:kimiw@mail.ulsan.ac.kr)

Recently, the photovoltaic of the ferroelectric materials, such as  $\text{Pb}(\text{Zr},\text{Ti})\text{O}_3$  (PZT),  $\text{BiFeO}_3$  (BFO), and  $\text{BaTiO}_3$  family, has become a research focus because it favors device miniaturization and exhibits ultraviolet (UV) regions with the potential applications for optical microsensing and microactuation in microelectromechanical systems (MEMS).

We have deposited  $(\text{Na}_{0.82}\text{K}_{0.18})_{0.5}\text{Bi}_{4.5}\text{Ti}_4\text{O}_{15}$  [NKBiT15] ferroelectric thin films by chemical solution deposition method and investigated photovoltaic behavior with different top electrodes of Pt and ITO sandwiched Bi-layered structure. The observed photocurrent of NKBiT15 films strongly depends on the wavelength of incident light beam. Maximum photocurrent of ITO/NKBiT15/Pt was obtained  $-27.75 \text{ nA/cm}^2$  at 352 nm and the band gap energy of NKBiT15 thin films was 3.52 eV. The maximum power conversion efficiency  $\eta$  for Pt/NKBiT15/Pt and ITO/NKBiT15/Pt capacitors are 0.010 and 0.035 % at the incident light beam intensity of  $300 \text{ mW/m}^2$ . The power conversion efficiency of ITO top electrode capacitor is 3.5 times larger than that of the Pt top electrode capacitor.

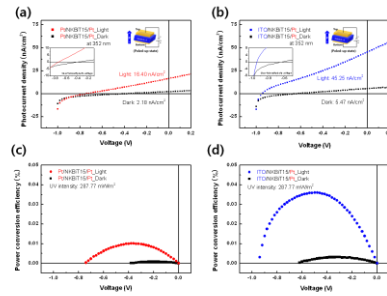


Figure show the typical photocurrent density of NKBiT15 thin films with top-electrodes (Pt and ITO) in poled-up state at wavelength of incident light beam from 300 to 500 nm. The inset of figure exhibits a schematic diagram of the experimental setup with poled up state.

## **Lead free piezoelectric AD layer for micro actuator**

Jun Akedo\*, Jae-Hyuk Park, and Muneyasu Suzuki

*National Institute of Advanced Industrial Science and Technology (AIST) 1-2-1 Namiki, Tsukuba  
305-8564 Japan*

High performance micro optical scanner with wide scanning angle, high speed scanning and large mirror size is strongly demanded for laser projection system and human detective sensor, which are expected huge market as piezoelectric actuator in the world. We demonstrate the lamb wave resonant optical scanning devices actuated by piezoelectric AD film and report their temperature properties and durability. Metal-based structure was introduced to reduce the production cost and to improve the optical scanning performance, simultaneously. The optical scanner with large mirror size of 1~5 mm square as well as high scanning angle of over 90 degree were fabricated. A high optical scanning angle (over 60 °) and high resonant frequency (over 30kHz) were achieved in ambient air without vacuum packaging. The resonant frequency and scanning angle of scanner were not change during life test for over 50,000 hours. In this report, BTO thick film as a lead free piezoelectric material was prepared by aerosol deposition (AD) method for fabrication of scanner devices. Piezoelectric  $d_{31}$  of BTO-AD film was approximately -138 pm/V. Also, the performance of optical scanner driven by AD-BTO thick film was compared with that by BTO bulk material and AD-PZT thick film. As the results, AD-BTO film can be used to practical applications.

## BiFeO<sub>3</sub> Thin Films for Photocatalytic Water Splitting

Wei Ji<sup>1,2</sup>, Kui Yao<sup>1\*</sup>, Yee Fun Lim<sup>1</sup> and Yung C. Liang<sup>2</sup>

<sup>1</sup>Institute of Materials Research and Engineering (IMRE), A\*STAR (Agency for Science, Technology and Research), 3 Research Link, Singapore 117602

<sup>2</sup>Department of Electrical and Computer Engineering, National University of Singapore, Kent Ridge, Singapore 119260

\*Email: k-yao@imre.a-star.edu.sg

Photoelectrolysis of water into hydrogen and oxygen is an attractive way to harvest the solar energy. It converts the solar energy into chemical energy, which is much easier to store than electricity. Semiconductor metal oxides have been widely used as photoanodes in photoelectrolytic cells due to their electrochemical stability. An ideal photoelectrolytic cell should be able to drive both the hydrogen and the oxygen evolutions without any external bias. However, the conduction bands in most of the oxides studied so far are too positive to drive the hydrogen evolution. Many of them also have a wide bandgap larger than 3 eV. Consequently, they are not able to absorb the visible region of the solar spectrum. New suitable materials are desired to achieve unassisted water splitting.

Ferroelectric BiFeO<sub>3</sub> (BFO) has a direct bandgap of about 2.7 eV. Previous studies have demonstrated its catalytic effects for water splitting under visible light<sup>379</sup>. However, the ferroelectric properties of BFO have not been explored in all these earlier reports. As has been shown in our earlier works, ferroelectric polarizations can significantly affect the photovoltaic (PV) process in epitaxial BFO thin films. The photocurrent direction can be switched by poling the BFO films in different directions<sup>380</sup>. This suggests that the ferroelectric polarization can be used to enhance the catalytic properties. In this work, we studied the photoelectrolytic water splitting reaction in high quality epitaxial BFO films. Significant anodic current is observed. The onset of the anodic photocurrent is at 0.210 V for the 223-nm-thick films. This is shifted to -0.036 V<sub>Ag/AgCl</sub> in the 112-nm-thick films. The thinner films minimize Ohmic losses and lead to the cathodic shift of the photocurrent onset. Furthermore, XPS measurements show that the band edges of BFO straddle the water redox levels. By considering both the energy band positions and the ferroelectric properties, we propose that BFO can potentially be used to achieve unassisted water splitting in a monolithic cell.

<sup>379</sup> F. Gao, et. al., "Visible-light photocatalytic properties of weak magnetic BiFeO<sub>3</sub> nanoparticles", *Adv. Mater.*, vol. 19, p. 2889-2892, 2007. J. Deng, et. al., "Bismuth iron oxide nanoparticles as photocatalyst for solar hydrogen generation from water", *J. Fund. Renew. Energ.*, vol. 1, p. 1-10, 2011.

<sup>380</sup> W. Ji, et. al., "Bulk photovoltaic effect at visible wavelength in epitaxial ferroelectric BiFeO<sub>3</sub> thin films", *Adv. Mater.*, vol. 22, p. 1763-1766, 2010.

## Actuator for precision positioning based on single crystalline lithium niobate

Ilya Kubasov<sup>1</sup>, Mikhail Malinkovich<sup>1</sup>, Aleksander Bykov<sup>1</sup>, Sedrak Grigoryan<sup>1</sup>

<sup>1</sup>National University of Science and Technology "MISIS", Moscow, Russian Federation

Email: kbasov.ilya@gmail.com

Bimorphs are widely used in actuators designed for precise positioning. Usually they are made of lead zirconate-titanate ( $\text{Pb}(\text{Zr}_x\text{Ti}_{1-x})\text{O}_3$ , PZT) piezoelectric ceramics because of its high piezoelectric coefficients values and high electromechanical conversion coefficient. At the same time PZT ceramics have low Curie temperature, high hysteresis, considerable temperature dependence of the piezoelectric modules, and creep. This disadvantages limit usage of the PZT made bimorphs and also make additional scanners calibration necessary.

In our previous work the ability to use single crystalline lithium niobate (LN) in the devices for precise displacement has been considered<sup>381</sup>. To realize bimorph structure it's necessary to form two domains with the opposite orientation of spontaneous polarization vector in a crystal plate. The bimorph based on LN single crystal has stability in wide temperature range due to  $T_c$  about 1200 °C, the absence of hysteresis and creep.

In this study bimorphs were made of single crystal LN plates by using non-uniform thermal field. Magnetron sputtering was used to make gold electrodes on the bimorph surface. Cantilevered bending displacements of the 6 cm LN bimorph were  $\approx \pm 20 \mu\text{m}$  in the voltage within  $\pm 300 \text{ V}$ . Single crystal LN bimorph actuators can be used for exact positioning in probe microscope techniques, for laser resonators adjustment and as wave guides with exact variable geometrical characteristics.

---

<sup>381</sup> Antipov V.V., Bykov A.S., Malinkovich M.D., Parkhomenko Y.N., "Formation of bidomain structure in lithium niobate single crystals by electrothermal method", *Ferroelectrics*, vol. 374, p. 701–708, 2008.

# NUMERICAL SIMULATION ANALYSIS FOR A NOVEL SHAPES OF PIEZOELECTRIC COUPLED WITH TUBE TO INCREASE THE RADIAL DISPLACEMENT

Yung Ting, Tzung-Shiuan Tsai, Amelia Sugondo and Yen-Lung Lee

Department of Mechanical Engineering, Chung Yuan Christian University, 200, Chung Pei Rd. Chung Li, Taiwan 32023, ROC

Email: yung@cycu.edu.tw

In this paper, piezoelectric actuators that constructed with a ring or several equal sectional type of piezoelectric ceramics attached to a thin tube are designed. The generated amplitude in the radial vibration of tube and other characteristics is investigated. Finite element method (FEM) is used to analyze the mode shape, resonance frequency and amplitude. The analytical and experimental results show a good agreement. From the results, there is no significant difference of the resonance frequency between the ring-type and sectional-type ceramic actuators. However, the sectional-type one is able to generate more radial amplitude. In particular, the sectional-type ceramic actuator with arc  $60^\circ$  and with equal clearance between the neighboring actuators performs the best.

**Key words:** piezoelectric tube, piece-by-piece piezoelectric, radially polarization, amplitude

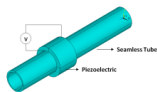
## Design of Piezoelectric Actuator

### A. Resonance Frequency

For a general tube structure, resonance frequency can be calculated by  $f_r = C/2\pi L$  where  $f_r$  is the resonance frequency,  $L$  is the length of the device, and  $C$  is the speed of sound. It indicates longer length of the structure would reduce the resonance frequency.

### B. Vibration Amplitude

Piezoelectric actuator is mounted on the tube as illustrated in Figure 1. Two types of piezoelectric actuators, ring and sectional, are depicted in Figure 2. A ring type piezoelectric actuator encircled the tube with no clearance is shown in Figure 2(a), named TYPE I. Two cases, with arc  $120^\circ$  and  $60^\circ$  of each section of piezoelectric actuator with equivalent clearance in between the actuators for the sectional type are illustrated in Figure 2(b) and 2(c), named TYPE II and TYPE III respectively. All the ring and sectional types of piezoelectric actuators are made of PZT-5A higher piezoelectric coefficient  $d_{31}$  and  $d_{33}$  in comparison with PZT-4 at room temperature. The tube is made of stainless steel because of high tensile strength as well as elastic limit that is suitable for high power ultrasound design.



## Simulation and Experiment Result

Note that, mode shape of tube with half wavelength is the design purpose. Using ANSYS, an example of appropriate mode shape is found and deformation with applied voltage of 50V is shown in Figure 3. As expected, resonance frequency decreases when the length of the tube increases. Also, resonance frequency is inversely proportional to the length of the tube. The first mode of simple axisymmetric deformation generating half wave is chosen to determine the resonance frequency by the modal analysis. Harmonic analysis is used to examine the vibration amplitude at the chosen resonance frequency. Figure 4 shows the harmonic simulation and experiment results employed with, for example 50V and 150V. The simulation results show that amplitude of radial vibration of the tube is very small for the ring type (TYPE I) but quite large for the sectional type. Compared to the amplitude of TYPE I, TYPE II is about one thousand times, and TYPE III is about twenty thousand times. As seen, amplitude of TYPE I presents with very small difference as tube length is changed, and amplitude of TYPE II is varying, and, amplitude of TYPE III is increased for longer tube but there is a maximum value for the length of about 47.5mm.

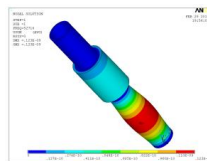




Fig. 1 Tube encircled with piezoelectric actuator

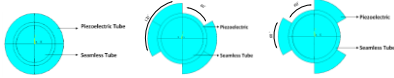
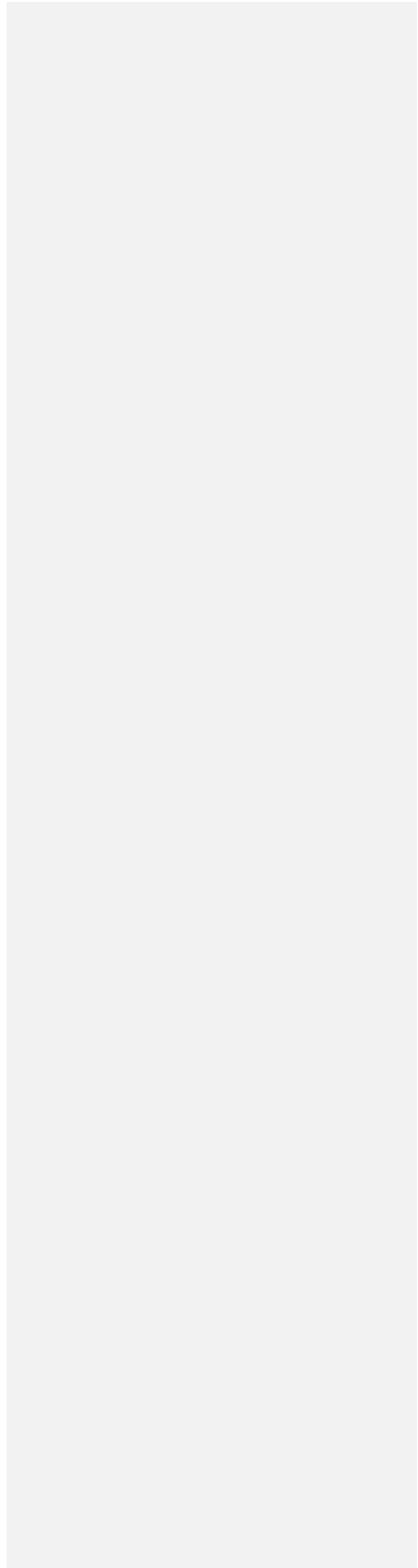


Fig. 2. Type and structure implementation of piezoelectric actuator: (a) Ring-type piezoelectric actuator encircles the tube, (b) Sectional-type (120°) piezoelectric actuator, (c) Sectional-type (60°) piezoelectric actuator

Fig. 3. Amplitude for the length of tube 50 mm

Fig. 4. Amplitude vs. Length for Ring and Sectional type



## Using *d14* FOR A New Wedge-Type Piezoelectric Motor

Yung Ting, Yun-Jui Shieh, Bing-Kuan Hou, Chin-CHih Yeh, Chih-Hao Lin  
[yung@cycu.edu.tw](mailto:yung@cycu.edu.tw)

Different from the usually designed ceramic actuators using *d33* or *d15*, ceramics *d14* is selected to build a high speed piezoelectric motor. Since the *d14* has good merits of polarization, it will be different from *d15*, for example, that needs to increase the thickness along the polarization direction for the purpose of generating more speed and force output. Therefore, using *d14* has the advantage of lower driving voltage required, and only by increasing the length can to achieve the target of obtaining high speed and large torque. Ceramics S-6 with high quality factor greater than that of ceramics PZT-8 is used for design of high speed wedge-type motor. Entire surface is fully in contact with the driven platform or stage.

Analytical simulation in ANSYS and experiment are carried out to investigate the resonance frequency and vibration mode shape as well as amplitude. Both results have close approximation. For a single piece of a built sample actuator with 150V applied voltage, it is able to generate vertical and transverse vibration amplitude of about  $0.4\mu\text{m}$  and  $2.0\mu\text{m}$  respectively. Associated with appropriate mechanism and assembly work as well as employed with an appropriate signal, the maximum linear speed is measured about 150mm/sec. As expected, with larger length or structural integration of more pieces in a series, higher speed would be achieved.

Keywords: wedge-type piezoelectric motor, *d14* and *d15* ceramics.

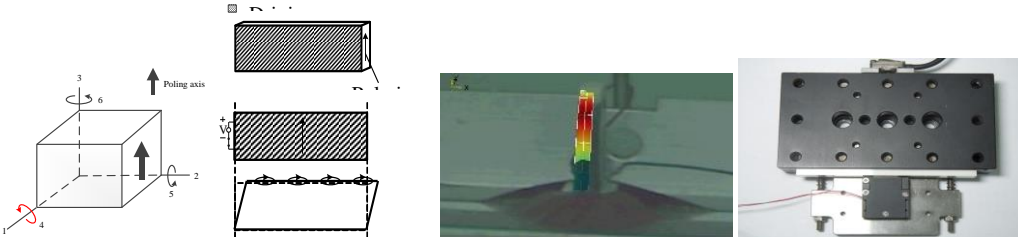


Fig. 1 Ceramics construction and poling

Fig. 2 Polarization and motion of *d14*

Fig. 3 Motion profile

Fig. 4 Motor integrated with stage

## Electrocaloric properties in relaxor ferroelectric PMN-PT system

Jani Peräntie<sup>1</sup>, Hamel Taylor<sup>2</sup>, Juha Hagberg<sup>1</sup>, Heli Jantunen<sup>1</sup>, and Zuo-Guang Ye<sup>2</sup>

<sup>1</sup>Microelectronics and Materials Physics Laboratories, University of Oulu, P.O.Box 4500, 90014 Oulu, Finland

<sup>2</sup>Department of Chemistry & 4D LABS, Simon Fraser University, Burnaby, BC, V5A 1S6, Canada

Email: jani@ee.oulu.fi

Various ferroic materials show large caloric effects, such as magneto- and electrocaloric effects, which can be induced reversibly by different external fields to achieve solid-state cooling cycles<sup>382</sup>. Due to new findings<sup>383,384</sup> the electrocaloric effect has regained attraction for a potential application in a new generation of solid-state cooling devices capable of challenging some existing refrigeration solutions. In particular, previous electrocaloric results on polymers and oxides have shown that relaxor ferroelectrics exhibit some interesting and enhanced electrocaloric properties. However, a lack of direct measurement data on the electrocaloric effect largely restricts our understanding of its behavior and properties.

The  $\text{Pb}(\text{Mg}_{1/3}\text{Nb}_{2/3})\text{O}_3\text{-PbTiO}_3$  (PMN-PT) relaxor ferroelectric solid-solution has been one of the most studied electrocaloric systems and its potential has been emphasized. However, the behaviour and mechanisms of electrocaloric effect in the PMN-PT system are still unclear due to a limited amount of results. Additionally, some discrepancies exist among both directly and indirectly measured electrocaloric data.

In the present work the electrocaloric effect is studied in the  $(1-x)\text{PMN-}x\text{PT}$  ( $x \leq 30\%$ ) relaxor ferroelectric system in the form of bulk by means of direct temperature measurements, which enables the observation of detailed electrocaloric behavior as a function of electric field, temperature and composition (see Fig.1 for an example). Specifically, the previous observations of high responsivity  $\Delta T/E$  around the critical point<sup>385</sup> and development of the “dual-peak” with higher electric fields<sup>386,387</sup> are investigated in detail.

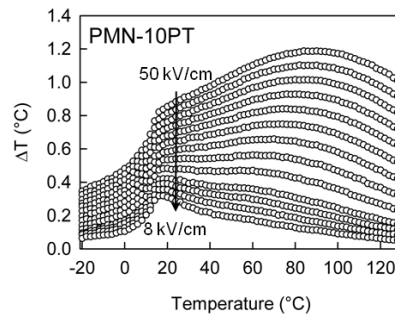


Fig. 127: Electrocaloric effect in PMN-10PT as a function of temperature and electric field.

<sup>382</sup> S. Fähler et al., “Caloric effects in ferroic materials: new concepts for cooling”, *Adv. Eng. Mater.* 14, 10-19, 2012.

<sup>383</sup> A. Mischenko et al., “Giant electrocaloric effect in thin film  $\text{PbZr}_{0.95}\text{Ti}_{0.05}\text{O}_3$ ”, *Science* 311, 1270-71, 2006.

<sup>384</sup> B. Neese et al., “Large electrocaloric effect in ferroelectric polymers near room temperature”, *Science* 321, 821-823, 2008.

<sup>385</sup> B. Rožič et al., “Influence of the critical point on the electrocaloric response of relaxor ferroelectrics”, *J. Appl. Phys.* 110, 064118, 2011.

<sup>386</sup> J. Hagberg et al., “Electrocaloric characteristics in reactive sintered  $0.87\text{Pb}(\text{Mg}_{1/3}\text{Nb}_{2/3})\text{O}_3\text{-}0.13\text{PbTiO}_3$ ”, *Appl. Phys. Lett.* 92, 132909, 2008.

## Design of Wall-plug Efficiency Optimized Semi-active Piezoelectric Shunt Damping Systems

Jan Václavík<sup>1</sup>, Pavel Mokry<sup>1</sup>, Pavel Márton<sup>1</sup>

<sup>1</sup> Institute of Mechatronics and Computer Engineering, Technical University of Liberec  
Studentská 2, Liberec, Czech Republic, CZ-46117

Email: pavel.mokry@tul.cz

Semi-active vibration control devices based on the principle of Piezoelectric Shunt Damping (PSD) represent a very promising possibility for efficient vibration transmission suppression with minimal demands on electronics. In the semi-active vibration control device (see Fig. 1), the piezoelectric actuator is attached to the vibrating structure and connected to an active analog electrical shunt that behaves as a negative capacitor. The word 'active' means that the electrical shunt consists of a power supply and an operational amplifier in the electrical network. In this arrangement, it is possible to highly efficiently control the vibration transmission from the source of vibrations through the piezoelectric element. It is achieved by actively tuned mechanical impedance of the piezoelectric actuator. Unfortunately, the efficiency of the electrical part of the device is rather low, since the electric power transfer in the system has a large reactive component, which is dissipated on the transistors of the operational amplifier, which is used in the negative capacitor. This yields a situation, where wall-plug efficiency, i.e. the ratio of mechanical power reflected or absorbed by the actively shunted piezoelectric actuator over the input electrical power, is extremely low.

The aforementioned issues have motivated the work presented in this Paper. The mechanical and electric energy flows in two semi-active vibration control systems have been analyzed in detail. The vibration control systems have been designed and realized to suppress the vibration transmission in narrow and broad frequency ranges, respectively. The results of our measurements indicate that the average apparent electrical power in the electric part of the vibration control device is about 100 times larger than the mechanical power, which is supplied to the system from the source of vibrations. Such a situation puts specific requirements on the design of the negative capacitor electronics.

In this paper, there will be analyzed strengths and weaknesses of the typical realizations of the semi-active vibration control devices and discussed principles that can enhance their wall-plug efficiency. Optimized concepts that eliminate weaknesses of the aforementioned devices will be presented. The rules for designing the highly efficient and low-power electronic parts of semiactive vibration control systems are discussed.

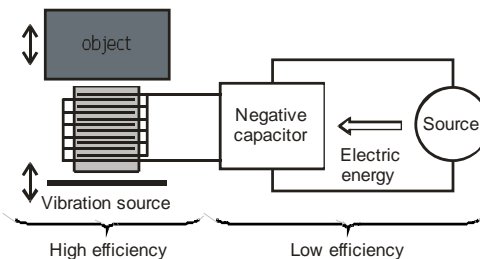


Fig. 128: Semi-active vibration control device, which consists of a piezoelectric actuator and a negative capacitor.

<sup>387</sup> L.J. Dunne et al., "Statistical mechanical lattice model of the dual-peak electrocaloric effect in ferroelectric relaxors and the role of pressure", J. Phys. D: Appl. Phys. 44, 375404, 2011

## Efficiency measurement in piezoelectric vibration energy harvesters.

P. M. Weaver<sup>1</sup>, P. Woolliams<sup>1</sup>, M.G. Cain<sup>1</sup>, M. Stewart<sup>1</sup>

<sup>1</sup>National Physical Laboratory, Teddington, UK

Email: paul.weaver@npl.co.uk

Vibrational energy harvesters convert energy from vibrations and movement in the environment into electrical energy which can be used to power a device such as a wireless sensor node. The energy source is often considered as “waste” energy and energy harvesting performance is typically characterised by power output under specified conditions of vibration amplitude and frequency. This takes no account of the energy extracted from or available from the source. This is important where account needs to be taken of the loading of the source by the harvester. This includes “parasitic” harvesting where the energy derived from the source is not “free” or wasted, and use of the energy harvester increases the power consumed by the source. Examples include human or vehicle powered applications where it is the availability of the energy source rather than energy saving that is the main motivation. It is also important in situations where the power from the source is limited. In these cases, the ratio of power out to power in, or the efficiency needs to be known.

Measuring efficiency is more complex than measuring power out under well-defined vibration conditions, because of the requirement to measure the power transferred from the source to the energy harvester. Often the harvested power is a small fraction of the total power delivered by the system. We are not aware of any published reports of measurement of efficiency, although it is discussed in some mathematical models of energy harvesters.

In this paper we describe an experimental method of measuring efficiency for resonant piezoelectric cantilever energy harvesters based on a damped oscillator response to an impulse input. Experimental results for typical energy harvesting devices are presented.

This work has been performed in the framework of the joint research project “Metrology for Energy Harvesting”, which is supported by the European Metrology Research Programme (EMRP), jointly funded by the EMRP participating countries within EURAMET and the European Union.

## SiO<sub>2</sub>/SiN Infrared Absorbing Films for Uncooled Pyroelectric Sensor and its Fabrication and Evaluation

Koji Oishi<sup>1</sup>, Daisuke Akai<sup>2</sup>, Makoto Ishida<sup>1,2</sup>

<sup>1</sup>Electric and Electronic Information Engineering, Toyohashi University of Technology, Toyohashi, Aichi, Japan

<sup>2</sup>Electronics-Inspired Interdisciplinary Research Institute (EIIRIS), Toyohashi University of Technology, Toyohashi, Aichi, Japan

Email: oishi-k@int.ee.tut.ac.jp

Uncooled Infrared sensor is widely used for human detection. The pyroelectric sensor has advantage of high sensitivity and is possible to integrate on Si substrate with MEMS technology, and it possesses possibility for improvement in many ways. Our approach to improving sensor is to control crystalline orientation of Pb(Zr, Ti)O<sub>3</sub> (PZT) film using epitaxial  $\gamma$ -Al<sub>2</sub>O<sub>3</sub> grown on Si substrate. Other sensor consisting material such as electrode is also grown with crystalline orientation controlled<sup>388</sup>. Absorption of infrared that convert to heat is also the key factor for the improving sensitivity. We proposed new absorbing film using SiO<sub>2</sub> and SiN for our PZT thin film pyroelectric infrared sensor. We have researched the fabrication and evaluation of the absorbing film and the sensor.

Our sensor structure is PZT capacitor consists of SrRuO<sub>3</sub>(SRO)/PZT/SRO/Pt/ $\gamma$ -Al<sub>2</sub>O<sub>3</sub>/Si. SRO is crystalline electrode that used for buffer layer for interface of PZT and Pt that adhesion is very weak, which cause fabrication failure.(Fig.1) Absorbing film is fabricated by plasma enhanced chemical vapor deposition, and SiO<sub>2</sub>(550nm) is deposited on SiN(850nm). These film possess specific absorption in wavelength range of 8-14 $\mu$ m, often used for human detection. The film is also CMOS material and easy to fabricate. The infrared absorption is confirmed both calculation and measurement, and they show the similarity in target wavelength. Result shows over 70% of average absorption is obtained from proposed absorbing film.(Fig.2)

SiO<sub>2</sub>/SiN absorbing films is deposited on sensor structure without fabrication failure. The responsivity (R<sub>v</sub>) of sensor with absorbing film is measured with source follower (JFET and 47k $\Omega$  resistor) and lock-in amplifier. The R<sub>v</sub> of 176 V/W is achieved on chopping frequency of 10 Hz.

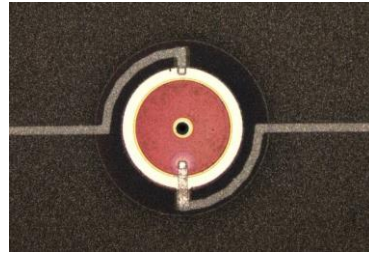


Fig. 129: Absorbing film on fabricated sensor. Fabrication is successfully completed without

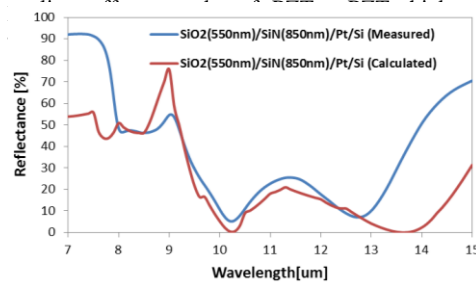


Fig. 2: Reflectance of SiO<sub>2</sub>/SiN double layer absorbing film on Pt/Si. The Pt does not transmit infrared therefore the reflectance shows absorption characteristics.

<sup>388</sup>D. Akai et al., Applied Physics Letter, 86 (2005) 202906

# Effect of Dome-shaped Asymmetric Piezoelectric Multimorph Ceramic on Frequency Response Characteristics of Piezoelectric Acoustic Actuator

Hye Jin Kim<sup>1</sup> and Woo Seok Yang<sup>1</sup>

<sup>1</sup>Nano Convergence Sensor Research Section, IT Materials and Components Lab., Electronics and Telecommunications Research Institute (ETRI), Daejeon, South Korea

Email: nolawara@etri.re.kr

Recently, the piezoelectric acoustic actuators have attracted a great deal of attention owing to their several benefits of being thinner, more power-efficient and lighter than the traditional dynamic speakers. However, they have still suffered from the bad sound quality due to their fluctuating output sound pressure and high total harmonic distortion characteristics. In this paper, the dome-shaped asymmetric piezoelectric multimorph ceramics are proposed to achieve good sound quality of the piezoelectric acoustic actuators which means flat and smooth frequency response characteristics on a wide playing frequency range. In order to investigate the effect of asymmetric piezoelectric multimorph ceramic on the frequency response characteristics of the piezoelectric acoustic actuator, we simulated and analyzed the vibrational and output acoustic spectrums using the finite-element analysis (FEA) and the laser scanning vibrometer (LSV) and B&K pulse analyzer equipment.

The fabricated piezoelectric acoustic actuator was comprised of a PZT ceramic membrane and an acoustic diaphragm. Herein, PZT piezoelectric ceramic sheet was prepared to have an asymmetric triple-layered multimorph structure, which is composed of three piezoelectric layers: upper and lower piezoelectric active layers and a dummy layer. The upper and lower piezoelectric active layers consisted of 2 and 4 individual piezoelectric element layers, respectively.

As shown in Fig. 1, it is observed that the measured output sound pressure of the fabricated piezoelectric acoustic actuator was quite improved to be flat and smooth spectrum by the dome-shaped asymmetric piezoelectric ceramic. Especially, the significant dip at 3.35 kHz was dramatically enhanced by about 15 dB. This result is due to the dome-shaped structure of the asymmetric triple-layered multimorph, which is obtained by the polarization process. From the polarization process, the proposed asymmetric piezoelectric ceramic was bended to the arched profile due to the difference of the lateral shrinkages between upper and lower active layers, which can possess both large displacement and loading ability performance. This paper presents that the dome-shaped asymmetric piezoelectric triple-layered multimorph ceramic can not only improve the sound quality of the piezoelectric acoustic actuator by a flat and smooth frequency response characteristics but also allow high sound pressure characteristics comparable to the commercial piezoelectric acoustic actuator.

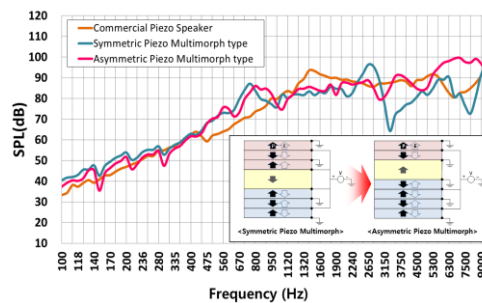


Fig. 130: The output sound pressure levels of the fabricated piezoelectric acoustic actuator with the dome-shaped asymmetric multimorph ceramic, compared to the flat symmetric triple-layered ceramic and commercial piezoelectric speakers.

## AlN cantilever for differential pressure sensor

Yutaka Tomimatsu<sup>1,2</sup>, Hidetoshi Takahashi<sup>3</sup>, Takeshi Kobayashi<sup>1,4</sup>, Kiyoshi Matsumoto<sup>3</sup>,  
Isao Shimoyama<sup>3</sup>, Toshihiro Itoh<sup>1,4</sup> and Ryutaro Maeda<sup>1,4</sup>

<sup>1</sup>NMEMS Technology Research Organization, JAPAN

<sup>2</sup>Seiko Instruments Inc., JAPAN

<sup>3</sup>The University of Tokyo, JAPAN

<sup>4</sup>National Institute of Advanced Industrial Science and Technology (AIST), JAPAN

Email: ytomimatsu@nmems.or.jp

MEMS cantilever type force sensors have been widely developed for many applications<sup>389,390</sup>. Among them, a cantilever type differential pressure sensor has a higher sensitivity than traditional diaphragm type sensors because only the base part of the cantilever is fixed. Previous sensor uses a piezoresistor for the sensing element. Thus, the sensor needs power consumption of several milliwatts to apply the bias voltage.

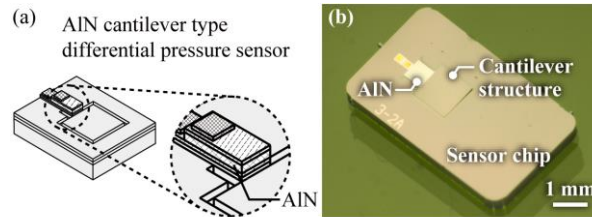


Fig. 131: (a) Concept of the differential pressure sensor using a AlN cantilever. (b) Photograph of the fabricated sensor chip.

We propose a piezoelectric cantilever type differential pressure sensor as shown in Fig. 1(a). A piezoelectric type sensor does not require power consumption to drive the sensing element. Thus, a differential pressure sensor with high sensitivity and low power consumption is achieved.

In this research, Aluminum nitride (AlN) was used as the piezoelectric material due to its chemical stability and small dielectric constant<sup>391</sup>. We designed and fabricated the AlN cantilever, and the force sensitivity of the fabricated sensor was evaluated.

Fig.1(b) shows a photograph of the fabricated cantilever. The cantilever was fabricated from the multilayer of Pt/Ti/AlN/Pt/Ti/SiO<sub>2</sub> deposited on a silicon on insulator (SOI) wafer. The cantilever, which is formed on the center of the sensor chip, is 1500 μm × 1000 μm × 2 μm in size. The AlN layer is formed on the base of the cantilever where strain is concentrated. The spring constant is designed to be 0.27 N/m. The capacitance of the fabricated cantilever is 70 pF.

The displacement sensitivity of the fabricated cantilever was measured by moving a PZT actuator that touched the center of the cantilever. The piezoelectric voltage was generated according to the displacement of the actuator. Based on this measurement, the displacement sensitivity was calculated to be 3.3 mV/μm. From the result and the calculated spring constant, the force sensitivity was obtained to be 12 mV/μN.

<sup>389</sup> M. Tortonese *et al.*, "Atomic resolution with an atomic force microscope using piezoresistive detection," *Applied Physics Letters*, vol. 62, pp. 834-836, 1993.

<sup>390</sup> H. Takahashi *et al.*, "Differential pressure sensor using a piezoresistive cantilever," *Journal of Micromechanics and Microengineering*, vol. 22, pp. 055015, 2012.

<sup>391</sup> V. Cimalla, *et al.*, "Group III nitride and SiC based MEMS and NEMS: materials properties, technology and applications," *Journal of Physics D: Applied Physics*, vol. 40, no. 20, pp. 6386-6434, 2007.



## Application driven design, fabrication and characterization of piezoelectric energy scavenger for cardiac pacemakers

Mikael Colin, Libor Rufer, Skandar Basrour

TIMA (CNRS, G-INP, UJF), Grenoble, FRANCE

Email: Libor.Rufer@imag.fr

The disruptive innovation in pacemakers and implantable cardioverter defibrillators (ICDs) will provide implants that do not require electrical leads. Main actors in the field of cardiac rhythm management (CRM) implants prepare miniaturized and autonomous leadless implants, which could be directly placed inside a human heart. Several concepts for powering stand-alone cardiac implants were proposed<sup>392</sup> in the past, and recently the first study of an energy scavenging system placed in the human heart has been presented<sup>393</sup>. The study was conducted for a relatively large system operating at 40 Hz. We will demonstrate, that according to the heart beat acceleration spectrum obtained by placing accelerometers inside several heart cavities<sup>394</sup>, the useful vibration energy is rather localized at lower frequencies (15 to 30 Hz). We will also detail the dimensional restrictions in the case of a leadless pacemaker. Since it has to be placed into a heart through veins, the device is expected to be of cylindrical shape with a diameter of about 6 mm.

We will present the design, simulation, fabrication and characterization of piezoelectric vibration energy scavenger for cardiac implants. We will discuss the energy content of the heart vibration spectrum in a view of energy harvesting. We will place emphasis on the nature of the spectrum, the energy frequencies and corresponding amplitudes. We will present an application driven design of a resonant piezoelectric energy scavenger aiming at powering a leadless pacemaker with a useable energy of few  $\mu\text{J}$  per heartbeat. Such an energy scavenger consists of a piezoelectric bimorph cantilever with 20  $\mu\text{m}$  thick  $\text{Pb}(\text{Zr}_x\text{Ti}_{1-x})\text{O}_3$  layers. A simulation study in both ANSYS® and Simulink® environments, has shown that the proposed design delivers the required energy.

However, none of the current fabrication processes can be used for manufacturing such PZT thick films. Using processes derived from the microelectronic field such as Sol Gel deposition or sputtering, the maximum achievable thickness is about 2 to 5  $\mu\text{m}$ . In contrary, using co-firing techniques, the PZT plates can hardly be thinner than 100  $\mu\text{m}$ . As a consequence, the manufacturing of the above-described piezoelectric scavenger corresponds to an actual process window. In this paper, we present the fabrication of an low-frequency device (15 Hz) using optimized grinding polishing techniques. The obtained experimental results are good agreement with our analytical and numerical modeling (Figure 1).

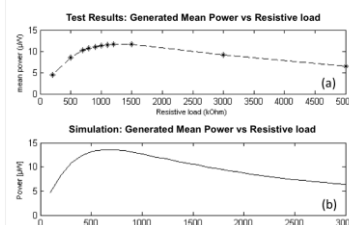


Fig.1: Experiment/simulation results

blind  
ultra  
and  
in

<sup>392</sup> W. H. Ko, "Piezoelectric energy converter for electronic implants", *US patent* 3,456,134, 1969.

<sup>393</sup> M. A. Karami, D. J. Inman, "Powering Pacemakers from heartbeat vibration using linear and non linear energy harvester", *Applied Physics Letters*, vol. 100, 042901, 2012.

<sup>394</sup> M. Deterre, B. Bouteaud, R. DalMolin, S. Boisseau, J-J. Chaillout, E. Lefeuvre, E. Dufour-Gergam, "Energy harvesting system for cardiac implant applications", *Symposium on the Design, Test, Integration and Packaging of MEMS/MOEMS (DTIP)*, May 11-13, 2011, pp. 387-391.

## Impact of domain depth on SAW generation by acoustic superlattice transducers in 128° YX-cut lithium niobate

Didit Yudistira<sup>1</sup>, Andreas Boes<sup>1,2</sup>, Amgad Rezk<sup>1</sup>, Tristan Crasto<sup>1,2</sup>, Hendrik Steigerwald<sup>1,2</sup>, Elisabeth Soergel<sup>3</sup>, James Friend<sup>1</sup>, Arnan Mitchell<sup>1,2</sup>

<sup>1</sup>Electrical and Computer Engineering, RMIT University, VIC 3001, Melbourne, Australia

<sup>2</sup>Center for Ultra-high Bandwidth Devices for Optical Systems (CUDOS)

<sup>3</sup>Institute of Physics, University of Bonn, Wegelerstr. 8, 53115 Bonn, Germany

Email: didit.yudistira@rmit.edu.au

Acoustic superlattice (ASL) transducers comprising periodic domain inversion on Z-cut lithium niobate (LN) achieved with electric field poling, and coplanar electrode have been demonstrated as an alternative means of surface acoustic wave (SAW) generation beside more common interdigitated transducer<sup>395</sup>. While its applications in the integrated optics have been reported<sup>396</sup>, in many other SAW applications such as in Microfluidics, 128 YX LN is preferable because it has the largest coupling constant (5.3%) compared to Z-cut (0.53%). However, to achieve domain inversion on this cut using electric field poling is relatively difficult because of its inclined polarization axis. In our distinct submission to this conference, for the first time periodic domain inversion on 128 YX LN has been achieved by means of UV direct writing. However,

these engineered domains can be quite shallow. Here, we analyse SAW generation on 128 YX cut LN studying in particular the impact of domain depth.

The studied structure is presented in the inset of Fig. 1(a) with domains of constant period  $\Lambda$  and variable depth  $\delta$ . We define the normalized parameter  $\tau = \delta/\Lambda$ . The

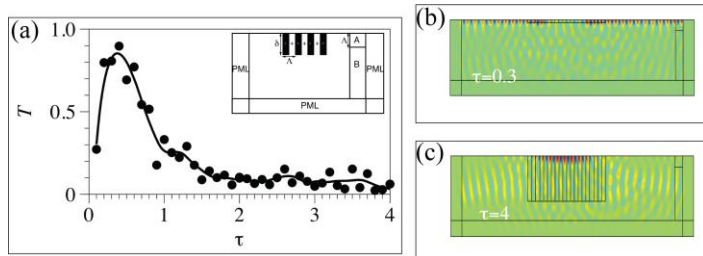


Fig. 132: (a) Out-going surface bound acoustic energy ( $T$ ) vs normalized domain depth ( $\tau$ ), displacement profiles with: (b)  $\tau=0.3$ , and (c)  $\tau=4$ .

structure, was simulated using the finite element method assuming a stress free boundary condition (BC) on the surface except at the periodic domain surface where Dirichlet BC,  $V_{RF}=1$  V, is imposed. The remaining boundaries are terminated with Perfectly-matched layers. Figure 1(a) shows the fraction of the total acoustic energy leaving the transducer that passes through region A and indicates that a bound SAW is achieved when  $\tau \approx 0.3$  as clearly shown in Fig. 1(b). If the depth is further increased beyond the lattice period  $\Lambda$  ( $\tau > 1$ ), the generated SAW is more localized within the periodic domain, as shown in Fig. 1(c).

These predictions show that efficient propagating SAW generation on shallow-depth 128 YX acoustic superlattice should be possible, provided the domain depth is 30% of the lattice period. Such an aspect ratio is quite achievable with the UV domain writing approach.

<sup>395</sup>D. Yudistira, S. Benchabane, D. Janner, and V. Pruneri, Applied Physics Letters, **95**, 052901 (2009).

<sup>396</sup>D. Yudistira, D. Janner, S. Benchabane, and V. Pruneri, Optics Express, **18**, 21781 (2010).

## Improved Microwave Dielectric Properties of $\text{Nd}(\text{Mg}_{0.5}\text{Sn}_{0.5})\text{O}_3$ Ceramics with Ba Substitution

Yih-Chien Chen and Min-Zhe Weng

Department of Electrical Engineering, Lunghwa University of Science and Technology, Gueishan Shiang, Taoyuan County, Taiwan

Email: ycchencku@yahoo.com.tw

Many investigations of  $\text{Nd}(\text{Mg}_{0.5}\text{Sn}_{0.5})\text{O}_3$  ceramics have investigated their potential application in modern communication systems. A dielectric constant of 19.3 and a  $Q \times f$  of 43,300 GHz were obtained for  $\text{Nd}(\text{Mg}_{0.5}\text{Sn}_{0.5})\text{O}_3$  ceramics that were sintered at 1550 °C for 4 h<sup>397</sup>. Since the ionic radius of  $\text{Ca}^{2+}$  (0.100 nm) exceeds that of  $\text{Mg}^{2+}$  (0.072 nm),  $\text{La}(\text{Mg}_{0.5-x}\text{Ca}_x\text{Sn}_{0.5})\text{O}_3$  ceramics have better microwave dielectric properties than  $\text{La}(\text{Mg}_{0.5}\text{Sn}_{0.5})\text{O}_3$  ceramics<sup>398</sup>. This fact motivated this study of the effect of the substitution of  $\text{Mg}^{2+}$  ions (0.072 nm) by  $\text{Ba}^{2+}$  ions (0.135 nm) to form  $\text{Nd}(\text{Mg}_{0.5-x}\text{Ba}_x\text{Sn}_{0.5})\text{O}_3$  (NMBS) ceramics. The effect of the sintering temperature on the microwave dielectric properties of NMBS ceramics was investigated. The microwave dielectric properties of NMBS ceramics were found to vary with the extent of  $\text{Ba}^{2+}$  substitution and sintering temperature. The microwave dielectric properties were further analyzed by densification, X-ray diffraction patterns, and observation of their microstructures. **The X-ray diffraction patterns of the  $\text{Nd}(\text{Mg}_{0.47}\text{Ba}_{0.03}\text{Sn}_{0.5})\text{O}_3$  ceramics revealed no significant variation of phase with sintering temperatures.  $\text{Nd}(\text{Mg}_{0.47}\text{Ba}_{0.03}\text{Sn}_{0.5})\text{O}_3$  ceramics that were sintered at 1600 °C for 4 h had an apparent density of 6.91 g/cm<sup>3</sup>, a dielectric constant of 19.14, a  $Q \times f$  of 97,500 GHz, and a  $\tau_f$  of -65.4 ppm/°C. The density and formation of  $\text{Nd}_2\text{Sn}_2\text{O}_7$  affected the dielectric constant and  $Q \times f$  of NMBS ceramics. The dielectric constant of NMBS ceramics was also depended on the ionic polarization.**

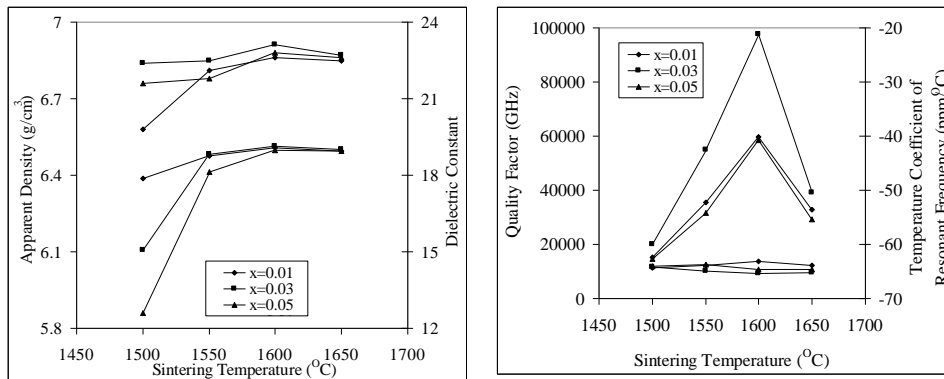


Fig. 1. Microwave dielectric properties of  $\text{Nd}(\text{Mg}_{0.5-x}\text{Ba}_x\text{Sn}_{0.5})\text{O}_3$  ceramics.

<sup>397</sup> Y.C. Chen, R.J. Tsai, Mater. Chem. Phys. vol. 129, p.116-120, 2011.

<sup>398</sup> Y.C. Chen, M.D. Chen, J. Phys. Chem. Solids vol. 72 p. 1447-1451, 2011.

## Analysis of guided wave propagation in (1-x)Pb(In<sub>1/2</sub>Nb<sub>1/2</sub>)(Mg<sub>2/3</sub>Nb<sub>1/3</sub>)O<sub>3</sub>-xPbTiO<sub>3</sub> piezoelectric media

H. Wang<sup>1</sup>, T. Baron<sup>1</sup>, W. Daniau<sup>1</sup>, B. Dulmet<sup>1</sup>, S. Ballandras<sup>2</sup>

<sup>1</sup> FEMTO-ST Institute, UMR 6174, Université Franche-Comté, CNRS, ENSMM, UTBM, 32 avenue de l'observatoire, 25000 Besançon cedex, France

<sup>2</sup> Frecn|sys SAS, 18 rue Alain Savary, 25000 Besançon cedex, France

Email: haixia.wang@femto-st.fr

Currently the different piezoelectric materials with superior high electromechanical coupling coefficient have been found such as (1-x)Pb(Mg<sub>1/3</sub>Nb<sub>1/3</sub>)O<sub>3</sub>-xPbTiO<sub>3</sub> (PMNT) crystal<sup>399</sup>. It was also discovered that the coupling factor of shear mode can be larger if these crystals are polarized properly<sup>400</sup>, compared with the commonly used piezoceramics and crystals. It means that these crystals may trigger a revolution in the performance of next generation electromechanical devices. Therefore, a thorough theoretical investigation on the guided wave propagation in these piezoelectrics is very useful both for a fundamental understanding on wave phenomena and for potential applications.

Our theoretical studies focus on the validation of guided wave with pure horizontal shear mode in piezoelectric orthorhombic media with mm2 symmetry, and how  $k^2$  of these modes change when a uniform metal layer is deposited in the surface. The investigation elucidated the necessary condition for the existence of pure shear Bleustein-Gulyaev wave in mm2 even with large coupling factor and also general condition  $V < V_{th}$  required for all materials. The velocity function and dispersion relation have been deduced in materials with mm2 and also 4mm symmetry. With the measured parameters in the PIMNT crystal we found that the existence of Bleustein-Gulyaev wave in both symmetries is validated and this wave is totally decoupled from Rayleigh wave. The maximum coupling factor  $k^2$  about 50% at around 37°YX with velocity  $V_m=1696\text{m/s}$  and  $V_r=2273\text{m/s}$  can be obtained in crystal with mm2 symmetry. The corresponding measurements and applications will be further investigated under the optimum choice of layered structure with metal and insulator film deposited on the top of substrate without badly sacrificing  $k^2$  for the response, since one can expect that devices based on these guided waves may be useful in the near future.

<sup>399</sup> Service R F 1997 Science 275 1878

<sup>400</sup> Zhang R, Jiang B, Jiang W H and Cao W W 2006 Appl. Phys. Lett. 89 242908

## Measurement of Radiant Energy using Pyroelectric Polymer/Ceramic Composite

Edinilton Morais Cavalcante<sup>1</sup>, Darcy Hiroe Fujii Kanda<sup>1</sup>, Washington Luiz de Barros Melo<sup>2</sup>, Gilberto de Campos Fuzari Jr.<sup>3</sup>, Walter Katsumi Sakamoto<sup>1</sup>

<sup>1</sup>Departamento de Física e Química, Universidade Estadual Paulista – UNESP, Ilha Solteira, São Paulo, Brazil.

<sup>2</sup>Empresa Brasileira de Pesquisa Agropecuária – EMBRAPA, São Carlos, São Paulo, Brazil.

<sup>3</sup>Instituto de Ciências Exatas e da Terra, Universidade Federal de Mato Grosso – UFMT, Barra do Garças, Mato Grosso, Brazil.

Email: sakamoto@dfq.feis.unesp.br

Monitoring non-ionizing radiant energy is increasingly demanded for many applications such as automobile, biomedical and security system. Thermal type infrared (IR) sensors can operate at room temperature and pyroelectric materials have high sensitivity and accuracy for that application. Working as thermal transducer pyroelectric sensor converts the non-quantified thermal flux into the output measurable quantity of electrical charge, voltage or current. In the present study the composite made of poly(vinylidene fluoride) – PVDF and lead zirconate titanate (PZT) partially recovered with polyaniline (PAni) conductor polymer has been used as sensor element. The pyroelectric coefficient  $p(T)$  was obtained by measuring the pyroelectric reversible current, i.e., measuring the thermally stimulated depolarization current (TSDC) after removing all irreversible contribution to the current such as injected charge during polarization of the sample. The scheme in Figure 1 shows the experimental setup to analyze the sensing property of the pyroelectric material. In that scheme, the sensor is irradiated by a high power light source (halogen lamp of 250 W) that is chopped providing a modulated radiation. A device assembled in the laboratory is used to change the light intensity sensor, an aluminum strip having openings with diameters ranging from 1 to 10 mm incremented by one millimeter. The sensor element is assembled between two electrodes while its frontal surface is painted black ink to maximize the light absorption. The signal from the sensor is measured by a Lock-In amplifier model SR530 – Stanford Research Systems. Figure 2 shows the behavior of the output voltage for an input power at several frequencies for PZT-PAni/PVDF (30/70 vol%) composite. The signal amplitude follows the inverse power law ( $1/f$ ) and the linearity can be observed in the frequency range used.

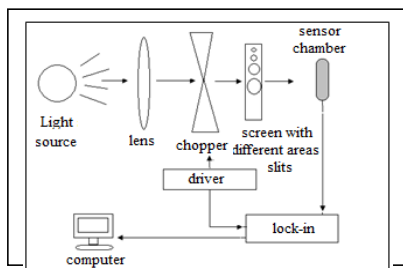


Fig. 1 - Block diagram of the photopyroelectric detection.

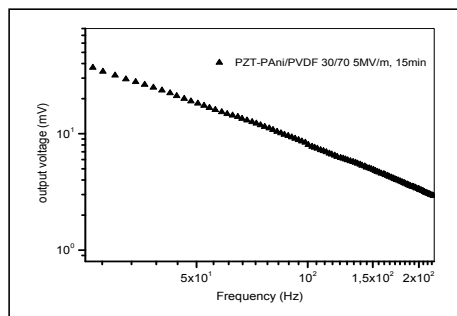


Fig. 2 – photopyroelectric response as a function of frequency.

## Tunability and Sensitivity Modification by Poling on PZT Film of Frequency-Tunable Ultrasonic Microsensors

Kaoru Yamashita, Hikaru Tanaka, Atsushi Morimoto, Yang Yi, Minoru Noda

Graduate School of Science and Technology, Kyoto Institute of Technology, Kyoto, Japan

Email: yamashita.kaoru@kit.ac.jp

Frequency-tunable piezoelectric ultrasonic microsensors have been fabricated and tested in terms of tunability and sensitivity changes induced by poling. Figure 1 shows a schematic illustration of the sensor structure. Sol-gel derived lead-zirconate-titanate (PZT) thin film capacitors are formed on silicon-dioxide diaphragms. The top electrode of the capacitor is divided into the inner part for sensing and the outer part for resonant frequency tuning<sup>401</sup>. The tunable sensors are utilized to multiple-frequency technique for high resolution and ghost suppressive ultrasonic measurement on a sparse phased array<sup>402</sup>. The resonant frequency draws a butterfly curve<sup>1</sup>, as shown in Fig. 2 (a), reflecting ferroelectric polarization hysteresis to the applied tuning voltage, similar to the cases of piezoelectric diaphragm actuators<sup>403</sup>.

Although the poling onto the sol-gel PZT film is known to improve the piezoelectric property<sup>404</sup>, the interference between the poling and the tuning on the tunable sensors was not clear. In this work, the sensor performance has been characterized upon poling voltage application on the sensing electrode. The results are shown in Fig. 2, where the poling state is initial (before poling), poled at 8 V and decreased poling voltage to 0 V as illustrated in the insets. The butterfly curve shifts to slightly higher frequency by the 8 V-poling due to additional converse piezoelectric stress and maintains the shift after the poling voltage is decreased to 0 V, as shown in Fig. 2 (a). The frequency shift slightly decreases the tunability but it is still enough for the dual-frequency measurement technique. Figure 2 (b) shows improvement of sensitivity by the poling at 8 V and also it is maintained after the poling voltage is decreased to 0 V. Although a tensile stress to the poled sol-gel PZT was reported to increase its piezoelectric coefficient  $e_{31,f}$ <sup>405</sup>, the sensitivity of the poled sensor raises much higher than that by the  $e_{31,f}$  increase at a higher tuning voltage range, while that of the unpoled sensor shows a low sensitivity with the reversed response to the tuning voltage due to less aligned polarizations toward possibly the reversed direction. As the result, we can utilize the tunability up to 200% by selecting tuning voltages as 1 V and 6 V for a dual-frequency technique, avoiding polarization reversal, and the improved sensitivity by five times through poling on the sensing electrode at 0 V through 8 V.

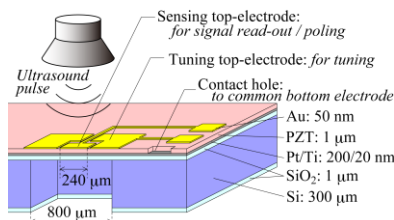


Fig. 1: A schematic illustration of the sensor structure and electrode configuration.

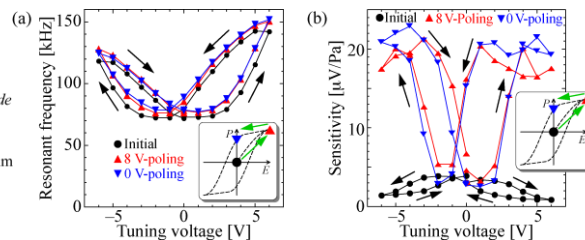


Fig. 2: Sensor performance at the initial, after poled at 8 V and then decreased poling voltage to 0 V; (a) for the tunability and (b) for the sensitivity.

<sup>1</sup> K. Yamashita, K. Tomiyama, K. Yoshikawa, M. Noda, M. Okuyama, *Ferroelectrics*, vol. 408, p. 48–54, 2010.

<sup>402</sup> K. Yamashita, K. Tomiyama, K. Yoshikawa, M. Noda, *Procedia Chem.*, vol. 1, p. 540–543, 2009.

<sup>403</sup> P. Muralt, A. Kholkin, M. Kohli, T. Maeder, *Sens. Actuat. A*, vol. 53, p. 398–404, 1996.

<sup>404</sup> K. Yamashita, M. Okuyama, *IEEE Trans. SM*, vol. 124, p. 124–128, 2004.

<sup>405</sup> M. A. Dubois, P. Muralt, *Sens. Actuat. A*, vol. 77, p. 106–112, 1999.

## Switchable bandpass filters using acoustically coupled ferroelectric FBARs

Andrei Vorobiev and Spartak Gevorgian

Department of Microtechnology and Nanoscience, Chalmers University of Technology,  
Gothenburg, Sweden

[andrei.vorobiev@chalmers.se](mailto:andrei.vorobiev@chalmers.se); [spartak.gevorgian@chalmers.se](mailto:spartak.gevorgian@chalmers.se)

In multiband-multichannel microwave communications systems filters are one of the most critical components affecting the cost, performance and form factor of the handsets and systems. Tunable and switchable filters are considered as a possible solution to the problem. Intrinsically switchable and tunable Film Bulk Acoustic Wave resonators (FBAR) based on ferroelectrics (utilize electric field induced piezoelectric effect) appear to be one of the most promising technologies for these applications. Recently attempts are made to improve the performance of these filters in terms of low losses and high out-of-band rejection<sup>406, 407</sup>. While for the lower insertion losses FBARs with high Q-factors are required, the out-of-band rejection and steepness of the skirts in ladder filters may be improved by using inductors in series with the shunt resonators<sup>2</sup> and by using acoustic coupling between the series resonators<sup>1</sup>. The filter using acoustically coupled resonators having rectangular or polygon form often suffer from spurious resonances<sup>1</sup>.

In this work voltage switchable bandpass filters based on acoustically coupled FBARs are considered. To avoid generation of the spurious resonances FBARs having semicircular electrodes are used, Fig.1a. The filter makes use of BiFeO<sub>3</sub>-BaTiO<sub>3</sub> films. A 100 nm thick Pt film is used as the bottom electrodes. The top electrode is made of 100 nm Al. Details of fabrication and measurements are reported in an article<sup>408</sup>.

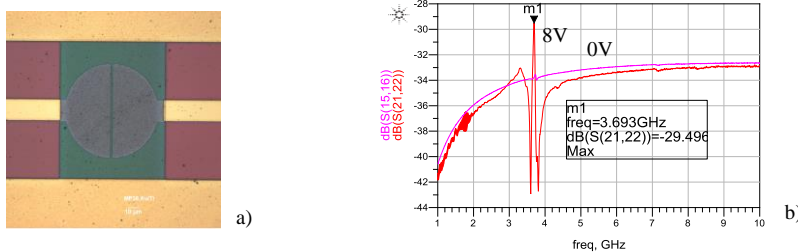


Fig.1 Microphotograph (a) and measured off ( $V_{\text{bias}}=0$ ) and on ( $V_{\text{bias}}=8\text{V}$ ) state S21. Diameter of electrodes is 60  $\mu\text{m}$ , slotwidth is 1.0  $\mu\text{m}$ .

Filters with different sizes and slotwidth between the semicircular electrodes are fabricated and measured. The Q-factor of the resonators is estimated to be about 80 at resonant frequency of 3,695 GHz under DC bias voltage 8V applied to each of the resonators. As is seen in Fig.1b the filter is free of spurious resonances with a clear 3dB pass band of 3%. The return losses are -13dB. However, the coupling is still weak and the losses in input/output strips are high which result in higher dumping in the passband. The future plans include optimization of the designs/coupling strength.

This work is supported by Swedish Science Council Vetenskapsrådet via project VR-FBAR.

<sup>406</sup> S. Sis, V. Lee and A. Mortazawi, "Intrinsically Switchable, BST-on-Silicon Composite FBARs", IEEE IMS'2011, pp.1-4

<sup>407</sup> S. Gevorgian, A. Tagantsev and A. Vorobiev, Tuneable Film Bulk Acoustic Wave Resonators, Springer 2013

<sup>408</sup> A.Vorobiev etc. "Intrinsically tunable 0.67BiFeO<sub>3</sub>-0.33BaTiO<sub>3</sub> thin film bulk acoustic wave resonators", Appl. Phys. Lett., vol. 101, p. 232903-5, 2012

## Piezoelectric energy harvesting device using PZT nanorods with single crystal structure

Seok-Jin Yoon, Woo-Suk Jung, Chong-Yun Kang

Electronic Materials Research Center, Korea Institute of Science and Technology (KIST),  
Hwarangno 14-gil 5, Seongbuk-gu, Seoul, Korea

Email: jws7216@gmail.com

Piezoelectric nanocomposite generator (NCG) is realized with PZT nanorods and Polydimethylsiloxane (PDMS) polymer. The PZT nanorods were fabricated by hydrothermal method, resulting in a single crystal structure and the epitaxial growth of the nanorods. The PDMS was utilized for the flexibility of the nanogenerator and mixture of Ag nanowires with PZT-PDMS composite for the enhancement of power generation. A power generation principle of the PZT-PDMS NCG and the role of the Ag nanowires were verified from the comparison of output performances from the generators. The NCC generator produces a peak voltage of  $\sim 2.5$  V and current of 200 nA. The piezoelectric nanocomposite technique reported here successfully overcomes the size-related restrictions and enables simple, low-cost, and large-scale stabled generator. These results represent a critical step in the realization of self-powering nanotechnology that harvests electricity such as wireless sensors, implantable devices, personal electronics, MEMS, and so on.

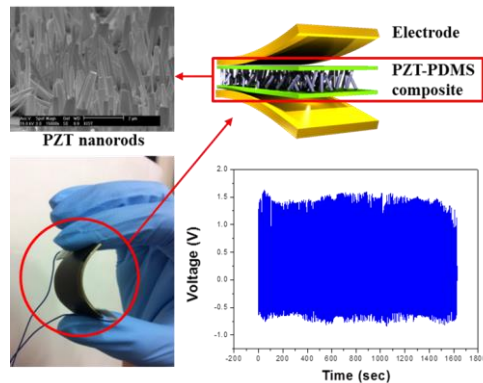


Fig. 133: Fabricated PZT-PDMS nanocomposite generator and its output performance.



## Remanent polarization and electromechanical properties of LTCC-PZT monomorphs

Sobocinski Maciej, Juuti Jari, Jantunen Heli

Microelectronics and Materials Physics Laboratories, University of Oulu, Finland

Email: maciej.sobocinski@ee.oulu.fi

Poling is a crucial stage in polycrystalline ceramic in order to exhibit piezoelectric properties. In the case of Low Temperature Co-fired Ceramic embedded piezoelectric bulk structures, poling is necessary step of manufacturing as elevated temperature of the process is far above the Curie temperature of common PZT compositions. In previous works by the authors<sup>409,410,411</sup>, LTCC embedded structures were poled with 1.6 kV/mm and higher fields were restricted by occurring electrical breakdown during the poling. Although sufficient remanent polarization has been obtained, further improvement of poling should be emphasized. This paper focuses on optimization of the poling conditions for LTCC-PZT unimorph structures. The problem of occurring electrical breakdown has been solved by applying additional dielectric layer at the edges of the structure. Hysteresis measurements were done from 0.1 V/ $\mu\text{m}$  to 3 V/ $\mu\text{m}$  for three temperatures: 25 °C, 75 °C and 125 °C. Remanent polarization of 22  $\mu\text{C}/\text{cm}^2$  was obtained for the monomorph structure with 3.7 V/ $\mu\text{m}$  poling field at 125 °C. Subsequently LTCC-PZT samples were poled in the optimal conditions and electrical and electro-mechanical properties was measured and compared to previous results. Higher remanent polarization and planar coupling effect was obtained.

<sup>409</sup> Σοβοχινσκι Μ., Λεινονεν Μ., Ξυυτι Ξ., Ξαντυνεν Η. □Πιεζοελεχτριχ αχτιπε μιρρορ συσπενσιον εμβεδδεδ ιντο Λοω Τεμπερατυρε Χο-φιρεδ Χεραμιχ□, IEEE Τρανσαχτιονσ ον Υλτρασονιχσ, Φερροελεχτριχσ, ανδ Φρεθυενχψ Χοντρολ ζολ. 59, νυμ. 9, π. 1990–1995, 2012

<sup>410</sup> Σοβοχινσκι Μ., Λεινονεν Μ., Ξυυτι Ξ., Ξαντυνεν Η., □Μονομορπη πι εζοελεχτριχ ωιδεβανδ ενεργψ ηαρπεστερ ιντεγρατεδ ιντο ΛΤΧΧ□, Ξου ρναλ οφ τηε Ευροπεαν Χεραμιχ Σοχιετυ, ζολυμε 31, Ισσυε 5, π. 789–794, 2011

<sup>411</sup> Σοβοχι)σκι Μ., Ζοιερζ Ρ., Ξυυτι Ξ., Ξαντυνεν Η., Γολονκα Λ., □Ελεχτριχ αλ ανδ ελεχτρομεηανιχαλ χηαραχτεριστιχσ οφ ΛΤΧΧ εμβεδδεδ πι εζοελεχτριχ βυλκ αχτυατορσ.□, Ξουρναλ οφ Αδωανχεσ ιν Αππλιεδ Χεραμιχ, πολ. 109, νο. 3, ππ. 135–138, 2010

## Stress-modified phase transitions in polarized PMN-PIN-PT, KN and KNL-NTS single crystals/textured ceramics: thermal expansion and Raman scattering studies

Aneta Slodczyk<sup>1</sup>, Gwénael Gouadec<sup>1</sup>, Philippe Colomban<sup>1</sup>, Mai Pham Thi<sup>2</sup>

<sup>1</sup> LADIR, umr7075 CNRS - UPMC, Paris, France

<sup>2</sup> THALES Research & Technology-France, 91767 Palaiseau, France

Email: philippe.colomban@upmc.fr

Due to their high application potential various piezoelectric single crystals are widely investigated. Since, their outstanding properties result from very complex physical and chemical behavior usually limited to the local structure/nanostructure, specific methods of analysis are necessary. Consequently, we have performed the thermal expansion and Raman scattering studies of lead based PMN-PIN-PT relaxor ferroelectric single crystals and a lead-free KN or KNL-NTS ( $\text{K}_{0,38}\text{Na}_{0,52}\text{Li}_{0,04}\text{(Nb}_{0,86}\text{Ta}_{0,10}\text{Sb}_{0,04})\text{O}_{2,97}$ ) ferroelectric solid solution single crystal/textured ceramic. The used techniques probe well the local nano-heterogeneity and allow detecting the structural phase transitions as a function of temperature and applied stress. Since, the polarization plays a key role in the behavior of complex, multi-domains (relaxor) ferroelectrics, the single crystals were preliminary poled along the [001] and [101] crystallographic directions. A sequence of two 1<sup>st</sup> order structural phase transitions is clearly seen in the case of KNN solid solution whereas more complex structural modifications: contraction/expansion (as a function crystallographic direction) are also detected at 70°C (KN) and 121°C (PMN-PIN-PT), respectively. The dependence of phase transition character/force and temperatures on applied stress/pressure is discussed. The phase transitions determined by dilatometry are in good agreement with the results of Raman scattering recorded as a function of temperature/pressure in a wide (Stokes and anti-Stokes) wavenumber range. For example, such analysis revealed the presence of strong soft mode behavior in the case of KN single crystal.

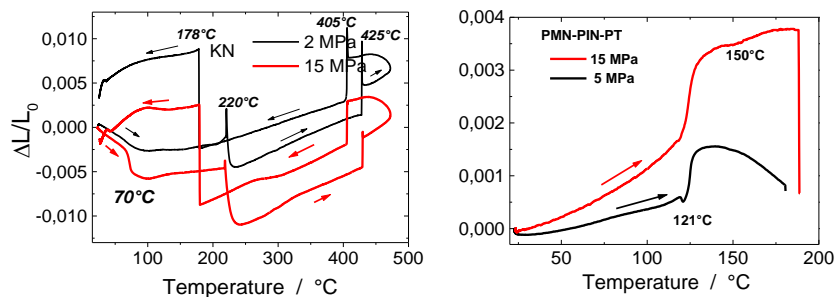


Fig. 1. Thermal expansion curves of polarized KN and PMN-PIN-PT single crystals measured parallel to [001] under various stress (2/5 and 15MPa).

Raman spectra recorded while rotating the sample around the microscope optical axis allowed determining the Raman modes sensitive to the symmetry/polarization changes. Raman mapping were recorded with (VV and VH) and without selection of the scattered light polarization before and after various temperature/pressure cycles for samples in polarized and depolarized states.

## Investigation of poling behavior under complex loading conditions

Sophia Eßlinger<sup>1</sup>, Rostislav Svidler<sup>1</sup>, Peter Neumeister<sup>1</sup>, Andreas Schönecker<sup>1</sup>

<sup>1</sup>Fraunhofer-IKTS, Dresden, Germany

Email: Sophia.Esslinger@ikts.fraunhofer.de

Piezoceramic transducers are key components in smart structures, providing the desired active functions. The integration of the active material during manufacturing often has thermal or mechanical impact on the piezoelectric material, altering its properties. Thus, knowledge of the effects of these influences on the piezoelectric ceramic is essential to optimize manufacturing and to predict material behavior.

The polarization of ceramics is a key step in activating the piezoelectric coupling. Former measurements of switchable polarization of soft piezoelectric ceramics disclosed a characteristic dependency of the remanent polarization  $P_r$  on the applied electric field strength  $E$  and the temperature  $T$ <sup>1</sup>. The correlations between remanent polarization and performance data for unclamped transducers are empirically known. Polarization measurements under compressive<sup>2</sup> and tensile loadings<sup>3</sup> are reported for piezoelectric ceramics, whereas measurements on compressive loading orthogonal to the electric field and polarization are only rarely reported in the literature<sup>4</sup>. The considered manufacturing technologies of our research imply orthogonal compressive load, motivating us to extent measurements of polarization and related functional data in this condition. For being able to do systematic studies on various samples, a test set-up allowing for orthogonal uniaxial, orthogonal biaxial and orthogonal isotropic loading is currently developed, see Fig.1.

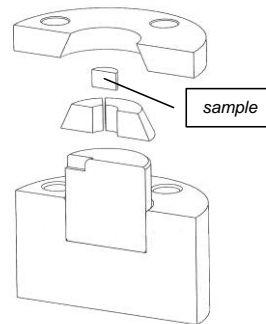


Fig. 1: Exploded view of the sample holder (cross section) allowing for orthogonal isotropic loading

<sup>1</sup>M. Nicolai, S. Uhlig, A. Schönecker, A. Michaelis, "Experimental Investigation of Non-linear Behavior of PZT Piezoceramics at Low Temperatures", Advances in Science and Technology Vol. 56 (2008) pp 105-110.

<sup>2</sup>Zhou, D.: Experimental Investigation of Non-linear Constitutive Behavior of PZT Piezoceramics. Dissertation. Universität Karlsruhe, Karlsruhe, 2003.

<sup>3</sup>Guillon, O.; Thiebaud, F.; Delobelle, P.; Perreux, D.: Tensile behavior of PZT in short and open-circuit conditions. In Materials Letters 58 (6), 2004, pp. 986–990.

<sup>4</sup>Kounga Njiwa, A. B.; Aulbach, E.; Granzow, T.; Rödel, J.: Influence of radial stress on the poling behaviour of lead zirconate titanate ceramics, Acta Materialia 55 (2007) 675–680.

## **Stability study of [011] ternary PIN-PMN-PT relaxor ferroelectric single crystals under high electric field and compressive stress**

Th.Pastureaud<sup>1</sup>, M. Dosi<sup>1</sup>, F-X Launay<sup>1</sup>, R. Thannberger<sup>1</sup>, P. Finkel<sup>2</sup>, H. Robinson<sup>2</sup>, J. State<sup>2</sup>,  
C.Murphy<sup>2</sup>, E. Leveugle<sup>3</sup> and M. Pham-Ti<sup>3</sup>

<sup>1</sup>Thales Underwater System, Acoustic & Mechanical Competence Centre, 525 route des dolines, BP 157, 06903 Sophia-Antipolis cedex, France

<sup>2</sup>Naval Undersea Warfare Center - Devices, Sensors & Materials R&D, 1176 Howell Street, Newport, RI 02841

<sup>3</sup>Thales Research and Technology, Campus Polytechnique, 1 Avenue Auguste Fresnel, 91767 Palaiseau Cedex, France

Email: thomas.pastureaud@fr.thalesgroup.com

Piezoelectric properties of [011] poled 32 mode 24PIN-48PMN-28PT single crystals have been studied under temperature, large stress and electric field. Dielectric drift measurement shows good stability up to field of 350 Vrms/mm, which appears consistent with polarization field loop measured at room temperature. Room temperature elastic and piezoelectric responses, measured independently, display strong and sharp discontinuity at approximately 17 MPa compressive stress that is associated with the stress induced phase transition. These results agree with previous data supporting the conclusion that in ternaries this instability is likely related to the ferroelectric rhombohedral (R) – orthorhombic (O) phase transition. In good agreement with existing model, we observe the destabilization of the (R) phase by applying DC electric field along the poling direction. Stability stress-field-temperature diagrams defining the linear regions for the crystal are constructed.

PZT materials with compositions at the morphotropic phase boundary (MPB) between the tetragonal (P4mm) and rhombohedral (R3m) phase fields exhibit very high dielectric and piezoelectric properties which are intensively used for technological applications (sensors and actuators, microelectromechanical systems, and high frequency devices) [1]. We recently reported an *in situ* description of the origin of the ferroelectric properties as a function of the applied electric field E based on a synchrotron X-ray diffraction study [2]. The monoclinic (pseudo-rhombohedral)/ tetragonal phase ratio was found to increase with electric field which strongly supported the hypothesis of Noheda *et al.*, who explained the strong piezoelectric properties of PZT by the presence of a monoclinic phase [3] based on a polarization rotation mechanism [4]. Additionally, polarization flipping of polar lead atoms could unambiguously be characterized by a maximum in the disorder of lead ( $B_{\text{iso}}(\text{Pb})_{\text{m}}$ ) for the positive-negative value of the coercive field ( $E_{\text{c}}$ ) in the  $P_{\text{s}} - E$  hysteresis cycle. Here, we present a structural description of the macroscopic piezo- and ferroelectric properties in the important technological material Lead Zirconate Titanate (PZT) by *in situ* synchrotron X-ray and Neutron diffraction. In addition to a technically applied material, we investigated the poling behavior of different composition series in the vicinity of the MPB. The structural changes were either induced by variations of the lead oxide content during sintering or different titanium / zirconium ratios. Stroboscopic pump-probe measurements down to 250  $\mu\text{s}$  time resolution reveal differences in poling kinetics depending on composition. For the technically applied material they spectacularly comfort our interpretations and clearly show the time structure characterizing the ferroelectric poling response.

[1] B. Jaffe, W. R. Cook, H. Jaffe, *Piezoelectric Ceramics*, Academic, London (1971).

[2] M. Hinterstein *et al.* *Phys. Rev. Lett.* **107**, 077602 (2011).

[3] B. Noheda, D. E. Cox, G. Shirane, J. A. Gonzalo, L. E. Cross, and S.-E. Park, *Appl. Phys. Lett.* **74**, 2059 (1999).

[4] R. Guo, L. E. Cross, S.-E. Park, B. Noheda, D. E. Cox, and G. Shirane, *Phys. Rev. Lett.* **84**, 5423 (2000).

## Study on Electric-field induced Strain and Dielectric Properties of PMN-PT Ceramics

Wei Zhao<sup>1,2</sup>, Wei Ruan<sup>1</sup>, Lizhu Huang<sup>1,2</sup>, Jiangtao Zeng<sup>1</sup>, Liaoying Zheng, Huarong Zeng, Guorong Li<sup>1</sup>

<sup>1</sup>Shanghai Institute of Ceramics, Chinese Academy of Sciences, Shanghai, China

<sup>2</sup>University of Chinese Academy of Sciences, Beijing, China

E-mail: zjt@mail.sic.ac.cn

The (1-x)PMN-xPT ( $0.1 \leq x \leq 0.35$ ) ceramics were prepared by columbite method. The correlation of the ferroelectric/piezoelectric properties with domain structure was studied systemically. As the PT content increases, the ferroelectric state of PMN-PT system transforms gradually from the relaxor ferroelectric state to the normal ferroelectric state, accompanied with the change of electric-field induced strain, ferroelectric and dielectric properties. Electric-field induced strain reaches the maximum value of 0.25% at 32 kV/cm for the sample 70/30 due to its piezoelectric character. The *P-E* loop and dielectric property of (1-x)PMN-xPT clarify domain's contribution to the large strain. The dielectric behavior is found to have a thermal hysteresis due to the hysteresis of domains state changing between microdomain and macrodomain.

## Temperature-Dependent Strain Properties of Nb-doped $\text{Bi}_{1/2}(\text{Na}_{0.84}\text{K}_{0.16})_{1/2}\text{TiO}_3$ – $\text{SrTiO}_3$ Lead-Free Piezoelectrics

Rizwan Malik<sup>1</sup>, Thi Hinh Dinh<sup>1</sup>, Changhyo Hong<sup>1</sup>, Hyoung-Su Han<sup>1</sup>, Wook Jo<sup>2</sup>, Ali Hussain<sup>3</sup> and Jae-Shin Lee<sup>1</sup>

<sup>1</sup>School of Material Science and Engineering, University of Ulsan, Ulsan, Republic of Korea

<sup>2</sup>Institute of Materials Science, Technische Universität Darmstadt, Darmstadt, Germany

<sup>3</sup>School of Nano and Advanced Materials Engineering, Changwon National University, Gyeongnam, Republic of Korea

Email: bestkorean01@hotmail.com

Recently,  $0.82(\text{Bi}_{1/2}\text{Na}_{1/2})\text{TiO}_3$ - $0.18(\text{Bi}_{1/2}\text{K}_{1/2})\text{TiO}_3$  solid solution (BNKT) ceramics and their modified ones have attracted great attention because of their large electric field-induced strains (EFIS). However, BNKT retains a crucial problem of showing high strain values only near room temperature. Meanwhile, actuators for practical applications are required to maintain high strain over a wide temperature range dependent on their operating environment and self-heating.

In this study, lead-free  $0.96[\text{Bi}_{1/2}(\text{Na}_{0.84}\text{K}_{0.16})_{1/2}\text{TiO}_3]$ - $0.04\text{SrTiO}_3$  (BNKT-ST) ceramics and Nb-doped BNKT-ST (BNKNT-ST) were fabricated by the conventional solid-state method, and their dielectric and piezoelectric properties were investigated as functions of Nb doping level and temperature. The normalized strain ( $S_{\text{max}}/E_{\text{max}}$ ) of BNKT-ST was 246 pm/V at room temperature, rapidly increased up to  $110^\circ\text{C}$ , and reached its highest value of 742 pm/V. In contrast, the BNKTN-ST showed quite different  $S_{\text{max}}/E_{\text{max}}$  values compared with BNKT-ST. The  $S_{\text{max}}/E_{\text{max}}$  was started as 726 pm/V at room temperature. After that, as rising temperature it decreased gradually and the value was still remaining 560 pm/V at  $110^\circ\text{C}$ .

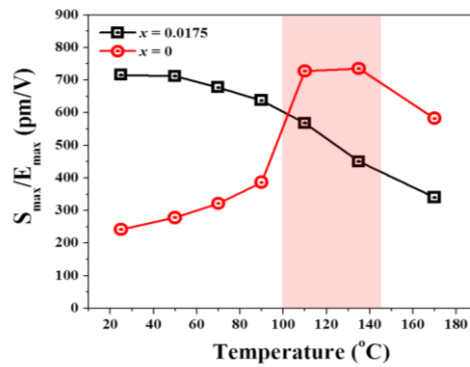


Fig. 134: Comparison of temperature dependence of  $S_{\text{max}}/E_{\text{max}}$  between undoped and Nb-doped BNKT-ST ceramics.

## Comparative study of electrical properties of PbLaZrTiOx capacitors with Al-doped ZnO and ITO top electrodes

Yoko Takada, Toru Tsuji, Naoki Okamoto, Takeyasu Saito, Kazuo Kondo, Takeshi Yoshimura<sup>a</sup>, Norifumi Fujimura<sup>a</sup>, Koji Higuchi<sup>b</sup>, Akira Kitajima<sup>b</sup>, and Akihiro Oshima<sup>b</sup>

Dept. of Chem. Eng., Osaka Prefecture University, Sakai, Osaka, JAPAN

<sup>a</sup> Dept. of Phys. Electro., Osaka Prefecture University, Sakai, Osaka, JAPAN

<sup>b</sup> Inst. of Sci. and Ind. Res., Osaka University, Ibaraki, Osaka, JAPAN

Email: [ytakada@chemeng.osakafu-u.ac.jp](mailto:ytakada@chemeng.osakafu-u.ac.jp)

Ferroelectric Random Access Memory (FeRAM) has attracted much attention and it is believed to be next generation non-volatile memory for its high operation (read/write) speed and low power consumption<sup>1</sup>. For example, the application of FeRAM includes transportation IC tags, mobile cards, and so on. However, conventional noble metal electrodes for ferroelectric materials, Pt, Ir or IrO<sub>2</sub>, causes price and resource issues for FeRAM device fabrication. In this study, we used conductive Al-doped ZnO (AZO)<sup>2</sup> and Sn-doped In<sub>2</sub>O<sub>3</sub> (ITO)<sup>3</sup> as an alternative for Pt top electrodes of PbLa(Zr,Ti)O<sub>3</sub> (PLZT) capacitors and evaluated the ferroelectric properties.

The substrates were highly (111)-oriented sputtered Pt as lower electrodes. PLZT (Pb:La:Zr:Ti=113:3:30:70) films (500 nm) were prepared by the sol-gel method. The films were deposited on Pt substrate by spin coating, at 3000 rpm for 20 s. Then, the gel-films were dried at 200°C for 2 min in order to eliminate the solvent, and pyrolyzed at 300°C for 10 min, in air for organic components removal. The films were prepared by repeating (3 times) the deposition and pyrolysis cycle. The prepared thickness was 500 nm. The coated films were finally calcined in air at 750°C, 10 min, in air for achieving crystallization. Pt top electrodes were deposited by sputtering. AZO and ITO top electrodes were deposited by Pulsed Laser Deposition (PLD). These deposition were performed with a metal through mask having 50 μm ~ 500 μm diameter. The composition of AZO and ITO targets were ZnO:Al<sub>2</sub>O<sub>3</sub>=98.5:1.5 wt.% and In<sub>2</sub>O<sub>3</sub>:SnO<sub>2</sub>=95.0:5.0 wt.%, respectively.

Initial polarization values of PLZT capacitors with Pt, AZO and ITO as top electrodes were 24.1 μC/cm<sup>2</sup>, 20.2 μC/cm<sup>2</sup>, 16.2 μC/cm<sup>2</sup>, respectively. Fig. 1 shows the polarization ratio of PLZT capacitors with Pt, AZO and ITO electrodes after heating in 200°C, 1 Torr, 3% hydrogen atmosphere. polarization ratio of PLZT capacitors with Pt AZO and ITO electrodes after 45 minutes were 0.23, 0.28, and 0.28, respectively. The implementation of AZO was promising in terms of hydrogen degradation.

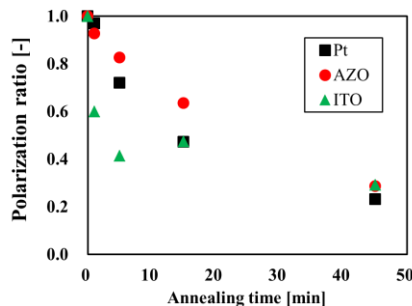


Fig. 1 Changes in polarization ratio of PLZT capacitors with Pt, AZO and ITO top electrodes at 15 V.

### References

- 1) M.M. Zhang *et al.*, Solid-State Electronics, Vol. 53, p. 473 (2009).
- 2) A. Suzuki *et al.*, Thin Solid Films, Vol. 517, p. 1478 (2008).
- 3) A.V. Rao *et al.*, Materials Letters, Vol. 29, p. 255 (1996).

and

The



## Leakage Currents in Sol-Gel PZT Films

Alexander Sigov, Yury Podgorny, Konstantin Vorotilov, Alexey Vishnevskiy

Moscow State Technical University of Radioengineering, Electronics and Automation (MIREA),  
Moscow, Russia

Email: rector@mirea.ru

Ferroelectrics are used in the capacitor structures of memory devices, therefore leakage currents and electrical breakdown represent potential problems which should be solved to provide the required operating characteristics. The study of the current–voltage ( $I$ – $V$ ) characteristics permits to obtain information on charge transport mechanisms in PZT films and film–electrode interfaces.

Possible conduction mechanisms in ferroelectric films (dielectrics) are the Schottky and Poole–Frenkel emissions, the Fowler–Nordheim tunneling, the ohmic, space–charge–limited, hopping conductivity, and conductivity via the grain boundaries<sup>412,413</sup>.

The objective of this research is to study the conduction mechanisms in PZT ferroelectric thin films prepared by the sol–gel method on silicon substrates with platinum bottom electrode for different voltage ramp speed and electric fields strengths. Long–term (tens of minutes) depolarization processes in metal–ferroelectric–metal (MFM) structure are studied as well.

Main mechanisms of leakage currents in thin PZT ferroelectric films prepared by the sol–gel method are discussed. Four specific regions are determined in  $I$ – $V$  dependences. At very weak fields (10–20 kV/cm) the current falls with the voltage increase as a result of depolarization. In the low field region (about 70–100 kV/cm), the leakage current decreases with decreasing voltage ramp speed, and its components are the ohmic and displacement currents. In the high field region ( $\geq 130$  kV/cm) the leakage current increases with decreasing step voltage ramp, in contrast to the previous case. Possible conductivity mechanisms are the Pool–Frenkel emission and hopping conduction. In the transition region between abovementioned ones (from 80–90 to  $\sim 130$  kV/cm), an abrupt unstable current increase is observed caused by breakdown of reverse bias Schottky barrier.

Depolarization current is given by a decreasing function which can be approximated by the sum of two exponents with different relaxation times. As an example, depolarization currents for sol–gel PZT thin films prepared at different annealing temperatures are studied. It is shown that both absolute and relative values of depolarization currents are increased with the increase of annealing temperature caused by film–substrate interface distortion.

---

<sup>412</sup> R. Waser, M. Klee, “Theory of conduction and breakdown in perovskite thin films”, *Integr. Ferroelectrics*, vol. 2, p. 23–40, 1992.

<sup>413</sup> M. Dawber, K.M. Rabe, J.F. Scott, “Physics of thin–film ferroelectric oxides”, *Rev. Mod. Phys.*, vol. 77, p. 1083–1130, 2005.

## Simultaneous piezoelectric and ferroelectric characterization of thin films for MEMS actuators

Andrea Mazzalai<sup>1</sup>, Davide Balma<sup>1</sup>, Nachiappan Chidambaram<sup>1</sup>, Paul Murali<sup>1</sup>

<sup>1</sup>Ceramics Laboratory, École Polytechnique Fédérale de Lausanne – EPFL,  
Lausanne, Switzerland

Email: andrea.mazzalai@epfl.ch

Recent improvements of piezoelectric thin films, like lead zirconate titanate  $\text{Pb}(\text{Zr}_x\text{Ti}_{1-x})\text{O}_3$  (PZT), are driven by high volume applications that will lead to an exponential increase of the piezo-MEMS market. Many devices of interest like inkjet print-heads or autofocus lenses are actuators relying on the transverse converse piezoelectric effect of ferroelectric thin films sandwiched between a parallel-plate capacitor structure. For the purpose of film development, we need to measure the in-plane stress ( $T_1$ ) and the ferroelectric polarization (P) loops. In this work, we have set up a cheap, versatile and easy to use tool that is based on an optical probe, a charge amplifier, a XYZ manipulator stage, and suitable cantilever samples that may have the full wafer thickness. The derivative of the obtained stress loop gives directly the converse piezoelectric coefficient  $e_{31,f} = \frac{\partial T_1}{\partial E_3}$  at a given voltage for an arbitrary waveform.

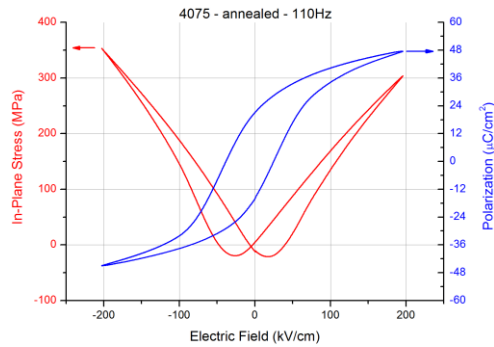


Figure 135. Simultaneous measurement of polarization and stress loops at a sol-gel deposited PZT thin film. The curves are averages of 500 continuous cycles made at a repetition rate of 110Hz.

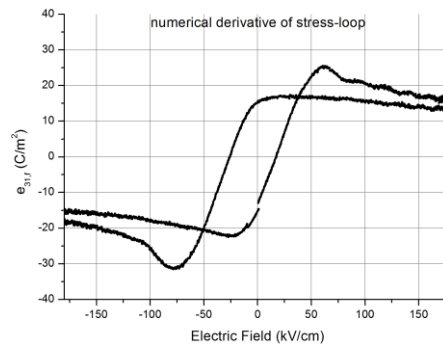


Figure 136. Numerical derivative of the averaged stress loop yields the effective converse piezoelectric coefficient  $e_{31,f}$  as a function of the electric field.

Figure 1 shows the measurement obtained with a  $1.18\mu\text{m}$  thick, sol-gel PZT thin film annealed after top electrode deposition. The remnant effective piezoelectric coefficient  $e_{31,f}$  was measured as  $14.7 \text{ C/m}^2$  with this set-up, and is identical to the direct  $e_{31,f}$  measured with the set up for the direct effect (as explained in refs <sup>414</sup>, <sup>415</sup>). We shall present the calculation of the in-plane stress from the cantilever deflection and report on a detailed study about the impact of the sample geometry and set-up parameters on accuracy and precision of the measurement.

<sup>414</sup> Dubois et. al. Sensors and Actuator A 77 (1999), p. 106

<sup>415</sup> Ledermann et. al. Sensors and Actuators A 105 (2003), p 162



## Effect of Polarization on Mechanical Properties of PZT Ceramics

Yao Yu, Xusheng Wang, Xi Yao

Functional Materials Research Laboratory, Tongji University, 1239 Siping Road, Shanghai200092, PR  
China

Email: yuyao9903@126.com

**Abstract:** The dynamic mechanical properties (storage modulus and internal friction) of PZT-5H and PZT-8 ceramics with temperature were investigated before and after polarization at different vibration load of 0.1, 0.5, 1, 5 and 10Hz by Dynamic Mechanical Analysis (DMA). The Curie temperature of PZT-5H and PZT-8 ceramics tested by DMA are 438K and 548K. The relaxation peak emerges in internal friction curves, and their position and intensity vary in different laws for PZT-5H and PZT-8.

The relaxation processes were studied according to Arrhenius law. The activation energies of unpolarized and polarized PZT-5H ceramics are 1.29eV and 1.36eV, the activation energies of unpolarized and polarized PZT-8 ceramics are 1.05eV and 1.08eV.

- <sup>i</sup> F. Cordero, F. Trequattrini, F. Craciun, and C. Galassi, *J Phys Condens Matter* **23**, 415901 (2011).
- <sup>ii</sup> M. A. Carpenter, J. F. Bryson, G. Catalan, S. J. Zhang, and N. J. Donnelly, *J Phys Condens Matter* **24**, 045902 (2012).
- <sup>iii</sup> W. Schranz, H. Kabelka, A. Sarras, and M. Burock, *Applied Physics Letters* **101**, 141913 (2012).
- <sup>iv</sup> A. Bouzid, E. M. Bourim, M. Gabbay, and G. Fantozzi, *Journal of the European Ceramic Society* **25**, 3213 (2005).
- <sup>v</sup> S. A. T. Redfern, C. Wang, J. W. Hong, G. Catalan, and J. F. Scott, *Journal of Physics-Condensed Matter* **20**, 452205 (2008).
- <sup>vi</sup> G. Picht, K. G. Webber, Y. Zhang, H. Kungl, D. Damjanovic, and M. J. Hoffmann, *Journal of Applied Physics* **112**, 124101 (2012).
- <sup>vii</sup> S. Sarkar, X. Ren, and K. Otsuka, *Physical Review Letters* **95**, 205702 (2005).
- <sup>viii</sup> E. Buixaderas, D. Nuzhnyy, J. Petzelt, L. Jin, and D. Damjanovic, *Physical Review B* **84**, 184302 (2011).
- <sup>ix</sup> J. Weerasinghe, D. W. Wang, and L. Bellaiche, *Physical Review B* **85**, 014301 (2012).
- <sup>x</sup> M. Wehnacht, A. Sotnikov, H. Schmidt, E. Smirnova, and S. Ktitorov, *Proceedings of the 2011 IEEE International Symposium on Applications of Ferroelectrics (ISAF)*, Vancouver, July 2011.
- <sup>xi</sup> J. Hlinka, J. Petzelt, S. Kamba, D. Noujni, T. Ostapchuk, "Infrared dielectric response of relaxor ferroelectrics", *Phase Transition*, vol. 101, pp. 167402(1-4), 2008.
- <sup>xii</sup> F. Jona, G. Shirane, F. Mazzi, and R. Pepinsky, "X-Ray and Neutron diffraction study of antiferroelectric lead zirconate,  $\text{PbZrO}_3$ ", *Phys. Rev.*, vol. 105, pp. 849-856, 1957.
- <sup>xiii</sup> T. Ostapchuk, J. Petzelt, V. Železný, S. Kamba, B. Malič, M. Kosec, L. Čakare, K. Roleder, J. Dec, "Infrared spectroscopy of lead zirconate single crystal, ceramics and films", *Ferroelectrics*, vol. 239, pp.109-115, 2000.
- <sup>xiv</sup> T. Ostapchuk, J. Petzelt, V. Železný, S. Kamba, V. Bovtun, V. Porokhonsky, A. Pashkin, P. Kuzel, M.D. Glinchuk, I.P. Bykov, B. Gorshunov, M. Dressel, "Polar phonons and central mode in antiferroelectric  $\text{PbZrO}_3$  ceramics", *J. Phys.: Condens. Matter*, vol. 13, pp.2677-2689, 2001.
- <sup>xv</sup> J. Hlinka, T. Ostapchuk, D. Nuzhnyy, J. Petzelt, P. Kuzel, C. Kadlec, P. Vanek, I. Ponomareva, L. Bellaiche, "Coexistence of the phonon and relaxation soft modes in the terahertz dielectric response of tetragonal  $\text{BaTiO}_3$ ", *Phys. Rev. Lett.*, vol. 101, pp. 167402(1-4), 2008.
- <sup>xvi</sup> Yang, S. Y. et al., *Nature Nanotechnology*, 2010, 5, 143-147
- <sup>xvii</sup> Alexe, M., *Nano Letters*, 2012, 12, 2193-2198
- <sup>xviii</sup> Matthias B. and Remeika J.P., *Phys. Rev.* 1949, 76, 1886.
- <sup>xix</sup> Bollmann W. and Stöhr H.J., *Physica Status Solidi A* 1977, 39, 477.
- <sup>xx</sup> Bagotsky V.S., *Fundamentals of Electrochemistry*; Wiley 2006.

<sup>1</sup> V. Ya. Shur, E. L. Rumyantsev, S. D. Makarov, "Kinetics of phase transformations in real finite systems: Application to switching in ferroelectrics", *J. Appl. Phys.*, vol. 84, p. 445-451, 1998.

<sup>xxii</sup> J. Hlinka *et al.*, *Phys. Rev. B*, vol. 83, article no. 020101(R), 2011.

<sup>xxiii</sup> ...

<sup>xxiv</sup> J. Hlinka, B. Hehlen, A. Kania and I. Gregora, "Soft mode in cubic  $\text{PbTiO}_3$  by hyper-Raman scattering", *Phys. Rev. B*, vol. 87, p. 064101 (1-4), 2013

---

<sup>xxv</sup> I. Tomeno, J.A. Fernandez-Baca, K.J. Mary, K. Oka, Y. Tsunoda, “Simultaneous softening of acoustic and optical modes in cubic PbTiO<sub>3</sub>”, Phys. Rev. B, vol. 86, p. 134306(1-15), 2012.

<sup>xxvi</sup> Goto, T., Kimura, T., Lawes, G., Ramirez, a. P., & Tokura, Y., Physical Review Letters, 92, 257201 (2004).

<sup>xxvii</sup> Hu, C., Physical Review B, 77, 174418 (2008).

<sup>xxviii</sup> Mochizuki, M., Furukawa, N., & Nagaosa, N., Physical Review B, 84, 144409 (2011).

<sup>xxix</sup> K. Nakamura and H. Shimizu, Ferroelectrics **93**, 211 (1989)

<sup>xxx</sup> V.D. Kugel, G. Rosenman, and D. Shur, J. Appl. Phys. **78**, 5592 (1995).

<sup>xxxi</sup> A.A. Grekov, A.A. Adonin, N.P. Protsenko, Ferroelectrics **13**, 483 (1976).

<sup>xxxii</sup> J. Seidel, et al., Nature Materials **8**, 229 (2009).

<sup>xxxiii</sup> H. Ishizuki, I. Shoji and T. Taira, Appl. Phys. Lett. **82**, 4062 (2003).

<sup>xxxiv</sup> M. Schröder, et al., Adv. Funct. Mater. **22**, 3936 (2012).

<sup>xxxv</sup> V.Ya. Shur et al., Appl. Phys. Lett. **77**, 3636 (2000).